

A Role for Opioid Neuropeptides in L-DOPA-Induced Dyskinesias in Parkinson's Disease

A thesis submitted to the University of Manchester for the degree of Doctor of Philosophy in the Faculty of Medicine

1997

Brian Henry

**Division of Neuroscience
School of Biological Sciences**

ProQuest Number: 10758128

All rights reserved

INFORMATION TO ALL USERS

The quality of this reproduction is dependent upon the quality of the copy submitted.

In the unlikely event that the author did not send a complete manuscript and there are missing pages, these will be noted. Also, if material had to be removed, a note will indicate the deletion.



ProQuest 10758128

Published by ProQuest LLC (2018). Copyright of the Dissertation is held by the Author.

All rights reserved.

This work is protected against unauthorized copying under Title 17, United States Code
Microform Edition © ProQuest LLC.

ProQuest LLC.
789 East Eisenhower Parkway
P.O. Box 1346
Ann Arbor, MI 48106 – 1346

5596301x
11 19962
(D C T M A)



Abstract

The dopamine precursor L-3,4-dihydroxyphenylalanine (L-DOPA) and other dopamine-replacing agents have been used in the treatment of Parkinson's disease for over 30 years. However, long-term L-DOPA-treatment is associated with many disabling side-effects, most notably the abnormal involuntary movements termed L-DOPA-induced dyskinesias. To date, the neural mechanisms underlying L-DOPA-induced dyskinesias remain unknown. In this thesis a possible role for opioid neuropeptides derived from the large molecular weight precursors pre-proenkephalin-A (PPE-A) and pre-proenkephalin-B (PPE-B) in mediating the neural mechanisms underlying L-DOPA-induced dyskinesias has been investigated. These proteins are the precursors for enkephalin and dynorphin which are the endogenous ligands for delta and kappa opioid receptors, respectively.

A novel rodent model of L-DOPA-induced dyskinesia has been characterised. Thus, following repeated L-DOPA-administration in the unilateral 6-hydroxydopamine-lesioned rat model of Parkinson's disease, an enhancement of the rotational response elicited by a given dose of L-DOPA was observed. This enhanced behavioural response has been characterised pharmacologically, and it was demonstrated that non-dopaminergic drugs known to reduce L-DOPA-induced dyskinesia in both patients and MPTP-treated macaques displaying L-DOPA-induced dyskinesias also attenuate the enhanced behavioural response observed in this rat model. This enhanced behavioural response was not seen following *de novo* administration of anti-parkinsonian drugs, such as bromocriptine or lisuride, known not to cause dyskinesias in either patients or MPTP-treated macaques.

Northern blot hybridisation was used to investigate the expression of PPE-A and PPE-B in the rodent model of L-DOPA-induced dyskinesia. Following repeated L-DOPA-administration, a significant increase in PPE-A (165%) and PPE-B (988%) expression was observed in the dopamine-depleted striatum when compared to the unlesioned striatum. This increase was not observed following vehicle treatment. In further behavioural experiments, co-administration of opioid receptor antagonists selective for delta and kappa opioid receptors reduced the enhanced response to L-DOPA seen in long-term treated 6-OHDA-lesioned rats by 38% and 37% respectively.

These data suggest that, following repeated L-DOPA-administration, the precursors for both enkephalin and dynorphin are increased selectively in the dopamine-depleted striatum and that opioid receptor activation underlies a significant part of the hyperkinesia observed in this rat model of L-DOPA-induced dyskinesia. *In situ* hybridisation was employed to study the topography of PPE-A and PPE-B expression in 6-OHDA-lesioned rats and changes induced by repeated L-DOPA, bromocriptine or lisuride treatment. Following lesion and repeated vehicle administration a significant increase in PPE-A expression is observed (maximal 78%). No alteration in PPE-B expression was observed throughout the rostrocaudal extent of the striatum. Following repeated L-DOPA-administration a significant increase in both PPE-A and PPE-B expression was observed in dorsolateral areas of the rostral striatum (128% and 2150%, respectively). Conversely, following repeated high dose therapeutically-active bromocriptine or lisuride administration, the lesion-induced increase observed in PPE-A expression was reduced to unlesioned levels and no alteration in PPE-B expression was observed. Topographical analysis of PPE-A and

PPE-B synthesis was also performed in MPTP-treated macaques with dopamine receptor agonist-induced dyskinesias. Increased PPE-A expression in both sensorimotor and associative areas of the rostral striatum was observed (24% and 30%, respectively, compared with MPTP-treated non-dyskinetic). PPE-B expression was also increased in the dyskinetic group (maximal 85% in the striosomal compartment and 62% in matrix).

Enhanced opioid peptide transmission in striatal efferent projections, may therefore provide a mechanism by which long-term dopamine-replacement therapy leads to the appearance of dyskinetic side-effects. The data described in this thesis suggest that a therapy combining selective kappa and/or delta opioid receptor antagonists, with traditional anti-parkinsonian agents such as L-DOPA, may be associated with a lower incidence of dyskinesia than currently-available treatments.

Declaration

No portion of the work referred to in this thesis has been submitted in support of an application for another degree or qualification at this or any other institution of learning.

Statement of Copyright

Copyright in text of this thesis rests with the Author. Copies (by any process) either in full, or of extracts, may be made **only** in accordance with instructions given by the Author and lodged in the John Rylands University Library of Manchester. Details may be obtained from the Librarian. This page must form part of any such copies made. Further copies (by any process) of copies made in accordance with such instructions may not be made without the permission (in writing) of the Author.

The ownership of any intellectual property rights which may be described in this thesis is vested in the University of Manchester, subject to any prior agreement to the contrary, and may not be made available for use by third parties without the written permission of the University, which will prescribe the terms and conditions of any such agreement.

Further information on the conditions under which disclosures and exploitation may take place is available from the Head of the Department of Neuroscience.

Acknowledgements

The work presented in this thesis was carried out within the Division of Neuroscience, School of Biological Sciences at the University of Manchester. I am grateful to Professor Alan R. Crossman for his guidance, supervision and the opportunity to carry out this work.

I would also like to thank Dr Jonathan M. Brotchie for his supervision and tireless-enthusiasm which has provided enough faith and energy in this project for both of us (several times over!). I am also indebted to Jon for providing me with an alternative scientific environment in which to work which proves that 'left to their own devices they probably would'.

Special thanks to Yann for showing me the ropes (and pointing me in the right direction of the brain) in those hazy early days. I would also like to thank Neill for making the transition to Manchester all the easier, Dave and Steve for all their help and encouragement and Billy for his constant theorising and perseverance with the Calbindin. Thanks to Mick, Chris, Sue and Oggy (and Jon and Yann again!) for making the many years spent in the lab the most enjoyable period of my life (so far)!

I would also like to thank Helen, Des, Jackie, Cha and Sandra for providing me with a sense of normality and reminded me that there is life outside the lab (or at least distracting me long enough to actually have one!). Thanks to my Mum and Dad for providing me with the freedom to pursue whatever I wanted and the encouragement to 'stick at it'.

Love and special thanks goes to Mitchy for her encouragement and for looking after and enduring me throughout my unendurable phase of the last year - I don't know how you did it!

Contents

Chapter 1:

General Introduction	17
1.1 Functional anatomy of the basal ganglia - an overview	18
1.1.1 Neostriatum	18
1.1.2 Globus pallidus	30
1.1.3 Subthalamic nucleus	33
1.1.4 Substantia nigra	36
1.1.5 VA/VL Thalamus	38
1.1.6 Superior colliculus	40
1.1.7 Pedunculopontine nucleus (PPN) and related nuclei	41
1.1.8 Synaptic connectivity of the basal ganglia	43
1.2 Dysfunction of the basal ganglia	46
1.2.1 Parkinson's disease	46
1.2.2 Aetiology of idiopathic Parkinson's Disease	47
1.2.3 Non-idiopathic parkinsonism	54
1.2.4 Animal models of Parkinson's disease	56
1.2.5 Pathophysiology of Parkinson's disease	63
1.3 Treatments for Parkinson's disease	66
1.3.1 Anti-cholinergic compounds	67
1.3.2 Amantidine and related compounds	68
1.3.3 Dopamine-replacing agents	69
1.3.4 Other pharmacological interventions	71
1.3.5 Surgical interventions	73
1.3.6 High frequency stimulation	75
1.3.7 Surgical transplantation	76
1.3.8 Summary of treatments for Parkinson's disease	77

1.4 L-DOPA-induced dyskinesias	78
1.4.1 Hyperkinetic movement disorders (chorea and dystonia)	80
1.4.2 Animal models of dyskinesias	82
1.4.3 Pathophysiology of dyskinesias	87
1.4.4 Clinical management of L-DOPA-induced dyskinesias	92
1.5 Opioid neuropeptides	94
1.5.1 Molecular biology of opioid peptides	96
1.5.2 Structure of opioid peptides	98
1.5.3 Opioid receptors	99
1.5.4 Functional significance of opioid receptor stimulation	102
1.5.5 Peptide neurotransmission	103
1.5.6 Opioid peptide modulation of neurotransmission within the basal ganglia	104
1.6 Opioid peptide alterations in dopamine-depleted animals and parkinsonian patients	107
1.7 Opioid peptide alterations following dopamine receptor stimulation in dopamine-depleted animals and parkinsonian patients	112
1.8 Aims of study	116
 Chapter 2:	
Characterisation of a rodent model of L-DOPA-induced dyskinesia in Parkinson's disease	117
2.1 Introduction	118
2.2 Methods	121
2.2.1 Unilateral 6-OHDA-lesion of the medial forebrain bundle	121
2.2.2 Drug treatment and behavioural analysis	121
2.2.3 High dose L-DOPA-treatment	122

2.2.4 Low dose L-DOPA-treatment	122
2.2.5 Calculation of L-DOPA 'on-time' in the 6-OHDA-lesioned rat	123
2.2.6 Calculation of rotations/minute during 'on-time'	123
2.2.7 Time course of L-DOPA-induced rotations following repeated low dose L-DOPA administration in the 6-OHDA-lesioned rat model of Parkinson's disease on days 14-21	123
2.2.8 Bromocriptine-treatment in the 6-OHDA-lesioned rat model of Parkinson's disease	123
2.2.9 Lisuride-treatment in the 6-OHDA-lesioned rat model of Parkinson's disease	124
2.2.10 Effect of non-dopaminergic drugs on L-DOPA-induced rotation in the 6-OHDA-lesioned rat model of Parkinson's disease following repeated L-DOPA treatment	124
2.2.11 Cresyl violet histological staining	125
2.2.12 Spontaneous locomotion following administration of non -dopaminergic drugs in normal, non-dopamine depleted, rats	126
2.2.13 Statistical analysis	127
2.3 Results	128
2.3.1 Verification of the specificity of a 6-OHDA-lesion injected into the medial forebrain bundle for dopaminergic cells	128
2.3.2 Effects of dopaminergic agents on rotational locomotion in the 6-OHDA-lesioned rat	130
2.3.3 Pharmacokinetics of repeated L-DOPA administration with respect to rotational response in the 6-OHDA-lesioned rat model of Parkinson's disease	133
2.3.4 Effect of co-administration of non-dopaminergic drugs on L-DOPA-induced rotational locomotion in the 6-OHDA- lesioned rat following repeated L-DOPA administration	138
2.3.5 Effect of non-dopaminergic drugs on spontaneous locomotion in normal, non-dopamine depleted, rats	144
2.4 Discussion	151

Chapter 3:

Striatal opioid peptide precursor expression and antagonism of opioid peptide transmission in the rodent model of L-DOPA-induced dyskinesia 157

3.1 Introduction 158

3.2 Methods 161

3.2.1 Northern Blot Hybridisation 161

3.2.2 Reserpine-treated rat model of Parkinson's disease 171

3.2.3 6-OHDA-lesioned rodent model of Parkinson's disease 173

3.2.4 Functional antagonism of opioid receptors in the rat model of L-DOPA-induced dyskinesia 174

3.2.5 Statistical analysis 175

3.3 Results 176

3.3.1 Methodological optimisation of Northern blot hybridisation 176

3.3.2 Pre-proenkephalin-A mRNA expression in the reserpine-treated rat model of Parkinson's disease 186

3.3.3 Pre-proenkephalin-A and Pre-proenkephalin-B mRNA expression in the rat model of L-DOPA-induced dyskinesia 188

3.3.4 Effect of functional antagonism of opioid receptors in the rat model of L-DOPA-induced dyskinesia 199

3.4 Discussion 204

Chapter 4:

Topographical distribution of striatal pre-proenkephalin-A and pre-proenkephalin-B mRNA in the 6-OHDA-lesioned rat following repeated treatment with L-DOPA, bromocriptine or lisuride 213

4.1 Introduction 214

4.2 Methods	216
4.2.1 <i>In situ</i> hybridisation	216
4.2.2 Drug treatment and behavioural analysis in 6-OHDA-lesioned rats following repeated vehicle, L-DOPA, bromocriptine or lisuride administration	220
4.2.3 Assessment of lesion : [³ H] Mazindol binding	221
4.2.4 <i>In situ</i> hybridisation	223
4.2.5 Statistical analysis	227
4.3 Results	228
4.3.1 Methodological results	228
4.3.2 Rodent model of L-DOPA-induced dyskinesia	234
4.3.3 Assessment of lesion : ³ H Mazindol binding	238
4.3.4 Topographical distribution of striatal pre-proenkephalin-A mRNA in the 6-OHDA-lesioned rat following repeated treatment with vehicle, L-DOPA, bromocriptine or lisuride	239
4.3.5 Topographical distribution of striatal pre-proenkephalin-B mRNA in the 6-OHDA-lesioned rat following repeated treatment with vehicle, L-DOPA, bromocriptine or lisuride	262
4.4 Discussion	285
 Chapter 5:	
Topographical distribution of striatal pre-proenkephalin-A and pre- proenkephalin-B mRNA in the MPTP-treated non-human primate following dopamine-replacement therapy	296
5.1 Introduction	297
5.2 Methods	298
5.2.1 Production of dopamine agonist-induced dyskinesia in the MPTP-treated non-human primate model of Parkinson's disease	298
5.2.2 <i>In situ</i> hybridisation	299

5.2.3 Acetylcholinesterase histochemistry	301
5.2.4 Calbindin immunocytochemistry	301
5.2.5 Analysis of <i>in situ</i> hybridisation signal	303
5.2.6 Statistical analysis	305
5.3 Results	306
5.3.1 Production of dopamine agonist-induced dyskinesia in the MPTP-treated non-human primate model of Parkinson's disease	306
5.3.2 Methodological considerations	306
5.3.3 Topographical distribution of pre-proenkephalin-A (PPE-A) in the MPTP-treated non-human primate model of dopamine-induced dyskinesia	308
5.3.4 Topographical distribution of pre-proenkephalin-B (PPE-B) in the MPTP-treated non-human primate model of dopamine-induced dyskinesia	317
5.4 Discussion	328
Chapter 6:	
General Discussion	335
References	343

Abbreviations

2-DG	2-deoxyglucose
5-HT	5-hydroxytryptamine
5-MDOT	5-methoxy 5-N,N-dimethyl-tryptamine
6-OHDA	6-hydroxydopamine
ANOVA	analysis of variance
AP-1	activator protein-1
cAMP	cyclic adenosine monophosphate
b.d.	<i>bi die</i> (twice-daily)
CM	centromedian thalamic nucleus
COMT	catechol-o-methyl-transferase
CREB	cAMP response binding element
D-I-D	dystonia-improvement-dystonia
D1	dopamine D1 receptor
D2	dopamine D2 receptor
DA	dopamine
DATATOP	deprenyl and tocopherol antioxidant therapy for parkinsonism
dATP	deoxyadenosine triphosphate
DEPC	diethylpyrocarbonate
DNA	deoxyribonucleic acid
EDTA	ethylenediaminetetraacetic acid
G-protein	GTP binding regulatory protein
G3PDH	glyceraldehyde-3-phosphate
GABA	gamma-aminobutyric acid
GAD	glutamic acid decarboxylase
GPI	lateral segment of the globus pallidus
GPm	medial segment of the globus pallidus
HPLC	high performance liquid chromatography
i.m.	intramuscular
i.p.	intraperitoneal

i.v.	intravenous
IDPN	iminodipropionitrile
i.O.D.	integrated optical density
L-DOPA	L-3,4-dihydroxyphenylalanine
MANOVA	multiple analysis of variance
MAO-B	monoamine oxidase A
MLR	mesencephalic locomotor region
MPDP	1-methyl-4-phenyl-2,3-dihydropyridinium
MPP ⁺	1-methyl-4-phenylpyridinium
MPPP	1-Methyl-4-phenyl-4-propionoxypiperidine
MPTP	1-methyl-4-phenyl-1,2,3,6-tetrahydropyridine
MR 2034	(-) 5, 9-dimethyl-2' -OH-2 tetrahydrofurfuryl-6, 7-benzomorphan
mRNA	messenger ribonucleic acid
NAc	nucleus accumbens
NADPH	nicotinamide adenine dinucleotide phosphate
NMDA	N-methyl-D-aspartate
<i>nor</i> -BNI	<i>nor</i> -binaltorphimine
OD	optical density
PF	parafasicular nucleus of the thalamus
PHNO	(+)-4-propyl-9-hydroxynaphthoxazine
PPE-A	pre-proenkephalin-A (pro-enkephalin)
PPE-B	pre-proenkephalin-B (pro-dynorphin)
PPN	pedunculopontine nucleus
rpm	revolutions per minute
RNAse	ribonuclease
SCH 23390	R(+)-7-cholro-8-hydroxy-1-phenyl-2,3,4,5-tetrahydro-1H-3-benzazepine
SCH 32615	3-amino-2-methyl-8-phenylmethoxyimidazo [1,2-a]pyrazine hydrochloride
SDS	sodium dodecyl sulphate
SEM	standard error of the mean

SKF 38393	(±)-1-phenyl-2,3,4,5-tetrahydro-(1H)-3-benzazepine-7,8-diol
SNpc	substantia nigra pars compacta
SNpr	substantia nigra pars reticulata
SSC	standard sodium citrate
T _m	melting temperature
U50 488H	trans-3, 4-dichloro-N-methyl-N-[2-(1-pyrrolidinyl)-cyclohexyl] benzeneacetamide methanesulfonate hydrate
VA	ventral anterior nucleus of the thalamus
VAmc	ventral anterior pars magnocellularis
VApc	ventral anterior pars principlis
VCM	vacuous chewing movement
Vim	ventral intermediate nucleus of the thalamus
VL	ventral lateral nucleus of the thalamus
VLc	ventrolateral pars caudalis
VLm	ventrolateral pars medialis
VLo	ventrolateral pars oralis
VM	ventromedial nucleus of the thalamus
MTA	ventral tegmental area

Chapter 1:

General Introduction

1.1 Functional anatomy of the basal ganglia - an overview

The basal ganglia are a group of functionally-related sub-cortical nuclei involved in both the planning and control of voluntary movement. The basal ganglia integrate and process information from all areas of the cerebral cortex as part of the process that provides spatially and temporally co-ordinated movement. Dysfunction of the basal ganglia results in a range of movement disorders. These consist of both hypokinetic disorders such as Parkinson's disease and hyperkinetic disorders such as Huntington's chorea and hemiballism.

The complex functional anatomy of the basal ganglia has been delineated by utilising a variety of techniques such as histochemistry, neuroanatomical tracing, neurochemistry, lesioning studies, immunocytochemistry, molecular biology and functional imaging. The basal ganglia consist of: the substantia nigra, which can be subdivided into two distinct components, namely the compacta, and the ventrally located, reticulata; the neostriatum; the pallidal complex (comprising two parts, a medial and lateral segment (GPM and GPI) in primates and the rodent homologue the entopeduncular nucleus and globus pallidus, respectively); and the subthalamic nucleus. The major nuclei of the basal ganglia are outlined in the following chapter.

1.1.1 Neostriatum

Gross morphology

The neostriatum is the major input structure of the whole basal ganglia complex. The neostriatum consists of the caudate nucleus, putamen and nucleus accumbens. In this thesis, the term striatum is used to denote the caudate nucleus and putamen of the primate, and dorsal neostriatum of the rat, with the nucleus accumbens referred to as a distinct entity.

In the primate brain, the caudate nucleus and putamen rostrally form one continuous entity. However, in the primate more caudally, they become two distinct structures, separated by the internal capsule. In the rat brain, the caudate nucleus and

putamen form one continuous entity throughout the rostro-caudal extent, termed the striatum.

Rostrally, the caudate nucleus lies in a dorsal position with the putamen situated more ventrolaterally. Caudally, the putamen lies lateral to the internal capsule and globus pallidus and it is separated from the globus pallidus by a thin lamina of nerve fibres known as the lateral medullary lamina. Caudally, the caudate lies dorsal and medial to the internal capsule. In the rodent brain there is no segregation of the caudate and putamen, and therefore forms one continuous structure, termed the striatum.

The caudate nucleus consists of a large rostral head and a tapering curved tail. The tail of the caudate passes caudally, gradually tapering as it does so, following the curvature of the lateral ventricle, where it descends into the temporal lobe. At the temporal extremity of the tail of the caudate lies the amygdala which is associated with limbic functions. In a similar manner, the nucleus accumbens is also associated with limbic functions and lies adjacent to medial and ventral portions of the rostral caudate-putamen.

Nucleus accumbens

The nucleus accumbens (NAc) is located ventral to the anterior commissure comprising the anterior, ventromedial part of the striatum that surrounds the anterior horn of the lateral ventricle and extends dorsally into the lateral part of the septum. The NAc is considered by many authors to be a part of the striatum as it does share many common afferent and efferent connections. However, although the NAc shares similarities in both afferent, efferent connections (Nauta and Domesick, 1978; Groenewegen and Russchen, 1984), and immunohistochemical characteristics (Pert *et al.*, 1976; Wamsley *et al.*, 1980) the prominent features that identifies the NAc as a distinct entity is the preferential input from limbic regions such as the hippocampus and the amygdala (Groenewegen *et al.*, 1990; Heimer *et al.*, 1991) and by certain unique features of its neurochemical organisation.

The NAc shows a compartmentalisation depending on immunohistological staining techniques and afferent and efferent projections. This compartmentalisation is known as the 'core' and 'shell' of the NAc. The first demonstration of this division within the NAc was the observation that atypical striatal projections to the

hypothalamus originated within a central 'core' region of the NAc (Groenewegen and Russchen, 1984).

Subsequent studies labelling cholecystokinin, zinc and acetylcholinesterase indicated that two distinct regions were present in the NAc (Zaborszky *et al.*, 1985). From these studies a central 'core' region was apparent surrounded on the medial, ventral and lateral sides by a 'shell' region. These regions show further differences in receptor binding, dopamine metabolism and electrophysiological properties (Zaborszky *et al.*, 1985; Zahm, 1989; Deutch and Cameron, 1992; Pennartz *et al.*, 1992; Brog *et al.*, 1993). The afferent and efferent connections of the NAc also remain distinct between either the core or shell compartments (Brog *et al.*, 1993). Afferent connections from the hippocampus, the paraventricular nucleus of the thalamus and the infralimbic cortex are predominantly associated with the shell, whereas fibres originating from the intermediodorsal nucleus of the thalamus, the prelimbic and dorsal insular cortices innervate predominantly the core (Kelley and Domesick, 1982; Groenewegen *et al.*, 1987; Berendse and Groenewegen, 1990; Berendse *et al.*, 1992). With respect to efferent connections, neurons in the shell of the NAc project mainly to the ventromedial part of the ventral pallidum, the ventral tegmental area and the retrorubral area. Neurons of the core innervate the dorsolateral part of the ventral pallidum and medial parts of the substantia nigra, both pars compacta and reticulata (Zahm, 1989; Groenewegen *et al.*, 1990; Heimer *et al.*, 1991; Berendse *et al.*, 1992). Within the core and shell compartments, the classical striosome-matrix compartmentalisation of the striatum (as described by Graybiel and Ragsdale (1979) and later in this section) becomes less well defined, with some, but not all identifying features maintained (Zahm and Brog, 1992; Jongen-Relo *et al.*, 1993). Recently, calbindin-D_{28k} has also been used to delineate the core and shell regions of rat, marmoset (*Callithrix jacchus*), rhesus (*Macaca mulatta*) and human nucleus accumbens (Meredith *et al.*, 1996).

Embryology of the neostriatum

Within the striatum the majority of the neurons are projection neurons, termed medium spiny neurons. In rodents, the medium spiny neurons, develop from the secondary germinal matrix derived from the neuroepithelium in the inferior horn of the lateral ventricle between developmental days E16 - E 22. Distinct neurogenic gradients

exist within striatal development, with ventrolateral neurons forming first and dorsomedial neurons later (Bayer and Altman, 1987). In the primate brain, the two components of the striatum appear to develop from two distinct embryological origins which accounts for the structural distinction in the adult. The caudate nucleus and putamen are telencephalic derivatives which develop from different parts of the striatal ridge and follow distinct migratory paths (Hamilton and Mossman, 1972).

Neuronal organisation of the neostriatum

The major neuronal type within the striatum are the medium spiny neurons which, in the rat, constitute 90-95% of all striatal neurons, while in the primate they represent 80-90% (Graveland and Di Figlia, 1985). Medium spiny neurons are the output neurons of the striatum and contain the inhibitory transmitter γ -aminobutyric acid (GABA, Fonnum *et al.*, 1978; Aroni *et al.*, 1984). Medium spiny neurons, as their name suggests, have a medium-sized cell body (approx. 15 μm in diameter), from which radiate 4-5 dendrites. These dendrites arborise and become densely covered with spines. Axons from medium spiny neurons give rise to several collaterals before leaving the area of the cell body. These collaterals show extensive arborisation, following two different patterns (Wilson and Groves, 1980).

The most common pattern is characterised by the neuron synapsing with either the dendritic domain of the cell of origin, or a nearby cell. This organisation allows local interactions within the striatum (Park *et al.*, 1980). The pattern less-commonly observed is characterised by a much larger and more extended arborisation which extends beyond, and often does not synapse with, the cell of origin (Kawaguchi *et al.*, 1990).

All medium spiny projection neurons utilise the neuropeptides enkephalin, dynorphin, substance P, and neurotensin, associated with GABA.

Afferents of the neostriatum

The striatum receives two major afferents, one a dopaminergic afferent mainly from the substantia nigra pars compacta (SNpc), the other a glutamatergic afferent from all regions of the cerebral cortex. The striatum also receives smaller inputs from the

thalamus (glutamatergic), the dorsal and medial raphe nucleus (serotonergic) and the subthalamic nucleus (glutamatergic). These will now be considered in greater detail.

Dopaminergic afferents

The striatum receives a large dopaminergic projection from the ipsilateral mesencephalon. This arises from the substantia nigra pars compacta (SNpc, A9), ventral tegmental area (VTA, A10) and retrorubral area (A8, Carpenter and Peter, 1972; Gerfen, 1985; Jimenez-Castellanos and Graybiel, 1987). These dopaminergic projections are topographically-arranged (Fallon and Moore, 1978a, b). The neurons of the SNpc are darkly pigmented in primate due to the presence of neuromelanin, a by-product of dopamine synthesis. The nucleus accumbens, receives dopaminergic input predominantly from the VTA. This projection is known as the mesostriatal pathway. The dopaminergic projection to the striatum from the SNpc and retrorubral areas is termed the nigrostriatal pathway.

The majority of dopaminergic afferent projections from the SNpc, VTA and retrorubral areas make synapses with the base of dendritic spines of medium spiny neurons. However, such synapses are only made with spines that also receive cortical input (Bouyer *et al.*, 1984). Other less prominent connections are made directly with the cell bodies and the dendritic shaft. Dopamine also innervates the terminals of the cortico-striatal fibres (Freund *et al.*, 1984; Smith and Bolam, 1991).

Corticostriatal afferents

Several studies have demonstrated the existence of an extensive excitatory glutamatergic projection from virtually all regions of the cerebral cortex to the neostriatum. This projection is predominantly, but not exclusively, from the ipsilateral hemisphere (Kurnzle, 1975; Kurnzel, 1977; Smith and Bolam, 1991). This projection is excitatory utilising glutamate as transmitter (Kim *et al.*, 1977; Young *et al.*, 1981; Hassler *et al.*, 1982; Errami and Nieoullon, 1986; Spencer, 1986).

In the primate, the motor cortex projects preferentially to the putamen, where the body is represented in an inverted, somatotopic manner. More anterior regions of the

frontal lobe and other association areas of the cerebral cortex, project predominantly to the caudate nucleus (Kurnzel, 1975).

The neostriatum of the primate brain can be divided into associative, sensorimotor or limbic territories depending on the input it receives from the cerebral cortex. The associative territory comprises input from the various association cortices in the frontal, temporal and parietal lobes (Kurnzel, 1977; Goldman and Nauta, 1977; Ragsdale and Graybiel, 1981).

The sensorimotor territory receives input from the primary motor and somatosensory cortices (Kurnzel, 1978; Liles and Updyke, 1985), while the limbic territory receives input from the limbic and paralimbic cortices as well as from the amygdala and hippocampus (Russchen and Price, 1984; Phillipson and Griffith, 1985; Haber *et al.*, 1990). In a similar manner to the primate, the rodent neostriatum can also be divided in associative, sensorimotor and limbic territories (McGeorge and Faull, 1989). The most ventral area of the rostral neostriatum, i.e. the nucleus accumbens, receives input from the limbic-associated areas and the remaining striatum can now be easily segregated into associative and sensorimotor inputs. The dorsolateral, and to a lesser extent the ventrolateral, area of the rodent striatum receives input from the sensorimotor areas of the cortex, while the remaining striatum receives associative input.

Afferent connections from the cerebral cortex to the medium spiny neurons contact mainly the distal portion of the dendritic spines of the medium spiny neuron (Bouyer *et al.*, 1984; Kemp and Powell, 1970; 1971).

Thalamostriatal projections

The striatum receives a further glutamatergic input from the ipsilateral thalamus (Kitai *et al.*, 1976). In the primate, the centromedian (CM) thalamic nuclei project preferentially to the putamen, whilst the parafacicular (PF) thalamic nuclei project to the caudate nucleus and nucleus accumbens (Powell and Cowen, 1956; Sadikot *et al.*, 1990). In the rat, the striatal innervation from the thalamus is less well-defined with CM/PF projections to all areas of the striatum (Herkenham and Pert, 1981; Berendse and Groenewegen, 1990).

The striatal afferents from the thalamus and cerebral cortex do not appear to converge on the same striatal spiny neurons (Dube *et al.*, 1988). The projection from the thalamus to the medium spiny neurons form synapses principally with the distal part of the dendritic spine, in a similar manner to the glutamatergic projection from the cerebral cortex. However, thalamic inputs can also directly synapse on the dendritic shaft (Dube *et al.*, 1988).

Striatal afferents from the raphe nuclei

The striatum receives serotonergic afferents from both the dorsal and median raphe nuclei (Dray *et al.*, 1978; Parent *et al.*, 1981; Soghomonian *et al.*, 1989; Vertes, 1991). These ipsilateral 5-HT-containing fibres innervate the striatum, pallidal complex and the substantia nigra pars reticulata (Pasik *et al.*, 1984; Azmitia and Gannon, 1986). This high degree of innervation arises from collateralisation of axons (van der Kooy and Hattori, 1980a). However, a certain level of topography is maintained (Imai *et al.*, 1986; Tork, 1990).

Subthalamostriatal projections

The striatum receives a further glutamatergic input from the subthalamic nucleus (Beckstead, 1983a; Royce and Laine, 1984; Kita and Kitai, 1987). There are also some small reciprocal connections between the ventral striatum and the medial part of the subthalamic nucleus in the rat (Groenewegen and Berendse, 1990).

Amygdalostriatal projections

The striatum receives projections from the amygdala, predominantly from the basal lateral amygdaloid nucleus (De Olmos and Ingeram, 1972). Rostral to the anterior commissure this projection is dense only in the nucleus accumbens, whereas the caudal part of the striatum receives a widespread amygdaloid projection (Kelley and Domesick, 1982). Amygdalostriatal projections are in general bilateral, with ipsilateral predominance (McGeorge and Faull, 1989). These projections from the amygdala to the striatum are topographically organised. A large number of amygdalostriatal projections

have collateral projections to prefrontal cortical areas (McDonald, 1991; Shinonaga *et al.*, 1994).

Intrinsic connections of the neostriatum

Within the striatum, a subset (5-10% in rat, 10-20% in primate) of neurons are the striatal interneurons (Gerfen 1985; Graveland and Di Figlia, 1985; Graveland *et al.*, 1985). Unlike the medium spiny projection neurons, the majority of synaptic connections made by striatal interneurons are not with themselves but are made with the medium spiny projection neurons. Interneurons are grouped into two main categories, giant aspiny interneurons and the medium-sized interneurons.

Giant aspiny interneurons

The giant aspiny interneurons have large elongated cell bodies (approx. 60 μm x 25 μm) from which several dendrites branch radially. These dendrites can extend through the striatum for up to several hundred micrometers from the cell body. Extensively-branched axons arise from these dendrites. The resulting arborisation produces a dense network of extremely fine axonal branches, thus producing a large surface area of contact with the medium spiny neurons (Phelps and Vauhn, 1986; Izzo and Bolam, 1988). The giant aspiny interneurons contain acetylcholine (Fonnum *et al.*, 1978; Butcher and Hodge, 1976). These cells have been shown not to project to the output structures of the basal ganglia but synapse with virtually all of the medium spiny projection neurons in this vicinity (Izzo and Bolam, 1988). As previously described, medium spiny projection neurons project, via collaterals, back onto the cholinergic interneurons.

Dopaminergic neurons also synapse directly on the cholinergic interneurons (Kubota *et al.*, 1987; Chang, 1988). The cholinergic interneurons can also be directly stimulated via projections from the cerebral cortex and thalamus (Wilson *et al.*, 1990; Lapper and Bolam, 1992). Cholinergic interneurons are found in both the striosome and matrix boundaries of the striatum (discussed in more detail in this section, Graybiel, 1986; Kawaguchi, 1993; Kubota and Kawaguchi, 1993).

Medium-sized interneurons

The medium-sized interneurons are subdivided into categories depending on their neurotransmitter content.

The first type of medium-sized aspiny interneurons contain GABA and parvalbumin, a calcium binding protein, and constitute 3-5% of the total striatal cell population in the rat (Gerfen, 1985). They are characterised by a round cell body (approx. 15 μm in diameter) with 5-8 dendrites that branch close to the cell body. These interneurons, like the acetylcholine-containing aspiny interneurons, are located in both the patch and matrix compartments of the striatum (Cowan *et al.*, 1990; Kita and Kitai, 1990). Parvalbumin-containing interneurons receive a significant projection from the cerebral cortex (Kita and Kitai, 1990). These interneurons also make significant connections between themselves. These connections have been suggested to be inhibitory (Kita and Kitai, 1990).

A second type of medium-sized interneuron contains somatostatin and neuropeptide Y but not, or at least very low levels of, GABA (Kawaguchi, 1993). These neurons also contain the enzyme nicotinamide adenine dinucleotide phosphate (NADPH)-diaphorase, the nitric oxide synthase involved in the production of nitric oxide. These somatostatin-containing interneurons are characterised by a spheroid cell body (approx. 12 μm in diameter) with 3-4 dendrites. These dendrites extend for approximately 100-200 μm in length and show an extensive arborisation of spine-like appendages (Di Figlia and Aronin, 1982). Although their cell bodies are found in both striosome and matrix compartments, these cells comprise 1-2% of striatal neurons and innervate mainly the matrix compartment (Gerfen, 1984; Chesselet and Graybiel, 1986). Somatostatin interneurons receive a direct connection from the cerebral cortex (Vuillet *et al.*, 1989a), and cholinergic and dopaminergic innervation (Vuillet *et al.*, 1989b, 1992; Kubota *et al.*, 1988; Aoki and Pickel, 1988).

The third type of smaller medium-sized interneuron, containing GABA and calretinin, is also present within the striatum. Calretinin is a calcium-binding protein with strong homology to calbindin D_{28K} (Bennett and Bolam, 1993). The function and properties of these interneurons remains to be elucidated.

Striosome-matrix striatal compartmentalisation

As will be discussed later, the major difference between the medium spiny neurons is their efferent projections. However, another subclassification within the striatum exists which differentiates medium spiny neurons. This subclassification is known as the striosome-matrix (Graybiel and Ragsdale, 1979) or patch-matrix compartmentalisation (Gerfen, 1984). This compartmentalisation is based on enzyme staining, afferent and efferent projections and to a certain degree neurochemical parameters. This arrangement will now be considered in more detail.

Historical delineation

The first reports of striosome-matrix compartmentalisation was derived on the basis of histochemical markers and radioligand binding studies. In the adult rat striatum patches enriched in μ opioid receptor binding were described (Pert *et al.*, 1976). Later it was described that acetylcholinesterase staining was weak in zones that were termed striosomes (Butcher and Hodge, 1976). These acetylcholinesterase weak areas exactly coincided with the μ opioid binding patches. These markers, together with somatostatin-containing fibres and calbindin-immunoreactive neurons (which both are located in the matrix) designate the 'striosome-matrix' compartmentalisation.

Afferent compartmentalisation - an overview

The striatal striosome and matrix regions receive differential afferent connections, both with respect to glutamatergic input from the cerebral cortex and dopaminergic input from the substantia nigra pars compacta, ventral tegmental area and retrorubral area. These afferent connections will now be discussed in more detail.

Corticostriatal compartmentalisation

With regard to the patch-matrix compartmentalisation, few projections from areas of the cerebral cortex appear to project to more than one striatal compartment (Gerfen, 1985; McGeorge and Faull, 1989).

Striosome compartments receive inputs from deep layer V and VI of the prefrontal and limbic cortices, whereas the matrix receives inputs from layer V and the supragranular layers of areas including the cingulate cortex, sensory cortex, motor cortex and certain prefrontal areas (Gerfen, 1984; McGeorge and Faull, 1989; Eblen and Graybiel, 1995).

Therefore, due to this pattern of cortical input, the striatal striosome-matrix organisation has been related to limbic and non-limbic functions, whereby, inputs to the striosomes originate from the limbic-related areas such as the amygdala and prelimbic cortex, while to the matrix from the sensorimotor cortical areas.

Dopaminergic compartmentalisation

The striosome and matrix compartments also receive different dopaminergic afferents. In the rat, the matrix receives dopaminergic input from the VTA, the dorsal portion of the substantia nigra pars compacta (SNpc) and the retrorubral area, whereas, striosomes receive dopaminergic input from the ventral tier of the SNpc (Gerfen, 1985). In the primate, Jimenez-Castellanos and Graybiel in 1987 used different terminology to describe the projections from the SNpc to striosome-matrix compartments. They described the striosomal afferents as arising in the 'denso-cellular zone' of both the substantia nigra pars compacta and reticulata, whereas the 'cell-sparse zone' of the substantia nigra pars compacta, ventral tegmental area (A10) and retrorubral areas (A8) projected to the matrix (Jimenez-Castellanos and Graybiel, 1987a, b).

Striosome-matrix efferent compartmentalisation

In the rat, medium spiny neurons within striosomes project to the dopaminergic cells of the SNpc, while those from the matrix project to the GABAergic cells of the SNpr and entopeduncular nucleus (Gerfen, 1985). However, in the primate, the striosomal neurons project not only to the SNpc but also to the SNpr and pallidal segments (Jimenez-Amaya and Graybiel, 1990). Projections to the two pallidal segments in the primate arise mainly from the matrix and are organised in 'clusters' of cells within the matrix termed 'non-striosomal but striosome-like compartments' (Jimenez-Castellanos and Graybiel, 1987b; 1989) or 'matrosomes' (Flaherty and Graybiel, 1993). However, some overlap in these matrosomes has been detected

(Flaherty and Graybiel, 1993). The dendrites of the striosomes and matrix projection neurons are restricted to the compartment of their parent cell body (Walker *et al.*, 1993).

Neuropeptide compartmentalisation

In the rat, it is generally accepted that medium spiny neurons projecting to the SNpr and entopeduncular nucleus (the rodent equivalent of the medial segment of the globus pallidus) express the neuropeptides dynorphin and substance P, while those to the globus pallidus express enkephalin (Cuello and Paxinos, 1978; Haber and Elde, 1981; Del Fiaccio *et al.*, 1982; Vincent and Hokfelt, 1982; Inagaki and Parent, 1984a; 1984b; Beckstead and Kersey, 1985; Gerfen and Young, 1988; Gerfen *et al.*, 1991). This neuropeptide expression within the medium spiny neurons, in the rat, does not follow any striosome-matrix compartmentalisation, with roughly equal numbers of medium spiny striatal neurons expressing enkephalin (65% in striosome neurons and 58% of matrix neurons) and dynorphin in both compartments (52% of striosome neurons and 45% of matrix neurons, Gerfen and Young, 1988).

However, in the primate a higher degree of segregation occurs with between 200-900% more dynorphin precursor mRNA within the striosomal compartment compared to the matrix (Hurd and Herkenham, 1995). Moreover, as will be discussed later, the efferent projection neurons of the primate neostriatum, containing enkephalin or dynorphin, are not as compartmentally-segregated as in the rat (Gerfen and Young, 1988).

Efferents of the neostriatum

The two main output pathways from the striatum project to both segments of the pallidal complex, and both segments of the substantia nigra (pars compacta and reticulata). Projections to the globus pallidus originate primarily in the putamen, while those to the substantia nigra pars reticulata arise in the caudate nucleus (Parent *et al.*, 1984, Feger and Crossman, 1984). The efferent connections of the striatum will be discussed in more detail in sections 1.1.2 and 1.1.4.

1.1.2 Globus pallidus

The globus pallidus is a wedge-shaped nuclear mass located between the medial surface of the putamen and the internal capsule. In the primate, the pallidal complex is sub-divided into two different structures known as the lateral (GPI) and medial segment of the globus pallidus (GPm) by a lamina of white matter known as the medial medullary lamina. The rodent homologues of these functionally-distinct structures are the globus pallidus and the entopeduncular nucleus, respectively. Whilst the rodent entopeduncular nucleus does not show great complexity in circuitry or compartmentalisation, in terms of overall function, connections and transmitters are thought to be equivalent to the primate GPm (van der Kooy and Carter, 1981).

In the primate, the smaller medial segment of the globus pallidus shares many cytological and connectional similarities with the SNpr. Although both the medial segment of the globus pallidus and the SNpr are separated by the internal capsule, they are best regarded as a single entity in the functional sense. Both the medial and lateral segments of the globus pallidus will now be considered separately, although both segments of the pallidal complex are reciprocally connected via inhibitory GABAergic neurons (Hasrati *et al.*, 1990; Kincaid *et al.*, 1991).

In the rodent, the cells of the entopeduncular nucleus originate before any other cells of the pallidum, between developmental days E12 - E14, with cells in the core maturing earlier than those in either the anterior or posterior poles. Neurons of the entopeduncular nucleus develop from the neuroepithelium of the third ventricle and are recognisable as entopeduncular nucleus as early as E13 (Bayer and Altman, 1987).

The neurons of the globus pallidus of the rodent originate between E13 and E16 in a complex neurogenic gradient. Posteriorventral neurons of the globus pallidus are the oldest, with younger neurons located more anteromedially (Bayer, 1985). The germinal source of the globus pallidus is thought to be the neuroepithelium in the ventromedial basal telencephalon, where the globus pallidus is apposed to the neuroepithelium of the third ventricle, the source of the entopeduncular nucleus (Bayer and Altman, 1987). In the primate brain, both segments of the globus pallidus are thought to be diencephalic derivatives arising from a dorsal lateral cell column of the hypothalamus, referred to as the 'subthalamic longitudinal zone' (Kuhlenbeck, 1948; Kuhlenbeck and Haymaker, 1949). The majority of this differentiation takes place in the

third foetal month when the lateral segment of the globus pallidus migrates rostromedially to contact the medial surface of the putamen (Carpenter, 1984).

Afferents of the lateral segment of the globus pallidus

The major afferent to the lateral segment of the globus pallidus (GPl) is from the striatum. The striatal efferents to the GPl are GABAergic in nature and co-express the opioid neuropeptide enkephalin (Cuello and Paxinos, 1978, Del Fiacco *et al.*, 1982; Beckstead and Kersey, 1985; Gerfen and Young, 1988). The medium spiny neurons that project to the GPl predominantly express the D2 dopamine receptor (Gerfen, 1990, Le Moine *et al.*, 1990, Le Moine and Bloch, 1995). However, recently all medium spiny neurons investigated were shown to express all dopamine receptor subtype classes (Surmeier *et al.*, 1996). The projection from the striatum to the lateral segment of the globus pallidus is topographically-arranged, such that, projections from the caudate nucleus terminate in the dorsomedial third of the GPl, while those projections from the putamen terminate in the ventrolateral two-thirds of the GPl (Hazrati and Parent, 1992a; Parent and Hazrati, 1994). Rostrocaudal and mediolateral topography is maintained throughout the striato-pallidal projection (Parent and Hazrati, 1994).

The GPl also receives glutamatergic input from the subthalamic nucleus (Palkoutis and Jakobowitz, 1974; Carpenter *et al.*, 1981), a 5-HT input from the dorsal raphe nucleus (Saavedra, 1977), dopaminergic projection from the SNpc (Parent and Smith, 1987a) and cholinergic input from the basal nucleus of Meynert (Soghomonian *et al.*; 1989).

Efferents of the lateral segment of the globus pallidus

The lateral segment of the globus pallidus projects predominantly to the subthalamic nucleus (Carpenter *et al.*, 1981), although inputs to the reticular nucleus of the thalamus (Hazrati and Parent, 1991), substantia nigra (Kincaid *et al.*, 1991) and the medial segment of the globus pallidus (Hazrati *et al.*, 1990) have also been described. These neurons utilise GABA as transmitter (Fonnum and Paulsen, 1990; Smith *et al.*, 1990; Berendse and Groenewegen, 1991) and, due to their spontaneous rate of discharge, tonically inhibit the subthalamic nucleus.

Afferents of the medial segment of the globus pallidus

The major afferent to the medial segment of the globus pallidus (GPM) arises from the striatum. The striatal efferents to the GPM are GABAergic in nature and co-express the neuropeptides dynorphin and substance P (Vincent and Hokfelt, 1982b; Beckstead and Kersey, 1985; Gerfen *et al.*, 1988; Gerfen and Young, 1990). The medium spiny neurons that project to the GPM predominantly express the D1 dopamine receptor (Gerfen, 1990; Le Moine and Bloch, 1995). However, evidence suggests that although these cells express predominantly dopamine D1 receptors, they also express other classes of dopamine receptors (Surmeier *et al.*, 1996). Topographical projections from the striatum exist in a similar manner to the lateral segment of the globus pallidus, such that the dorsal GPM receives input from predominantly the associative territories of the striatum, while the ventral portion of the GPM receives input from the sensorimotor areas of the striatum. Projections from the limbic territories of the striatum terminate predominantly in the medial tip of the GPM (Parent and Hazati, 1995a).

The GPM also receives an excitatory glutamatergic input from the subthalamic nucleus (Kita and Kitai, 1987; Robledo and Feger, 1990; Brochie and Crossman, 1991). This input is much more prominent than the projection to the lateral segment of the globus pallidus.

Retrograde tracing studies have shown that the medial part of the GPM receives afferents from the medial and ventrolateral part of the subthalamic nucleus (Smith *et al.*, 1990). The lateral part of the GPM receives inputs from the lateral part of the subthalamic nucleus (Berendse and Groenewegen, 1991).

Less prominent afferents originate from the substantia nigra pars compacta (Haber *et al.*, 1985), dorsal raphe nucleus (Soghomonian *et al.*, 1989; Vertes, 1991) and a cholinergic input via the basal nucleus of Meynert (De Vito and Anderson, 1982; Gonya-Magee and Anderson, 1983; Parent and De Bellefeuille, 1983).

Efferents of the medial segment of the globus pallidus

In the primate, the medial segment of the globus pallidus projects predominantly to the ventral anterior and ventral lateral thalamus (VA/VL). All these efferents have been demonstrated to be GABAergic (Pan *et al.*, 1983; Araki *et al.*, 1984). GABAergic

efferents from the GPM to the centromedian (CM) and parafascicular (PF) nuclei of the thalamus, the lateral habenula, and the pedunculopontine nucleus (PPN) have all been described (Nauta and Mehler, 1966; Carter and Fibiger, 1978; De Vito and Anderson, 1982; Gonya-Magee and Anderson, 1983).

The main projection of the entopeduncular nucleus of the rat is to the central area of the ventromedial nucleus (VM) of the thalamus. The lateral habenula, the parafascicular nucleus, the centromedian nucleus and the PPN have also been described as receiving inputs from the entopeduncular nucleus in the rat (Carter and Fibiger, 1978).

1.1.3 Subthalamic nucleus

The subthalamic nucleus is a small nuclear mass that lies along the dorsomedial surface of the internal capsule. The subthalamic nucleus consists mainly of projection neurons, although some (Rafols and Fox, 1976; Iwahori, 1978; Chang *et al.*, 1983), but not all studies (Yelnik and Percheron, 1979) have described interneurons.

The subthalamic nucleus of the rodent develops from a portion of the neuroepithelium in the anteriodorsal part of the mammillary recess between developmental days E13 - E15 (Bayer and Altman, 1987). In the primate brain, the subthalamic nucleus develops from the same area as the pallidal complex in the most caudal part of the area known as the 'subthalamic longitudinal zone' (Kuhlenbeck, 1948; Kuhlenbeck and Haymaker, 1949). In the third foetal month the subthalamic nucleus is prevented from migrating laterally by a group of fibres known as the hemispheric stalk. Although the subthalamic nucleus becomes separated from the pallidal complex by the fibres of the internal capsule, anatomical connections between these structures of common origin are maintained by fibres which traverse the peduncular part of the internal capsule (Carpenter, 1984).

The subthalamic nucleus receives its blood supply via the anterior choroidal artery, and also in part, from the posteromedial central arteries. The delicate nature of this supply leaves the subthalamic nucleus vulnerable to ischemic damage.

The subthalamic nucleus provides the only intrinsic excitatory projection within the basal ganglia and is of the utmost importance in the control of movement, a fact highlighted by the fact that any lesion of the subthalamic nucleus, via ischemic damage

or head trauma, causes hemiballism (Martin, 1927; Whittier, 1947; Carpenter, 1950, 1955). Furthermore, it has been demonstrated that overactivity within the subthalamic nucleus is central to the symptoms of Parkinson's disease (Bergman *et al.*, 1990; Brotchie *et al.*, 1991; Aziz *et al.*, 1991, 1992).

Subthalamic nucleus afferents

The major afferent connections of the subthalamic nucleus arise from the cerebral cortex (tonically exciting the subthalamic nucleus via a glutamatergic projection), and from the lateral segment of the globus pallidus (inhibiting the subthalamic nucleus via an inhibitory GABAergic projection).

In both the rat and primate, the subthalamic nucleus receives a large glutamatergic input from all areas of the cerebral cortex (Rouzaire-Dubois and Scarnati, 1985). The principle projection arises from the motor cortex. This projection is somatotopically-arranged, with clear representations of the leg, arm, and face terminating in the dorsolateral sector of the subthalamic nucleus (Kurnzle, 1978; Monakow *et al.*, 1978; Carpenter *et al.*, 1981; Jurgens, 1984). Neurons in the dorsolateral area of the subthalamic nucleus respond somatotopically to peripheral sensory stimulus (Wichmann *et al.*, 1993). Premotor cortical projections terminate principally in the ventromedial area of the subthalamic nucleus (Huerta *et al.*, 1985; Stanton *et al.*, 1988). The supplementary motor cortex and frontal eye fields also project to more ventromedial areas of the subthalamic nucleus. The subthalamic nucleus also receives inputs from limbic-associated areas, namely the amygdala and hippocampus (DeLong *et al.*, 1985; Parent and Smith, 1987b; Groenewegen and Berendse, 1990; Smith *et al.*, 1990). In the rat, this limbic projection appears to terminate in the medial tip of the subthalamic nucleus (Groenewegen and Berendse, 1990).

The largest input to the subthalamic nucleus, as described previously, arises from the lateral segment of the globus pallidus and is inhibitory in nature (Vincent *et al.*, 1982a; Oertel *et al.*, 1984; Smith *et al.*, 1987a; Canteras *et al.*, 1990; Fonnum *et al.*, 1990; Smith *et al.*, 1990). This inhibitory innervation is topographically-arranged. In rodents, this projection innervates all regions of the subthalamic nucleus and shows a mediolateral and rostrocaudal topography, with neurons in the lateral portion of the GPI innervating the lateral two-thirds of the subthalamic nucleus, whereas those in the

medial part of the GPI terminate in the remaining ventromedial third of the subthalamic nucleus.

In the primate, the GPI projects to the entire rostralateral two-thirds of the subthalamic nucleus (Carpenter *et al.*, 1981). It has been suggested that in the primate, the GPI projects principally to the rostralateral region of the subthalamic nucleus, that contains neurons projecting back to the GPI and not the caudomedial region of the subthalamic nucleus containing the neurons that project to the GPM (Parent and Hazrati, 1995b).

Subthalamic nucleus efferents

As already mentioned, subthalamic nucleus efferents provide the only excitatory pathway intrinsic to the basal ganglia, exerting a glutamate-mediated excitation of the substantia nigra pars reticulata and both segments of the globus pallidus.

In the primate, the projections to the GPI and GPM largely arise from separate subthalamic neurons, with only 10% of subthalamic nucleus cells exhibiting axon collaterals (Parent and Smith, 1987; Parent *et al.*, 1989). In the rat the majority of efferent projections (96%) to the SNpr and pallidal complex arise as axon collaterals (van der Kooy and Hattori, 1980b; Kita *et al.*, 1983). These efferent neurons from the subthalamic nucleus can be divided into distinct sensorimotor, associative and limbic regions (DeLong *et al.*, 1985; Parent and Smith, 1987; Groenwegen and Berendse, 1990; Smith *et al.*, 1990). It has been shown that the projection to the SNpr from the subthalamic nucleus arises from the dorsal and ventral surface of the subthalamic nucleus, and again is topographical-arranged (Whittier and Mettler, 1949a, b; Carpenter and Strominger, 1967). A small population of subthalamic neurons, located within a thin lateral strip of the nucleus, project to the pedunculopontine nucleus (Takada *et al.*, 1988).

Neurons from the medial tip of the subthalamic nucleus project to the limbic-associated regions of the ventral tegmental area and adjacent area of the SNpc. Through these connections, the subthalamic nucleus could effect the dopaminergic input to the striatum and may set the overall membrane excitability within the striatum. A smaller direct projection from the subthalamic nucleus to the striatum has been demonstrated (Beckstead, 1983a; Royce and Laine, 1984; Kita and Kitai, 1987; Parent and Smith,

1987; Smith *et al.*, 1990). Subthalamic nucleus neurons projecting to the caudate nucleus are located in the ventromedial area of the subthalamic nucleus, whereas those projecting to the putamen arise from the dorsolateral area of the subthalamic nucleus (Nauta and Cole, 1978; Parent and Smith, 1987b; Smith *et al.*, 1990).

A further, smaller projection has been demonstrated to arise from the subthalamic nucleus and project directly to the spinal cord (Takada *et al.*, 1987, 1988; Mizuno *et al.*, 1988).

1.1.4 Substantia nigra

The substantia nigra is an important component of the motor system with the dorsally-located substantia nigra pars compacta providing the dopaminergic input to the neostriatum. The substantia nigra pars reticulata, together with the GPM, forms the major output structures of the basal ganglia. In the rodent, the cells of the substantia nigra are derived from a primordial cell group in the ventral mesencephalon, which is first detectable by catecholamine fluorescence (Cooper, 1946; Seiger and Olson, 1973) and TH-immunoreactivity (Specht *et al.*, 1981a; 1981b) at approximately embryonic day E12. This cell group divides to form the SNpc, the VTA and retrorubral area cell groups by E17. In the primate brain, the cells of the substantia nigra divide on foetal days 36-43. Neurons of the substantia nigra develop from the neuroepithelium of the basal plate of the midbrain and migrate ventrally towards the cerebral peduncle (Shaner, 1936; Cooper, 1946; Hanaway *et al.*, 1971). The SNpc and SNpr will now be discussed separately.

Afferents of the substantia nigra pars compacta

Major inputs to the SNpc arise from the GABAergic medium-sized spiny neurons of the striatal striosomes (Gerfen, 1992). A smaller GABAergic connection to the SNpc also arises from the globus pallidus (Smith and Bolam, 1990, 1991). Other projections to the SNpc arise from the amygdala (Vankova *et al.*, 1992; Shinonaga *et al.* 1994), hypothalamus (Nauta and Domesick, 1978), preoptic area, and cortex, especially from the frontal and cingulate cortical areas (Wyss and Sripanidkulchai, 1984; Hurley *et al.* 1991; Sesack and Pickel, 1992).

Efferents of the substantia nigra pars compacta

The major output projection of the SNpc is the dopaminergic projection to the striatum. As already mentioned in section 1.1.1, dopaminergic projections from the SNpc and related nuclei (VTA and retrorubral area) project to the striatum in a topographical manner. Dopaminergic projections to all areas of the cerebral cortex are also present. This projection arises from the most dorsal tier of the SNpc. Many other smaller projections from the SNpc to other areas exist, including both the dorsal and medial raphe nuclei, ventral pallidum, locus coeruleus and hippocampus (Fallon and Moore, 1979; Gasbarri *et al.*, 1991; Klitenick *et al.*, 1992).

Afferents of the substantia nigra pars reticulata

The substantia nigra pars reticulata (SNpr) receives inputs from both the striatum (Somogyi and Smith, 1979; Somogyi *et al.*, 1979) and the subthalamic nucleus (Kita and Kitai, 1987). The striatal input is, as described previously (see section 1.1.1), GABAergic and co-expresses the neuropeptides dynorphin and substance P (Vincent *et al.*, 1982b; Beckstead and Kersey, 1985; Gerfen *et al.*, 1988; Gerfen and Young, 1990). This projection is topographically-arranged. In primates, the largest projection to the SNpr arises from the caudate nucleus. This projection terminates predominantly in the rostromedial two-thirds of the SNpr. Projections from the putamen terminate in the caudolateral third of the SNpr. However, this projection is less dense than the projection from the caudate nucleus. The nucleus accumbens projects to the medial SNpr. However, fibres also extend laterally and caudally (Haber *et al.*, 1990; Francois *et al.*, 1994).

In the rodent, striatonigral projections are also topographically arranged, with a similar mediolateral arrangement. However, the dorsoventral arrangement is inverted (Gerfen, 1985). The SNpr input from the subthalamic nucleus (Whittier and Mettler, 1949; Nauta and Cole, 1978; van der Kooy and Hattori, 1980b) is excitatory utilising glutamate as transmitter (Robledo and Feger, 1990; Brochie and Crossman, 1991).

Additionally, the SNpr receives less prominent projections from the globus pallidus (Smith and Bolam, 1989) and a serotonergic projection from the dorsal raphe nucleus (Dray *et al.*, 1978; Lavoie and Parent, 1990).

Efferents of the substantia nigra pars reticulata

The major efferent pathway of the SNpr (and as already discussed, the medial segment of the globus pallidus) is to the ventral anterior and ventro lateral areas of the thalamus (Carpenter and Peter, 1972; Beckstead, 1983b; Pare *et al.*, 1990). The SNpr also sends projections to the superior colliculus (see section 1.1.6, Graybiel, 1987) and to the pedunclopontine nucleus (see section 1.1.7, Jackson and Crossman, 1983; Moon-Edley and Graybiel, 1983).

All SNpr efferents are GABAergic in nature (Kilpatrick *et al.*, 1980) and fire tonically at a low rate due to the inhibitory nature of the striatonigral afferent and a low rate of excitation from the subthalamic nucleus. Taken together inhibition of SNpr outputs release the thalamic nuclei from their GABA-mediated inhibition, thus allowing movement.

1.1.5 VA/VL Thalamus

The thalamus represents the major target of the basal ganglia. The thalamus consists of a wide variety of cell types, with most of these cells having reciprocal links with the cerebral cortex (Schell and Strick, 1984).

The thalamus is divided by a thin layer of fibres known as the internal medullary lamina. This Y-shaped structure divides the thalamus into anterior, medial and lateral segments. The lateral nuclei are divided into a ventral tier and a dorsal tier, from which further subdivisions into individually-named nuclei are made.

The thalamic reticular nucleus is a thin layer of neurons interpose between the internal capsule laterally, and the external medullary lamina medially and covers the rostral and lateral aspects of the thalamus. This nucleus receives inputs from collaterals of both corticothalamic and thalamocortical axons (Jones, 1975). Cells of this nucleus in turn send their axons back into the thalamus, and innervate both relay cells and local GABAergic interneurons (Steriade and Deschenes, 1984). All thalamic nuclei, except for the reticular nucleus project to the ipsilateral cerebral cortex. Therefore the whole of the cerebral cortex receives input from the thalamus, with reciprocal connection from the cerebral cortex back to the thalamic nuclei.

The two major thalamic nuclei functionally-related to the basal ganglia are the ventral anterior (VA) nucleus and the ventral lateral (VL) nucleus (Grofova and Rinvik, 1974; Asanuma *et al.*, 1983a; Kultas-Ilinsky and Ilinsky, 1990).

In general, these nuclei receive input from both the cerebellum and basal ganglia and connect with motor regions of the frontal lobe, they also transmit information to the sensory, associative and limbic areas or the cerebral cortex.

The VA nucleus occupies the rostral part of the lateral nuclear mass. It is comprised of two subdivisions, the larger principle part (VApc) and the smaller magnocellular part (VAmc). The principle subcortical afferents to this regions are from the ipsilateral Gpm and SNpr. Fibres from the globus pallidus terminate in the VApc, while those from the SNpr terminate in the VAmc (Ilinsky *et al.*, 1985; Hazrati and Parent, 1991). The VA thalamus has, as already mentioned, reciprocal connections with motor regions of the frontal lobe, in particular the premotor and supplementary motor cortices.

The VL nucleus lies immediately caudal to the VA in the ventral tier of the lateral nuclear complex. It consists of three subdivisions: pars oralis (VLo); pars medialis (VLm); and pars caudalis (VLc). Major afferents to the VL thalamus arise from the ipsilateral globus pallidus and SNpr. Smaller connections also arise from the contralateral cerebellum. Pallidal and reticulata afferents terminate in the VLo and VLm, while inputs from the contralateral cerebellum terminate in the VLc.

The VL nucleus, in a similar manner to the VA nucleus, has reciprocal connections with motor areas of the frontal lobe, especially with the primary motor cortex. Excitatory thalamocortical fibres project to distinct frontal premotor cortical areas, whereas all connections from the SNpr and globus pallidus are GABAergic in nature (Uno and Yoshida, 1975; Pan *et al.*, 1983; Araki *et al.*, 1984).

A group of nuclei collectively known as the intralaminar nuclei of the thalamus have significant reciprocal connections with the cerebral cortex and project to both the caudate nucleus and putamen (Vogt and Vogt, 1941; Powell and Cowan, 1954; 1956). It has been demonstrated that two of these nuclei, namely the centre median nucleus (CN) and parafascicular nucleus (PN), project to the neostriatum. These projections are thought to be excitatory in nature (Buchwald *et al.*, 1973; Kitai, 1981). It has been suggested that the projections to the cerebral cortex (which are thought to utilise

glutamate) provide an 'enabling' excitatory signal to the cortex allowing movements generated in the cortex to be executed (Hoover and Strick, 1993).

Neurosurgical anatomy of the ventral thalamus

A nomenclature, distinct from that based on morphological characteristics described above, is often used by neurosurgeons to perform thalamotomies. Thus the ventralis intermedius or the ventral intermediate nucleus (Vim) is a common target to relieve tremor, and to some degree akinesia, in Parkinson's disease (see section 1.3.5). This area is the part of the thalamus that sends the majority of its axons to the motor cortex. The neurosurgical criteria used to define the Vim are high background activity with tremorosynchronicity (Ohye, 1978; 1990). In fact the Vim contains cells with the highest discharge potentials of any cells within the thalamus, probably corresponding to the large size of these cells (Hirai *et al.*, 1982; 1989). The exact extent and location of the 'stereotactic surgeons Vim' remains controversial (Ohye and Narabayashi, 1979; Lenz *et al.*, 1988; Ohye *et al.* 1989).

1.1.6 Superior colliculus

As previously mentioned in section 1.1.4, the superior colliculus receives a large afferent connection from the substantia nigra pars reticulata (Beckstead *et al.*, 1979; Gerfen *et al.*, 1982, Deniau and Chevalier, 1992). The superior colliculus is the major target of retinal ganglion cells (Linden and Perry, 1983; Beckstead and Frankfurter, 1983) and is concerned with the control of eye movements and the planned aspects of this movement, namely saccades (Cools *et al.*, 1984). Lesions of the superior colliculus produce visual and other sensory neglect (Krauthamer *et al.*, 1992) and deficits in visual search patterns (Haywood and Cowey, 1987). The efferent projections of the superior colliculus can be divided into two major divisions. The cells in the deep layers of the superior colliculus project predominantly to the ipsilateral spinal cord, pons and medulla. These deep layer cells also project to the intralaminar nuclei (Yamasaki *et al.*, 1986). These nuclei also receive input from other visually-related areas such as the visual cortical areas, the frontal eye fields and the pretectal complex. The second major projection from the superior colliculus arise from the predorsal bundle and innervates

predominantly the contralateral gaze centers in the midbrain concerned with orientating reactions (Redgrave *et al.*, 1986, 1987).

1.1.7 Pedunculopontine nucleus (PPN) and related nuclei

Together with the thalamus, the areas known as the pedunculopontine nucleus (PPN), midbrain extrapyramidal area (MEA), and mesencephalic locomotor region (MLR) represent the major regions receiving outputs from the basal ganglia. These areas lie in the caudal mesencephalon and are relay nuclei involved in the integration of basal ganglia, cerebral cortex, cerebellum and spinal signals associated with movement. The PPN is the most prominent of these nuclei and will therefore be described in more detail.

In the primate brain, the PPN consists of large, darkly-staining neurons that lie in close association with the superior cerebellar peduncle (Carpenter, 1984). The PPN consists of mainly cholinergic and glutamatergic neurons (Mesulam *et al.*, 1989; Lavoie and Parent, 1994a, b, c; Futami *et al.*, 1995). Separate populations of neurons exist, those utilising only acetylcholine, those utilising only glutamate and those expressing both as neurotransmitters (Lavoie and Parent, 1994a).

The rodent homologue of the primate PPN was defined by Rye *et al.* in 1987 as a collection of large, darkly-staining neurons in close association with the ascending limb of the superior cerebellar peduncle that extends from the caudal pole of the red nucleus to the rostral parabrachial nucleus. These PPN neurons were found to correspond entirely to the distribution of cholinergic neurons as visualised with choline acetyltransferase immunocytochemistry (Rye *et al.*, 1987). Before this definition, the PPN was considered as a much larger, ill-defined, more heterogeneous region of the mesopontine tegmentum. The region lying medially adjacent to the PPN has been defined as the rodent homologue of the midbrain extrapyramidal area (MEA).

Afferent connections of the PPN

The major afferents to the PPN arise from the medial segment of the globus pallidus (entopeduncular nucleus in the rat) (Kim *et al.*, 1976, Jackson and Crossman, 1983; Moon-Edley and Graybiel, 1983), the SNpr (Carpenter *et al.*, 1981; Jackson and

Crossman, 1983; Moon-Edley and Graybiel, 1983) and the subthalamic nucleus (Jackson and Crossman, 1981; Nauta and Cole, 1987; Groenewegen and Berendse, 1990). The PPN also receives smaller connections from the cerebral cortex (Moon-Edley and Graybiel, 1983) and cerebellum (Hazrati and Parent, 1992).

Efferent connections of the PPN

In the primate, the PPN projects to the medial segment of the globus pallidus and the SNpr (Carpenter *et al.*, 1981), and similarly to the entopeduncular nucleus and SNpr in the rat (Jackson and Crossman, 1981; Spann and Grofova, 1989). Furthermore, efferent connections to the pons, medulla, and spinal cord arise from the medial area of the PPN (Moon-Edley and Graybiel, 1983; Spann and Grofova, 1989). An efferent connection to the nucleus accumbens has also been described (Lavoie *et al.*, 1994b).

The major connections of the basal ganglia are summarised in diagrammatic form in figure 1.1.

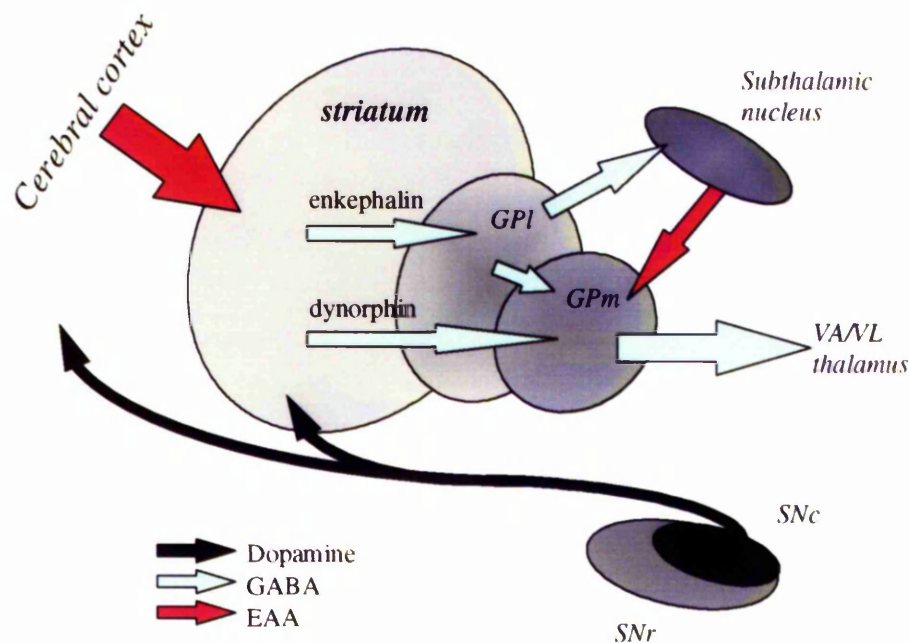


Figure 1.1 Functional circuitry of the basal ganglia

The neostriatum receives major inputs from both the cerebral cortex (glutamatergic) and the SNpc (dopaminergic). Efferent medium spiny projection neurons of the neostriatum utilise the inhibitory neurotransmitter GABA. Two major pathways exist termed the 'direct' or 'indirect' pathways. Neurons of the 'direct' pathway co-express the neuropeptides dynorphin and substance P and project directly to the output nuclei of the basal ganglia i.e. the medial segment of the globus pallidus (GPe) and substantia nigra pars reticulata (SNr). Neurons of the 'indirect' pathway co-express the opioid neuropeptide enkephalin and project to the lateral segment of the globus pallidus (GPi). The GPi is connected to the GPe and SNr via the subthalamic nucleus, thus providing an indirect route for striatal neurons to influence the output of the basal ganglia.

1.1.7 Synaptic connectivity of the basal ganglia

It was originally proposed that the striatum served to 'funnel' the input from the whole cerebral cortex to the thalamic nuclei, where it met the ascending projections from the cerebellum which synapsed in the same nuclei, so integrating the two separate

influences. It was proposed that following this integration of signals, the thalamus would send a unified projection from these two influences to back to the motor cortex.

However, a body of experimental evidence began to mount suggesting that this model is incorrect. Therefore, it was proposed that the basal ganglia were organised such that they did not funnel and thus converge information from the cerebral cortex, but in fact contained distinct channels or 'loops' which existed through the basal ganglia and thalamus back to the cerebral cortex (DeLong *et al.*, 1981). Furthermore, evidence suggested that the thalamic projection targets of the basal ganglia and cerebellum were in fact located on different nuclei (Asanuma *et al.*, 1983b; Ilinsky and Kultas-Llinsky, 1987). Therefore the concept emerged that information flowed through the basal ganglia in 'closed circuits' or loops. Recently, this model has been refined to suggest that these loops, although remaining distinct, are in fact interconnected with each other (DeLong *et al.*, 1981, 1984; Alexander *et al.*, 1986; Alexander *et al.*, 1990).

At least four distinct loops have been identified. These include the 'motor', 'occulomotor', 'prefrontal', and 'limbic' (DeLong and Georgopoulos, 1979; DeLong *et al.*, 1983). These loops maintain their segregation throughout both the nuclei of the basal ganglia and the thalamus, back to the cerebral cortex, in a manner known as parallel connectivity. Due to these segregated loops the caudate nucleus and putamen can be cordoned into distinct areas depending on their cortical innervation, these areas will now be described in more detail in both the rat and primate.

Parallel organisation in the primate

The neostriatum of the primate can be divided into associative, sensorimotor or limbic territories depending on the cerebral cortical input it receives. The associative territory comprises input from the various association cortices in the frontal, temporal and parietal lobes (Kurnzle, 1975; Goldman and Nauta, 1977; Ragsdale and Graybiel, 1981). The sensorimotor territory receives input from the primary motor and somatosensory cortices (Kurnzle, 1975; Liles and Updyke, 1985), while the limbic territory receives input from the limbic and paralimbic cortices as well as from the amygdala and hippocampus (Liles and Updyke, 1985; Alheid and Heimer, 1988; Graybiel *et al.*, 1994).

The most rostral region of the neostriatum receives associative inputs. More caudally as the striatum is separable into the caudate nucleus and putamen, the majority of the striatum remains associative, with only the most dorsal tip of both the caudate and putamen receiving sensorimotor input, while the limbic input projects to the nucleus accumbens.

More caudally, at the level of the anterior commissure, when the caudate and putamen are completely separated, the caudate nucleus receives input predominantly from the associative areas of the cortex, while the putamen is influenced by sensorimotor regions. In the caudal areas of the striatum the majority of the input is sensorimotor.

Electrophysiologically, neurons within the region of the striatum with inputs from the sensorimotor areas will respond in relation to movement. Neurons in associative regions will respond in relation to environmental stimuli and produce the initiation of behavioural responses, while neurons within the nucleus accumbens that receive limbic information from the amygdala and hippocampus respond to stimuli associated with reinforcement to novel stimuli or emotional and behavioural responses.

Therefore the striatal complex contains considerable segregation of function depending on the area of cerebral cortex projecting to it. This segregation of function is, as described previously, maintained throughout the nuclei of the basal ganglia.

Parallel organisation in the rat

Within the rodent neostriatum, a similar topographically-arranged cerebral cortical input to the striatum exists, although this arrangement is not as complex.

As already described, the rodent striatum does not show a delineation between caudate nucleus and putamen. However, in a similar manner to the primate, the most ventral area of the neostriatum, i.e. the nucleus accumbens, receives input from the limbic-associated areas. The remaining striatum can now be easily segregated into associative and sensorimotor inputs.

The dorsolateral, and to a less extent the ventrolateral, area of the rodent striatum receives input from the sensorimotor areas of the cortex, while the remaining striatum receives associative input. It is thought that although a similar arrangement occurs in

both the rodent and primate brain, the rodent brain shows a lower degree of functional segregation when compared to the primate (McGeorge and Faull, 1989).

1.2 Dysfunction of the Basal Ganglia

Dysfunction of the basal ganglia can result in a vast array of movement disorders. These movement disorders can be broadly classed into two main categories; the hypokinetic disorders and the hyperkinetic disorders. Hypokinetic disorders are characterised by a poverty in movement and hypertonia e.g. Parkinson's disease while the hyperkinetic disorders (dyskinesias) are characterised by an overactivity of movement e.g. Huntington's disease or hemiballism. Dystonia is an interesting condition characterised by increased movements but hypertonia i.e. an intermediate condition caused by co-contraction of antagonistic muscles.

1.2.1 Parkinson's Disease

Symptomatology

In 1817 James Parkinson described the symptoms of 'shaking palsy'. This was characterised by impairments in movement initiation (hypokinesia), slowness of voluntary movement (bradykinesia), muscular rigidity, postural abnormalities and tremor. Even though the disease, later to take his name, was described over 150 years ago, the underlying aetiology remains unknown. Parkinson's disease is a neurodegenerative disease characterised by a loss of dopamine cells of the substantia nigra pars compacta, with the formation of dense neuronal inclusions, composed of structurally altered neurofilament, termed Lewy bodies in both the SNpc and other brain areas (Gibb and Lees, 1988). Parkinson's disease is a disease with major socio-economic implications affecting 1 in 1000 of the general population, this rises to 1 in 100 in the population over the age of 50 (Marttila and Rinne, 1981, Marsden, 1994). Therefore, in the United Kingdom alone there are about 60 000-80 000 people suffering from Parkinson's disease (Marsden, 1994).

The major advance made in understanding the underlying cause of Parkinson's disease was the discovery of the central role played by dopamine. This was discovered via two different lines of evidence.

The pivotal role for dopamine in the generation of the symptoms of Parkinson's disease was discovered in the late 1950s when Carlsson *et al.* (1957) demonstrated that reserpine-induced akinesia and muscular rigidity in mice was reversible by the administration of the dopamine precursor L-3,4-dihydroxyphenylalanine (L-DOPA). Dopamine-depletion was subsequently observed, *post-mortem*, in the substantia nigra pars compacta of Parkinson's disease patients (Hornykiewicz, 1966). The dopamine-depletion observed in parkinsonian patients was thought to underlie the akinesia seen in these patients. However, other neurotransmitters are also reduced in these patients including noradrenaline and serotonin in the hypothalamus, hippocampus and other brain areas (Hornykiewicz, 1966; Javoy-Agid *et al.*, 1984) which was thought to underlie the psychiatric and cognitive disturbances seen in Parkinson's disease (Agid *et al.*, 1984; Stern and Langston, 1985). To better understand Parkinson's disease and to develop novel symptomatic, and possibly pre-symptomatic treatments, the most valuable asset is a useful animal model. This enables the researcher to investigate, under experimental conditions, the disease process and define the exact mechanism of novel anti-parkinsonian treatments, while allowing extrapolation to possible effects on both the disease progression and possible therapeutic benefits. The development of animal models that mimic aspects of the symptomatology and biochemical changes seen in idiopathic Parkinson's disease has taken a considerable amount of time. Furthermore, as will be discussed later, the model which mimics the symptoms of Parkinson's disease most reliably was in fact discovered through serendipity.

1.2.2 Aetiology of idiopathic Parkinson's Disease

The primary pathology of Parkinson's disease is widely recognised as the degeneration of the pigmented dopaminergic cells of the SNpc that project to the striatum. Despite the understanding of the underlying pathology, the cause of this selective degeneration remains unknown. Several candidates have been proposed. However, since only 75% of clinically diagnosed cases of Parkinson's disease are actually true cases of Parkinson's disease when followed up with *post-mortem* studies,

the ability to find common factors between patients remains elusive. The major hypothesised causes underlying the aetiology of idiopathic Parkinson's disease are outlined below.

Virus infection

Over 30 years ago it was suggested that the underlying cause of Parkinson's disease was a viral infection, particularly the virus that caused encephalitis lethargica, with the resultant postencephalitic parkinsonian state (Poskanzer and Schwab, 1963; Ravenholt and Foege, 1982). However, it has been impossible to transmit Parkinson's disease to animals by virus administration. Recently, an infectious aetiology involving an intra-uterine influenza again proposed as a possible mechanism (Mattock, 1988). However, these studies have not been confirmed (Ebmeier *et al.*, 1989).

Other factors such as an infection during childhood, or even the lack of an infection during childhood, have been proposed to pre-dispose a patient to Parkinson's disease. However, any evidence supporting these ideas has been inconclusive.

Therefore, in summary it seems that, due to the lack of evidence, a purely viral mechanism underlying idiopathic Parkinson's disease is unlikely, although it may possibly play a small role in a few limited cases.

Genetic component

Several neurodegenerative diseases, for example Huntington's disease and spinal cerebellar ataxia, have been shown to be linked to a genetic defect (Harding, 1981, 1982; HD Collaborative Research Group, 1993). Huntington's disease is an autosomal dominant neurodegenerative disease characterised by the selective degeneration of neurons of the striatum, cerebral cortex and other brain regions. Huntington's disease is associated with the overexpression of trinucleotide 'CAG' sequence in the IT15 Huntingtin gene (HD Collaborative Research Group, 1993) encoding glutamine. However, for Parkinson's disease no genetic mutation or sequence abnormality has been reported.

A hereditary component had seemed to be ruled out by studies in twins showing little concordance for Parkinson's disease among monozygotic twins (Ward *et al.* 1983,

Marttila *et al.*, 1988a). But reanalyses of the twin data concluded that the number of twins studied was too small to exclude a genetic factor, this was further complicated by *post-mortem* data showing misdiagnosis of Parkinson's disease in some of the cases (Golbe, 1990; Johnson *et al.* 1990). However, a large number of family members with inherited Parkinson's disease has been reported (Golbe, 1990). Clinical studies have increasingly emphasised some inherited component to Parkinson's disease, termed 'familial' Parkinson's disease (Maraganore *et al.*, 1992). Recently, studies in first-degree relatives of patients with Parkinson's disease has shown that first-degree relatives are 2.3 times more likely to develop Parkinson's disease compared to age-matched controls, with men at higher risk (Marder *et al.*, 1996).

It is possible that a genetic component plays a role in a multifactorial causation process in Parkinson's disease. The initial interpretation of the low concordance of Parkinson's disease in identical twins focused attention upon some exogenous cause, in particular environmental toxins. However, from recent evidence from both twin studies, and following families with a history of Parkinson's disease, it has now become clear that the genetic component of Parkinson's disease can be subdivided into two main classification of 'familial' and 'non-familial' Parkinson's disease.

Free radical damage

One of the leading hypothesis on the cause of Parkinson's disease suggests that the underlying neurodegeneration of the cells of the substantia nigra pars compacta is due to free radical damage.

Neuronal cell loss, with ageing, is known to occur in all animal species. From this it is easy to extrapolate an explanation as to why dopamine-containing cells of the SNpc would be preferentially lost at a more rapid rate. The main feature of these cells that would make them more susceptible to free radical damage is the fact that they synthesise dopamine. The chemical process of enzymatic oxidation of monoamines leads to the formation of one mole of hydrogen peroxide for each mole of amine that is oxidised (Cohen, 1983). The oxidation of catecholamines leads to the formation of cytotoxic quinones as well as hydrogen peroxide (Graham, 1984). Hydrogen peroxide can be converted to superoxide and hydroxyl radicals which are, through a variety of mechanisms, toxic to cells.

In 1983, Cohen proposed that free radicals derived from hydrogen peroxide generated from oxidation of dopamine, contribute to the pathology of Parkinson's disease, and that dopamine turnover can produce oxidative stress (Spina and Cohen, 1989).

In the brain, the major pathway for scavenging hydrogen peroxide is via reduced glutathione and glutathione peroxidase. Levels of reduced glutathione in the substantia nigra are depleted in Parkinson's disease (Perry *et al.* 1982; Jenner *et al.*, 1992), with no change in oxidised glutathione.

Depletion of reduced glutathione may be a critical abnormality in the substantia nigra in Parkinson's disease. One consequence of this change would be the failure to detoxify hydrogen peroxide, with subsequent excessive formation of toxic hydroxy radicals.

Fe^{2+} , which is present in high concentrations within the basal ganglia reacts via the fenton reaction to ultimately form Fe^{3+} , hydroxyl radicals, hydrogen peroxide and hydroxyl ions (Youdim, 1989). It has been demonstrated that in Parkinson's disease there is an excessive amount of iron in the substantia nigra (Linert, 1996; Owen *et al.*, 1996; Ye *et al.*, 1996). Thus, the combination of depleted glutathione and excessive iron could accelerate hydroxy radical formation in the substantia nigra in Parkinson's disease.

Free radicals cause peroxidation of membrane lipids, which can lead to cell death. An increase of malondialdehyde, an intermediate in the lipid peroxidation process, and lipid hydroperoxides have also been found in the substantia nigra in Parkinson's disease (Dexter *et al.*, 1989; Jenner *et al.*, 1992).

Evidence against the involvement of free radicals in the aetiology of Parkinson's disease comes from studies suggesting that there is an increase in superoxide dismutase, the enzyme that degrades superoxide radicals, in the substantia nigra of Parkinson's disease patients. It has been proposed that this may occur as a compensatory mechanism (Ceballos *et al.* 1990). Furthermore, it has been shown that an increase of brain superoxide dismutase protects against MPTP-induced toxicity (Przedborski *et al.* 1992).

Even if increased free radical formation leads to the degeneration seen in Parkinson's disease, the underlying cause of this increase has still to be determined.

One possibility is that there is an increased turnover of dopamine as a compensation to a reduction in dopamine-containing neurons (Hornykiewicz, 1982) via

one of the other proposed mechanisms for SNpc degeneration outlined in this thesis (section 1.2.2) e.g. head trauma or viral infection. This increase in dopamine turnover may put excess strain on the normal scavenging mechanism. Alternatively, a decrease in scavengers, especially reduced glutathione, possibly due to a genetic or environmental factor, causes an increased accumulation of free radicals, thus producing cellular damage.

The neuronal loss within the SNpc of Parkinson's disease patients is not uniform, but is most pronounced in certain regions of the SNpc (Gibb and Lees, 1991; Damier *et al.*, 1996). This suggests that within the compacta certain regions may not be able to sustain the sufficient oxy-radical scavenging required. This hypothesis is supported by studies showing that the region that is most severely affected in the SNpc in Parkinson's disease (i.e. the ventro-lateral zone) differs from that affected by ageing (Fearnley and Lees, 1990).

Therefore in summary, *post-mortem* pathological data of Parkinson's disease patients supports the hypothesis that oxygen free radicals play a role in the specific destruction of these neurons. However it could be argued that these changes reflect the dopamine-depletion and are not the underlying cause of the degeneration.

Mitochondrial deficiencies

Several neurodegenerative diseases are known to be caused by mitochondrial mutations which result in degeneration of various areas of the basal ganglia. It has been proposed that the degeneration seen in the SNpc in Parkinson's disease also may be caused by a mitochondrial deficiency. This hypothesis was strengthened by the finding that the enzyme activity of complex I in mitochondria of the substantia nigra in patients with Parkinson's disease is reduced (Schapira *et al.*, 1990). The reduction in mitochondrial complex I seen in the substantia nigra is not seen in any other parts of the brain in patients with Parkinson's disease, or in other diseases causing equal or greater nigral cell loss e.g. Multiple system atrophy (MSA). More evidence for the importance of complex I of the mitochondrial respiratory chain in Parkinson's disease is the fact that the inhibition of complex I is the final mechanism in the toxicity of MPP⁺, derived from MPTP.

Similarly, point mutations at nucleotide 7237 of the CO1 subunit of cytochrome-c-oxydase (complex IV) in mitochondria have been reported in the striatum of Parkinson's disease patients (Ozawa *et al.*, 1991; Di Mauro *et al.*, 1993). However, recent studies from SNpc of Parkinson's disease patients has failed to support this observation (Lucking *et al.*, 1995).

The selective reduction in nigral complex I activity could be due to an exogenous toxin such as MPTP, or to a genetic or other endogenous effect.

If there is an association between the reduction in glutathione or mitochondrial complex activity and Parkinson's disease, it has still to be established if one is a consequence of the other. For example, oxidative stress, depleting reduced glutathione, may damage mitochondria and reduce complex I. Alternatively, reduced complex I activity is known to generate oxidative stress, which could deplete reduced glutathione. Which process initiates the changes, if they are in fact linked, is unknown. Moreover, whether they have an active role in the aetiology of idiopathic Parkinson's disease has still to be elucidated.

Environmental and endogenous toxins

Several lines of evidence have supported the concept that several toxic substances, especially the heavy metals and pesticides, may underlie the pathology of Parkinson's disease. One of the earliest findings to suggest such a hypothesis was by Sofic in 1988 in which it was found that in *post-mortem* examination of Parkinson's disease brains, the levels of iron were substantially higher when compared to age-matched controls. This led to the hypothesis that metal deposition in the substantia nigra may lead to the degeneration of the compacta cells. Also epidemiological studies showed that, in areas with a high metal content in drinking water, there was an increased incidence of Parkinson's disease (Wong, 1991). Similarly, several studies have shown that, in experimental animals, intranigral injection of iron, copper or aluminium produce degeneration of the SNpc and a decrease in striatal dopamine levels (Youdim and Riederer, 1989).

Furthermore, the iron chelator deferoxamine partially prevents SNpc lesion by 6-hydroxydopamine (Ben-Shachar *et al.*, 1991). These results suggest that iron may play a crucial role in the process of dopaminergic neurodegeneration.

Another finding which points to the possibility of an environmental toxin underlying Parkinson's disease concerns cytochrome P450 mono-oxygenases. Cytochrome P450 mono-oxygenases metabolise several environmental and endogenous chemicals. Barbeau *et al.* (1985) first suggested the possibility that Parkinson's disease may result from a combination of inherited differences in metabolism and environmental exposure to neurotoxins, specifically via the impairment of a cytochrome P450 enzyme desbrisoquine 4-hydroxylase (CYP2D6). CYP2D6 shows polymorphism, with some alleles causing impaired desbrisoquine metabolism. Some poor metaboliser CYP2D6 alleles have been found to be about 2.5 times more frequent in Parkinson's disease patients when compared to controls (Armstrong *et al.* 1992; Smith *et al.* 1992). However, other studies contradict these results showing no correlation (Benitez *et al.*, 1990; Gudjonsson *et al.*, 1990). A significant association between the 'poor metabolisers' phenotype and a young age of onset was established in one study (Poirier *et al.*, 1987), but not in another (Sandy *et al.*, 1996).

Despite some contradictory evidence, reduced CYP2D6 remains a likely candidate due to the fact that MPTP and MPP⁺, bind to, and can be metabolised to non-toxic compounds by CYP2D6 (Fonne-Pfister *et al.*, 1987), suggesting that poor metabolisers, i.e. with the mutant CYP2D6, may be subject to excessive loads if exposed to a toxin. Other toxins may act in a similar manner and thus fail to be metabolised properly, resulting in neurodegeneration.

Although recent studies have failed to show a lack of association between inactive CYP2D6 and an increased risk of Parkinson's disease, other factors should be considered. For example, several polymorphs may exist that produce active protein products with reduced catalytic capabilities or protein stability. Further studies on the various phenotypes of CYP2D6 may help elucidate a metabolic predictor for Parkinson's disease.

It has been hypothesised that exposure to a rural environment may be of significance (Barbeau *et al.*, 1987; Koller *et al.*, 1990). This theory has been supported by the high degree of similarity between the neurotoxin MPTP and many pesticides and fertiliser compounds (Bocchetta and Corsini, 1986). However, no common environmental toxin has been identified.

Head trauma

It is well known that viral infection and restriction of blood supply can lead to the degeneration of the SNpc. It has therefore been suggested that any head trauma, either as a major or relatively small insult, can either damage cells of the SNpc or accelerate the speed of natural degeneration. However, there are many problems in investigating such ideas as it is impossible to accurately record all minor head insults and then identify how such insults correlate with the development of Parkinson's disease. Furthermore patients with Parkinson's disease will exhibit 'recall bias', whereas controls may not recall a similar head injury.

Therefore at present no direct correlation between head trauma and Parkinson's disease can be assumed.

Summary

No specific cause of neurodegeneration in Parkinson's disease has been identified. However, from the data available, the most probable hypothesis is that patients with Parkinson's disease may be at risk due to a genetic disposition preventing the disposal of toxins (e.g. CYP2D6), such that, if exposed to a toxin, at risk patients would be unable to detoxify this and so progress to Parkinson's disease. The fact that many environmental toxins may exist, coupled with the fact that deficiencies in many anti-oxidant enzymes may exist, complicates the search for any specific aetiology of Parkinson's disease.

1.2.3 Non-idiopathic parkinsonism

Several causative agents and neurological disorders can produce parkinsonian symptoms including akinesia, bradykinesia and tremor. However, these cases are not examples of idiopathic Parkinson's disease. These can be grouped under the general term of Parkinson-plus syndromes.

One of the most common of the Parkinson-plus syndromes is neuroleptic-induced parkinsonism. These symptoms of akinesia, rigidity and bradykinesia occur following treatment for schizophrenia with neuroleptics e.g. haloperidol. These side-

effects are due to the long-term blockade of dopamine receptors. However, a dose reduction, or removal of the drug altogether rarely helps reduce the symptoms, with the parkinsonism persisting for up a year following drug removal (Bateman *et al.*, 1986; section 1.4.1 on tardive dyskinesia). Similarly, following treatment for depression several serotonin uptake inhibitors e.g. fluoxetine, can also produce parkinsonian symptoms. This phenomena is termed 'serotonin syndrome'. Again, drug withdrawal does not immediately reverse the symptoms which can persist for up to several years.

Several cases of parkinsonism have been known to occur following either a viral or bacterial infection, especially when infection crosses the blood brain barrier and infects the cerebral spinal fluid. One of the most common forms of this type of parkinsonism is termed 'post-encephalitic parkinsonism'. Most of these cases occurred in the 1920s when it was observed that an increased number of younger people were developing symptoms of Parkinson's disease. This was thought to coincide with exposure to 'encephalitis lethargica' (retrospective analysis, Marmot, 1981). Several infectious agents, which are known to cause parkinsonian symptoms, have now been identified including measles, poliovirus and western equine encephalitis (Meyer, 1943; Duvosin and Yahr, 1965).

Head trauma is also known to damage the cells of the SNpc thus causing parkinsonian symptoms, with especially high incidence in individuals subjected to chronic head trauma e.g. boxers. These cases develop an encephalopathy in which parkinsonian symptoms are prominent. Anti-parkinsonian therapies are of use in these cases, although in a similar manner to idiopathic Parkinson's disease the symptoms are progressive (Calne *et al.*, 1984).

Several neurodegenerative atrophies can also produce the parkinsonian symptoms of akinesia, bradykinesia and slow shuffling gait which leads to the misdiagnosis of Parkinson's disease. These include, Progressive Supranuclear Palsy, Multiple System Atrophy (Shy-Drager Syndrome), and in some cases Alzheimer's disease. In some of these atrophies dopamine agonists and anti-cholinergic treatments are effective for a short period to time. However, these drugs fail to provide any meaningful level of improvement in the long-term.

1.2.4 Animal models of Parkinson's disease

A number of animal models exist which replicate, both behaviourally and biochemically, Parkinson's disease to varying degrees. These models have been instrumental in delineating the neural mechanisms underlying both the pathology and pathophysiology of movement disorders.

The various animal models available in which to study Parkinson's disease will now be discussed.

Reserpine-treated rodent model of Parkinson's disease

Systemic administration of the alkaloid reserpine induces central and peripheral blockade of reuptake of catecholamines into vesicles. This causes depletion of monoamines (dopamine, serotonin and noradrenaline) from intracellular storage granules into the cytoplasm where they are degraded by monoamine oxidases, ultimately producing a reduction in the levels of all catecholamines.

In rats, reserpine administration produces symptoms similar to Parkinson's disease patients including akinesia, rigidity, with postural flexion of the back, limbs and digits (Carlsson *et al.*, 1957; Uretsky and Seiden, 1969). Reserpine-induced monoamine depletion is reversible as the nigrostriatal dopaminergic neurons remain intact, thus the parkinsonian symptoms are short lived.

Due to the transient nature of the parkinsonian symptoms this model does not mimic the pathology of Parkinson's disease. Reserpine also has central effects including hypothermia, sedation and decreases in goal-directed activity such as feeding and mating (Jurna, 1968).

The reserpine model is of use mainly in a behavioural respect, as dopamine agonists that are of use in the clinical situation such as apomorphine, lisuride, and of course L-DOPA, also reverse the locomotor deficiency in the reserpine-treated rodent model of Parkinson's disease. Therefore, this model is of use in developing and determining the effectiveness of novel anti-parkinsonian agents (Cooper *et al.*, 1984; Koller *et al.*, 1987; Maj *et al.*, 1990).

A major limitation of the reserpine-treated animal model of Parkinson's disease is the transient nature of the symptoms and therefore duration of action. Since Parkinson's

disease is a chronic progressive disease, many other receptor and transmitter systems undergo alterations. Due to the short duration of action of reserpine, these alterations do not take place.

Therefore in summary, due to the transient nature of the induced dopamine-depletion the reserpine-treated rodent model of Parkinson's disease is useful only for investigations founded on acute behavioural effects or the effects of acute monoamine depletion.

Unilateral 6-hydroxydopamine-lesioned models of Parkinson's disease

The unilateral 6-hydroxydopamine (6-OHDA)-lesioned model has several advantages over the reserpine-treated model, mainly due to it producing a long-term lesion of the dopamine neurons of the substantia nigra pars compacta (Ungerstedt, 1968, Ungerstedt, 1971). Five major administration routes for the neurotoxin 6-OHDA have been described:

- peripheral
- intraventricular
- striatal
- direct SNpc
- medial forebrain bundle.

The most useful at producing a large targeted lesion of the whole dopaminergic system is the medial forebrain bundle (MFB) route of administration. Unilateral administration into the MFB is the most useful site of administration for two reasons. Firstly, all ascending nigrostriatal dopaminergic fibres pass via the medial forebrain bundle. Such lesions therefore destroy not only the SNpc but also the VTA and retrorubral area. Secondly, the full rostral-caudal extent of the mesencephalic dopaminergic system will be lesioned. When coupled with administration of noradrenaline uptake inhibitors, 6-OHDA causes selective destruction of all dopamine containing cells to the neostriatum, which mimics the loss of the dopaminergic cells in Parkinson's disease (Hornykiewicz, 1966). Thus, 6-OHDA can mimic the major pathological change of Parkinson's disease.

However, there are several limitations of the 6-OHDA-lesioned model. The first obvious disadvantage of this model is the unilateral nature of the lesion. The animals show little hypokinesia (although a reduction in spontaneous locomotion is observed) or rigidity as the contralateral intact dopaminergic compacta permits behavioural compensation. A further problem with this model is the non-progressive nature of the lesion. Within 7 hours of injection of 6-OHDA into the medial forebrain bundle, the cells of the SNpc begin to die. With optimal doses, this continues until about 14 days, when virtually all of the compacta cells (>95%) have undergone degeneration. By 21 days no further degeneration takes place (Jeon *et al*, 1995; Labandeira-Garcia *et al*, 1996). This termination of any further degeneration is unlike the progressive nature seen in idiopathic Parkinson's disease. A further limitation of the 6-OHDA-lesioned rat is that unlike Parkinson's disease, there is no loss of 5-HT or, due to the addition of noradrenaline uptake blockers, noradrenaline (Waddington, 1980).

Following unilateral 6-OHDA-lesion of the medium forebrain bundle a postural and directional asymmetry is produced. Although the behavioural deficit witnessed in the 6-OHDA-lesioned rat is not as marked as either that seen in reserpine-treated rodents, or that seen in patients with advanced Parkinson's disease, it still affords two useful purposes. One is that the long-term biochemical changes that occur following dopamine-depletion can be investigated, and secondly 6-OHDA-lesioned rats display a spontaneous ipsiversive rotational response (Pycock, 1980). The utility of this ipsiversive rotational response arises from the fact that, when challenged with either L-DOPA or a direct dopamine receptor agonist, the ipsiversive rotational response is either abolished, following low dose treatment, or, following a higher dose or repeated treatment, converted to contraversive rotation. The contraversive rotation is dose-dependent and can be reliably quantified (Arbuthnought and Ungerstedt, 1970; Ungerstedt, 1971). Contraversive rotational behaviour has been very useful in defining novel dopamine-replacing drugs (Pycock, 1980).

Annett *et al*. (1992) produced unilateral 6-OHDA-lesions of the medial forebrain bundle in common marmosets (*Callithrix Jacchus*). However, these marmosets showed only unilateral deficits and when challenged with dopamine agonists, exhibited contralateral movement which was difficult to quantify as a mark of anti-parkinsonian action.

Bilateral 6-hydroxydopamine-lesioned models of Parkinson's disease

In attempts to model the hyperkinesia seen in idiopathic Parkinson's disease, several groups have investigated the possibility of employing bilateral 6-OHDA-lesions in both rodents and primates.

In two rodent studies, bilateral 6-OHDA-lesions of the medial forebrain bundle caused chronic akinesia leading to adipsia, aphagia and finally death within 2-4 days post-operatively (Ungerstedt, 1970). Recently, one study has shown that with post-operative intragastric feeding, it is possible to maintain bilateral 6-OHDA-lesioned rats (Sakai and Gash, 1994). However, these animals show severe aphagia and adipsia and 30% post-operative mortality was observed. For these reasons, to date, the bilateral 6-OHDA-lesioned rodent model has been of little use as a model of Parkinson's disease. In the case of primate models there has been more, though limited success.

A two stage bilateral 6-OHDA-lesioned primate model of Parkinson's disease was developed by Mitchell *et al.* (1995). This model has both advantages and disadvantages. The bilateral 6-OHDA-lesioned marmoset model provides a stable parkinsonian model with no signs of behavioural recovery for up to 6 months. Due to its bilateral nature, the hypokinesia shown in these primates models the behavioural deficits in Parkinson's disease with more accuracy than the unilateral 6-OHDA lesion. Furthermore, following dopamine agonist administration these animals show a bilateral reversal of hypokinesia, that can be easily quantified.

However, there are several limitations to this model. Since the route of neurotoxin administration is not systemic, two identical lesions of the midbrain dopaminergic neurons must be produced. An uneven bilateral lesion causes a unilateral akinetic bias, which becomes more pronounced when anti-parkinsonian agents are administered, with the animals developing a rotational behaviour, similar to a unilateral lesion. Another problem with this bilateral 6-OHDA-lesioned marmoset model is that post-operatively the animals are unable to spontaneously feed, drink or groom themselves. Thus, the marmosets require hand feeding in the initial weeks of postoperative recovery period (Mitchell *et al.*, 1995).

Electrolytic and radiofrequency-lesioned primate models of Parkinson's disease

Electrolytic or radiofrequency lesions of the brainstems of monkeys have been employed to induce experimental parkinsonism, especially tremor. Early studies had shown that electro-coagulation lesions within the midbrain and ventral tegmentum, produced varying degrees of tremor and hypokinesia (Poirier, 1960).

Again bilateral lesions proved difficult to induce without animals dying of aphasia and adipsia. Motor abnormalities appeared to vary markedly between animals, presumably reflecting the precise location of the lesion. The extent of pathology and biochemical changes again did not mimic that of Parkinson's disease and the model did not provide a useful model of Parkinson's disease. This method of lesion generation was superseded by 6-OHDA-lesions.

1-Methyl-4-phenyl-1,2,3,6-tetrahydropyridine (MPTP)-treated models of Parkinson's disease

The serendipitous discovery of the neurotoxin 1-methyl-4-phenyl-1,2,3,6-tetrahydropyridine (MPTP) by drug abusers in 1982 provided a giant leap forward in Parkinson's disease research. Chemists trying to manufacture the heroin substitute 1-methyl-4-phenyl-4-propionoxypiperidine (MPPP), which due to its novel structure, would escape legal control, inadvertently produced MPTP. When injected, MPTP induces symptoms identical to Parkinson's disease (Ballard *et al.*, 1985). *Post-mortem* examination of the brain of one of the MPTP-injected drug addicts revealed marked cell loss in the SNpc, indicating a pathology identical to idiopathic Parkinson's disease.

When injected into adult rhesus primates (*macaca mulatta*), MPTP produced the symptomology of akinesia, rigidity, and resting tremor (Burns *et al.*, 1983). This condition was reversible by L-DOPA and *post-mortem* examination showed selective degeneration of the SNpc (Burns *et al.*, 1983) and reduction in noradrenaline content of the locus coeruleus mimicking Parkinson's disease (Javoy-Agid *et al.*, 1984). Chemical analysis of dopamine, noradrenaline, and 5-HT levels in MPTP-treated non-human primates showed marked reductions in dopamine, with some reduction in both 5-HT and noradrenaline levels (Javoy-Agid *et al.*, 1984; Forno *et al.*, 1993).

Several weeks following MPTP administration ($1-8 \text{ mg kg}^{-1}$), non-human primates show reduced spontaneous movement (Burns *et al.*, 1983). Complex movements are poorly co-ordinated and the range of movements produced limited. All of these motor defects are reversible by administration of L-DOPA or direct dopamine receptor agonists (Crossman *et al.*, 1987).

As previously mentioned, following MPTP-administration, the cells within the SNpc are selectively destroyed. Within the substantia nigra those cells in the centrolateral area are more damaged than those in the medial portion. This closely resembles pathological findings in the substantia nigra of *post-mortem* parkinsonian patients (Varastet *et al.*, 1994).

There has been some controversy as to how accurately the MPTP model resembles idiopathic Parkinson's disease. In younger primates two pathological differences between MPTP-lesioned primates and patients with idiopathic Parkinson's disease were described. Firstly, degeneration of the ventral tegmental area (VTA), locus coeruleus, and raphe nucleus was not apparent in young MPTP-treated non-human primates (Gupta *et al.*, 1984). All these areas show degeneration in *post-mortem* idiopathic Parkinson's disease (Hornykiewicz, 1964). Secondly, MPTP-treated primates showed a lack of Lewy bodies (Forno *et al.*, 1986). However, pathological findings from older primates treated with MPTP has shown both damage in the VTA, locus coeruleus and raphe nucleus and Lewy-like bodies have been described in various brain areas (Mitchell *et al.*, 1985; Forno *et al.*, 1988, 1993; Ovadia *et al.*, 1995).

In other primate species, MPTP-administration can produce parkinsonism to varying degrees. Following acute systemic administration of MPTP, marmosets show behavioural recovery within 3-4 weeks. Therefore, due to the short term action and recovery observed in these animals, this does not effectively model Parkinson's disease. Recently, a method of chronic MPTP-administration in marmosets has been shown to induce parkinsonism with only a small amount of behavioural recovery seen in the first few weeks, and then a stable parkinsonism is observed without further behavioural recovery for up to 12 months (Pearce, 1995). However, larger 'old-world' primates still afford the best model of Parkinson's disease, without any behavioural recovery (Burns *et al.*, 1983).

Rats have been shown to be resistant to MPTP with no evidence of persistent parkinsonian symptoms (Boyce *et al.*, 1984; Chiueh *et al.*, 1984). However,

administration of MPTP to some strains of mice produces a substantial loss of dopamine-containing cells in the SNpc (Heikkila *et al.*, 1985a,b).

The mechanism by which MPTP produces its actions were delineated by investigating the mode of resistance in rats. It was shown that MPTP was metabolised by MAO-B to 1-methyl-4-phenylpyridine (MPP⁺), via an intermediate 1-methyl-4-phenyl-2,3-dihydropyridine (MPDP, Chiba *et al.*, 1984).

MAO-B oxidises MPTP rapidly, MAO-B inhibitors (e.g. deprenyl and pargyline) prevent the neurotoxic effects of MPTP (Heikkila, 1985b,c). Since MAO-B is mainly localised in glial cells and 5-HT neurons of the brain (Westlung *et al.*, 1985) it was initially not clear why the formation of MPP⁺ in non-dopaminergic cells could cause neuronal death selectively in the SNpc.

It was demonstrated that the toxic metabolite of MPTP, MPP⁺, was accumulated in striatal synaptosomes, via active transport across the membrane, in a way similar to dopamine. Unlike MPTP, treatment with deprenyl was unable to prevent MPP⁺ toxicity in the mouse (Bradbury *et al.*, 1985). However, dopamine uptake blockers were able to prevent dopamine-depletion in the striatum caused by MPTP (Ricaurte *et al.*, 1985). This led to the hypothesis that MPTP is oxidised by MAO-B within glial cells and 5-HT terminals, and is transformed to MPP⁺, which is then accumulated preferentially in the dopaminergic terminals via the specific dopamine uptake mechanism.

It has been proposed that cell bodies can be protected preferentially by the presence of surrounding catecholamine terminals. Thus, the neurons of the locus coeruleus, which express dopamine uptake sites, also receive a dense catecholaminergic innervation, which may provide protection from MPTP toxicity, as the surrounding terminals accumulated MPP⁺. The cell bodies of the SNpc do not possess the same protection, and thus are highly susceptible to MPP⁺ toxicity.

Several suggestions have been proposed to explain the resistance of rats to MPTP toxicity. One major finding concerns clearance rates which are quicker in rats than in primates. The half-life of MPP⁺ in rhesus monkeys has been estimated at about 10 days, whereas in the rat it is only 3 hours (Johannessen *et al.*, 1985). It has also been suggested that in the rat, due to a rat-specific vesicular amine transporter, MPP⁺ is actively transported into intracellular vesicles, where it is stored and broken down, and is therefore unable to damage mitochondria causing cell death (Liu *et al.*, 1992).

In summary, the MPTP-treated monkey mimics idiopathic Parkinson's disease closely and is the best behavioural and biochemical animal model of Parkinson's disease to date. However, due to the non-progressive nature, and the lack of Lewy bodies in young primates, it is probably of limited usefulness in studying the progression of Parkinson's disease.

1.2.5 Pathophysiology of Parkinson's disease

The use of the animal models described above have proved useful in defining the neural mechanisms underlying the behavioural changes seen in Parkinson's disease. These are summarised in figure 1.2 and are outlined below.

Summary of basal ganglia pathway changes in Parkinson's disease

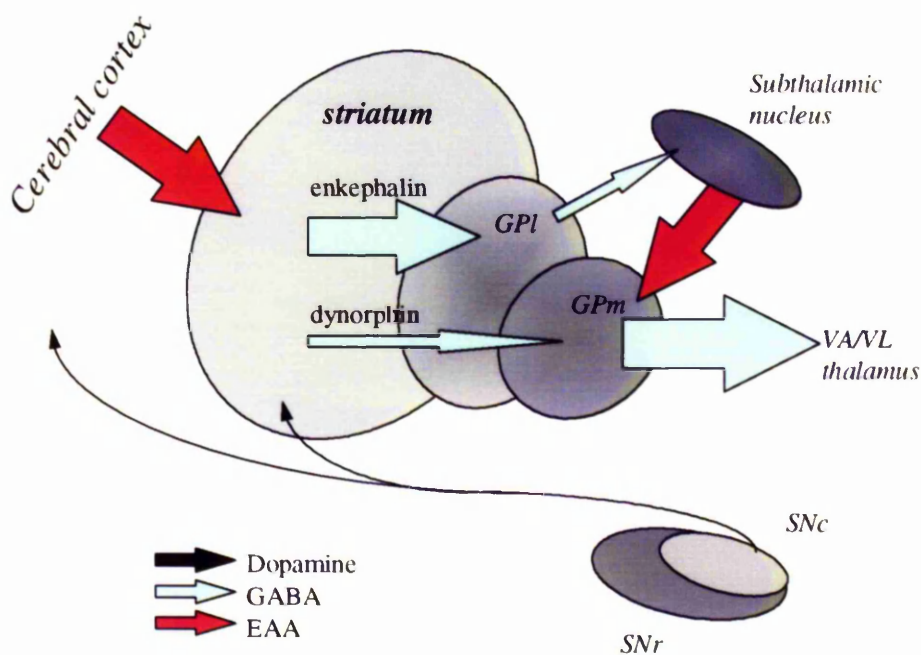


Figure 1.2 Functional circuitry of the basal ganglia in Parkinson's disease

Following dopamine-depletion, the 'direct' GABAergic pathway to the medial segment of the globus pallidus and SNpr becomes underactive. The 'indirect' GABAergic pathway to the lateral segment of the globus pallidus is released from inhibition by dopamine and becomes overactive. Overactivity of the 'indirect' pathway reduces GPi activity. GABAergic GPi efferents to the subthalamic nucleus are therefore underactive, thus increasing subthalamic nucleus activity. Overactivity of the glutamatergic subthalamic nucleus efferents overstimulates the GPe and SNpr. Thus, overactive GPe and SNpr efferents inhibit the VAVL thalamus and so terminate voluntary movement.

■ Decreased dopamine levels in the striatum

As already described, several lines of evidence indicate that the underlying cause of Parkinson's disease is dopamine-depletion of the striatum. Carlsson *et al.*, in 1957, showed that reserpine-induced akinesia could be reversed by administration of the dopamine precursor L-DOPA (Carlsson *et al.*, 1957). Studies from *post-mortem* tissue showed a dopamine deficiency within the striatum and degeneration of SNpc cells in patients with Parkinson's disease (Hornykeiwicz, 1966). More recently, positron emission tomography (PET) studies utilising fluorodopa have shown a progressive loss of dopamine terminals within the striatum as idiopathic Parkinson's disease progresses (Morrish *et al.*, 1996).

■ Decreased activity of the lateral segment of the globus pallidus

Several lines of evidence suggest that the lateral segment of the globus pallidus is underactive due to increased activity of the striatopallidal pathway in Parkinson's disease. In the 6-OHDA-lesioned rat, flunitrazepam binding demonstrated a downregulation of GABA receptor numbers in the rodent globus pallidus, consistent with an increase in striatopallidal activity (Pan *et al.*, 1985; Gnanalingham and Robertson, 1993). Similarly in both MPTP-treated primates and in human *post-mortem* tissue, flunitrazepam binding is reduced suggesting overactivity in the GABAergic striatopallidal pathway (Griffiths *et al.*, 1990; Calon *et al.*, 1995). Electrophysiological recordings from cells within the lateral segment of the globus pallidus in MPTP-treated non-human primates showed a decrease in activity compared with non-parkinsonian, consistent with an overactive GABAergic pathway from the striatum (Miller and DeLong, 1987). Studies utilising the metabolic tracer [^3H] 2-deoxyglucose (2-DG) showed increased accumulation of 2-DG in the lateral segment of the globus pallidus. 2-DG becomes preferentially accumulated in active nerve terminals. Increased 2-DG accumulation in the GPi thus provides evidence of an overactive striatopallidal pathway (Mitchell *et al.*, 1989). Reserpine-induced parkinsonism in rats can be alleviated by intracerebral injection of the GABA antagonist bicuculline in the globus pallidus (Maneuf *et al.*, 1995). Direct evidence for the overactivity of the striatopallidal pathway,

comes from work by Roberston *et al.* (1991), utilising intracerebral microdialysis. Following MPTP-treatment in non-human primates, the extracellular levels of GABA released in the GPI was significantly increased. However, recently the underactivity of the GPI has been questioned due to evidence from cytochrome oxidase subunit mRNA studies (as a marker of long-term neuronal activity) in which GPI neurons displayed a non-significantly increased expression of cytochrome oxidase in parkinsonian MPTP-treated macaques, suggesting an increase in neuronal activity (Vila *et al.*, 1997). It has been suggested that this increase in cytochrome oxidase subunit mRNA may be due to increased excitation from the hyperactive subthalamic nucleus efferents to the GPI.

■ Increased activity of the subthalamic nucleus

Due to the underactivity of the lateral segment of the globus pallidus described above, the subthalamic nucleus is released from inhibition and becomes overactive in parkinsonism. 2-DG accumulation in the subthalamic nucleus is decreased, suggesting a reduction in the activity of GABAergic projection to the subthalamic nucleus, (Mitchell *et al.*, 1989).

Several lines of evidence point to overactivity of the subthalamic nucleus as being critical for the underlying symptoms of akinesia seen in parkinsonism. In the MPTP-treated primate model of Parkinson's disease, the firing rate of subthalamic nucleus neurons is increased (Miller and DeLong, 1987). Blockade of excitatory amino acids from subthalamic nucleus efferents within the SNpr and GPM can alleviate parkinsonism in rodent models (Brotchie *et al.* 1991; Robertson *et al.* 1991). Similarly, electrolytic lesion or high frequency stimulation of the subthalamic nucleus can alleviate parkinsonism in both MPTP-treated non-human primates (Bergman *et al.*, 1990; Aziz *et al.*, 1991, 1992) and in patients with Parkinson's disease (Bergman *et al.*, 1990; Limousin *et al.*, 1995). Recently, more evidence for the overactivity of the subthalamic nucleus in Parkinson's disease has been demonstrated utilising cytochrome oxidase subunit mRNA studies (as a marker of long-term neuronal activity) in which subthalamic nucleus neurons displayed a significant increase in expression of cytochrome oxidase in parkinsonian MPTP-treated macaques, suggesting an increase in neuronal activity (Vila *et al.*, 1997).

■ Increased activity of the medial segment of the globus pallidus

Whilst increased activity of the subthalamic nucleus would, by glutamatergic excitation, increase the activity of the GPM and SNpr, as described above there is also evidence for a decrease in activity of the inhibitory GABAergic input to the GPM and SNpr. Increased flunitrazepam binding is observed in 6-OHDA-lesioned rats in the SNpr and the entopeduncular nucleus on the lesioned side (Pan *et al.*, 1985; Gnanalingham and Robertson, 1993), and in the GPM of the MPTP-treated non-human primate (Calon *et al.*, 1995). This decrease in GABA inhibition may arise from the direct pathway. Recently, more evidence for the overactivity of the medial segment of the globus pallidus in Parkinson's disease has been demonstrated utilising cytochrome oxidase subunit mRNA studies, in which GPM neurons displayed a significant increase in expression of cytochrome oxidase in parkinsonian MPTP-treated macaques (Vila *et al.*, 1997).

■ Underactivity of the VA/VL thalamus

Mitchell *et al.* (1992b) showed an, albeit non-significant, increase in 2-DG accumulation within the nuclei of the VA/VL thalamus, suggesting the GABAergic input from the medial segment of the globus pallidus to the thalamus was overactive in parkinsonism, thereby inhibiting the activity of the thalamic neurons which consequently reduces movement. Further evidence for the overactive GABAergic input to the thalamus arises from neurosurgical evidence, suggesting that thalamotomies can alleviate parkinsonian symptoms in both non-human primates and patients (Hariz, 1990; Wester and Hauglie-Hanssen, 1990).

1.3 Treatments for Parkinson's Disease

Until the discovery, in the 1960s, that the major pathology underlying the symptoms of Parkinson's disease was the degeneration of the dopaminergic cells of the SNpc (Hornykewicz, 1966) and that it was possible to reverse the symptoms by administration of the dopamine precursor L-DOPA (Carlsson, 1957), the only treatment

for the symptomatic relief of Parkinson's disease were anti-cholinergic compounds and the antiviral agent amantidine. At that time, the mode of action of these compounds was unknown. These compounds provided, albeit limited, relief from the symptoms of Parkinson's disease, especially of tremor.

1.3.1 Anti-cholinergic compounds

The anti-cholinergic drugs trihexyphenidyl and benzhexol (Artane) are most effective at reducing tremor and rigidity but have little effect on akinesia. The overall improvement in hypokinesia with anti-cholinergics is thought to be in the region of 10-15%. Studies to investigate the efficacy of anti-cholinergics as monotherapy compared to L-DOPA (Parkes *et al.*, 1974) showed L-DOPA to be more beneficial. However, one study reported that anti-cholinergics are at least as effective as L-DOPA in controlling tremor, with a maximal reduction of 50% (Duvosin, 1967; Koller, 1986). Van der Drift (1977) showed a clear improvement in hypokinesia, rigidity and tremor for up to 30 months following initiation of treatment. Therefore, anti-cholinergics may provide symptomatic relief when administered as a monotherapy in the early stages of the disease. There is also evidence that anti-cholinergics may provide a useful adjunct to L-DOPA (Horrocks *et al.*, 1973). There have also been reports of anti-cholinergic drugs reducing L-DOPA-induced dyskinesias and 'on-off' fluctuations in both human trials (Lang and Blair, 1989) and in some non-human primate studies (Pearce *et al.*, 1996). It is known that dopamine exerts a tonic inhibitory action on acetylcholine release from cholinergic interneurons within the striatum (Lehmann and Langer, 1983). Following the loss of dopaminergic stimulation within the striatum in Parkinson's disease, acetylcholine transmission becomes overactive. It is therefore thought that anti-cholinergics exert their anti-parkinsonian effects through decreasing the acetylcholine-dopamine imbalance within the striatum (Stoof *et al.*, 1982b, 1987). Side-effects of anti-cholinergics in the treatment of Parkinson's disease range from impairment of memory and hallucinations, to urinary retention and vasodilation (Jankovic and Marsden, 1988).

Therefore in summary, anti-cholinergics are useful as a monotherapy in the early stages of Parkinson's disease, especially if resting tremor is the most prominent symptom. Furthermore, anti-cholinergics may be useful adjuncts to L-DOPA in

reducing or smoothing 'on-off' fluctuations and may help reduce L-DOPA-induced dyskinesias.

1.3.2 Amantidine and related compounds

Amantidine (Symmetrel), was serendipitously discovered to be a useful anti-parkinsonian agent in 1967 by a patient with influenza (Schwab *et al.* 1969a,b). While receiving amantidine for influenza, this patient observed a marked improvement in their symptoms. This finding was subsequently followed up with a larger study that showed improvement in two thirds of 166 parkinsonian patients. This improvement lasted up to 8 months and when amantidine was withdrawn, a rapid deterioration was seen (Schwab *et al.*, 1972). Amantidine administered with L-DOPA is more beneficial than L-DOPA alone, and allows a reduction in the dose of L-DOPA required. However, the usefulness of amantidine is short-lived with efficacy only up to a maximum of one year reported (Parkes *et al.*, 1971). Memantine, has also been used in the treatment of Parkinson's disease (Wesemann *et al.*, 1980). It was originally thought that amantidine worked by increasing the synthesis and release of dopamine (Stromberg and Svensson, 1971; Von Voigtlander and Moore, 1971). However, it has been demonstrated that amantidine can, at therapeutic concentrations, bind to the MK-801 binding site of the NMDA receptor in *post-mortem* human frontal cortex (Kornhuber *et al.*, 1991), suggesting NMDA receptor antagonist properties. Several studies have demonstrated the ability of NMDA receptor antagonists to be capable of alleviating the akinesia observed in both rodent and non-human primate models of Parkinson's disease (Graham *et al.*, 1990a; Klockgether and Turski, 1990; Brotchie *et al.*, 1991; Loschmann *et al.*, 1991; Carroll *et al.*, 1995; Mitchell *et al.*, 1995). These studies suggest a role for amantidine in reducing the effects of overactive glutamate release within the basal ganglia. Psychosis and memory impairment are the major problems associated with glutamate antagonists (Riederer *et al.*, 1991).

In summary, amantidine and memantidine can be an effective monotherapy in the early stages of Parkinson's disease. However, they have a small therapeutic window and are susceptible at causing memory impairment and psychosis.

1.3.3 Dopamine-replacing agents

In 1967, the introduction of the dopamine precursor L-DOPA as a treatment for Parkinson's disease was a mile-stone in the treatment of Parkinson's disease (Cotzias *et al.*, 1967). Despite much research into direct dopamine agonists, L-DOPA remains the 'gold standard' for the treatment of Parkinson's disease. Systemically-administered L-DOPA is decarboxylated to dopamine by the enzyme L-amino acid decarboxylase (AADC), thus producing an anti-parkinsonian effect. However, L-DOPA is not without disadvantages, including 'on-off' fluctuations, wearing off of efficacy, non-responsiveness and, most disturbing of all, the involuntary abnormal movements of L-DOPA-induced dyskinesias (these will be discussed in detail in section 1.4).

In an attempt to combat these side-effects and enhance the efficacy, L-DOPA has been produced in a variety of formulations to modulate delivery pharmacokinetics so as to achieve a more constant plasma level, rather than the usual peaks in plasma concentrations evident following administration of a single dose formulation.

L-DOPA is also usually administered with a peripheral decarboxylase inhibitor (carbidopa or benserazide) to inhibit decarboxylation to dopamine before crossing the blood-brain barrier, thereby reducing peripheral side-effects, such as nausea, vomiting, anorexia and cardiovascular effects (Brogden *et al.*, 1982; Langdon *et al.*, 1986).

The most common L-DOPA formulations are 'Sinemet' which consists of L-DOPA and carbidopa (in a ratio 10:1 or 4:1) and 'Madopar' composed of L-DOPA and benserazide in a 4:1 ratio. The plasma half life of L-DOPA is only 1.3 hours (Gancher *et al.*, 1987), therefore controlled-release preparations have been developed to try and even out the plasma levels of L-DOPA. Sinemet CR contains 200 mg of L-DOPA and 50 mg of carbidopa, this causes fewer fluctuations in plasma levels and gives a smoother therapeutic response. Madopar CR is also available. However, there is considerable variability between patients with such controlled release preparations and often with a slow response on the first dose of each day (Burton and Calne, 1984).

Due to the problems encountered with the long-term use of L-DOPA, many other direct dopamine receptor agonists have been developed. These are utilised in the treatment of Parkinson's disease, both as monotherapy and in conjunction with L-DOPA to assist in symptomatic relief. Clinically-applied agonists include apomorphine (Cotzias *et al.*, 1976; Agid *et al.*, 1979), bromocriptine (Parkes, 1979; Lieberman *et al.*,

1979), pergolide (Le Witt *et al.*, 1983), PHNO (Stoessl *et al.*, 1985), lisuride (Parkes *et al.*, 1981), and the newly-available cabergoline (Lera *et al.*, 1993; Inzelberg *et al.*, 1995), ropinirole (Brooks *et al.*, 1995), and pramipexole (Hubble *et al.*, 1995).

The first clinical trials of the dopamine D1 and D2 receptor agonist apomorphine (*n*-propyl-norapomorphine) were disappointing due to low patient tolerance (Cotzias *et al.*, 1976). However, in 1974, bromocriptine, a dopamine D2 receptor agonist ergot derivative was introduced as the first clinically useful-dopamine receptor agonist (Calne *et al.*, 1974, 1978). Bromocriptine was successful in smoothing out L-DOPA-induced fluctuations and caused no dyskinesias when used as a monotherapy (Lees and Stern, 1981). The success of bromocriptine was attributed to a long half life of over 8 hours. Unfortunately, bromocriptine is not useful in all patients as many exhibit non-responsiveness and psychiatric problems including visual hallucinations (Calne *et al.*, 1978; Hoehn, 1985). Later, pergolide (a D2 dopamine receptor agonists with possible D1 agonist properties) and lisuride (a D2 dopamine agonist) were developed which act in a similar way to bromocriptine, with half lives of 12, and 3 hours respectively (Parkes *et al.*, 1981; LeWitt *et al.*, 1983).

PHNO, a non-ergoline agonist is a potent post-synaptic D2 receptor agonist (Stoessl *et al.*, 1985) with the added advantage that it can be administered transcutaneously. However, PHNO, due a lack of licence, is seldom used clinically.

All direct dopamine receptor agonists reverse the symptoms of akinesia, rigidity, and to some extent tremor by mimicking the effects of endogenous dopamine. The advantage for most of the compounds over L-DOPA is the fact that they have extended plasma half lives and therefore behave more like the controlled-release preparations with lower plasma fluctuations. Recently cabergoline, with a half life of 72 hours, has been introduced for the treatment of Parkinson's disease with reported successes in both smoother 'on-off' periods, less dyskinesias and longer 'on' periods. Similarly, novel dopamine agonists ropinirole (Rascol *et al.*, 1996) and pramipexole (Molho *et al.*, 1995) have been introduced as a novel therapeutic strategy with purported less complications. However, due to the novelty of these compounds, the lack of complications suggested by relatively few clinical trials to date cannot be fully assessed until longer term trials have been carried out. Already, side-effects of carbergoline have been reported (Geminiani *et al.*, 1996).

1.3.4 Other pharmacological interventions

Other strategies in the treatment of Parkinson's disease include: increasing dopamine synthesis via stimulation of tyrosine hydroxylase (Le Witt *et al.*, 1983); enhancement of dopamine release with amphetamine-type drugs (Parkes *et al.*, 1975); and blockade of dopamine uptake (Bedard *et al.*, 1977; Sandyk, 1985). However, these treatments have little if any use in the treatment of Parkinson's disease. Blockade of dopamine uptake has only a modest anti-parkinsonian effect but may be useful in the treatment of depression in Parkinson's disease.

Other therapeutic approaches utilised which have had more success in the treatment of Parkinson's disease have been those compounds that inhibit dopamine catabolism. Degradation of L-DOPA involves two enzymes, catechol-o-methyl-transferase (COMT) and monoamine oxidase (MAO).

Early studies using COMT inhibitors found many adverse effects with little efficacy in the treatment of Parkinson's disease. (Ericsson *et al.*, 1971; Reches *et al.*, 1982). However, more recently with the development of the more selective COMT-inhibitors entacapone and tolcapone, a renewed interest in COMT inhibitors has been evident. Entacapone, which does not cross the blood-brain barrier, was shown in a single dose study to increase the patients 'on-time' with a concomitant increase in plasma levels of L-DOPA (Merello *et al.*, 1994). Similar results with entacapone were found in a longer trial of four weeks i.e. decrease L-DOPA intake with increased 'on-time' (Ruottinen and Rinne, 1996). In a longer chronic dose study (8 weeks), L-DOPA doses were reduced by 27% while the mean plasma concentrations were increased by 23% (Nutt *et al.*, 1994). A 77% increase in 'on-time' was also noted. Combination therapy consisting of L-DOPA, the MAO-B inhibitor selegiline and a novel COMT-inhibitor tolcapone, again increase the anti-parkinsonian effects of L-DOPA with nausea as the only adverse effects (Davis *et al.*, 1995). However, longer clinical trials are required to establish the effectiveness of combined COMT- inhibitors and L-DOPA therapy.

More success was reported with the MAO-inhibitors. MAO-B inhibitors in conjunction with L-DOPA had originally been found to be more beneficial than COMT-inhibitors in the treatment of Parkinson's disease, without adverse effects. The most commonly prescribed MAO-B inhibitor in use today is selegiline (deprenyl/eldepryl).

MAO-B inhibitors inhibit the breakdown of dopamine, thereby increasing the local concentration of dopamine in the striatum. Since the appearance of the symptoms of Parkinson's disease requires a large depletion of striatal dopamine (>70-90% reduction), dopamine concentration within the striatum only has to be increased above this critical level to reverse the symptoms of Parkinson's disease. Several early studies showed that MAO-B inhibitors may be able to delay the need for L-DOPA or dopamine agonist therapy by up to one year compared to those receiving the placebo (Parkinson Study group, 1989; 1993).

It was thought that by reducing the oxidative metabolism of dopamine, and concomitant reduction in free radical formation, MAO-B inhibitors would prove to be neuroprotective (Olanow, 1993). However, neuroprotective effects of MAO-B inhibitors have not been shown (Parkinson Study Group, 1993). To investigate this possible neuroprotective role, a large prospective study was carried out in the U.S.; the DATATOP study (deprenyl and tocopherol antioxidant therapy for parkinsonism). Recently, it has been reported from this trial that deprenyl did not improve the progression of the disease nor was the delay in the time required for L-DOPA therapy maintained over an extended period (Parkinson Study Group, 1996). Similarly, another arm of the study investigating the effects of deprenyl in conjunction with L-DOPA, showed no advantage of concurrent deprenyl treatment with regards to the development of L-DOPA-induced complications, such as L-DOPA-induced dyskinesias and 'on-off' fluctuations (Parkinson Study Group, 1996). Moreover, recent reports of increased morbidity rates in Parkinson's disease patients treated with the MAO-B inhibitor deprenyl, (60% higher than those patients receiving L-DOPA monotherapy) has led to its controversial removal from some patient treatments (Lees, 1995). However, the high mortality rate seen in both selegiline-treated and non selegiline-treated patients has left this study open to criticism (Olanow *et al.*, 1996).

Therefore, benefits of both COMT-inhibitors, due to the lack of long-term prospective studies, and of MAO-B inhibitors, due to the recent studies reporting no long-term benefit and possible increased morbidity, in the long-term management of Parkinson's disease still remains controversial.

1.3.5 Surgical interventions

Recently, the problems associated with long-term L-DOPA therapy, have led to a resurgence of interest in surgical techniques for the symptomatic relief of Parkinson's disease. These techniques fall into two broad categories.

The first involves specific deactivation of specific brain nuclei, through either non-reversible electrolytic lesioning, or reversibly 'deactivating' these nuclei via high frequency stimulation in the technique known as deep brain stimulation.

The second surgical technique involves implantation of dopamine-producing cells, directly into the caudate nucleus or putamen to reverse the dopamine deficiency seen in Parkinson's disease. These will now be considered separately.

Surgical lesioning

In the early part of this century, destruction of various brain areas has been used in an attempt to correct neurological disorders (Bucy, 1937; Myers, 1940; Putnam, 1940; Spiegel and Wycis, 1950). However, until the 1950s, these lesions were mostly unsuccessful as they were not targeted to specific nuclei. In the 1950s, work by Narabayashi and others, made possible by advances in both imaging techniques and lesion-generating electrodes, were able to target lesions more specifically. These not only alleviated symptoms, but helped delineate the function of these various brain nuclei.

The advent of modern drug development reduced the need for direct lesioning of brain structures and pharmacological intervention became the approach of choice. However, it became obvious that the early promise of L-DOPA therapy for Parkinson's disease was not met due to the vast array of complications. In the 1980s, when both information concerning the mechanisms underlying movement disorders and intracellular recording techniques had improved, stereotactic lesioning once again became a useful therapeutic tool.

In studies on both non-human primates and humans, not only did these techniques show therapeutic benefit to patients but they also gave further insight into the mechanisms underlying various movement disorders.

Early studies by Narabayashi *et al.* in the 1950s showed that stereotactic lesions of the medial segment of the globus pallidus could alleviate both rigidity and tremor in Parkinson's disease (Narabayashi *et al.*, 1956). However, subsequent studies showed that thalamic lesions produced greater benefit (Cooper and Bravo, 1958). In these studies, lesions in the thalamus were found to abolish contralateral tremor and rigidity.

Many of these studies contradict present theories of basal ganglia function. For instance, the thalamus is thought to be overly inhibited in Parkinson's disease and so thalamic lesions would be expected to enhance motor deficits. One explanation of this apparent discrepancy is that enhancement of parkinsonism only occur following thalamic lesions if the whole of the basal ganglia-related thalamus is lesioned bilaterally. This speculation leads to the hypothesis that only a small amount of the VA/VL thalamus is actually required for normal functioning of the motor circuit. Another possibility for a lack of increased motor impairment following thalamic lesions is that the descending pathways to the PPN and the SNpr to the brainstem are spared thus maintaining some degree of voluntary movement.

The development of stereotatic radiofrequency ablation allowed lesions of just a few millimetres in diameter to be produced. These can be targeted to highly specific locations by utilising advances in electrophysiological recording and stimulation procedures. Advances in imaging techniques, such as computer-based integration of radiological, magnetic resonance tomography and blood vessel location via angiographic studies, has further increased the specificity of targets for lesions. Together these approaches have succeeded in giving neurosurgeons a higher degree of success and to lesion selective areas of the brain with a reduced number of complications.

To date, ablative thalamic surgery is primarily only performed in patients with tremor that does not respond to pharmacological intervention. Albe-Fessard *et al.* (1962, cited in Albe-Fessard *et al.*, 1996), using intrathalamic recording techniques, demonstrated that rhythmic discharges were present in the ventral thalamus that were time-locked with the spontaneous contralateral tremor. This pointed to the ventral intermediate nucleus of the thalamus as the most obvious target for parkinsonian tremor. The ventral lateral nuclei or the ventral intermediate nucleus (Vim) of the thalamus remains the primary target for lesions to control parkinsonian tremor (Narabayashi, 1989).

Recently, two new target sites have been described to alleviate parkinsonian symptoms, namely the medial segment of the globus pallidus (pallidotomy) and the subthalamic nucleus (subthalamotomy). Pallidotomies and subthalamotomies have been performed in both MPTP-treated non-human primates (Aziz *et al.*, 1991, 1992; Bergman *et al.*, 1990) and in patients (Dogali *et al.*, 1995; Lozano *et al.*, 1995; Baron *et al.*, 1996). However, subthalamotomies are associated with a higher degree of risk than either pallidotomies or thalamotomies due to the relatively small size and rich blood supply of the nucleus, which therefore increases the risk of haemorrhaging (Linazasoro *et al.*, 1996).

1.3.6 High frequency stimulation

More recently, a less destructive, nonetheless invasive, non-permanent inactivation of brain structures has been produced using high frequency stimulators (Benabid *et al.*, 1987). This technique has allowed the stereotatic implantation of high frequency stimulators into the Vim nucleus of the thalamus to control parkinsonian tremor. The effects of chronic stimulation are maintained over an extended period (Benabid *et al.*, 1991, 1993). Recently, subthalamic stimulations have been carried out to alleviate parkinsonism in both MPTP-treated primates (Boraud *et al.*, 1996) and patients (Limousin *et al.* 1995). The procedure offers several advantages over traditional electrolytic ablation techniques. The high frequency stimulating electrode can be removed with relatively little damage to the implanted nuclei. The stimulator can be switched on and off via a magnetic plate implanted subcutaneously on the patients chest, allowing greater flexibility. The patient can also turn off the stimulator during sleep, thus reducing the possible long-term effects of chronic over-stimulation. The latest generation of stimulators contain multiple channels which can be programmed to stimulate in a particular sequence thus allowing the stimulator to be 'tailor-made' to each patients requirements, thus giving maximum therapeutic benefit. This programmable element also allows the stimulator to be 'fine-tuned' over time to maximise the benefit gained without the need for further operations, unlike traditional pallido- and thalamotomies. The only reported problems with the use of high frequency stimulators are the small risk of infection and in some cases, especially when implanted in the subthalamic nucleus, haemorrhaging (Linazasoro *et al.*, 1996).

In summary, advances in both electrode generators and imaging techniques, coupled with the advances in understanding the neural mechanisms underlying movement disorders, has led to both pallido- and thalamotomies being useful additions in the treatment of Parkinson's disease, especially in the treatment of tremor. Recently, it has become apparent that subthalamotomies and pallidotomies may also be useful in controlling the detrimental side-effects of L-DOPA-treatment, namely L-DOPA-induced dyskinesias. However, the mechanism by which this reduction in dyskinesias comes about remains to be elucidated and current models of basal ganglia function do not explain these observations. It has been suggested that since only a small area of either the subthalamic nucleus or medial pallidal segment is lesioned the increase in dyskinesias that would be expected is not observed (Marsden and Obeso 1995). The use of high-frequency stimulators may provide a safer more controllable alternative to lesions. Furthermore, the development of more advanced electrodes should offer an invaluable therapeutic tool for the control of movement disorders.

1.3.7 Surgical Transplantation

Neural transplantation of cellular material from either foetal tissue or transfected cell lines has proved to be a more successful therapeutic approach than most would have expected. In 1976, Stenevi *et al.* reported that they had successfully transplanted both central and peripheral monoamine neurons into the rat brain. Further advances were made when it was shown that foetal rat nigral cells could be transplanted into the substantia nigra of rats with a degenerated substantia nigra after a 6-OHDA-lesion (Perlow *et al.*, 1979).

Bjorklund *et al.*, 1980, demonstrated that a suspension of nigral cells could be stereotactically implanted in the desired site with survival. The dopaminergic cells not only survived and synthesised dopamine but in fact exhibited spontaneous electrical firing activity, produced axons and showed dendritic arborisation, increased the concentration of dopamine within the striatum, and improved motor and behavioural abnormalities in parkinsonian rats (Freed *et al.*, 1983; Rose *et al.*, 1985; Stromberg *et al.*, 1985). Utilising foetal substantia nigra cells, neural transplants were carried out in the MPTP-treated non-human primate model of Parkinson's disease, with similar success (Bakay *et al.*, 1985; Redmond *et al.*, 1986).

Madrazo *et al.* in 1988 implanted human substantia nigra cells from aborted foetal tissue into two patients with Parkinson's disease. During a 6 months follow up, the patients had improved in both their off-motor score disability and by a lowering of the amount of L-DOPA required. Subsequently, a Swedish group also reported improvement in two patients with idiopathic Parkinson's disease (Lindvall *et al.*, 1989) and later in the heroin addicts with MPTP-induced parkinsonism. These studies have highlighted the success of such neural implantation techniques. However, several problems still exist.

There is a large ethical question involved, with many countries banning the use of foetal material. Furthermore, the transplantation procedure is very labour intensive, requiring the expertise of cell biologists, neurologists, and neurosurgeons. Recent studies utilising genetically-transformed cell lines expressing dopamine (Date and Ohmoto, 1996) or xenographs (Lindvall, 1995; Folkerth, 1996) have highlighted the possibility of a more reliable and ethically-acceptable transplantational material.

In summary, both lesion, inactivation and transplantation techniques can aid in the symptomatic relief of Parkinson's disease, especially in the later stages of the disease when drugs are less efficacious. However, due to the labour intensity, risk of haemorrhage, rejection and/or ethical considerations, drug intervention seems to likely to remain the most desirable therapeutic strategy in Parkinson's disease.

1.3.8 Summary of treatments for Parkinson's disease

Several therapeutic strategies are available for the symptomatic relief of Parkinson's disease. In the early stages of the disease, anti-cholinergic or anti-glutamatergic agents may reduce the symptoms of tremor and rigidity. However, following disease progression, dopamine-replacement becomes necessary. Bromocriptine and other direct dopamine agonists, if tolerated by the patient, gives the most therapeutic benefit with lower incidence of dyskinesia. Eventually, L-DOPA plus a peripheral decarboxylase inhibitor, either with or without a MAO-B or COMT-inhibitor, will be required. Following the appearance of inevitable side-effects of long-term L-DOPA therapy, stereotactic surgery, high-frequency stimulation or neural transplantation may provide symptomatic relief in the later stages of the disease.

However, for the foreseeable future, L-DOPA will remain the most effective treatment for Parkinson's disease in spite of the high incidence of complications. Therefore, by understanding the pathophysiology of L-DOPA-induced dyskinesias, it may be possible to provide symptomatic relief of Parkinson's disease with L-DOPA without the complicated and disabling side-effects of L-DOPA-induced dyskinesias.

1.4 L-DOPA-induced dyskinesias

With the discovery of the therapeutic benefit of the endogenous dopamine precursor L-DOPA in the late 1960s, the symptomatic problems of Parkinson's disease seemed concluded. However, shortly after the introduction of L-DOPA it became apparent that L-DOPA was not going to be as useful as was first hoped, and that repeated L-DOPA therapy was associated with a number of detrimental side-effects. These included a wearing-off of efficacy, 'on-off' fluctuation (Nutt *et al.*, 1984), and most commonly, the inappropriate involuntary movements of L-DOPA-induced dyskinesias (Barbeau, 1969; Barbeau, 1974; Marsden and Parkes, 1976; Barbeau, 1980; Nutt, 1990). These will now be discussed in detail.

Clinical manifestations of L-DOPA-induced dyskinesias

L-DOPA-induced dyskinesias, eventually affect up to 80% of patients with Parkinson's disease, and are characterised by chorea and dystonia, both at peak plasma levels following L-DOPA administration and also during 'off' periods. These dyskinesias eventually become as debilitating as Parkinson's disease itself (Nutt, 1990).

Clinically, L-DOPA-induced dyskinesias present themselves in a variety of forms. In most patients, dyskinesia is of greatest severity at the time of optimum improvement from L-DOPA, and are therefore referred to as peak-dose dyskinesias. These mainly involve choreic movements, although can also be dystonic in nature, occurring when the administered L-DOPA has reached maximal plasma levels and should therefore be expected to be producing maximal anti-parkinsonian response. Dyskinesias can also occur as 'beginning and end-of-dose dyskinesias' or more commonly termed 'diphasic

dyskinesias'. Diphasic dyskinesia develops as the plasma levels of L-DOPA are rising or falling, but not during the peak plasma levels (Tolosa *et al.*, 1975a, 1975b).

However, in some patients only the beginning or end dose dyskinesia is apparent. Most of the affected patients with this form of dyskinesia have dystonia as their pattern of dyskinesia, though some have choreic movements, and others have a mixture of the two types. These diphasic dyskinesias are also described as 'D-I-D' phenomenon for 'Dystonia-improvement-dystonia' (Muentert *et al.*, 1977).

The group most severely affected by L-DOPA-induced dyskinesias exhibit so-called 'square wave' dyskinesias, whereby patients exhibit signs of dyskinesia for the full duration of the anti-parkinsonian effects of the L-DOPA.

Clinically therefore, in the vast majority of patients, dopamine-replacement therapy for the treatment of Parkinson's disease is inevitably associated with dyskinetic side-effects. Unfortunately, all the other direct dopamine receptor agonists have limited value as they also elicit dyskinesia when given either with low doses of L-DOPA, or when given alone to patients previously treated with L-DOPA.

Only one dopaminergic treatment, bromocriptine, has been successful in alleviating the symptoms of Parkinson's disease without eliciting dyskinesia. Non-human primates rendered parkinsonian with MPTP and subsequently treated with bromocriptine *de novo*, do not develop dyskinesias (Bedard, 1986). Similar clinical studies suggest that bromocriptine can also alleviate parkinsonian symptoms in previously untreated patients with no, or a much reduced incidence of, dyskinesia (Kartzinel *et al.*, 1976; Parkes *et al.*, 1976; Lees and Stern, 1981).

Unfortunately, only about 30% of patients respond to the anti-parkinsonian effects of bromocriptine (Fahn *et al.*, 1979; Lees, 1993). Patients also suffer from psychiatric side-effects including confusion, visual hallucinations, and paranoia (Calne *et al.*, 1978; Harris, 1984) and therefore require either, bromocriptine in combination with L-DOPA, or L-DOPA therapy alone, both regimes eventually resulting in dyskinesia (Rinne, 1987).

1.4.1 Hyperkinetic movement disorders (chorea and dystonia)

Huntington's disease

As previously described in section 1.2.2, Huntington's disease is a genetically-inherited disorder, characterised clinically by chorea and genetically by a repeated trinucleotide expansion of 'CAG' producing the 'huntingtin' protein. The underlying cause of the clinical manifestation of chorea is degeneration of the caudate nucleus and putamen. Initially, the medium spiny neurons of the indirect pathway to the lateral segment of the globus pallidus degenerate, followed by degeneration of the direct pathway to the medial segment of the globus pallidus (Sapp *et al.*, 1995). This degeneration of the striatum is accompanied with the appearance of amyloid protein 'plaques' in the cerebral cortex and other brain regions with concomitant dementia. The only symptomatic treatment for the chorea in Huntington's disease is monoamine-depleting drugs such as reserpine. However, these drugs increase depression, sedation and can cause parkinsonism (Jankovic and Orman, 1988). It has been suggested from animal models that NMDA receptor antagonists, enzymes that aid mitochondrial energy metabolism (coenzyme Q₁₀) and nitric oxide synthase inhibitors, may slow the progression of Huntington's disease. However, data from clinical trials has not yet been obtained. Intrastratial implantation techniques, similar to those used in Parkinson's disease (see section 1.3.5), utilising genetically engineered or foetal cells, may also provide a future therapeutic strategy.

Tourette's syndrome

Gilles de la Tourette's syndrome is a genetically-inherited neurological disorder which presents itself as motor and vocal tics (Pauls *et al.*, 1991). This syndrome usually presents itself in childhood and is often accompanied by obsessive-compulsive disorders (Jankovic, 1987). The cause of Tourette's syndrome remains unknown, although due to increased [³H]-mazindol radioligand binding, increased dopaminergic transmission within the nucleus accumbens has been suggested (Singer *et al.*, 1989, 1990). Since the nucleus accumbens is associated with the limbic system, this may explain the clinical

manifestations of disorders of both behaviour and the vocal tics. The main treatment for Tourette's syndrome is dopamine antagonists, although haloperidol can often cause side effect of tardive dyskinesia and neuroleptic-induced dyskinesia. Fluphenazine is often used as it causes less drug-induced side-effects. Most patient's suffering from Tourette's syndrome undergo a remission with age.

Tardive dyskinesia

Tardive dyskinesia was first described in 1957 in patients who were being treated for schizophrenia with antipsychotics (Schonecker, 1957; cited in Fahn, 1994). Tardive dyskinesia is a movement disorder of abnormal involuntary movements, mainly orofacial but also involving limbs and axial musculature. Tardive dyskinesia is caused by long-term treatment by dopamine receptor antagonists and persists for months or even years after the dopamine antagonists are stopped (Polizos *et al.*, 1973; Casey, 1986; Jeste, 1988).

Dystonia

Dystonia is characterised by involuntary, unusually held, or twisted, postures, usually of the limbs, but also involving axial, trunk and orofacial musculature. These dystonias are often permanent and can be extremely painful for the patient. Several forms of dystonia exist, including the most general form of idiopathic torsion dystonia, dopa-responsive dystonia (an inherited dystonia that responds to low doses of L-DOPA), and several subdivisions of juvenile-onset dystonia and myoclonic dystonia.

Drug therapies for dystonia are usually not very successful. Anti-cholinergics and benzodiazepines have been noted to improve some forms of dystonia, although side-effects are common. For localised dystonia, injections of botulinum toxins, to relax the muscle groups underlying the dystonia by inhibiting acetylcholine release, can provide symptomatic relief in many cases. In the most advanced and disabling cases of generalised dystonia, surgery can also be of benefit, with the main target being the thalamus. However, post-operative complications including hypokinesia and speech deterioration are common (Tasker *et al.*, 1988).

1.4.2 Animal models of dyskinesias

As with Parkinson's disease, the most useful asset for both understanding the pathophysiology and the development of effective treatments is the animal model. In primates, several models have been useful in investigating the neural mechanisms underlying dyskinesias. In rodents, certain types of dyskinesia have been modelled, including tardive dyskinesia, serotonin syndrome, and dystonia. However, no model to date has been able to reproduce the symptoms of L-DOPA-induced dyskinesia in rodents.

Rodent Models of dyskinesias

Behavioural correlates of dyskinesia have proved difficult to produce and interpret in the rodent, mainly due to the more limited set of movements afforded by the rodent anatomy.

Vacuous chewing movements

One model of dyskinesia reported in rodents are the so called 'vacuous chewing movements' produced following chronic administration of neuroleptics. Following several months neuroleptic treatment (e.g. haloperidol), rats develop inappropriate vacuous chewing movements (VCMs), which are maintained following withdrawal of treatment. VCMs are classically considered to be a rodent model of tardive dyskinesia.

Similar VCMs coupled with increase sniffing and grooming behaviour can also be produced following chronic amphetamine or apomorphine treatment in clinically-normal rats (Murray *et al.*, 1989). These VCMs are thought to model oral dyskinesia seen in various dyskinesias (Waddington and Gamble, 1980; Waddington *et al.*, 1983). Due to the subtle nature of behaviours such as VCMs and increased sniffing or grooming, detection and quantification is difficult. However, VCM is at present the best rodent model of tardive dyskinesia. However, chronic amphetamine or apomorphine treatment probably does not afford a useful model of L-DOPA-induced dyskinesias as the rats develop these dyskinesias without the long-term dopamine-depletion associated with Parkinson's disease.

Iminodipropionitrile-induced dyskinesia

Several investigators have highlighted the dyskinetic properties of mice, rats and cats treated with iminodipropionitrile, resulting in a persistent dyskinesia (Przedborski *et al.*, 1989, 1990; Kawada *et al.*, 1995). Chronic administration of the neurotoxin iminodipropionitrile (IDPN) to rodents causes the dyskinetic symptoms of lateral and vertical neck dyskinesia, random circling and hyperexcitability. The dyskinetic symptoms induced by IDPN closely resemble those of idiopathic dyskinesia in humans, in that they are permanent, are aggravated by stress, and subside during sleep.

This toxin has been reported to disrupt microtubular vesicle transportation in axons, predominantly in serotonergic neurons (Cadet *et al.*, 1989; Ogawa *et al.*, 1990). Chemical and receptor changes seen in the serotonin systems of these animals leads to the hypothesis that this animal model is probably more analogous to the so called 'serotonin syndrome' seen in patients following long-term serotonin uptake blockers e.g. fluoxetine for depression (Przedborski *et al.*, 1989, 1990). Therefore, although the behavioural symptoms can be described as dyskinetic, due to its differing iatrogenic aetiology, with lack of dopamine involvement, this rodent model of dyskinesia cannot be considered a useful correlate of L-DOPA-induced dyskinesia.

Rodent model of Huntington's disease

Quinolinic or ibotenic acid infused into the neostriatum of rodents produces a biochemical and behavioural model of Huntington's disease by destroying cells of the neostriatum (Figueredo-Cardenas *et al.*, 1994). These animals do not display the clinical symptoms of chorea or dystonia, but they do display a hyperkinetic behaviour (Figueredo-Cardenas *et al.*, 1994). However, due to the acute damage caused by the lesion, without preferential selectivity for the enkephalinergic cells initially seen in the disease (Sapp *et al.*, 1995; Richfield *et al.*, 1995) and the non-progressive nature of the lesion makes this model of limited use (Hantraye *et al.*, 1990).

Genetically dystonic rodents

A mutant strain of Syrian Golden hamsters (dt^{82}) was discovered which, following stress, develop sustained dystonia of the limbs and trunk with distorted body postures (Loscher *et al.*, 1988). These dystonic hamsters have been investigated to elucidate whether the mechanism underlying this genetic mutation may cause a disturbance in the neural pathways in a similar manner to either focal dystonia, familiar dystonia or even L-DOPA-induced dystonia. However, utilising both 2-deoxyglucose methods and *in situ* hybridisation, this model seems to be one of Hereditary Progressive Dystonia (Segawa's disease) or transient paroxysmal dystonia. Investigations have shown little link to basal ganglia dysfunction and therefore are of little use in investigating L-DOPA-induced dystonia. An autosomal recessive mutant dystonic rat (dt) has also been described. These dystonic rats share features of idiopathic torsion dystonia. These symptoms have been localised to a cerebellar disorder of the serotonergic system, and symptoms can be reversed by cerebellectomy (Wieland and Lucki, 1991; Le Doux *et al.*, 1993; Le Doux *et al.*, 1994).

L-DOPA-induced dyskinesia

In 1991 Carey described an 'L-DOPA-induced overstimulation' rat model. This model consisted of the 6-OHDA-lesioned rat model of Parkinson's disease following repeated doses of L-DOPA. A marked enhancement in contraversive rotations elicited by treatment, with increasing time of treatment was noted. This was described as being analogous to the supersensitivity to dopamine agonists seen in patients following repeated treatment in Parkinson's disease. This behavioural supersensitivity has also been described in the 6-OHDA-lesioned rat, following repeated apomorphine administration (Bevan, 1983). In terms of mechanisms inducing this behaviour, this is the best rodent model of L-DOPA-induced dyskinesia. However, the validity of this model is unclear as the symptoms expressed are not choreiform or dystonic and it is not known whether the pharmacology of this dyskinesia is similar to that of L-DOPA-induced dyskinesia. Studies in chapter 2 will address this issue.

Non-human primate models of dyskinesias

As already mentioned, several primate models exist in which it has proved possible to study the neural mechanisms underlying dyskinesias. These will now be outlined below.

Non-human primate model of tardive dyskinesia

Long-term systemic administration of various neuroleptic compounds, such as haloperidol or fluphenazine deconate, accurately mimics the dyskinesias seen in patients treated with these drugs for psychiatric disorders. These dyskinesias are mainly orofacial with some limb and axial musculature involved. The dyskinesia seen in these animals, like that seen in patients, persists following drug removal (Gunne and Barany, 1976). This model provides a useful and accurate non-human primate model of tardive dyskinesia.

Non-human primate models of hemiballism, chorea and dystonia

Several studies have shown that intracerebral injection of various antagonists in differing parts of the basal ganglia nuclei can induce experimental hemiballism and dystonia. Early studies by Whittier, 1949 and Carpenter in 1950, demonstrated hemiballism following lesion of the subthalamic nucleus. Similarly, in more recent studies, injection of the GABA receptor antagonist bicuculline into the subthalamic nucleus also elicits hemiballism (Crossman *et al.*, 1980; Crossman *et al.*, 1984). Injection of bicuculline into the lateral segment of the globus pallidus in the primate causes chorea (Jackson and Crossman, 1984; Crossman *et al.*, 1988; Mitchell *et al.*, 1989) while injection of the glutamate antagonist kynurenate into the GPM causes chorea and dystonia (Robertson *et al.*, 1989). The induction of experimental hemiballism and dystonia has been invaluable in investigating and understanding the neural mechanisms underlying both normal functioning of the basal ganglia nuclei and the pathophysiology of movement disorders (Crossman *et al.*, 1990). However, while providing an invaluable framework for extrapolation to L-DOPA-induced dyskinesia this model is of little use in understanding the cellular, molecular and biochemical mechanisms of L-DOPA-induced dyskinesia.

Non-human primate model of Huntington's disease

Ibotenic acid infused into the neostriatum of non-human primates produces a biochemical and behavioural model of Huntington's disease, by destroying cells of the caudate nucleus and putamen (Isacson *et al.*, 1989). These animals display the clinical symptoms of chorea and dystonia when challenged with dopamine receptor agonists such as apomorphine (Hantraye *et al.*, 1990). However, due to the acute damage caused by the lesion, without preferential selectivity for the enkephalinergic cells initially seen in the disease (Richfield *et al.*, 1995; Sapp *et al.*, 1995), and the non-progressive nature of the lesion makes this model of limited use in understanding the mechanisms underlying the pathology of Huntington's disease (Hantraye *et al.*, 1990).

Non-human primate model of L-DOPA-induced dyskinesia

The animal model which most closely mimics the symptomatology and clinical manifestations of L-DOPA-induced dyskinesias, is the MPTP-treated parkinsonian non-human primate following repeated L-DOPA or dopamine receptor agonist treatment. Primates rendered parkinsonian by MPTP-administration develop dyskinesias in weeks to months, following repeated administration of either L-DOPA or apomorphine (Bedard *et al.*, 1986; Clarke *et al.*, 1987). The symptoms of these dyskinesias are similar to those seen in Parkinson's disease patients following several years of L-DOPA therapy. Similarly, dopaminergic drugs that do not cause dyskinesias in parkinsonian patients, such as bromocriptine and lisuride, do not produce dyskinesias in this primate model (Gomez-Mancilla and Bedard, 1993).

This primate model of L-DOPA-induced dyskinesia exhibits the full range of dyskinetic symptoms including chorea, ballism, dystonia, vacuous chewing movements, and in some incidences increased abnormal vocalisations. This model provides the perfect system for, not only the evaluation of anti-dyskinetic therapies, but also evaluating the pro-dyskinetic potential of novel anti-parkinsonian agents. The L-DOPA-induced dyskinetic primate has been an invaluable model in the delineation of the neural mechanisms underlying L-DOPA-induced dyskinesias.

Recent reports have suggested that following repeated treatment with L-DOPA, or direct dopamine receptor agonists, it is possible to induce dyskinesias in MPTP-

treated common marmosets (*Callithrix Jacchus*, Pearce *et al.*, 1995). However, the doses of L-DOPA required to produce the dyskinesia in this model are far greater than 'therapeutic' doses, and the marmosets display hyperlocomotor responses at the beginning of the dosing regime. This model has not yet been substantiated by other groups. However, if it is possible to produce dyskinesias in a common marmoset following MPTP-treatment with subsequent repeated dopamine agonist treatment, this model will provide a useful addition to the small number of animal models available in which to study L-DOPA-induced dyskinesia. Although this model may be a welcome addition, it seems likely to replace the larger 'old world' primate model for all but the most rudimentary studies into L-DOPA-induced dyskinesias, as the larger primates afford a much more complex range of movements, making them indistinguishable from patients with L-DOPA-induced dyskinesias, and show dyskinesias following treatment protocols that would be applied clinically.

Summary

In summary, rodent models are available for several types of dyskinesias, including tardive dyskinesias, 'Serotonin syndrome', and Hereditary Progressive Dystonia (Segawa's disease). The 6-OHDA-lesioned rat model of Parkinson's disease following repeated L-DOPA administration may be a plausible rodent model of L-DOPA-induced dyskinesia. In MPTP-treated non-human primates an excellent model of L-DOPA-induced dyskinesia can be produced. This non-human primate model of L-DOPA-induced dyskinesia displays the full range of clinical symptoms seen in patients with Parkinson's disease following long-term L-DOPA therapy.

1.4.3 Pathophysiology of dyskinesias

The neural mechanisms underlying L-DOPA-induced dyskinesias remain largely unknown. However, a wide variety of studies have suggested that a common mechanism may underlie all forms of dyskinesias. Thus, in all forms of dyskinesia, changes in basal ganglia function results in a massive reduction in basal ganglia outputs. The evidence for this delineation will now be outlined below and are summarised in figure 1.3.

Summary of basal ganglia pathway changes in L-DOPA-induced dyskinesia in Parkinson's disease

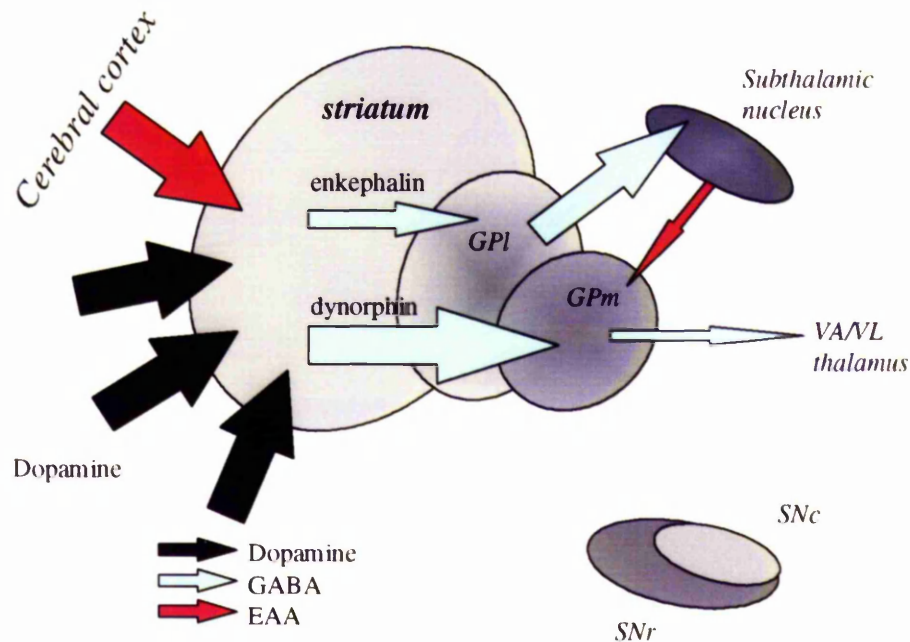


Figure 1.3 Functional circuitry of the basal ganglia in L-DOPA-induced dyskinesias in Parkinson's disease

Following dopamine-replacement in the dopamine-depleted striatum, the 'direct' GABAergic pathway to the medial segment of the globus pallidus and SNpr becomes functionally overactive. The 'indirect' GABAergic pathway to the lateral segment of the globus pallidus becomes underactive. Underactivity of the 'indirect' pathway increases GPe activity. GABAergic GPe efferents to the subthalamic nucleus are therefore overactive, thus decreasing subthalamic nucleus activity. Underactivity of the glutamatergic subthalamic nucleus efferents reduces GPi and SNpr activity. Thus, underactive GPi and SNpr efferents disinhibit the VA/VL thalamus and thus elicits dyskinesia.

■ Overactivity of the lateral segment of the globus pallidus

Experimental chorea can be produced in non-human primates by injection of the GABA receptor antagonist bicuculline into the lateral segment of the globus pallidus, suggesting that overactivity of the lateral segment of the globus pallidus may be important in the genesis of dyskinesias (Jackson and Crossman, 1984; Crossman *et al.*, 1988). Furthermore, 2-deoxyglucose metabolism investigation in these animals, showed increased uptake in the subthalamic nucleus, suggesting the inhibitory GABAergic terminals projecting to the subthalamic nucleus are overactive in these animals (Mitchell *et al.*, 1992).

■ Underactivity of the subthalamic nucleus

One of the most important observations common to all dyskinesias seems to be the underactivity of the subthalamic nucleus. Martin in 1927, described the clinical symptoms of hemiballism following haemorrhaging and subsequent lesion of the subthalamic nucleus. Later in 1942, Papez *et al.* described hemiballism following lesion of the lateral segment of the globus pallidus, although this lesion encompassed both afferent and efferent projections of the subthalamic nucleus. Experimental lesions of the subthalamic nucleus in clinically-normal non-human primates was also demonstrated to elicit hemiballism and chorea (Whittier, 1949a, 1949b).

From anatomical studies showing the extensive innervation of the subthalamic nucleus by inhibitory GABAergic efferents from the lateral segment of the globus pallidus, Jackson and Crossman (1984) demonstrated that the GABA receptor antagonist bicuculline, injected into the lateral segment of the globus pallidus (thus releasing the GPI from the inhibitory input from the striatum and increasing GABAergic transmission to the subthalamic nucleus), caused contralateral choreic movements in the conscious monkey. Furthermore, 2-deoxyglucose studies in monkeys displaying these bicuculline-induced dyskinesia showed most activity in the terminals (from the GPI) to the dorsolateral region of the subthalamic nucleus (Mitchell *et al.*, 1989).

Further 2-deoxyglucose studies in MPTP-treated non-human primates displaying L-DOPA-induced dyskinesias, demonstrated that the subthalamic nucleus was

underactive in the primates displaying dyskinesia compared to both clinically normal and parkinsonian primates (Mitchell *et al.*, 1992). In this study, it was also noted that the animals displaying peak-dose dystonia compared to peak-dose chorea showed the greatest increase in subthalamic nucleus labelling, predominantly in the ventral tip of the subthalamic nucleus, i.e. in the dystonic primates the subthalamic nucleus was under greatest inhibition via GABAergic terminals from the lateral segment of the globus pallidus.

In MPTP-treated non-human primates, ibotenic acid lesion of the subthalamic nucleus not only caused reversal of akinesia, which was the major finding of the paper, but also induced dyskinesias (Bergman *et al.*, 1990). Following lesioning, both animals described developed dyskinesias, one of the primates displayed transient dyskinesia which reduced 7 days post-operatively, the second primate retained dyskinetic symptoms until it was sacrificed 3 weeks later.

Other evidence implicating subthalamic nucleus underactivity in the manifestations of dyskinesias comes from work carried out on *post-mortem* tissue from patients suffering from Huntington's chorea. In these patients, the pathway to the lateral segment of the globus pallidus was shown to degenerate first (at the time when most choreic symptoms are observed). Degeneration of the 'indirect' striatopallidal pathway to the GPi would release it from GABAergic inhibition, thus increasing the GABAergic pathway to the subthalamic nucleus, therefore reducing the activity of the subthalamic nucleus (Richfield *et al.*, 1995; Sapp *et al.*, 1995).

Recent evidence from electrophysiological recordings in bicuculline-induced dyskinesia in non-human primates (injected into the lateral segment of the globus pallidus), has shown hyperactivity in a subset of GPi neurons projecting to the subthalamic nucleus. However, some neurons are seen to be underactive. Furthermore, the firing patterns of the GPi neurons changed, with long periods of silence recorded. This would contradict evidence that the subthalamic nucleus is underactive in dyskinesia. However, both the topographical projections of these neurons and drug effects on collaterals axons, may account for the differences in the firing patterns observed (Matsumura *et al.*, 1995).

Further indirect evidence for possible underactivity of the striato-pallidal pathway, is the fact that following L-DOPA-treatment and subsequent dyskinesia in the MPTP-treated non-human primate, a subset of striatal projection neurons show an

increased expression of both isoforms of the GABA synthesising enzyme, glutamic acid decarboxylase (GAD), namely GAD₆₇ and GAD₆₅. This contrasts with the increase in GAD₆₇ expression only in the MPTP-treated parkinsonian primates. This would suggest an increase in GABAergic transmission in striatal outputs. However, it is not known which subset of striatal projection neurons are responsible for this increase (Levy *et al.*, 1995a; Soghomonian *et al.*, 1996). Recently, evidence from *post-mortem* studies in parkinsonian patients, following long-term L-DOPA treatment and all displaying L-DOPA-induced dyskinesia, suggested that there is also increased GAD₆₇ mRNA expression within cells of the lateral segment of the globus pallidus, indicating the overactivity of efferent projections to the subthalamic nucleus from the lateral segment of the globus pallidus (Nisbet *et al.*, 1996).

■ Underactivity of the medial segment of the globus pallidus

Decreased activity of the subthalamic nucleus would be expected to result in less excitation of the medial segment of the globus pallidus. This has been confirmed by 2-deoxyglucose metabolism studies in both experimentally-induced chorea in non-human primates (Mitchell *et al.*, 1989) and in MPTP-treated non-human primates displaying dyskinesia following repeated L-DOPA administration (Mitchell *et al.*, 1992).

■ Overactivity of the VA/VL thalamus

[³H]2-Deoxyglucose studies in non-human primates displaying experimentally-induced dyskinesia, tardive dyskinesia or L-DOPA-induced dyskinesia in MPTP-treated non-human primates, have all shown a non-significant reduction in uptake in the ventral anterior and ventrolateral nuclei of the thalamus (Mitchell *et al.*, 1989; Mitchell *et al.*, 1992a; Mitchell *et al.*, 1992b). This would suggest that the output from the GPm to the VA/VL thalamus is underactive in all these forms of dyskinesias.

1.4.4 Clinical management of L-DOPA-induced dyskinesias in Parkinson's disease

Presently there is no way to alleviate the L-DOPA-induced dyskinesias observed following repeated L-DOPA therapy in the treatment of Parkinson's disease. However, several authors have suggested both strategies and compounds that may help attenuate some of the dyskinesias. These will now be considered in more detail.

Drug holidays

When L-DOPA-induced complications were first reported it was thought that if patients were given 'drug holidays' i.e. a period of time without L-DOPA administration, when the treatment was resumed, the L-DOPA would be as effective as when the patients were first exposed to L-DOPA. Early reports suggested that this was the case (Sweet *et al.*, 1972; Weiner *et al.*, 1984). However, further studies showed that when patients resumed their L-DOPA therapy, the dyskinesias and on-off freezing episodes soon returned (Nutt *et al.*, 1994).

Controlled L-DOPA-release preparations

As previously mentioned in section 1.3.3, evidence from animals models suggested that continuous infusion of L-DOPA resulted in a marked decrease in L-DOPA-induced dyskinesias (Schuh and Bennett, 1993; Blanchet *et al.*, 1995). This led to the development of controlled release preparations of L-DOPA. These preparations did reduce and delay the complications of long-term L-DOPA treatment in some studies (Koller and Pahwa, 1994). However, although these preparations may prolong the usefulness of L-DOPA therapy, they do eventually result in dyskinesias and other complications (Vaamonde *et al.*, 1991).

Surgery

As already discussed in section 1.3.5, both pallidotomies, thalamotomies and subthalamotomies have been shown to reduce L-DOPA-induced dyskinesias in both experimental non-human primates and patients (Andy, 1983; Narabayashi *et al.*, 1984;

Caparros-Lefebvre *et al.*, 1993). Similarly, high frequency stimulation of the thalamus and the subthalamic nucleus has also been reported to improve L-DOPA-induced dyskinesias (Benabid *et al.*, 1987, 1991; Pollack *et al.*, 1993; Limousine *et al.*, 1995; Boraud *et al.*, 1996). The mechanism by which these treatments alleviate the L-DOPA-induced dyskinesias, without a concomitant reduction on the L-DOPA efficacy, remains elusive. It has been speculated that since these surgical interventions are for the most part unilateral, the expected akinesia and worsening of parkinsonian symptoms are not observed.

Adjuncts to L-DOPA

From observations in non-human primates displaying L-DOPA-induced dyskinesias, several candidate compounds have been proposed which may ameliorate the iatrogenic consequences of L-DOPA therapy.

Reduction in the dose of L-DOPA by introduction of a direct dopamine agonist such as bromocriptine, has been shown to improve L-DOPA-induced dyskinesias (Lees, 1993). Both anti-cholinergics and NMDA receptor antagonists administered with L-DOPA, have been shown to improve L-DOPA-induced dyskinesias in both non-human primate models (Papa and Chase, 1996; Pearce *et al.*, 1996) and in patients (Clough *et al.*, 1984; Verhagen-Metman *et al.*, 1996). The atypical neuroleptic clozapine, which is predominantly a dopamine receptor antagonist with higher affinity for the D1 and D4 dopamine receptor than the D2 dopamine receptor but also has affinity for serotonergic receptors (Meltzer *et al.*, 1989), has been shown to reduce L-DOPA-induced dyskinesias (Bennett *et al.*, 1993; Schuh and Bennett, 1993a; Bennett *et al.*, 1994), improve tremor (Friedman and Lannon, 1990) and psychotic symptoms (Pinter and Helscher, 1993).

Similarly, co-administration of the beta-adrenergic receptor antagonist propranolol with L-DOPA, has been shown to reduce L-DOPA-induced dyskinesias in both experimental primates (Gomez-Mancilla and Bedard, 1993) and, in a small scale study, patients (Carpentier *et al.*, 1996).

Targeting serotonergic transmission may provide a useful strategy in the treatment of L-DOPA-induced dyskinesias. Several reports have indicated that increasing serotonergic transmission can reduce L-DOPA-induced dyskinesias in

patients. This has been achieved by increasing transmission via the serotonin uptake blocker fluoxetine (Durif *et al.*, 1995) and by direct agonism of the 5-HT_{1a} receptor using buspirone (Bonifati *et al.*, 1994).

In experimentally-induced L-DOPA-induced dyskinesias in MPTP-treated non-human primates, the α_2 -adrenergic receptor antagonist yohimbine has been shown to reduce L-DOPA-induced dyskinesias without loss of anti-parkinsonian response (Gomez-Mancilla and Bedard, 1993), although no clinical data has been reported on their effect in patients with L-DOPA-induced dyskinesias.

Reducing opioid neuropeptide transmission by administration of naloxone or the longer acting analogue naltrexone, has been shown to either improve (Trabucchi *et al.*, 1982; Sandyk and Snider, 1986) or have no effect on L-DOPA-induced dyskinesias in patients (Rascol *et al.*, 1994) and experimental primates (Gomez-Mancilla *et al.*, 1993).

Therefore in summary, several adjuncts to L-DOPA have been reported, both in experimentally-induced non-human primate models, and in patients with idiopathic Parkinson's disease, to decrease the symptoms of L-DOPA-induced dyskinesias. However, as yet no solid scientific rational exists to guide the selection of potentially useful adjuncts, and no large scale clinical trials have been carried out to support these observations.

The elucidation of the neural mechanisms underlying L-DOPA-induced dyskinesias may help to develop a useful adjunct to L-DOPA, thus improve Parkinson's disease symptoms without the complications of L-DOPA-induced dyskinesias following long-term therapy.

1.5 Opioid neuropeptides

The opioid peptides are a group of structurally-homologous short amino acid peptides derived from three precursor molecules, namely pre-proenkephalin-A (proenkephalin), pre-proenkephalin-B (prodynorphin), and pro-opiomelanocortin. Historically, the discovery of the opioid peptides, or endorphins, arose from two lines of evidence.

The first was derived from the analgesic properties of opiates, the class of drugs with opium-like or morphine-like properties. The analgesic effects of morphine

suggested the existence of an endogenous receptor. The partial reversal of this analgesia by naloxone led to the hypothesis that the endogenous pain-inhibitory system may have opiate-like properties (Akil, 1980).

The second route to the discovery of the opioid peptides, was the suggestion that due to the structure of both opioid agonists and antagonists an endogenous receptor must exist (Goldstein, 1973). The discovery of functional receptors in peripheral tissues (Kosterlitz, 1972), lead to subsequent discovery of such receptors in the central nervous system (Simon *et al.*, 1973; Terenius, 1973; Pfeiffer and Hertz, 1981).

The discovery of enkephalins (Hughes *et al.*, 1975a, b, c) and subsequently other endogenous opioids, brought together the two lines of evidence, providing an endogenous ligand for the opioid receptor and a set of neurotransmitters that explained the mechanism underlying the actions of morphine.

Many levels of complexity exist within the opioid system. This complexity arises from both the number of opioid peptides and receptors, the anatomical distribution of both these peptides and receptors, receptor interactions, and their regulatory mechanisms. Since their discovery over twenty years ago, understanding the diverse roles which opioid neuropeptides play in both signalling and modulation of other 'classical' neurotransmitters is only now becoming clear.

It has taken so long to elucidate the vast array of opioid neuropeptide functions, mainly due to their unusual mode of synthesis. Opioid peptides are synthesised from a larger inactive protein precursor molecule, which can subsequently undergo cleavage by a series of proteolytic steps to generate various smaller biologically-active neuropeptides or fragments. Further complications arise by the fact that these opioid peptides half-lives are controlled by endopeptidases.

The major advance in understanding the opioid peptides has been through the advent of molecular cloning. Cloning and sequencing of both the opioid peptide precursors and their receptors, has allowed delineation of opioid function. The molecular biology of the opioid peptides will now be discussed in more detail.

1.5.1 Molecular biology of opioid neuropeptides

The opioid peptides show great diversity, deriving from three separate multifunctional precursors (Bloom, 1983; Costa *et al.*, 1987). These precursors show a 60-80% structural homology both at the genomic and protein precursor level, suggesting a common ancestral gene. The three genes: pro-opiomelanocortin; pre-proenkephalin-A (proenkephalin); and pre-proenkephalin-B (prodynorphin) have been identified and cloned from several species.

Pro-opiomelanocortin has been cloned and sequenced from brain tissue of bovine (Nakanishi *et al.*, 1979), rat (Drouin *et al.*, 1985), and mouse (Uhler *et al.*, 1983). Pre-proenkephalin-A (proenkephalin) has been cloned and sequenced from brain tissue of human (Comb *et al.*, 1982), bovine (Noda *et al.*, 1982), rat (Howells *et al.*, 1984) and mouse (Zurawski *et al.*, 1986). Pre-proenkephalin-B (prodynorphin) has been cloned and sequenced from brain tissue from human (Horikawa *et al.*, 1983), porcine (Kakidani *et al.*, 1982) and rat (Douglass *et al.*, 1989).

Pro-opiomelanocortin is the precursor of β -endorphin, adrenocorticotrophic hormone (ACTH), α -, β -, and γ -melanocyte-stimulating hormone (MSH) and corticotrophin (Nakanishi *et al.*, 1979). Pro-opiomelanocortin and the peptides derived from it are found mainly in the pituitary gland and hypothalamus. β -endorphin is probably the most studied opioid peptide, with the structure being highly-conserved in all mammalian species.

Pre-proenkephalin-A in higher species contains six copies of methionine-enkephalin and one copy of leucine-enkephalin, where the terminal methionine is replaced by a leucine. Two of the pentapeptide methionine-enkephalins are extended to form the heptapeptide methionine-enkephalin-Arg⁶-Phe⁷ and the octapeptide methionine-enkephalin-Arg⁶-Glu⁷-Leu⁸ (Pittius *et al.*, 1983; Zamir *et al.*, 1984a; Beaumont *et al.*, 1985; White *et al.*, 1986; Schiller *et al.*, 1995).

Pre-proenkephalin-B has three copies of leucine-enkephalin which are the starting sequence for the extended dynorphins (dynorphin A₁₋₁₇ and B₁₋₁₃) and α -neoendorphin. These longer peptides are metabolically more stable within the brain and have a different receptor profile than the enkephalins. The enkephalin pentapeptides represent the minimum-sized fragments with opioid activity. Both dynorphin A and B can be further processed by proteolytic cleavage into the smaller fragment

dynorphin A₁₋₈ and several enkephalin pentapeptides (Seizinger *et al.*, 1984; Breslin *et al.*, 1993; Dupuy *et al.*, 1994; Berman *et al.*, 1995).

The mechanism by which enkephalin and dynorphin are regulated has been studied extensively utilising the striatum as a model system. It has been known for some time that dopamine, via the two main dopamine receptor subtypes, i.e. the D1 dopamine receptor and D2 dopamine receptor, plays a pivotal role in the regulation of opioid peptides within the striatum. Following chronic dopamine receptor blockade by haloperidol, an increase in pre-proenkephalin-A is observed. This has been shown to be blocked by co-administration of dopamine D2 receptor agonists (Le Moline *et al.*, 1990). This increase in pre-proenkephalin has also been demonstrated following repeated D2 dopamine receptor antagonist administration but not a D1 dopamine receptor antagonist (Jiang *et al.*, 1990).

Cell culture studies utilising primary striatal cells, have shown that the application of dopamine to these cells reduces the levels of enkephalin precursor mRNA (Weiss *et al.*, 1985). These studies suggest that pre-proenkephalin-A expression and synthesis is under the control of dopamine D2 receptors and is tonically inhibited by dopamine D2 activation.

Therefore, reduced D2 dopamine receptor activation by direct dopamine D2 receptor antagonism leads to an increase in pre-proenkephalin-A synthesis. This increase in enkephalin synthesis is probably mediated through cAMP. The 5'-flanking region of pre-proenkephalin-A contains two cAMP and phorbol ester response elements termed ENKCRE-1 and ENKCRE-2. These bind distinct trans-acting factors (Comb *et al.*, 1986, 1988). Both pre-proenkephalin-A and pre-proenkephalin-B contain immediate early gene recognition sites or enhancer elements within the 5'-flanking regions of their genes. c-Fos and c-Jun can bind to this region of pre-proenkephalin-A and stimulate transcription (Sonnenberg *et al.*, 1989).

The dynorphin precursor contains a promoter similar to cAMP response element-like (CRE) or AP-1-like site termed DYNCRE3 in the 5'-flanking region of the pre-proenkephalin-B gene. DYNCRE3 is similar to the ENKCRE-2 promoter site on pre-proenkephalin-A (Messersmith *et al.*, 1996). These can mediate transcriptional responses to both cAMP and phorbol esters, via binding of both AP-1- and CREB-like proteins (Douglass *et al.*, 1994; Messersmith *et al.*, 1994). Via these mechanisms

transcriptional control of both pre-proenkephalin-A and pre-proenkephalin-B expression is regulated.

1.5.2 Structure of opioid peptides

As described above, the opioid peptides are small peptides containing 5-17 amino acids which are proteolytically cleaved from larger precursors. This proteolytic cleavage produces smaller fragments with maintained activity (Holt, 1986). These proteolytic enzymes are co-packaged with the peptide precursors in the Golgi apparatus. This mechanism allows the cell a further level of modulatory control, thus by a post-transcriptional method the amount of peptides stored and released is regulated. For example the dynorphin family of peptides can be transformed into both smaller fragments of dynorphin and enkephalins by dynorphin-converting enzymes (Zamir *et al.*, 1984b). As will be seen below this differential transformation obviously effects the type of receptor activated by the products of a given precursor. The release dynamics of such proteolytic cleavage steps remain to be elucidated.

Following release, the opioid peptides are degraded by several enzymes (Nyberg and Terenius, 1991). Ubiquitously distributed, these aminopeptidases inactivate the peptides by removing their N-terminal tyrosine. Carboxy- or endopeptidases are also important in the control of opioid peptide function. Neutral endopeptidase 24.11 or enkephalinase, is the endopeptidase which inactivates enkephalins. To date, three neutral endopeptidases 24.11 have been cloned from human, suggesting these endopeptidases are more specific than once thought (Kenny *et al.*, 1986).

Blockade of endopeptidase 24.11 activity, in otherwise drug-naïve animals, increases enkephalin levels and induces opioid tolerance (Roques and Nobel, 1995). Similarly, the novel enkephalinase inhibitor, SCH 32615, has been shown to modulate the effects of predominantly, dopamine D2 receptors. SCH 32615 was shown to decrease both dopamine D1 and D2 receptor antagonist-induced catalepsy, while it increased dopamine D2 receptor agonist-induced stereotypies (Marin and Chase, 1995). These studies suggest that endopeptidase degradation is an important mechanism in the control of opioid peptide activity and that alterations in enkephalinergic and dynorphinergic transmission may dramatically effect a vast array of behavioural function.

1.5.3 Opioid neuropeptide receptors

It was first hypothesised in 1954, by Beckett *et al.*, that different opioid receptors with various binding sites may exist. Martin in 1967 proposed the existence of multiple types of opioid receptors. Three subtypes of opioid receptors were suggested: mu; kappa; and delta. This was based on the interaction of morphine and nalorphine, together with structure-activity studies of Portoghese (1965).

Since the discovery of opioid receptors in 1973 (Pert and Snyder, 1973), it has proved difficult to elucidate the number and anatomical distribution of different subtypes of receptors. Recently, molecular cloning, *in situ* hybridisation, and radiolabelling studies have permitted the isolation and location of the three major opioid receptor types, mu, kappa and delta opioid receptors (Lord *et al.*, 1977; Goldstein and Naidu, 1989). The three opioid receptors are present on different chromosomes in both mouse and human. In the human, the gene encoding the kappa opioid receptor is located on the proximal long arm of chromosome 8, the delta opioid receptor to the distal part of the short arm of chromosome 1 and the mu opioid receptor to the distal part of the long arm of chromosome 6 (Miotto *et al.*, 1995). All of the opioid receptor genes contain introns, suggesting the possibility that several alternatively-spliced variants of each receptor may exist (Bare *et al.*, 1994; Min *et al.*, 1994). Alternatively-spliced variants of opioid receptors have been shown to be preferentially localised in anatomically-distinct regions (Mansour *et al.*, 1994, 1995).

The opioid peptides, at high concentrations, do not show complete selectivity for a single receptor. However, they do show preferential selectivity towards a specific receptor and it is thought that at physiological concentrations selectivity for receptors is shown (Wuster, 1979). Enkephalin has been shown to interact with delta receptors with high specificity (Lord *et al.*, 1977; Goldstein and Naidu, 1989). However, enkephalin also interacts with mu receptors at higher concentrations. Dynorphin shows high affinity for the kappa receptor and has been shown to be the endogenous ligand for this receptor (Lord *et al.*, 1977; Chavkin *et al.*, 1982; Corbett *et al.*, 1982). β -endorphin has been shown to be the endogenous ligand for the mu opioid receptor (Lord *et al.*, 1977; Goldstein and Naidu, 1989). Within the three types of opioid receptors there are various receptor subtypes. It was first recognised that several subtypes may exist, when autoradiographic studies utilising various ligands resulted in differing distributions.

Autoradiographic binding studies utilising the specific kappa receptor agonist U50 488H identified the kappa₁ receptor (Kosterlitz *et al.*, 1981). Utilising various antagonists, kappa₂ receptors were identified in 1988 (Zukin *et al.*, 1988). However, the pharmacology of kappa₂ receptors remains largely unresolved. Kappa₃ receptors have been well characterised pharmacologically and in binding studies, and are present in high concentrations within the brain (Clark *et al.*, 1989; Kinouchi and Pasternak, 1991; Cheng *et al.*, 1992).

Binding studies using both enkephalin analogues and morphine identified the mu opioid receptor subtypes. It was demonstrated that when both morphine and enkephalin binding were carried out, more receptors labelled than with morphine alone (Pasternak and Wood, 1986). These were classified mu₁ (morphine and enkephalin binding) and mu₂ (morphine binding alone).

Similarly, pharmacological evidence suggests that there are at least two subtypes of the delta receptor, delta₁ and delta₂ delineated on the basis of interactions with both agonists and antagonists. Thus delta₁ is defined as the site sensitive to antagonism by [D-Ala²,Leu⁵,Cys⁶]enkephalin (DALCE) and activated by [D-Pen²,D-Pen⁵]enkephalin (DPDPE), while the delta₂ site was sensitive to antagonism by naltrindole 5'-isothiocyanate (5'-NTTII) and activated by [D-ALA²-Glu⁴]deltorphan (Mattia *et al.*, 1991). It remains unknown whether these different subtypes arise due post-transcriptional modification or whether they are different gene products. In addition to the differences in pharmacology there are localisation and functional differences between the subtypes (Mansour *et al.*, 1995).

Opioid receptor-like receptors

Recently, a novel opioid receptor was cloned which shares 65% structural homology to the other classical opioid receptors. The seven-transmembrane regions and features common to G protein-linked receptors negatively-linked to adenylyl cyclase, are the most homologous regions. However, this novel receptor does not bind classical opioid ligands. The receptor, termed the orphanin receptor (ORL1), was cloned from rat (Bunzow *et al.*, 1994), mouse (Nishi *et al.*, 1994), and human brain (Mollereau *et al.*, 1994). Homology data suggests that the orphanin receptor may in fact be a splice variant of the kappa₃ receptor (Bunzow *et al.*, 1994; Mollereau *et al.*, 1994).

Recently, an endogenous ligand for the orphanin receptor was cloned from porcine hypothalamus (Reinscheid *et al.*, 1995) and rat brain (Meunier *et al.*, 1995). This novel pentapeptide has been termed orphanin-FQ or nociceptin (Meunier *et al.*, 1995; Reinscheid *et al.*, 1995). Nociceptin has a sequence that closely resembles dynorphin A. In transfected cells, nociceptin binds orphanin with high affinity and inhibits forskolin-stimulated adenylyl cyclase (Meunier *et al.*, 1995; Reinscheid *et al.*, 1995). *In vivo*, intraventricular administration of nociceptin has been shown to induce hypolocomotion (Reinscheid *et al.*, 1995) and hyperalgesia (Reinscheid *et al.*, 1995). Using *in situ* hybridisation studies, orphanin has been shown to be distributed in limbic and hypothalamic structures (Bunzow *et al.* 1994; Mollereau *et al.*, 1994). Due to its localisation, nociceptin has been proposed to be implicated in emotional and motivational functions.

Three further, non-classical, opioid receptors have been identified termed epsilon, sigma and zeta opioid receptors.

Epsilon opioid receptors are labelled by β -endorphin in rat vas deferens tissue. These receptors are tolerant to the effects of mu, kappa and delta receptor agonists but retain a response to β -endorphin (Wuster *et al.*, 1979). These receptors have been cloned and functionally-expressed in *Xenopus* oocytes. Their expression in the adult brain remains controversial and they have very low affinity for morphine.

Sigma opioid receptors respond to benzomorphans (compounds lacking the carbon ring present in morphine e.g. MR 2034, bremazosin), in an opioid receptor-like manner, although these effects are not blocked by high concentrations of naloxone (Stringer *et al.*, 1983), which has led to them being defined as non-opioid receptors. They contain a high affinity binding site for phencyclidine and related compounds. Classically, opioid receptors are stereo-selective for (-)-isomers of opioid receptor agonists and antagonists, whereas sigma receptors are stereo-selective for the corresponding (+)-isomers.

Zeta opioid receptors are present during development but are not expressed in the adult brain (Zagon *et al.*, 1992). Therefore they are thought to be involved in the development of the nervous system (Zagon *et al.*, 1992). Zeta opioid receptors interact with methionine-enkephalin, the proposed opioid growth factor, and is thought to serve as an inhibitory influence on the developing nervous system (Zagon *et al.*, 1989).

1.5.4 Functional significance of opioid receptor stimulation

The recent cloning of the opioid receptors suggests that they are members of the superfamily of seven transmembrane G-protein-coupled receptors. The mu, delta, and kappa receptors are homologous to one another (65-70%) at both the nucleic acid and amino acid level, and are highly conserved in the regions of the transmembrane spanning domains and intracellular loops. Mu, delta and kappa opioid receptors are most divergent in the extracellular domain which may be important for the functional differences of the receptors and their selectivity for particular ligands.

All three cloned receptors have been expressed in cell lines and their pharmacological properties investigated. Most neuronal cells respond to direct application of opioids by hyperpolarisation, a decrease in cell firing and a reduction in transmitter release (Werz *et al.*, 1984; Cohen *et al.*, 1992).

Transfection studies indicate that mu, kappa and delta receptors are negatively coupled to adenylyl cyclase via Gi i.e. all three receptors inhibit cAMP formation (Chen *et al.* 1993; Izenwasser *et al.*, 1993). All three receptors have been found to couple indirectly (either via cAMP and protein kinase C or via phospholipase C, arachidonic acid and phospholipase A2/5) to K⁺ channels (Alrgja *et al.*, 1993; Avidoe-Reiss *et al.*, 1995; Tsu *et al.*, 1995; Ueda *et al.*, 1995a, 1995b; Fukuda *et al.*, 1996; Murthy and Makhoulf, 1996; Smart and Lambert, 1996). Activation results in an outward K⁺ current and hence hyperpolarisation at resting membrane potentials (Williams *et al.*, 1982).

Kappa receptors are thought to interact with voltage-dependent Ca²⁺ channels and may be directly coupled to them (Werz *et al.*, 1983). Activation of kappa receptors depresses calcium entry, thereby reducing neurotransmitter release. The coupling of the kappa receptors to adenylyl cyclase and ionic conductance channels are thought to involve Gi and/or Go.

Utilising the sequence data from the cloned opioid receptors, together with radioligand binding studies, a detailed picture of the various opioid neuropeptide circuits within the brain can now be built up. Once these have been established their involvement in both clinically-normal and pathological conditions can be investigated.

1.5.5 Peptide neurotransmission

As already noted, the first indication that there was an endogenous opioid-like substance with a receptor resulted from studies on pain, with the fact that the effects of morphine could be blocked by naloxone (Martin, 1967).

Peptidergic neurotransmission is similar to that of classical transmitters in that peptides are synthesised and packaged into vesicles and are released from the nerve terminal via a calcium-dependent manner (Verhage *et al.* 1992).

However, there are two major differences between classical neurotransmitters and peptides. The first is that classical neurotransmitters are localised in small clear vesicles located near the plasma membrane of the nerve terminal, whereas peptides are located in dense vesicles containing both peptide and classical neurotransmitter (Lundberg *et al.*, 1982; Fried *et al.*, 1985; Matteoli *et al.* 1988). The majority of these vesicles are located further from the plasma membrane of the nerve terminal. This implies a further level of modulation. It has been demonstrated that following low frequency depolarisation only classical neurotransmitter is released. However, following rapid high-frequency stimulation both peptide and classical neurotransmitter are released. This has led to the suggestion that high frequency stimulation may be required to activate peptide-containing vesicles (Lundberg *et al.*, 1982; Iverfeldt *et al.*, 1989; Whim *et al.*, 1989; Bean *et al.*, 1991).

The second major difference that is apparent between classical neurotransmitters and peptides, is in their mode of inactivation following release. Most classical neurotransmitters have re-uptake sites, or transporters, located on the nerve terminals or adjacent glia. These transporters actively transport the transmitter back into the nerve terminal and repackage the transmitter into vesicles, ready to be re-released following depolarisation. In contrast, peptides are not actively reuptaken by transporters but are degraded within the synapse by endopeptidases, or removed from the synapse via diffusion. Due to the lack of active transport and re-uptake of peptides, it has been suggested that opioid peptides may act like local hormones, i.e. provide an action at a distant site from the site of release (Duggan *et al.*, 1990; Fuxe and Agnati, 1991).

One other difference between classical neurotransmission and peptide transmission is the action that they have on post-synaptic cells. In general, classical neurotransmitters exert a rapid short-acting local response, whereas peptide responses

are generally of longer duration and take place over a wider area than just the synapse. Some authors have suggested that peptide release does not take place at the nerve terminal but at an extrasynaptic area (Golding and Bayraktaroglu, 1984; Thureson-Klien and Klein, 1990).

1.5.6 Opioid peptide modulation of neurotransmission within the basal ganglia

Many studies have demonstrated the modulatory roles that opioid peptides can play on 'classical' neurotransmitter systems. This has led to the hypothesis that one function of the opioid peptides, and indeed co-transmission itself, is as a regulatory mechanism to modulate 'classical' neurotransmission. This will now be considered in more detail with relevance to the basal ganglia.

Within the basal ganglia, a high degree of opioid peptide co-transmission exists. Many studies have now confirmed that 'classical transmitters' such as glutamate and GABA can be modulated by the action of opioid neuropeptides both within the basal ganglia and other brain regions. Two early studies demonstrated that dynorphin, via activation of kappa receptors, could inhibit synaptic transmission in hippocampal mossy fibre long-term potentiation studies (Gannon and Terrian, 1991a, 1991b; Wagner *et al.*, 1993; Weisskopf *et al.*, 1993a, 1993b).

Kappa opioid receptors within the basal ganglia

Dynorphin, the endogenous ligand for the kappa opioid receptor, is present in large amounts in the SNpr of the rat, and to a lesser extent, the primate (Zamir *et al.* 1985; Gerfen, 1988). These data led to the suggestion that opioid peptides may be involved in the control of dopamine release within the basal ganglia. There have been many investigations into the role of kappa opioid receptor stimulation in the control of dopamine release within the striatum. Receptor-radioligand binding studies have demonstrated kappa opioid receptors to be localised within the striatum. *In situ* hybridisation studies have localised the kappa opioid receptor mRNA to the SNpc (Mansour *et al.*, 1994). A proportion of kappa opioid receptor binding seen in the striatum, is subsequently lost following a 6-OHDA lesion of the SNpc, thus some of the

kappa opioid receptors seen in the striatum are present on pre-synaptic terminals of the nigrostriatal pathway (Smith *et al.*, 1993).

Several studies have investigated the role of kappa opioid receptors on dopamine release within the striatum. Utilising striatal slice preparations and measuring the release of [³H] dopamine, kappa opioid receptor agonists have been shown to reduce dopamine release (Mulder *et al.*, 1984; Gauchy *et al.*, 1991). Similarly, several *in vivo* microdialysis studies have demonstrated a reduction in dopamine release following intrastriatal or intracumbal administration of kappa opioid receptor agonists (Herrera-Marschitz *et al.*, 1986; Di Chiara and Imperato, 1988; Reid *et al.*, 1988; Spanagel *et al.*, 1990, 1992). Systemic administration of kappa opioid receptor agonists has been shown to decrease both spontaneous locomotion and the release of mesolimbic dopamine in the nucleus accumbens (Di Chiara and Imperato, 1988).

Several studies have demonstrated that intranigral administration of kappa opioid receptor agonists can induce behavioural responses, in locomotion (expressed as a rotational response), exploratory behaviour, sniffing, and rearing behaviour (Herrera-Marschitz *et al.*, 1983, 1984). However, this effect is independent of the striatonigral dopaminergic system, and in fact the response is enhanced following a 6-OHDA-lesion (Matsumoto *et al.*, 1988a, 1988b). This suggests that the locomotor response to kappa opioid receptor stimulation is in fact dopamine-independent and must be causing these observed effects through another mechanism.

Recently, it has been shown that kappa opioid receptor agonists can inhibit glutamate release both in substantia nigra pars reticulata slices (Maneuf *et al.*, 1995) and in a synaptosomal preparation from both rat and primate striatum (Hill and Brotchie, 1995; Hill *et al.*, 1996). This evidence suggests that kappa opioid receptor agonist induced reduction in glutamate release is mediated through pre-synaptic kappa opioid receptors on corticostriatal efferents.

It has been reported that in the human brain the subthalamic nucleus contains one of the highest levels of kappa opioid receptor mRNA (Zhu *et al.*, 1995). Furthermore, it has been demonstrated that stimulation of kappa opioid receptors can reduce excitatory amino acid release in regions of the basal ganglia receiving input from the subthalamic nucleus (Maneuf *et al.*, 1995). Due to the pivotal role the subthalamic nucleus plays in the control of movement (see section 1.1.3), coupled with the evidence

that kappa opioid receptor activation can modulate glutamate release, changes in opioid expression may have major consequences for the functioning of the basal ganglia.

Delta opioid receptors within the basal ganglia

The concentration of methionine-enkephalin in the lateral globus pallidus is highest in both the rodent and primate brain (Emson *et al.* 1980; Zamir *et al.* 1985). In contrast to kappa opioid receptors, delta opioid receptor agonists have been shown to both increase spontaneous locomotion, and mesolimbic dopamine concentration when injected into the nucleus accumbens of rats (Di Chiara and Imperato, 1988). However, direct application of delta agonists to SNpc neurons has no effect on the firing rate of the cells (Collingridge and Davis, 1982; Homer and Pert, 1983). In a similar manner to kappa opioid receptor agonists, delta opioid receptor agonists injected into the SNpc also cause a contraversive circling response. However, unlike the kappa opioid-mediated effect, following dopamine-depletion following a 6-OHDA-lesion, the delta opioid receptor effect is markedly reduced. This suggests the delta opioid receptor effect on behaviour is mediated by dopaminergic cells within the SNpc (Matsumoto *et al.*, 1988a).

It has been demonstrated that enkephalin activation of delta opioid receptors can block GABA inhibition in hippocampal neurons (Cohen *et al.*, 1992) and more recently that enkephalin reduces GABA release, via activation of opioid receptors in the globus pallidus of the rat (Maneuf *et al.*, 1994, 1995).

Delta opioid receptors have been shown to be highly expressed on the efferent terminals from the striatum to the globus pallidus (Mansour *et al.*, 1995). These GABAergic efferents co-express enkephalin. Thus, alterations in enkephalinergic transmission may alter GABA release within the globus pallidus, ultimately this would have important consequences for the control of movement.

Mu opioid receptors within the basal ganglia

Mu opioid receptors are found at high concentration within the basal ganglia and are activated by both β -endorphin and, at higher concentrations, enkephalin (Lord *et al.*, 1977). Mu opioid receptors are found in especially high abundance within the

striosomes of the neostriatum (see section 1.1.1, Graybiel 1986; Mansour 1995). In contrast to kappa, but similar to delta, mu opioid receptors stimulate striatal dopamine release following either systemic administration or following intranigral administration (Homer and Pert, 1983; Walker *et al.*, 1987; Di Chiara and Imprato, 1988). A proportion of mu receptors are lost following 6-OHDA-lesion of the dopamine containing cells of the SNpc (Smith *et al.*, 1993), and when injected directly into the nigra, in a similar manner to the delta opioid agonists, cause contraversive rotational behaviour that is subsequently lost following 6-OHDA-lesion, suggesting a dopamine-mediated effect (Matsumoto *et al.*, 1988).

Therefore, in summary, from the evidence to date, enkephalin and dynorphin can produce a marked modulatory effect on other neurotransmitters. Therefore, it is apparent that any alterations in these opioid neuropeptides may have substantial consequences for the functioning of the basal ganglia and effect the control of voluntary movement.

1.6 Opioid peptide alterations in dopamine-depleted animals and parkinsonian patients

Pre-proenkephalin-A expression and enkephalin peptide levels following dopamine denervation

Many studies have investigated the effects of dopamine depletion on striatal opioid neuropeptides. The earliest of these studies were carried out in rodents chronically treated with neuroleptics. In such studies, it was demonstrated that following 21 day haloperidol treatment, there was an increase in methionine-enkephalin levels in the striatum (Hong *et al.*, 1980) with later studies confirming similar increases in pre-proenkephalin-A (PPE-A) mRNA expression (Tang *et al.*, 1983; Jaber *et al.*, 1994).

Following further investigation, it became clear that this neuroleptic-induced increase in enkephalin synthesis was due to dopamine D2 receptor blockade, as both typical and atypical neuroleptics, lacking D1 receptor antagonism, also elevated enkephalin synthesis (Angulo *et al.*, 1987).

Following the delineation of the pivotal role of dopamine D2 receptors in the control of enkephalin synthesis, it was proposed that these changes in enkephalin

synthesis may also take place following dopamine depletion in pathological conditions such as Parkinson's disease. Therefore, investigation of enkephalin levels in both animal models of Parkinson's disease and in human parkinsonian *post-mortem* brain tissue were performed.

It was found that lesioning the dopaminergic substantia nigra pars compacta cells with the neurotoxin 6-hydroxydopamine in rodents (Angulo *et al.*, 1986; Voorn *et al.*, 1987) or by catecholamine depletion via systemic administration of reserpine (Jaber *et al.*, 1992; Jaber *et al.*, 1995) increased the levels of both PPE-A mRNA and enkephalin peptide levels.

The development of more specific D1 and D2 dopamine receptor antagonists allowed a clearer understanding of the involvement of the both the D1 and D2 dopamine receptor subtypes in the control of enkephalin synthesis.

In all studies it was found that D2 dopamine receptor antagonists produced an increase in enkephalin synthesis (Mocchetti *et al.*, 1987; Morris *et al.*, 1989; Angulo *et al.*, 1992; Jaber *et al.*, 1994). The results from studies involving D1 antagonists have been inconclusive (Mocchetti *et al.*, 1987; Morris *et al.*, 1988; Caboche *et al.*, 1991), possibly due to dosage, routes of administration and different drugs used. Therefore, it is still unclear whether the dopamine D1 receptor may in some way modulate the influence of dopamine D2 receptor antagonists on enkephalin synthesis. In contrast to the antagonist, dopamine D2 agonists (quinpirole) have been shown to decrease levels of enkephalin (Angulo *et al.*, 1992). However, it is still not clear whether the D1 modulatory effect of D2 regulation of enkephalin synthesis is through a direct mechanism or an indirect mechanism via interneurons.

To investigate whether enkephalin synthesis was altered in animal models of Parkinson's disease, initial studies were carried out 2 weeks following a 6-OHDA-lesion of the SNpc in rat. These studies demonstrated that PPE-A mRNA expression was significantly increased in the striatum (Young *et al.*, 1986). Several such studies utilising both Northern blot hybridisation (Jaber *et al.*, 1994), *in situ* hybridisation (Gerfen *et al.*, 1991; Jaber *et al.*, 1995) and by measuring enkephalin peptide levels via either high-performance liquid chromatography (HPLC) (Taylor *et al.*, 1992) or radioimmunoassay (Engber *et al.*, 1991), have confirmed such an increase in enkephalin synthesis within the striatum or efferent projection sites following dopamine-denervation via lesion of the SNpc.

Studies using human *post-mortem* tissue comparing control and parkinsonian brains has been less conclusive. De Ceballos *et al.* (1993) showed using both HPLC and radioimmunoassay, that although all patients had a dopamine-deficiency within the whole neostriatum (>90% compared to controls), when the caudate nucleus was considered alone, two subgroups were evident, patients with a dopamine deficiency of greater than 80% within the caudate, and patients with a dopamine deficiency of approximately 50% within the caudate nucleus. In the patients with a 80% decrease in dopamine concentrations within the caudate there was an 3 fold increase in enkephalin peptide levels seen in the medial segment of the globus pallidus. However, in patients with approximately a 50% decrease in dopamine levels within the caudate nucleus there was a decrease in enkephalin peptide levels in the medial segment of the globus pallidus.

In studying the mRNA levels from control and parkinsonian human *post-mortem* brains, Nisbet *et al.* (1995) observed a 109% increase in PPE-A expression levels in the caudate and a 55% increase in the putamen of parkinsonian brains. However, in contrast, Levy *et al.* (1995b) showed no significant difference in mRNA levels encoding PPE-A between control and parkinsonian brains. However, this sample size was considerably smaller than the previous studies carried out by De Ceballos *et al.* (1993) and Nisbet *et al.* (1995).

Changes in both mRNA expression for PPE-A and enkephalin peptide levels have been further investigated in the MPTP-treated non-human primate model of Parkinson's disease.

The first of such studies were carried out in MPTP-treated non-human primate brains (1-5 months following the last administration of MPTP). Utilising radioimmunoassay, the peptide levels of methionine-enkephalin, substance P, and dynorphin were measured from various brain regions (Zamir *et al.*, 1984). This study demonstrated that following MPTP administration (0.35 mg kg^{-1} i.v. for 5 days) there was a decrease in striatal methionine-enkephalin. However, in the globus pallidus there was an increase in all opioid peptides. Similarly, pre-proenkephalin-A mRNA levels have been shown to increase in both the hemi-parkinsonian MPTP-treated non-human primate (*Macacca fascicularis*, Augood *et al.*, 1989; Frayne *et al.*, 1991) and by 40-190% in the MPTP-treated squirrel monkey (*saimiri sciureus*, Asselin *et al.*, 1994).

More recently, in a study utilising the common marmoset (*Cathithrix jacchus*) there was a 60-65% increase in PPE-A mRNA expression in the rostral striatum in marmosets chronically-treated with MPTP (sacrificed 7 days after the last MPTP injection). This increased level of PPE-A expression decreases to 30-50% if the marmosets are allowed to recover for 18 months following the last MPTP administration (Jolkkonen *et al.*, 1995a). Similarly, in the cynomolgus (*macacca fascicularis*) non-human primate, severely parkinsonian animals were sacrificed 3 months following the final MPTP injection, PPE-A expression was increased by 40-50% in the rostral striatum (Herrero *et al.*, 1995).

Following dopamine depletion in lesioned animal models, this enkephalin increase can be modulated by various non-dopaminergic agents.

It has been demonstrated that an intact corticostriatal pathway i.e. excitation via glutamatergic pathway is required for the increase in enkephalin synthesis to be maintained. Several studies have shown that physical deafferentation via a knife cut of the corticostriatal pathway, decortication or via pharmacological intervention using NMDA receptor antagonists (Uhl *et al.*, 1988; Somers and Beckstead, 1992; Campbell and Bjorklund, 1994; Angulo *et al.*, 1995; Hajji *et al.*, 1996) reduces a 6-OHDA-lesion-induced increase in enkephalin synthesis. This suggests that striatal cells require not only to be released from the tonic inhibition of dopamine, acting via dopamine D2 receptors, but also require excitation via NMDA receptors from the corticostriatal pathway to maintain the elevated enkephalin synthesis.

In a similar manner, anti-cholinergics have also been shown to attenuate the 6-OHDA-lesion-induced increase in enkephalin synthesis (Pollack and Wooten, 1992). It is presumed that this action is mediated via the giant aspiny interneurons as these axons arborise densely throughout the striatum. The modulatory actions of acetylcholine suggest that the actions of dopamine on enkephalin expression are positively-modulated by cholinergic neurons.

Recently, it has been demonstrated that bilateral SNpc destruction by 6-OHDA in the rat does not produce the elevated pre-proenkephalin-A increase seen in all areas of the striatum following unilateral SNpc destruction (Salin *et al.*, 1996). However, a dorsolateral strip of cells within the striatum does show a significant increase above controls. The authors suggest that a complex interhemispheric adaptive process may take place in the unilateral model. However, in this study the ventral tegmental area and

retrotrubral areas remained intact. Since the sensorimotor regions of the striatum, the area which receives the dopaminergic projection from the substantia nigra pars compacta, shows a similar increase in PPE-A expression seen in the unilateral lesioned animal, it is tempting to speculate that the intact VTA and retrotrubral areas may account for the lack of PPE-A increase seen in the bilateral model. However, since both MPTP-treated non-human primate models and human *post-mortem* studies show increased enkephalin precursor expression, this study may suggest that alterations in the bilateral lesioned rat are not as widespread as in the primate. This coupled with the intact VTA and retrotrubral areas may account for the differences observed.

Pre-proenkephalin-B expression and dynorphin peptide levels following dopamine denervation

In contrast to enkephalin which is tonically inhibited by dopamine, dynorphin synthesis is tonically stimulated by dopamine. This has been substantiated, in a similar manner to enkephalin, by both pharmacological and lesion studies.

Daily injections of the dopamine receptor agonist apomorphine in clinically-normal rats, increased dynorphin levels in the striatum in a dose-dependent manner. This increase was blocked by co-administration of a dopamine D1 receptor antagonist (Li *et al.*, 1986). Similar increases are also seen in PPE-B mRNA levels within the striatum (Li *et al.*, 1988). It has also been shown that increasing dopamine concentrations via d-amphetamine administration results in increased PPE-B expression (Li *et al.* 1986; Li *et al.* 1988). Utilising more selective dopamine receptor subtype antagonists it has been demonstrated that the dopamine D1 receptor subtype antagonist SCH 23390 can block the d-amphetamine increase in PPE-B, suggesting that the D1 dopamine receptor has a much greater effect on the regulation of dynorphin synthesis than the D2 receptor (Angulo *et al.* 1992).

In contrast with enkephalin, all studies in rodent models of Parkinson's disease have shown a decrease in both PPE-B mRNA expression and peptide levels (Li *et al.*, 1988; Jiang *et al.*, 1990; Li *et al.*, 1990; Gerfen *et al.*, 1991).

Only one study to date has investigated dynorphin levels in parkinsonian *post-mortem* brains using the radioimmunoassay method (Zamir *et al.*, 1984). This study showed a decrease in dynorphin B peptide levels in both the caudate, putamen and the

SNpr, similar to the changes seen in the rat model. However, this study has not been confirmed. To date, the only study to investigate dynorphin precursor expression (PPE-B) in the MPTP-treated non-human primate also suggests a 10-15% decrease in the levels of expression throughout the neostriatum (Parent *et al.*, 1996).

1.7 Opioid peptide alterations following dopamine receptor stimulation in dopamine-depleted animals and parkinsonian patients

As previously described, following dopamine denervation in animal models of Parkinson's disease, several alterations take place which requires both dopamine-depletion coupled with glutamatergic and acetylcholine innervation. However, when dopamine is replaced in such models the elevation in enkephalin and reduction in dynorphin is not simply reversed, but undergoes further alteration.

Pre-proenkephalin-A expresion and enkephalin levels following dopamine receptor stimulation following dopamine depletion

Increased enkephalin expression following dopamine denervation can be differentially modulated by dopamine receptor agonists depending on the mode of administration.

Continuous treatment of the 6-OHDA-lesioned rat, via an osmotic minipump, with the dopamine D2 receptor agonist quinpirole (for 21 days), reduces PPE-A expression to control values. However, intermittent treatment (i.e. single daily injections for 21 days) with the same agonist, causes PPE-A levels to remain elevated (Gerfen *et al.*, 1990). A differing pattern of enkephalin change following either continuous infusion or intermittent administration has been shown for L-DOPA administration. In these studies, enkephalin peptide levels in the globus pallidus of the 6-OHDA-lesion rat were measured, four weeks postoperatively followed by 21 day L-DOPA treatment (either as a continuous infusion 100 mg kg⁻¹ per day, or intermittent i.e. two 50 mg kg⁻¹ injections per day). This study show that enkephalin peptide levels remain elevated in the intermittently-treated group and were further, significantly, increased in the continuously-infused group (Engber *et al.*, 1991).

It is difficult to extrapolate from any studies carried out on *post-mortem* parkinsonian brains with regards peptide changes following dopamine replacement for several reasons. Most patients will have been treated for several years with various dopamine precursors or receptor agonists, and it is difficult to normalise patients with regards to both treatment regimes and long-term treatment complications. Coupled with the fact that no parkinsonian 'untreated' groups are generally available, it is hard to draw any conclusions with regards to dopamine-replacement from human *post-mortem* studies.

However, in the MPTP-treated non-human primate this question may be better addressed. Two recent studies have evaluated the levels of enkephalin following dopamine replacement. In an MPTP-treated marmoset study, PPE-A expression levels following L-DOPA treatment (12.5 mg kg^{-1} twice daily for four weeks) were unchanged from the MPTP-treated alone (Jolkkonen *et al.*, 1995).

In an MPTP-treated macaque study, 4 months treatment with 50 mg kg^{-1} oral L-DOPA, showed a slight, non-significant, reduction in PPE-A mRNA expression compared with the severely parkinsonian MPTP-treated primates. However, these macaques had been parkinsonian for four months longer than the MPTP-treated group and this may account for some of the decrease in enkephalin observed (Herrero *et al.*, 1995). These findings contradict earlier observations by Frayne *et al.* (1991) which demonstrated that in the hemi-parkinsonian MPTP-treated non-human primate, following repeated apomorphine treatment with the development of peak-dose dystonia, further increases in PPE-A expression were observed on the parkinsonian side.

Pre-proenkephalin-B expression and dynorphin levels following dopamine receptor stimulation following dopamine depletion

As previously discussed in section 1.6, following dopamine denervation in rodent models of Parkinson's disease both PPE-B mRNA expression and dynorphin peptide levels are decreased. However, when dopamine is replaced in such models, the decrease in dynorphin is not simply reversed but undergoes a massive upregulation (Li *et al.*, 1988; Gerfen *et al.*, 1990; Jiang *et al.*, 1990; Li *et al.*, 1990; Engber *et al.*, 1991).

This upregulation of dynorphin synthesis, in similar manner to enkephalin, can be differentially modulated by dopamine receptor agonists depending on the mode of administration.

Intermittent treatment (i.e. single daily injections for 21 days) with a dopamine D1 receptor agonist (SKF 38393) for 21 days increases the levels of PPE-B mRNA. This contrasts with continuous treatment via an osmotic minipump with the same agonist (for 21 days), where PPE-B levels were unchanged from the lesion alone values (Gerfen *et al.*, 1990).

A differing pattern of dynorphin change following either continuous infusion or intermittent administration has also been shown for L-DOPA administration. In these studies dynorphin peptide levels in the substantia nigra of the 6-OHDA-lesioned rat were measured, four weeks following 6-OHDA-lesion, followed by 21 day L-DOPA treatment (either as a continuous infusion $100 \text{ mg kg day}^{-1}$, or intermittent i.e. two 50 mg kg^{-1} injections per day). This study showed that dynorphin peptide levels remain decreased compared to the unlesioned side when treated continuously with L-DOPA but displayed a significant increase following intermittent treatment (Engber *et al.*, 1991).

To date, no studies have investigated dynorphin changes in parkinsonian *post-mortem* brain tissue specifically following treatment.

Similarly, no studies investigating dynorphin expression or peptide levels in MPTP-treated non-human primates, following repeated L-DOPA or dopamine receptor agonist treatment, have been reported.

Summary

It has been demonstrated that following dopamine denervation, there is an increase in enkephalin synthesis and a decrease in dynorphin synthesis in the medium spiny projection neurons of the striatum. In the 6-OHDA-lesioned rat model of Parkinson's disease, there is an increase in both striatal enkephalin mRNA and peptide levels. Conversely, there is a decrease in both striatal dynorphin mRNA and peptide levels.

Following intermittent L-DOPA-treatment, in the 6-OHDA-lesioned rat, there no change in mRNA expression levels or a small increase in enkephalin peptide levels and a significant increase in both dynorphin mRNA and peptide levels. However, in the

6-OHDA-lesioned rat, continuous treatment with L-DOPA causes a further increase in enkephalin peptide levels and no change in dynorphin levels. To date, there is no topographical data regarding these changes, or data on other, clinically relevant, dopamine agonists with regards to peptide alterations.

It has been reported in the MPTP-treated non-human primate model of Parkinson's disease, that there are increased levels of enkephalin and decreased levels of dynorphin mRNA synthesis within the neostriatum, which are unaltered by the development of dyskinesias following repeated dopamine receptor agonist treatment. This finding has also been confirmed by *post-mortem* studies from parkinsonian brain tissue. Decreased levels of dynorphin mRNA expression have been reported in MPTP-treated non-human primates. There is currently no data available for dynorphin mRNA alterations in parkinsonian *post-mortem* tissue. Furthermore, there are presently no data on topographical changes in either enkephalin or dynorphin mRNA expression, following either MPTP-induced parkinsonism or following dopamine agonist-induced dyskinesias in the non-human primate.

1.8 Aims

The aims of the experiments described in this thesis were to investigate the role played by opioid neuropeptides in striatal efferents in the generation of symptoms in iatrogenic dyskinesias caused by dopamine-replacement therapies in Parkinson's disease.

■ In chapter 2 a series of behavioural studies have been performed to develop and characterise a rodent model of L-DOPA-induced dyskinesia.

■ In chapter 3 a series of experiments have been performed applying the technique of Northern blot hybridisation to assess the synthesis of opioid peptides in the striatum in a rodent model of L-DOPA-induced dyskinesia and to assess the role of opioid transmission in the rodent model of L-DOPA-induced dyskinesia.

■ In chapter 4 a series of experiments are described using the technique of *in situ* hybridisation to investigate the topography of changes in opioid neuropeptide synthesis in the striatum in a rodent model of Parkinson's disease following repeated L-DOPA, bromocriptine or lisuride treatment.

■ In chapter 5 a series of experiments are described that investigate the topography of changes in opioid neuropeptide synthesis in the striatum of the MPTP-treated non-human primate model of L-DOPA-induced dyskinesia.

Chapter 2:

Characterisation of a rodent model of L-DOPA-induced dyskinesia in Parkinson's disease

2.1 Introduction

The most effective and most commonly-prescribed treatment for Parkinson's disease is the dopamine precursor L-3,4-dihydroxyphenylalanine (L-DOPA, Cotzias *et al.*, 1969). This treatment is highly successful in reversing the symptoms of Parkinson's disease in the initial few years of treatment. However, following repeated treatment, over an extended period many complications are seen. These include 'on-off' fluctuations, freezing episodes, non-responsiveness or 'wearing-off' (Marsden and Parkes, 1976; Barbeau, 1969; Shaw *et al.*, 1980), and the abnormal involuntary movements of L-DOPA-induced dyskinesia (Barbeau, 1980). Following 5 years of L-DOPA-treatment in Parkinson's disease, up to 80% of patients develop some symptoms of L-DOPA-induced dyskinesia (Nutt, 1990). These dyskinetic side-effects can become as debilitating as the Parkinson's disease itself. Conversely, *de novo* administration of bromocriptine or lisuride to both patients and MPTP-treated macaques, does not lead to the development of dyskinesia (Lees and Stern, 1981; Bedard *et al.*, 1986). Unfortunately, only about 30% of patients respond to the anti-parkinsonian effects of bromocriptine (Lees, 1993). Patients who receive bromocriptine monotherapy may also experience psychiatric adverse effects, including confusion, visual hallucinations and paranoia (Calne *et al.*, 1978; Hoehn, 1985) and therefore require either bromocriptine plus L-DOPA or L-DOPA monotherapy. Both of these latter regimens eventually result in dyskinesia (Rinne, 1987).

To understand the neural mechanisms underlying L-DOPA-induced dyskinesia; investigate and develop effective adjunct therapies for L-DOPA-induced dyskinesia; and to screen for novel anti-parkinsonian drugs that do not cause dyskinesias, the most valuable asset is an effective animal model which replicates the molecular, cellular, biochemical and symptomatic changes seen in parkinsonian patients displaying L-DOPA-induced dyskinesia. To date the only animal model which achieves this aim with respect to L-DOPA-induced dyskinesia has been the MPTP-treated macaque following repeated L-DOPA or dopamine-agonist administration (Mitchell *et al.*, 1986). This is an excellent model in almost all respects and will remain the 'gold standard' for the investigation of L-DOPA-induced dyskinesia. Recently, it has been suggested that MPTP-treated marmosets may also be capable of eliciting L-DOPA-

induced dyskinesias (Pearce *et al.*, 1995). However, ethical and logistical considerations must lead to us to consider non-primate models that might permit useful advances towards understanding the neural mechanisms underlying L-DOPA-induced dyskinesias. Therefore, a rodent model that replicates the biochemical, molecular and neural mechanisms underlying L-DOPA-induced dyskinesia would be of great advantage to not only further our understanding of the neural mechanisms underlying L-DOPA-induced dyskinesia, but also to investigate new anti-parkinsonian drugs for their pro-dyskinetic properties and to screen for novel anti-dyskinetic compounds. Additionally, a rodent model would be less expensive, allow several compounds to be tested *de novo* in a short period of time, and allow subsequent molecular, biochemical or receptor changes to be investigated following these treatments. No rodent model of L-DOPA-induced dyskinesia has been described to date. However, several authors have described a behavioural enhancement to the effects of apomorphine and L-DOPA following repeated administration in 6-OHDA-lesioned rats (Bevan, 1984; Carey, 1991; Gancher *et al.*, 1995). Thus, 6-OHDA-lesioned rats, when treated repeatedly show an enhanced level of rotational behaviour in response to treatment with increasing length of treatment. In this chapter a rodent model produced by lesioning the dopaminergic cells of the SNpc, VTA and retrorubral areas, followed by subsequent repeated low-dose L-DOPA administration will be used.

The aim of the experiments described in this chapter were to: investigate the possible development of a rodent model of L-DOPA-induced dyskinesia by characterisation of the behavioural response to repeated administration of a low dose of L-DOPA; investigate the modification of this behavioural response by drugs known to reduced L-DOPA-induced dyskinesia when co-administered with L-DOPA, in both patients and MPTP-treated non-human primates (see table 2.1, Gomez-Mancilla and Bedard, 1993; Bennett *et al.*, 1994; Bonifati *et al.*, 1994; Durif *et al.*, 1995; Carpentier *et al.*, 1996); investigate the response to *de novo* administration of drugs known not to cause dyskinesias in patients and MPTP-treated non-human primates.

Non-dopaminergic drug (mg kg ⁻¹) co-administered with L-DOPA (50 mg kg ⁻¹)	% reduction in dyskinesia	% reduction in anti- parkinsonian efficacy
Yohimbine (0.01)	32 % *	0%
(0.1)	71 % *	10%
Naloxone (0.02)	-19 %	5%
(0.04)	6 %	12%
Clonidine (0.1)	97 % *	95% *
5-MDOT (0.1)	26 %	42%
(1.0)	42 % *	54% *
Propranolol (10)	74 % *	46% *

Table 2.1 Anti-dyskinetic properties of various non-dopaminergic drugs in the MPTP-treated non-human primate model of Parkinson's disease

Following repeated L-DOPA administration MPTP-treated non-human primates display L-DOPA-induced dyskinesias. This table summarises the anti-dyskinetic effects, and any reduction in anti-parkinsonian efficacy of L-DOPA (expressed as a percentage reduction), produced by co-administration of various non-dopaminergic drugs with L-DOPA, ($P < 0.05$, Friedman's test, $n=4$, modified from Gomez-Mancilla and Bedard, 1993).*

2.2 Methods

2.2.1 Unilateral 6-OHDA-lesion of the medial forebrain bundle

Male Sprague Dawley rats (250-300g) were obtained from Charles River (UK), maintained in standard housing conditions with constant temperature ($22 \pm 1^\circ\text{C}$), humidity (relative, 30%), 12 hour light/dark cycles (light period 8 a.m./8 p.m.) and were allowed free access to food (Standard pellets, B & K Universal) and water. Thirty minutes prior to surgery animals were injected intraperitoneally (i.p.) with pargyline (5 mg kg^{-1} , Sigma) (to inhibit monoamine oxidase-B activity and therefore enhance the dopamine-depletion by 6-hydroxydopamine) and desipramine (25 mg kg^{-1} , Sigma) (a noradrenaline uptake inhibitor to minimise damage to noradrenergic neurons) both dissolved in sterile 0.9% w/v sodium chloride (Braun Medical) and injected at a volume of 1 ml kg^{-1} of body weight. Rats were placed in a stereotactic frame, under sodium pentobarbitone anaesthesia (60 mg kg^{-1} , i.p., Sagatal, Rhone-Merieux). Each animal received a unilateral injection of $2.5 \mu\text{l}$ 6-hydroxydopamine HCl (Sigma, 5 mg ml^{-1} in sterile water (Braun Medical) with 0.1% ascorbic acid (Sigma) into the right medial forebrain bundle at co-ordinates -2.8 mm from Bregma, 2 mm lateral to the midline and 9 mm below the skull according to the atlas of Paxinos and Watson (1986). The injection was made, by hand, over a 5 minute period using a $5 \mu\text{l}$ Hamilton syringe. Sham-lesions were carried out as above, with the exception that only $2.5 \mu\text{l}$ of 0.1% ascorbic acid was injected. Post-operatively, all animals were placed on heated pads and received a subcutaneous injection of 12 ml sterile glucose-saline (0.18% w/v sodium chloride, 4% w/v glucose, Intraven, IVEX Pharmaceuticals) to prevent post-operative dehydration.

2.2.2 Drug treatment and behavioural analysis

Day 0-sterile water injection

To investigate the ipsiversive rotational behaviour produced by the stress involved in an i.p. injection of sterile water, 21 days post-operation the 6-

hydroxydopamine-lesioned rats were removed from their home cage, injected with sterile water (1 mg ml^{-1} , i.p., Braun Medical) at 9 a.m., and placed immediately in a 40 cm diameter stainless-steel bowl (day 0). Behaviour was recorded on videotape for 3 hours. Videotapes were analysed and the number of complete 360° rotations ipsiversive and contraversive to the lesion (or sham injection) were counted over a 2 hour period, immediately post-injection. 6-hydroxydopamine lesioned animals obtaining a net ipsiversive rotation less than 30 rotations in 2 hours were removed from the experimental groups.

2.2.3 High dose L-DOPA-treatment

Rats were injected i.p. with either L-DOPA or vehicle twice-daily at 9 a.m. and 5 p.m. L-DOPA (100 mg kg^{-1}) was administered as the methyl ester form of L-DOPA, L-3,4 dihydroxyphenylalanine methyl ester (L-DOPA, Sigma), a more stable and soluble pro-drug whose ester moiety is rapidly hydrolysed by non-specific esterases to form L-DOPA (Cooper *et al.*, 1984), with 25 mg kg^{-1} benserazide (Sigma) (both dissolved in 0.05% ethanol (BDH) and 0.1% ascorbic acid (Sigma) in sterile water (Braun Medical) and injected at a volume of 1 ml kg^{-1} of body weight). Vehicle consisted of 0.05% ethanol (BDH) and 0.1% ascorbic acid (Sigma) in sterile water (Braun Medical) and injected at a volume of 1 ml kg^{-1} of body weight. Behavioural analysis was carried out as described in 2.2.2 immediately following the 9 a.m. injection on days 1, 3, 5, 7, and 10. Rats were removed from the stainless-steel bowls 3 hours following the 9 a.m. injection.

2.2.4 Low dose L-DOPA-treatment

Rats were injected i.p. with either L-DOPA or vehicle twice a day at 9 a.m. and 5 p.m. L-DOPA (6.5 mg kg^{-1}) was administered as the methyl ester form with 1.5 mg kg^{-1} benserazide (Sigma) (dissolved in 0.05% ethanol (BDH) and 0.1% ascorbic acid (Sigma) in sterile water (Braun Medical) and injected at a volume of 1 ml kg^{-1} of body weight. Behavioural analysis was carried out as described in 2.2.2 immediately following the 9 a.m. injection on days 1, 3, 5, 7, 10, 14, 17 and 21. Rats were removed from the stainless-steel bowls 3 hours following the 9 a.m. injection.

2.2.5 Calculation of L-DOPA 'on-time' in the 6-OHDA-lesioned rat

Following L-DOPA administration on days 1, 3, 5, 7, 10, 14, 17 and 21 rotational behaviour was assessed for 2 hours immediately following the L-DOPA-injection. This 2 hour time period was divided into 5 minute time-bins. Five rotations, contraversive to the lesion, in any 5 minute time-bin was established as a threshold of 'on' effects of L-DOPA.

2.2.6 Calculation of rotations/minute during 'on-time'

During the L-DOPA 'on-time' period, as defined in section 2.2.5, net rotations contraversive to the 6-OHDA-lesion per minute were assessed on days 0, 1, 3, 5, 7, 10, 14, 17 and 21.

2.2.7 Time course of L-DOPA-induced rotations following repeated low dose L-DOPA administration in the 6-OHDA-lesioned rat model of Parkinson's disease on days 14-21

Following repeated, twice-daily, L-DOPA (6.5 mg kg^{-1}) and benserazide (1.5 mg kg^{-1}) treatment, on days 14-21, rotations contraversive to the 6-OHDA-lesion made in the 2 hour time period immediately following the L-DOPA injection were assessed. This 2 hour time period was divided into 5 minute time-bins. Mean rotations, per 5 minutes on days 14-21, contraversive to the lesion were plotted over the 120 minute time period following L-DOPA administration. Rats were removed from the stainless-steel bowls 3 hours following the 9 a.m. injection.

2.2.8 Bromocriptine-treatment in the 6-OHDA-lesioned rat model of Parkinson's disease

Rats were injected with 2-bromo- α -ergocryptine (bromocriptine, Sigma), twice-daily, at 9 a.m. and 5 p.m. Bromocriptine (5 mg kg^{-1} , i.p.) was dissolved in 0.05% ethanol (BDH) and 0.1% ascorbic acid (Sigma) in sterile water (Braun Medical) and injected at a volume of 1 ml kg^{-1} of body weight. Behavioural analysis

was carried out as described in 2.2.2. Rats were removed from the stainless-steel bowls 3 hours following the 9 a.m. injection. Net rotations contraversive to the 6-OHDA-lesion were assessed, for 2 hours, beginning 1 hour following the 9 a.m. injection on days 1, 3, 5, 7, 10, 14, 17 and 21.

2.2.9 Lisuride-treatment in the 6-OHDA-lesioned rat model of Parkinson's disease

Rats were injected i.p. with R(+)-lisuride hydrogen maleate (lisuride, Research Biochemicals International) twice a day at 9 a.m. and 5 p.m. Lisuride (0.1 mg kg^{-1} , i.p) was dissolved in 0.05% ethanol (BDH) and 0.1% ascorbic acid (Sigma) in sterile water (Braun Medical). Behavioural analysis was carried out as described in 2.2.2 immediately following the 9 a.m. injection on days 1, 3, 5, 7, 10, 14, 17 and 21. Rats were removed from the stainless-steel bowls 3 hours following the 9 a.m. injection.

2.2.10 Effect of non-dopaminergic drugs on L-DOPA-induced rotation in the 6-OHDA-lesioned rat model of Parkinson's disease following repeated L-DOPA treatment

Three weeks post 6-hydroxydopamine lesion, rats were treated with L-DOPA (6.5 mg kg^{-1}) and benserazide (1.5 mg kg^{-1}) for 14 days (twice-daily) as described in 2.2.4. L-DOPA treatment was continued for days 14-21. However, additional treatment with non-dopaminergic agents (or vehicle) was administered in concert with the 9 a.m. injection of L-DOPA. The non-dopaminergic drugs were administered 40 minutes after L-DOPA, to give a maximal effect at approximately 45 minutes after the L-DOPA-administration (In preliminary studies it was shown that this time represented the peak effect of L-DOPA, Figure 2.3.3.3). Rats were placed in 40 cm stainless-steel bowls immediately following the L-DOPA injection, and remained in the bowls for 3 hours. Rotational locomotion was assessed for 15 minutes, between 45 minutes to 60 minutes following L-DOPA injection. Appropriate vehicle plus L-DOPA injections were made on the following day. To investigate the stability of response and effect of sterile water injections during the 45-60 minute period post L-DOPA, following 13-21 days L-DOPA administration, the percentage change in

rotational behaviour (i.e. % hyperkinesia) in response to co-administration of sterile water 40 minutes following L-DOPA-administration on days 13 to 21 were assessed. Rotations, contraversive to the 6-OHDA-lesion in the 15 minute time period (45-60 minutes post L-DOPA/benserazide injection) were assessed on days 13 to 21. Rotations made in this 15 minute period were expressed as a percentage of the corresponding time period for the L-DOPA-sterile water treatment on the following day.

Drugs tested were: the α_2 -adrenergic receptor antagonist yohimbine (0.03-10 mg kg⁻¹, Sigma); the non-selective opioid receptor antagonist naloxone (0.01- 0.03 mg kg⁻¹, Sigma); the α_2 -adrenergic receptor agonist clonidine (1 mg kg⁻¹, Sigma); the 5-HT uptake inhibitor 5-methoxy 5-N,N-dimethyl-tryptamine (5-MDOT, 0.5, 2 mg kg⁻¹, Sigma); the β -adrenergic receptor antagonist and 5-HT₁ agonist, propranolol (10 mg kg⁻¹, Sigma), all dissolved in sterile water (Braun Medical) and injected at a volume of 1 ml kg⁻¹. Net rotations, ipsiversive and contraversive to the lesion, were recorded in the 15 minutes from 45 minutes to 60 minutes post L-DOPA/benserazide administration and were expressed as a percentage of the corresponding time period for the L-DOPA-vehicle treatment on the following day. The animals were used for up to 4 non-dopaminergic treatments with each second day as a vehicle control. Following 21 days of L-DOPA treatment the animals were sacrificed by stunning and cervical dislocation.

2.2.11 Cresyl violet histological staining

Following sacrifice, the animals brains were removed and snap frozen in isopentane cooled to -42°C. Coronal brain sections (15 μ m thick) were cut using a cryostat (OTF, Bright UK) at -19°C and thaw mounted onto gelatin/chromalum coated slides. To verify lesion of the substantia nigra pars compacta 15 mm sections through the substantia nigra were taken (-5.30 mm from bregma). To verify the dorsal raphe nucleus and locus coeruleus remained intact, sections through both these nuclei were cut (-8.0 mm and -9.8 mm from bregma, respectively). Sections were allowed to dry in a hybridisation oven (Mini 10, Hybaid) for 1 hour at 37°C and then fixed in 10% neutral buffered formalin (Sigma) overnight. Following a 30 second rinse in distilled

water, sections were placed in 40%, 70% and then 95% ethanol (BDH) for 1 minute each. Sections were placed in xylene for 5 minutes, then 95%, 70% and finally 40% ethanol for 1 minute. Sections were transferred to 0.1% cresly violet acetate (9-amino-5-imino-5H-benzo[a]phenoxazine acetate salt, Sigma) for 1 hour at room temperature. Following incubation the sections were rinsed in water, 70% ethanol and placed in 95% ethanol for 10 minutes. Sections were then placed in 100% ethanol for 2 minutes and transferred to xylene. The sections were then mounted in 'Practamount' a xylene-based mount, and allowed to dry.

2.2.12 Spontaneous locomotion following administration of non-dopaminergic drugs in normal, non-dopamine depleted, rats

Twenty four male Sprague Dawley rats (250-300g) were obtained from Charles River (UK), maintained in standard housing conditions with constant temperature ($22 \pm 1^\circ\text{C}$), humidity (relative, 30%), 12 hour light/dark cycles (light period 8 a.m./8 p.m.) and were allowed free access to food (Standard pellets, B & K Universal) and water. Rats were assigned to two groups, 12 vehicle-treated rats and 12 drug-treated rats. Both groups were injected with sterile water (1 ml kg^{-1} , i.p., Braun Medical, on day 1). Following a 5 min recovery period in their home cage, rats were placed in locomotion boxes (perspex boxes $52 \times 36 \text{ cm}$, with infra-red detectors at 2.5 cm intervals along the bottom, 4 cm from floor of the box, Amlogger, Linton Instruments) for 30 min and mobile counts, defined as the time in seconds that the rat is active i.e. its central position changes by more than two grids in any one second, were recorded. On days 2, 4, 6, 8 and 10 non-dopaminergic drugs were administered at the maximal doses tested in the L-DOPA-treated 6-OHDA-lesioned rat as previously described (2.2.10). Rats were administered either drug or the appropriate vehicle and following a 5 minute recovery period in their home cage, rats were placed in locomotion boxes. Drugs tested were: yohimbine (10 mg kg^{-1}); naloxone (5 mg kg^{-1}); clonidine (1 mg kg^{-1}); 5-MDOT (2 mg kg^{-1}); propranolol (10 mg kg^{-1}), all dissolved in sterile water (Braun Medical) and injected at 1 ml kg^{-1} of body weight. On the day following each drug-trial day (i.e. days 3, 5, 7, 9 and 11), all rats were injected with sterile water (1 ml kg^{-1} , i.p., Braun Medical), and spontaneous

locomotion (mobile counts) assessed to insure no drug or vehicle effects (on spontaneous locomotion) lasted more than 24 hours.

2.2.13 Statistical analysis

Data are expressed as mean \pm standard error of the mean (SEM) values. Rotational behavioural data, following repeated drug administration, were analysed by multiple analysis of variance (MANOVA), followed by Student-Newman-Keuls post hoc analysis or unpaired student's t-test. Analysis of the effects of repeated L-DOPA administration on rotational behaviour were analysed using one-way analysis of variance (ANOVA), followed by Student-Newman-Keuls post hoc analysis. Effect of drug or vehicle administration on L-DOPA-induced hyperkinesia were analysed using one-way analysis of variance (ANOVA) followed by Dunnett's, Student-Newman-Keuls post hoc analysis or paired Student's t-test where appropriate. Spontaneous locomotion following non-dopaminergic drug or vehicle administration in normal, non-dopamine depleted, rats were analysed using unpaired Student's t-test. In all tests significance was assigned when $P < 0.05$.

2.3 Results

2.3.1 Verification of the specificity of a 6-OHDA-lesion injected into the medial forebrain bundle for dopaminergic cells

To verify that injection of the neurotoxin 6-OHDA into the medial forebrain bundle, coupled with the noradrenaline uptake inhibitor desipramine (25 mg kg⁻¹, injected 30 minutes prior to surgery) remained selective for only dopaminergic cells of the substantia nigra pars compacta, cresyl violet histological staining was performed on coronal sections through the substantia nigra pars compacta, the dorsal raphe nucleus and the locus coeruleus. Figure 2.3.1.1 shows loss of substantia nigra pars compacta cells in the lesioned hemisphere, with intact cells in the dorsal raphe nucleus and locus coeruleus (Figures 2.3.1.2, 2.3.1.3, respectively).

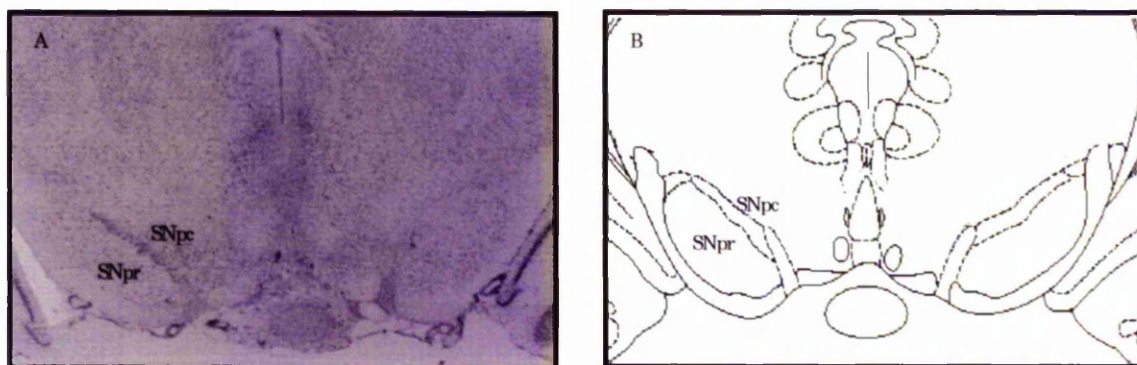


Figure 2.3.1.1 Cresyl violet stained coronal rat brain section (-5.3 mm from bregma) demonstrating loss of substantia nigra pars compacta cells (SNpc) on the lesioned hemisphere (right hand side) following unilateral injection of 6-OHDA into the medial forebrain bundle (A). Diagrammatic representation of the substantia nigra pars compacta (SNpc) and substantia nigra pars reticulata (SNpr) in a coronal rat brain section (-5.3 mm from bregma, B).

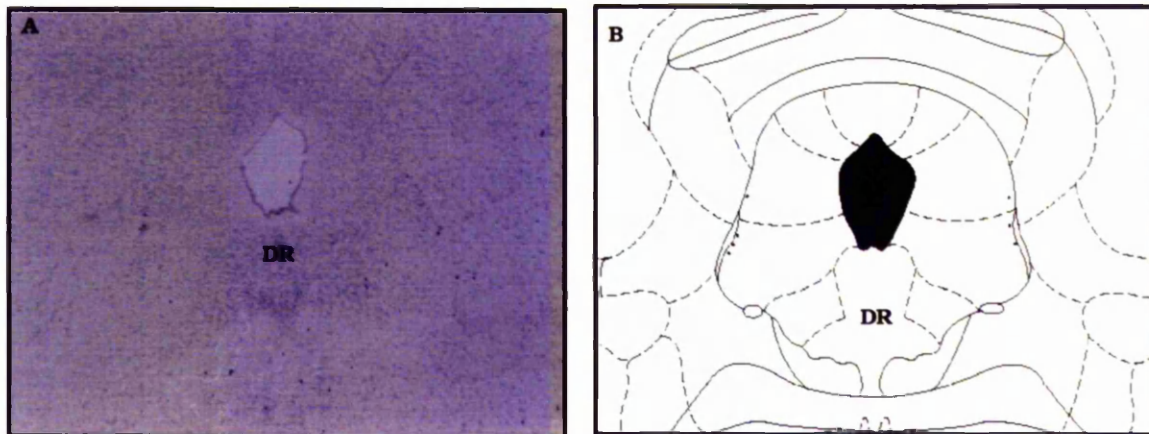


Figure 2.3.1.2 *Cresyl violet stained coronal rat brain section (-8.0 mm from bregma) demonstrating intact cells of the dorsal raphe nucleus (DR) following unilateral injection of 6-OHDA into the right hand side medial forebrain bundle (A). Diagrammatic representation of the dorsal raphe nucleus (DR) in a coronal rat brain section (-8.0 mm from bregma, B).*

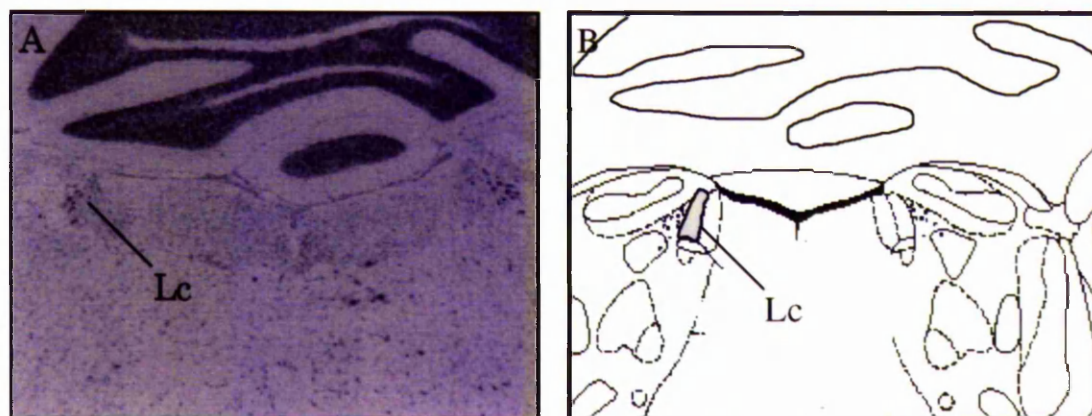


Figure 2.3.1.3 *Cresyl violet stained coronal section (-9.8 mm from bregma) demonstrating intact cells of the locus coeruleus (Lc) following unilateral injection of 6-OHDA into the right hand side medial forebrain bundle (A). Diagrammatic representation of the locus coeruleus (Lc) in a coronal rat brain section (-9.8 mm from bregma, B).*

2.3.2 Effects of dopaminergic agents on rotational locomotion in the 6-OHDA-lesioned rat

High dose administration

The effects of various dopaminergic agents on rotational locomotion of the 6-OHDA-lesioned rat model of Parkinson's disease were investigated. Following injection of 1 ml kg⁻¹ sterile water (day 0) all 6-OHDA-lesioned rats showed spontaneous rotation ipsiversive to the 6-OHDA-lesion (Figures 2.3.2.1). Following a single injection of L-DOPA (100 mg kg⁻¹, b.d.) on day 1, rotation contraversive to the 6-OHDA-lesion was observed (210 ± 51.9). This rotational response showed a marked potentiation following subsequent injections, rising rapidly and reaching a plateau by approximately day 7. By the end of the treatment period (day 10) a 500% increase in the rotational response to the same dose of L-DOPA was observed (Figure 2.3.2.1). Following repeated vehicle administration no behavioural alterations were observed, with a low level of rotation ipsiversive to the 6-OHDA-lesion observed throughout the test period (Figure 2.3.2.1).

Low dose administration

Twice-daily injection of the lower dose of 6.5 mg kg⁻¹ of L-DOPA showed a more gradual potentiated response (Figure 2.3.2.2). A rotational response, contraversive to the 6-OHDA-lesion, was not seen until day 7. However, following 7 days treatment a rapid increase was observed following subsequent injections. This potentiated behavioural response reaches a plateau by day 14 (741 ± 114). Again, by the end of the treatment period (21 days), approximately a 500% increase in the rotational response was observed when compared to the initial (day 1) L-DOPA administration. Following 21 days vehicle administration, no alteration in behavioural response was observed with only a low level of rotations ipsiversive to the 6-OHDA-lesion observed (figure 2.3.2.2).

Bromocriptine and lisuride administration

Following 21 day, twice-daily, bromocriptine (5 mg kg^{-1}) administration rotation, contraversive to the 6-OHDA-lesion, was observed, becoming significantly different from the vehicle group by day 3 (58 ± 20). However, unlike the response to L-DOPA this behaviour was not significantly potentiated following subsequent injections and by 21 days bromocriptine administration 133.7 ± 51 rotations contraversive to the 6-OHDA-lesion were observed. A qualitatively similar pattern was observed following, twice-daily, 21 days lisuride (0.1 mg kg^{-1}) treatment. (Figure 2.3.2.2).

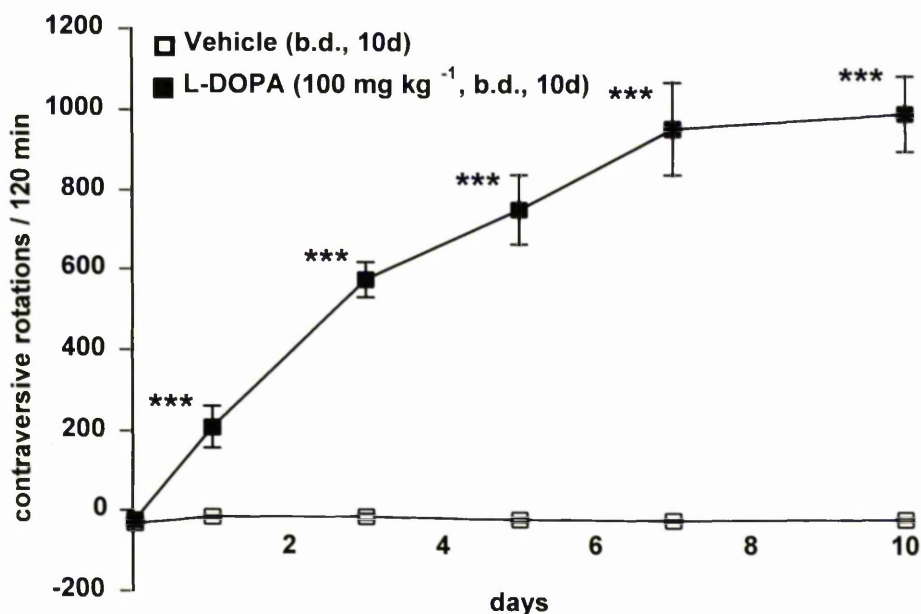


Figure 2.3.2.1 Effect of repeated high dose L-DOPA-administration on rotational behaviour in the 6-OHDA-lesioned rat

Rotational behaviour was measured in 6-OHDA-lesioned rats receiving twice-daily injection of L-DOPA (100 mg kg^{-1}) and benserazide (25 mg kg^{-1}) (■) or vehicle (□). Locomotion was assessed for 2 hours following the 9 a.m. injection on days 0, 1, 3, 5, 7, and 10. Data are expressed as mean (\pm SEM) net rotations contraversive to the 6-OHDA-lesion ($n = 6$, effect of drug $P < 0.001$, $F_{1,10} = 1810.88$, MANOVA, effect of drug over time $P < 0.001$, $F_{5,48} = 14.29$, MANOVA, *** $P < 0.001$ cf vehicle group, unpaired Student's *t*-test).

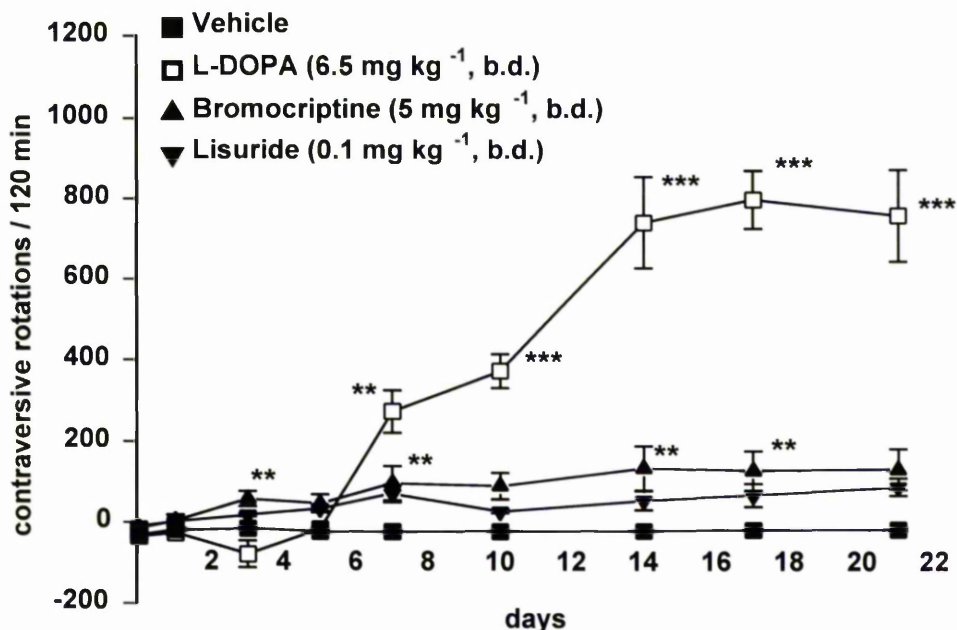


Figure 2.3.2.2 Effect of repeated vehicle, bromocriptine, lisuride or low-dose L-DOPA on rotational behaviour in the 6-OHDA-lesioned rat

Rotational behaviour was measured in 6-OHDA-lesioned rats receiving twice-daily injection of vehicle (■), bromocriptine (5 mg kg^{-1} , ▲), lisuride (0.1 mg kg^{-1} , ▼) or L-DOPA (6.5 mg kg^{-1}) and benserazide (1.5 mg kg^{-1}) (□). Locomotion was assessed for 2 hours immediately following the 9 a.m. injection on days 0, 1, 3, 5, 7, 10, 12, 14, 17, and 21 in the vehicle, lisuride and L-DOPA and benserazide groups whereas the bromocriptine group was assessed, for 2 hours, 1 hour post injection. Data are expressed as mean (\pm SEM) net rotations contraversive to the 6-OHDA-lesion ($n = 6$, effect of drug $P < 0.001$, $F_{3, 20} = 230.94$ MANOVA, effect of drug over time $P < 0.001$, $F_{24, 160} = 25.59$, MANOVA, $** P < 0.05$ cf vehicle group, $*** P < 0.001$ cf vehicle group, one-way analysis of variance, Student-Newman-Keuls post hoc analysis).

2.3.3 Pharmacokinetics of repeated L-DOPA administration with respect to rotational response in the 6-OHDA-lesioned rat model of Parkinson's disease

The effect of repeated low dose L-DOPA-administration (6.5 mg kg^{-1}) on the rotational response to L-DOPA in the 6-OHDA-lesioned rat was investigated with respect to the pharmacokinetics of the behavioural response. When the 'on-time' of L-DOPA was considered, as defined as time when rotations contraversive to the 6-OHDA-lesion were greater than 5 rotations per minute, 'on-time' increased in a similar manner to the potentiated behavioural response, that is, until day 5 there was no significant effect of L-DOPA on rotation, and therefore on 'on-time'. However, by day 5 an 'on-time' of 14.7 ± 7.6 minutes was observed. This 'on-time' increased following subsequent injections until the effect of L-DOPA 'on-time' was 80-90 minutes between days 14-21 (Figure 2.3.3.1). This effect was reflected in the response to repeated L-DOPA administration by the number of rotations per minute during the 'on-time', that is, at day 5, the rats show very few rotations per minute. However, by day 21 this had potentiated to a maximal 10 rotations per minute by day 17 (Figure 2.3.3.2).

Following L-DOPA-administration on days 14 to 21, there was a rapid increase in the rotational response, peaking at approximately 25 minutes. This begins to decrease and stabilises between 40 and 60 minutes (Figure 2.3.3.3). Following 60 minutes the effects of L-DOPA on rotational behaviour began to decline, until 120 minutes, when no rotational response was observed.

To investigate the stability of response and effect of sterile water injections during the 45-60 minute period post L-DOPA, following 13-21 days L-DOPA administration, the percentage change in rotational behaviour (i.e. % hyperkinesia) in response to co-administration of vehicle 40 minutes following L-DOPA-administration on days 13 to 21 was assessed. No significant alterations in hyperkinetic response between days 13 to 21 following vehicle administration were observed (Figure 2.3.3.4).

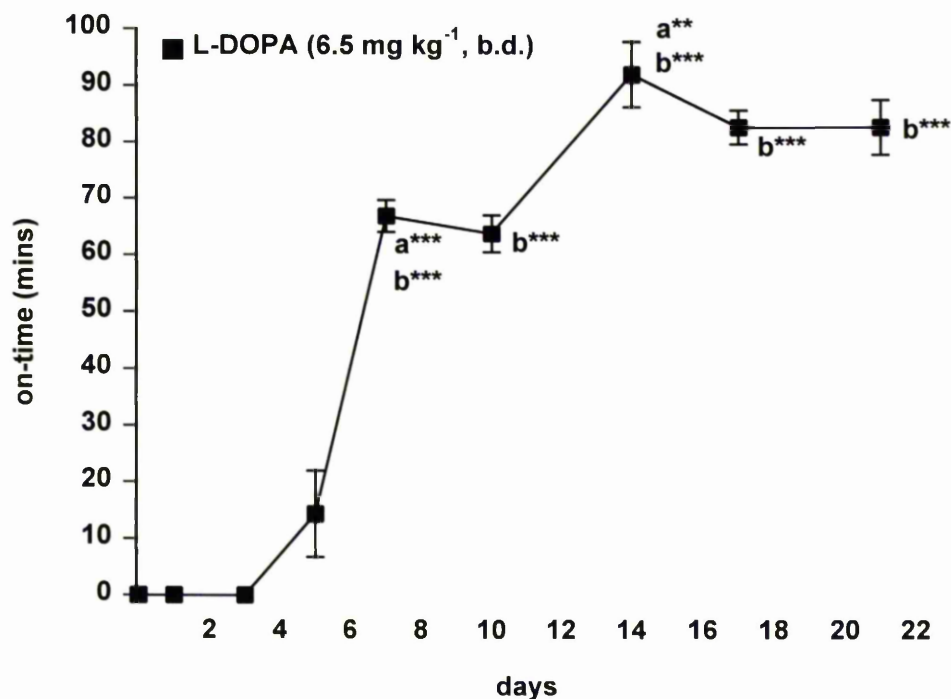


Figure 2.3.3.1 Effect of repeated L-DOPA administration on 'on-time' in the 6-OHDA-lesioned rat

Graph illustrating time in minutes in which 6-OHDA-lesioned rats achieved net rotations contraversive to the 6-OHDA-lesion greater than 5 rotations per 5 minutes following twice-daily injection of L-DOPA (6.5 mg kg^{-1}) and benserazide (1.5 mg kg^{-1}) (■). Data are expressed as mean (\pm SEM) time in minutes ($n=8$, $a^{**} P < 0.01$ cf previous time point, $a^{***} P < 0.001$ cf previous time point, $b^{***} P < 0.001$ cf day 1, $F_{8, 63} = 64.15$, one-way analysis of variance, Student-Newman-Keuls post hoc analysis).

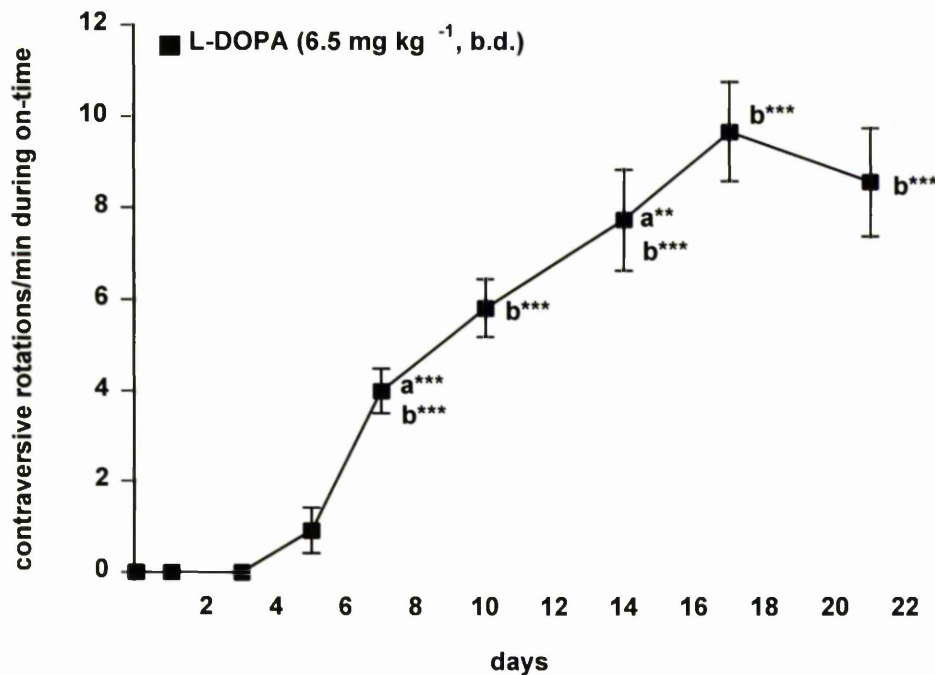


Figure 2.3.3.2 Effect of repeated L-DOPA administration on rotations/minute during 'on-time' in the 6-OHDA-lesioned rat

Net 360° rotations contraversive to the 6-OHDA-lesion following twice-daily injections of L-DOPA (6.5 mg kg⁻¹) and benserazide (1.5 mg kg⁻¹) (■) in the 6-OHDA-lesioned rat model of Parkinson's disease. Rats were filmed for 2 hours immediately following the 9 a.m. injection on days 0, 1, 3, 5, 7, 10, 12, 14, 17, and 21. Rotations per minute during 'on-time' (i.e. the period in which 6-OHDA-lesioned rats achieved net rotations contraversive to the 6-OHDA-lesion greater than 5 rotations in 5 minutes) are expressed as mean (± SEM) time in minutes (n=8, a** P < 0.01 cf previous time point, a*** P < 0.001 cf previous time point, b *** P < 0.001 cf day 1, F_{8, 63} = 32.87, one-way analysis of variance, Student-Newman-Keuls post hoc analysis).

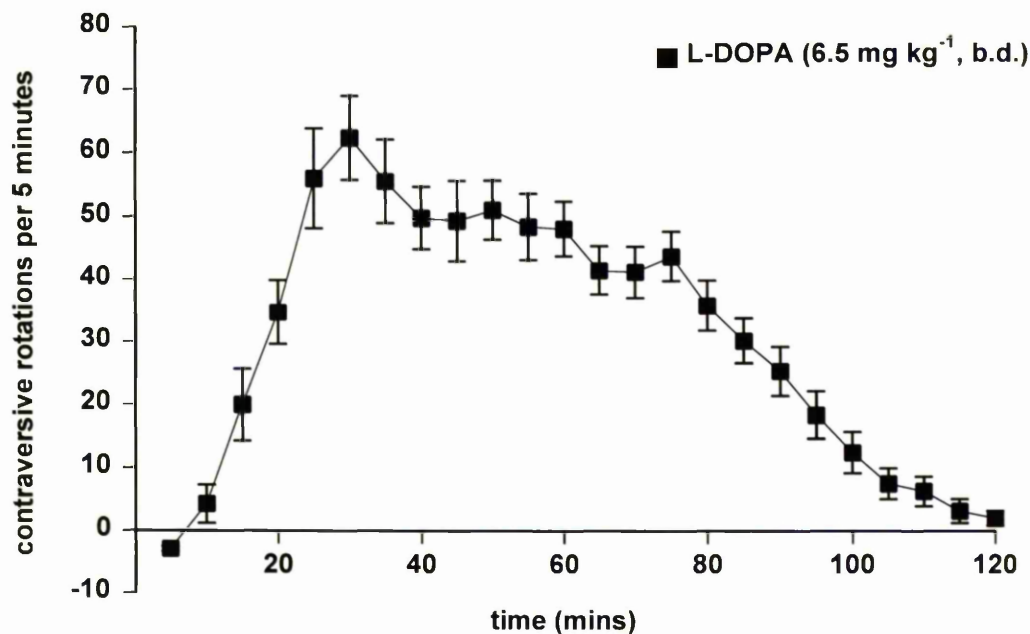


Figure 2.3.3.3 Time course of L-DOPA-induced rotations following repeated L-DOPA-administration in the 6-OHDA-lesioned rat model of Parkinson's disease on days 14-21

This figure illustrates the rotational behaviour following twice-daily injections of L-DOPA (6.5 mg kg^{-1}) and benserazide (1.5 mg kg^{-1}) (■) in 6-OHDA-lesioned rats that had previously received 13 days treatment with L-DOPA/benserazide. Locomotion was assessed for 2 hours immediately following the 9 a.m. injection on days 14 to 21. The net number of rotations, contraversive to the 6-OHDA-lesion, made in 5 minute time-bins were assessed on days 14 to 21. Data are expressed as mean (\pm SEM) net rotations, per 5 minutes, contraversive to the 6-OHDA-lesion ($n=8$).

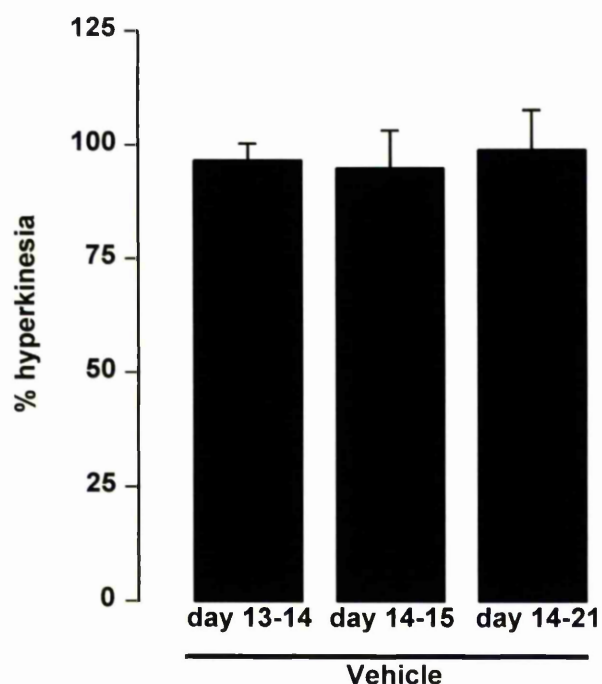


Figure 2.3.3.4 Effect of repeated vehicle administration on L-DOPA-induced hyperkinesia in the 6-OHDA-lesioned rat

This figure illustrates the ratio of the net contraversive rotations elicited by L-DOPA/benserazide and sterile water injections on rotation contraversive to the 6-OHDA-lesion, in the period in which potential anti-dyskinetic treatments were tested. Rotations were assessed as a 15 minute period beginning 45 minutes following 6.5 mg kg⁻¹ L-DOPA and 1.5 mg kg⁻¹ benserazide, on days 13 to 21 (following repeated doses of 6.5 mg kg⁻¹ L-DOPA and 1.5 mg kg⁻¹ benserazide twice-daily for the previous 12 days). 40 minutes following L-DOPA/benserazide administration rats were i.p. injected with sterile water (1 ml kg⁻¹). The hyperkinesia is expressed as a percentage of the following days sterile water injection (for days 13-15) and as a percentage change between day 13 and 21 in the final bar of the graph. Net 360° rotations contraversive to the 6-OHDA-lesion in 15 minutes, 45 minutes post L-DOPA injection (i.e. 45 - 60 min post i.p. L-DOPA and benserazide) are expressed as a percentage of the following day sterile water injection. Data are expressed as mean (± SEM) rotations, contraversive to the 6-OHDA-lesion (n=8, ns, $P > 0.05$, $F_{3, 21} = 0.144$, one-way analysis of variance, Student-Newman-Keuls post hoc analysis).

2.3.4 Effect of co-administration of non-dopaminergic drugs on L-DOPA-induced rotational locomotion in the 6-OHDA-lesioned rat following repeated L-DOPA administration

Between 14 and 21 days L-DOPA-administration, the effects of non-dopaminergic drugs on L-DOPA-induced rotation were investigated. Following co-administration of the α_2 -adrenergic receptor antagonist yohimbine a dose-dependent reduction in the L-DOPA-induced hyperkinesia was observed compared to vehicle (Figure 2.3.4.1). Administration of 10 mg kg^{-1} yohimbine completely abolished the L-DOPA-induced hyperkinesia (98.3% reduction, $P < 0.01$). Low doses of the non-selective opioid receptor antagonist naloxone had no significant effect on the L-DOPA-induced hyperkinesia (Figure 2.3.4.2). Clonidine the α_2 -adrenergic receptor agonist, at a dose of 1 mg kg^{-1} , significantly reduced the L-DOPA-induced hyperkinesia seen following repeated L-DOPA administration in the 6-OHDA-lesioned rat by 95% ($P < 0.001$, Figure 2.3.4.3). Similarly, the 5-HT uptake inhibitor 5-MDOT, at both 0.5 and 2 mg kg^{-1} , significantly reduced the hyperkinesia by 93% and 98%, respectively ($P < 0.001$, Figure 2.3.3.4). Propranolol, the beta-adrenergic receptor antagonist reduced L-DOPA-induced hyperkinesia by 35%, but this was not significant ($P > 0.05$, Figure 2.3.4.5).

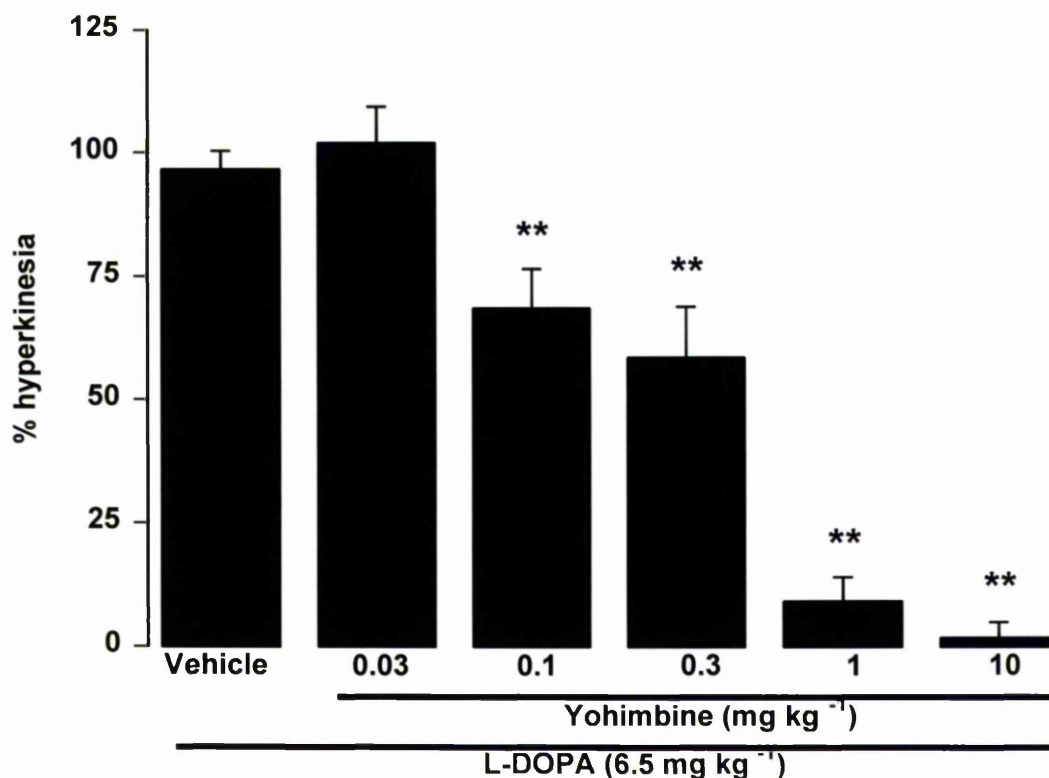


Figure 2.3.4.1 Effect of yohimbine on hyperkinesia induced by repeated L-DOPA treatment in the 6-OHDA-lesioned rat

Hyperkinesia was induced by repeated injections of L-DOPA 6.5mg kg⁻¹ and 1.5 mg kg⁻¹ benserazide (twice-daily) for 13 days. On days 14-21 rats were injected with L-DOPA/benserazide. 40 minutes following the L-DOPA/benserazide injection rats were injected with the α_2 -adrenergic receptor antagonist yohimbine (0.03 - 10 mg kg⁻¹, i.p.). Net 360° rotations contraversive to the 6-OHDA-lesion, in the 15 minute period (45 minutes post L-DOPA injection) are expressed as a percentage of that observed following vehicle injection 40 minutes after L-DOPA/benserazide treatment on the following day. Data are expressed as mean (\pm SEM) hyperkinesia ($n=4-8$, ** $P < 0.01$ cf vehicle administration, $F_{5, 27} = 62.68$, one-way analysis of variance, Dunnett's post hoc comparison).

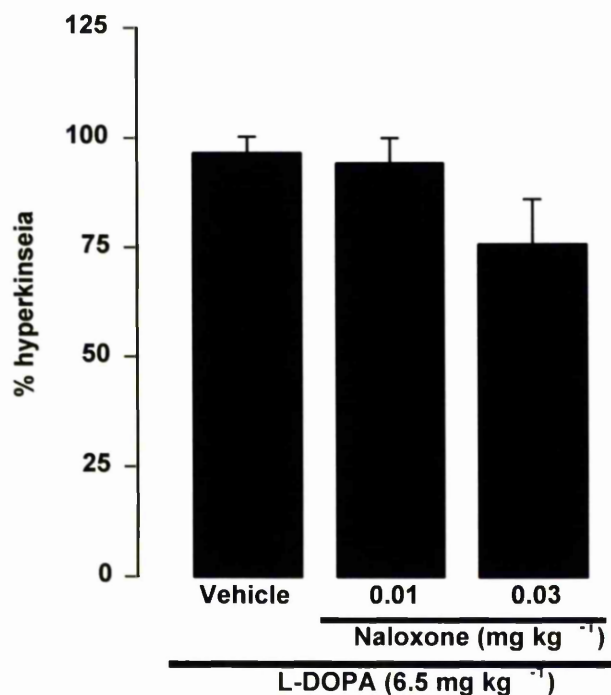


Figure 2.3.4.2 Effect of low dose naloxone on hyperkinesia induced by repeated L-DOPA treatment in the 6-OHDA-lesioned rat

Hyperkinesia was induced by repeated injections of L-DOPA 6.5 mg kg⁻¹ and 1.5 mg kg⁻¹ benserazide (twice-daily) for 13 days. On days 14-21 rats were injected with L-DOPA/benserazide. 40 minutes following L-DOPA/benserazide administration rats were injected with the non-selective opioid receptor antagonist naloxone (0.01, 0.03 mg kg⁻¹, i.p). Net 360° rotations contraversive to the 6-OHDA-lesion, in the 15 minute period, (45 minutes post L-DOPA injection) are expressed as a percentage of that observed following vehicle injection 40 minutes after L-DOPA/benserazide treatment the following day. Data are expressed as mean (\pm SEM) hyperkinesia ($n=7-8$, ns, $P > 0.05$, $F_{2, 19} = 1.75$, cf vehicle administration, one-way analysis of variance, Dunnett's post hoc comparison).

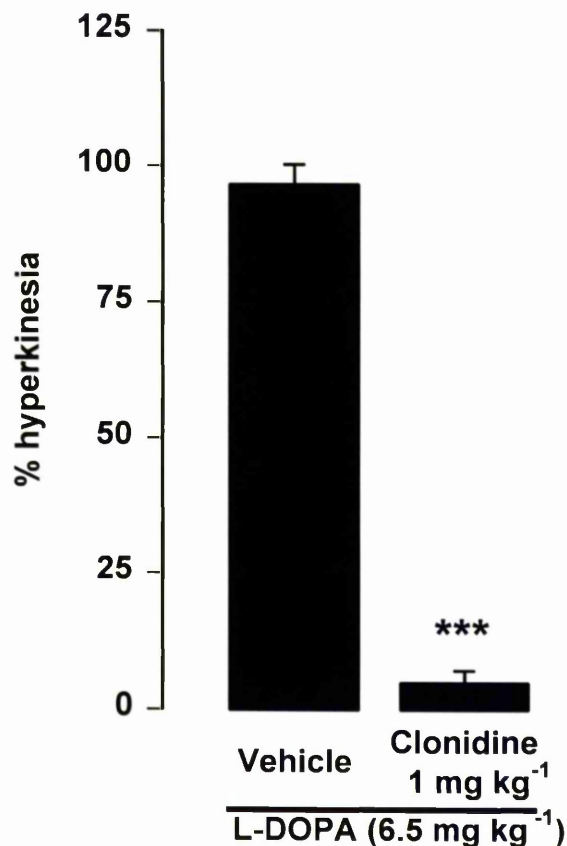


Figure 2.3.4.3 Effect of clonidine on hyperkinesia induced by repeated L-DOPA treatment in the 6-OHDA-lesioned rat

*Hyperkinesia was induced by repeated injections of L-DOPA 6.5 mg kg⁻¹ and 1.5 mg kg⁻¹ benserazide (twice-daily) for 13 days. On days 14-21 rats were injected with L-DOPA/benserazide. 40 minutes following L-DOPA/benserazide administration rats were injected with the α_2 - adrenergic receptor agonist clonidine (1 mg kg⁻¹, i.p.). Net 360° rotations contraversive to the 6-OHDA-lesion, in the 15 minute period, (45 minutes post L-DOPA injection) are expressed as a percentage of that observed following vehicle injection 40 minutes after L-DOPA/benserazide treatment the following day. Data are expressed as mean (\pm SEM) hyperkinesia ($n=6$, *** $P < 0.001$ cf vehicle administration, paired Student's's t -test).*

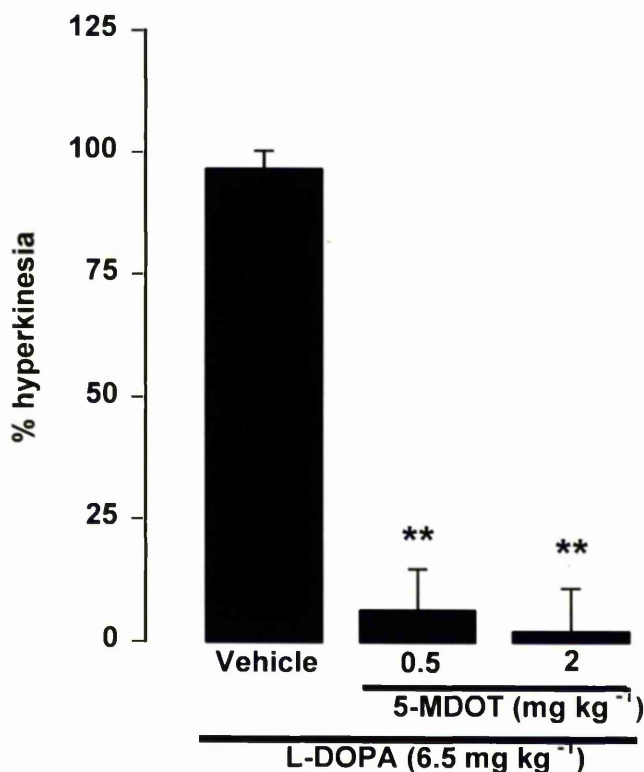


Figure 2.3.4.4 Effect of the 5-HT uptake inhibitor 5-MDOT on hyperkinesia induced by repeated L-DOPA treatment in the 6-OHDA-lesioned rat

*Hyperkinesia was induced by repeated injections of L-DOPA 6.5 mg kg⁻¹ and 1.5 mg kg⁻¹ benserazide (twice-daily) for 13 days. On days 14-21 rats were injected with L-DOPA/benserazide. 40 minutes following L-DOPA/benserazide administration, rats were injected with the 5-HT uptake inhibitor 5-methoxy 5-N,N dimethyl-tryptamine (5-MDOT, 0.5, 2 mg kg⁻¹, i.p.). Net 360° rotations contraversive to the 6-OHDA-lesion, in the 15 minute period, (45 minutes post L-DOPA injection) are expressed as a percentage of that observed following vehicle injection 40 minutes after L-DOPA/benserazide treatment the following day. Data are expressed as mean (\pm SEM) hyperkinesia ($n=6-8$, ** $P < 0.01$, $F_{2,17} = 47.64$, cf vehicle administration, one-way analysis of variance, Dunnett's post hoc comparison).*

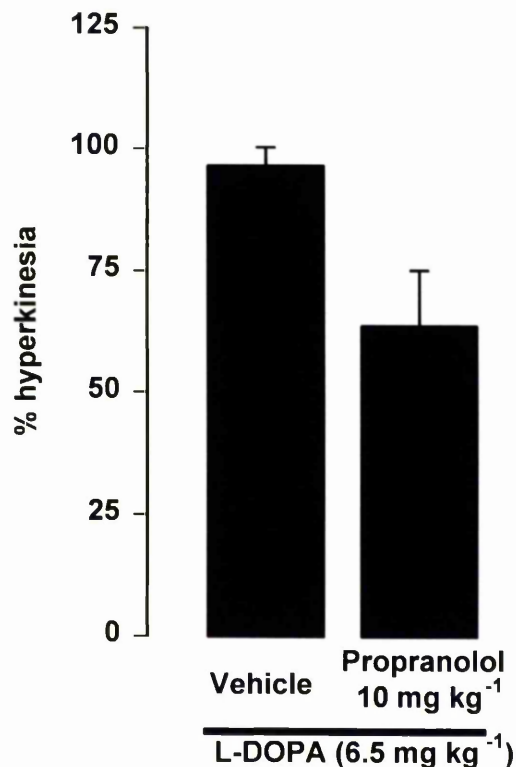


Figure 2.3.4.5 Effect of propranolol on hyperkinesia induced by repeated L-DOPA treatment in the 6-OHDA-lesioned rat

Hyperkinesia was induced by repeated injections of L-DOPA 6.5 mg kg⁻¹ and 1.5 mg kg⁻¹ benserazide (twice-daily) for 13 days. On days 14-21 rats were injected with L-DOPA/benserazide. 40 minutes following L-DOPA/benserazide administration rats were injected with the beta-adrenergic receptor antagonist and 5-HT₁ receptor antagonist propranolol (10 mg kg⁻¹, i.p.). Net 360° rotations contraversive to the 6-OHDA-lesion, in the 15 minute period, (45 minutes post L-DOPA injection) are expressed as a percentage of that observed following vehicle injection 40 minutes after L-DOPA/benserazide treatment the following day. Data are expressed as mean (± SEM) hyperkinesia (n=6, ns, P > 0.05, paired Student's t-test).

2.3.5 Effect of non-dopaminergic drugs on spontaneous locomotion in normal, non-dopamine depleted, rats

To assess whether the effects of non-dopaminergic drugs on L-DOPA-induced hyperkinesia in the hyperkinetic 6-OHDA-lesioned rat, were due to a general reduction in spontaneous locomotion, the drugs tested in 2.3.4 were administered to normal (i.e. non-dopamine depleted) rats and the spontaneous locomotion assessed on alternate days following drug or vehicle administration.

To ensure that no effect of any of the drugs remained after 24 hours, sterile water injections were given on the day following a drug test day. Spontaneous locomotion, as measured by mobile counts, was unaltered on the following day by any of the drug treatments. However, a reduction in locomotion was seen with repeated injections (Figure 2.3.5.1).

Following administration of the α_2 -adrenergic receptor antagonist yohimbine (10 mg kg^{-1}), a significant 200% increase in spontaneous locomotion was observed (vehicle 1176.5 ± 189.8 , yohimbine 2516.8 ± 355.5 , $P < 0.001$, Figure 2.3.5.1). Naloxone (Figure 2.3.5.2), 5-MDOT (Figure 2.3.5.4), and propranolol (Figure 2.3.5.5) had no effect on the spontaneous locomotion of normal rats. However, clonidine (1 mg kg^{-1}) showed a marked 80% reduction in spontaneous locomotion (vehicle 1301.5 ± 201 , clonidine 300.7 ± 59.6 , $P < 0.001$, Figure 2.3.5.3).

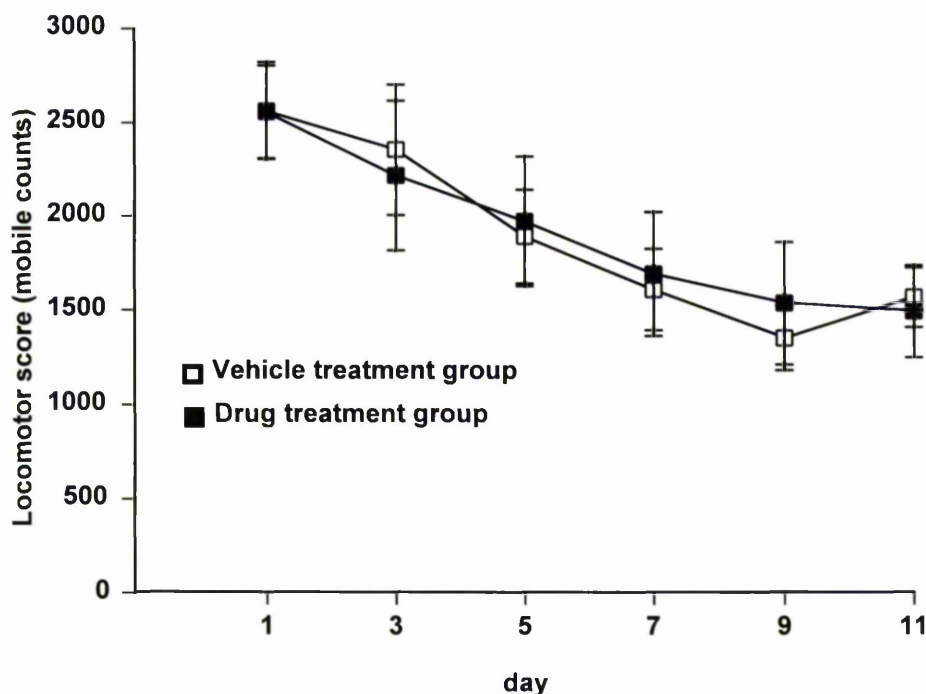


Figure 2.3.5.1 Effect of sterile water injections on spontaneous locomotion in normal rats on the day following non-dopaminergic drug administration

Spontaneous locomotion was measured in normal rats on the day following non-dopaminergic drug administration. Spontaneous locomotion was assessed in normal rats following injection of sterile water (1 ml kg^{-1} , day 1). On days 2, 4, 6, 8, and 10 various non-dopaminergic drugs were administered and the spontaneous locomotion assessed as described in 2.2.12. On days 3, 5, 7, 8 and 11 normal rats were injected with 1 ml kg^{-1} sterile water. Five minutes post injection rats were placed in an open field arena and locomotor scores were recorded for 30 minutes as described in section 2.2.12. Data are expressed as mean (\pm SEM) locomotor score (mobile counts, $n = 12$, ns, $P > 0.05$, unpaired Student's t -test).

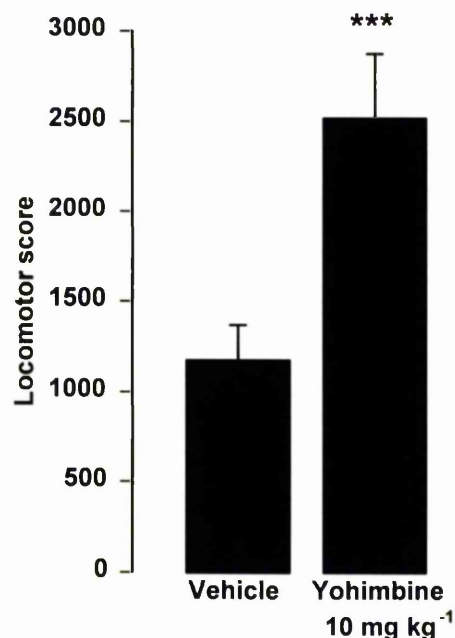


Figure 2.3.5.2 Effect of the α_2 -adrenergic receptor antagonist yohimbine on locomotion in normal rats

Spontaneous locomotion was measured in normal rats following injection of the α_2 -adrenergic receptor antagonist yohimbine (10 mg kg^{-1} , i.p.) or vehicle. Five minutes post injection rats were placed in an open field arena and locomotor scores were recorded for 30 minutes as described in section 2.2.12. Data are expressed as mean (\pm SEM) locomotor score (mobile counts, $n=12$, *** $P < 0.001$ cf vehicle group, unpaired Student's t -test).

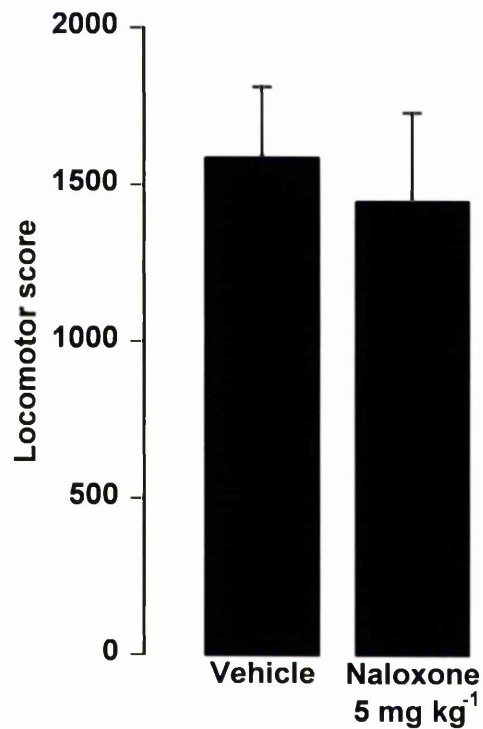


Figure 2.3.5.3 Effect of the non-selective opioid receptor antagonist naloxone on locomotion in normal rats

Spontaneous locomotion was measured in normal rats following injection of the non-selective opioid receptor antagonist naloxone (5 mg kg⁻¹, i.p.) or vehicle. Five minutes post injection rats were placed in an open field arena and locomotor scores were recorded for 30 minutes as described in section 2.2.12. Data are expressed as mean (\pm SEM) locomotor score (mobile counts, $n=12$, ns, $P > 0.05$ cf vehicle group, unpaired Student's t -test).

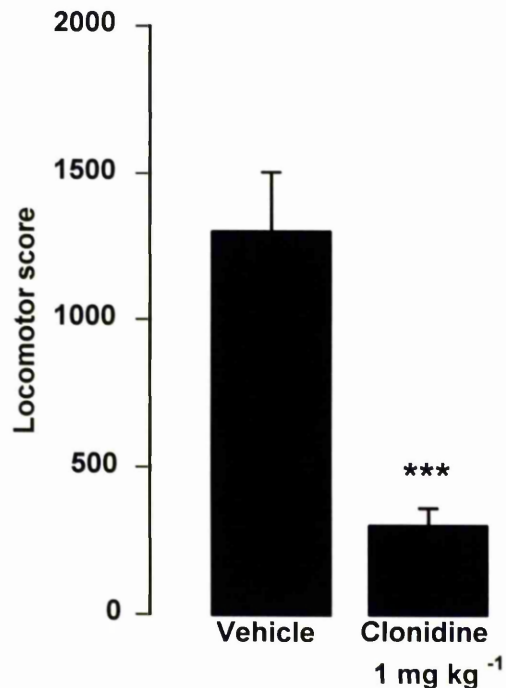


Figure 2.3.5.4 Effect of the α_2 -adrenergic receptor agonist clonidine on locomotion in normal rats

*Spontaneous locomotion was measured in normal rats following injection of the α_2 -adrenergic receptor agonist clonidine (1 mg kg^{-1} , i.p.) or vehicle. Five minutes post injection rats were placed in an open field arena and locomotor scores were recorded for 30 minutes as described in section 2.2.12. Data are expressed as mean (\pm SEM) locomotor score (mobile counts, $n=12$, *** $P < 0.001$ cf vehicle group, unpaired Student's t -test).*

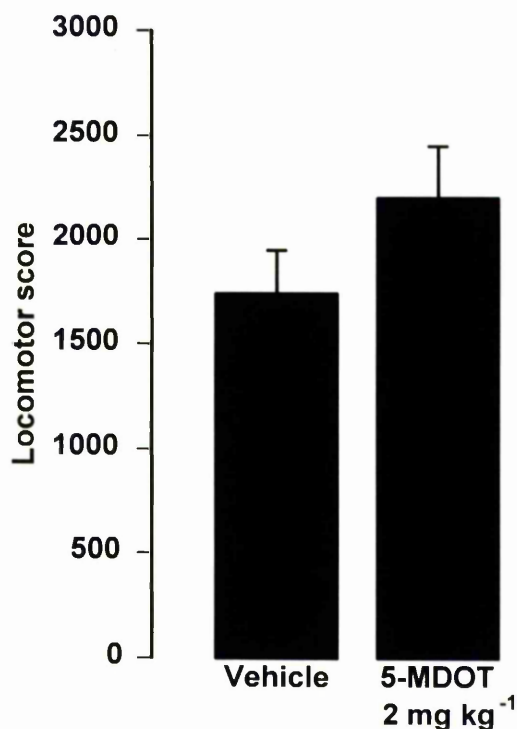


Figure 2.3.5.5 Effect of the 5-HT uptake inhibitor 5-MDOT on locomotion in normal rats

Spontaneous locomotion was measured in normal rats following injection of the 5-HT uptake inhibitor 5-methoxy 5-N,N dimethyl-tryptamine (5-MDOT, 2 mg kg⁻¹, i.p) or vehicle. Five minutes post injection rats were placed in an open field arena and locomotor scores were recorded for 30 minutes as described in section 2.2.12. Data are expressed as mean (\pm SEM) locomotor score (mobile counts, $n=12$, ns, $P > 0.05$ cf vehicle group, unpaired Student's t -test).

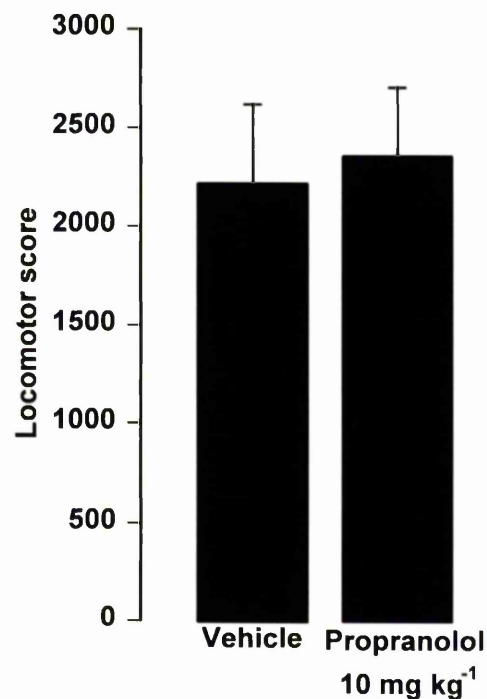


Figure 2.3.5.6 Effect of the beta-adrenergic receptor antagonist propranolol on locomotion in normal rats

*Spontaneous locomotion was measured in normal rats following injection of the beta-adrenergic receptor antagonist and 5-HT₁ antagonist propranolol (10 mg kg⁻¹, i.p.) or vehicle. Five minutes post injection rats were placed in an open field arena and locomotor scores were recorded for 30 minutes as described in section 2.2.12. Data are expressed as mean (± SEM) locomotor score (mobile counts, n=12, ns $P > 0.05$ cf vehicle group, unpaired Student's *t*-test).*

2.4 Discussion

Methodological considerations

The data presented in this chapter were aimed at developing and characterising, at the pharmacological level, a rodent model in which it might be possible to study the molecular and neural mechanisms underlying L-DOPA-induced dyskinesia in Parkinson's disease. The model used was based upon the well-characterised 6-OHDA-lesioned rat model of Parkinson's disease (Ungerstedt, 1971). The 6-OHDA-injection was targeted to the medial forebrain bundle as a method for destruction of dopaminergic cells in the VTA, SNpc and retrorubral area (A8-A10, Ungerstedt, 1968, 1971). The medial forebrain bundle (MFB) was targeted rather than a direct lesion of the SNpc for two reasons. Firstly, a lesion placed in the fibres of the MFB will be taken up by dopamine uptake sites on the axons of dopamine-containing neurons and be retrogradely transported to the cells of the SNpc, VTA and retrorubral areas, thus lesioning all dopaminergic cells in the A8-A10 complex. Secondly, since the SNpc is extended in the rostral-caudal axis, lesions placed in the MFB will destroy all cells of the SNpc, not only a small localised area that may be produced by a direct SNpc lesion. The extent of the loss of dopaminergic cells can be achieved by assessing the loss of dopaminergic terminals in the striatum through either mazindol radioligand binding studies (binds to dopamine uptake sites) or tyrosine hydroxylase immunocytochemistry (the enzyme involved in the processing of endogenous L-tyrosine to L-DOPA). Loss of cells of the substantia nigra pars compacta can also be visualised by cresyl violet histological staining (Figure 2.3.1.1).

It has been reported that 6-OHDA administration alone does not produce a lesion that is specific for dopamine neurons, but that 6-OHDA is also transported by noradrenaline and 5-HT axons, and can lesion noradrenaline and 5-HT-utilising neurons (Hokfelt and Ungerstedt, 1973).

The noradrenaline uptake inhibitor desipramine has previously been shown, to protect noradrenaline-containing cells (Fuchs and Coper, 1980; Waddington, 1980; Wooten and Collins, 1981). In the present study steps were not taken to specifically

protect 5-HT utilising cells as the vast majority of serotonergic afferents to the nuclei of the basal ganglia, from the medial and dorsal raphe nuclei, do not ascend through the MFB (Dray, 1978). Indeed, it has previously been demonstrated that following a similar lesion, there is no significant reduction in striatal 5-HT levels (Breese and Traylor, 1970). Utilising the noradrenaline uptake inhibitor desipramine (administered 30 minutes prior to the surgery), specifically targeting the MFB does not result in damage to the locus coeruleus or dorsal raphe nucleus, as demonstrated by cresyl violet staining of coronal sections from 6-OHDA-lesioned rats (Figures 2.3.1.2, 2.3.1.3).

Pargyline was administered pre-operatively to inhibit monoamine oxidase activity and thus the deamination of the 6-OHDA, to enhance the ability of the 6-OHDA to produce the lesion (Breese *et al.*, 1968; Breese and Traylor, 1970). Rats were left for 21 days post-operatively before any further experimentation was performed. This was to allow the full development of the lesion to occur. It has previously been shown that 3-4 days following lesion up to 80% of SNpc degeneration has taken place. By 14 days, all 90-95% of the degeneration of the SNpc neurons has taken place (Jeon *et al.*, 1995; Labandeira-Garcia *et al.*, 1996).

For behavioural testing, rats were placed in circular bowls. This has been described as the most suitable testing environment for the study of rotation by several authors (Ungerstedt and Arbuthnott, 1970; Carey 1991). The rats activity was filmed following the a.m. rather than at the p.m. injection, when the animals are more active and responses more variable, as any subtle changes in rotation due to the increase in spontaneous activity may have been masked. Twenty one days post-operatively, the rats were injected with 1 ml kg⁻¹ sterile water and the behaviour recorded for 2 hours post injection. Within the first 30 minutes, animals that were later identified by mazindol binding as having a greater than 95% lesion, were spontaneously active making only ipsiversive rotations.

Repeated treatment with both low (6.5 mg kg⁻¹) and high (100 mg kg⁻¹) dose L-DOPA-administration in 6-OHDA-lesioned rats elicited (by the end of the test period) a contraversive circling response that was qualitatively similar to that previously been demonstrated by several authors (Bevan, 1983; Carey, 1991, Figures 2.3.1.2, 2.3.1.3). The low dose of L-DOPA used for repeated treatment in these studies was determined by calculating a 'therapeutic' dose in patients. Thus, an average dose of

800 mg of levodopa in a 70 kg patient was used as an average daily dose (Calne, 1984), therefore, 13 mg kg⁻¹ a day L-DOPA was used as a 'low therapeutic' dose administered to the rats. To better mimic the plasma concentration fluctuations of dopamine seen in parkinsonian patients treated with oral L-DOPA tablets, this was divided into two injections, a 9 a.m. and 5 p.m. injection of 6.5 mg kg⁻¹ for 21 days. This dose of L-DOPA is much lower than any previous studies in 6-OHDA-lesioned rats, with the majority of studies administering 10-250 mg kg⁻¹. (Engber *et al.*, 1991; Taylor *et al.*, 1992; Jolkkonen *et al.*, 1995; Zeng *et al.*, 1995). The 'high dose' L-DOPA, bromocriptine and lisuride were determined from previous studies carried out in rats from the literature (Fletcher and Starr, 1987; Silverman, 1993). Twenty one days administration was determined as a standard test period from similar studies in the literature (Gerfen, 1990; Engber *et al.*, 1991).

Characterisation of behavioural response to repeated dopamine-replacement therapy in the 6-OHDA-lesioned rat model of Parkinson's disease

Repeated dopamine-replacement therapy in the 6-OHDA-lesioned rat models, on the neurochemical level, the mechanism for production of L-DOPA-induced dyskinesia in parkinsonian patients i.e. dopamine-depletion of the striatum and subsequent artificial exogenous re-introduction in a pulsatile manner. However, due to the rat's limited anatomical range of movements, chorea and dystonia are not seen and it is unclear superficially as to how well the functioning of the basal ganglia might model the neural mechanism underlying symptom generation seen in the patient. Nonetheless, a novel behaviour was observed whereby the rotational response to L-DOPA was markedly enhanced with repeated treatment. Comparison of the pharmacology of the enhanced response with that of L-DOPA-induced dyskinesia in humans and non-human primates has allowed the assessment of the relevance of this rat model in the study of L-DOPA-induced dyskinesias.

Dopamine-replacing agents

High dose L-DOPA administration (100 mg kg⁻¹, b.d.) produced the well-characterised contraversive rotational response in the 6-OHDA-lesioned rats. However, this rotation showed marked potentiation in response to further treatment, reaching a plateau by day 7 (Figure 2.3.1.1). Similarly, following low dose L-DOPA administration (6.5 mg kg⁻¹, b.d.), a behavioural potentiation in rotational response was observed, which reached a plateau following 14 days administration (Figure 2.3.1.2). The rate of onset and magnitude of this behavioural change was, like dyskinetic symptoms clinically, related to the dose and duration of treatment (Figures 2.3.1.1, 2.3.1.2).

To investigate whether the potentiated rotational response seen in these animals following repeated low-dose L-DOPA administration might in fact represent a rodent equivalent of L-DOPA-induced dyskinesia seen in both parkinsonian patients and MPTP-treated non-human primates following repeated L-DOPA-administration, the response to drugs known not to cause dyskinesia when administered *de novo* and co-administration of drugs known to reduced L-DOPA-induced dyskinesia were investigated (Kartzinel *et al.*, 1976; Parkes *et al.*, 1976; Lees and Stern, 1981; Gomez-mancilla and Bedard, 1993). No potentiation in rotational behaviour was observed following repeated bromocriptine or lisuride treatment (figure 2.3.1.2).

The reasons why L-DOPA leads to dyskinesias and bromocriptine and lisuride do not will be further addressed in chapter 4.

Characterisation of behavioural response to co-administration of non-dopaminergic drugs with L-DOPA following repeated dopamine-replacement therapy in the 6-OHDA-lesioned rat model of Parkinson's disease

Previous studies in MPTP-treated primates, have shown that several non-dopaminergic agents can reduce L-DOPA-induced dyskinesia (Gomez-Mancilla and Bedard, 1993). Co-administration of these compounds with L-DOPA was performed in the 6-OHDA-lesioned rat following repeated low dose L-DOPA-treatment. All compound were administered at time and dose to produce maximal effects at the peak of the L-DOPA response. As in the case with L-DOPA-induced dyskinesia in the

MPTP-treated primate, the α_2 -adrenergic receptor antagonist yohimbine, the α_2 -adrenergic receptor agonist clonidine, and the 5-HT uptake inhibitor 5-MDOT completely abolished the potentiated rotational response. Propranolol, the beta-adrenergic receptor antagonist, non-significantly reduced the potentiated rotational response, while low doses of the non-selective opioid receptor antagonist naloxone had no effect on the potentiated rotational response (Figures 2.3.4.1-5).

Therefore, both α_2 -adrenergic receptor agonists and antagonists, 5-HT uptake inhibitors and beta-adrenergic receptor antagonists reduced the potentiated response of repeated L-DOPA-administration to 6-OHDA-lesioned rats, when co-administered with L-DOPA, in a similar manner to L-DOPA-induced dyskinesia seen in MPTP-treated non-human primates following repeated L-DOPA administration.

To test that compounds that reduced the potentiated rotational response were not simply affecting overall locomotion, all compounds that reduced the potentiated rotational response in the 6-OHDA-lesioned rat model following repeated L-DOPA-treatment were administered to normal, non-dopamine depleted rats and the spontaneous locomotion investigated. All drugs were administered at the highest doses used in the 'anti-dyskinetic' investigations in the 6-OHDA-lesioned rat. In contrast to the reduction seen in the potentiated response in the rat model of L-DOPA-induced dyskinesia, yohimbine significantly increased locomotion, whereas 5-MDOT and propranolol had no effect on spontaneous locomotion. Conversely, clonidine significantly reduced spontaneous locomotion in normal rats, thus indicating that the reduction in the potentiated response to L-DOPA was not specific but a more general reduction in locomotion. This generalised reduction in locomotion by clonidine was also observed in the dyskinetic MPTP-treated non-human primate study (Gomez-Mancilla and Bedard, 1993, Table 2.1).

In summary, while the 6-OHDA-lesioned rat following repeated L-DOPA treatment does not show symptoms characteristic of chorea or dystonia, it does demonstrate an enhanced rotational behaviour with a pharmacological profile identical to that of L-DOPA-induced dyskinesias. The non-human primate model will no doubt remain the 'gold-standard' animal model for investigating L-DOPA-induced dyskinesia. However, this novel rodent model of L-DOPA-induced dyskinesia will provide a useful addition to investigate possible novel anti-parkinsonian compounds for their dyskinesia-producing properties, understanding the molecular and neural

mechanisms underlying L-DOPA-induced dyskinesia, and developing adjuncts to dopamine agonists that may reduced the symptoms of L-DOPA-induced dyskinesia seen following long-term L-DOPA therapy in Parkinson's disease.

Chapter 3:

**Striatal opioid peptide precursor expression and antagonism
of opioid peptide transmission in the rodent model of L-
DOPA-induced dyskinesia**

3.1 Introduction

As discussed in detail in this thesis (section 1.4), following repeated L-DOPA or dopamine agonist administration in Parkinson's disease, following 5 years of treatment, up to 80% of patients develop the abnormal involuntary movements termed L-DOPA-induced dyskinesia. These dyskinesias are choreiform and/or dystonic in nature and can become as debilitating as the Parkinson's disease itself (Nutt, 1990). From work carried out in both experimentally-induced chorea or dystonia (Crossman *et al.*, 1980; Crossman *et al.*, 1984; Jackson and Crossman, 1984; Robertson *et al.*, 1989; Crossman *et al.*, 1988) and from 2-deoxyglucose (2-DG) studies in MPTP-treated macaques displaying L-DOPA-induced dyskinesias following repeated dopamine-replacement therapy (Mitchell *et al.*, 1990), the neural mechanisms underlying L-DOPA have been partially delineated. The common mechanism underlying all forms of dyskinesias are thought to involve underactivity of the subthalamic nucleus and medial segment of the globus pallidus (GPM; Crossman, 1987; Mitchell *et al.*, 1990). In L-DOPA-induced dyskinesia, underactivity of the subthalamic nucleus is thought to be due in part to overactivity of the inhibitory projection from the lateral segment of the globus pallidus to the subthalamic nucleus. Thus, in L-DOPA-induced dyskinesia, the subthalamic nucleus is observed to have a higher 2-DG accumulation and thus terminal afferent activity than in animals where L-DOPA has reversed symptoms. However, when considering 2-DG accumulation in the lateral segment of the globus pallidus, no difference was seen between animals with L-DOPA-induced dyskinesia and those in which L-DOPA has reversed parkinsonian symptoms (Mitchell *et al.*, 1990). Since the change in GPi activity cannot be explained simply by changes in terminal activity, it suggests the possible involvement of neuromodulators in striatal efferents.

In the medial segment of the globus pallidus, the situation is more difficult to interpret given a larger number of afferents. Again no changes in 2-DG accumulation were seen in L-DOPA-induced dyskinesia compared to treated parkinsonian, though it is widely-held that medial segment of the globus pallidus is underactive in L-DOPA-induced dyskinesia. The possibility that abnormalities in the mechanisms modulating amino acid transmission may underlie changes in activity is also attractive. Two

powerful neuromodulators found in striatal efferents are the opioid neuropeptides enkephalin and dynorphin.

Enkephalin and dynorphin are found in high concentrations within the basal ganglia, specifically in the efferent projections from the striatum to both segments of the globus pallidus and substantia nigra pars reticulata (Del Fiacco *et al.*, 1982; Vincent and Hokfelt, 1982; Beckstead and Kersey, 1985; Gerfen and Young, 1988). Recent studies have shown that enkephalin can reduce GABA transmission in the globus pallidus via activation of delta opioid receptors (Maneuf *et al.*, 1994; Hill *et al.*, 1996), while dynorphin reduces glutamate release in the substantia nigra and striatum via kappa opioid receptors (Maneuf *et al.*, 1995; Hill and Brochie, 1995; Hill *et al.*, 1996).

Therefore, increased opioid peptide transmission may act to reduce GABA and glutamate release within basal ganglia. Changes in peptidergic transmission within the basal ganglia, may explain why no further 2-DG alterations are seen in the GPI during peak-dose dyskinesia in the MPTP-treated macaque, following repeated dopamine-receptor stimulation, while the subthalamic nucleus undergoes a further reduction. This mechanism would permit changes in basal ganglia nuclei, without necessarily changing afferent terminal activity.

To investigate the possible involvement of opioid peptide neurotransmission in L-DOPA-induced dyskinesia, Northern blot analysis was employed to investigate alterations in the precursors of enkephalin (pre-proenkephalin-A, PPE-A) and dynorphin (pre-proenkephalin-B, PPE-B) in the striatum of 6-OHDA-lesioned rats following repeated L-DOPA treatment, as previously described in chapter 2. Northern blot hybridisation has been described as a useful technique to quantify the total amount of a specific mRNA transcript within a specific tissue (Sambrook *et al.*, 1986).

Although there is substantial evidence to suggest that alterations in mRNA provides an accurate indicator of peptide levels, one cannot automatically presume that alterations in mRNA will be reflected in altered levels of neurotransmission. To address this problem and begin to show a causal relationship, functional antagonism by pharmacological blockade of the receptors for the endogenous peptides enkephalin and dynorphin were investigated in the rat model of L-DOPA-induced dyskinesia. Thus, the effect of opioid receptor antagonists on behaviour, with respect to the behavioural potentiation seen following repeated low-dose L-DOPA administration was investigated. The non-selective opioid receptor antagonist naloxone (Martin, 1967), the

kappa opioid receptor-selective antagonist, nor-binaltorphimine (*nor*-BNI, Portoghese *et al.*, 1987); the delta opioid receptor-selective antagonist, naltrindole (Portoghese *et al.*, 1988); and the mu opioid receptor-selective antagonist, cyprodime (Schmidhammer *et al.*, 1989) were thus administered acutely with L-DOPA in rats with established L-DOPA-induced hyperkinesia.

3.2 Methods

3.2.1 Northern Blot Hybridisation

3.2.1.1 Maintenance of ribonuclease-free conditions

Ribonucleases are DNA- and RNA-degrading enzymes that are present in all living cells. In order to successfully extract, isolate and manipulate RNA from tissue the laboratory environment must be free from ribonuclease (RNase) contamination. All apparatus and solutions were therefore treated to remove RNase activity. All solutions and water used were treated first with a 0.1% solution of diethyl pyrocarbonate (DEPC, Sigma). DEPC solutions were incubated at 37°C for 2 hours. DEPC treatment strongly inhibits RNase activity. However, DEPC also effects RNA by carboxymethylation modification of purine residues. Carboxymethylation reduces the ability to form DNA:DNA and RNA:RNA. To prevent this, DEPC solutions are autoclaved at 124°C for 40 min. This converts DEPC to carbon dioxide and water. All glassware was also treated by incubation for at least 2 hours at 37°C in a 0.1% solution of DEPC, followed by autoclaving as described. All plastics were either purchased 'bio-pure' i.e. free from any ribonuclease activity, or were autoclaved at 124°C for 15 minutes.

3.2.1.2 Extraction of total RNA from rat striatum

To optimise isolation of mRNA from rat striata, various techniques for the extraction and purification of mRNA were used. These were assessed to determine the optimum procedure for isolation by evaluating the purity of the extracted RNA. Purity was evaluated by measurement of both the ratio of absorption of light at 260:280 nm and by observing degradation by running the various extracts on agarose gels, stained with ethidium bromide. In all extraction methods, male Sprague Dawley rats 250-300g in weight, were maintained in standard housing conditions with constant temperature ($22 \pm 1^\circ\text{C}$), humidity (relative, 30%), 12 hour light/dark cycles (light period 8 a.m./8 p.m.) and were allowed free access to food (Standard pellets, B & K Universal) and water. Animals were sacrificed by cervical dislocation, brains were removed and the

striatum dissected out on ice. The striatum was placed in extraction buffer (see sections 3.2.1.3; 3.2.1.4; 3.2.1.5), homogenised using an Ultra-Turrex homogeniser (T25, labortechnik, 24 000 rpm for 1 minute) and transferred to aliquots. Three different extraction procedures were employed and are outlined below.

3.2.1.3 Chomczynski and Sacchi phenol-chloroform method for total RNA extraction

The first method of RNA extraction employed was the Chomczynski and Sacchi phenol-chloroform extraction method (Chomczynski and Sacchi, 1987). A single striatum was homogenised in 5 ml of the RNase inhibitor solution (4M guanidium thiocyanate (Sigma), 25 mM sodium citrate pH 7 (Sigma), 0.5% sarcosyl (Sigma), and 0.1 M 2-mercaptoethanol, Sigma) using an Ultra-Turrex (T25, labortechnik, 24 000 rpm for 1 minute). Once homogenised, this solution was aliquoted into 10 x 0.5 ml aliquots in 1.5 ml microcentrifuge tubes (Eppendorf) and 0.1 ml of 2 M sodium acetate (pH 4), 1ml of phenol (Sigma) and 0.2 ml of chloroform-iso-amyl alcohol (Sigma) were added. The solution was mixed through inversion and allowed to stand on ice for 15 minutes. Microcentrifuge tubes were centrifuged at 10 000 g_{av} for 15 minutes (Centrifuge 4515, Eppendorf). Following centrifugation, three distinct layers were seen: the lower phenol phase; the interphase containing DNA and proteins; and the upper aqueous phase, containing the RNA.

The upper aqueous phase was removed and placed in a fresh microcentrifuge, mixed with 1 ml of isopropanol and stored at -20°C for one hour to precipitate the RNA. Following centrifugation at 10 000 g_{av} for 20 min (Centrifuge 4515, Eppendorf) a white RNA precipitate became visible. The supernatant was removed and the pellet redissolved in 0.3 ml of the original RNase inhibitor solution. RNA was again precipitated by addition of 0.3 ml isopropanol (Sigma) at -20°C for one hour. Following centrifugation at 10 000 g_{av} for 10 min (Centrifuge 4515, Eppendorf), the supernatant was removed and the RNA pellet resuspended in 75% ethanol (BDH), re-sedimented through centrifugation (5 000 g_{av} , 5 min, Centrifuge 4515, Eppendorf) and once the supernatant was removed, vacuum freeze-dried for 15 min (-60°C, 600 Pa). Following freeze drying, the pellet was dissolved in 50 μ l of 1 mM ethylenediaminetetraacetic acid (EDTA, Sigma) at 65°C for 10 minutes.

From each 50 µl aliquot of isolated RNA, 3 µl was removed and added to 3 ml of DEPC-treated water. 3 µl of 1 mM EDTA was added to 3 ml DEPC-treated water and used as a control to autozero the spectrophotometer. Quantification of total RNA was achieved by measuring optical density (O.D.) at a wavelength of 260 nm using a spectrophotometer (Lambda Bio UV/VIS, Perkin Elmer). The concentration of RNA was calculated as (O.D. reading at 260 nm x 40) since an O.D. reading of 1 unit is equal to 40 µg ml⁻¹ of RNA. Contamination of the RNA with protein and DNA was assessed by taking O.D. readings at 280 nm. Absorbance ratio between 260:280 nm were calculated. Ratios between 1.8 and 2 were taken to be acceptably pure and free of DNA/protein contamination (Sambrook *et al.*, 1986). These samples were subsequently used for gel electrophoresis. RNA was stored at -20°C until use.

3.2.1.4 RNazol B extraction method for total RNA extraction

The second method for mRNA extraction, employed the commercially-available RNA extraction solution RNazol B (Biogene) which contains similar reagents to the Chomczynski and Sacchi phenol-chloroform extraction. A single rat striatum was placed in 1 ml of RNazol B solution and was homogenised using an Ultra-Turrex homogeniser (T25, labortechnik, 24 000 rpm for 1 minute). Following homogenisation, 0.1 ml chloroform (BDH) was added, the sample shaken vigorously for 15 seconds and left on ice for 15 minutes. Samples were then centrifuged at 12 000 g_{av} for 15 minutes (Centrifuge 4515, Eppendorf). The homogenate then forms three phases: the lower blue phenol-chloroform phase; the interphase containing DNA and proteins; and the colourless upper aqueous phase containing RNA. The aqueous phase was carefully removed and transferred to a new RNase free microcentrifuge tube (Eppendorf) to which an equal volume of isopropanol (Sigma) was added and the sample stored at 4°C for 15 minutes. Samples were then centrifuged at 12 000 g_{av} (4°C) for 15 minutes (Z382K, Hermel) to form a white precipitated pellet of RNA. The supernatant was removed and the pellet washed by vortexing with 1 ml of 75% ethanol, with subsequent centrifugation at 7 500 g_{av} for 8 minutes at 4°C (Z382K, Hermel). The resultant supernatant (i.e. 75% ethanol wash) was removed and the RNA pellet vacuum freeze-dried for 15 minutes (-60°C, 600 Pa). Following freeze drying, the pellet was re-dissolved in 50 µl of 1 mM ethylenediaminetetraacetic acid (EDTA, Sigma) at pH 7, by

vortexing and incubation at 60°C for 15 minutes. The resultant mRNA solution was then quantified and purity assessed using spectrophotometry as described in 3.2.1.3. RNA was stored at -20°C until use.

3.2.1.5 RNazol B extraction followed by poly-A purification via oligotex columns

The third extraction technique involved extraction of only poly-A mRNA from the striatum using a commercially-available oligotex mRNA midi kit (Qiagen). Transcribed mRNA in eukaryotic cells terminate in a homopolymer of 20-250 adenosine nucleotides, commonly known as a poly-A tail. Poly-A mRNA only accounts for 5-10% of eukaryotic cell expression, therefore the total poly-A mRNA extracted from the striatum is extremely low, though highly concentrated. This purification technique is useful when the expression of the transcript of interest is low. Initially, total RNA was extracted as described in 3.2.1.4 by the RNazol B extraction method. Following total RNA extraction, DEPC-treated water was added to make a total volume of 360 µl. The oligotex solution contains small polystyrene latex beads (1.1 mm in diameter) with oligonucleotides covalently linked to the surface of the beads. These oligonucleotides are 30 bases long and consist of thymidine polymers (dT₃₀). Under the correct conditions (37°C) these oligonucleotides hybridise the poly-A tails. These can then be purified from remaining non-poly-A RNA by centrifugation through purification columns. These purification columns consist of a series of filters with pores less than 1 mm, thus stopping the latex beads, and hybridised poly-A mRNA from elution. The poly-A can then be eluted and collected separately. The oligotex solution is pre-heated to 37°C and vortexed prior to use. 15 µl of oligotex solution was added to the mRNA/DEPC solution with 75 µl binding buffer (10 mM Tris HCl, 500 mM NaCl, 1 mM EDTA, 0.1% SDS, 0.1% NaN₃ and 10 % (w/v) (0.1 mg µl⁻¹) suspension of oligotex particles). This mixture was heated to 65°C for 3 minutes and allowed to cool to room temperature to allow hybridisation of the poly-A tails to the beads. The suspension was then centrifuged for 2 minutes at 15 000 g_{av} (Centrifuge 4515, Eppendorf) to pellet the beads and poly-A mRNA. This pellet was resuspended in 400 µl wash buffer (10 mM Tris HCl (pH 7.5) 150 mM NaCl, 1 mM EDTA), vortexed and transferred to the purification column. The column was then centrifuged at 15 000 g_{av} for 30 seconds (Z382K, Hermel), 450 µl wash buffer was added, centrifuged again at

15 000 g_{av} for 30 seconds (Z382K, Hermel) and the elute discarded. Finally the microcentrifuge tube (Eppendorf) was replaced and 20 μ l of elution buffer (5 mM Tris HCl (pH 7.5), pre-warmed to 80°C) added and the column centrifuged at 15000 g_{av} for 30 seconds (Z382K, Hermel). The eluted poly-A mRNA solution was collected and quantified by 260:280 nm absorbance ratio as described in 3.2.1.3. Poly-A mRNA was then stored at -20°C until use.

3.2.1.6 Isolation of total striatal RNA for Northern blot hybridisation

Both right and left striata were dissected out and placed in separate 50 ml round bottomed centrifuge tubes (Falcon) in 5 ml RNazol B solution (Biogene). The striata were homogenised using an Ultra-Turrax homogeniser (T25, labortechnik, 24 000 rpm for 1 minute). The striatal suspension was divided into 1 ml samples and kept on ice. Total mRNA was extracted and quantified as described for the RNazol B protocol in 3.2.1.4. Each pellet was resuspended in 50 μ l of 1 mM ethylenediaminetetraacetic acid (EDTA), pH 7 and incubated at 65°C for 15 minutes. RNA suspensions isolated from the same striatal tissue were then recombined into one microcentrifuge tube (Eppendorf) and stored at -20°C.

3.2.1.7 Preparation of samples for gel electrophoresis

Each RNA sample to be loaded consisted of 10 μ g of total striatal RNA and 15.5 μ l of sample loading buffer. The end lane of each gel contained 3 μ l of 0.24 - 9.5 Kb RNA markers (Gibco, BRL), also with 15.5 μ l of sample loading buffer added. This loading buffer consisted of 2 μ l of 5 x formaldehyde gel running buffer (20.6 g of 3-[N-morpholino]propanesulfonic acid (MOPS), in 800 ml of 50 mM sodium acetate, 20 ml of 250 mM EDTA, 34.5 ml of 1 M sodium hydroxide and 145.5 ml of DEPC treated water, pH 7), 3.5 μ l of formaldehyde (37% solution, Sigma) and 10 μ l of formamide (Sigma). Samples were incubated at 65°C for 15 minutes (to denature the RNA), then transferred to ice. Once cooled, 4 μ l of gel loading buffer was added to each sample. Gel loading buffer contained the visual marker 0.01% bromophenol blue which enables the sample front to be followed, 50% glycerol (Sigma) and 5% Ficoll 400 (Pharmacia Biotech), to increase the density of the sample.

3.2.1.8 Agarose gel electrophoresis

10 µg of total RNA from striata from each animal were adjacently loaded on a 12 lane, 1.2% agarose (Sigma) formaldehyde gel in an RNAase-free electrophoresis tank (Hybaid). The gel consisted of 2.88 g of agarose (Sigma) dissolved in 150 ml of DEPC-treated water by heating for 2 minutes at 800 W in a microwave (NN-5452, Panasonic). To this, 42.84 ml of formaldehyde (Sigma) and 47.13 ml of 5x formaldehyde gel running buffer (described in 3.2.1.7) was added. The agarose was poured into a gel casting tray (Hybaid) and allowed to cool. Following solidification, the gel was submerged in 1500 ml gel running buffer and samples were electrophoresised at 80V for 3 hours until the bromophenol blue marker had run three-quarters of the length of the gel. A peristaltic mini-pump (Masterflex) circulating at 50 ml per minute was used to reduce any heat build-up and recirculate ions from the negative electrode to the positive electrode, therefore reducing any pH gradient build up.

Following electrophoresis, the gel was removed from the tank, rinsed in DEPC-treated water and stained for 20 minutes in a 1 µg ml⁻¹ solution of ethidium bromide (Sigma). The gel was then destained overnight in DEPC-treated water. Ethidium bromide binds to RNA and allows visualisation, due to the high concentration of the 18S and 28S ribosomal RNA fragments at 1.8 kilobases (Kb) and 4.4 Kb respectively. The RNA was observed on a U.V. transilluminator (IBI-Kodak), and the gel photographed using a direct screen instant camera (model DS34, with a DSH-7 extension hood, Polaroid) with instant black and white film (667, Polapan ISO 3000, Polaroid) to give a permanent record of the amount of RNA in each lane. This allowed qualitative verification of equal loading between lanes and observation of degradation.

3.2.1.9 RNA transfer to nylon membrane

The gel was washed in 20 x standard sodium citrate (SSC, 3M sodium chloride, 0.3 M sodium citrate) for 45 minutes to remove remaining formaldehyde. The RNA was transferred from the gel to a nylon hybridisation membrane (Biodyne biosupport membranes, Pall) overnight by capillary action (Sambrook *et al.*, 1986). The gel was inverted and placed in contact with the nylon hybridisation membrane, pre-soaked in 20 x SSC, on a solid support in an ascending flow of buffer. This ascending flow was

achieved by placing the gel on 3 MM CHR Whatman paper (Whatman International) which is placed with both ends in the reservoir of 20 x SSC transfer buffer. The buffer is drawn up through the gel and nylon membrane via capillary action, carrying the RNA with it. Capillary action was achieved by placing two layers of 17 MM CHR Whatman paper, (pre-cut to the identical size of the nylon membrane) above the nylon membrane, followed by several layers of paper towel (also pre-cut to the size of the nylon membrane). Finally, a glass plate and a 500 g weight was placed on top of the paper towels to ensure a tight connection between the layers of materials used in the transfer system. Following transfer, the RNA was U.V. crosslinked to the membrane using an ultraviolet crosslinker with 120 J cm^{-2} exposure (UVC-508 ultraviolet crosslinker, Anachem). The membrane was observed under U.V. using a handheld U.V. lamp (UVP-mineral light lamp, UVGL-58) to confirm successful RNA transfer and enabling lanes and 18S and 28S ribosomal RNA to be marked on the membrane. Membranes were wrapped in saran-wrap and stored in a humidified sealed container at 4°C until hybridisation.

3.2.1.10 Pre-hybridisation

To block any non-specific binding sites on the membrane, a prehybridisation step was carried out. Membranes were rinsed in 2 x SSC to remove any residual formaldehyde and placed in rotating hybridisation tubes (Hybaid). Membranes were pre-hybridised overnight at 42°C in hybridisation buffer containing 25 ml of formamide (Sigma), 5 ml of 50 x Denhardt's solution (1% Ficoll type 400, Pharmacia Biotech, 1% polyvinylpyrrolidone (Sigma), 1% Bovine serum Albumin (Fraction V, Sigma)), 12.5 ml of 20 x SSC, 1.25 ml of 20% Sodium dodecyl sulphate (SDS), ? ml of 10 mg ml^{-1} Salmon testes DNA (Sigma), 0.5 ml of 5 mg ml^{-1} polyadenylic acid (Sigma).

3.2.1.11 Radiolabelling of oligonucleotide probes for Northern blot hybridisation

Synthetic oligonucleotide probes (30-45 bases in length) were synthesised by Gibco BRL, complementary to the sequence coding the rat sequence for pre-proenkephalin-A (PPE-A), pre-proenkephalin-B (PPE-B) and 18S ribosomal subunit. Specificity of these probe sequences was checked using the UK Human Genome

Mapping Project Resource Center database (both EMBL and GenBank databases, BLAST search, Altschul *et al.*, 1990) to verify that the selected sequences would not hybridise to any other known sequences. The PPE-A oligonucleotide probe was complementary to the sequence coding for bases 343-384 of the rat PPE-A gene (Accession number M28263, Howells *et al.* 1984) sequence 5'- CTT CAT GAA GCC TCC ATA CCG TTT CAT GAA CCC TCC ATA CTT -3'. The PPE-B oligonucleotide probe was complementary to the sequence coding for bases 754-798 of the rat PPE-B gene (Accession number RNEKB M10088, Civelli *et al.*, 1985) sequence 5'- GCT CCT CTT GGG GTA TTT GCG CAA AAA GCC GCC ATA GAG TTT GGC -3'. The 18S ribosomal subunit oligonucleotide probe was used as a control probe in all Northern blot hybridisations. This probe is complementary to nucleotides 519-550 of the human 18S ribosomal gene (98.8% homologous to the rat), sequence 5'- TTT CTC AGG CTC CCT CTC CGG AAT CGA ACC -3' (Torczynski *et al.*, 1985; 1983).

3'-end labelling of each oligonucleotide probe was carried out using [α 32 P]-dATP. 1 μ l of the oligonucleotide at a concentration of 20 ng μ l $^{-1}$ was labelled by the isotope at an incubation temperature of 37°C in a mixture containing 9 μ l sterile water, 12.5 μ l reaction buffer (sodium cocodylate pH 7.2 and dithiothreitol), 2.5 μ l cobalt chloride, and 2 μ l terminal deoxynucleotide transferase, pH 7.2 (all reagents DuPont/NEN) with 8 μ l of [α 32 P]-dATP (NEN). Following a 30 minute incubation at 37°C the reaction was stopped by addition of 50 μ l of ice-cold sterile water. The labelled probe was subsequently purified (to separate out unincorporated isotope from the labelled probe) using Bio-spin chromatography columns (Bio-Rad) centrifuged at 1 100 g_{av} for 4 minutes (Z382K, Hermel). 32 P-labelled probes were kept on ice until use. 1 μ l of the labelled oligonucleotide probe was removed, added to 5 ml scintillation fluid (Ecoscint A, Mensura) and counted in a liquid scintillation beta-counter (Tricarb 1500, Packard) for 2 min to assess the efficiency of radioactive labelling. Counts above 500 000 counts per minute per μ l were considered to be acceptable for hybridisation.

3.2.1.12 Hybridisation

Following pre-hybridisation, hybridisation was carried out by addition of 4000 counts per minute per μ l of hybridisation buffer of 32 P-dATP-labelled oligonucleotide to the pre-hybridisation buffer.

Depending on the sequence, length, guanosine and cytosine content of the oligonucleotide probe, concentration of monovalent cations and formamide in the hybridisation solution, the optimal hybridisation conditions for each probe will vary. This is called the probe melting temperature (T_m). T_m for each probe was calculated using the following calculation (Wilkinson, 1992):

$$T_m = 79.8 + 18.5 \log (\text{molarity of monovalent cations}) + 0.58 (\%GC \text{ content of the probe}) + 0.12 (\% GC \text{ content})^2 - 820/(\text{length of probe in bases}) - 0.35 (\% \text{ formamide})$$

This T_m calculation is only an approximation, with hybridisation usually carried out at 20-25°C below the calculated T_m , therefore the optimal hybridisation temperature was calculated empirically. Hybridisation temperatures both above and below that of the calculated T_m were employed. Using this formula the calculated T_m for pre-proenkephalin-A, pre-proenkephalin-B, and 18S were 68.8°C, 73.7°C and 75.5°C respectively. Pre-proenkephalin-A (PPE-A) and pre-proenkephalin-B (PPE-B) oligonucleotides were hybridised for 18 hours (overnight) at 32°C, 42°C and 52°C to determine the optimal hybridisation temperature for both of the oligonucleotide probes.

3.2.1.13 Membrane wash

Following hybridisation, membranes were washed briefly with 1 x SSC containing 0.1% SDS at room temperature, followed by a 30 minute wash with 1 x SSC and 0.1% SDS at room temperature, then a further 30 minute wash at 55°C with 1 x SSC and 0.1% SDS. To optimise specific vs non-specific hybridisation signal, the final wash temperature for each oligonucleotide probe was determined, experimentally. Thus, a final 10 minute wash with 0.1 x SSC and 0.1% SDS at various temperatures (37°C, 55°C and 65°C) was performed. Following this final wash, membranes were wrapped in saran-wrap and exposed to Hyperfilm-MP (Amersham) between hyper-intensifying screens (Fastspeed, Amersham) at -70°C for 1-14 days.

3.2.1.14 Hyperfilm-MP autoradiographic film exposure time for specific probes

Depending on the abundance of the mRNA transcript and hence probe concentration, varying exposure times are required. Various exposure times for the probe signal were employed to optimise the exposure time for each probe. For each probe, the exposure time was varied and the film developed at 24 hours, 7 days and 14 days post-hybridisation. For each probe the optimum exposure time was calculated by measuring integrated optical density (i.O.D.) readings of 10 µg of electrophoresed striatal RNA. Optimal exposure times were defined as when the i.O.D. reading were within the specified linear part of the films response (as determined in section 3.2.1.16).

3.2.1.15 Autoradiographic film development

Hyperfilm-MP autoradiographic films were developed in D-19 developer (Kodak) for 6 minutes, rinsed in cold tap water then fixed in Unifix (Kodak) for 15 minutes, given a final rinse, and left to dry at room temperature.

3.2.1.16 Linearity of Hyperfilm-MP autoradiographic film response

To check the linearity of the response of Hyperfilm-MP (Amersham) film to the amount of radioactivity and therefore ensure that even with the most abundant signal, any alterations in signal could be distinguished, a concentration gradient of mRNA (2.5 - 20 µg of RNA) was prepared and probed using the 18S oligonucleotide probe (the most abundant transcript to be investigated). This membrane was then exposed for 12 hours, 24 hours and 48 hours. The integrated optical density values (i.O.D) for each of the lanes (2.5-20µg), for each of the exposure time periods were measured and plotted against the concentration of mRNA. This was used to investigate the linearity of the Hyperfilm-MP autoradiographic film in relation to the probe signal. An integrated optical density (i.O.D.) range was determined over which the response of the film remained linear. This range was used in the subsequent Northern blot hybridisations.

3.2.1.17 Re-probing of membranes

To re-hybridise membranes with different probes, the membranes were stripped at a high stringency consisting of a 30 minute period in boiling 0.1 x SSC and 0.1% SDS. Membranes were re-exposed to the Hyperfilm-MP (Amersham) film to check no probe signal remained, then re-hybridised. To ensure this stripping was a valid procedure, and ensure no loss of signal resulted from the stripping procedure, membranes were probed with pre-proenkephalin-A (PPE-A) and pre-proenkephalin-B (PPE-B) and exposed to Hyperfilm-MP autoradiographic film for 7 and 14 days respectively. The films were developed and fixed as described in 3.2.1.15. The probes were then stripped from the membranes by boiling in 0.1x SSC and 0.1% SDS for 30 minutes. The membranes were then re-exposed to film, left for the same time period, after which the film was developed and fixed as described in 3.2.1.15. The membranes were then pre-hybridised, re-hybridised and exposed to film as described in 3.2.1.10-15 and left for the same time period as above. Finally, the films were developed and fixed as described in 3.2.1.15. The integrated optical density for both probes was measured for the first hybridisation, following stripping and then for the second hybridisation.

3.2.1.18 Analysis of integrated optical density signal

Seescan Image Analysis equipment (Seescan, Inc.) was used to quantify the integrated optical density (i.O.D.) value from the Hyperfilm-MP autoradiographic film. A value for both the probe of investigation (pre-proenkephalin-A (PPE-A) or pre-proenkephalin-B (PPE-B)) and the 18S ribosomal subunit was measured and a ratio of PPE-A to 18S or PPE-B to 18S was determined.

3.2.2 Reserpine-treated rat model of Parkinson's disease

3.2.2.1 Animals and drug treatment

Male Sprague Dawley rats (250-300g) were obtained from Charles River, maintained in standard housing conditions with constant temperature ($22 \pm 1^\circ\text{C}$), humidity (relative, 30%), 12 hour light/dark cycles (light period 8 a.m./8 p.m.) and were

allowed free access to food (Standard pellets, B & K Universal) and water. Twelve rats were placed into 2 experimental groups. All animals were anaesthetised with halothane (Fluorothane, Zeneca) and injected subcutaneously with either 8 mg kg⁻¹ reserpine (80 mg reserpine (Sigma) dissolved by addition of 80 µl glacial acetic acid (BDH) dropwise and by sonication, then diluted to 10 ml with sterile water (Braun Medical), or vehicle (80 µl glacial acetic acid (BDH) in 10 ml sterile water (Braun Medical) both injected at a volume of 1 ml kg⁻¹ of body weight.

3.2.2.2 Behavioural analysis

Eighteen hours post-subcutaneous injection of either reserpine (8 mg kg⁻¹) or vehicle, rats were placed in open field arena locomotor boxes (Amlogger) and the locomotor score recorded for 30 minutes as described in 2.2.11.

3.2.2.3 Total mRNA extraction

Twenty hours post-subcutaneous injection of either reserpine (8 mg kg⁻¹) or vehicle rats were killed by cervical dislocation and the striatum quickly dissected out, on ice, and placed in RNazol B solution as in 3.2.1.4. Total mRNA was extracted as described in 3.2.1.6.

3.2.2.4 Northern blot hybridisation of reserpine-treated animals

Gel electrophoresis, transferral to membrane and Northern blot hybridisation was carried out as described in 3.2.1.8, 3.2.1.9 and 3.2.1.10-15, respectively. Lanes were loaded with 10 µg of mRNA from the striatum of either reserpine or vehicle treated animals, placed in alternating lanes. Membranes were hybridised using an oligonucleotide probe targeted against pre-proenkephalin-A (PPE-A) transcript, then stripped (as described in 3.2.1.17) and re-probed using an oligonucleotide probe targeted against the 18S ribosomal subunit transcript. Membranes were exposed to Hyperfilm-MP autoradiographic film as described in 3.2.1.13 and were developed as in 3.2.1.15. Integrated optical density was measured for both probes and the ratio of PPE-A to 18S control probe was determined.

3.2.3 6-OHDA-lesioned rodent model of Parkinson's disease

3.2.3.1 Animals and drug treatment

Twenty four male Sprague Dawley rats (250-300 g) were obtained from Charles River, maintained in standard housing conditions with constant temperature ($22 \pm 1^\circ\text{C}$), humidity (relative, 30%), 12 hour light/dark cycles (light period 8 a.m./8 p.m.) and were allowed free access to food (Standard pellets, B & K Universal) and water. 12 rats received unilateral 6-hydroxydopamine lesions of the medial forebrain bundle, while 12 rats received sham-lesions as described in 2.1.1.

3.2.3. Behavioural analysis

Twenty one days post-operatively both the 6-hydroxydopamine-lesioned and sham-lesioned rats were removed from their home cage and, following an i.p injection of sterile water (1 ml kg^{-1}), placed in a 40 cm diameter stainless-steel bowl with a video camera placed above to record activity. Both full ipsiversive and contraversive rotations were recorded over a two hour period. 6-hydroxydopamine lesioned animals obtaining a net ipsiversive rotation greater than 30 rotations/hour were then divided into two experimental groups. One group received an i.p. injection of 0.1% ascorbic acid (vehicle group), the other received co-injections of 6.5 mg kg^{-1} L-DOPA and 1.5 mg kg^{-1} benserazide both dissolved in 0.1% ascorbic acid (L-DOPA group), both injected at 1 ml kg^{-1} of body weight. Sham-lesioned animals were also divided into two experimental groups one receiving L-DOPA and the other vehicle as described above. All animals received two injection per day 8 hours apart (9 a.m. and 5 p.m). Behavioural analysis was carried out 2 hours following the a.m. injection on days 0, 1, 3, 5, 7, 10, 14, 17, and 21 of injection. Following 21 days of treatment, two hours following the final p.m. injection the animals were killed by stunning and cervical dislocation, the brains were removed and following hemitranssection the striatum was dissected and lesioned and unlesioned or sham-operated or sham-unoperated striatum placed separately in 5 ml RNazol B for further processing and extraction of total RNA as described in 3.2.1.4.

3.2.2.7 Northern Blot hybridisation of 6-OHDA-lesioned or sham-lesioned animals

Gel electrophoresis and Northern blot hybridisation was carried out as described in 3.2.1.8-15. Ten lanes were loaded with 10 µg of mRNA from either lesioned or unlesioned and sham-lesioned or sham-unoperated striatum, and placed in alternating lanes. Membranes were hybridised using oligonucleotide probes targeted against the dynorphin precursor pre-proenkephalin-B (PPE-B), stripped and re-probed for the enkephalin precursor, pre-proenkephalin-A (PPE-A). Finally membranes were stripped and re-probed for the 18S ribosomal subunit. Membranes were exposed to Hyperfilm-MP autoradiographic film as described in 3.2.1.13 and were developed as in 3.2.1.15. Integrated optical density was measured for all probes and the ratio of PPE-A and PPE-B to 18S control probe were determined.

3.2.4 Functional antagonism of opioid receptors in the rat model of L-DOPA-induced dyskinesia

3.2.4.1 6-OHDA-lesioned rodent model of Parkinson's disease

Male Sprague Dawley rats (250-300g) were obtained from Charles River UK, maintained in standard housing conditions with constant temperature ($22 \pm 1^\circ\text{C}$), humidity (relative, 30%), 12 hour light/dark cycles (light period 8 a.m./8 p.m.) and were allowed free access to food (Standard pellets, B & K Universal) and water. Rats received unilateral 6-hydroxydopamine lesions of the medial forebrain bundle as described in 2.2.1.

3.2.4.2 Drug treatment and behavioural analysis

Twenty one days post-operation the 6-hydroxydopamine-lesioned rats were removed from their home cage and injected with sterile water (1 ml kg^{-1} , i.p.) and placed in a 40 cm diameter stainless-steel bowl. Behaviour was recorded on videotape. Videotapes were analysed and the number of complete 360° rotations ipsiversive and contraversive to the lesion were counted over a 2 hour period. 6-hydroxydopamine lesioned animals obtaining a net ipsiversive rotation less than 30 rotations/hour were

removed from the experimental group. Animals received injections of 6.5 mg kg^{-1} L-DOPA (Sigma) and 1.5 mg kg^{-1} benserazide (Sigma) both dissolved in 0.1% ascorbic acid (Sigma) and injected at a volume of 1 ml kg^{-1} of body weight. All animals received two injection per day (9 a.m. and 5 p.m.). Behavioural assessment was carried out for 2 hours following the 9 a.m. injection. Following 14 days of treatment the animals were co-injected with various opioid receptor antagonists to give maximal effect at 45 minutes following L-DOPA injection and filmed for a further 30 minutes. Antagonists tested were; the non-selective opioid receptor antagonist naloxone (Sigma) at doses 0.01 mg kg^{-1} , 0.03 mg kg^{-1} , 0.05 mg kg^{-1} , 0.5 mg kg^{-1} , 5 mg kg^{-1} ; the selective delta opioid receptor antagonist naltrindole (Sigma) at 10 mg kg^{-1} ; the selective kappa opioid receptor antagonist *nor*-binaltorphamine (Research Biochemicals International) at 20 mg kg^{-1} and the selective mu opioid receptor antagonist cyprodime (Research Biochemicals International) at 10 mg kg^{-1} , all dissolved in 0.1% ethanol (BDH) and injected at 1 ml kg^{-1} of body weight. Net ipsiversive and contraversive rotations were recorded from 45 minutes to 60 minutes post L-DOPA/benserazide and expressed as a percentage compared to the same time period for the vehicle control on the following day. The animals were tested for up to 21 days with each second day as a wash-out control day.

3.2.5 Statistical analysis

Data are expressed as mean \pm standard error of the mean (SEM) values. Integrated optical density values of hybridisation signal following re-probing of membranes were analysed by paired Student's t-test. Spontaneous locomotion following reserpine administration and integrated optical density values following Northern blot hybridisation were analysed by unpaired Student's t-test. Rotational behavioural data, following repeated drug or vehicle administration, were analysed by multiple analysis of variance (MANOVA), followed by unpaired student's t-test. Integrated optical density values from Northern blot hybridisation following repeated L-DOPA or vehicle administration were analysed by paired Student's t-test. Effect of drug or vehicle administration on L-DOPA-induced hyperkinesia were analysed using one-way analysis of variance (ANOVA) followed by Dunnett's or Student-Newman-Keuls post hoc analysis where appropriate. In all tests significance was assigned when $P < 0.05$.

3.3 Results

3.3.1 Methodological optimisation of Northern blot hybridisation

To optimise the extraction procedure for rat striatal RNA, three extraction procedures were employed. The first technique involved making all buffers using the Chomczynski and Sacchi (1987) method, the second by use of the commercially-available RNazol B (Biogene) and the third involved further purification of the total RNA extracted by the RNazol B method by poly-A purification to purify mRNA (Oligotex mRNA mini kit, Qiagen). Contamination of RNA extracts can be detected by utilising the absorption of the extract at both 260 and 280 nm, by calculating the ratio of 260:280 nm, ratios between 1.8 and 2 have been reported to be relatively pure and free from DNA and protein contamination (Sambrook *et al.*, 1986). The optimal extraction procedure to isolate both a useful amount of RNA, with little contamination by proteins and DNA (as indicated by the 260:280 nm absorption ratio) was the RNazol B method. The Chomczynski and Sacchi method isolated 45% less RNA than the RNazol B extraction procedure and qualitatively the extracted RNA was poor. RNazol B extraction followed by poly-A purification, produced relatively pure mRNA, though a yield that was insufficient to run more than one lane per sample (Table 3.1). Therefore, in all subsequent Northern blot hybridisation experiments the RNazol B extraction method was used to isolate RNA.

Extraction method	RNA type	RNA ($\mu\text{g } \mu\text{l}^{-1}$)	Ratio 260:280	Total yield (μg)
Chomczynski and Sacchi Phenol-Chloroform	total RNA	0.89 ± 0.16	1.6 ± 0.11	17.4 ± 3.3
RNazol B	total RNA	1.96 ± 0.08	1.89 ± 0.04	39.3 ± 1.6
RNazol B followed by Poly-A purification	poly-A mRNA	$2.7 \times 10^{-3} \pm 2.2 \times 10^{-4}$	2.1 ± 0.14	1.37 ± 0.11

Table 3.1 Optimisation of striatal RNA extraction procedure

Total RNA was extracted from rat striatum using either the Chomczynski and Sacchi method or the commercially-available RNazol B solution. Extracted striatal RNA was resuspended in 20 μl of 1 mM EDTA. 1 μl of this solution was removed and the purity of the extract, via the ratio of 260:280 absorbance and the total yield per striatum are shown (mean \pm SEM, $n = 12$). Also shown is amount of RNA isolated following further poly-A mRNA purification with purity and total yield (mean \pm SEM, $n = 12$).

Following gel electrophoresis and transfer to nylon membrane, the hybridisation conditions for each oligonucleotide probe were optimised by altering a variety of conditions. The first condition critical for optimal binding of oligonucleotide probes to transcript mRNA is the temperature of hybridisation (Sambrook *et al.*, 1986). The hybridisation temperature was varied using parameters defined from Northern blot hybridisation studies in the literature (Sambrook *et al.*, 1986). Hybridisation was performed at temperatures of 37°C, 42°C or 52° for both pre-proenkephalin-A (PPE-A) and pre-proenkephalin-B (PPE-B) oligonucleotide probes.

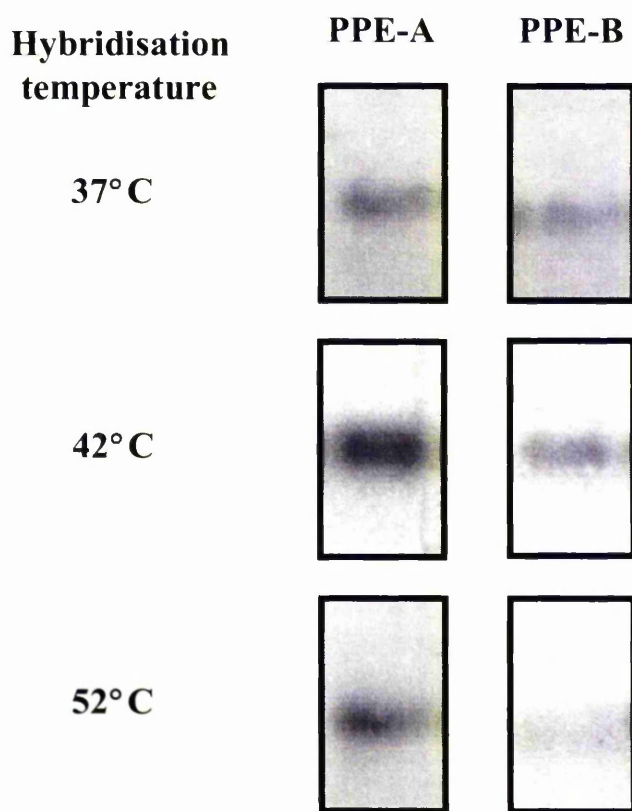


Figure 3.3.1.1 Northern blot autoradiographs of oligonucleotide probes targeted to pre-proenkephalin-A and pre-proenkephalin-B transcripts illustrating the effect of varying hybridisation temperature

10 µg of striatal RNA was hybridised with oligonucleotide probes targeted against pre-proenkephalin-A (PPE-A) and pre-proenkephalin-B (PPE-B) mRNA transcripts at 37°C, 42°C and 52°C for 18 hours and exposed to Hyperfilm-MP for 7-14 days as described in table 3.2.

Once hybridised, the membranes were exposed to film and developed after 24 hours, 7 days, or 14 days for 18S, PPE-A and PPE-B, respectively (Table 3.4). Following integrated optical density measurements of hybridisation signal, it can be seen that hybridisation at 42°C gave the maximal signal for both probes (Figure 3.3.1.1, Table 3.2). This was used in all subsequent experiments.

Hybridisation temperature (°C)	PPE-A (i.O.D. x 10 ⁻³)	PPE-B (i.O.D. x 10 ⁻³)
37	1.523 ± 0.02	8.983 ± 0.02
42	3.438 ± 0.01	15.23 ± 0.02
52	1.819 ± 0.03	7.983 ± 0.02

Table 3.2 Effect of varying hybridisation temperature on integrated optical density signal: optimisation of hybridisation temperature

Table showing integrated optical density (i.O.D.) measurements following various hybridisation temperatures. 10 µg of isolated striatal RNA, were hybridised with oligonucleotide probes targeted against pre-proenkephalin-A (PPE-A) and pre-proenkephalin-B (PPE-B) mRNA transcripts, at 37°C, 42°C and 52°C, for 18 hours as described in section 3.2.1.14. Membranes were washed as described in 3.2.1.15. Integrated optical density is expressed as mean (±SEM)(n=3).

Another critical factor for optimal hybridisation in Northern blot hybridisation, is the temperature of the final wash to remove non-specific hybridisation. Following a final wash temperature of 55°C, a hybridisation signal is detected with very low non-specific binding (Figure 3.3.1.2, Table 3.3). At 37°C high levels of non-specific binding are detected and at the higher temperature of 65°C, neither non-specific nor specific hybridisation signal are detected (Figure 3.3.1.2, Table 3.3). A final wash temperature of 55°C was used in all subsequent experiments.

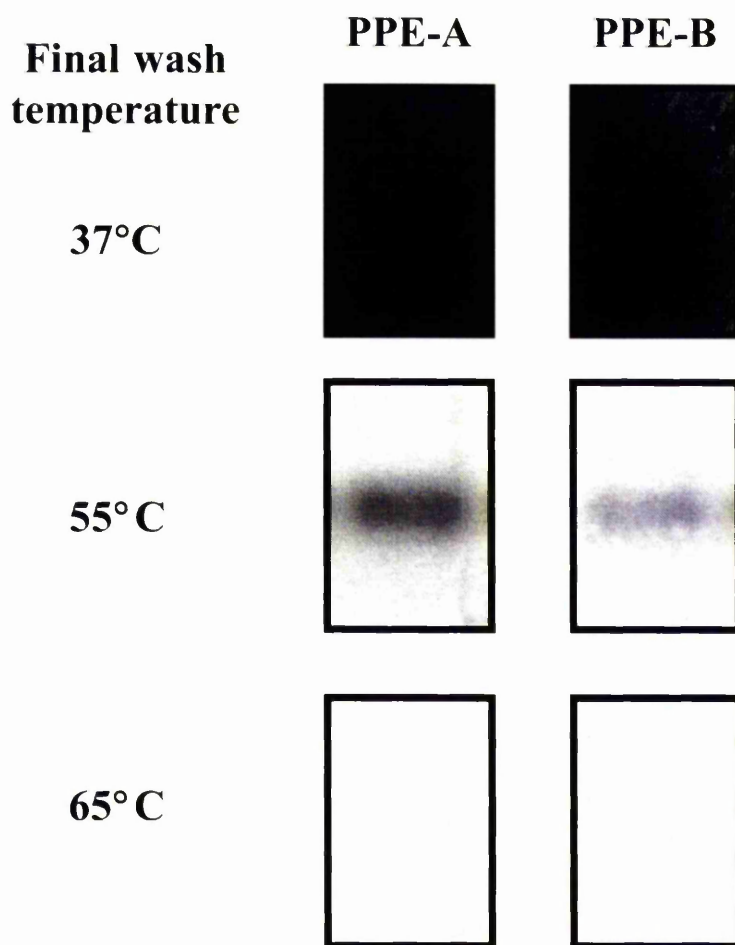


Figure 3.3.1.2 Northern blot autoradiographs of oligonucleotide probes targeted against pre-proenkephalin-A (PPE-A) and pre-proenkephalin-B (PPE-B) mRNA transcripts: illustrating effects of varying post-hybridisation wash stringency

Northern blot hybridisation signal utilising oligonucleotide probes targeted against PPE-A and PPE-B mRNA transcripts, following increasing stringency of washes. Membranes were hybridised at 42°C for 18 hours as described in section 3.2.1.10-15, washed and exposed to Hyperfilm-MP autoradiographic film following a range of washes of differing stringency. All membranes were washed initially with 1 x SSC and 0.1% SDS for 30 minutes at room temperature, 1 x SSC and 0.1% SDS at 55°C for 30 minutes. A final ten minute wash with 0.1 x SSC and 0.1% SDS were performed at either 37°C, 55°C or 65°C.

Final wash temperature (°C)	PPE-A (i.O.D.)	PPE-B (i.O.D.)
37	$6.09 \times 10^{-4} \pm 1.44 \times 10^{-5}$	$4.25 \times 10^{-4} \pm 1.25 \times 10^{-5}$
55	$1.508 \times 10^{-3} \pm 1.3 \times 10^{-4}$	$8.767 \times 10^{-4} \pm 5.5 \times 10^{-5}$
65	$< 1.0 \times 10^{-6}$	$< 1.0 \times 10^{-6}$

Table 3.3 Northern analysis of oligonucleotide probes targeted against pre-proenkephalin-A (PPE-A) and pre-proenkephalin-B (PPE-B) mRNA transcripts: Integrated optical density following increased wash stringency

Table showing integrated optical density measurements following increased stringency of washes. Membranes were hybridised with oligonucleotide probes targeted against PPE-A and PPE-B mRNA transcripts at 42°C for 18 hours as described in section 3.2.1.10-15., washed and exposed to Hyperfilm-MP autoradiographic film following a range of washes with differing stringency. All membranes were washed initially with 1 x SSC and 0.1% SDS for 30 minutes at room temperature, 1 x SSC and 0.1% SDS at 55°C for 30 minutes. A final ten minute wash with 0.1 x SSC and 0.1% SDS were performed at either 37°C, 55°C or 65°C. Integrated optical density values are expressed as mean (\pm SEM) (n=3).

To verify the specificity of the oligonucleotide probes for both PPE-A, PPE-B and the control probe 18S, 10 μ g of rat striatal RNA was electrophoresed with RNA molecular weight markers in the adjacent lanes. Following hybridisation, all oligonucleotide probes displayed a single band (indicating specificity for a single target), with each running at a different molecular weight: PPE-A at 1.4 Kb; PPE-B at 2.4 Kb; and 18S at 1.8 Kb (Figure 3.3.1.3).

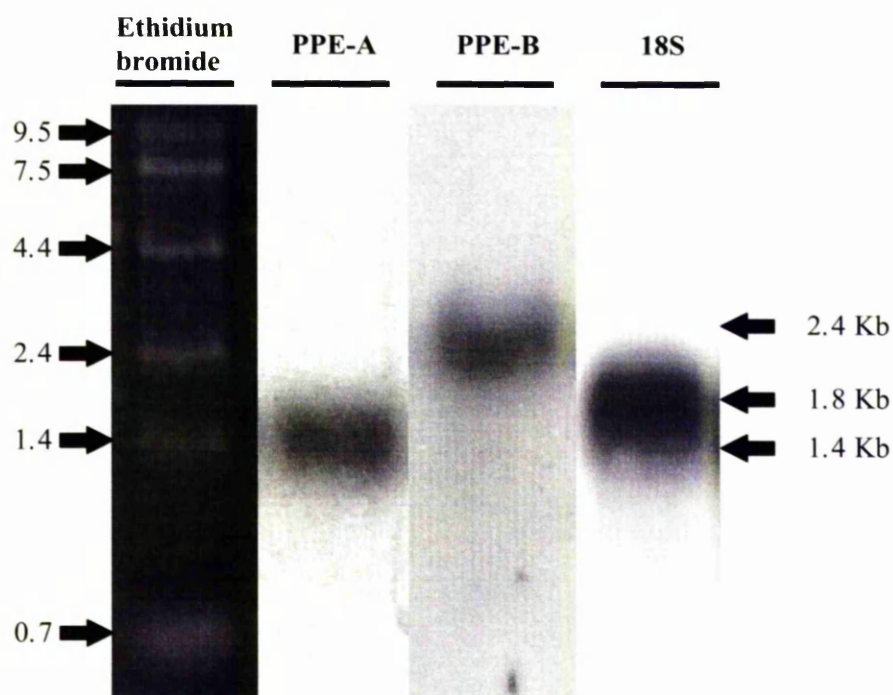


Figure 3.3.1.3 Northern blot of striatal mRNA hybridised with oligonucleotides targeted against pre-proenkephalin-A, pre-proenkephalin-B and 18S control probe transcripts: determination of the molecular weight utilising ethidium bromide stained RNA markers

Northern blot hybridisation signal utilising oligonucleotide probes targeted against the mRNA transcripts encoding pre-proenkephalin-A (the enkephalin precursor, PPE-A), pre-proenkephalin-B (the dynorphin precursor, PPE-B) and the 18S ribosomal subunit (18S). Membranes were hybridised at 42°C for 18 hours as described in 3.2.1.10-15, washed and exposed to Hyperfilm-MP autoradiographic film for 1-14 days as described in table 3.4. Membranes also indicated molecular markers (0.7-9.5 Kb) as determined by ethidium bromide staining, illuminated by ultra violet light.

The linearity of the film response to the hybridisation signal, was investigated by hybridisation of a concentration gradient of RNA with an oligonucleotide probe targeted to the control probe 18S transcript. Once hybridised, this membrane was exposed to Hyperfilm-MP for varying time periods. The film response, as measured by integrated optical density, remained linear in relation to the signal, up to the maximal time period and concentration of RNA used (Figure 3.3.1.4). Hyperfilm-MP exposure times for oligonucleotide probes targeted against PPE-A, PPE-B and 18S control probe were optimised to produced a signal on the linear part of the films

response (i.e. between 0.025 - 8.925×10^{-3}). The optimal time period of exposure for each probe was therefore identified as being 7 days for the PPE-A oligonucleotide probe, 14 days for the PPE-B oligonucleotide probe and 24 hours for the 18S control oligonucleotide probe (Figure 3.3.1.5).

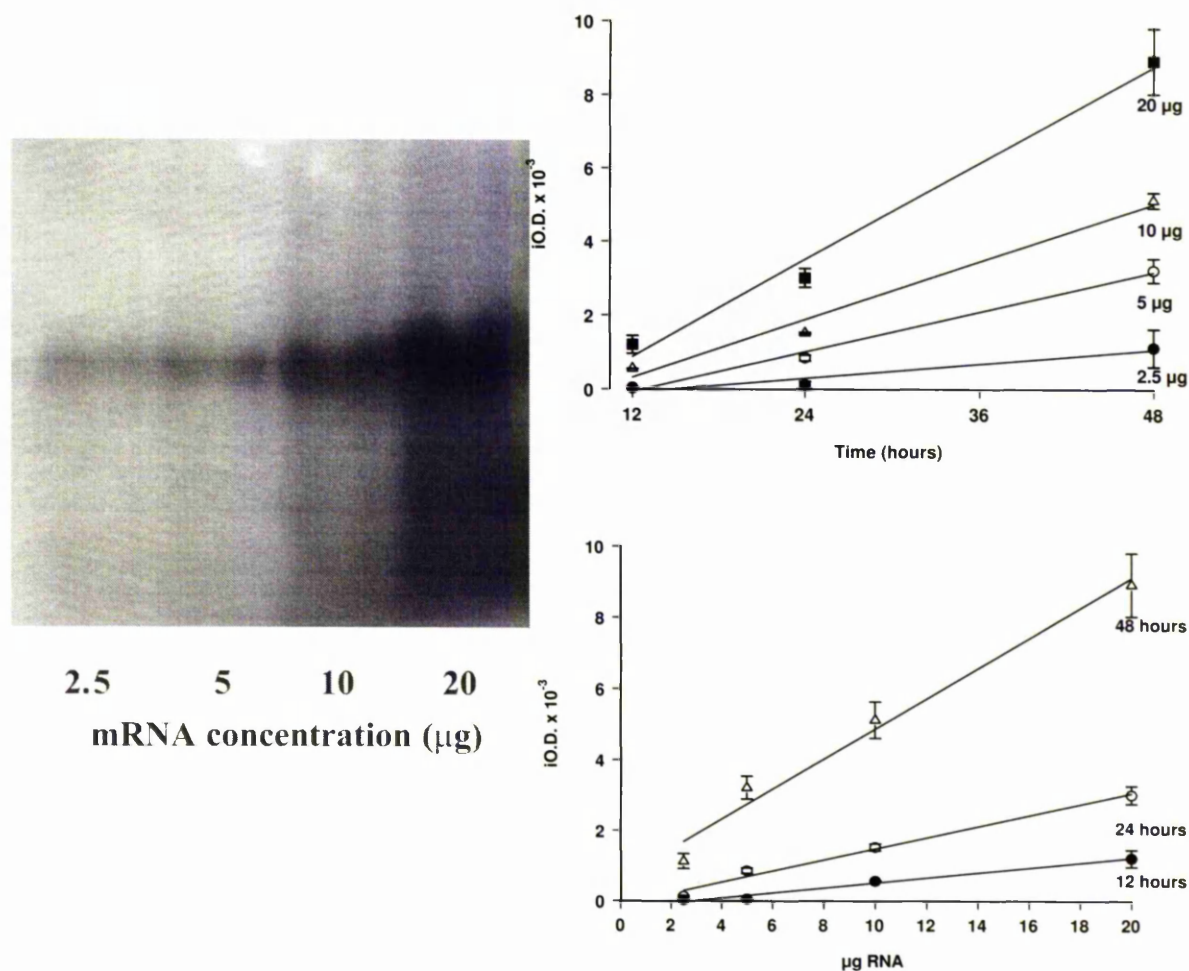


Figure 3.3.1.4 Effect of exposure time and mRNA concentration on oligonucleotide probe signal targeted against 18S ribosomal subunit, utilising Hyperfilm-MP autoradiographic film

A range of concentrations of striatal RNA (2.5-20 µg) was hybridised with an oligonucleotide probe targeted against the 18S ribosomal subunit RNA as described in section 3.2.1.16 and exposed to Hyperfilm-MP for 12, 24, 36 and 48 hours. Integrated optical density of each band was measured at these time points. Integrated optical density values are expressed as mean (\pm SEM) ($n=3$).

Oligonucleotide probe	Integrated optical density of hybridisation signal (i.O.D.)		
	Exposure time		
	24 hours	7 days	14 days
PPE-A	$< 1.0 \times 10^{-6}$	2.198×10^{-3} $\pm 9.071 \times 10^{-5}$	5.923×10^{-2} $\pm 5.124 \times 10^{-3}$
PPE-B	$< 1.0 \times 10^{-6}$	1.604×10^{-5} $\pm 3.087 \times 10^{-6}$	1.734×10^{-3} $\pm 5.875 \times 10^{-4}$
18S	2.235×10^{-3} $\pm 5.425 \times 10^{-4}$	0.133 $\pm 1.047 \times 10^{-2}$	0.189 $\pm 5.855 \times 10^{-3}$

Table 3.4 Optimisation of exposure times utilising oligonucleotide probes targeted against striatal mRNA transcripts, encoding the opioid peptide precursors pre-proenkephalin-A, pre-proenkephalin-B and the ribosomal subunit 18S

Oligonucleotide probes targeted against pre-proenkephalin-A (PPE-A), pre-proenkephalin-B (PPE-B) and 18S ribosomal subunit, at a concentration of 4000 cpm per μ l of hybridisation solution, were exposed to Hyperfilm-MP autoradiographic film using hyperscreen intensifying screens, for 24 hours, 7 days and 14 days, to determine the optimal exposure time for membranes probed with each oligonucleotide probe. Optimal exposure times were determined as being within the range $0.025 - 8.925 \times 10^{-3}$. PPE-A exposed for 7 days, PPE-B for 14 days and 18S for 24 hours all gave a hybridisation signal within the linear detection range for the Hyperfilm-MP. Integrated optical density values are expressed as mean (\pm SEM) ($n=3$).

To perform more accurate quantification of Northern blot hybridisation the ratio to a control probe was carried out, to control for unequal loading or degradation between lanes. To investigate more than one probe and to re-hybridise for the control probe, one assumes there is no loss of signal through the membrane stripping procedure. To demonstrate that membranes could be stripped following a first hybridisation, then successfully re-probed without any loss of signal, 10 μ g of striatal RNA was hybridised with oligonucleotide probe targeted to PPE-A and PPE-B mRNA transcripts and exposed to film (Figure 3.3.1.5, A). Following development of the film, the membranes were stripped and re-exposed to Hyperfilm to check the oligonucleotide probe had been removed (Figure 3.3.1.5, B). The membrane was then

re-probed without any significant loss of signal, indicating that re-probing the same membrane for a different probe would not result in any loss of signal (Figure 3.3.1.5, Table 3.5).

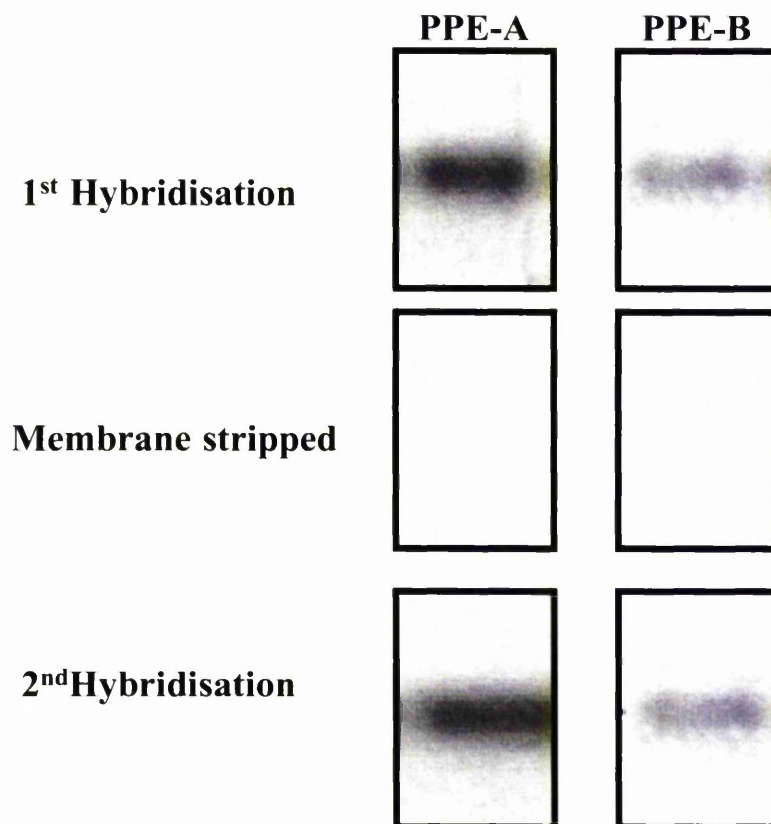


Figure 3.3.1.5 Stripping and re-probing of oligonucleotide probes targeted to pre-proenkephalin-A and pre-proenkephalin-B mRNA transcripts

Membranes were hybridised with oligonucleotide probes targeted against mRNA transcripts encoding the opioid precursor pre-proenkephalin-A (PPE-A) and pre-proenkephalin-B (PPE-B), exposed to Hyperfilm-MP autoradiographic film and developed. Membranes were then stripped, re-exposed to Hyperfilm-MP film and developed as before to check the successful stripping of the probe. Membranes were then re-probed with the same oligonucleotide probe, exposed to the Hyperfilm-MP autoradiographic film and developed as before.

Oligonucleotide probe	integrated optical density of hybridisation signal (i.O.D.)		
	1 st hybridisation	stripped	2 nd hybridisation
PPE-A	2.036×10^{-3} $\pm 3.001 \times 10^{-5}$	$< 1.0 \times 10^{-6}$	1.986×10^{-3} $\pm 1.33 \times 10^{-5}$
PPE-B	7.983×10^{-4} $\pm 3.528 \times 10^{-5}$	$< 1.0 \times 10^{-6}$	7.214×10^{-4} $\pm 2.154 \times 10^{-5}$

Table 3.5 Effect of stripping and re-probing of oligonucleotide probes targeted against pre-proenkephalin-A and pre-proenkephalin-B mRNA transcripts on signal detection

Integrated optical density values are shown for first hybridisation, following stripping and second hybridisation. No degradation or loss of signal due to stripping and re-probing was observed. Integrated optical density values are expressed as mean (\pm SEM). No significant difference was observed between the signal obtained on the first or second hybridisation for either probe ($n=6$, ns, $P > 0.5$, paired Student's t -test).

3.3.2 Pre-proenkephalin-A mRNA expression in the reserpine-treated rat model of Parkinson's disease

Pre-proenkephalin-A (PPE-A) expression was measured in the reserpine-treated rat model of Parkinson's disease. Eighteen hours following reserpine administration, rats showed a marked decrease in spontaneous locomotion (Figure 3.3.2.1).

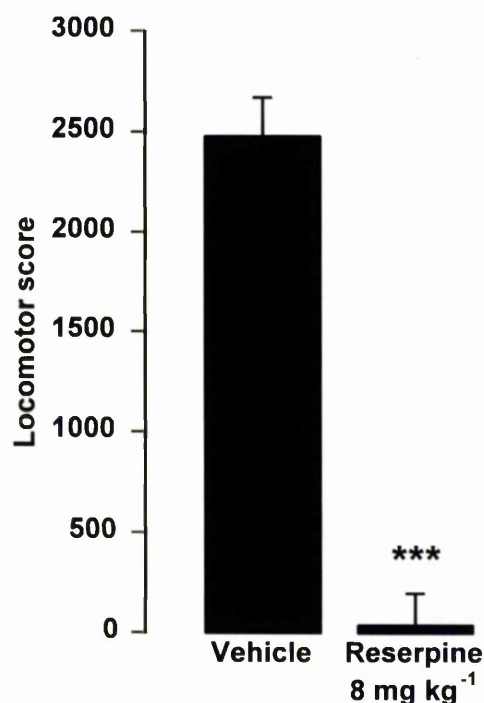


Figure 3.3.2.1 Spontaneous locomotion in rats 18 hours following reserpine-administration

*Rats were injected with reserpine (8 mg kg⁻¹, s.c.) or vehicle (both injected at 1 ml kg⁻¹ of body weight). Eighteen hours later, rats were placed in an open field arena (52 x 36 cm) and locomotion assessed for 30 minutes. Locomotion is expressed as mean (± SEM) locomotor score (n=6, *** P < 0.01, unpaired Student's t-test).*

Twenty hours following reserpine administration, striatal RNA was extracted and 10 µg of RNA from reserpine-treated or vehicle-treated rats were electrophoresed on a 1.2% agarose gel. Ethidium bromide staining of the gel indicated equal loading of the lanes (Figure 3.3.2.2). Following hybridisation with an oligonucleotide probe

targeted against the PPE-A mRNA transcript, a marked increase in PPE-A expression is seen in the reserpine-treated group when compared to vehicle-treated. No changes in the 18S control probe indicated equal loading of all lanes on the gel (Figure 3.3.2.2). Following optical density analysis, a 75% increase in PPE-A expression is observed ($P < 0.05$, Figure 3.3.2.3).

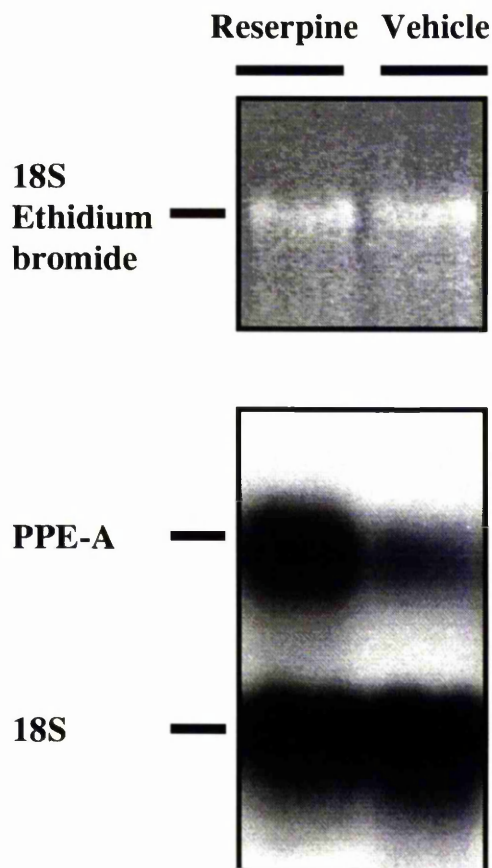


Figure 3.3.2.2 Northern blot hybridisation utilising oligonucleotide probes targeted against pre-proenkephalin-A and 18S mRNA transcripts, 20 hours following reserpine-administration in the reserpine-treated rat model of Parkinson's disease

Northern blot hybridisation utilising oligonucleotide probes targeted against pre-proenkephalin-A (PPE-A) and 18S control probe mRNA transcripts from striatal RNA extracted 20 hours following reserpine (8 mg kg⁻¹) or vehicle administration. 10 µg of total striatal RNA is present in each lane, as indicated by ethidium bromide stain under ultraviolet light following gel electrophoresis, showing both intact RNA and equal loading of lanes.

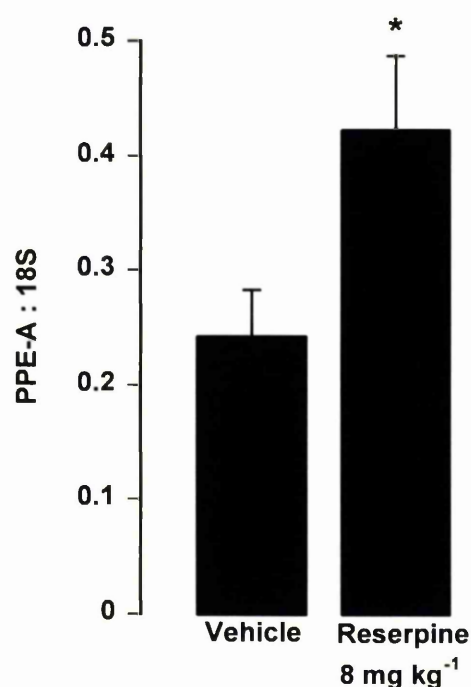


Figure 3.3.2.3 Ratio of striatal pre-proenkephalin-A:18S expression 20 hours following reserpine-administration

*Rat striatal RNA was extracted and Northern blot hybridisation carried out utilising oligonucleotide probes targeted against pre-proenkephalin-A (PPE-A) and 18S ribosomal subunit mRNA transcripts, 20 hours following reserpine (8 mg kg⁻¹) or vehicle administration. PPE:18S expression is expressed as mean (± SEM) (n=6, * P < 0.05, unpaired Student's t-test).*

3.3.3 Pre-proenkephalin-A and Pre-proenkephalin-B mRNA expression in the rat model of L-DOPA-induced dyskinesia

Alterations in pre-proenkephalin-A (PPE-A) and pre-proenkephalin-B (PPE-B) were investigated in the 6-OHDA-lesioned rat following repeated L-DOPA or vehicle treatment, utilising Northern blot hybridisation. To ensure that any alterations seen in this model were not simply due to drug administration, sham-operated control rats were also investigated. Following repeated L-DOPA administration in sham-operated rats, no significant alteration in the rats behavioural response (as measured by rotational behaviour), was observed as compared to repeated vehicle-treated sham-operated groups (Figure 3.3.3.1). In the 6-OHDA-lesioned rats, following repeated L-

DOPA (6.5 mg kg^{-1}) and benserazide (1.5 mg kg^{-1}) administration, a marked increase in rotation, contraversive to the 6-OHDA-lesion, is observed. This potentiated behavioural response is not seen following repeated vehicle administration in either the 6-OHDA-lesioned or sham-lesioned rats (Figure 3.3.3.2).

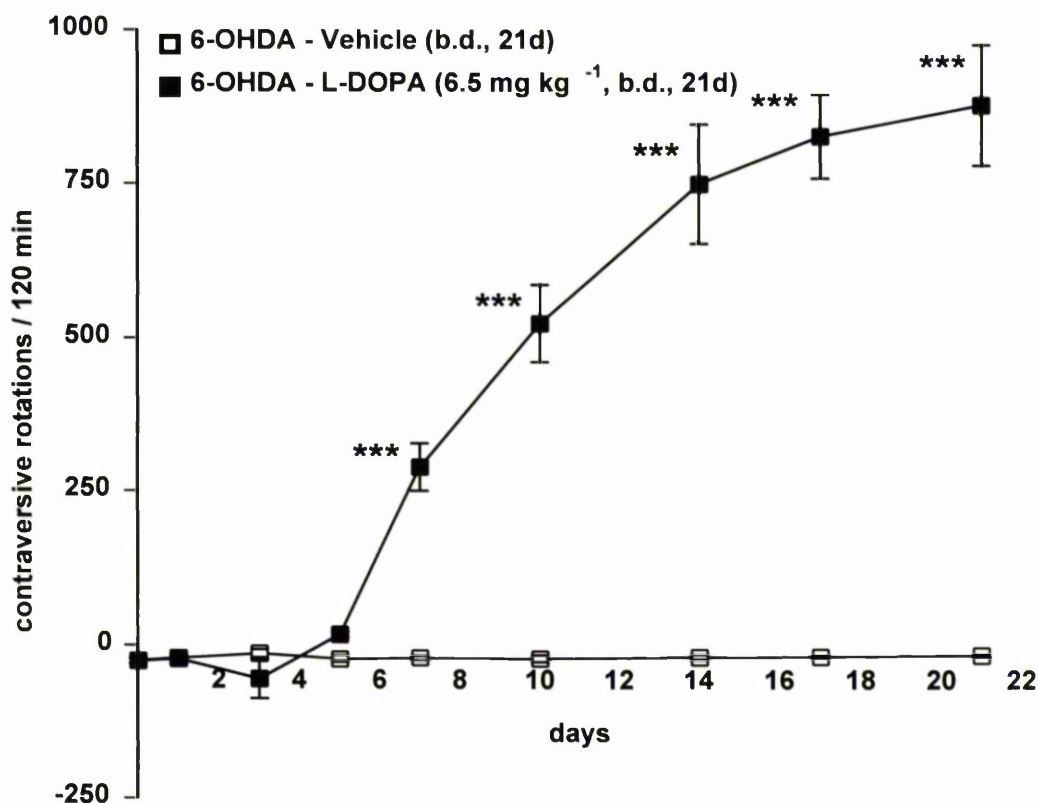


Figure 3.3.3.1 Rotational locomotion following repeated vehicle or low dose L-DOPA treatment in the 6-OHDA-lesioned rat

Net rotations, contraversive to the 6-OHDA-lesion, following repeated (twice daily, 21 days) i.p. injections of L-DOPA (6.5 mg kg^{-1}) and benserazide (1.5 mg kg^{-1}) (■) or vehicle (□) in the 6-OHDA-lesioned rat model of Parkinson's disease are shown. Locomotion was assessed for 2 hours following the 9 a.m. injection on days 0, 1, 3, 5, 7, 10, 14, 17 and 21. Data are expressed as mean (\pm SEM) complete rotations contraversive to the lesion ($n=6$, effect of drug $P < 0.001$, $F_{1, 10} = 457.20$, MANOVA, effect of drug over time $P < 0.001$, $F_{8, 80} = 41.21$, MANOVA, *** $P < 0.001$ cf vehicle group, unpaired Student's t -test).

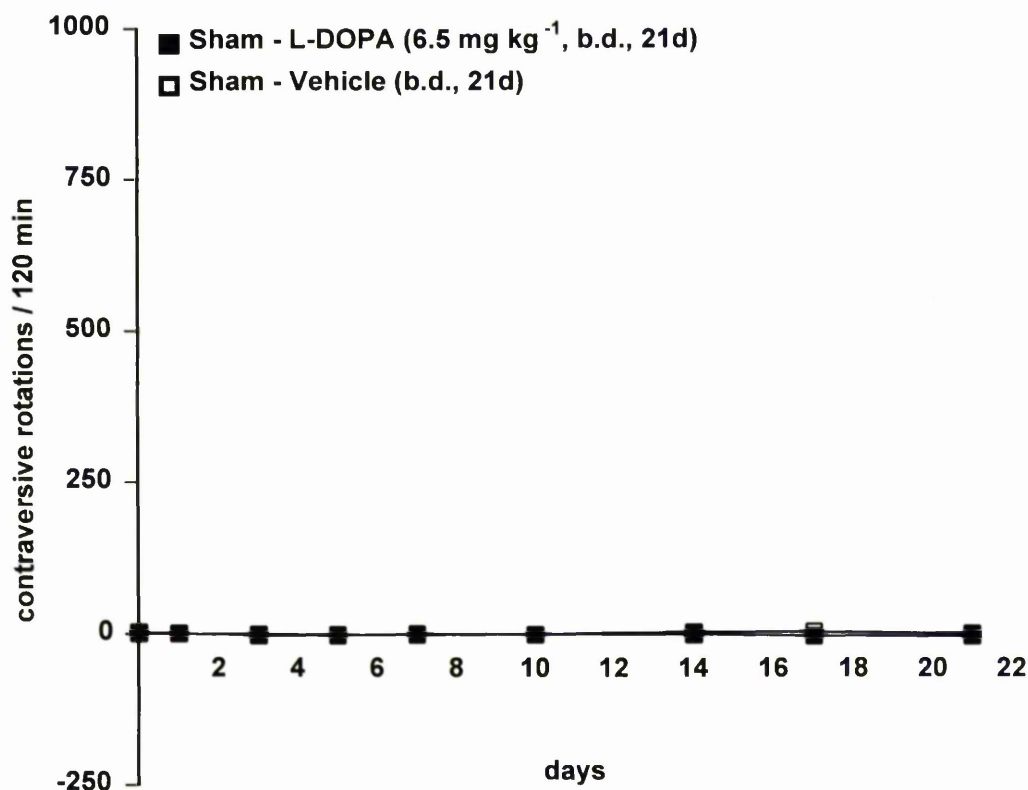


Figure 3.3.3.2 Rotational locomotion following repeated vehicle or low dose L-DOPA administration in sham-lesioned rats

Net rotations, contraversive to the sham-lesion, following repeated (twice daily, 21 days) i.p. injections of L-DOPA (6.5 mg kg⁻¹) and benserazide (1.5 mg kg⁻¹) (■) or vehicle (□) in the sham-lesioned rat model of Parkinson's disease are shown. Locomotion was assessed for 2 hours following the 9 a.m. injection on days 0, 1, 3, 5, 7, 10, 14, 17 and 21. Data are expressed as mean (\pm SEM) complete rotations contraversive to the sham-lesion ($n=6$, effect of drug, ns, $P > 0.05$, $F_{1, 10} = 2.85$, MANOVA, effect of drug over time, ns, $P < 0.05$, $F_{8, 80} = 1.04$, MANOVA, ns, $P > 0.05$ cf vehicle group, unpaired Student's t -test).

In the 6-OHDA-lesioned rat, Northern blot hybridisation of striatal RNA utilising an oligonucleotide probe targeted against PPE-A mRNA transcripts, shows a marked increase in the lesioned striatum, compared to the unlesioned and sham-operated following both L-DOPA and vehicle treatment. Following integrated optical density analysis, no significant difference is observed in the sham-operated rats following either L-DOPA or vehicle treatment (Figures 3.3.3.5, 3.3.3.6). Following 6-OHDA-lesion and vehicle treatment a non-significant 153% increase in mean PPE-

A:18S expression is observed in the lesioned striatum when compared to the unlesioned striatum ($P > 0.05$). However, in the 6-OHDA-lesioned rat, following repeated L-DOPA treatment, a further (12%) increase in PPE-A expression is observed (165% when compared to unlesioned striatum, $P < 0.05$, figures 3.3.3.3, 3.3.3.4).

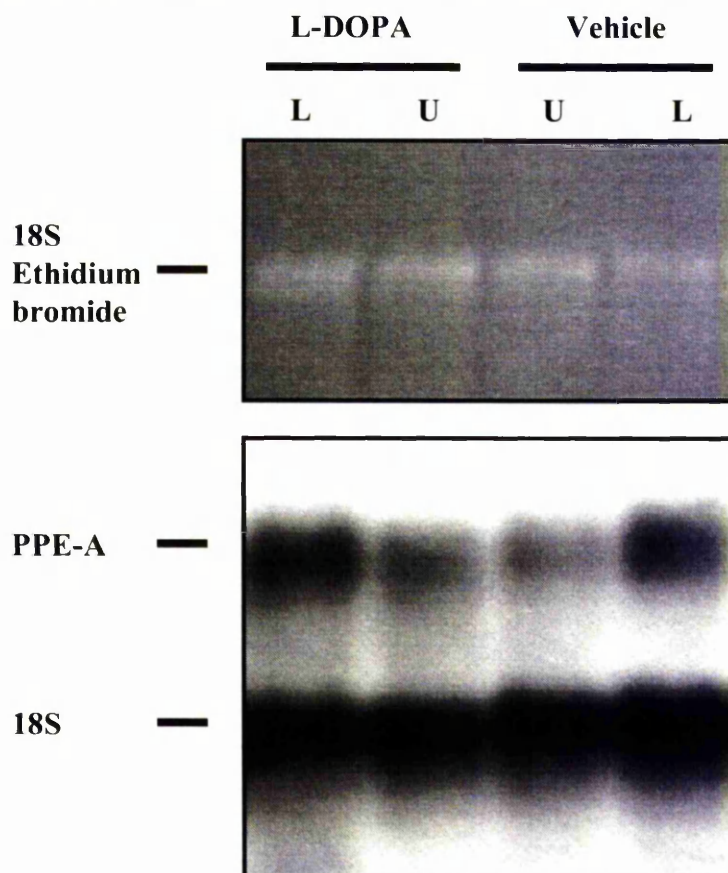


Figure 3.3.3.3 Northern blot hybridisation utilising oligonucleotide probes targeted against pre-proenkephalin-A and 18S striatal mRNA transcripts in the 6-OHDA-lesioned rat following repeated L-DOPA or vehicle treatment

Northern blot hybridisation of RNA extracted from lesioned (L) or unoperated (U) striatum in the 6-OHDA-lesioned rat model of Parkinson's disease following repeated vehicle or L-DOPA-administration. Pre-proenkephalin-A (PPE-A) and 18S control probe mRNA expression levels are shown following 21 day, twice daily, vehicle or L-DOPA (6.5 mg kg^{-1}) and benserazide (1.5 mg kg^{-1}) treatment. $10 \mu\text{g}$ of total striatal RNA is present in each lane, as indicated by ethidium bromide stain under ultraviolet light following gel electrophoresis of RNA, showing both intact RNA and equal loading of lanes.

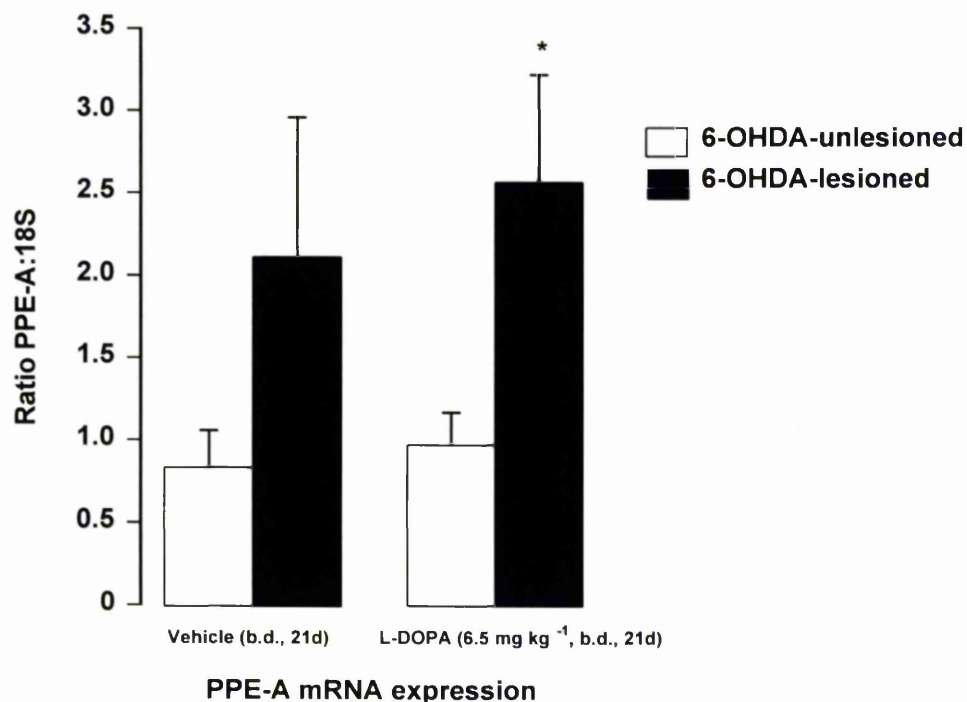


Figure 3.3.3.4 Pre-proenkephalin-A:18S expression in 6-OHDA-lesioned rats following repeated vehicle or L-DOPA administration

Ratio of pre-proenkephalin-A (PPE-A) mRNA to 18S control probe i.O.D. in 6-OHDA-lesioned (■) striatum and unlesioned (□) striatum following 21 day, b.d., vehicle or L-DOPA (6.5 mg kg⁻¹) and benserazide (1.5 mg kg) treatment. Ratio of PPE-A:18S is expressed as mean (\pm SEM) ($n=8$, * $P < 0.05$, paired Student's t -test).

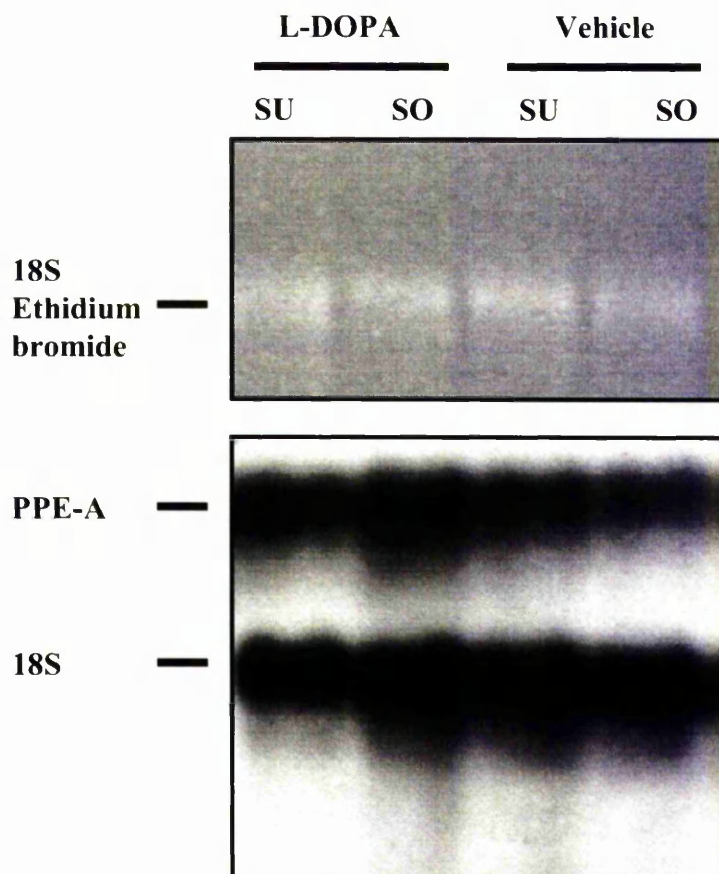


Figure 3.3.3.5 Northern blot hybridisation utilising oligonucleotide probes targeted against pre-proenkephalin-A and 18S striatal transcripts in the sham-lesioned rat following repeated L-DOPA or vehicle treatment

Northern blot hybridisation of RNA extracted from sham-operated (SO) or sham-unoperated (SU) striatum in the sham-lesioned rat model of Parkinson's disease. Pre-proenkephalin-A (PPE-A) and 18S control probe mRNA expression levels are shown following 21 day, twice daily, vehicle or L-DOPA (6.5 mg kg⁻¹) and benserazide (1.5 mg kg⁻¹) treatment. 10 µg of total striatal RNA is present in each lane, as indicated by ethidium bromide stain under ultraviolet light following gel electrophoresis of RNA, showing both intact RNA and equal loading of lanes.

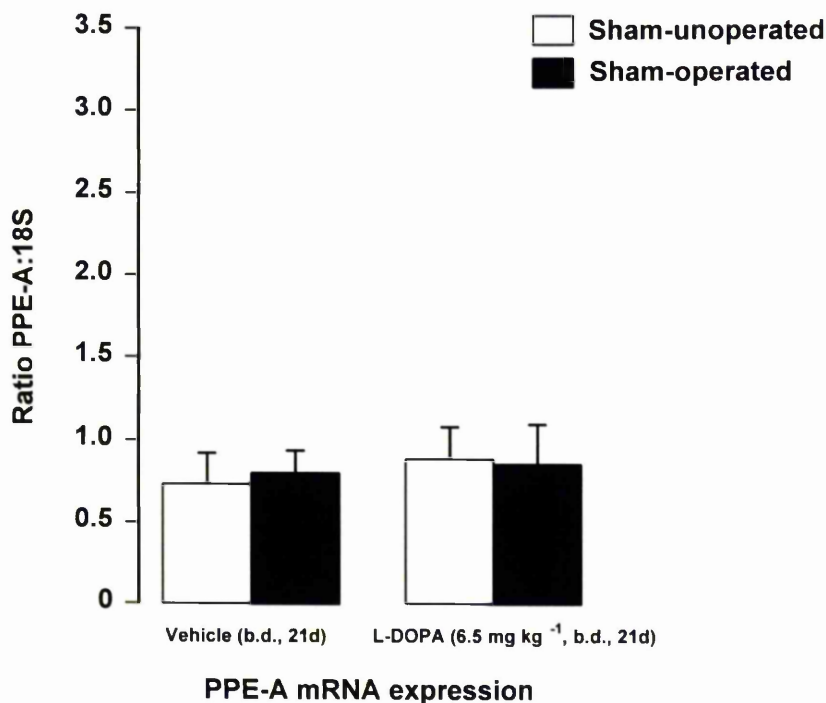


Figure 3.3.3.6 Pre-proenkephalin-A:18S expression in sham-lesioned rats following repeated vehicle or L-DOPA administration

Ratio of pre-proenkephalin-A (PPE-A) mRNA to 18S control probe i.O.D. in sham-operated (■) striatum and sham-unoperated (□) striatum following 21 day, b.d., vehicle or L-DOPA (6.5 mg kg⁻¹) and benserazide (1.5 mg kg⁻¹) treatment. Ratio of PPE-A:18S is expressed as mean (\pm SEM) ($n=8$, ns, $P > 0.05$, paired Student's t -test).

Northern blot hybridisation of striatal RNA, utilising an oligonucleotide probe targeted to the PPE-B mRNA transcript in the 6-OHDA-lesioned rat, shows no alteration following vehicle administration. However, a 988% increase in the ratio of PPE-B:18S was observed following repeated L-DOPA-administration ($P < 0.01$, figures 3.3.3.7, 3.3.3.8). This rise in PPE-B expression is not seen in the sham-operated rats following repeated L-DOPA- or vehicle-administration (Figures 3.3.3.9, 3.3.3.10).

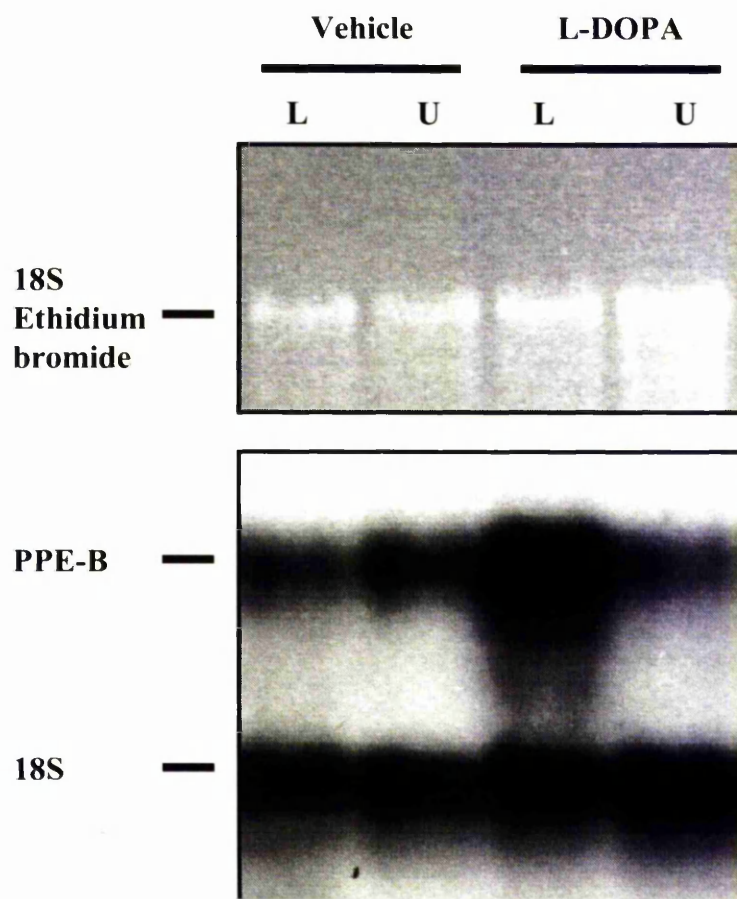


Figure 3.3.3.7 Northern blot hybridisation utilising oligonucleotide probes targeted against pre-proenkephalin-B and 18S striatal transcripts in the 6-OHDA-lesioned rat following repeated L-DOPA or vehicle treatment

Northern blot hybridisation of RNA extracted from lesioned (L) or unoperated (U) striatum in the 6-OHDA-lesioned rat model of Parkinson's disease following repeated vehicle or L-DOPA-administration. Pre-proenkephalin-B (PPE-B) and 18S control probe mRNA expression levels are shown following 21 day, twice daily, vehicle or L-DOPA (6.5 mg kg^{-1}) and benserazide (1.5 mg kg^{-1}) treatment. $10 \mu\text{g}$ of total striatal RNA is present in each lane, as indicated by ethidium bromide stain under ultraviolet light following gel electrophoresis of RNA, showing both intact RNA and equal loading of lanes.

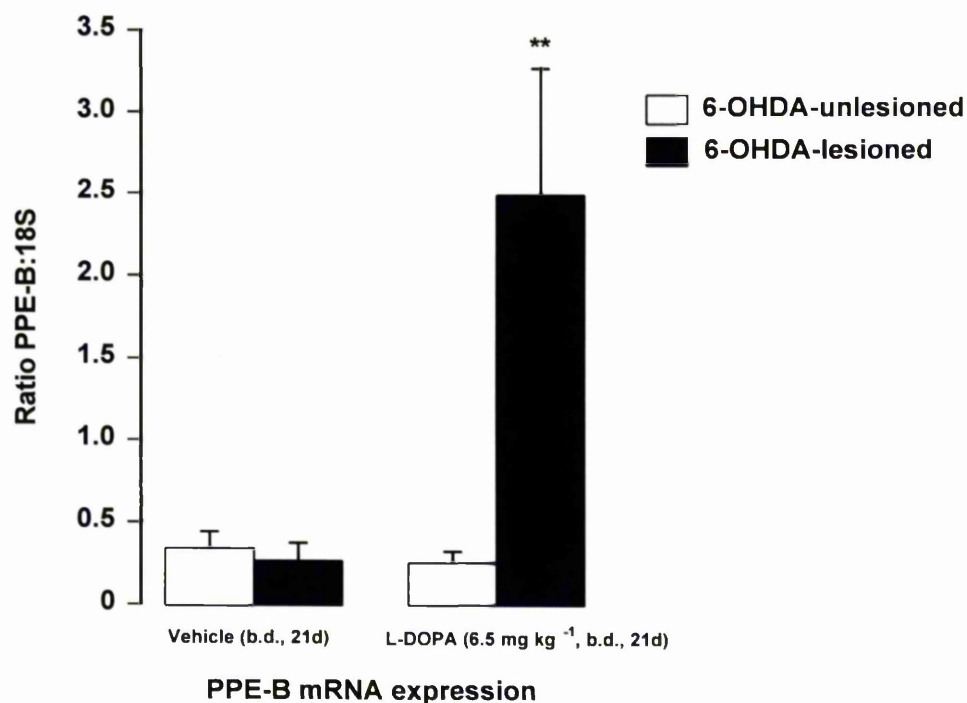


Figure 3.3.3.8 Pre-proenkephalin-B:18S expression in 6-OHDA-lesioned rats following repeated vehicle or L-DOPA administration

Ratio of pre-proenkephalin-B (PPE-B) mRNA to 18S control probe i.O.D. in 6-OHDA-lesioned (■) striatum and unlesioned (□) striatum following 21 day, b.d., vehicle or L-DOPA (6.5 mg kg⁻¹) and benserazide (1.5 mg kg⁻¹) treatment. Ratio of PPE-B:18S is expressed as mean (\pm SEM) ($n=8$, ** $P < 0.01$, paired Student's t -test).

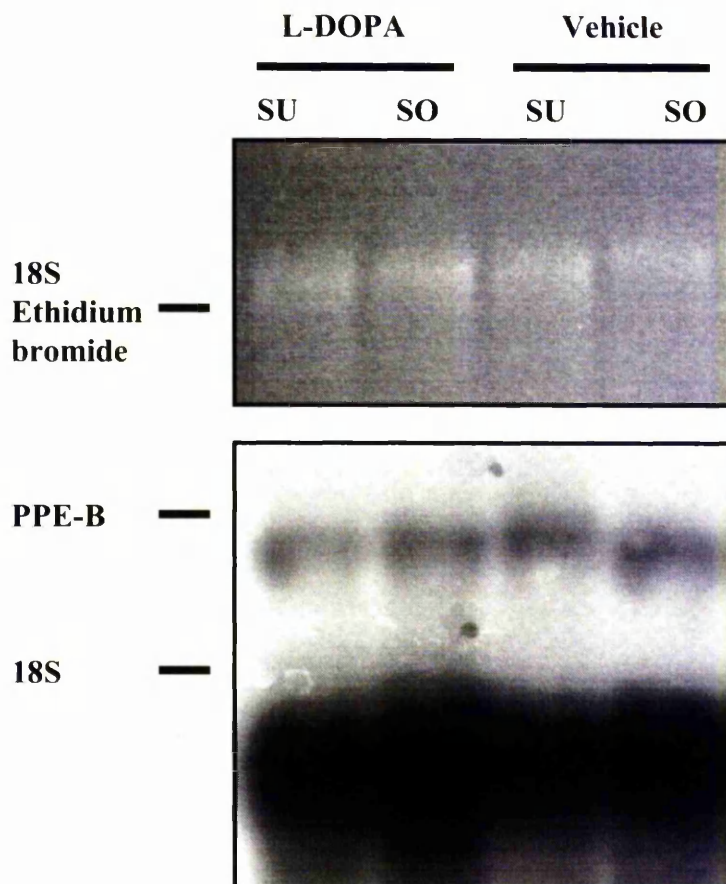


Figure 3.3.3.9 Northern blot hybridisation utilising oligonucleotide probes targeted against pre-proenkephalin-B and 18S striatal transcripts in the sham-lesioned rat following repeated L-DOPA or vehicle treatment

Northern blot hybridisation of RNA extracted from sham-operated (SO) or sham-unoperated (SU) striatum in sham-lesioned rats. Pre-proenkephalin-B (PPE-B) and 18S control probe mRNA expression levels are shown following 21 day, twice daily, vehicle or L-DOPA (6.5 mg kg^{-1}) and benserazide (1.5 mg kg^{-1}) treatment. $10 \mu\text{g}$ of total striatal RNA is present in each lane, as indicated by ethidium bromide stain under ultraviolet light following gel electrophoresis of RNA, showing both intact RNA and equal loading of lanes.

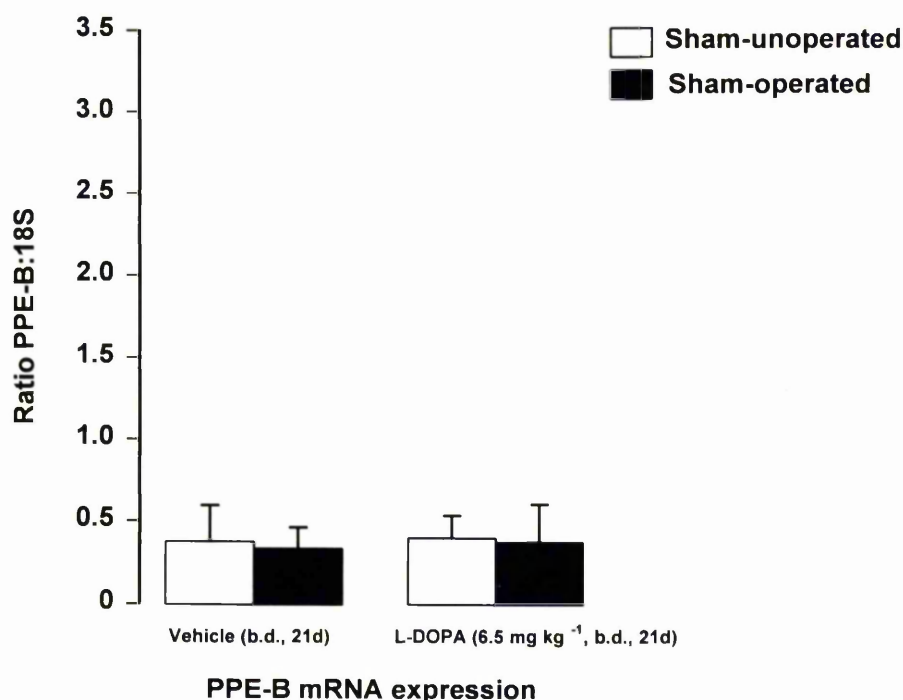


Figure 3.3.3.10 Pre-proenkephalin-B:18S expression in sham-lesioned rats following repeated vehicle or L-DOPA administration

Ratio of pre-proenkephalin-B (PPE-B) mRNA to 18S control probe i.O.D. in sham-operated (■) striatum and sham-unoperated (□) striatum following 21 day, b.d., vehicle or L-DOPA (6.5 mg kg⁻¹) and benserazide (1.5 mg kg⁻¹) treatment. Ratio of PPE-B:18S is expressed as mean (\pm SEM) ($n=8$, ns, $P > 0.05$, paired Student's t -test).

3.3.4 Effect of functional antagonism of opioid receptors in the rat model of L-DOPA-induced dyskinesia

Following repeated L-DOPA-administration in the 6-OHDA-lesioned rat model of Parkinson's disease, a marked potentiation in the behavioural response was observed (as previously described in chapter 2). In this rat model of L-DOPA-induced dyskinesia, co-administration of the non-selective opioid antagonist naloxone, dose-dependently reduced hyperkinesia seen following repeated L-DOPA-administration. At the highest dose of naloxone co-administered with L-DOPA (5 mg kg⁻¹), hyperkinesia was reduced by 39% (Figure 3.3.4.1). Following co-administration of the selective delta opioid receptor antagonist naltrindole, a 38% reduction in L-DOPA-induced hyperkinesia was observed in the rat model of L-DOPA-induced dyskinesia (Figure 3.3.4.2). Similarly, following co-administration of the selective kappa opioid receptor antagonist, *nor*-binaltorphamine, a 37% reduction in L-DOPA-induced hyperkinesia was observed (Figure 3.3.4.3). However, following co-administration of the selective mu opioid receptor antagonist cyprodime, no significant alteration in L-DOPA-induced hyperkinesia was observed (Figure 3.3.4.4).

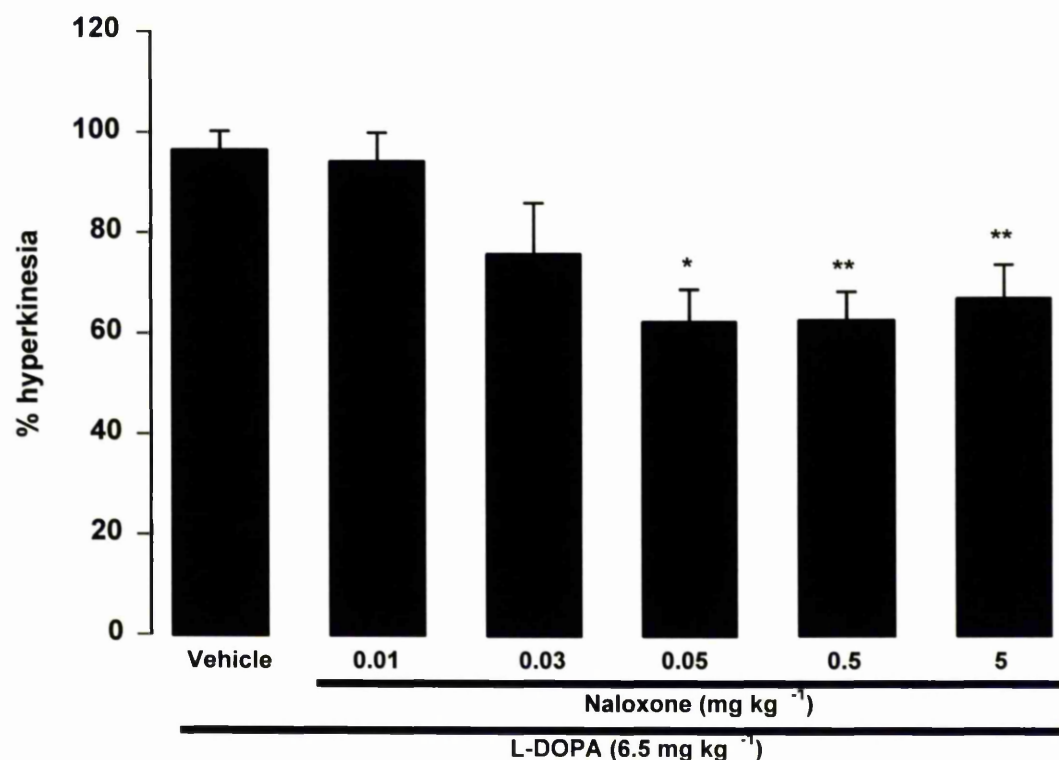


Figure 3.3.4.1 Effect of naloxone on hyperkinesia induced by repeated L-DOPA treatment in the 6-OHDA-lesioned rat

Hyperkinesia was induced by repeated, twice-daily, injections of L-DOPA (6.5 mg kg^{-1}) and benserazide (1.5 mg kg^{-1}) for 13 days. On days 14-21, rats were injected with L-DOPA, 40 minutes later rats were injected with the broad spectrum opioid antagonist naloxone ($0.01 - 5 \text{ mg kg}^{-1}$). Net rotations, contraversive to the lesion, in the 15 minute period, 45 minutes post L-DOPA injection is expressed as a percentage of that observed following vehicle injection 40 minutes after L-DOPA/benserazide treatment the following day. Percent hyperkinesia is expressed as mean ($\pm \text{SEM}$) ($n=5-12$, * $P < 0.05$, ** $P < 0.01$, $F_{5, 44} = 5.185$, one-way analysis of variance, Dunnett's post hoc comparison).

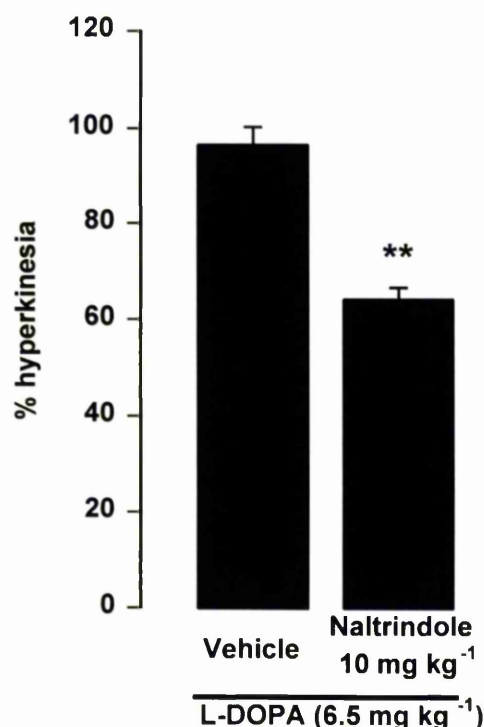


Figure 3.3.4.2 Effect of the delta opioid receptor antagonist naltrindole on hyperkinesia induced by repeated L-DOPA treatment in the 6-OHDA-lesioned rat

Hyperkinesia was induced by repeated, twice-daily, injections of L-DOPA (6.5 mg kg⁻¹) and benserazide (1.5 mg kg⁻¹) for 13 days. On days 14-21, rats were injected with L-DOPA, 40 minutes later, rats were injected with the delta opioid receptor specific antagonist naltrindole (10 mg kg⁻¹). Net rotations, contraversive to the lesion, in the 15 minute period, 45 minutes post L-DOPA injection, is expressed as a percentage of that observed following vehicle injection 40 minutes after L-DOPA/benserazide treatment the following day. Percent hyperkinesia is expressed as mean (\pm SEM) ($n=4$, ** $P < 0.01$, $F_{3,12} = 10.84$, one-way analysis of variance, Dunnett's post hoc comparison).

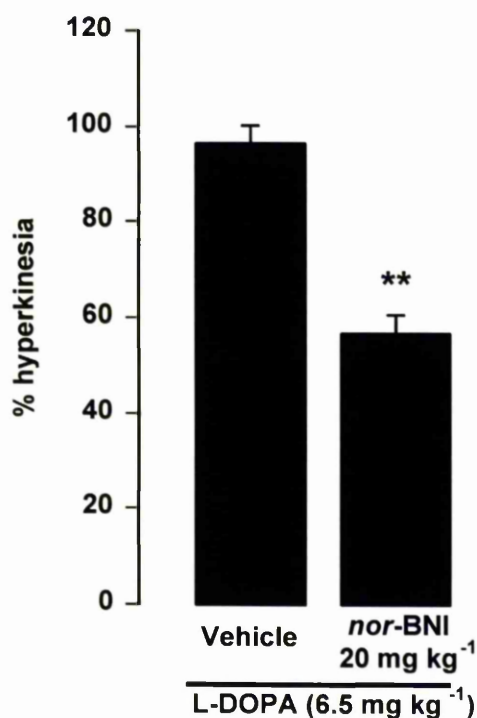


Figure 3.3.4.3 Effect of the kappa opioid receptor antagonist nor-binaltorphimine on hyperkinesia induced by repeated L-DOPA treatment in the 6-OHDA-lesioned rat

*Hyperkinesia was induced by repeated, twice-daily, injections of L-DOPA (6.5 mg kg⁻¹) and benserazide (1.5 mg kg⁻¹) for 13 days. On days 14-21, rats were injected with L-DOPA, 40 minutes later, rats were injected with the kappa opioid receptor specific antagonist nor-binaltorphimine (20 mg kg⁻¹). Net rotations, contraversive to the lesion, in the 15 minute period, 45 minutes post L-DOPA injection, is expressed as a percentage of that observed following vehicle injection 40 minutes after L-DOPA/benserazide treatment the following day. Percent hyperkinesia is expressed as mean (\pm SEM) ($n=4$, ** $P < 0.01$, $F_{3,12} = 10.84$, one-way analysis of variance, Dunnett's post hoc comparison).*

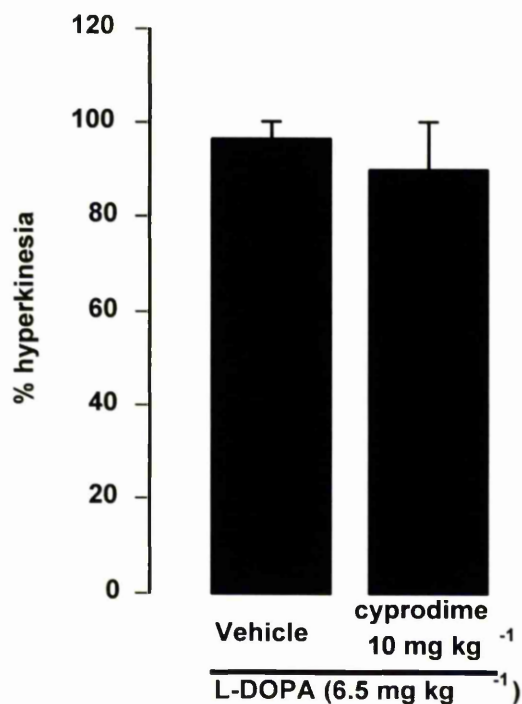


Figure 3.3.4.4 Effect of the mu opioid receptor specific antagonist cyprodime on hyperkinesia induced by repeated L-DOPA treatment in the 6-OHDA-lesioned rat

Hyperkinesia was induced by repeated injections of L-DOPA (6.5 mg kg⁻¹) and benserazide (1.5 mg kg⁻¹) for 13 days. On days 14-21, rats were injected with L-DOPA, 40 minutes later, rats were injected with the mu opioid receptor specific antagonist cyprodime (10 mg kg⁻¹). Net rotations, contraversive to the lesion, in the 15 minute period, 45 minutes post L-DOPA injection, is expressed as a percentage of that observed following vehicle injection 40 minutes after L-DOPA/benserazide treatment the following day. Percent hyperkinesia is expressed as mean (± SEM) (n=4, ns, $P > 0.5$, $F_{3,12} = 10.84$, one-way analysis of variance, Dunnett's post hoc comparison).

3.4 Discussion

Methodological considerations

To investigate the levels of the mRNA encoding the large molecular weight precursors for enkephalin and dynorphin, pre-proenkephalin-A (PPE-A) and pre-proenkephalin-B (PPE-B) respectively, in the rat model of L-DOPA-induced dyskinesia (as described in chapter 2), the technique of Northern blot analysis was employed. Oligonucleotide probe sequences were generated from previously published sequences (Howells *et al.*, 1984; Civelli *et al.*, 1985). The theoretical specificity of these oligonucleotide probes were verified by genbank and EMBL database searches, to indicate specificity for only the desired mRNA transcript (Altschul *et al.*, 1993). Specificity for a single mRNA transcript and previously reported molecular weight, was indicated the presence of only one band at molecular weights of 1.4 Kb, 2.4 Kb, and 1.8 Kb, for PPE-A, PPE-B and 18S respectively (Figure 3.3.1.3; Howells *et al.*, 1984; Civilli *et al.*, 1995; Torczynski *et al.*, 1983, 1985).

To investigate the specificity of the extraction procedure for RNA, the final extract was analysed in a spectrophotometer at both 260 nm and 280 nm wavelengths. Only RNA extractions with an absorption ratio between 1.8 and 2 were used in subsequent Northern blot hybridisation studies, as this demonstrates mRNA with acceptably low protein and DNA contamination (Sambrook *et al.*, 1986).

Although the T_m of each oligonucleotide probe can be calculated using sequence data, it must also be determined experimentally. To address this, both the hybridisation temperature and post-hybridisation wash temperatures were altered, in order to optimise the hybridisation signal. For all oligonucleotide probes used in this study, possibly due to the similar length of the oligonucleotide probes, an optimal hybridisation temperature of 42°C was determined. Similarly, for all probes used, a post-hybridisation wash temperature of 55°C was determined as the optimal temperature to produce specific binding (Figures 3.3.1.1, 3.3.1.2).

The ability to strip one oligonucleotide probe and re-probe for another mRNA transcript, without loss of signal, was also verified for both PPE-A and PPE-B oligonucleotide probes. This indicated that there was no loss of signal after stringent

probe removal wash conditions (Figure 3.3.1.5, Table 3.5). These measures allowed identification of specific transcripts, subsequent removal of this probe and re-probing for another transcript without any loss of signal.

To characterise the film response, and ensure oligonucleotide probe signals were within the linear response of the film, Northern blot hybridisation using an oligonucleotide probe for 18S control probe (mRNA transcript producing the highest signal) was carried out on a concentration gradient of striatal mRNA (2.5-20 µg). Post-hybridisation, this membrane was exposed to film for 12, 24, 36 and 48 hours. Following integrated optical density (i.O.D.) measurements, a clear linear response was to the film both over concentration of radiation and over time was demonstrated (Figure 3.3.1.4).

To demonstrate that this method of mRNA quantification was capable of detecting changes in mRNA expression from striatal tissue, a study on the reserpine-treated rat was performed. It has previously been reported that following catecholamine depletion by reserpine, an increase in pre-proenkephalin-A (the precursor for enkephalin) is observed (Jaber *et al.*, 1992; Jaber *et al.*, 1995). Eighteen hours following reserpine (8 mg kg⁻¹) administration in male Sprague Dawley rats, a marked decrease in spontaneous locomotion is observed, indicating, predominantly, a loss of dopaminergic transmission within the striatum (Figure 3.3.2.1). Twenty hours following reserpine administration, striatal mRNA was extracted from reserpine- or vehicle-treated rats and Northern blot hybridisation performed, utilising oligonucleotide probes targeted to the enkephalin precursor, PPE-A, and the 18S ribosomal subunit (as *p+28Xa control probe) mRNA transcripts. A 75% increase in mRNA expression for PPE-A was noted (Figure 3.3.2.3). This finding was in agreement with previous reports (Jaber *et al.*, 1992; Jaber *et al.*, 1995) and showed that the technique employed here could detect changes in opioid neuropeptide precursor following dopamine depletion.

Alterations in pre-proenkephalin-A and pre-proenkephalin-B expression in the rat model of L-DOPA-induced dyskinesia utilising Northern blot hybridisation

The expression of PPE-A and PPE-B were investigated in the 6-OHDA-lesioned rat following L-DOPA treatment. As discussed in chapter 2 this appears on many levels to provide a potentially useful model to study the cellular and molecular mechanisms

underlying L-DOPA-induced dyskinesia. Expression was also studied in 6-OHDA-lesioned rats receiving repeated vehicle treatment. Comparison to sham-operated rats, following either repeated L-DOPA or vehicle-administration were also made.

The dose of L-DOPA used in these experiments was determined by calculating a 'therapeutic' dose in patients. Thus, an average dose of 800 mg of levodopa in a 70 kg patient was used as an average daily dose (Calne, 1984). Therefore, 13 mg kg^{-1} a day L-DOPA was used as a 'low therapeutic' dose administered to the rats. To better mimic the plasma concentration fluctuations of dopamine seen in parkinsonian patients treated with oral L-DOPA tablets, this was divided into two injections, a 9 a.m. and 5 p.m. injection of 6.5 mg kg^{-1} for 21 days. In sham-lesioned rats, following either vehicle or L-DOPA-treatment, there was no significant alteration in the expression of either PPE-A or PPE-B (Figure 3.3.3.5, 3.3.3.9). As already demonstrated in chapter 2, following repeated L-DOPA administration in the 6-OHDA-lesioned rat, a novel behaviour was observed whereby the rotational response to L-DOPA was markedly enhanced with repeated treatment. The mechanism underlying this behavioural hyperkinesia will be discussed in more detail in chapter 4.

Following 6-OHDA-lesion and vehicle treatment there was a non-significant increase in PPE-A expression in the lesioned striatum. This is in keeping with similar studies reported in the literature (Gerfen, 1990; Jaber, 1992). However, following L-DOPA-treatment, a further rise in PPE-A expression is indicated by the fact that a significant elevation in the ratio of PPE-A:18S is seen in the lesioned striatum compared to the unlesioned striatum (Figure 3.3.3.3, 3.3.3.4). A further increase in enkephalin peptide levels has been previously described following repeated L-DOPA treatment (Engber *et al.*, 1991). However, further increases in PPE-A mRNA expression, by either Northern blot hybridisation or other means, has not been reported to date (Gerfen, 1990; Jaber *et al.*, 1992).

No change in PPE-B expression was observed following vehicle treatment in the 6-OHDA-lesioned rat or in either of the sham-operated groups. However, following L-DOPA treatment in the 6-OHDA-lesioned striatum, a significant increase in PPE-B expression is observed following L-DOPA treatment (Figure 3.3.3.7., 3.3.3.8).

Therefore, it is clear from this data that in the 6-OHDA-lesioned rodent model of Parkinson's disease, PPE-A expression is elevated, though non-significantly, while PPE-B expression is unchanged. However, in the rat model of L-DOPA-induced

dyskinesia, PPE-A expression is further increased and PPE-B expression undergoes a marked significant increase.

Regulation of pre-proenkephalin-A and pre-proenkephalin-B in the dopamine-denervated striatum following repeated dopamine-replacement therapy

The mechanism underlying the control of peptide expression, following dopamine-depletion and subsequent replacement, has not been investigated in this thesis. However several studies have investigated the role of dopamine on the regulation of expression of both PPE-A and PPE-B. The differential alteration in expression of PPE-A and PPE-B most probably arises from the reported differential effect of dopamine on the two major types of dopamine receptors within the striatum i.e. dopamine D1 and D2 receptors (Stoof and Kebabian, 1981, 1982; Lazareno *et al.*, 1985) and the subsequent co-localisation of PPE-A and PPE-B within different cells within the striatum (Gerfen, 1985; Le Moine *et al.*, 1990; Le Moine and Bloch, 1995). Recently, it has been reported that within all medium spiny neurons, both D1 and D2 dopamine receptors are expressed and are capable of playing a functional role in the control of medium spiny neurons within the striatum (Surmeier *et al.*, 1996). However, dopamine D2 receptors are preferentially localised on the PPE-A expressing neurons that project preferentially to the lateral segment of the globus pallidus (Del Fiacco *et al.*, 1982; Vincent and Hokfelt, 1982; Beckstead and Kersey, 1985; Gerfen and Young, 1988; Gerfen *et al.*, 1988). Dopamine D1 receptors are preferentially expressed on medium spiny neurons that co-localise PPE-B and project to the substantia nigra pars reticulata (SNpr) and entopeduncular nucleus (the rodent equivalent of the medial segment of the globus pallidus (GPM, Del Fiacco *et al.*, 1982; Vincent and Hokfelt, 1982; Beckstead and Kersey, 1985; Gerfen and Young, 1988; Gerfen *et al.*, 1988). Dopamine has been reported to have differential effects on each of these receptors, such that D2 dopamine receptors are negatively coupled to adenylyl cyclase, while dopamine D1 receptors are positively coupled to adenylyl cyclase (Stoof and Kebabian, 1981, 1982; Lazareno *et al.*, 1985).

Both PPE-A and PPE-B mRNA transcripts contain cAMP binding response elements (CREB) which can differentially modulate, in conjunction with AP-1 binding proteins, the expression of these peptides (Comb *et al.*, 1986, 1988; Sonnenberg *et al.*,

1989; Douglass *et al.*, 1994; Messersmith *et al.*, 1994, 1996). It is thought that in the medium spiny neurons of the neostriatum, D1 and D2 receptors work through an integrated mechanism, or 'co-operate' in the regulation of adenylyl cyclase to control gene regulation. Several lines of evidence suggest that following dopamine denervation this integrated or 'co-operative' mechanism is lost (Needhan *et al.*, 1993; Thomas *et al.*, 1992). Therefore, following dopamine denervation cells expressing predominantly the D2 dopamine receptor are released from inhibition of adenylyl cyclase. This increases the turnover of cAMP, thus upregulating the transcription of the enkephalin precursor, PPE-A. Conversely, following dopamine denervation, predominantly D1 dopamine receptor expressing cells within the striatum are released from tonic stimulation by dopamine, thus reduced the activity of adenylyl cyclase and therefore reduced the expression of the dynorphin precursor, PPE-B.

Following exogenous dopamine-replacement in the dopamine-denervated striatum, the explanation for the resultant changes seen are not as easily reconcilable. Following dopamine-replacement in the dopamine-denervated striatum, one would expect the predominantly dopamine D2 receptor expressing cells containing PPE-A to simply decrease adenylyl cyclase activity and thus decrease the transcription of PPE-A mRNA. However, Northern blot hybridisation studies carried out in this chapter demonstrate that, PPE-A expression does not simply return to pre-lesion levels but is further enhanced. One possibility for this further increase in PPE-A transcription could be the loss of co-operation between D1 and D2 receptors, such that, when dopamine is re-introduced to the denervated striatum, stimulation of D1 receptors increases adenylyl cyclase activity in the predominantly D2 containing cells, thus further increasing PPE-A expression. Similarly in the predominantly D1 containing cells, re-introduction of dopamine to these cells will cause an upregulation in adenylyl cyclase and thus of PPE-B expression. Furthermore, there is evidence to suggest a supersensitivity of dopamine D1 receptor coupling to adenylyl cyclase, without changes in receptor numbers or affinity following dopamine denervation (Cole *et al.*, 1994). This would again imply that following dopamine denervation D1 coupling to adenylyl cyclase becomes enhanced or supersensitive, thus, following re-introduction of dopamine to the denervated striatum, the loss of co-operation, coupled with the D1 dopamine receptors enhanced ability to stimulate adenylyl cyclase results in a massive up regulation of both PPE-A and PPE-B expression. This will be further discussed in chapter 4.

Functional antagonism of subtype-specific opioid receptors in the rat model of L-DOPA-induced dyskinesia

From the Northern blot hybridisation studies described in this chapter, it is clear that following repeated L-DOPA-administration in the 6-OHDA-lesioned rat model of Parkinson's disease, expression levels of both PPE-A and PPE-B are increased. To investigate whether these precursor changes in mRNA expression are translated into biologically active peptides, released and stimulate endogenous receptors, and possibly underlie the symptoms of the hyperkinesia seen in the rat model of L-DOPA-induced dyskinesia, behavioural investigations were carried out to determine the effect of blocking endogenous opioid receptor transmission on the hyperkinesia seen in the rat model of L-DOPA-induced dyskinesia. Enkephalin is the endogenous ligand for the delta opioid receptor (Lord *et al.*, 1977; Goldstein and Naidu, 1989), dynorphin for the kappa opioid receptor (Lord *et al.*, 1977; Chavkin *et al.*, 1982; Corbett *et al.*, 1982), and β -endorphin for the mu opioid receptor (Lord *et al.*, 1977; Goldstein and Naidu, 1989).

Administration of naloxone, the non-selective opioid receptor antagonist which, at high doses, functionally blocks all opioid peptide transmission (Martin, 1967), dose-dependently reduces the hyperkinesia seen in the rat model of L-DOPA-induced dyskinesia (Figure 3.3.4.1). When administered to clinically-normal rats, this dose of naloxone, produces no change in spontaneous locomotion (Figure 2.3.4.2), thus indicating specificity for hyperkinesia in the rat model of L-DOPA-induced dyskinesia. Utilising the subtype-selective opioid receptor antagonists *nor*-binaltorphimine, naltrindole and cyprodime for kappa, delta and mu opioid receptors respectively, the effects on behavioural hyperkinesia were investigated in the rat model of L-DOPA-induced dyskinesia.

All drugs were used at concentrations shown to both have central effects in other paradigms and remain selective for either the kappa, delta or mu receptor subtypes (Kieffer, 1995). Both the kappa and delta opioid receptor antagonists reduced the hyperkinesia up to a maximal 39%, while the mu opioid receptor antagonist had no effect on the L-DOPA-induced hyperkinesia (Figures 3.3.4.2, 3.3.4.3, 3.3.4.4). These data suggest that the increased mRNA expression seen in the Northern blot hybridisation studies are in fact translated into active opioid peptides. Furthermore, that the opioid peptides enkephalin and dynorphin are released, stimulate endogenous opioid

receptors, and underlie, at least a proportion, of the hyperkinesia seen in the rat model of L-DOPA-induced dyskinesia.

From these data it is also apparent that the mu selective opioid receptor antagonist cyprodime has no effect on the hyperkinesia induced by repeated L-DOPA-administration in the 6-OHDA-lesioned rat. Pro-opiomelanocortin (POMC) is the large molecular weight precursor of β -endorphin, the endogenous ligand for the mu opioid receptor which, together with enkephalin (with a much lower affinity), activate mu opioid receptors (Lord *et al.*, 1976; Nakanishi *et al.*, 1979). Pro-opiomelanocortin expression has not, either in this thesis nor in other reports in the literature, been studied in animal models of Parkinson's disease or following repeated L-DOPA or dopamine receptor agonist therapy in Parkinson's disease. However, several studies have shown, both in *in vivo* (Chen *et al.*, 1983; Jaber *et al.*, 1994) and *in vitro* cell culture (Cote *et al.*, 1986; Loeffler *et al.*, 1986; L'Hereault and Barden, 1991) that following dopamine receptor stimulation with dopamine receptor agonists, POMC expression is decreased. Conversely, following dopamine receptor blockade with antagonists such as haloperidol, POMC expression is increased (Jaber, 1994). This would suggest that in Parkinson's disease, reduced dopamine levels would increase POMC expression within the striatum. However, following repeated dopamine receptor agonist stimulation (e.g. in parkinsonian patients treated with dopamine-replacing agents), POMC expression, and hence β -endorphin, would be either normalised or decreased below normal levels. Evidence for such alterations come from work by Franceschi *et al.* (1986) who demonstrated that in untreated patients with Parkinson's disease, levels of plasma β -endorphin were increased in comparison to controls. However, following repeated L-DOPA administration, plasma levels of β -endorphin were decreased in comparison to controls. This reduction in β -endorphin levels may explain the lack of effect of the mu opioid receptor antagonist in reducing the hyperkinesia seen following repeated L-DOPA administration in the 6-OHDA-lesioned rat. Furthermore, intraventricular administration of β -endorphin has been shown to produce akinesia in rats (Bloom *et al.*, 1976; Jacquet and Marks 1976), suggesting little role for increased β -endorphin transmission in L-DOPA-induced hyperkinesia in rats, or L-DOPA-induced dyskinesias in patients. However, without measuring the levels of POMC in the 6-OHDA-lesioned rat following repeated L-DOPA treatment, it cannot be concluded that this is the reason

no effect on hyperkinesia was observed following mu opioid receptor antagonist administration.

A further interpretation that can be drawn from the lack of effect of the mu opioid receptor antagonist cyprodime on the hyperkinesia seen following repeated L-DOPA-administration in the 6-OHDA-lesioned rat is that increased enkephalin transmission resulting from increased PPE-A expression does not activate mu opioid receptors, and therefore plays no role in L-DOPA-induced hyperkinesia. Taken together these data suggest little role for the activation of mu opioid receptors underlying the symptoms of L-DOPA-induced dyskinesias following repeated L-DOPA administration in Parkinson's disease.

One of the most perplexing findings from the subtype-selective opioid receptor antagonist studies is that both kappa and delta opioid receptor antagonists, and at higher doses, the non-selective opioid receptor antagonist naloxone, all reduced L-DOPA-induced hyperkinesia in the 6-OHDA-lesioned rat by a similar maximal level.

Since all of the opioid receptor antagonists used in this experiment were administered systemically, it is impossible to determine the exact site of action of these compounds. One possibility to explain the fact that both kappa and delta and, at higher doses, the non-selective opioid receptor antagonist naloxone all reduce hyperkinesia to the same level is the fact that inhibition of opioid transmission in other, either basal ganglia or non-basal ganglia areas of the brain, may be responsible for the lack of differential effect of the selective subtype antagonists. Therefore, it may be possible that blocking either kappa, delta or other opioid receptors in other brain areas, may reduced the effectiveness of the inhibition of hyperkinesia. Therefore, without intracerebral administration of opioid receptor antagonists in the 6-OHDA-lesioned rat following repeated L-DOPA treatment, it is not possible to determine the exact location of the opioid transmission being effected by the systemically administered opioid receptor antagonists. The data from this rat model of L-DOPA-induced dyskinesias suggests that increased opioid peptide transmission in striatal efferent pathways may only be responsible for a maximal 40% of the increase in hyperkinesia observed in the rat. However, this does not preclude the possibility that in the primate this 40% decrease observed following blockade of opioid peptide transmission underlies L-DOPA-induced dyskinesia. In fact two small-scale clinical trials have suggested that the non-selective

opioid antagonist naloxone can reduced peak-dose L-DOPA-induced dyskinesias in patients with Parkinson's disease (Trabucchi *et al.*, 1982, Sandyk and Snider, 1986).

A limitation of Northern blot analysis is the fact that the topographical distribution of PPE-A and PPE-B mRNA changes within the striatum cannot be determined. Since the functional organisation of the striatum is topographically arranged, the rise in PPE-A and PPE-B expression observed following repeated L-DOPA administration may be restricted to a specific area of the striatum. This selective increase in PPE-A expression may play a pivotal role in the generation of hyperkinetic (in the rat) or dyskinetic symptoms (in the patient). Furthermore, identifying increased neuropeptide transmission within functionally segregated areas within the striatum may provide a framework in which the neural mechanisms underlying L-DOPA-induced dyskinesia may be understood. *In situ* hybridisation, does allow the topographical distribution of mRNA transcripts to be identified. Therefore, *in situ* hybridisation studies were carried out (described in chapter 4) to provide a better insight into the topographical distribution of both the further increase in PPE-A expression and of the PPE-B expression, possibly allowing for functional considerations of these peptide alterations to be better addressed.

Chapter 4:

Topographical distribution of striatal pre-proenkephalin-A and pre-proenkephalin-B mRNA in the 6-OHDA-lesioned rat following repeated treatment with L-DOPA, bromocriptine or lisuride

4.1 Introduction

The neural mechanisms underlying L-DOPA-induced dyskinesias remain largely unknown. It is thought that in common with all other forms of dyskinesia, the symptoms of L-DOPA-induced dyskinesia arise from underactivity of the subthalamic nucleus and hence the medial segment of the globus pallidus (Crossman, 1987; Mitchell *et al.*, 1992). In chapter 3 it was proposed that further decreases in basal ganglia output nuclei, namely the medial segment of the globus pallidus and substantia nigra pars reticulata, could be achieved by increased peptidergic transmission in striatal efferents. From the results of chapter 2, it is also clear that following repeated L-DOPA administration in the rat model of L-DOPA-induced dyskinesia, a further increase in pre-proenkephalin-A (PPE-A), the enkephalin precursor takes place. The topographical nature of this further increase, together with the topography of the pre-proenkephalin-B (PPE-B) increase remains unknown. Although several studies have investigated the changes in PPE-A and PPE-B in animal models of Parkinson's disease following repeated L-DOPA or dopamine receptor agonist treatment (Engber *et al.*, 1991; Jaber *et al.*, 1994), no study to date, has carried out a full topographical investigation into changes in PPE-A and PPE-B in animal models of L-DOPA-induced dyskinesia. Within the striatum many segregated functional areas exist with respect to cerebro-cortical innervation from sensorimotor, associative and limbic cortices. (see chapter 1, section 1.1.1). This topographical distribution may be useful in determining the functional implications of increased peptide expression within striatal efferents. Furthermore, from the results of chapter 2, it is clear that a proportion of the hyperkinesia seen in the rat model of L-DOPA-induced dyskinesia can be accounted for by increased opioid neuropeptide transmission, specifically acting at kappa and delta opioid receptors. As previously described, following *de novo* bromocriptine or lisuride administration to MPTP-treated non-human primates and parkinsonian patients, dyskinesias are not observed (Lees and Stern, 1981; Gomez-Mancilla *et al.*, 1993). In chapter 2, it was shown that following *de novo* treatment in the 6-OHDA-lesioned rat model of Parkinson's disease, unlike repeated treatment with L-DOPA, no potentiated behavioural hyperkinesia is observed. It may be possible that this behavioural potentiation is not seen as bromocriptine and lisuride normalise peptide alterations, while still providing dopaminergic stimulation to

alleviate the hypokinetic symptoms of Parkinson's disease. The present chapter addresses this question by topographically assessing the level of PPE-A and PPE-B expression in the 6-OHDA-lesioned rat following repeated *de novo* treatment of bromocriptine or lisuride. Furthermore, utilising *in situ* hybridisation studies, the full topographical nature of the increase of PPE-A and PPE-B expression observed following repeated L-DOPA administration in the rat model of L-DOPA-induced dyskinesia are investigated.

4.2 Methods

4.2.1 *In Situ* Hybridisation

4.2.1.1 Tissue preparation for *in situ* hybridisation methods

Tissue for all *in situ* hybridisation methodological studies were obtained from naive 250-300g male Sprague Dawley rats (Charles River, UK). Rats were maintained in standard housing conditions with constant temperature ($22 \pm 1^{\circ}\text{C}$), humidity (relative, 30%), 12 hour light/dark cycles (light period 8 a.m./8 p.m.) and were allowed free access to food (Standard rat pellets, B & K Universal) and water. Rats were killed by stunning and cervical dislocation, the brains were rapidly removed and snap frozen in isopentane cooled to -42°C . The brains were then stored at -70°C until further processing.

4.2.1.2 Synthetic oligonucleotide probes

Synthetic oligonucleotide probes (30-45 bases in length) were synthesised by Gibco BRL complementary to the sequence encoding the rat sequence for pre-proenkephalin-A (PPE-A) and pre-proenkephalin-B (PPE-B). Specificity of these probes were checked in two ways. First, the probe sequences were checked using the UK Human Genome Mapping Project Resource Centre database (both EMBL and GenBank databases, BLAST search, Altschul *et al.*, 1990) to check that the selected sequences would not hybridise to any other known sequence. Secondly, two probes for each target transcript were synthesised to check the specificity of the probes (see section 4.2.1.6).

The first probe targeted against PPE-A (PPE-A-1) was complementary to the sequence coding for bases 343-384 of the rat PPE-A gene (Accession number M28263, Howells *et al.* 1984) sequence 5'- CTT CAT GAA GCC TCC ATA CCG TTT CAT GAA CCC TCC ATA CTT -3'.

The second probe targeted against an alternative region of the rat PPE-A gene (PPE-A-2), was complementary to the sequence coding for bases 448-492 of the rat

PPE-A gene (Accession number M28263, Howells *et al.*, 1984) sequence 5'- CTG TCC CTC ATC TGC ATC CTT CTT CAT GAA ACC GCC ATA CCT CTT -3'.

The first probe targeted against PPE-B (PPE-B-1) was complementary to the sequence coding for bases 754-798 of the rat PPE-B gene (Accession number RNEKB M10088, Civelli *et al.*, 1985) sequence 5'- GCT CCT CTT GGG GTA TTT GCG CAA AAA GCC GCC ATA GAG TTT GGC -3'.

The second probe targeted against an alternative region of the rat PPE-B gene (PPE-B-2) was complementary to the sequence coding for bases 862-906 of the rat PPE-B gene (Accession number RNENKB M10088, Civelli *et al.*, 1985) sequence 5'- GTC CCA CTT AAG CTT GGG GCG AAT GCG CCG CAG GAA GCC CCC ATA -3'. The commercially available housekeeping gene glyceraldehyde 3-phosphate dehydrogenase (G3PDH, Clontech) was used as a control probe in all *in situ* hybridisations. This probe is complementary to nucleotides 734-763 of the G3PDH gene (G3PDH-1), sequence 5'- CAC GGA AGG CCA TGC CAG TGA GCT TCC CGT -3' (Arcari *et al.*, 1984). The second probe targeted to the sequence coding for bases 751-781 of the rat G3PDH gene (G3PDH-2), sequence 5'- TGC AAC CGT CAC CCC TGT GCC TTC CGG TAC -3' (Arcari *et al.*, 1984).

4.2.1.3 Radiolabelling of oligonucleotide probes

3'-end labelling of each oligonucleotide probe was carried out using ^{35}S -dATP. 1 μl of the oligonucleotide at a concentration of 20 ng μl^{-1} was tailed by the isotope at an incubation temperature of 37°C in a mixture containing 10 μl sterile water, 12.5 μl reaction buffer (sodium cocodylate pH 7.2 and dithiothreitol), 2.5 μl cobalt chloride, and 2 μl terminal deoxynucleotide transferase pH 7.2 (all reagents DuPont/NEN) with 7 μl of ^{35}S -dATP (NEN). Following 1 hour incubation, the reaction was stopped by addition of 50 μl of ice cold sterile water. The labelled probe was subsequently purified (to separate out unlabelled probe and isotope from the labelled probe) using Bio-spin chromatography columns (Bio-Rad) centrifuged at 1 100 g_{av} for 4 minutes (Z382K, Hermel). The volume of ^{35}S -dATP labelled probes eluted from the column was measured and 5 x volume of elute of 1 M dithiothreitol (DTT) added, to prevent sulphur bridge formation. 1 μl of the probe was removed and counted by a liquid scintillation

counter (Tricarb, 1500 Packard) beta-counter to assess the efficiency of radioactive labelling.

4.2.1.4 *In situ* hybridisation

Sections were thawed at room temperature for 30 minutes, then fixed in a 4% paraformaldehyde solution for 10 minutes, rinsed in DEPC treated water and incubated in 0.25% solution of acetic anhydride in 0.1M triethanolamine and 0.9% saline (pH 8.0) for a further 10 minutes. Sections were then dehydrated in a series of ascending concentrations of ethanol (1 min in 70%, 1 min in 80%, 2 min in 90%, and 1 min in 100%), defatted for 5 minutes in 100% chloroform, rehydrated for 1 min in 100% and 1 min in 95% ethanol and finally air dried at room temperature. Slides were then placed in an air-tight hybridisation box containing paper towels soaked in 50% formamide. Labelled probes were added to hybridisation solution (50% formamide, 4x standard sodium citrate (SSC), 10% dextran sulphate and 10mM dithiothreitol), to a final concentration of 3×10^6 counts per ml of hybridisation solution. 50 μ l of this solution was added to each of the sections, which were then covered with parafilm and incubated in an incubation oven (Mini 10, Hybaid) at 42°C for 18 hours. Following the incubation period, parafilm coverslips were floated off using 2 x SSC and the slides were returned to racks for further processing. Stringent washes were carried out for 30 minutes at room temperature in 1 x SSC, 30 minutes at 55°C in 1 x SSC, and 10 minutes at 55°C in 0.1 x SSC. Sections were then dehydrated for 2 minutes in 70% and 95% ethanol and allowed to air dry. Once dry, the sections were placed in a cassette and exposed to X-ray film (β -max Hyperfilm; Amersham) for 14 days at 4°C. An autoradiographic ^{14}C micro-scale (Amersham) of known radioactivity (range 31-833 nCi g^{-1}) was also placed in each cassette. The film was then developed in Kodak D-19 developer for 2-3 minutes, rinsed in cold tap water then fixed in Kodak unifix for 15 minutes, given a final rinse, and left to dry at room temperature.

4.2.1.5 RNase pre-treatment

After fixation in paraformaldehyde and incubation in acetic anhydride (see 4.2.1.4) tissue sections were washed in RNase A solution (ribonuclease A (Sigma) 10 $\mu\text{g ml}^{-1}$) at 37°C for 30 minutes prior to hybridisation. The sections were then processed for *in situ* hybridisation as normal i.e. hybridised with the experimental probes. Pre-treatment with RNase A solution should degrade all mRNA in the section and therefore following *in situ* hybridisation no signal (probe binding) should occur.

4.2.1.6 Specificity of anti-sense oligonucleotide probe sequence

Hybridisation using synthetic oligonucleotide anti-sense probes directed to an alternative region of the PPE-A and PPE-B mRNA was carried out. If binding is selective for a specific transcript, these probes should produce identical hybridisation signal to that achieved with the equivalent test probes. The synthetic oligonucleotide probe sequences used are described in section 4.2.1.2.

4.2.1.7 Sense oligonucleotide probes

Hybridisation using synthetic oligonucleotide sense probes which were identical in sequence to the mRNA regions targeted by the experimental probes i.e. the exact complement of the hybridisation probes, were used. These probes should produce only non-specific hybridisation. PPE-A sense probe: 5'- AAG TAT GGA GGG TTC ATG AAA CGG TAT GGA GGC TTC ATG AAG -3' i.e. complementary to PPE-A-1 oligonucleotide probe; PPE-B sense probe: 5'- GCC AAA CGC TAT GGC GGC TTT TTG CGC AAA TAC CCC AAG AGG AGC -3' i.e. complementary to PPE-B-1 oligonucleotide probe were synthesised by GIBCO, BRL.

4.2.2 Drug treatment and behavioural analysis in 6-OHDA-lesioned rats following repeated vehicle, L-DOPA, bromocriptine or lisuride administration

4.2.2.1 6-OHDA-lesion rat model of Parkinson's disease

Thirty six male Sprague Dawley rats (250-300g) were obtained from Charles River (UK), maintained in standard housing conditions with constant temperature ($22 \pm 1^\circ\text{C}$), humidity (relative, 30%), 12 hour light/dark cycles (light period 8 a.m./8 p.m.) and were allowed free access to food (Standard pellets, B & K Universal) and water. All rats received unilateral 6-hydroxydopamine lesions of the medial forebrain bundle as described in 2.2.1.

4.2.2.2 Drug treatment and behavioural analysis

Twenty one days post-operation, the 6-hydroxydopamine-lesioned rats were removed from their home cage, i.p. injected with sterile water (1 ml kg^{-1}) and placed in a 40 cm diameter bowl. Behaviour was recorded on videotape. Videotapes were analysed and the number of complete 360° rotations ipsiversive and contraversive to the lesion were counted over a 2 hour period. 6-hydroxydopamine lesioned animals obtaining a net ipsiversive rotation greater than 30 rotations/hour were then divided into 6 experimental groups containing 6 rats in each group. All animals received two injections per day at 9 a.m. and 5 p.m. for 21 days. Group 1 received an i.p. injection of 0.1% ethanol (BDH) and 0.1% ascorbic acid (Sigma) dissolved in sterile water (Braun Medical, vehicle group) and were filmed for 2 hours post injection. Group 2 received co-injections of 6.5 mg kg^{-1} L-DOPA (Sigma) and 1.5 mg kg^{-1} benserazide (Sigma) both dissolved in 0.1% ethanol and 0.1% ascorbic acid (Sigma) in sterile water (Braun Medical, L-DOPA group) and were filmed for 2 hours post injection. Group 3 received i.p. injections of 5 mg kg^{-1} bromocriptine (Sigma) dissolved in 0.1% ethanol and 0.1% ascorbic acid (Sigma) in sterile water (Braun Medical, high-dose bromocriptine group) and were filmed for 2 hours, 1 hour post i.p. injection. Group 4 received twice-daily i.p. injections of 1 mg kg^{-1} bromocriptine (Sigma) dissolved in 0.1% ethanol and 0.1% ascorbic acid (Sigma) in sterile water (Braun Medical, low-dose bromocriptine group) and were filmed for 2 hours, 1 hour post injection. Group 5 received i.p. injections of 0.1 mg kg^{-1}

lisuride (Research Biochemicals International) dissolved in 0.1% ethanol and 0.1% ascorbic acid (Sigma) in sterile water (Braun Medical, high-dose lisuride group) and were filmed for 2 hours post injection. Group 6 received i.p. injections of 0.01 mg kg^{-1} lisuride (Research Biochemicals International) dissolved in 0.1% ethanol and 0.1% ascorbic acid (Sigma) in sterile water (Braun Medical, low-dose lisuride group) and were filmed for two hours post injection. All drugs were injected at a volume of 1 ml kg^{-1} of body weight. Net rotations, contraversive to the 6-OHDA-lesion, were assessed 2 hours immediately (or 1 hour following bromocriptine injection) the a.m. injection on days 0, 1, 3, 5, 7, 10, 14, 17, and 21 of injection. Both full ipsiversive and contraversive rotations were recorded over this two hour period. Rats were removed from the stainless-steel bowls 3 hours following the 9 a.m. injection. Following 21 days of treatment, two hours following the final 5 p.m. injection, the animals (groups 1-6) were killed by stunning and cervical dislocation, the brains were rapidly removed and snap frozen in isopentane cooled to -42°C . The brains were then stored at -70°C until further processing.

4.2.2.3 Section processing

Coronal brain sections ($15 \mu\text{m}$ thick) were cut using a cryostat (OTF, Bright UK), at -19°C and thaw-mounted onto gelatin/chomalum coated glass slides. A series of 6 slides of equivalent triplicate sections were obtained from every animal. These were assigned into 4 levels depending on there localisation (see 4.2.4.4). Racks of slides were then wrapped in foil and stored desiccated at -70°C until required for mazindol receptor binding and subsequent *in situ* hybridisation.

4.2.3 Assessment of lesion : [^3H] Mazindol radioligand binding

4.2.3.1 Section processing

Coronal striatal sections ($15 \mu\text{m}$) thick were cut as in section 4.2.2.3. Sections were lyophilised for 18 hours in a freeze drier at -60°C , 600 Pa pressure.

4.2.3.2 [^3H]-mazindol radioligand binding

Mazindol radioligand binding was modified from a method previously described (Javitch *et al.*, 1985). Sections were pre-incubated in 50 mM Tris HCl buffer, pH 7.9 at 4 °C for 5 minutes. Incubation buffer consisted of 50 mM Tris HCl, 300 mM sodium chloride, 5 mM potassium chloride and 50 nM desipramine, to block noradrenergic uptake sites. Mazindol binds to both the noradrenaline and dopamine uptake sites on terminals within the striatum. Therefore, desipramine, a noradrenaline uptake inhibitor, was added to block binding to noradrenaline sites, only allowing binding to the dopaminergic sites and thus giving a true representation of dopamine-depletion within the striatum. Specific binding was defined as displacement by 100 μM nomifensine. Following pre-incubation the sections were quickly dried in a stream of cool air and placed in the incubation buffer with 10 nM [^3H]-mazindol (DuPont, NEN). Sections were incubated at 4°C for 50 minutes. Following incubation the sections were washed twice in incubation buffer for 1 minute and rinsed in distilled water. The sections were quickly dried in a stream of cool air. The sections were exposed to [^3H]-sensitive autoradiographic film (Hyperfilm, Amersham) with ^{14}C radioactive standards and stored at 4°C for 14 days. Autoradiographic film was developed and fixed as described in 4.2.1.4.

4.2.3.3 Image Analysis

Image analysis was carried out using Seescan Image Analysis equipment (Seescan, Inc). Optical density was measured from both lesioned and unlesioned striatum. Non-specific binding was subtracted for each side. Percentage lesion was defined as specific binding of the lesioned striatum over the specific binding from the unlesioned striatum. Only 6-OHDA-lesioned rats with a specific reduction in dopamine uptake sites of greater than 90% were further processed for *in situ* hybridisation studies.

4.2.4 *In situ* hybridisation

4.2.4.1 Anti-sense oligonucleotide probes

Synthetic 45-base oligonucleotide probes were synthesised complementary to the pre-proenkephalin-A and pre-proenkephalin-B transcripts as previously described 4.2.1.2. The commercially available 30-base oligonucleotide housekeeping gene glyceraldehyde 3-phosphate dehydrogenase (G3PDH, Clontech) was purchased. These oligonucleotide probes were subsequently used in the *in situ* hybridisation studies.

4.2.4.2 Radiolabelling of oligonucleotide probes

Synthetic oligonucleotide probes were 3'-end labelled with ^{35}S -dATP as previously described in 4.2.1.3

4.2.4.3 *In situ* hybridisation

In situ hybridisation was carried out as described in 4.2.1.4

4.2.4.4 Analysis of *in situ* hybridisation signal

Densitometric analysis of the pre-proenkephalin-A (PPE-A), pre-proenkephalin-B (PPE-B) and G3PDH autoradiographs was performed using a Seescan Image Analysis system (Seescan Inc.). Optical density (O.D.) measurements were obtained from 18 areas from both the lesioned and unlesioned neostriatum. These areas are illustrated in figures 4.1 to 4.4 (modified from Paxinos and Watson, 1986).

In levels 1 (1.7 mm anterior from bregma) and 2 (1 mm anterior from bregma), i.e. rostral striatum - level 1 and rostral striatum - level 2 respectively, the striatum and nucleus accumbens is divided into 6 areas as shown in figure 4.1 and 4.2. The caudate-putamen is divided into quarters (dorsolateral, dorsoventral, ventrolateral and ventromedial), the nucleus accumbens is divided into core and shell regions. The intermediate striatum (-0.26 mm posterior from bregma) is divided into quarters (dorsolateral, dorsoventral, ventrolateral and ventromedial) as shown in figure 4.3. The caudal striatum (-0.92 mm posterior from bregma) is divided in half (dorsal and ventral) as shown in figure 4.4. The hybridisation signal arising from non-specific binding (defined as the O.D. of the corpus callosum) was subtracted from all the O.D. values for both PPE-A and PPE-B oligonucleotide probe signals.

The mean values for each triplicate of sections were then calculated and subsequently corrected for any non-specific changes in transcription rate that occurred between animals, either due to non-specific RNase activity within the sections, temporal variations in preparation of the sections both due to *post-mortem* delay period and following cryostat cutting, mounting and re-freezing. This was achieved by dividing the mean of the probe of investigation values (PPE-A and PPE-B) from lesioned or unlesioned striatum, by the mean value of the control probe G3PDH over the whole striatum (both lesioned and unlesioned combined). The final value is therefore expressed as a ratio of the mean probe of investigation relative to the mean of the G3PDH probe. This ratio gives a semi-quantitative analysis of PPE-A and PPE-B mRNA expression in the neostriatum.

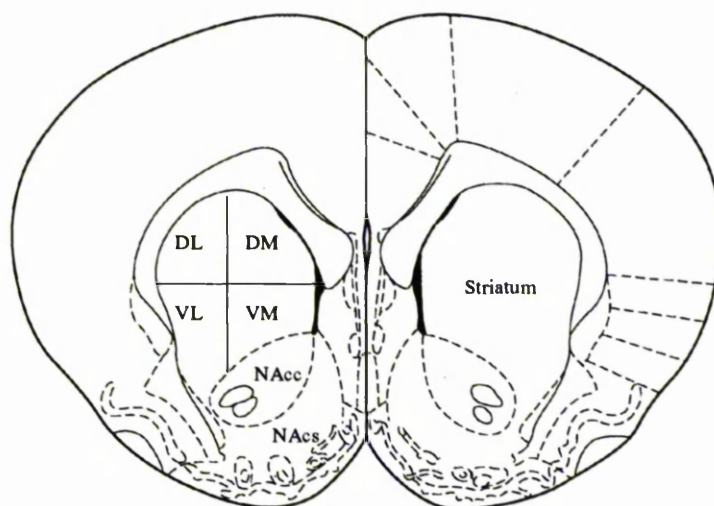


Figure 4.1 *Diagrammatic representation of rostral striatum - level 1. The striatum is divided into quarters (dorsolateral (DL), dorsomedial (DM), ventrolateral (VL) and ventromedial (VM)). The nucleus accumbens (NAc) is divided into core (NAcc) and shell (NAcs) regions.*

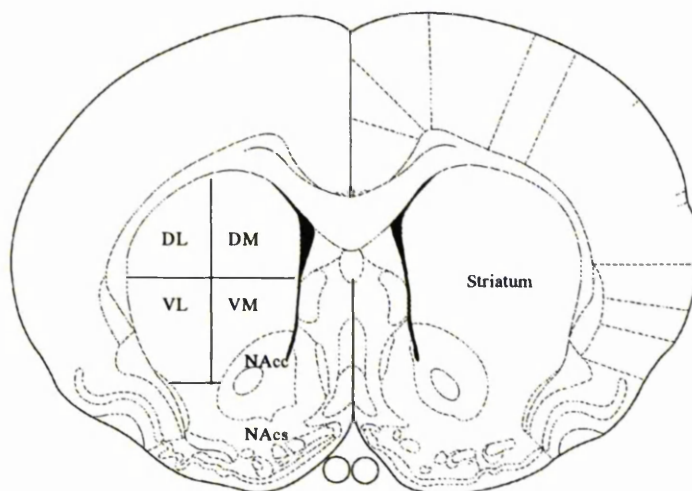


Figure 4.2 *Diagrammatic representation of rostral striatum - level 2. The striatum is divided into quarters (dorsolateral (DL), dorsomedial (DM), ventrolateral (VL) and ventromedial (VM)). The nucleus accumbens (NAc) is divided into core (NAcc) and shell (NAcs) regions.*

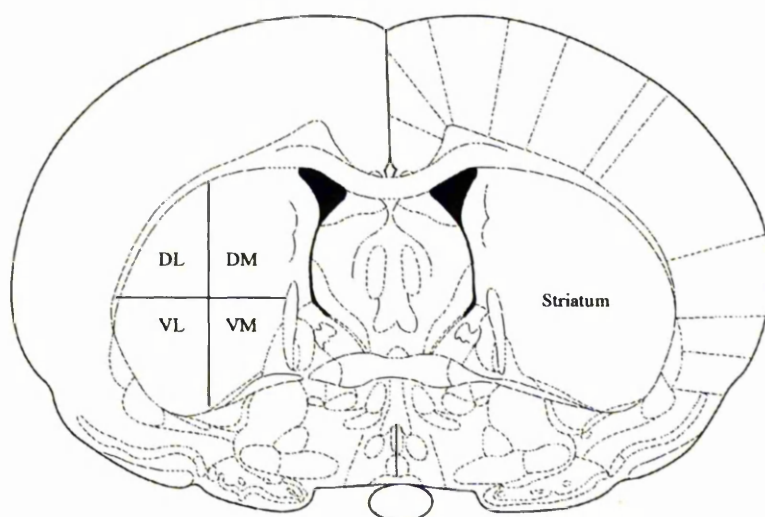


Figure 4.3 *Diagrammatic representation of the intermediate striatum. The striatum is divided into quarters (dorsolateral (DL), dorsomedial (DM), ventrolateral (VL) and ventromedial (VM)).*

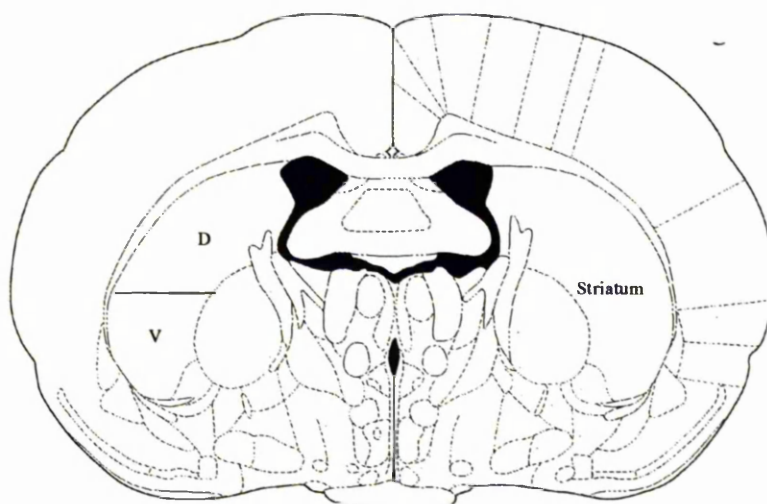


Figure 4.4 *Diagrammatic representation of caudal striatum. The striatum is divided in half (dorsal (D) and ventral (V)).*

4.2.5 Statistical analysis

Data are expressed as mean \pm SEM values. Rotational behavioural data, following repeated drug administration, were analysed by multiple analysis of variance (MANOVA), followed by unpaired student's t-test. Average optical density readings of *in situ* hybridisation signal were analysed between all identical areas within each rostral-caudal level from both the lesioned or unlesioned striatum for all drug groups using one-way analysis of variance (ANOVA), followed by Student-Newman-Keuls post hoc analysis. In all tests significance was assigned when $P < 0.05$.

4.3 Results

4.3.1 Methodological results

Following *in situ* hybridisation utilising an oligonucleotide probe specifically targeted to the mRNA transcript encoding the enkephalin precursor, pre-proenkephalin-A (PPE-A), a specific hybridisation signal restricted to the neostriatum (high to moderate), was observed (Figure 4.3.1.1, A). RNase pre-treatment prior to *in situ* hybridisation resulted in no hybridisation signal for PPE-A (Figure 4.3.1.1, B). Similarly, following *in situ* hybridisation utilising an oligonucleotide probe specifically targeted to the mRNA transcript encoding the dynorphin precursor, pre-proenkephalin-B (PPE-B), a specific hybridisation signal restricted to the neostriatum was observed, with moderate signal in the ventral neostriatum and lower signal in the dorsal striatum (Figure 4.3.1.2, A). RNase pre-treatment prior to *in situ* hybridisation, resulted in no hybridisation signal for PPE-B (Figure, 4.3.1.2, B). Following *in situ* hybridisation with an oligonucleotide probe targeted to the G3PDH mRNA transcript, signal was observed in all regions of the brain, with particularly high levels within the cerebral cortex (Figure 4.3.1.3, A). RNase pre-treatment prior to *in situ* hybridisation resulted in no hybridisation signal for G3PDH (Figure 4.3.1.3, B).

Two oligonucleotide probes targeted to different sites on the mRNA transcripts for PPE-A, PPE-B and G3PDH were designed. Following *in situ* hybridisation identical hybridisation signals for both oligonucleotide probes targeted to PPE-A (Figure 4.3.1.4), PPE-B (Figure 4.3.1.5) and G3PDH (Figure 4.3.1.6) were observed.

Sense oligonucleotide probes identical to the mRNA transcript signal for PPE-A, PPE-B and G3PDH were synthesised. *In situ* hybridisation with the antisense oligonucleotide probe produced a hybridisation signal identical to that already observed for PPE-A (Figure 4.3.1.7, A), PPE-B (Figure 4.3.1.8, A) and for G3PDH (Figure 4.3.1.9, A). However, *in situ* hybridisation with the sense oligonucleotide probes specific for PPE-A (Figure 4.3.1.7, B), PPE-B (Figure 4.3.1.8, B) and G3PDH (Figure 4.3.1.9, B), showed no hybridisation signal.

4.3.1.1 Effect of RNase pre-treatment

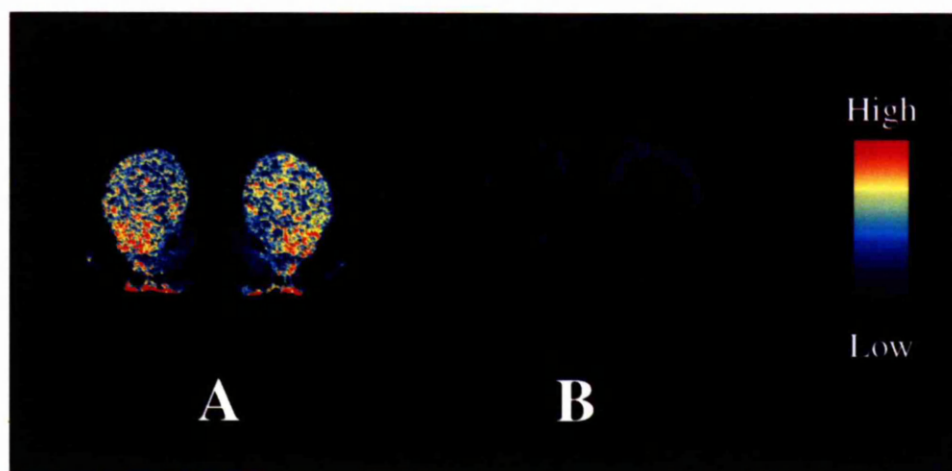


Figure 4.3.1.1 Pseudocolour transformation of an autoradiograph of an *in situ* hybridisation utilising an oligonucleotide probe targeted against pre-proenkephalin-A in the rodent striatum following RNase treatment

In situ hybridisation of (A) pre-proenkephalin (PPE-A) antisense oligonucleotide probe and (B) PPE-A antisense oligonucleotide probe following RNase-A treatment in the rat striatum.

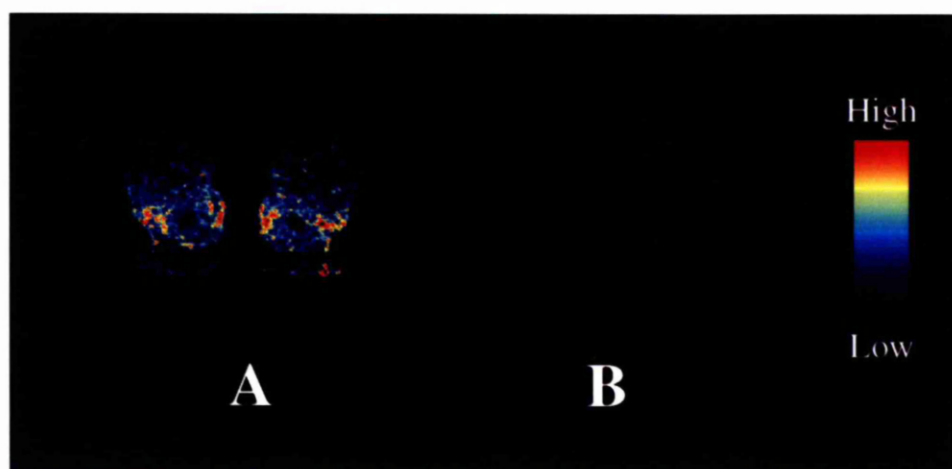


Figure 4.3.1.2 Pseudocolour transformation of an autoradiograph of an *in situ* hybridisation utilising an oligonucleotide probe targeted against pre-proenkephalin-B in the rodent striatum following RNase treatment

In situ hybridisation of (A) pre-proenkephalin-B (PPE-B) antisense oligonucleotide probe and (B) PPE-B antisense oligonucleotide probe following RNase-A treatment in the rat striatum.

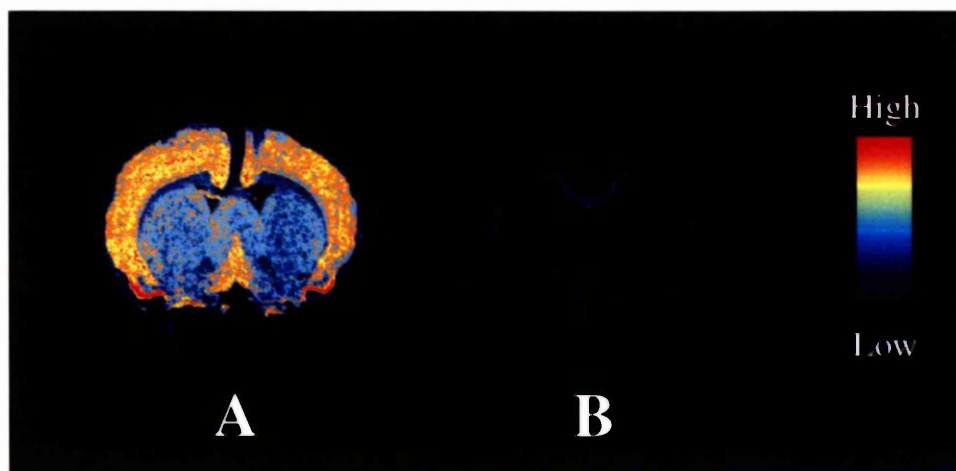


Figure 4.3.1.3 Pseudocolour transformation of an autoradiograph of an *in situ* hybridisation utilising an oligonucleotide probe targeted against G3PDH in the rodent striatum following RNase treatment

In situ hybridisation of (A) G3PDH antisense oligonucleotide probe and (B) G3PDH antisense oligonucleotide probe following RNase-A treatment in the rat striatum.

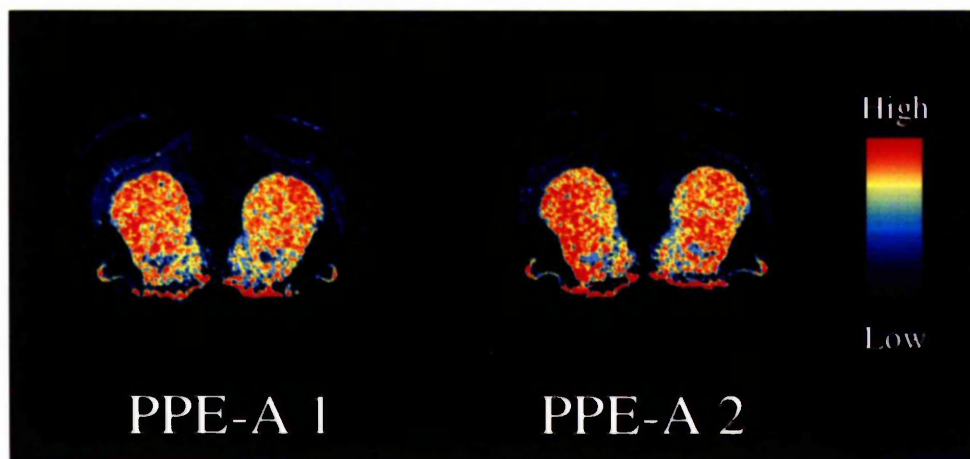


Figure 4.3.1.4 Pseudocolour transformation of an autoradiograph of an *in situ* hybridisation utilising oligonucleotide probes directed to different sites on the pre-proenkephalin-A transcript

In situ hybridisation of (A) the pre-proenkephalin-A (PPE-A-1, directed to codons 343-384) antisense oligonucleotide probe and (B) a PPE-A-2 antisense oligonucleotide probe directed towards a second region of the mRNA transcript (directed to codons 448-492).

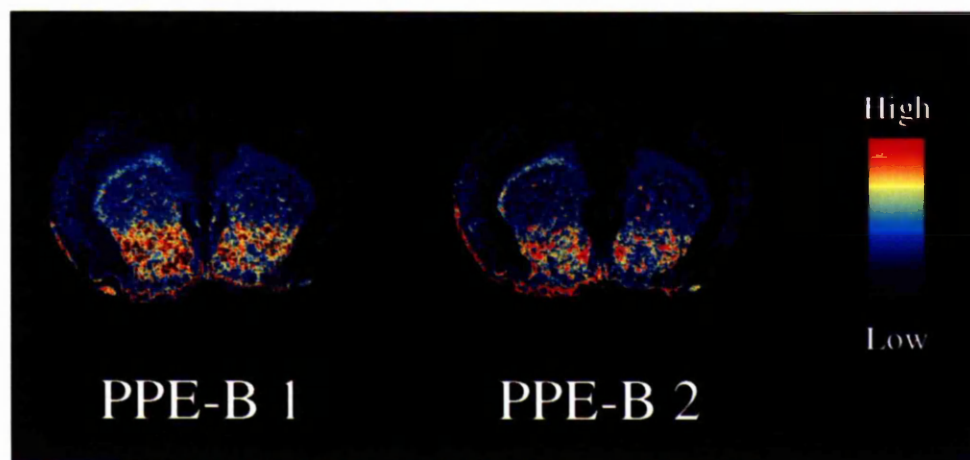


Figure 4.3.1.5 Pseudocolour transformation of an autoradiograph of an *in situ* hybridisation utilising oligonucleotide probes directed to different sites on the pre-proenkephalin-B transcript

In situ hybridisation of (A) the pre-proenkephalin-B (PPE-B-1, directed to codons 754-798) antisense oligonucleotide probe and (B) a PPE-B-2 antisense oligonucleotide probe directed towards a second region of the mRNA transcript (directed to codons 862-906).

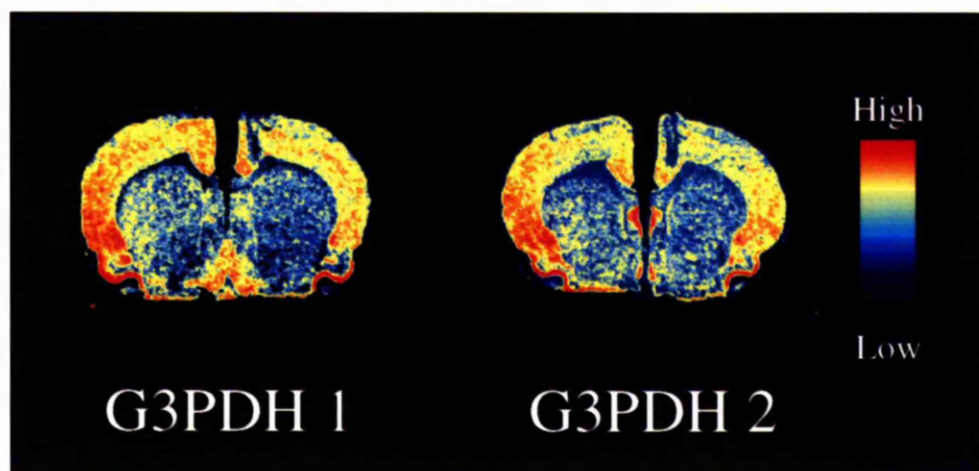


Figure 4.3.1.6 Pseudocolour transformation of an autoradiograph of an *in situ* hybridisation utilising oligonucleotide probes directed to different sites on the G3PDH transcript

In situ hybridisation of the commercially available G3PDH (G3PDH 1) oligonucleotide probe, directed to codons 734-763 and (B) an antisense oligonucleotide probe directed towards a second region of the mRNA transcript (G3PDH-2, directed to codons 751-781).

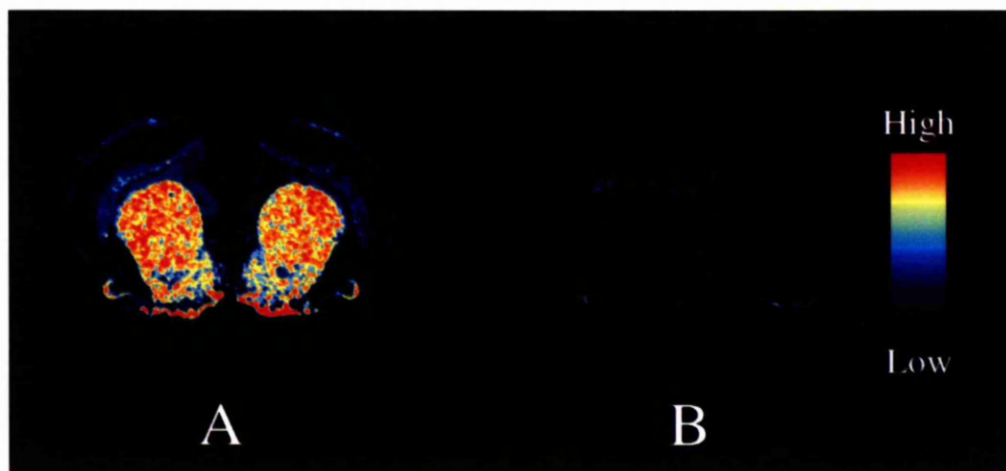


Figure 4.3.1.7 Pseudocolour transformation of an autoradiograph of a sense pre-proenkephalin-A oligonucleotide probe

In situ hybridisation of (A) pre-proenkephalin-A (PPE-A) antisense oligonucleotide probe and (B) PPE-A sense oligonucleotide probe.

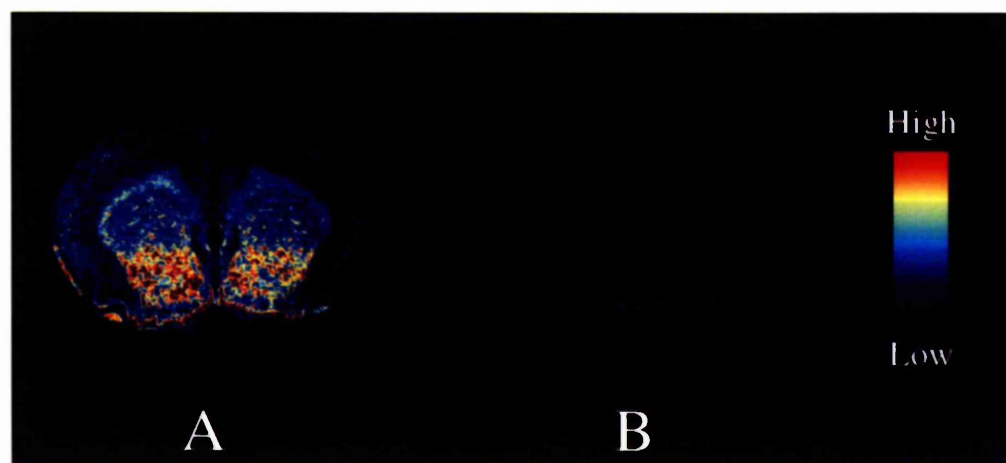


Figure 4.3.1.8 Pseudocolour transformation of an autoradiograph of a sense pre-proenkephalin-B oligonucleotide probe

In situ hybridisation of (A) pre-proenkephalin-B (PPE-B) antisense oligonucleotide probe and (B) PPE-B sense oligonucleotide probe.

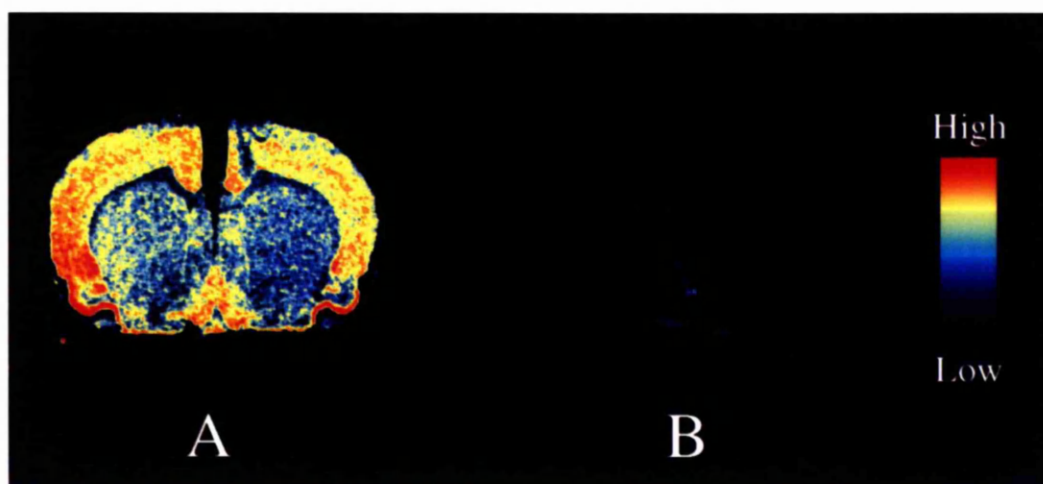


Figure 4.3.1.9 Pseudocolour transformation of an autoradiograph of a sense G3PDH oligonucleotide probe

In situ hybridisation of (A) pre-proenkephalin-B (PPE-B) antisense oligonucleotide probe and (B) PPE-B sense oligonucleotide probe.

4.3.2 Rodent model of L-DOPA-induced dyskinesia

Following repeated L-DOPA-administration in the 6-OHDA-lesioned rat model of Parkinson's disease, a potentiated behavioural response is observed (Figure 4.3.2.1). This behavioural potentiation does not occur following repeated vehicle treatment (Figure 4.3.2.1). Repeated *de novo* administration of bromocriptine at both 5 mg kg⁻¹ and 1 mg kg⁻¹ produced contraversive rotations. However, this response was not potentiated over the 21 day period (Figure 4.3.2.2). Similarly, repeated *de novo* administration of lisuride at both 0.1 mg kg⁻¹ and 0.01 mg kg⁻¹ also produced contraversive rotations that were not potentiated over the 21 day treatment period (Figure 4.3.2.3).

Following the 21 day behavioural analysis all rats were sacrificed. All brains were processed for both *in situ* hybridisation and mazindol binding. Before *in situ* hybridisation was performed, mazindol binding was carried out on all brains. Only rats with greater than 90% dopamine-depletion were used for further *in situ* hybridisation studies (Figure 4.3.3.1 and Table 4.1).

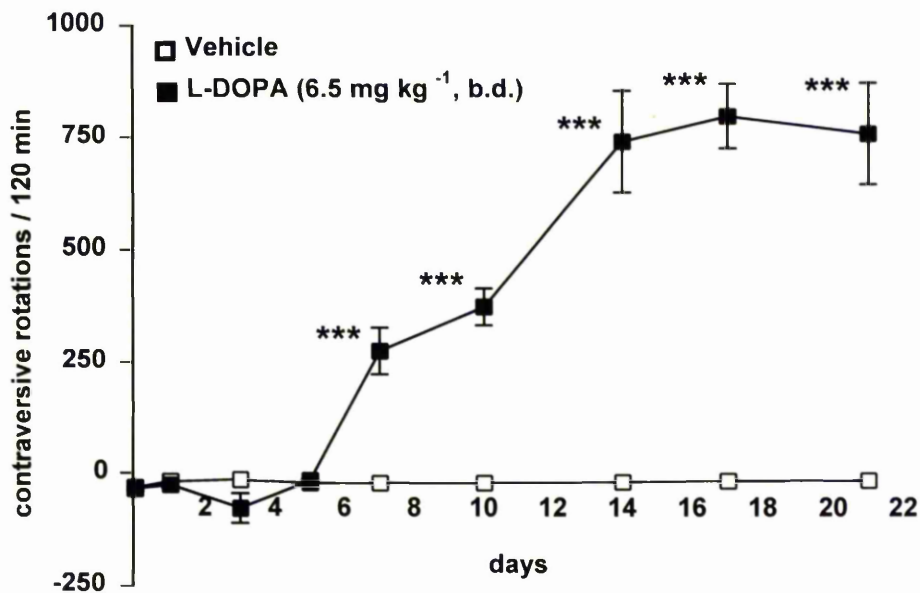


Figure 4.3.2.1 Rotational locomotion in 6-OHDA-lesioned rats following repeated vehicle or L-DOPA administration

Net rotations, contraversive to the 6-OHDA-lesion, in the 2 hours following repeated (21 days, b.d.) vehicle (□) or L-DOPA (6.5 mg kg⁻¹) and benserazide (1.5 mg kg⁻¹) (■) treatment in the 6-OHDA-lesioned rat model of Parkinson's disease. Locomotion was assessed in both vehicle and L-DOPA-treated rats 2 hours immediately following the 9 a.m. i.p. injection. Data are expressed as mean (\pm SEM) complete rotations contraversive to the lesion ($n = 6$, effect of drug $P < 0.001$, $F_{1, 10} = 297.64$, MANOVA, effect of drug over time $P < 0.001$, $F_{8, 80} = 28.02$, MANOVA, *** $P < 0.001$ cf vehicle group, unpaired Student's t -test).

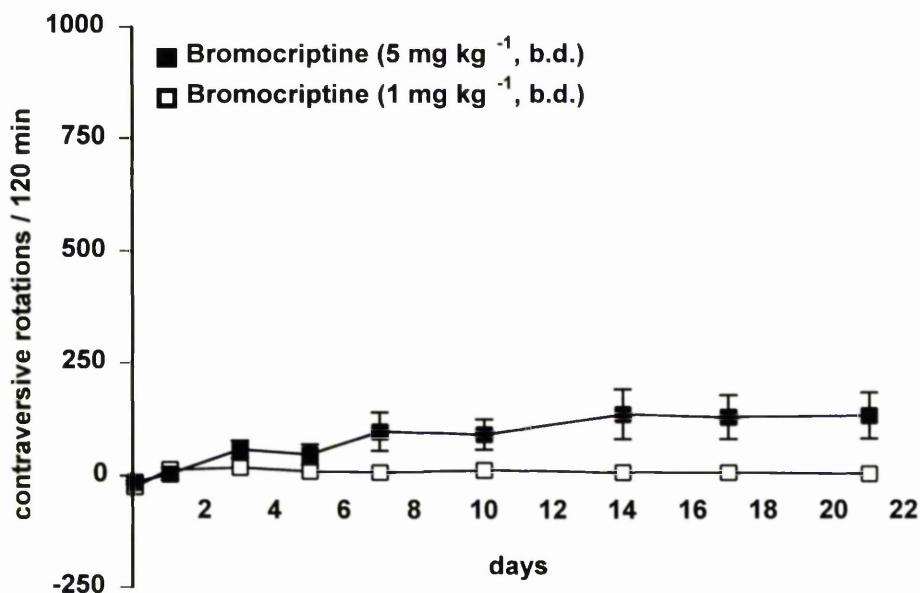


Figure 4.3.2.2 Rotational locomotion in 6-OHDA-lesioned rats following repeated bromocriptine treatment

Net rotations, contraversive to the 6-OHDA-lesion, in the 2 hours following repeated (21 days, b.d.) bromocriptine (5 mg kg⁻¹ (■), or 1 mg kg⁻¹ (□)) treatment in the 6-OHDA-lesioned rat model of Parkinson's disease. Locomotion was assessed in both bromocriptine-treated groups for 2 hours, 1 hour following the 9 a.m. i.p. injection. This 1 hour period following injection was to allow for differences in drug pharmacokinetics. Data are expressed as mean (\pm SEM) complete rotations contraversive to the lesion ($n = 6$, effect of drug $P < 0.001$, $F_{1, 10} = 84.25$, MANOVA, effect of drug over time $P < 0.001$, $F_{8, 80} = 6.42$, MANOVA, ns $P > 0.5$ cf vehicle group, unpaired Student's t -test).

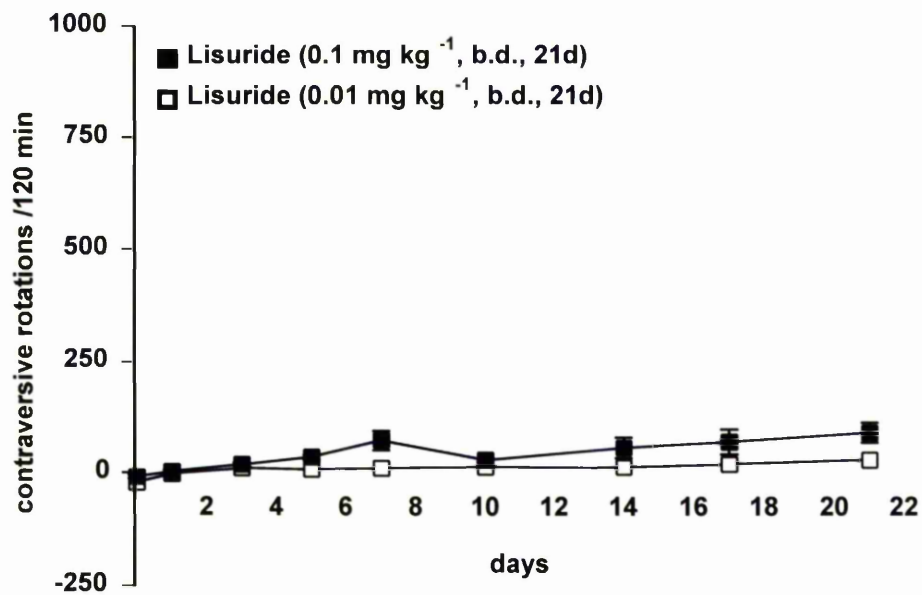


Figure 4.3.2.3 Rotational locomotion in 6-OHDA-lesioned rats following repeated lisuride administration

Net rotations, contraversive to the 6-OHDA-lesion, in the 2 hours following repeated (21 days, b.d) lisuride (0.1 mg kg⁻¹ (■), or 0.01 mg kg⁻¹ (□)) treatment in the 6-OHDA-lesioned rat model of Parkinson's disease. Locomotion was assessed in both lisuride-treated groups for 2 hours immediately following the 9 a.m. i.p. injection. Data are expressed as mean (\pm SEM) complete rotations contraversive to the lesion. ($n = 6$, effect of drug $P < 0.001$, $F_{1,10} = 74.06$, MANOVA, effect of drug over time $P < 0.001$, $F_{8,80} = 1470.80$, MANOVA, $P > 0.05$ cf vehicle group, unpaired Student's t -test).

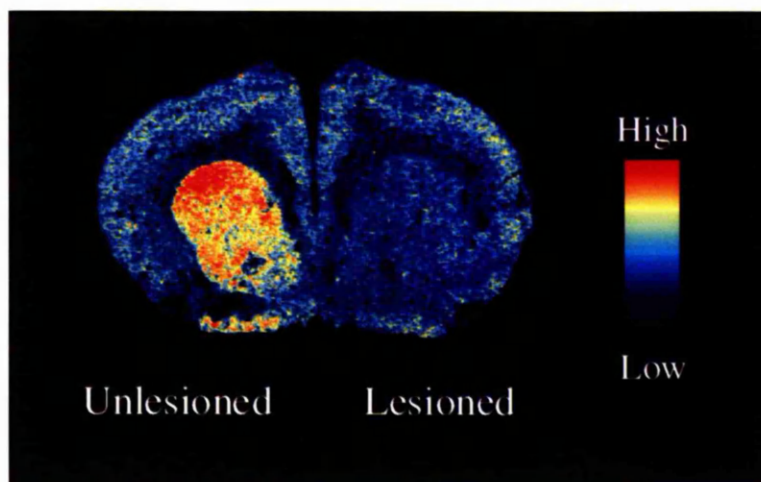
4.3.3 Assessment of lesion : ^3H Mazindol radioligand binding

Figure 4.3.3.1 Pseudocolour transformation of autoradiographs of [^3H] mazindol radioligand binding in a coronal striatal section of the rat brain following a 6-OHDA-lesion of the medial forebrain bundle.

6-OHDA-lesioned group	% reduction in specific [^3H]mazindol binding (Mean \pm SEM)
Vehicle	95.68 \pm 1.65
L-DOPA	98.24 \pm 2.35
Bromocriptine (5 mg kg $^{-1}$ group)	96.43 \pm 1.65
Bromocriptine (1 mg kg $^{-1}$ group)	95.32 \pm 2.11
Lisuride (0.1 mg kg $^{-1}$ group)	94.51 \pm 1.12
Lisuride (0.01 mg kg $^{-1}$ group)	96.74 \pm 2.31

Table 4.1 Table showing percentage reduction of specific mazindol binding in the striatum following 6-OHDA-lesions of the medium forebrain bundle in the vehicle-, L-DOPA-, bromocriptine and lisuride groups. Data are expressed as mean (\pm SEM) ($n=6$).

4.3.4 Topographical distribution of striatal pre-proenkephalin-A mRNA in the 6-OHDA-lesioned rat following repeated treatment with vehicle, L-DOPA, bromocriptine or lisuride

In situ hybridisation utilising an oligonucleotide probe targeted against the enkephalin precursor (pre-proenkephalin-A, PPE-A) was employed to investigate the topographical distribution of PPE-A in the striatum of 6-OHDA-lesioned rats following 21 day, twice daily treatment with either vehicle, L-DOPA (6.5 mg kg^{-1}), bromocriptine (5 mg kg^{-1} or 1 mg kg^{-1}) or lisuride (0.1 mg kg^{-1} or 0.01 mg kg^{-1}).

In the 6-OHDA-lesioned striatum, following 21 days vehicle administration, elevated levels of PPE-A expression were seen throughout the striatum. The highest significantly elevated levels of PPE-A expression were found in the rostral and dorsal striatum. Following 21 day L-DOPA (6.5 mg kg^{-1}) and benserazide (1.5 mg kg^{-1}) administration, the levels of PPE-A expression remained elevated throughout the striatum (Figures 4.3.4.1-4.3.4.22), with a significant further elevation in PPE-A expression seen in the rostral and dorsal striatum (Figures 4.3.4.2, 4.3.4.3). Following 21 day high-dose bromocriptine (5 mg kg^{-1}) administration the lesion-induced elevation in PPE-A was reduced to unlesioned levels throughout the striatum (Figures 4.3.4.1-4.3.4.22). Twenty one day low-dose administration of bromocriptine (1 mg kg^{-1}) had no significant effect on PPE-A expression compared to the L-DOPA-treated group (Figures 4.3.4.1-4.3.4.22).

Following 21 day high-dose lisuride administration (0.1 mg kg^{-1}), a reduction in the lesion-induced elevation in PPE-A expression was observed throughout the striatum. Low-dose lisuride (0.01 mg kg^{-1}) administration also produced a significant reduction in lesion-induced elevation of PPE-A throughout the striatum (Figures 4.3.4.1-4.3.4.22).

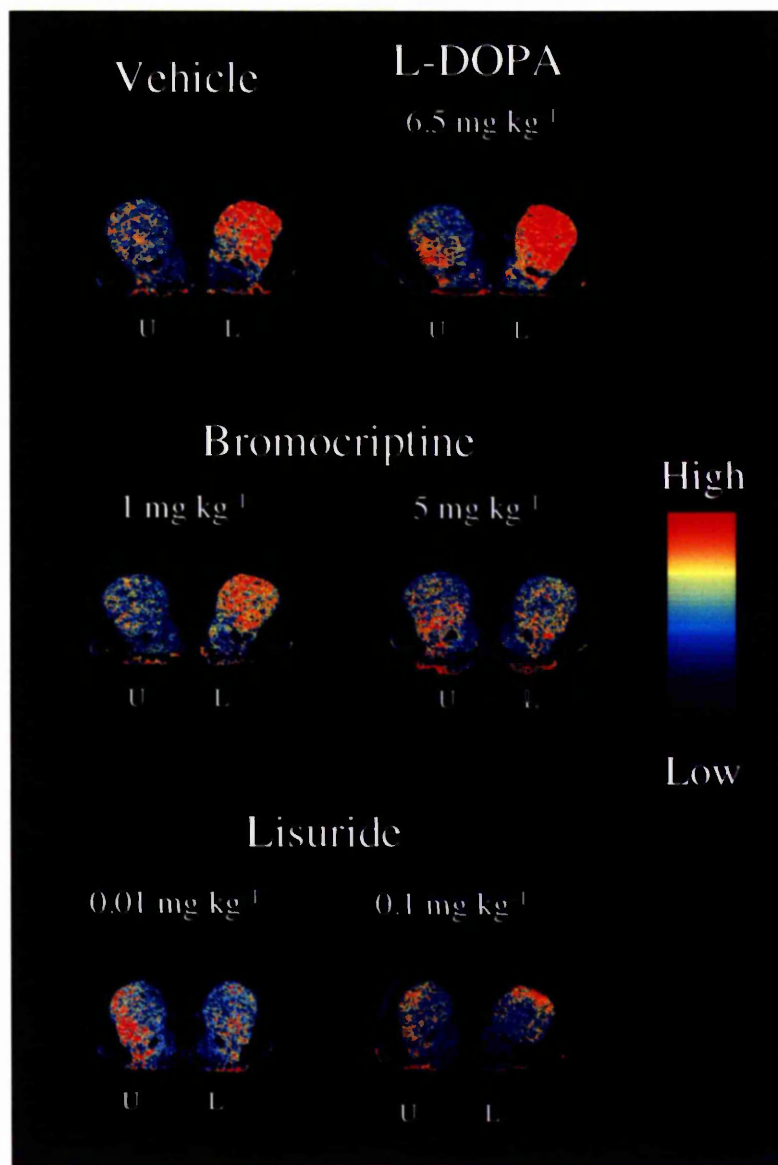


Figure 4.3.4.1 Pseudocolour transformations of autoradiographs of *in situ* hybridisation utilising an oligonucleotide probe targeted against pre-proenkephalin-A (PPE-A) in the lesioned (L) or unlesioned (U) rostral striatum (level 1) following 21 days, twice-daily, vehicle, L-DOPA (6.5 mg kg⁻¹) and benserazide (1.5 mg kg⁻¹), bromocriptine (5 or 1 mg kg⁻¹) or lisuride (0.1 or 0.01 mg kg⁻¹) treatment in the 6-OHDA-lesioned rat model of Parkinson's disease.

Pre-proenkephalin-A : G3PDH expression - Rostral Striatum - Level 1

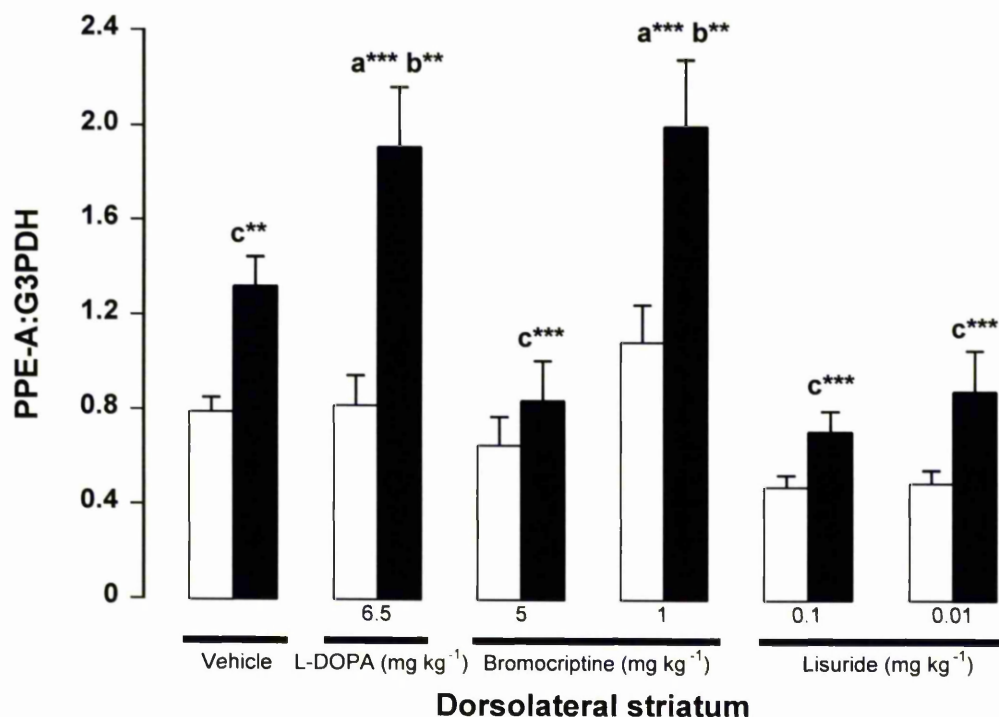


Figure 4.3.4.2 Ratio of pre-proenkephalin (PPE-A) to G3PDH mRNA expression in rostral striatum level 1 (dorsolateral) in the 6-OHDA-lesioned rat model of Parkinson's disease following 21 day, twice-daily, treatment with vehicle, L-DOPA (6.5 mg kg⁻¹) and benserazide (1.5 mg kg⁻¹), bromocriptine (5, 1 mg kg⁻¹, b.d.) or lisuride (0.1, 0.01 mg kg⁻¹, b.d.). Unlesioned (□) and lesioned (■) striatum are shown. Data are expressed as mean (\pm SEM) optical density ratios ($n=6$, $a^{***} P < 0.001$ cf unlesioned in same group, $b^{**} P < 0.01$ cf ipsi vehicle group, $c^{***} P < 0.001$ cf ipsi L-DOPA group, $c^{**} P < 0.01$ cf ipsi L-DOPA group, $F_{11, 60} = 10.53$, one-way analysis of variance, Student-Newman-Keuls post hoc analysis).

Pre-proenkephalin-A : G3PDH expression - Rostral Striatum - Level 1

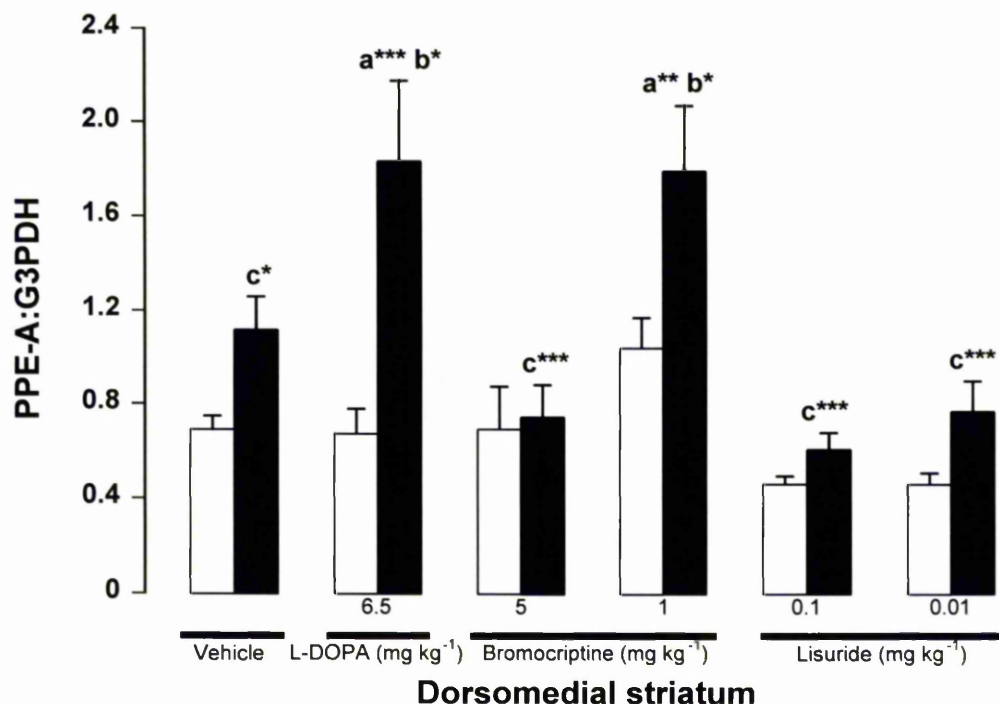


Figure 4.3.4.3 Ratio of pre-proenkephalin (PPE-A) to G3PDH mRNA expression in rostral striatum level 1 (dorsomedial) in the 6-OHDA-lesioned rat model of Parkinson's disease following 21 day, twice-daily, treatment with vehicle, L-DOPA (6.5 mg kg⁻¹) and benserazide (1.5 mg kg⁻¹), bromocriptine (5, 1 mg kg⁻¹, b.d.) or lisuride (0.1, 0.01 mg kg⁻¹, b.d.). Unlesioned (□) and lesioned (■) striatum are shown. Data are expressed as mean (\pm SEM) optical density ratios ($n=6$, a*** $P < 0.001$ cf unlesioned in same group, a** $P < 0.01$ cf unlesioned in same side, b* $P < 0.01$ cf ipsi vehicle group, c*** $P < 0.001$ cf ipsi L-DOPA group, c* $P < 0.05$ cf ipsi L-DOPA group, $F_{11, 60} = 8.23$, one-way analysis of variance, Student-Newman-Keuls post hoc analysis).

Pre-proenkephalin-A : G3PDH expression - Rostral Striatum - Level 1

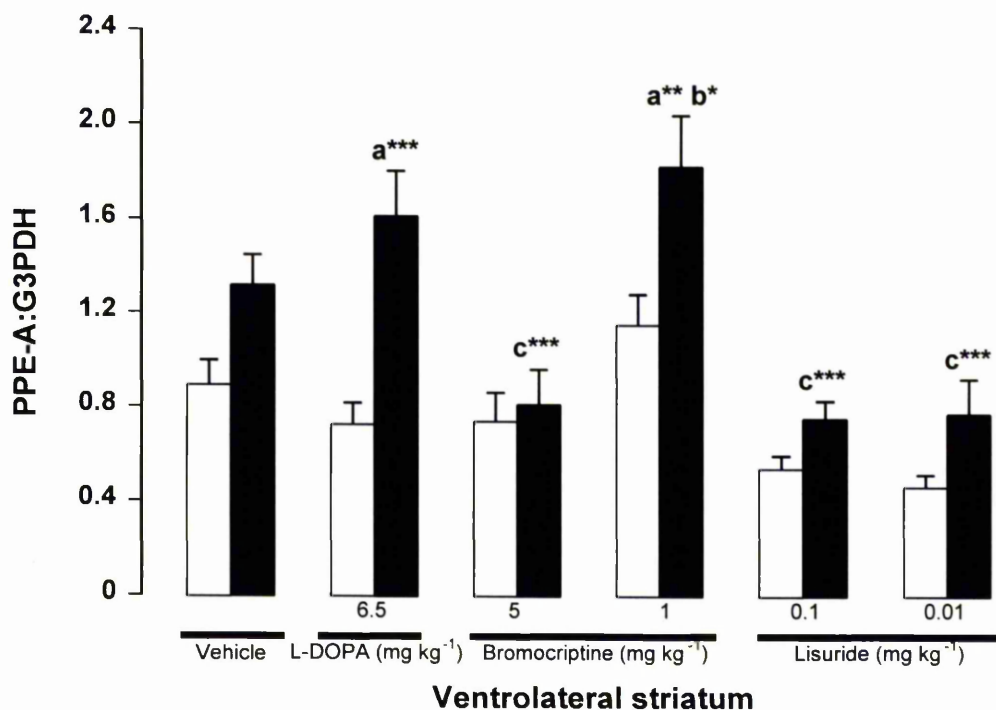


Figure 4.3.4.4 Ratio of pre-proenkephalin (PPE-A) to G3PDH mRNA expression in rostral striatum level 1 (ventrolateral) in the 6-OHDA-lesioned rat model of Parkinson's disease following 21 day, twice-daily, treatment with vehicle, L-DOPA (6.5 mg kg⁻¹) and benserazide (1.5 mg kg⁻¹), bromocriptine (5, 1 mg kg⁻¹, b.d.) or lisuride (0.1, 0.01 mg kg⁻¹, b.d.). Unlesioned (□) and lesioned (■) striatum are shown. Data are expressed as mean (\pm SEM) optical density ratios ($n=6$, a*** $P < 0.001$ cf unlesioned in same group, a** $P < 0.01$ cf unlesioned in same side, b* $P < 0.01$ cf ipsi vehicle group, c*** $P < 0.001$ cf ipsi L-DOPA group, $F_{11, 60} = 10.79$, one-way analysis of variance, Student-Newman-Keuls post hoc analysis).

Pre-proenkephalin-A : G3PDH expression - Rostral Striatum - Level 1

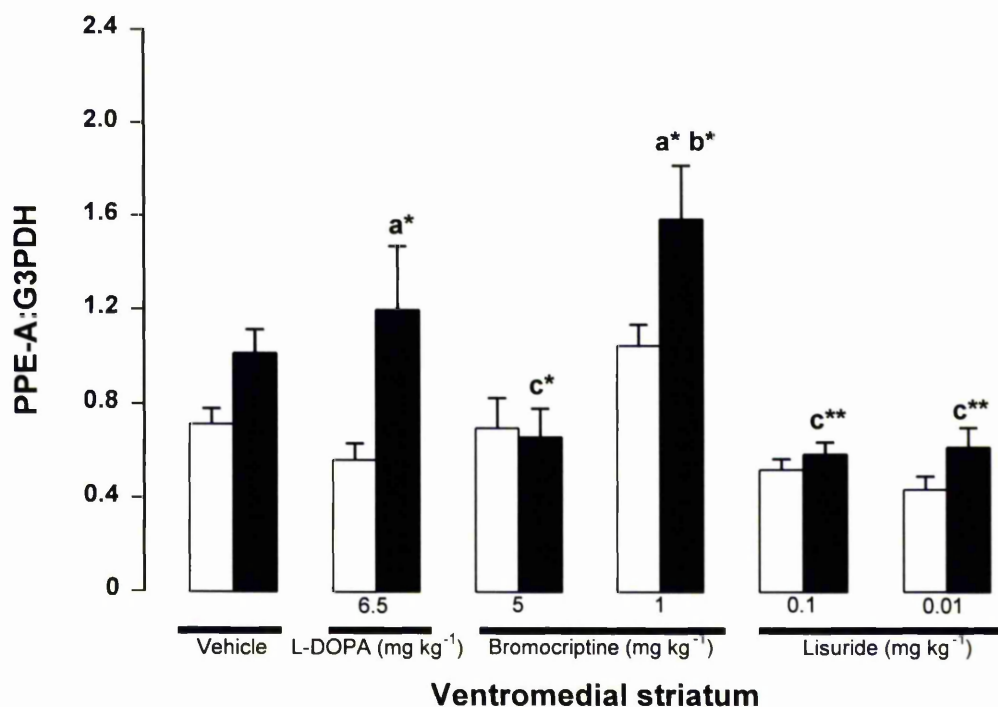


Figure 4.3.4.5 Ratio of pre-proenkephalin (PPE-A) to G3PDH mRNA expression in rostral striatum level 1 (ventromedial) in the 6-OHDA-lesioned rat model of Parkinson's disease following 21 day, twice-daily, treatment with vehicle, L-DOPA (6.5 mg kg⁻¹) and benserazide (1.5 mg kg⁻¹), bromocriptine (5, 1 mg kg⁻¹, b.d.) or lisuride (0.1, 0.01 mg kg⁻¹, b.d.). Unlesioned (□) and lesioned (■) striatum are shown. Data are expressed as mean (± SEM) optical density ratios (n=6, a* $P < 0.5$ cf unlesioned in same group, b* $P < 0.01$ cf ipsi vehicle group, c** $P < 0.01$ cf ipsi L-DOPA group, c* $P < 0.05$ cf ipsi L-DOPA group, $F_{11, 60} = 6.97$, one-way analysis of variance, Student-Newman-Keuls post hoc analysis).

Pre-proenkephalin-A : G3PDH expression - Rostral Striatum - Level 1

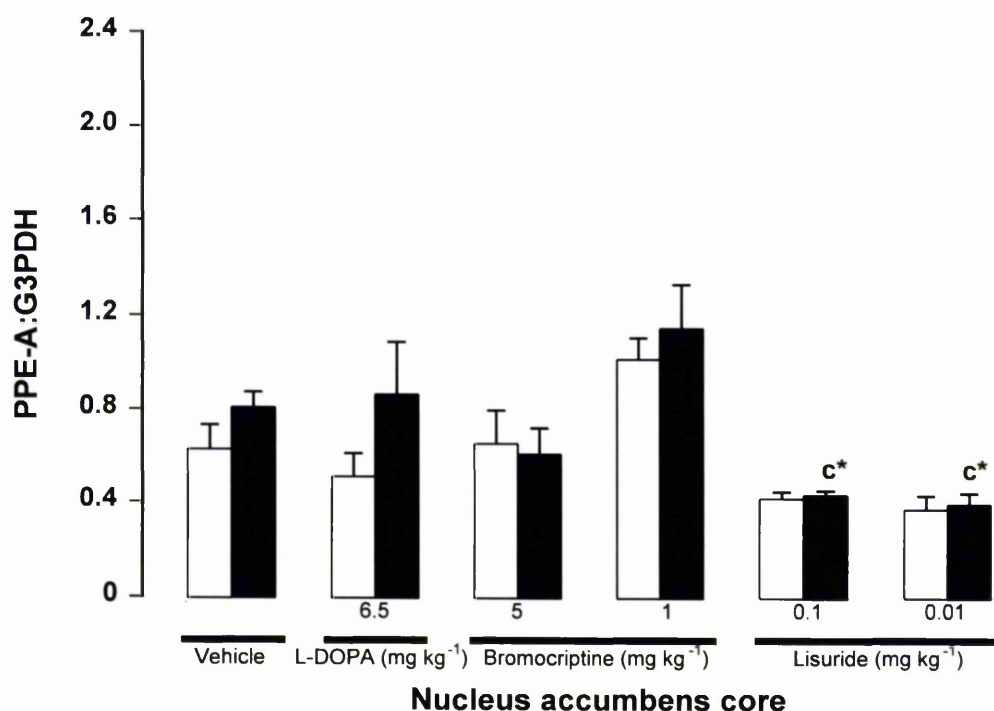


Figure 4.3.4.6 Ratio of pre-proenkephalin (PPE-A) to G3PDH mRNA expression in rostral striatum level 1 (Nucleus accumbens core) in the 6-OHDA-lesioned rat model of Parkinson's disease following 21 day, twice-daily, treatment with vehicle, L-DOPA (6.5 mg kg⁻¹) and benserazide (1.5 mg kg⁻¹), bromocriptine (5, 1 mg kg⁻¹, b.d.) or lisuride (0.1, 0.01 mg kg⁻¹, b.d.). Unlesioned (□) and lesioned (■) striatum are shown. Data are expressed as mean (\pm SEM) optical density ratios ($n=6$, c^* $P < 0.05$ cf ispi L-DOPA group, $F_{11, 60} = 4.95$, one-way analysis of variance, Student-Newman-Keuls post hoc analysis).

Pre-proenkephalin-A : G3PDH expression -Rostral Striatum - Level 1

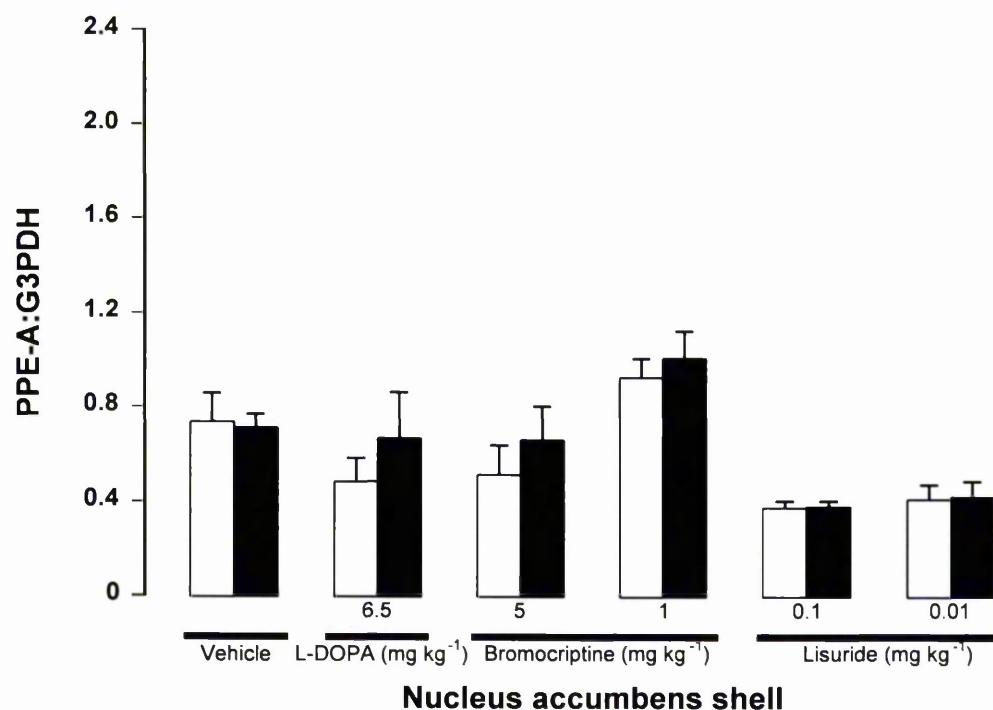


Figure 4.3.4.7 Ratio of pre-proenkephalin (PPE-A) to G3PDH mRNA expression in rostral striatum level 1 (Nucleus accumbens shell) in the 6-OHDA-lesioned rat model of Parkinson's disease following 21 day, twice-daily, treatment with vehicle, L-DOPA (6.5 mg kg⁻¹) and benserazide (1.5 mg kg⁻¹), bromocriptine (5, 1 mg kg⁻¹, b.d.) or lisuride (0.1, 0.01 mg kg⁻¹, b.d.). Unlesioned (□) and lesioned (■) striatum are shown. Data are expressed as mean (\pm SEM) optical density ratios ($n=6$, ns, $F_{11, 60} = 3.70$, one-way analysis of variance, Student-Newman-Keuls post hoc analysis).

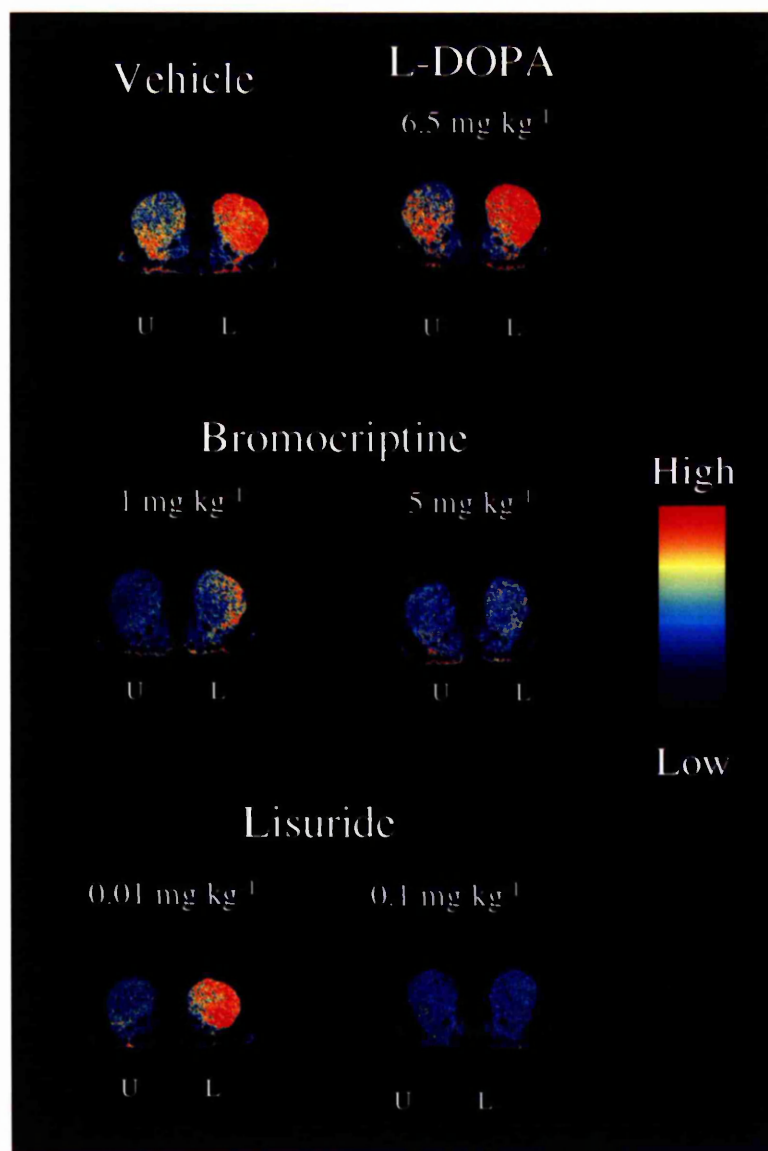


Figure 4.3.4.8 Pseudocolour transformations of autoradiographs of *in situ* hybridisation utilising an oligonucleotide probe targeted against pre-proenkephalin-A (PPE-A) in the lesioned (L) or unlesioned (U) rostral striatum (level 2) following 21 days, twice-daily, vehicle, L-DOPA (6.5 mg kg^{-1}) and benserazide (1.5 mg kg^{-1}), bromocriptine (5 or 1 mg kg^{-1}) or lisuride (0.1 or 0.01 mg kg^{-1}) treatment in the 6-OHDA-lesioned rat model of Parkinson's disease.

Pre-proenkephalin-A : G3PDH expression -Rostral Striatum - Level 2

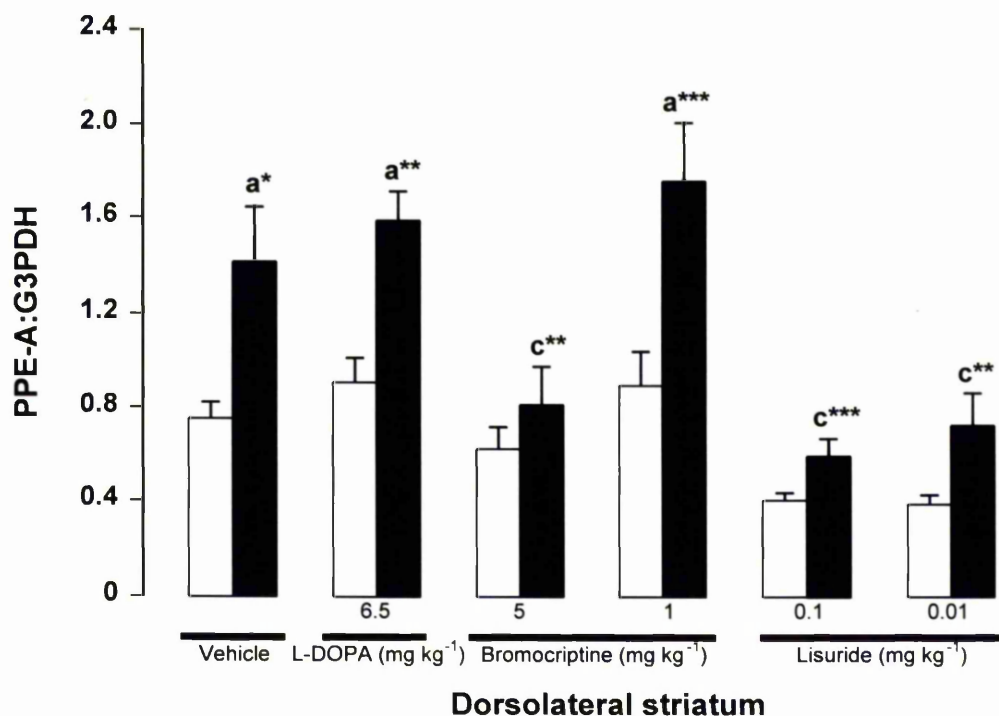


Figure 4.3.4.9 Ratio of pre-proenkephalin (PPE-A) to G3PDH mRNA expression in rostral striatum level 2 (dorsolateral) in the 6-OHDA-lesioned rat model of Parkinson's disease following 21 day, twice-daily, treatment with vehicle, L-DOPA (6.5 mg kg⁻¹) and benserazide (1.5 mg kg⁻¹), bromocriptine (5, 1 mg kg⁻¹, b.d.) or lisuride (0.1, 0.01 mg kg⁻¹, b.d.). Unlesioned (□) and lesioned (■) striatum are shown. Data are expressed as mean (\pm SEM) optical density ratios ($n=5-6$, $a^{***} P < 0.001$ cf unlesioned in same group, $a^{**} P < 0.01$ cf unlesioned in same side, $a^* P < 0.05$ cf unlesioned in same side, $c^{***} P < 0.001$ cf ipsi L-DOPA group, $c^{**} P < 0.01$ cf ipsi L-DOPA group, $F_{11, 58} = 9.84$, one-way analysis of variance, Student-Newman-Keuls post hoc analysis).

Pre-proenkephalin-A : G3PDH expression - Rostral Striatum - Level 2

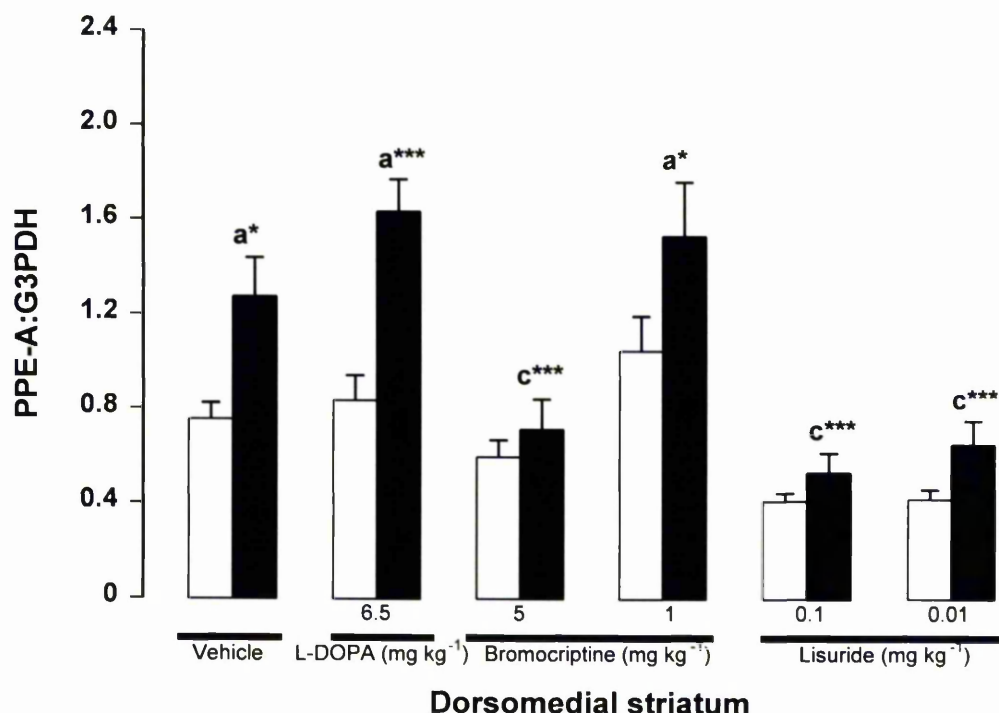


Figure 4.3.4.10 Ratio of pre-proenkephalin (PPE-A) to G3PDH mRNA expression in rostral striatum level 2 (dorsomedial) in the 6-OHDA-lesioned rat model of Parkinson's disease following 21 day, twice-daily, treatment with vehicle, L-DOPA (6.5 mg kg⁻¹) and benserazide (1.5 mg kg⁻¹), bromocriptine (5, 1 mg kg⁻¹, b.d.) or lisuride (0.1, 0.01 mg kg⁻¹, b.d.). Unlesioned (□) and lesioned (■) striatum are shown. Data are expressed as mean (\pm SEM) optical density ratios ($n=5-6$, a*** $P < 0.001$ cf unlesioned in same group, a* $P < 0.05$ cf unlesioned in same side, c*** $P < 0.001$ cf ipsi L-DOPA group, $F_{11, 58} = 11.15$, one-way analysis of variance, Student-Newman-Keuls post hoc analysis).

Pre-proenkephalin-A : G3PDH expression - Rostral Striatum - Level 2

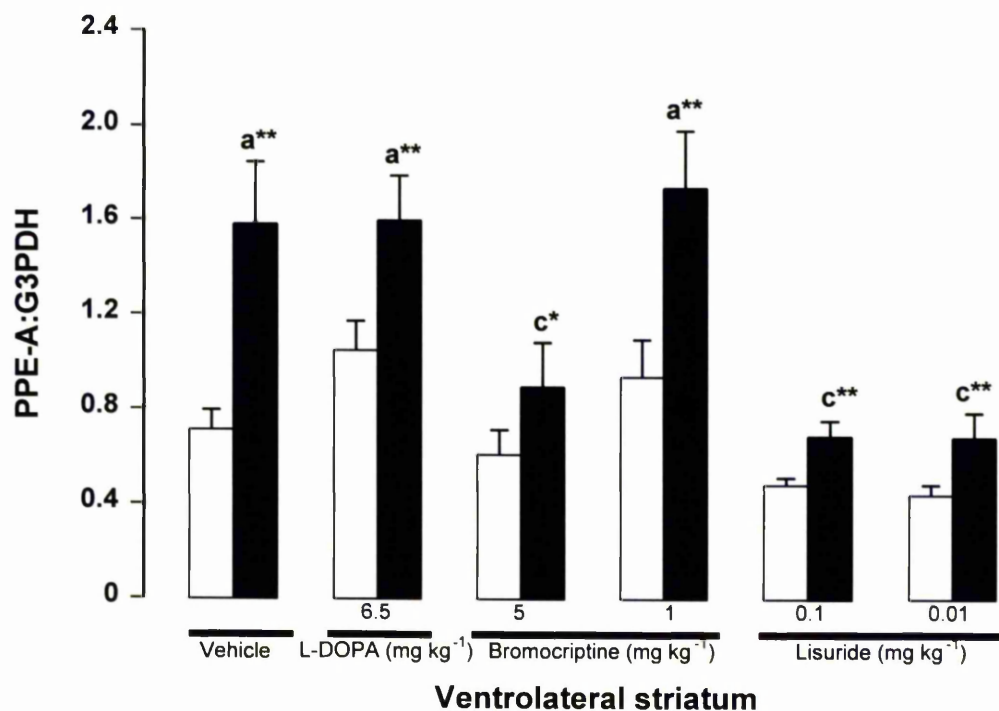


Figure 4.3.4.11 Ratio of pre-proenkephalin (PPE-A) to G3PDH mRNA expression in rostral striatum level 2 (ventrolateral) in the 6-OHDA-lesioned rat model of Parkinson's disease following 21 day, twice-daily, treatment with vehicle, L-DOPA (6.5 mg kg⁻¹) and benserazide (1.5 mg kg⁻¹), bromocriptine (5, 1 mg kg⁻¹, b.d.) or lisuride (0.1, 0.01 mg kg⁻¹, b.d.). Unlesioned (□) and lesioned (■) striatum are shown. Data are expressed as mean (\pm SEM) optical density ratios ($n=5-6$, a** $P < 0.01$ cf unlesioned in same group, c** $P < 0.01$ cf ipsi L-DOPA group, c* $P < 0.05$ cf ipsi L-DOPA group, $F_{11, 58} = 8.34$, one-way analysis of variance, Student-Newman-Keuls post hoc analysis).

Pre-proenkephalin-A : G3PDH expression - Rostral Striatum - Level 2

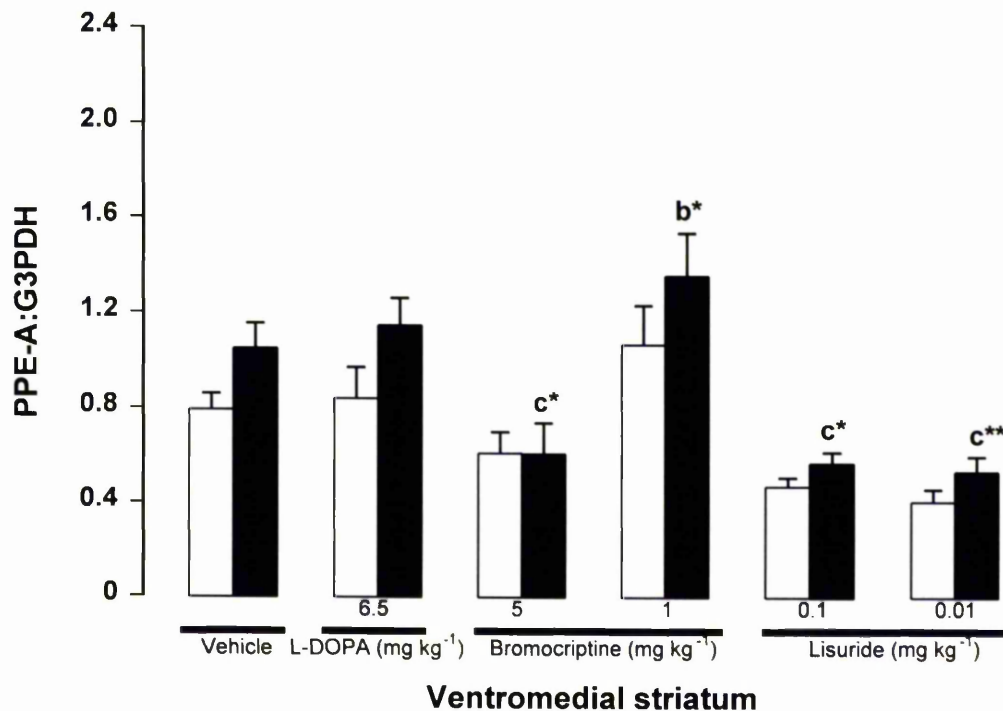


Figure 4.3.4.12 Ratio of pre-proenkephalin (PPE-A) to G3PDH mRNA expression in rostral striatum level 2 (ventromedial) in the 6-OHDA-lesioned rat model of Parkinson's disease following 21 day, twice-daily, treatment with vehicle, L-DOPA (6.5 mg kg⁻¹) and benserazide (1.5 mg kg⁻¹), bromocriptine (5, 1 mg kg⁻¹, b.d.) or lisuride (0.1, 0.01 mg kg⁻¹, b.d.). Unlesioned (□) and lesioned (■) striatum are shown. Data are expressed as mean (\pm SEM) optical density ratios ($n=5-6$, $b^* P < 0.05$ cf ipsi vehicle group, $c^{**} P < 0.01$ cf ipsi L-DOPA group, $c^* P < 0.05$ cf ipsi L-DOPA group, $F_{11, 58} = 7.52$, one-way analysis of variance, Student-Newman-Keuls post hoc analysis).

Pre-proenkephalin-A : G3PDH expression - Rostral Striatum - Level 2

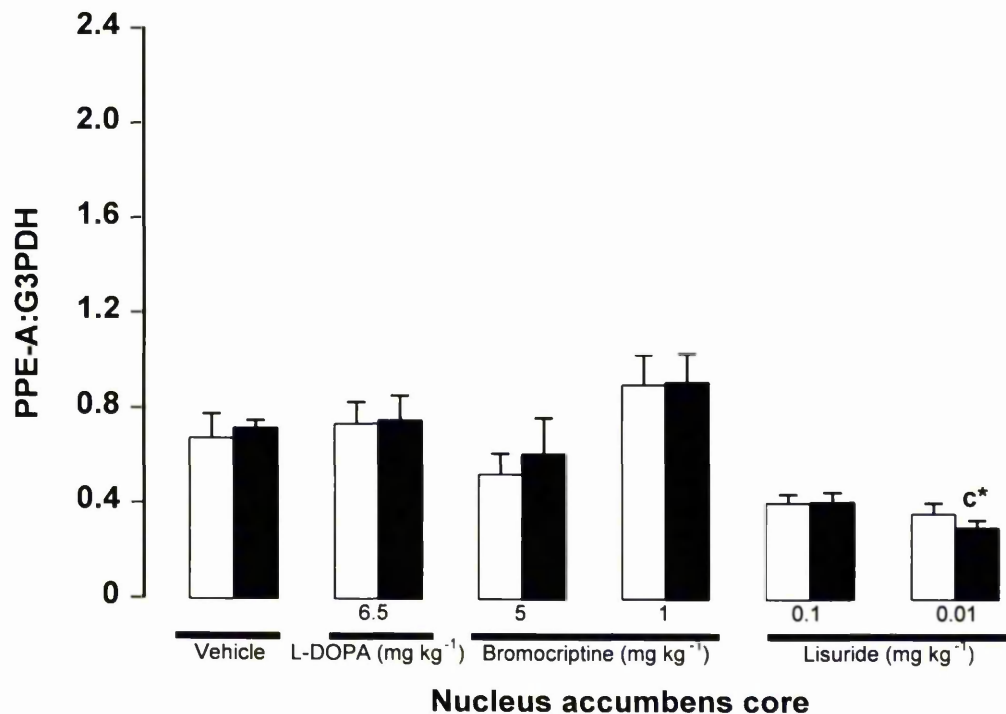


Figure 4.3.4.13 Ratio of pre-proenkephalin (PPE-A) to G3PDH mRNA expression in rostral striatum level 2 (Nucleus accumbens core) in the 6-OHDA-lesioned rat model of Parkinson's disease following 21 day, twice-daily, treatment with vehicle, L-DOPA (6.5 mg kg⁻¹) and benserazide (1.5 mg kg⁻¹), bromocriptine (5, 1 mg kg⁻¹, b.d.) or lisuride (0.1, 0.01 mg kg⁻¹, b.d.). Unlesioned (□) and lesioned (■) striatum are shown. Data are expressed as mean (\pm SEM) optical density ratios ($n=5-6$, $c^* P < 0.5$ cf ipsi L-DOPA group, $F_{11, 58} = 5.03$, one-way analysis of variance, Student-Newman-Keuls post hoc analysis).

Pre-proenkephalin-A : G3PDH expression - Rostral Striatum - Level 2

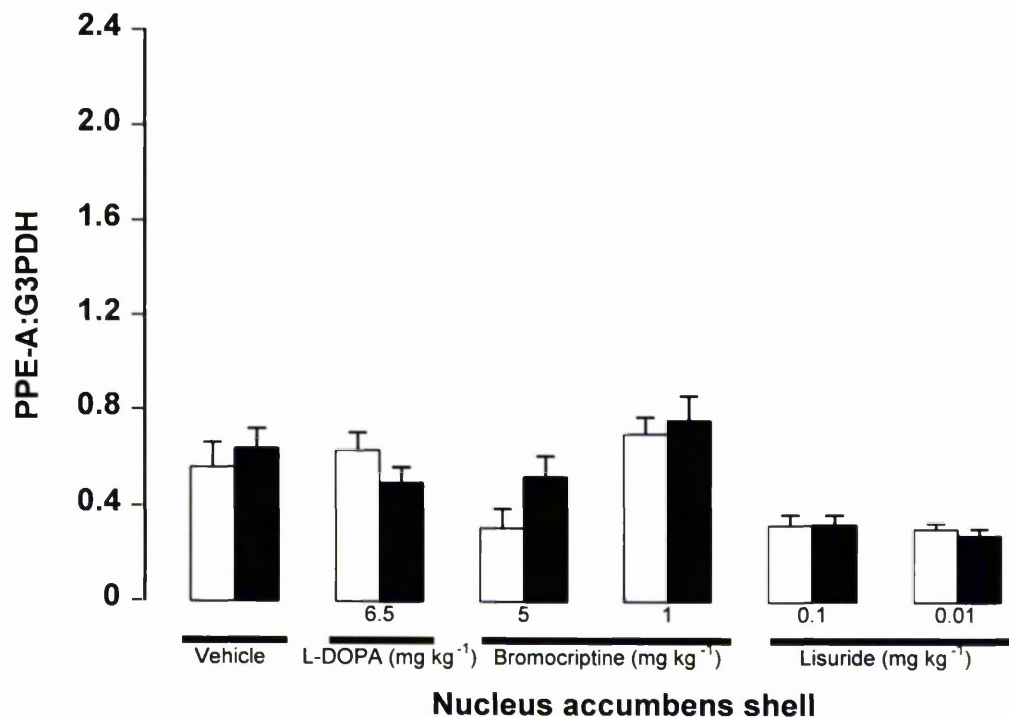


Figure 4.3.4.14 Ratio of pre-proenkephalin (PPE-A) to G3PDH mRNA expression in rostral striatum level 2 (Nucleus accumbens shell) in the 6-OHDA-lesioned rat model of Parkinson's disease following 21 day, twice-daily, treatment with vehicle, L-DOPA (6.5 mg kg⁻¹) and benserazide (1.5 mg kg⁻¹), bromocriptine (5, 1 mg kg⁻¹, b.d.) or lisuride (0.1, 0.01 mg kg⁻¹, b.d.). Unlesioned (□) and lesioned (■) striatum are shown. Data are expressed as mean (\pm SEM) optical density ratios ($n=5-6$, ns, $P > 0.05$, $F_{11, 58} = 5.64$, one-way analysis of variance, Student-Newman-Keuls post hoc analysis).

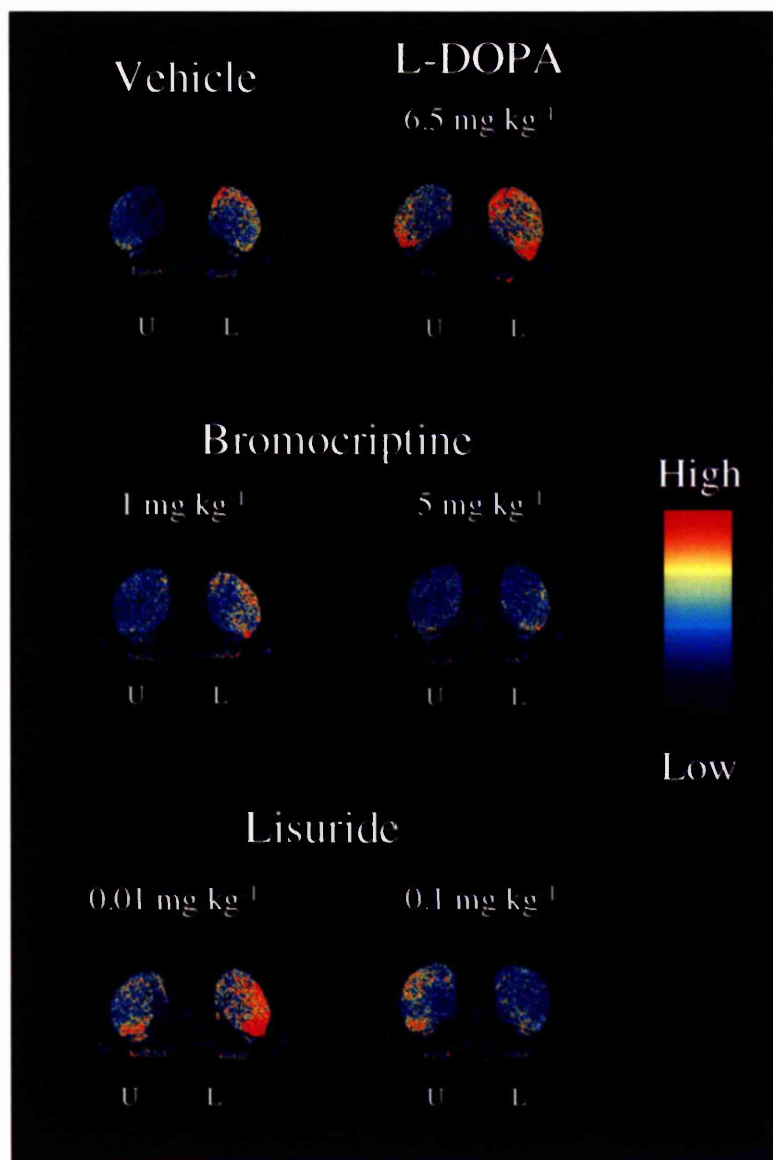


Figure 4.3.4.15 Pseudocolour transformations of autoradiographs of *in situ* hybridisation utilising an oligonucleotide probe targeted against pre-proenkephalin-A (PPE-A) in the lesioned (L) or unlesioned (U) intermediate striatum following 21 days, twice-daily, vehicle, L-DOPA (6.5 mg kg⁻¹) and benserazide (1.5 mg kg⁻¹), bromocriptine (5 or 1 mg kg⁻¹) or lisuride (0.1 or 0.01 mg kg⁻¹) treatment in the 6-OHDA-lesioned rat model of Parkinson's disease.

Pre-proenkephalin-A : G3PDH expression - Intermediate Striatum

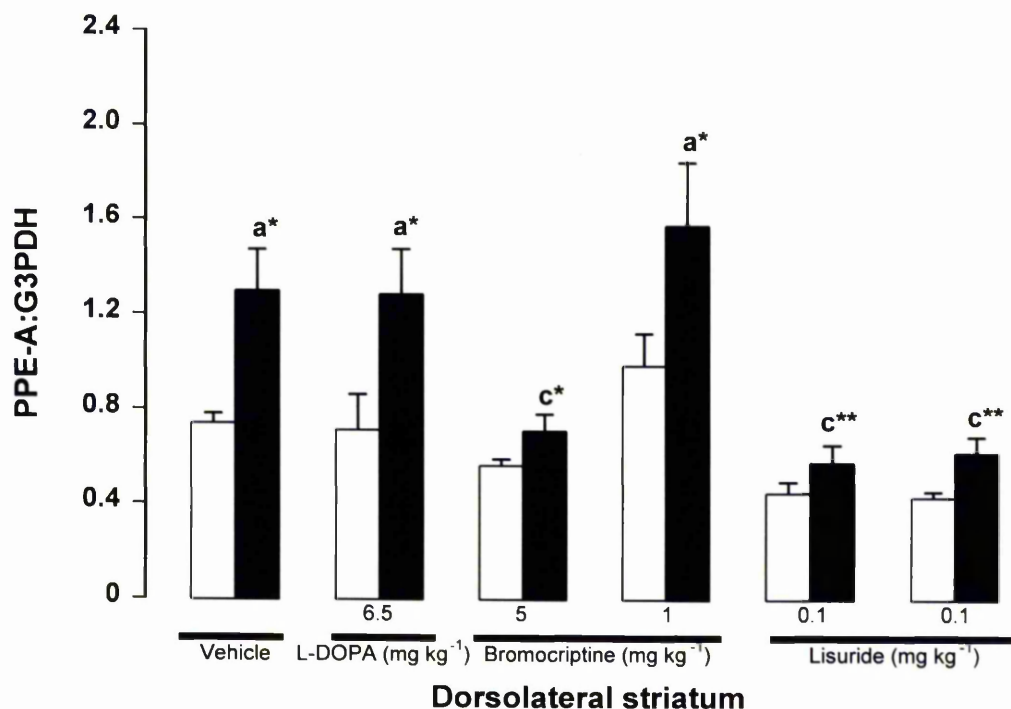


Figure 4.3.4.16 Ratio of pre-proenkephalin (PPE-A) to G3PDH mRNA expression in intermediate striatum (dorsolateral) in the 6-OHDA-lesioned rat model of Parkinson's disease following 21 day, twice-daily, treatment with vehicle, L-DOPA (6.5 mg kg⁻¹) and benserazide (1.5 mg kg⁻¹), bromocriptine (5, 1 mg kg⁻¹, b.d.) or lisuride (0.1, 0.01 mg kg⁻¹, b.d.). Unlesioned (□) and lesioned (■) striatum are shown. Data are expressed as mean (\pm SEM) optical density ratios ($n=6$, a^* $P < 0.05$ cf unlesioned in same group, c^{**} $P < 0.01$ cf ipsi L-DOPA group, c^* $P < 0.05$ cf ipsi L-DOPA group, $F_{11, 60} = 8.30$, one-way analysis of variance, Student-Newman-Keuls post hoc analysis).

Pre-proenkephalin-A : G3PDH expression - Intermediate Striatum

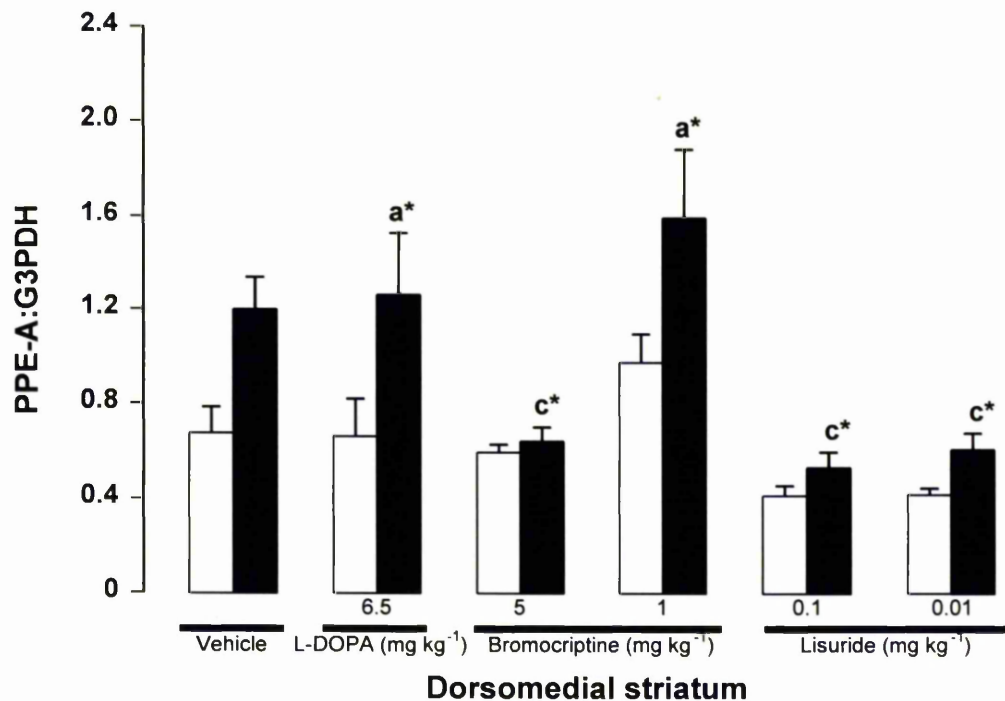


Figure 4.3.4.17 Ratio of pre-proenkephalin (PPE-A) to G3PDH mRNA expression in intermediate striatum (dorsomedial) in the 6-OHDA-lesioned rat model of Parkinson's disease following 21 day, twice-daily, treatment with vehicle, L-DOPA (6.5 mg kg⁻¹) and benserazide (1.5 mg kg⁻¹), bromocriptine (5, 1 mg kg⁻¹, b.d.) or lisuride (0.1, 0.01 mg kg⁻¹, b.d.). Unlesioned (□) and lesioned (■) striatum are shown. Data are expressed as mean (\pm SEM) optical density ratios ($n=6$, $a^* P < 0.5$ cf unlesioned in same group, $c^* P < 0.05$ cf ipsi L-DOPA group, $F_{11, 60} = 6.97$, one-way analysis of variance, Student-Newman-Keuls post hoc analysis).

Pre-proenkephalin-A : G3PDH expression - Intermediate Striatum

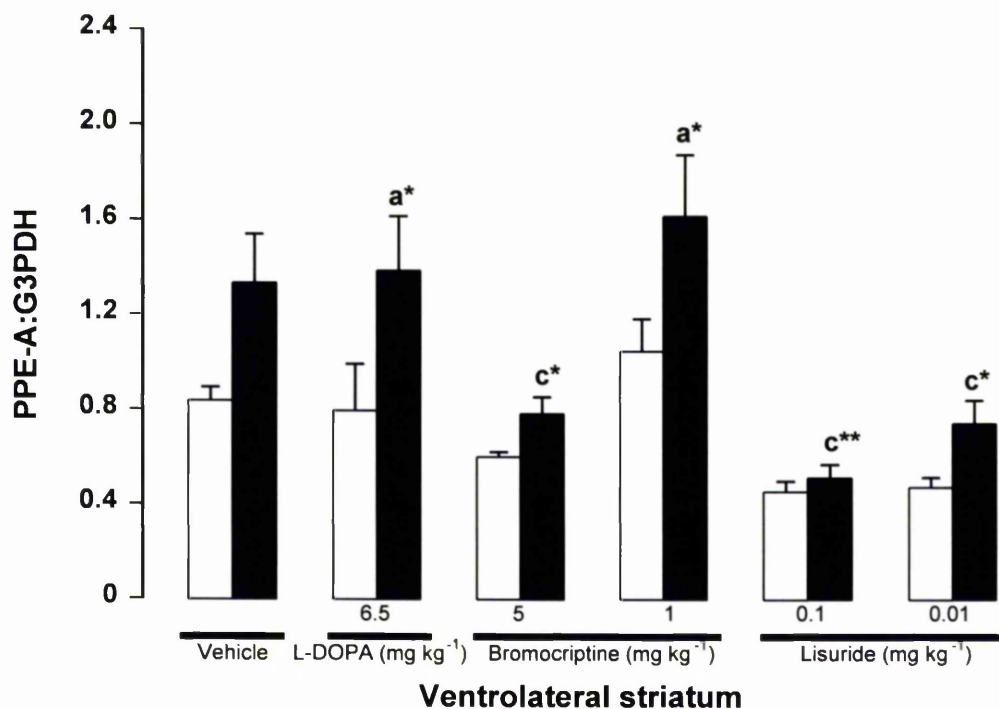


Figure 4.3.4.18 Ratio of pre-proenkephalin (PPE-A) to G3PDH mRNA expression in intermediate striatum (ventrolateral) in the 6-OHDA-lesioned rat model of Parkinson's disease following 21 day, twice-daily, treatment with vehicle, L-DOPA (6.5 mg kg⁻¹) and benserazide (1.5 mg kg⁻¹), bromocriptine (5, 1 mg kg⁻¹, b.d.) or lisuride (0.1, 0.01 mg kg⁻¹, b.d.). Unlesioned (□) and lesioned (■) striatum are shown. Data are expressed as mean (\pm SEM) optical density ratios ($n=6$, a^* $P < 0.5$ cf unlesioned in same group, c^{**} $P < 0.01$ cf ipsi L-DOPA group, c^* $P < 0.05$ cf ipsi L-DOPA group, $F_{11, 60} = 7.23$, one-way analysis of variance, Student-Newman-Keuls post hoc analysis).

Pre-proenkephalin-A : G3PDH expression - Intermediate Striatum

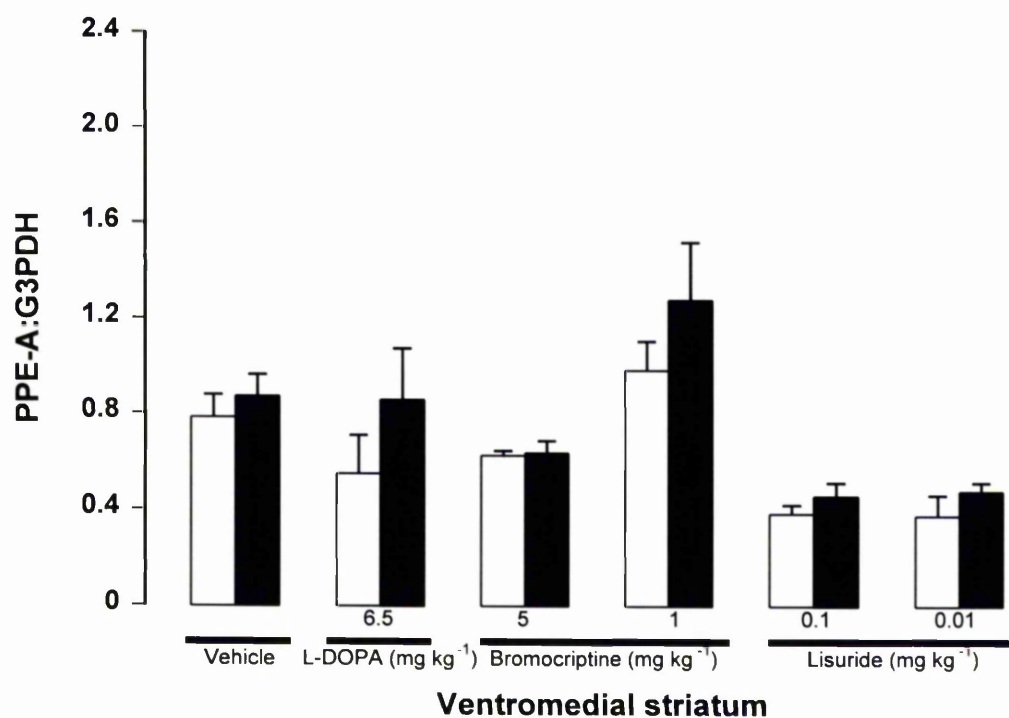


Figure 4.3.4.19 Ratio of pre-proenkephalin (PPE-A) to G3PDH mRNA expression in intermediate striatum (ventromedial) in the 6-OHDA-lesioned rat model of Parkinson's disease following 21 day, twice-daily, treatment with vehicle, L-DOPA (6.5 mg kg⁻¹) and benserazide (1.5 mg kg⁻¹), bromocriptine (5, 1 mg kg⁻¹, b.d.) or lisuride (0.1, 0.01 mg kg⁻¹, b.d.). Unlesioned (□) and lesioned (■) striatum are shown. Data are expressed as mean (\pm SEM) optical density ratios ($n=6$, ns, $P > 0.05$, $F_{11, 60} = 4.95$, one-way analysis of variance, Student-Newman-Keuls post hoc analysis).

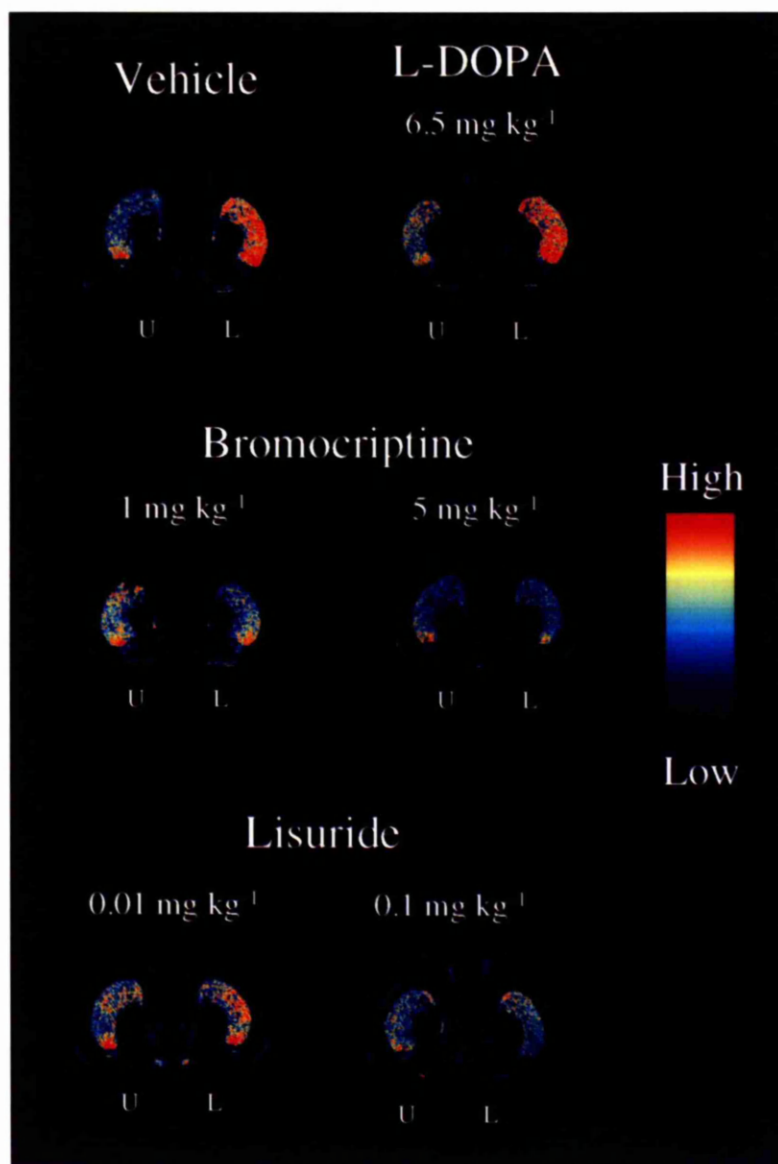


Figure 4.3.4.20 Pseudocolour transformations of autoradiographs of in situ hybridisation utilising an oligonucleotide probe targeted against pre-proenkephalin-A (PPE-A) in the lesioned (L) or unlesioned (U) caudal striatum following 21 days, twice-daily, vehicle, L-DOPA (6.5 mg kg⁻¹) and benserazide (1.5 mg kg⁻¹), bromocriptine (5 or 1 mg kg⁻¹) or lisuride (0.1 or 0.01 mg kg⁻¹) treatment in the 6-OHDA-lesioned rat model of Parkinson's disease.

Pre-proenkephalin-A : G3PDH expression - Caudal Striatum

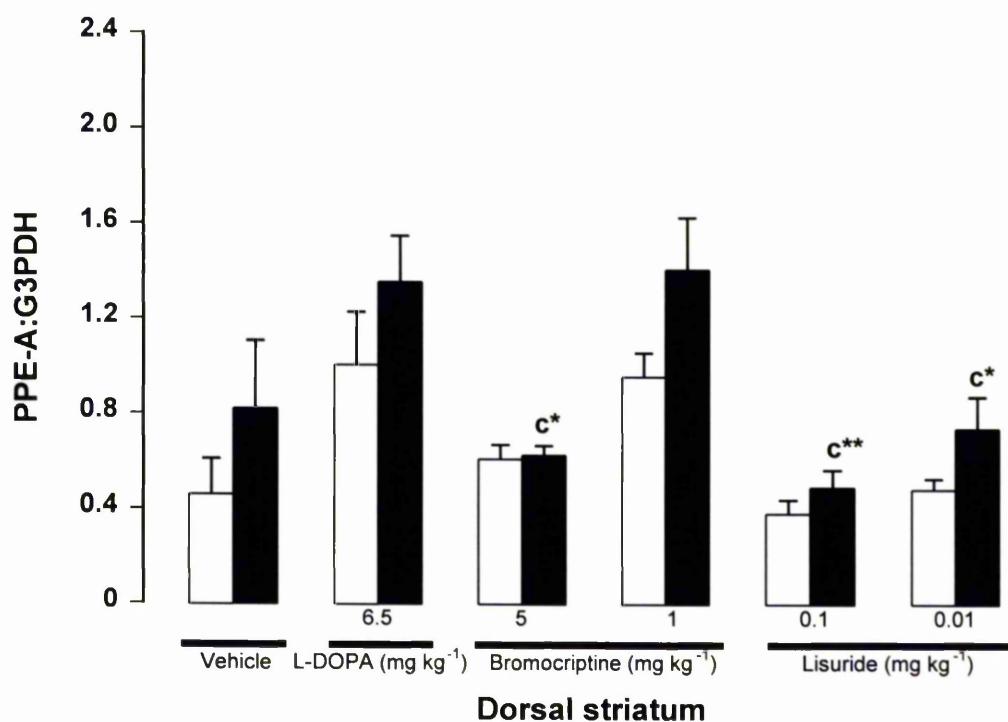


Figure 4.3.4.21 Ratio of pre-proenkephalin (PPE-A) to G3PDH mRNA expression in caudal striatum (dorsal) in the 6-OHDA-lesioned rat model of Parkinson's disease following 21 day, twice-daily, treatment with vehicle, L-DOPA (6.5 mg kg⁻¹) and benserazide (1.5 mg kg⁻¹), bromocriptine (5, 1 mg kg⁻¹, b.d.) or lisuride (0.1, 0.01 mg kg⁻¹, b.d.). Unlesioned (□) and lesioned (■) striatum are shown. Data are expressed as mean (\pm SEM) optical density ratios ($n=6$, $c^{**} P < 0.01$ cf ipsi L-DOPA group, $c^* P < 0.05$ cf ipsi L-DOPA group, $F_{11, 60} = 4.95$, one-way analysis of variance, Student-Newman-Keuls post hoc analysis).

Pre-proenkephalin-A : G3PDH expression - Caudal Striatum

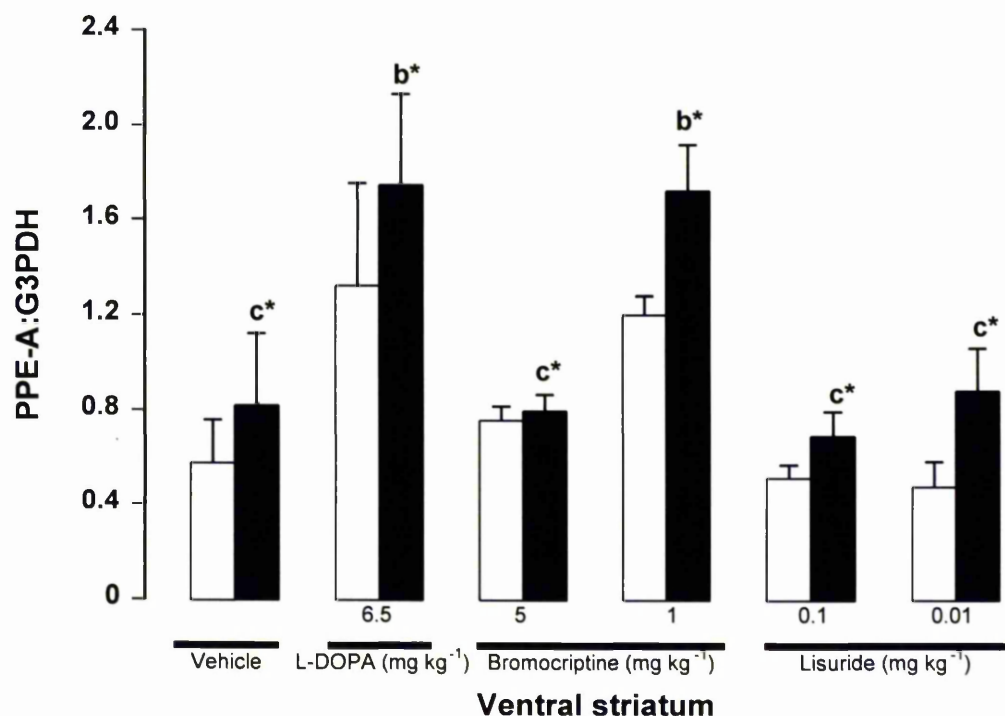


Figure 4.3.4.22 Ratio of pre-proenkephalin (PPE-A) to G3PDH mRNA expression in caudal striatum (ventral) in the 6-OHDA-lesioned rat model of Parkinson's disease following 21 day, twice-daily, treatment with vehicle, L-DOPA (6.5 mg kg⁻¹) and benserazide (1.5 mg kg⁻¹), bromocriptine (5, 1 mg kg⁻¹, b.d.) or lisuride (0.1, 0.01 mg kg⁻¹, b.d.). Unlesioned (□) and lesioned (■) striatum are shown. Data are expressed as mean (\pm SEM) optical density ratios ($n=6$, $b^* P < 0.05$ cf ipsi vehicle group, $c^* P < 0.05$ cf ipsi L-DOPA group, $F_{11, 60} = 3.98$, one-way analysis of variance, Student-Newman-Keuls post hoc analysis).

4.3.5 Topographical distribution of striatal pre-proenkephalin-B mRNA in the 6-OHDA-lesioned rat following repeated treatment with vehicle, L-DOPA, bromocriptine or lisuride

In situ hybridisation utilising an oligonucleotide probe targeted against the dynorphin precursor (pre-proenkephalin-B, PPE-B) was employed to investigate the topographical distribution of PPE-B in the striatum of 6-OHDA-lesioned rats following 21 day, twice-daily, treatment with either vehicle, L-DOPA (6.5 mg kg⁻¹), bromocriptine (5 mg kg⁻¹ or 1 mg kg⁻¹) or lisuride (0.1 mg kg⁻¹ or 0.01 mg kg⁻¹). Following 21 day vehicle administration, a non-significant decrease in PPE-B expression was observed in the unlesioned striatum throughout the striatum. Following 21 day, twice-daily, L-DOPA (6.5 mg kg⁻¹) and benserazide (1.5 mg kg⁻¹) administration, a maximal 2150% increase in PPE-B expression was observed on the lesioned striatum. This elevation was observed throughout the striatum (Figures 4.3.5.1-4.3.5.22). The greatest elevation was present in the rostral striatum, and displayed a mediolateral gradient, with highest expression seen in the lateral areas of the lesioned striatum. Following 21 day, twice-daily, administration of both bromocriptine and lisuride, at all doses administered, no elevation in PPE-B expression in any area of the striatum was observed. In fact, as with vehicle administration, a non-significant decrease in PPE-B expression was observed (Figure 4.3.5.1-4.3.5.22).

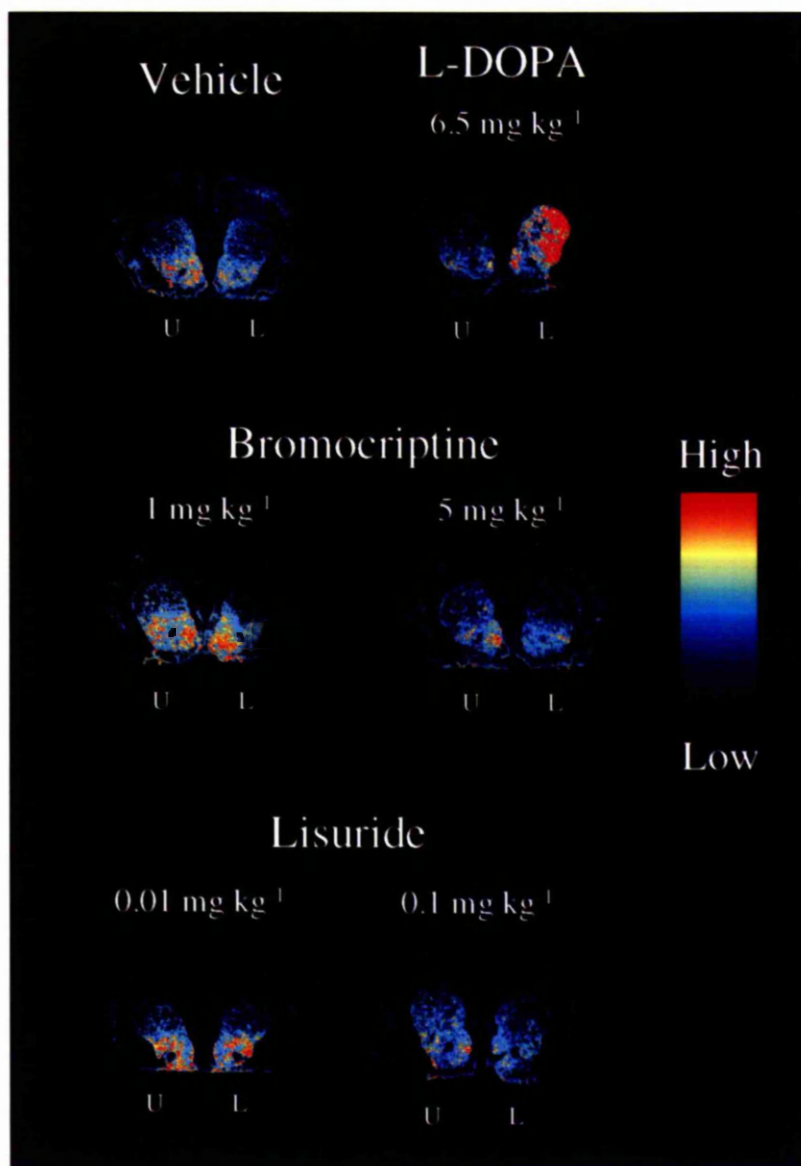


Figure 4.3.5.1 Pseudocolour transformations of autoradiographs of *in situ* hybridisation utilising an oligonucleotide probe targeted against pre-proenkephalin-B (PPE-B) in the lesioned (L) or unlesioned (U) rostral striatum (level 1) following 21 days, twice-daily, vehicle, L-DOPA (6.5 mg kg⁻¹) and benserazide (1.5 mg kg⁻¹), bromocriptine (5 or 1 mg kg⁻¹) or lisuride (0.1 or 0.01 mg kg⁻¹) treatment in the 6-OHDA-lesioned rat model of Parkinson's disease.

Pre-proenkephalin-B : G3PDH expression - Rostral Striatum - Level 1

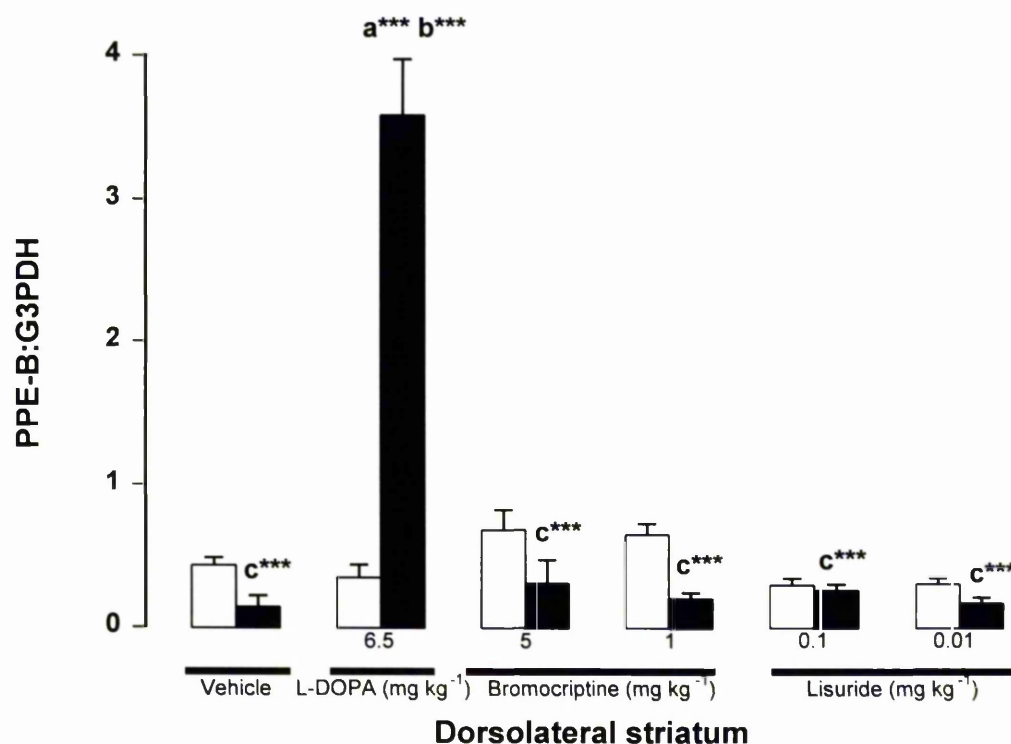


Figure 4.3.5.2 Ratio of pre-proenkephalin-B (PPE-B) to G3PDH mRNA expression in rostral striatum level 1 (dorsolateral) in the 6-OHDA-lesioned rat model of Parkinson's disease following 21 day, twice-daily, treatment with vehicle, L-DOPA (6.5 mg kg⁻¹) and benserazide (1.5 mg kg⁻¹), bromocriptine (5, 1 mg kg⁻¹, b.d.) or lisuride (0.1, 0.01 mg kg⁻¹, b.d.). Unlesioned (□) and lesioned (■) striatum are shown. Data are expressed as mean (\pm SEM) optical density ratios ($n=6$, a*** $P < 0.001$ cf unlesioned in same group, b*** $P < 0.001$ cf ipsi vehicle group, c*** $P < 0.001$ cf ipsi L-DOPA group, $F_{11, 60} = 47.66$, one-way analysis of variance, Student-Newman-Keuls post hoc analysis).

Pre-proenkephalin-B : G3PDH expression - Rostral Striatum - Level 1

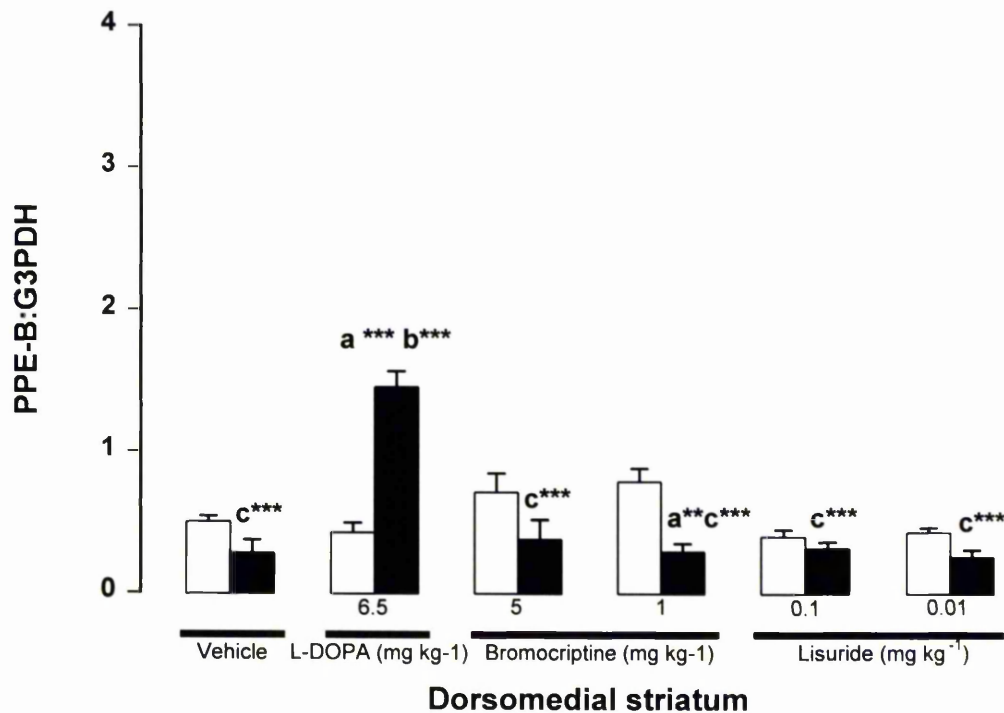


Figure 4.3.5.3 Ratio of pre-proenkephalin-B (PPE-B) to G3PDH mRNA expression in rostral striatum level 1 (dorsoventral) in the 6-OHDA-lesioned rat model of Parkinson's disease following 21 day, twice-daily, treatment with vehicle, L-DOPA (6.5 mg kg⁻¹) and benserazide (1.5 mg kg⁻¹), bromocriptine (5, 1 mg kg⁻¹, b.d.) or lisuride (0.1, 0.01 mg kg⁻¹, b.d.). Unlesioned (□) and lesioned (■) striatum are shown. Data are expressed as mean (\pm SEM) optical density ratios ($n=6$, a*** $P < 0.001$ cf unlesioned in same group, a** $P < 0.01$ cf unlesioned in same side, b*** $P < 0.001$ cf ipsi vehicle group, c*** $P < 0.001$ cf ipsi L-DOPA group, $F_{11, 60} = 15.85$, one-way analysis of variance, Student-Newman-Keuls post hoc analysis).

Pre-proenkephalin-B : G3PDH expression - Rostral Striatum - Level 1

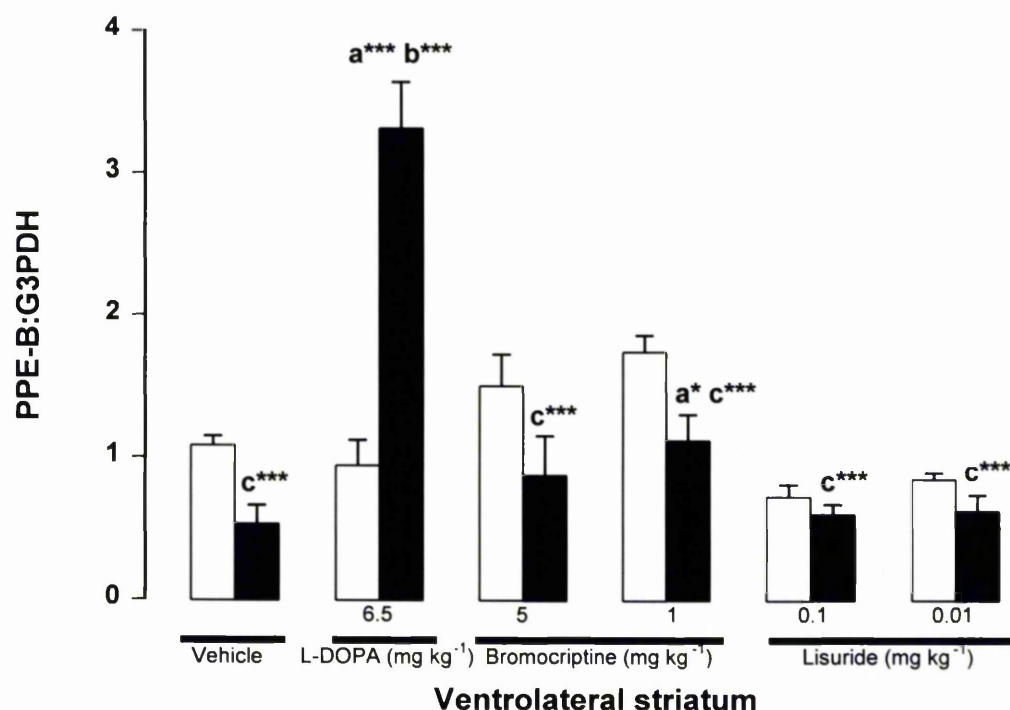


Figure 4.3.5.4 Ratio of pre-proenkephalin-B (PPE-B) to G3PDH mRNA expression in rostral striatum level 1 (ventrolateral) in the 6-OHDA-lesioned rat model of Parkinson's disease following 21 day, twice-daily, treatment with vehicle, L-DOPA (6.5 mg kg⁻¹) and benserazide (1.5 mg kg⁻¹), bromocriptine (5, 1 mg kg⁻¹, b.d.) or lisuride (0.1, 0.01 mg kg⁻¹, b.d.). Unlesioned (□) and lesioned (■) striatum are shown. Data are expressed as mean (\pm SEM) optical density ratios ($n=6$, a*** $P < 0.001$ cf unlesioned in same group, a* $P < 0.05$ cf unlesioned in same side, b*** $P < 0.001$ cf ipsi vehicle group, c*** $P < 0.001$ cf ipsi L-DOPA group, $F_{11, 60} = 19.45$, one-way analysis of variance, Student-Newman-Keuls post hoc analysis).

Pre-proenkephalin-B : G3PDH expression - Rostral Striatum - Level 1

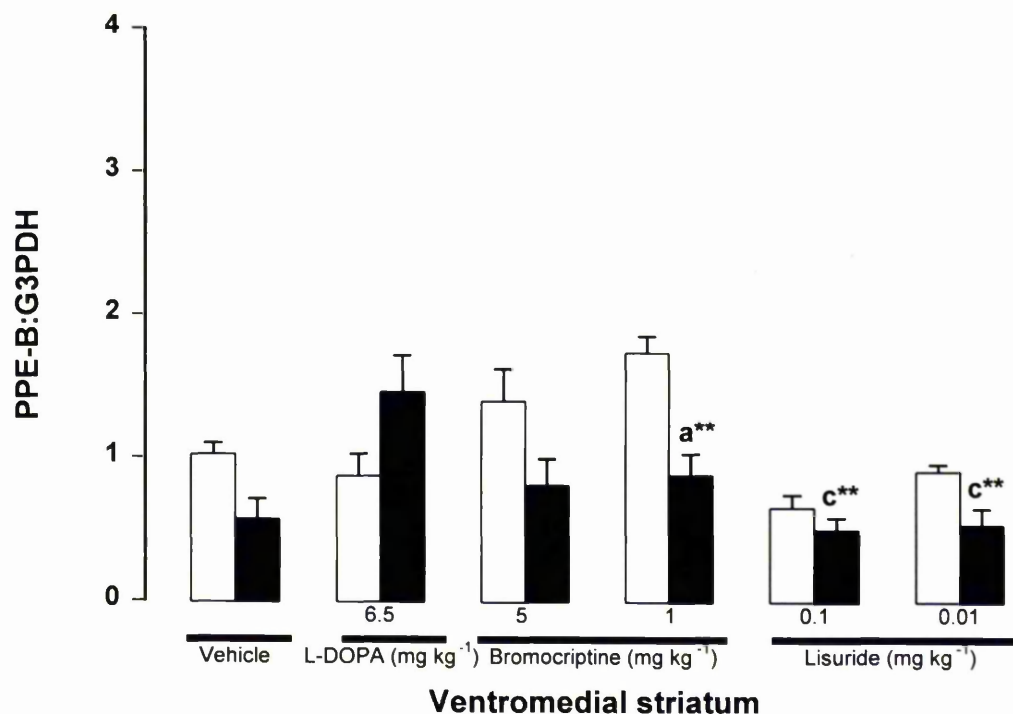


Figure 4.3.5.5 Ratio of pre-proenkephalin-B (PPE-B) to G3PDH mRNA expression in rostral striatum level 1 (ventromedial) in the 6-OHDA-lesioned rat model of Parkinson's disease following 21 day, twice-daily, treatment with vehicle, L-DOPA (6.5 mg kg⁻¹) and benserazide (1.5 mg kg⁻¹), bromocriptine (5, 1 mg kg⁻¹, b.d.) or lisuride (0.1, 0.01 mg kg⁻¹, b.d.). Unlesioned (□) and lesioned (■) striatum are shown. Data are expressed as mean (\pm SEM) optical density ratios ($n=6$, $a^{**} P < 0.01$ cf unlesioned in same group, $c^{**} P < 0.01$ cf ipsi L-DOPA group, $F_{11, 60} = 6.95$, one-way analysis of variance, Student-Newman-Keuls post hoc analysis).

Pre-proenkephalin-B : G3PDH expression - Rostral Striatum - Level 1

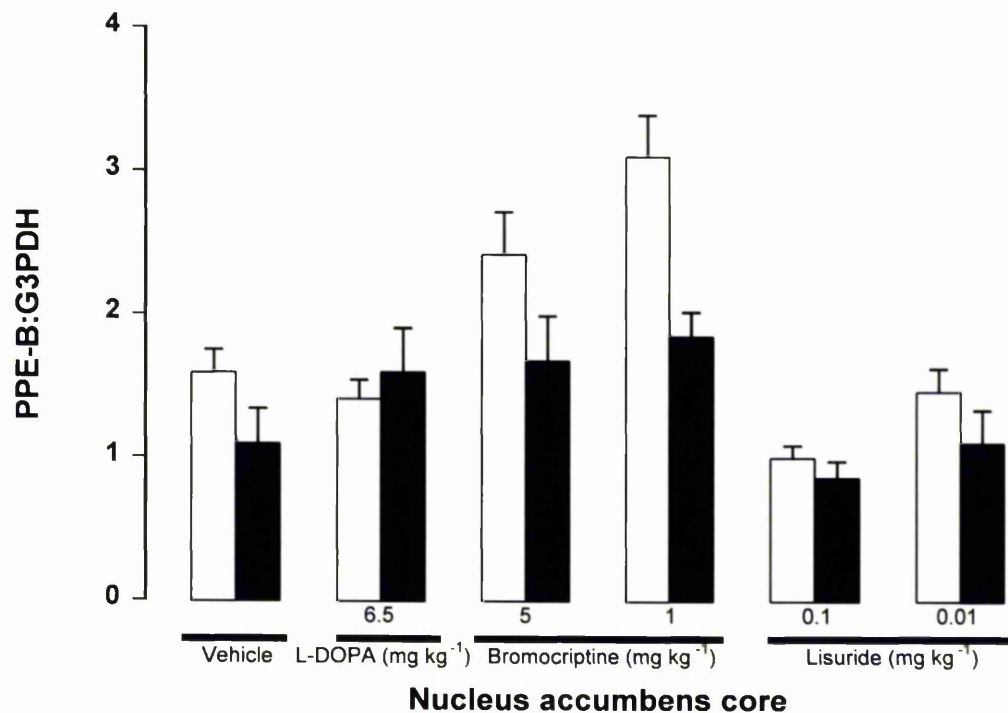


Figure 4.3.5.6 Ratio of pre-proenkephalin-B (PPE-B) to G3PDH mRNA expression in rostral striatum level 1 (Nucleus accumbens core) in the 6-OHDA-lesioned rat model of Parkinson's disease following 21 day, twice-daily, treatment with vehicle, L-DOPA (6.5 mg kg⁻¹) and benserazide (1.5 mg kg⁻¹), bromocriptine (5, 1 mg kg⁻¹, b.d.) or lisuride (0.1, 0.01 mg kg⁻¹, b.d.). Unlesioned (□) and lesioned (■) striatum are shown. Data are expressed as mean (\pm SEM) optical density ratios ($n=6$, ns $P > 0.05$, $F_{11, 60} = 8.04$, one-way analysis of variance, Student-Newman-Keuls post hoc analysis).

Pre-proenkephalin-B : G3PDH expression - Rostral Striatum - Level 1

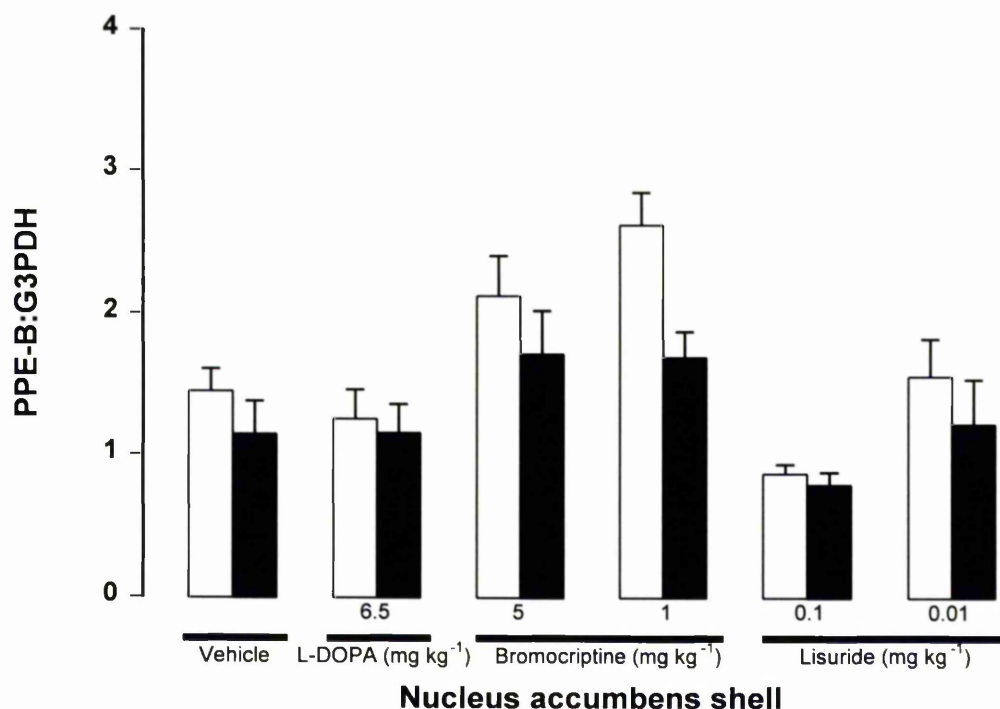


Figure 4.3.5.7 Ratio of pre-proenkephalin-B (PPE-B) to G3PDH mRNA expression in rostral striatum level 1 (Nucleus accumbens shell) in the 6-OHDA-lesioned rat model of Parkinson's disease following 21 day, twice-daily, treatment with vehicle, L-DOPA (6.5 mg kg⁻¹) and benserazide (1.5 mg kg⁻¹), bromocriptine (5, 1 mg kg⁻¹, b.d.) or lisuride (0.1, 0.01 mg kg⁻¹, b.d.). Unlesioned (□) and lesioned (■) striatum are shown. Data are expressed as mean (\pm SEM) optical density ratios ($n=6$, ns, $P > 0.05$, $F_{11, 60} = 8.04$, one-way analysis of variance, Student-Newman-Keuls post hoc analysis).

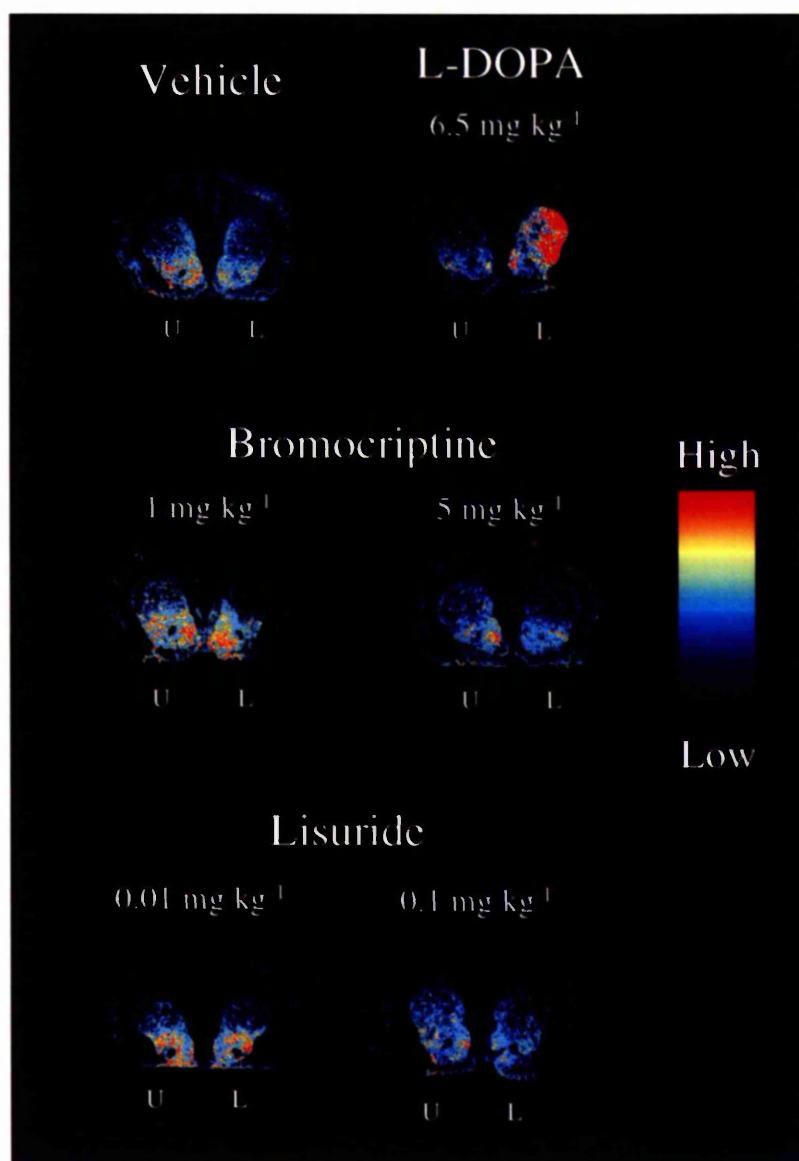


Figure 4.3.5.8 Pseudocolour transformations of autoradiographs of *in situ* hybridisation utilising an oligonucleotide probe targeted against pre-proenkephalin-B (PPE-B) in the lesioned (L) or unlesioned (U) rostral striatum (level 2) following 21 days, twice-daily, vehicle, L-DOPA (6.5 mg kg⁻¹) and benserazide (1.5 mg kg⁻¹), bromocriptine (5 or 1 mg kg⁻¹) or lisuride (0.1 or 0.01 mg kg⁻¹) treatment in the 6-OHDA-lesioned rat model of Parkinson's disease.

Pre-proenkephalin-B : G3PDH expression - Rostral Striatum - Level 2

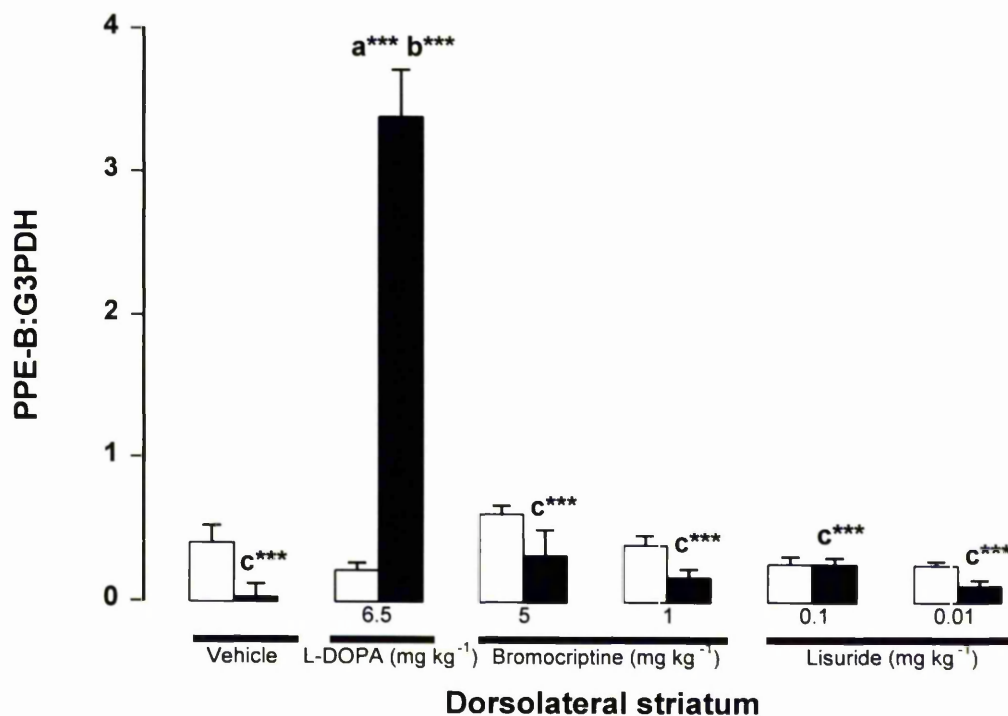


Figure 4.3.5.9 Ratio of pre-proenkephalin-B (PPE-B) to G3PDH mRNA expression in rostral level 2 (dorsolateral) in the 6-OHDA-lesioned rat model of Parkinson's disease following 21 day, twice-daily, treatment with vehicle, L-DOPA (6.5 mg kg⁻¹) and benserazide (1.5 mg kg⁻¹), bromocriptine (5, 1 mg kg⁻¹, b.d.) or lisuride (0.1, 0.01 mg kg⁻¹, b.d.). Unlesioned (□) and lesioned (■) striatum are shown. Data are expressed as mean (\pm SEM) optical density ratios ($n=5-6$, $a^{***} P < 0.001$ cf unlesioned in same group, $b^{***} P < 0.001$ cf ipsi vehicle group, $c^{***} P < 0.001$ cf ipsi L-DOPA group, $F_{11, 58} = 51.53$, one-way analysis of variance, Student-Newman-Keuls post hoc analysis).

Pre-proenkephalin-B : G3PDH expression - Rostral Striatum - Level 2

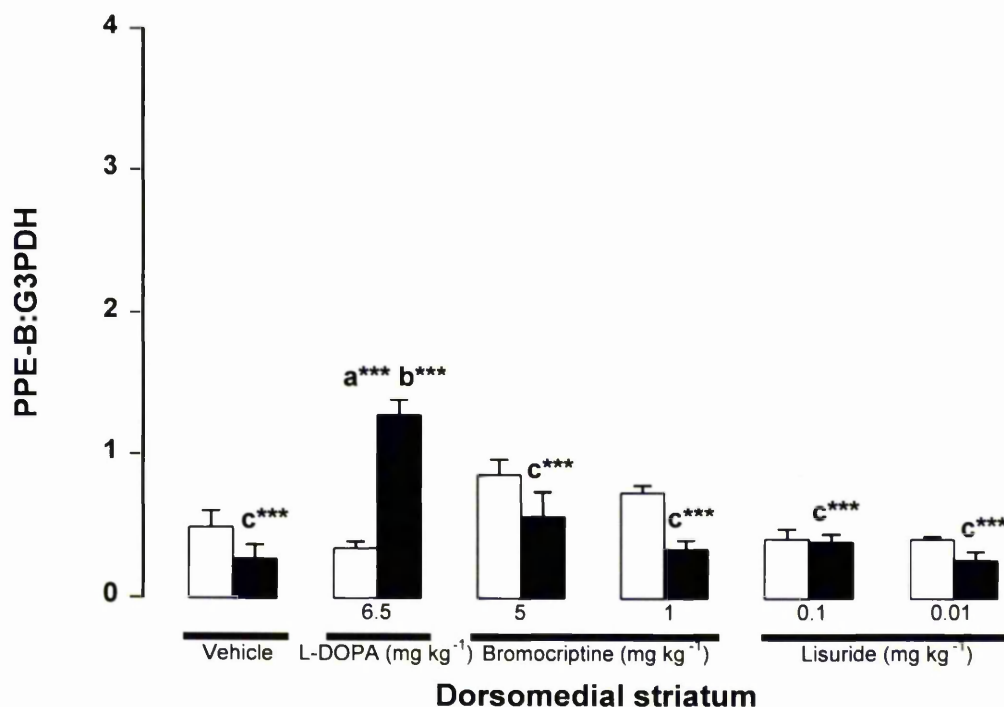


Figure 4.3.5.10 Ratio of pre-proenkephalin-B (PPE-B) to G3PDH mRNA expression in rostral level 2 (dorsomedial) in the 6-OHDA-lesioned rat model of Parkinson's disease following 21 day, twice-daily, treatment with vehicle, L-DOPA (6.5 mg kg⁻¹) and benserazide (1.5 mg kg⁻¹), bromocriptine (5, 1 mg kg⁻¹, b.d.) or lisuride (0.1, 0.01 mg kg⁻¹, b.d.). Unlesioned (□) and lesioned (■) striatum are shown. Data are expressed as mean (\pm SEM) optical density ratios ($n=5-6$, a*** $P < 0.001$ cf unlesioned in same group, b*** $P < 0.001$ cf ipsi vehicle group, c*** $P < 0.001$ cf ipsi L-DOPA group, $F_{11, 58} = 10.66$, one-way analysis of variance, Student-Newman-Keuls post hoc analysis).

Pre-proenkephalin-B : G3PDH expression - Rostral Striatum - Level 2

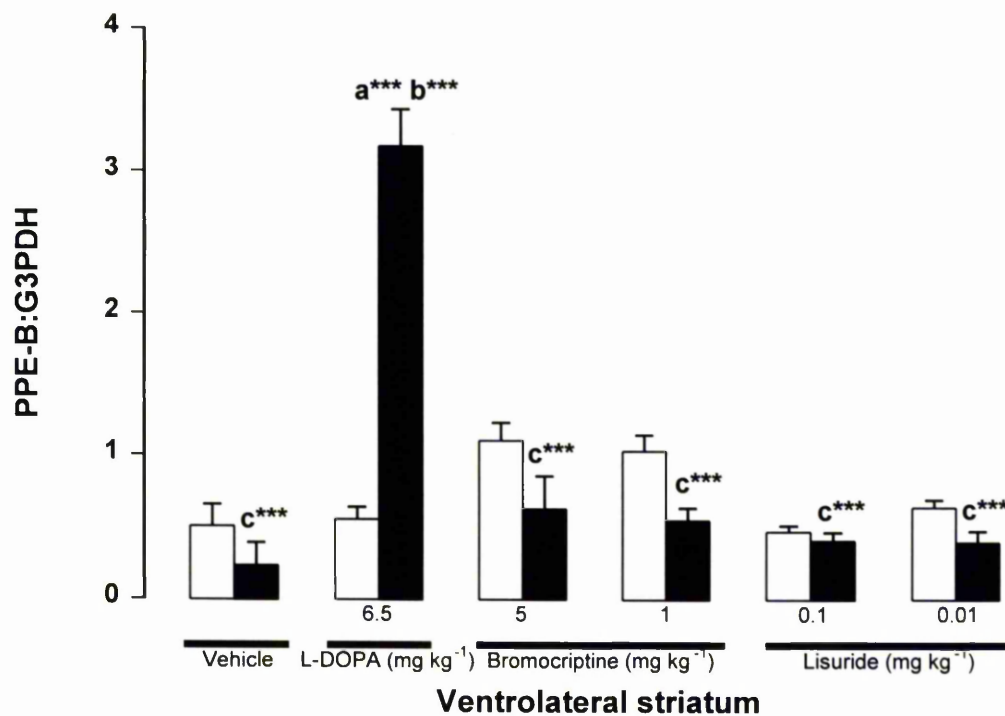


Figure 4.3.5.11 Ratio of pre-proenkephalin-B (PPE-B) to G3PDH mRNA expression in rostral level 2 (ventrolateral) in the 6-OHDA-lesioned rat model of Parkinson's disease following 21 day, twice-daily, treatment with vehicle, L-DOPA (6.5 mg kg⁻¹) and benserazide (1.5 mg kg⁻¹), bromocriptine (5, 1 mg kg⁻¹, b.d.) or lisuride (0.1, 0.01 mg kg⁻¹, b.d.). Unlesioned (□) and lesioned (■) striatum are shown. Data are expressed as mean (\pm SEM) optical density ratios ($n=5-6$, $a^{***} P < 0.001$ cf unlesioned in same group, $b^{***} P < 0.001$ cf ipsi vehicle group, $c^{***} P < 0.001$ cf ipsi L-DOPA group, $F_{11, 58} = 31.69$, one-way analysis of variance, Student-Newman-Keuls post hoc analysis).

Pre-proenkephalin-B : G3PDH expression - Rostral Striatum - Level 2

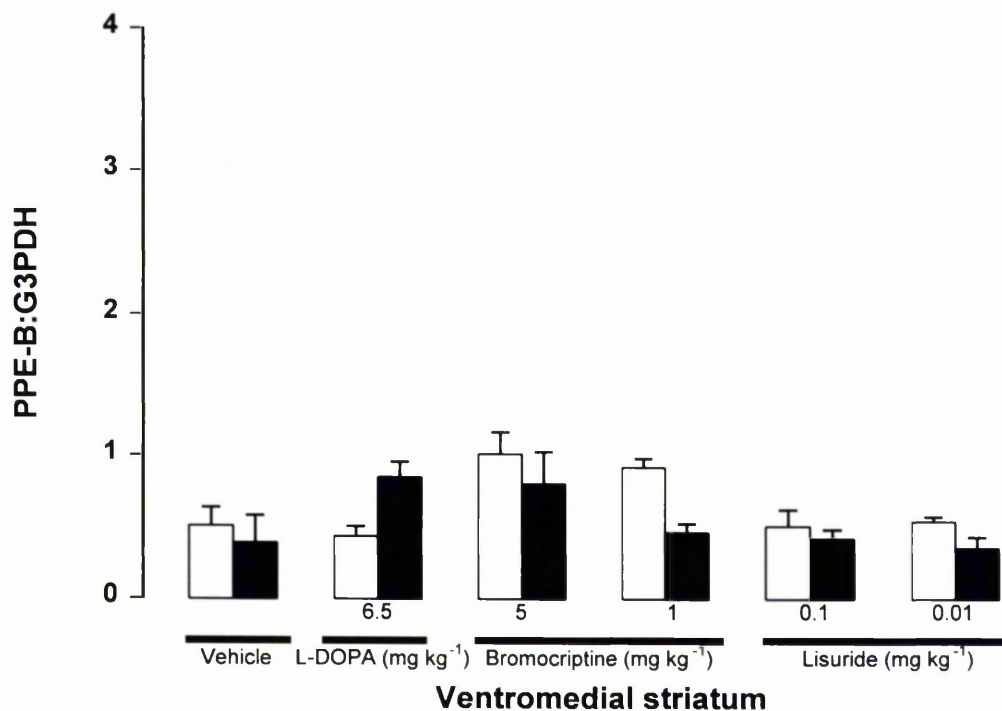


Figure 4.3.5.12 Ratio of pre-proenkephalin-B (PPE-B) to G3PDH mRNA expression in rostral level 2 (ventromedial) in the 6-OHDA-lesioned rat model of Parkinson's disease following 21 day, twice-daily, treatment with vehicle, L-DOPA (6.5 mg kg⁻¹) and benserazide (1.5 mg kg⁻¹), bromocriptine (5, 1 mg kg⁻¹, b.d.) or lisuride (0.1, 0.01 mg kg⁻¹, b.d.). Unlesioned (□) and lesioned (■) striatum are shown. Data are expressed as mean (\pm SEM) optical density ratios ($n=5-6$, ns, $P > 0.05$, $F_{11, 58} = 3.40$, one-way analysis of variance, Student-Newman-Keuls post hoc analysis).

Pre-proenkephalin-B : G3PDH expression - Rostral Striatum - Level 2

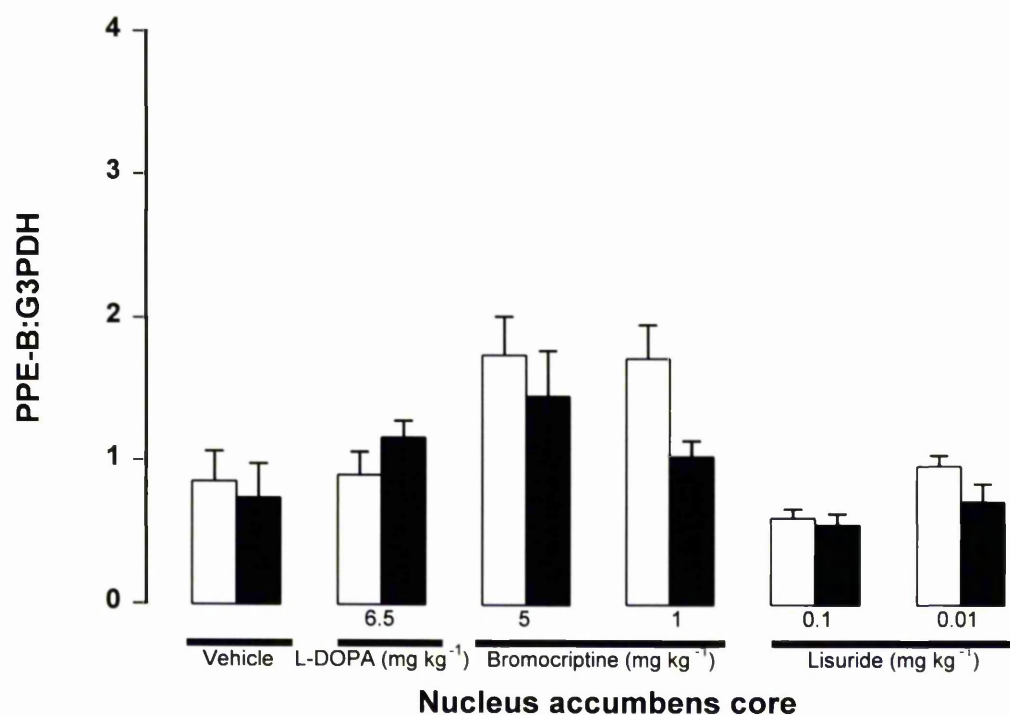


Figure 4.3.5.13 Ratio of pre-proenkephalin-B (PPE-B) to G3PDH mRNA expression in rostral level 2 (Nucleus accumbens core) in the 6-OHDA-lesioned rat model of Parkinson's disease following 21 day, twice-daily, treatment with vehicle, L-DOPA (6.5 mg kg⁻¹) and benserazide (1.5 mg kg⁻¹), bromocriptine (5, 1 mg kg⁻¹, b.d.) or lisuride (0.1, 0.01 mg kg⁻¹, b.d.). Unlesioned (□) and lesioned (■) striatum are shown. Data are expressed as mean (\pm SEM) optical density ratios ($n=5-6$, ns, $P > 0.05$, $F_{11, 58} = 4.41$, one-way analysis of variance, Student-Newman-Keuls post hoc analysis).

Pre-proenkephalin-B : G3PDH expression - Rostral Striatum - Level 2

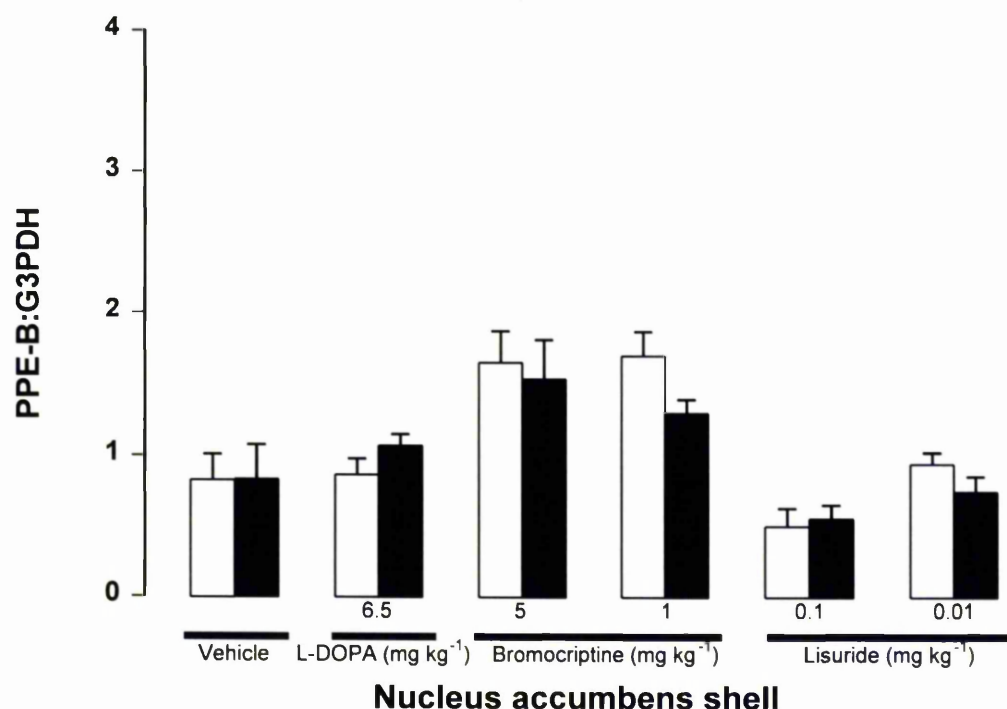


Figure 4.3.5.14 Ratio of pre-proenkephalin-B (PPE-B) to G3PDH mRNA expression in rostral level 2 (Nucleus accumbens shell) in the 6-OHDA-lesioned rat model of Parkinson's disease following 21 day, twice-daily, treatment with vehicle, L-DOPA (6.5 mg kg⁻¹) and benserazide (1.5 mg kg⁻¹), bromocriptine (5, 1 mg kg⁻¹, b.d.) or lisuride (0.1, 0.01 mg kg⁻¹, b.d.). Unlesioned (□) and lesioned (■) striatum are shown. Data are expressed as mean (\pm SEM) optical density ratios ($n=5-6$, ns, $P > 0.05$, $F_{11, 58} = 5.95$, one-way analysis of variance, Student-Newman-Keuls post hoc analysis).

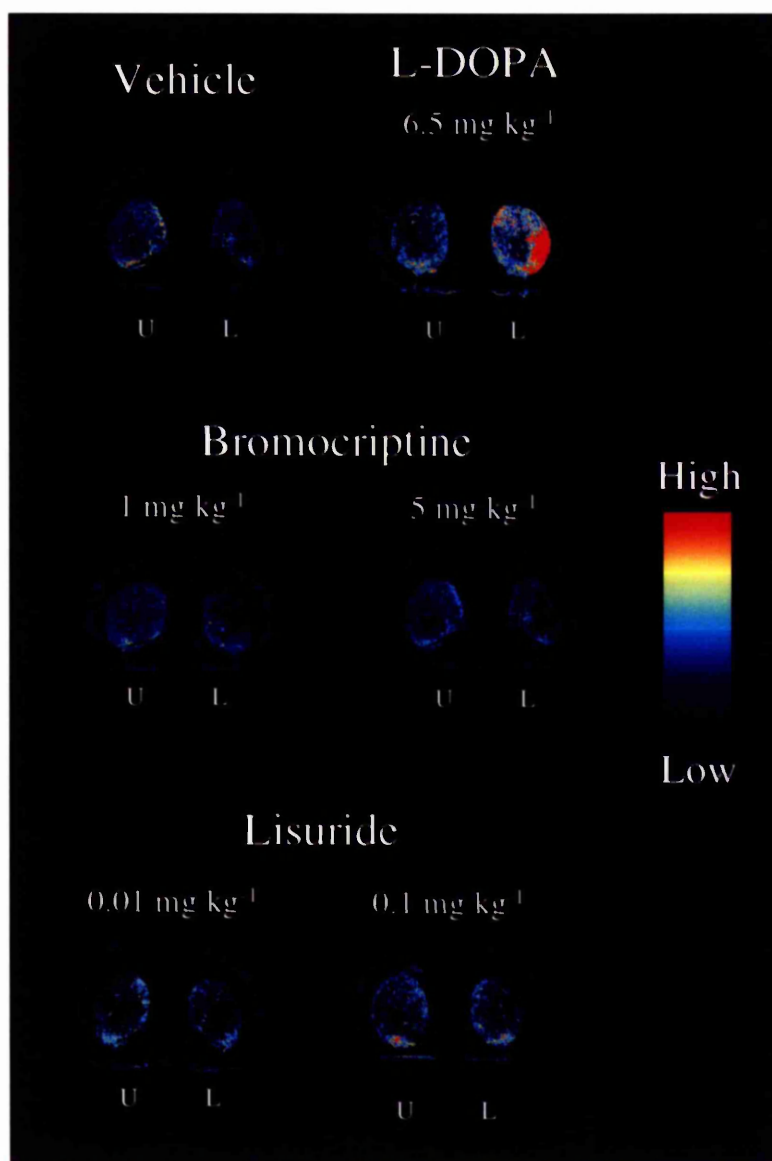


Figure 4.3.5.15 Pseudocolour transformations of autoradiographs of *in situ* hybridisation utilising an oligonucleotide probe targeted against pre-proenkephalin-B (PPE-B) in the lesioned (L) or unlesioned (U) intermediate striatum following 21 days, twice-daily, vehicle, L-DOPA (6.5 mg kg⁻¹) and benserazide (1.5 mg kg⁻¹), bromocriptine (5 or 1 mg kg⁻¹) or lisuride (0.1 or 0.01 mg kg⁻¹) treatment in the 6-OHDA-lesioned rat model of Parkinson's disease.

Pre-proenkephalin-B : G3PDH expression - Intermediate striatum

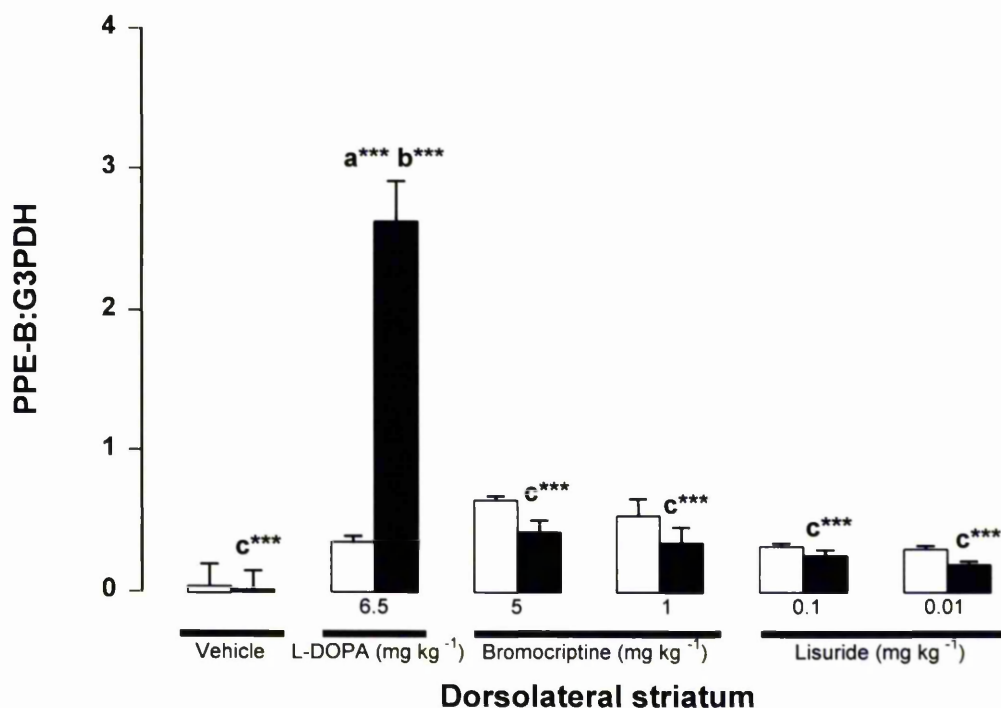


Figure 4.3.5.16 Ratio of pre-proenkephalin-B (PPE-B) to G3PDH mRNA expression in intermediate striatum (dorsolateral) in the 6-OHDA-lesioned rat model of Parkinson's disease following 21 day, twice-daily, treatment with vehicle, L-DOPA (6.5 mg kg⁻¹) and benzerazide (1.5 mg kg⁻¹), bromocriptine (5, 1 mg kg⁻¹, b.d.) or lisuride (0.1, 0.01 mg kg⁻¹, b.d.). Unlesioned (□) and lesioned (■) striatum are shown. Data are expressed as mean (\pm SEM) optical density ratios ($n=6$, a*** $P < 0.001$ cf unlesioned in same group, b*** $P < 0.001$ cf ipsi vehicle group, c*** $P < 0.001$ cf ipsi L-DOPA group, $F_{11,60} = 34.48$, one-way analysis of variance, Student-Newman-Keuls post hoc analysis).

Pre-proenkephalin-B : G3PDH expression - Intermediate striatum

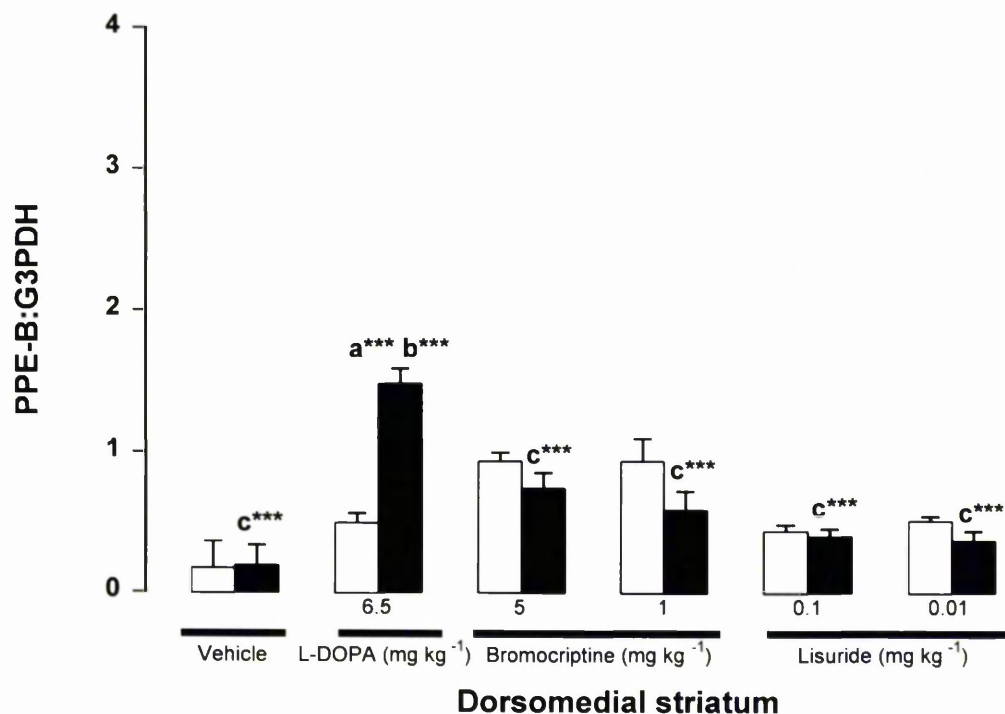


Figure 5.3.5.17 Ratio of pre-proenkephalin-B (PPE-B) to G3PDH mRNA expression in intermediate striatum (dorsomedial) in the 6-OHDA-lesioned rat model of Parkinson's disease following 21 day, twice-daily, treatment with vehicle, L-DOPA (6.5 mg kg⁻¹) and benserazide (1.5 mg kg⁻¹), bromocriptine (5, 1 mg kg⁻¹, b.d.) or lisuride (0.1, 0.01 mg kg⁻¹, b.d.). Unlesioned (□) and lesioned (■) striatum are shown. Data are expressed as mean (\pm SEM) optical density ratios ($n=6$, a*** $P < 0.001$ cf unlesioned in same group, b*** $P < 0.001$ cf ipsi vehicle group, c*** $P < 0.001$ cf ipsi L-DOPA group, $F_{11, 60} = 11.47$, one-way analysis of variance, Student-Newman-Keuls post hoc analysis).

Pre-proenkephalin-B : G3PDH expression - Intermediate striatum

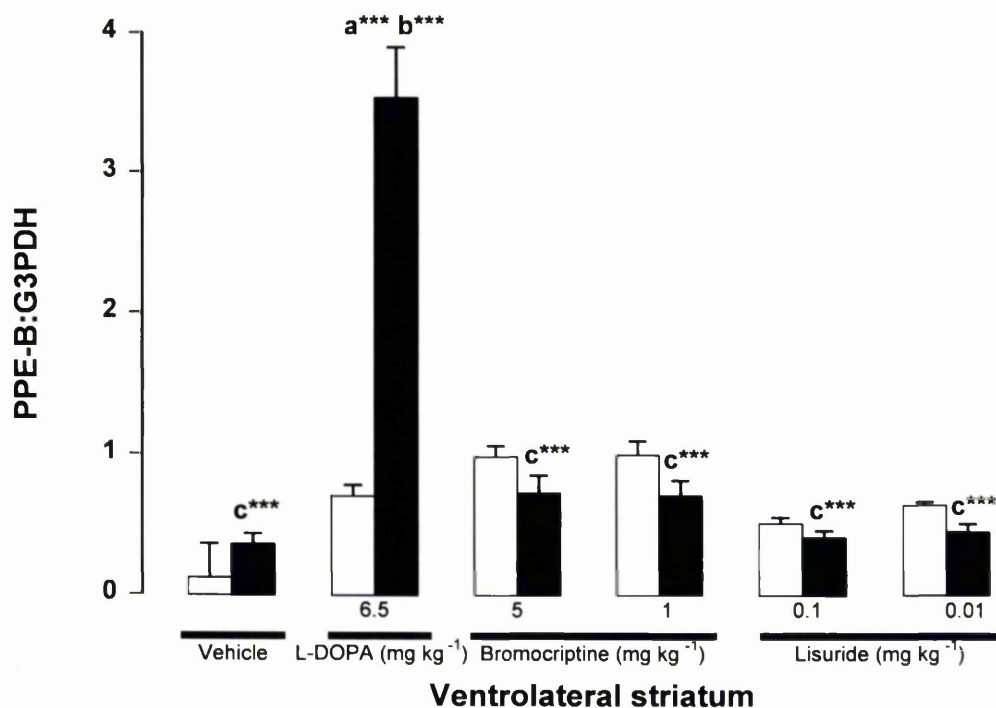


Figure 4.3.5.18 Ratio of pre-proenkephalin-B (PPE-B) to G3PDH mRNA expression in intermediate striatum (ventrolateral) in the 6-OHDA-lesioned rat model of Parkinson's disease following 21 day, twice-daily, treatment with vehicle, L-DOPA (6.5 mg kg⁻¹) and benserazide (1.5 mg kg⁻¹), bromocriptine (5, 1 mg kg⁻¹, b.d.) or lisuride (0.1, 0.01 mg kg⁻¹, b.d.). Unlesioned (□) and lesioned (■) striatum are shown. Data are expressed as mean (\pm SEM) optical density ratios ($n=6$, a*** $P < 0.001$ cf unlesioned in same group, b*** $P < 0.001$ cf ipsi vehicle group, c*** $P < 0.001$ cf ipsi L-DOPA group, $F_{11, 60} = 37.96$, one-way analysis of variance, Student-Newman-Keuls post hoc analysis).

Pre-proenkephalin-B : G3PDH expression - Intermediate striatum

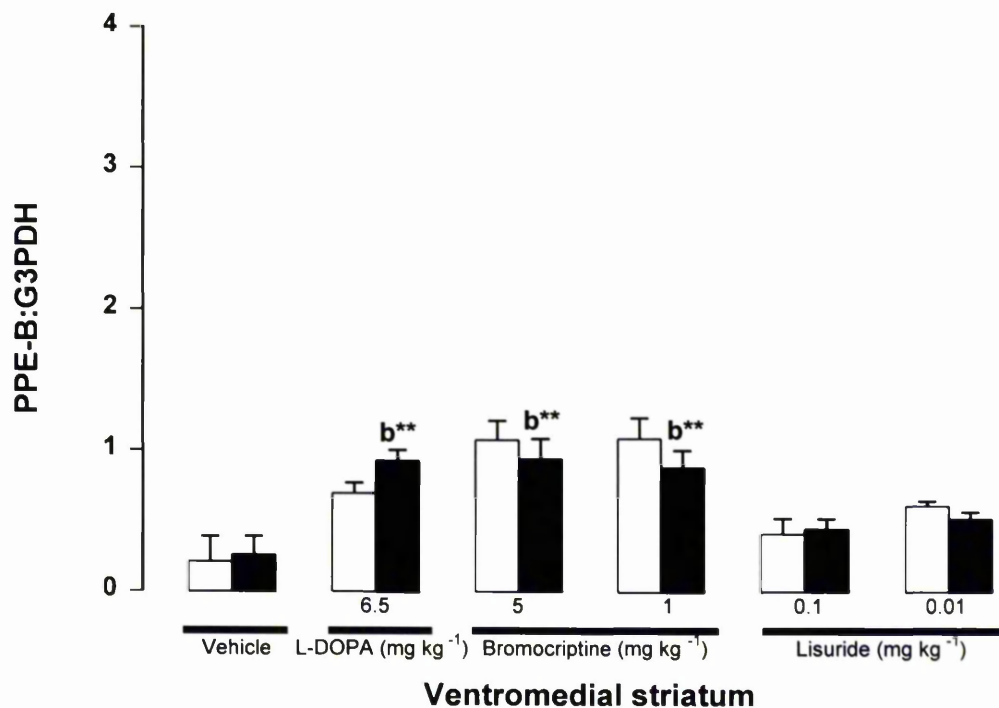


Figure 4.3.5.19 Ratio of pre-proenkephalin-B (PPE-B) to G3PDH mRNA expression in intermediate striatum (ventromedial) in the 6-OHDA-lesioned rat model of Parkinson's disease following 21 day, twice-daily, treatment with vehicle, L-DOPA (6.5 mg kg⁻¹) and benserazide (1.5 mg kg⁻¹), bromocriptine (5, 1 mg kg⁻¹, b.d.) or lisuride (0.1, 0.01 mg kg⁻¹, b.d.). Unlesioned (□) and lesioned (■) striatum are shown. Data are expressed as mean (\pm SEM) optical density ratios ($n=6$, $b^{**} P < 0.01$ cf ipsi vehicle group, $F_{11, 60} = 7.24$, one-way analysis of variance, Student-Newman-Keuls post hoc analysis).

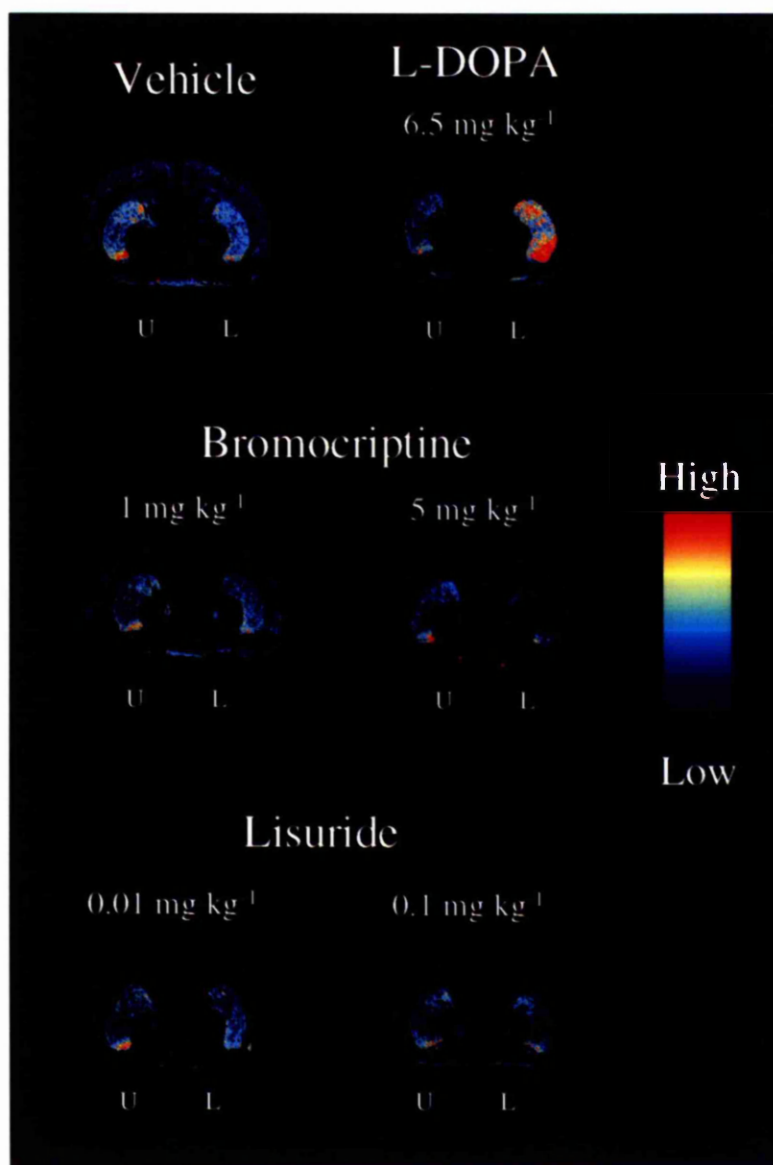


Figure 4.3.5.20 Pseudocolour transformations of autoradiographs of *in situ* hybridisation utilising an oligonucleotide probe targeted against pre-proenkephalin-B (PPE-B) in lesioned (L) or unlesioned (U) caudal striatum following 21 days, twice-daily, vehicle, L-DOPA (6.5 mg kg⁻¹) and benserazide (1.5 mg kg⁻¹), bromocriptine (5 or 1 mg kg⁻¹) or lisuride (0.1 or 0.01 mg kg⁻¹) treatment in the 6-OHDA-lesioned rat model of Parkinson's disease.

Pre-proenkephalin-B : G3PDH expression - Caudal striatum

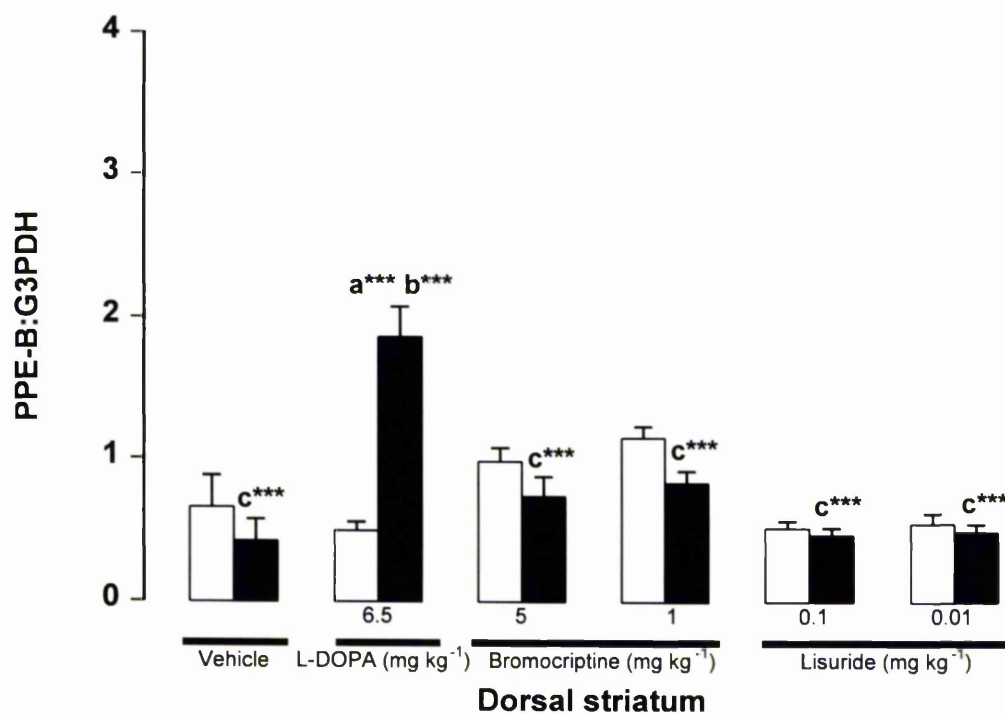


Figure 4.3.5.21 Ratio of pre-proenkephalin-B (PPE-B) to G3PDH mRNA expression in caudal striatum (dorsal) in the 6-OHDA-lesioned rat model of Parkinson's disease following 21 day, twice-daily, treatment with vehicle, L-DOPA (6.5 mg kg⁻¹) and benserazide (1.5 mg kg⁻¹), bromocriptine (1, 5 mg kg⁻¹, b.d.) or lisuride (0.1, 0.05 mg kg⁻¹, b.d.). Unlesioned (□) and lesioned (■) striatum are shown. Data are expressed as mean (\pm SEM) optical density ratios ($n=4-6$, a*** $P < 0.001$ cf unlesioned in same group, b*** $P < 0.001$ cf ipsi vehicle group, c*** $P < 0.001$ cf ipsi L-DOPA group, $F_{11, 56} = 15.28$, one-way analysis of variance, Student-Newman-Keuls post hoc analysis).

Pre-proenkephalin-B : G3PDH expression - Caudal striatum

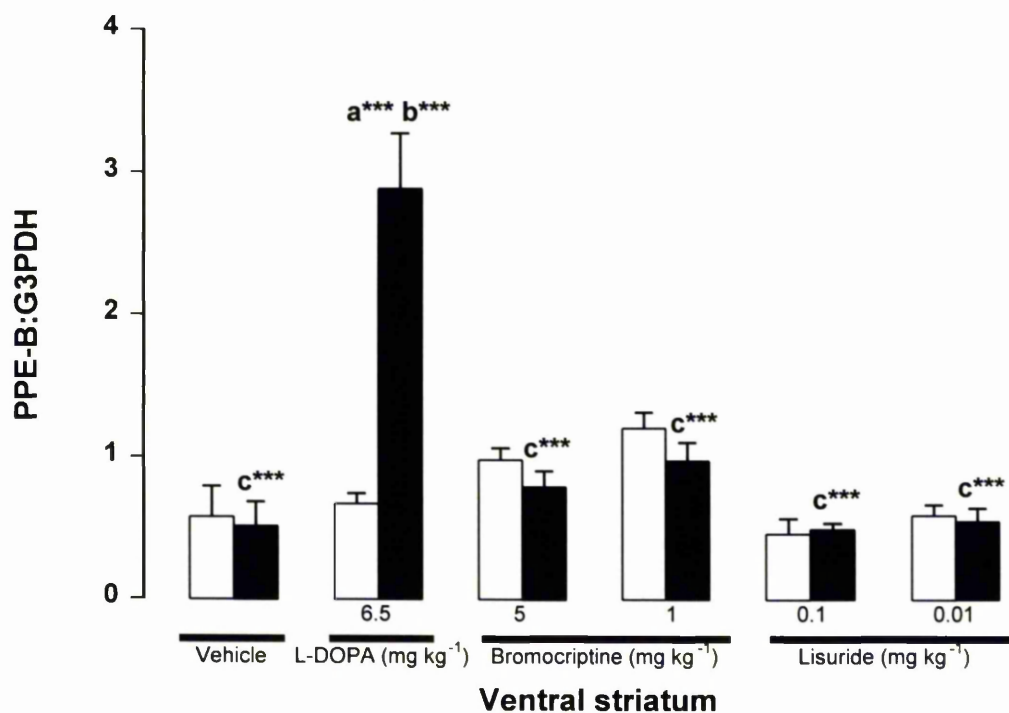


Figure 4.3.5.22 Ratio of pre-proenkephalin-B (PPE-B) to G3PDH mRNA expression in caudal striatum (ventral) in the 6-OHDA-lesioned rat model of Parkinson's disease following 21 day, twice-daily, treatment with vehicle, L-DOPA (6.5 mg kg⁻¹) and benserazide (1.5 mg kg⁻¹), bromocriptine (1, 5 mg kg⁻¹, b.d.) or lisuride (0.1, 0.05 mg kg⁻¹, b.d.). Unlesioned (□) and lesioned (■) striatum are shown. Data are expressed as mean (\pm SEM) optical density ratios ($n=4-6$, a*** $P < 0.001$ cf unlesioned in same group, b*** $P < 0.001$ cf ipsi vehicle group, c*** $P < 0.001$ cf ipsi L-DOPA group, $F_{11, 56} = 18.45$, one-way analysis of variance, Student-Newman-Keuls post hoc analysis).

4.4 Discussion

Methodological considerations

In a similar manner to northern blot hybridisation, the main uncertainty regarding the technique of *in situ* hybridisation is assessing the specificity of the oligonucleotide probe. To this end several methodological considerations have been employed to ensure the oligonucleotide probes used are specific for pre-proenkephalin-A (PPE-A) and pre-proenkephalin-B (PPE-B) mRNA transcripts. The first concern is the specificity of the oligonucleotide probe for RNA. To address this, pre-treatment with RNase, an enzyme that specifically degrades single-stranded RNA, completely abolished the signal for PPE-A, PPE-B and the control probe G3PDH (Figures 4.3.1.1, 4.3.1.2, 4.3.1.3). Secondly, the specificity of the oligonucleotide probe sequences were verified using genbank and EMBL databases (Altschul *et al.*, 1993). The third control for probe specificity, was the use of sense probes. Sense oligonucleotide probes are of identical sequence to the target mRNA transcripts. These were used to verify no non-specific binding occurs to DNA (Figures 4.3.1.7, 4.3.1.8, 4.3.1.9). The fourth control to verify the specificity of the probes for the target transcripts was by using two oligonucleotide probe sequences, distinct from each other, but targeted to the same transcript. Both these probes showed an identical binding pattern, thus indicating specificity for the target of interest (Figures 4.3.1.7, 4.3.1.8, 4.3.1.9). Taken together, these data confer the specificity of the oligonucleotide probes to the mRNA transcripts for PPE-A, PPE-B and G3PDH.

[³H]Mazindol radioligand binding on coronal striatal sections verified greater than 90% reduction in dopamine uptake sites in the striatum, ipsilateral to the 6-OHDA-lesion. Only rats with a reduction in dopamine uptake sites greater than 90% were included in the *in situ* hybridisation groups (Figure 4.3.3.1, Table 4.1).

Behavioural analysis following repeated, twice-daily, vehicle, L-DOPA, bromocriptine or lisuride in the 6-OHDA-lesioned rat model of Parkinson's disease

The rat model of L-DOPA-induced dyskinesia was prepared as in chapter 2. Four additional groups, consisting of low and high dose bromocriptine or lisuride treated rats were also investigated. The bromocriptine groups were filmed for 2 hours, 1 hour post injection, as previous reports on the pharmacokinetics of bromocriptine described a latency of therapeutic action (Rouillard *et al.*, 1987). All other groups were filmed for 2 hours immediately following injection. L-DOPA-treated rats showed a marked potentiation of behavioural hyperkinesia as previously described. Vehicle administration produced little change over the 21 day period, with only ipsiversive rotations noted (Figure 4.3.2.1). Both the high and low dose bromocriptine groups showed a rotational response, contraversive to the 6-OHDA-lesion. This rotational response was not potentiated throughout the 21 day period (Figure 4.3.2.2). The 5 mg kg⁻¹ (twice-daily, 21d) bromocriptine group showed a non-significantly increased number of rotations when compared to the 1 mg kg⁻¹ (twice-daily, 21d) group. Similarly, the high dose lisuride (0.1 mg kg⁻¹, twice-daily, 21d) group showed a slightly higher, non-significant, rate of contraversive rotational behaviour than the low dose group (0.01 mg kg⁻¹, twice-daily, 21d), with neither group showing any significant potentiation of the response (Figure 4.3.2.3).

Following 21 day vehicle administration, no alteration in the behavioural response was observed following repeated injections. A small number of rotations, ipsiversive to the 6-OHDA-lesion, were observed. This ipsiversive rotational behaviour, with body posturing ipsiversive to the lesion has been previously described and is thought to result from the dopamine-deficiency in the lesioned striatum (Bracha *et al.*, 1987; Olsson *et al.*, 1995). No alteration in the response to repeated vehicle administration was observed as no changes in dopaminergic transmission occurs. Following repeated low dose L-DOPA administration an enhanced response, characterised by an increased rotational behaviour, was observed. This increase in behavioural response has been previously reported following both repeated L-DOPA or apomorphine administration (Bevan, 1984; Carey, 1991; Gancher *et al.*, 1995). Several hypotheses have been proposed to explain this increase in behavioural

response. The most widely-held view is that following repeated dopamine-stimulation, dopamine receptors become supersensitive on the denervated striatum, either due to increased receptor numbers or increased affinity for dopamine. However, several studies have shown that following repeated dopamine stimulation by either L-DOPA or apomorphine, a decrease in dopamine receptor number and mRNA is observed (Gerfen *et al.*, 1990; Chritin *et al.*, 1993). Therefore, dopamine receptor number cannot explain the alterations in behavioural response following repeated L-DOPA administration. Dopamine D2 receptor supersensitivity has been reported following repeated apomorphine in 6-OHDA-lesioned rats (Bevan, 1984). Similarly dopamine D1 receptors have been demonstrated to become more effectively coupled to adenylyl cyclase following dopamine denervation, without changes in either affinity or number of dopamine D1 receptors (Thomas *et al.*, 1992). Therefore, alterations in dopamine receptor to intracellular second messenger coupling effector systems, has become one of the most attractive explanation by which enhanced behavioural response following repeated dopamine receptor stimulation occurs. Therefore, in the case of repeated bromocriptine or lisuride treatment, the lack of enhanced behavioural response following repeated dopamine-replacement therapy could be due to a lack of supersensitive second messenger coupling effector systems within the denervated striatum. In fact evidence from rat models of Parkinson's disease following repeated bromocriptine suggests such a loss of effector mechanism may take place following repeated bromocriptine treatment (Bedard *et al.*, 1986; Silverman, 1992).

Since bromocriptine and lisuride only activate dopamine D2 receptors, it has been suggested that both D1 and D2 dopamine receptor stimulation are required for the genesis of dyskinesia (Bedard, 1996). However, this seems unlikely since other 'pure' dopamine D2 receptor agonists, namely PHNO, have been shown to cause dyskinesia following *de novo* administration in MPTP-treated primates (Crossman 1992; Gomez-Mancilla and Bedard, 1992). The long acting nature of both bromocriptine and lisuride, with half-lives of 8 and 3 hours, respectively, may play a role in the lack of behavioural potentiation. Since L-DOPA has a plasma half-life of only 1.5 hours, plasma concentration in parkinsonian patients are highly variable throughout the treatment period. Therefore, dopamine receptor stimulation undergoes non-physiological fluctuations. Similarly, in the rat model of L-DOPA-induced dyskinesias, one of the contributing factors to the behavioural potentiation could be

the pulsatile nature of dopamine within the striatum. Again this seems unlikely as control-release preparations of L-DOPA also eventually develop dyskinesia (Rodnitzky, 1992; Koller and Pahwa, 1994). The lack of behavioural enhancement following repeated treatment of bromocriptine and lisuride may be due to dopamine receptor desensitisation. Evidence from several studies suggests that following repeated receptor stimulation, two possible mechanisms produced reductions in the response to continual receptor stimulation. The first mechanism involves the control of receptor numbers, the second, a loss of second messenger effector coupling. Evidence from the MPTP-treated non-human primate model suggests that following repeated dopamine receptor stimulation, following L-DOPA-administration, an increase in dopamine receptors is observed when compared to MPTP-treated parkinsonian primates. However, following repeated bromocriptine treatment this rise in dopamine receptor numbers is reduced (10 %, Bedard 1986). Studies carried out in 6-OHDA-lesioned rats suggest that following intermittent L-DOPA-administration or the D2 receptor agonist quinpirole, dopamine D2 receptor mRNA remains elevated above control values. However, following continual administration, utilising osmotic mini-pumps, the level of dopamine D2 receptor mRNA is decreased to basal (pre-lesion) levels (Gerfen, 1990). This would suggest that following repeated bromocriptine administration, dopamine D2 receptors are returned to pre-parkinsonian levels. This mechanism may account for the lack of behavioural potentiation following repeated bromocriptine or lisuride treatment.

A further possibility for the lack of behavioural potentiation observed following repeated bromocriptine or lisuride treatment is the possibility that bromocriptine and lisuride may be effecting other transmitter systems within the basal ganglia which alter the dyskinetic producing effects of D2 dopamine receptor stimulation. In fact bromocriptine and lisuride have been implicated in altering both noradrenaline and 5-HT levels in the brain following administration (Horowski and Wachter, 1976; Parkes, 1977; Morales-Olivas *et al.*, 1984).

As will now be discussed in more detail, a further possibility exists for the lack of behavioural hyperkinesia observed following repeated bromocriptine or lisuride administration, whereby the molecular and cellular changes that take place, with specific relevance to neuropeptide precursors within striatal efferents, cause

behavioural alterations different to those observed following repeated L-DOPA administration.

Topographical analysis of *in situ* hybridisation utilising oligonucleotide probes targeted against pre-proenkephalin-A and pre-proenkephalin-B mRNA transcripts in the 6-OHDA-lesioned rat following repeated vehicle, L-DOPA, bromocriptine or lisuride administration

The major finding from these studies was the fact that high doses of bromocriptine or lisuride did not elevate PPE-B levels and, in fact, reduced PPE-A expression to pre-lesioned levels. Qualitatively similar results were found with both the lower doses of bromocriptine and lisuride. Low dose bromocriptine administration did not increase PPE-B expression but produced only a slight, non-significant, decrease in the lesion-induced PPE-A expression. Further insights into the topographical alterations associated with PPE-A and PPE-B expression in the rat model of L-DOPA-induced dyskinesia were also made possible. These will now be discussed in context with the bromocriptine and lisuride data.

Following lesion and subsequent vehicle treatment, there was a non-significant increase in PPE-A expression in all areas of the rostral striatum (level 1, Figure 4.3.4.1-4.3.4.5). In the rostral level 2 striatum there was a similar increase in the all areas of the striatum. However, with significance only observed in the dorsolateral, dorsomedial and ventrolateral areas (Figures 4.3.4.9, 4.3.4.10, 4.3.4.11). No significant increases in PPE-A expression were seen in the ventromedial areas or core or shell regions of the nucleus accumbens of the rostral level 2 striatum (Figures 4.3.4.12, 4.3.4.13, 4.3.4.14). In the intermediate and rostral striatum, non-significant increases of PPE-A expression were observed in all areas.

Following repeated L-DOPA-treatment a similar pattern of PPE-A expression was seen, however PPE-A expression is further increased (over lesion followed by vehicle treatment) in dorsolateral and dorsomedial areas of rostral level 1 (Figures 4.3.4.2, 4.3.4.3).

Following repeated high dose bromocriptine treatment (5 mg kg⁻¹, twice-daily, 21d) lesion-induced increases in PPE-A expression levels were decreased and were not significantly different from the unlesioned side in any of the levels or areas

throughout the striatum (Figures 4.3.4.1-4.3.4.22). In contrast, following low dose bromocriptine treatment (1 mg kg^{-1} , twice-daily, 21d) this decrease in PPE-A expression was not observed, with significantly increased levels of PPE-A expression in all areas of rostral level 1 striatum (dorsolateral, dorsomedial, ventrolateral and ventromedial) and no change in either the core or shell regions of the nucleus accumbens (Figures 4.3.4.1-4.3.4.2). Similarly, in rostral level 2 following repeated low dose bromocriptine (1 mg kg^{-1} , twice-daily, 21d), PPE-A expression was significantly increase in all areas of the striatum (dorsolateral, dorsomedial, ventrolateral and ventromedial) with no changes in the core or shell regions of the nucleus accumbens (Figures 4.3.4.9, 4.3.4.14). In the intermediate striatum following low dose bromocriptine (1 mg kg^{-1} , twice-daily, 21d), PPE-A expression was significantly increased in the dorsolateral, dorsomedial and ventrolateral striatum, with a non-significant increase in the ventromedial area of the intermediate striatum (Figures 4.3.4.16, 4.3.4.17, 4.3.4.18). In the caudal striatum no significant difference in PPE-A expression between lesioned and unlesioned sides were apparent following low dose bromocriptine administration (Figures 4.3.4.21, 4.3.4.22).

Following both high (0.1 mg kg^{-1} , twice-daily, 21d) and low (0.01 mg kg^{-1} , twice-daily, 21d) dose lisuride treatment there was no significant difference between the lesioned and unlesioned striatum in any areas throughout the striatum (Figures 4.3.4.1, 4.3.1.22).

Following lesion and subsequent vehicle treatment, there was a non-significant decrease in PPE-B expression in all areas of the striatum and both core and shell regions of the nucleus accumbens in both rostral levels (levels 1 and 2, Figures 4.3.5.1-4.3.5.14). Similarly, in both the intermediate and caudal striatum, no significant difference between the lesioned and unlesioned side following vehicle treatment were observed in any area of the striatum or in either the core or shell of the nucleus accumbens (Figures 4.3.5.15-4.3.5.22). A similar pattern of non-significant decreases in PPE-B expression in the lesioned striata of both high and low dose bromocriptine or lisuride was also observed (Figures 4.3.5.1-4.3.5.22). Conversely, following repeated L-DOPA-treatment a marked significant increase in PPE-B expression was seen in the dorsolateral, dorsomedial and ventrolateral areas of the striatum in the rostral striatum (level 1, Figures 4.3.5.1-4.3.5.4). In the ventromedial striatum no significant increase in PPE-B expression was observed in the rostral

striatum (level 1, Figures 4.3.5.6-4.3.5.7). Similarly, no significant difference in PPE-B expression between lesioned and unlesioned sides were observed in either the core or shell of the nucleus accumbens (level 1, Figures 4.3.5.6, 4.3.5.7).

In the rostral striatum (level 2) a similar pattern of PPE-B expression was observed following L-DOPA-treatment. In the dorsolateral, dorsomedial and ventrolateral areas of the rostral (level 2, Figures 4.3.5.8-4.3.5.11) striatum a significant increase is observed on the lesioned side. No significant difference between lesioned and unlesioned striatum was apparent in the ventromedial striatum or the core or shell of the nucleus accumbens (Figures 4.3.5.12-4.3.5.14).

In the intermediate striatum, significant increases in PPE-B expression were observed in the dorsolateral, dorsomedial and ventrolateral areas (Figures 4.3.5.15-4.3.5.18), while no significant increase is observed in the ventromedial area (Figure 4.3.5.19). In the caudal striatum, significant increases in PPE-B expression were seen in both the dorsal and ventral areas of the caudal striatum (Figures 4.3.5.20-4.3.5.22).

In summary, following vehicle, bromocriptine or lisuride treatment there was a decrease in PPE-B expression on the lesioned side compared with the unlesioned side. However, following L-DOPA treatment there was a marked significant increase in PPE-B expression throughout the striatum, displaying a mediolateral gradient (with higher expression in the lateral areas of the lesioned striatum).

Topographical alterations in PPE-A and PPE-B expression following repeated bromocriptine or lisuride administration in the 6-OHDA-lesioned rat model of Parkinson's disease

There are two possible mechanism for the observed alteration in peptide precursors following repeated bromocriptine or lisuride treatment. Several studies have demonstrated that continuous administration of L-DOPA or the D2 dopamine receptor agonist quinpirole, through the use of osmotic minipumps, decreases the elevated PPE-A expression seen following 6-OHDA-lesion in rats (Gerfen, 1990; Engber *et al.*, 1991). While intermittent treatment, in a pulsatile manner (i.e. 2-3 injections per day) does not alter lesion-induced increases in PPE-A mRNA levels, or in fact undergoes a slight increase in enkephalin peptide levels (Engber *et al.*, 1991). Following continuous L-DOPA or quinpirole (by minipump infusion) administration

in 6-OHDA-lesioned rats, PPE-B expression is not altered, while intermittent treatment causes an upregulation in both mRNA transcription and dynorphin peptide levels (Gerfen, 1990). Both bromocriptine and lisuride are D2 dopamine receptor agonists known to have a long half-lives of about 8 hours and 3 hours, respectively (Aellig and Nuesch, 1977; Markey *et al.*, 1979; Parkes *et al.*, 1981). This may explain the decrease in PPE-A expression to basal levels and the lack of increase seen in PPE-B expression. Therefore, if two injections per day of the long-acting dopamine agonists bromocriptine or lisuride has the same effect as continuous treatment, this may account for the lack of peptide expression alterations observed. It has been reported that long half-life drugs, or continuous treatment through osmotic minipumps, and L-DOPA control-release preparations, elicit fewer dyskinetic side effects in both parkinsonian patients and in MPTP-treated non-human primates (Lieberman *et al.*, 1979; Parkes, 1979; Lees and Stern, 1981; Mancilla-Gomez and Bedard, 1993; Koller and Pahwa, 1994). It has been suggested that this may occur as the dopamine receptor stimulation is more physiological in these situations than either twice-daily oral tablet administration in patients or twice-daily injections in animal models of Parkinson's disease.

The second mechanism by which bromocriptine and lisuride may be causing the reduction in PPE-A and the lack of elevation in PPE-B is the fact that these compound may not in fact be pure dopamine D2 receptor agonists. In fact studies have shown that bromocriptine may in fact be a dopamine D1 receptor antagonist (Dolphin *et al.*, 1977; Schachter *et al.*, 1980). If bromocriptine and lisuride do have D1 dopamine receptor antagonistic properties it is possible that by only stimulating the D2 receptors on both PPE-A and PPE-B containing cells, with concomitant lack of D1 stimulation, PPE-A expression may be reduced and PPE-B expression remained unaltered. Recent evidence demonstrated that in the 6-OHDA-lesioned rat either L-DOPA or the D1 receptor agonist SKF 38393 both increased AP-1 and CREB DNA-binding activity, presumably through increasing adenylyl cyclase activity, whereas bromocriptine did not induced AP-1 or CREB DNA-binding activity (Kashihara *et al.*, 1996).

However, since intermittent administration of the direct dopamine D2 receptor agonist quinpirole also results in an elevation in both PPE-A and PPE-B, the lack of

D1 stimulation does not seem a plausible mechanism to explain normalisation of PPE-A and PPE-B by both bromocriptine and lisuride.

Topographical alterations in PPE-A and PPE-B following repeated vehicle or L-DOPA treatment in the 6-OHDA-lesioned rat model of Parkinson's disease

Following repeated L-DOPA administration in the 6-OHDA-lesioned rat model of Parkinson's disease a topographical distribution of PPE-A expression is observed, such that the greatest rise is seen in the rostral and, more specifically, the dorsolateral areas within the rostral neostriatum (Figures 4.3.4.2, 4.3.4.3). The mechanism underlying this topographical arrangement could arise from two possibilities.

It has been demonstrated that, both in normal, non-dopamine depleted rats and in rats following dopamine denervation, dopamine receptors are not homogeneously distributed throughout the neostriatum. Higher levels of D2 dopamine receptors have been reported in the most rostral striatum with a dorsolateral and mediolateral gradient (with higher levels in the dorsolateral region of the striatum, Tassin *et al.*, 1976; Doucet *et al.*, 1986; Graham *et al.*, 1989a). Following dopamine-replacement therapy in animal models of Parkinson's disease, preferential stimulation of these upregulated receptors may account for the further rise seen in PPE-A expression. This may also account for why a significant increase in PPE-A expression is only seen in this region of the striatum.

A second possible mechanism for the topographical changes observed in PPE-A expression following dopamine-replacement therapy in the lesioned striatum, may be the topographical compartmentalisation of functional cerebrocortical innervation. It is known that the sensorimotor area of the cerebral cortex in the rat innervates the striatum in predominantly in the rostral striatum, following a dorsolateral (highest innervation) to ventomedial (lowest innervation) gradient (McGeorge and Faull, 1989). This corresponds to the topographical density of dopamine receptors observed within the striatum (Tassin *et al.*, 1976; Doucet *et al.*, 1986; Graham *et al.*, 1989a). It has been demonstrated in several studies that a maintained cortical input, through activation of NMDA receptors, is required to maintain the elevated PPE-A expression following dopamine denervation (Uhl *et al.*, 1988; Campbell and Bjorklund, 1994;

Hajji *et al.*, 1996). This would imply that corticostriatal innervation plays a pivotal role in peptide expression.

It has been demonstrated that blockade of NMDA receptors increases the expression of dopamine D2 receptors (Lannes *et al.*, 1995). Therefore, increased corticostriatal NMDA transmission could effect the balance of D1 to D2 receptors present in medium spiny neurons of the striatum and thus effect adenylyl cyclase activity, ultimately resulting in altered peptide expression.

Therefore, following dopamine denervation of the striatum, with subsequent dopamine-replacement, cerebrocortical and corticostriatal activity may play a role in the topographical distribution of the PPE-A and PPE-B signal. If this is in fact the mechanism by which PPE-A and PPE-B expression is further increased following repeated L-DOPA-administration in the lesioned striatum, it would imply that the sensorimotor region of the cerebral cortex is overactive in L-DOPA-induced dyskinesia. In fact a recent study demonstrated, using single-photon emission tomography, an overactivity of the supplementary motor area and primary motor area in parkinsonian patients displaying L-DOPA-induced dyskinesia (Rascol, 1996). This may also account for the recent success in alleviating dyskinesias by utilising NMDA receptor antagonists in both MPTP-treated non-human primates (Chase *et al.*, 1995; Papa and Chase 1996) and in small scale clinical trials (Verhagen-Metman *et al.*, 1996).

Summary

The increased hyperkinesia seen in the rat model of L-DOPA-induced dyskinesia, with the concomitant expression of the opioid peptide precursors PPE-B and PPE-A as already described in chapter 3, can be blocked by the co-administration of L-DOPA with either the specific kappa opioid receptor antagonist, *nor*-binaltorphimine, or the specific delta opioid receptor antagonist, naltrindole. It has been proposed in this thesis that the mechanism underlying this opioid-induced hyperkinesia arises from two separate mechanisms, both of which ultimately result in underactivity of basal ganglia outputs and therefore decreased inhibition of the VA/VL thalamus (Crossman, 1987)

Increased enkephalin release in the direct striatopallidal pathway may act to further reduced GABA release in the GPI. This would cause increased GPI activity. Inhibitory GABAergic efferents to the subthalamic nucleus would become overactive, thus causing underactivity of the subthalamic nucleus. Underactivity of the subthalamic nucleus would decrease the excitatory glutamatergic projection to the medial segment of the globus pallidus. Decreased activity of the medial segment of the globus pallidus would lead to decreased inhibition of the VA/VL thalamus. Increased activity of the VA/VL thalamus would lead to increased excitation of the motor cortex and thus dyskinesia.

L-DOPA causes dyskinesia in both the clinic and in experimental primate models of Parkinson's disease. In the 6-OHDA-lesioned rat model of Parkinson's disease, repeated L-DOPA-administration is associated with an increase in expression of both PPE-A and PPE-B. Conversely, drugs known not to cause dyskinesias in both the clinic and in experimental animal models of Parkinson's disease, i.e. bromocriptine and lisuride, are not associated with increased expression in PPE-B and, in fact, decrease the lesion-induced elevation seen in PPE-A in the rat model of L-DOPA-induced dyskinesia. This correlation, in conjunction with the data demonstrating both kappa and delta opioid receptor subtype selective antagonists reduce the hyperkinesia observed in the rat model of L-DOPA-induced dyskinesia, suggests a role for opioid peptides in the genesis of L-DOPA-induced dyskinesia. To better address the question of the involvement of increased opioid peptide transmission in underlying L-DOPA-induced dyskinesias, the expression of the opioid peptide precursors (PPE-A and PPE-B) were investigated in the 'gold-standard' MPTP-treated non-human primate model of Parkinson's disease, following repeated dopamine-receptor stimulation to produced dyskinesias, indistinguishable from those seen in the clinical situation.

Chapter 5:

Topographical distribution of striatal pre-proenkephalin-A and pre-proenkephalin-B mRNA in the MPTP-treated non-human primate following dopamine-replacement therapy

5.1 Introduction

In the previous chapters it has been demonstrated that in a rodent model of L-DOPA-induced dyskinesia there is an increase in the large molecular weight opioid neuropeptide precursors pre-proenkephalin-A (PPE-A, proenkephalin) and pre-proenkephalin-B (PPE-B, prodynorphin). The increase seen following repeated L-DOPA administration is not observed following repeated treatment with drugs known not to cause dyskinesia in both MPTP-treated primates and patients i.e. bromocriptine or lisuride. Moreover, in chapter 3, it was demonstrated that functional antagonism of two of the receptors for the peptide transmitters derived from these precursors, namely kappa and delta opioid receptors, can reduce L-DOPA-induced hyperkinesia. This has led to the hypothesis that increased opioid peptide neurotransmission in striatal efferents, following repeated dopamine-agonist administration, may be involved in the genesis of dyskinetic symptoms in both MPTP-treated primates and patients. In this chapter, utilising *in situ* hybridisation, the topographical distributions of PPE-A and PPE-B expression within the striatum were investigated. mRNA levels were assessed both with respect to the segregation of function with regards sensorimotor, associative or limbic regions of the striatum and to striosome-matrix compartmentalisation. mRNA levels were assessed in MPTP-treated non-human primates following reversal of parkinsonian symptoms the dopamine-agonist apomorphine. One group of MPTP-treated macaques subsequently developed dopamine agonist-induced dyskinesias while the other did not. As discussed in chapter 4, it is clear that opioid neuropeptides do modulate both the classical neurotransmitters GABA and glutamate within the basal ganglia. Therefore, increased opioid peptide neurotransmission in striatal efferent pathways may modulate classical transmitters and could underlie the symptoms of dopamine agonist-induced dyskinesias following repeated treatment of Parkinson's disease. Analysis of the expression of opioid peptide precursor transcripts with respect to functional segregation and striosome-matrix compartmentalisation, a more comprehensive hypothesis for the involvement of opioid neuropeptides in the striatal efferent pathways may be proposed, in order to generate a greater understanding of the neural mechanisms underlying the genesis of dyskinetic side effects seen following dopamine-replacement therapy of Parkinson's disease.

5.2 Methods

5.2.1 Production of dopamine agonist-induced dyskinesia in the MPTP-treated non-human primate model of Parkinson's disease

Eight (male) rhesus macaques (*macaca mulatta*, mean age 60 ± 1 months) with body weights ranging between 5.1 kg to 12.5 kg (mean, 7.44 ± 0.8 kg) were obtained from Shamrock (UK). The macaques were housed in standard housing conditions with constant temperature ($25 \pm 1^\circ\text{C}$), humidity (relative, 50%) and 12 h light/dark cycles (light period 8 a.m/8 p.m). Macaques were allowed free access to food pellets (Masuri primate diet-E, Scientific Dietary Services, UK) and water. In addition, the macaques received fresh fruit supplements each day. Initially, all macaques were administered 0.03 mg kg^{-1} 1-methyl-4-phenyl-1,2,3,6-tetrahydropyridine (MPTP) hydrochloride (Research Biochemicals International) intravenously under ketamine anaesthesia (Vetalar, Parke Davis). Further incremental doses of MPTP, ranging between 0.3 mg kg^{-1} and 0.967 mg kg^{-1} , were given at approximately weekly intervals (between 2-12 weeks) until the animals were moderate to severely parkinsonian, similar to level III-IV on the Hoehn and Yahr human parkinsonian rating scale (1969). Total accumulated doses of MPTP ranged between 1.37 mg kg^{-1} and 6.87 mg kg^{-1} . On occasion apomorphine ($0.024 - 0.096 \text{ mg kg}^{-1}$, i.m.) was administered to encourage feeding and/or mobility. Following stabilisation of the parkinsonian symptoms all animals were able to feed and groom themselves.

Before any further experimentation was carried out, macaques remained in a stable parkinsonian state for a minimum of one month (mean 8 ± 1 months). The macaque's behaviour was assessed and the animals rated depending on parkinsonian disability (mean 3.2 ± 0.3). The macaques were then assigned into two groups of four, such that no significant difference in either the level or time of parkinsonism was observed (mean level of parkinsonism of non-dyskinetic group 3.3 ± 0.5 , dyskinetic group 3.1 ± 0.2 , not significantly different, $P > 0.5$, Mann-Whitney U-test, mean time of parkinsonism of non-dyskinetic group 29 ± 10 weeks, dyskinetic group 32 ± 5 weeks, not significantly different, $P > 0.05$, unpaired Student's t-test).

Four of the monkeys were selected to receive apomorphine injections to reverse parkinsonian symptoms (dose employed for each animal that produced the optimal therapeutic anti-parkinsonian response, 0.024-0.088 mg kg⁻¹, i.m.) 3 times a day until dyskinesia was observed after each dose (mean number of days of injection 4 ± 1). Apomorphine was chosen in preference to L-DOPA as it has previously been demonstrated that in the MPTP-treated primate apomorphine gives a more reliable anti-parkinsonian, and hence dyskinetic response, following every injection. L-DOPA administration often has dosing, administration, and plasma fluctuations that makes it unreliable in producing consistent dyskinesia in MPTP-treated primates. Following this period the monkeys received 3 injections of apomorphine per day, for 14 days. The remaining four MPTP-treated monkeys received a single dose of apomorphine (0.065-0.096 mg kg⁻¹) to reverse their parkinsonian symptoms on the day of the terminal procedure. All animals were killed by terminal anaesthesia (1 ml Vetalar, i.m., Parke Davis, followed by 10 ml, sodium pentobarbitone, i.v., Sagatal, Rhone-Merieux) 20 minutes post apomorphine injection. All final doses were given before the terminal anaesthesia to coincide with the maximal dyskinetic response previously observed, i.e. 20-25 minutes. At this point, macaques were decapitated and the heads immersed in isopentane at -35°C.

5.2.2 *In situ* hybridisation

5.2.2.1 Section processing

Brains were exposed by careful drilling of the skull no more than 3 days after the terminal procedure. Brains were stored at -70°C for a maximum of 24 weeks before sectioning. Cryostat-cut coronal sections (15 µm thick) were cut using a cryostat (OTF, Bright UK, at -19°C onto RNase-free gelatin/chromalum coated glass slides. Sections were then stored for a maximum of 48 weeks at -70°C until use.

5.2.2.2 Radiolabelling of oligonucleotide probes

Sequences complementary to the sequence coding the human sequence for pre-proenkephalin-A and pre-proenkephalin-B were designed using the UK Human Genome

Mapping Project Resource Centre database (both EMBL and GenBank databases, BLAST search, Altschul *et al.*, 1990) and thus ensure that the selected sequences would not hybridise to any other known sequence. These synthetic oligonucleotide probes (30-45 bases in length) were synthesised by Gibco BRL. The PPE-A oligonucleotide probe was complementary to the sequence coding for bases 191-232 of the human PPE-A gene (Accession number HSENK2 V00510, Noda *et al.* 1982) sequence 5'- CTT CAT GAA GCC TCC ATA CCT TTT CAT GAA GCC CCC ATA CCT -3'. The PPE-B oligonucleotide probe was complementary to the sequence coding for bases 418-462 of the human PPE-B gene (Accession number HSENK B21 K02268, Horikawa *et al.*, 1985) sequence 5'- GCT CCT CTT GGG GTA TTT GCG CAA AAA GCC CCC ATA GAG TTT GAC -3'. Glyceraldehyde 3-phosphate dehydrogenase (G3PDH, Clontech) was used as a control probe in all *in situ* hybridisations. This oligonucleotide probe is complementary to nucleotides 734-763 of the G3PDH gene, sequence 5'- CAC GGA AGG CCA TGC CAG TGA GCT TCC CGT -3' (Arcari *et al.*, 1984). All probes were 3'-end labelled with ³⁵S-dATP as described in 4.2.1.3.

5.2.2.3 *In situ* hybridisation

In situ hybridisation was carried out as described in section 4.2.1.4. Hybridisation buffer consisted of 50% formamide, 4 x SSC, 10% dextran sulphate, 5 x Denhardt's solution, 25mM denatured salmon sperm, 100 ml polyadenylic acid, 25 mM sodium phosphate, pH 7.0, and 1 mM sodium pyrophosphate. All probes were hybridised at 42°C and washed as described in 4.2.1.4. Sections were exposed to β-max Hyperfilm (Amersham) for various times depending on activity (14 days for PPE-A and G3PDH and 56 days for PPE-B, all at 4°C). An autoradiographic ¹⁴C micro-scale (Amersham) of known radioactivity (range 31-833 nCi g⁻¹) was also placed in each cassette. The film was developed as described in 4.2.1.4.

5.2.2.4 RNase pre-treatment

After fixation in paraformaldehyde and incubation in acetic anhydride (see 4.2.1.5) tissue sections were washed in RNase A solution (ribonuclease A (Sigma) 10 µg ml⁻¹) at 37°C for 30 minutes prior to hybridisation. The sections were then processed

for *in situ* hybridisation as normal i.e. hybridised with the experimental probes. Pre-treatment with RNase A solution should degrade all mRNA in the section and therefore following *in situ* hybridisation no signal (probe binding) should occur.

5.2.3 Acetylcholinesterase histochemistry

To determine the striosome-matrix compartmentalisation within the primate neostriatum, acetylcholinesterase histochemistry was performed. The method was modified from Graybiel and Ragsdale (1979). Sections adjacent to those used for *in situ* hybridisation were removed from the -70°C freezer and allowed to air dry at room temperature for one hour. Sections were then placed in the incubation medium consisting of the substrate solution (34.6 mM acetylthiocholine iodide (Sigma), 0.1 M hydrous copper sulphate (Sigma) in distilled water, this was then filtered (to remove the precipitate)), 16.5 mM glycine (Sigma) and 1 M hydrous sodium acetate (Sigma) in distilled water, pH 5.5. Sections were incubated in the incubation medium for 2 hours at room temperature. Following the two hour incubation period, sections were removed from the incubation medium and rinsed in distilled water for 1 minute. Post rinse, the sections were placed in 1% ammonium polysulfide solution for 1 minute, until a brown precipitate was observed. The sections were then removed from this solution and rinsed in distilled water for 1 minute, then allowed to air dry for 1 hour. The sections were then mounted in 'Practamount' a xylene-based mount, and allowed to dry.

5.2.4 Calbindin immunocytochemistry

A second complementary technique, calbindin immunocytochemistry, was employed to determine the striosome-matrix compartmentalisation within the primate neostriatum. Calbindin immunocytochemistry was performed on sections adjacent to the sections used for *in situ* hybridisation. Cryostat cut sections were removed from the -70°C freezer and brought up to room temperature over a period of 30 minutes. After ringing the sections with a water retentive pen (Dako) they were placed horizontally at 4°C and flooded with fixative (4% paraformaldehyde (Sigma) and 0.05% glutaraldehyde (Sigma) in 0.1 M sodium phosphate buffer (Sigma) containing 0.2% picric acid (Sigma), pH 7.4). The sections were held in this solution for 30 minutes at

4°C. Sections were washed in phosphate buffered saline over a 2 hour period to remove the picric acid and then placed in tris buffered saline, pH 7.4. Sections were incubated at room temperature unless otherwise stated. Sections were incubated in tris buffered saline with: 10% normal goat serum for 2 hours; mouse anti-calbindin antibody 1:200 (Sigma Chemicals) containing 2% normal goat serum, overnight at 4°C; normal goat serum for 1 hour at room temperature; goat anti-mouse Fab fragment, biotinylated 1:200 (Sigma) in tris buffered saline containing 2% normal goat serum for 2 hours; Vectastain ABC avidin-horseradish peroxidase kit, (Vector Laboratories) in tris buffered saline containing 2% normal goat serum for 1 hour 30 minutes. Signal development was conducted using diaminobenzidine and osmium tetroxide (Sigma). The sections were washed in 0.08M tris-buffer pH 7.4 and developed in 0.5 mg ml⁻¹ diaminobenzidine and 0.0002% hydrogen peroxide in tris buffer for 10 minutes. The sections were then washed in tris buffer, tris buffered saline and phosphate buffered saline prior to incubation overnight at 4°C in 0.005% osmium tetroxide in phosphate buffered saline. The sections were then washed and mounted in a glycerol based mountant.

5.2.5 Analysis of *in situ* hybridisation signal

Densitometric analysis of the PPE-A, PPE-B and G3PDH autoradiographs was performed using a Seescan Image Analysis system (Seescan Inc.). Average optical density measurements were made from both rostral and caudal levels for both PPE-A and PPE-B oligonucleotide probe hybridisations. Rostral and caudal levels of the striatum were divided into sensorimotor, associative and limbic regions as previously described (section 1.1.7, Parent *et al.*, 1996, Figures 5.1 and 5.2).

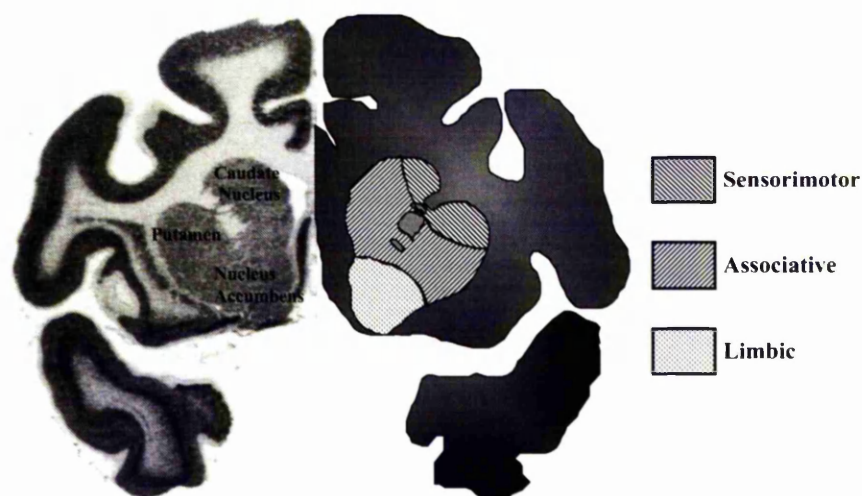


Figure 5.1 Diagrammatic representation of sensorimotor, associative and limbic regions in the rostral neostriatum of the macaque (*Macaca mulatta*)

Left hemisphere shows in situ hybridisation utilising an oligonucleotide probe targeted against G3PDH mRNA transcripts. Caudate nucleus, putamen and nucleus accumbens are shown. Right hemisphere shows a diagrammatic representation illustrating sensorimotor, associative or limbic functional segregation within the neostriatum of the macaque (Macaca mulatta).

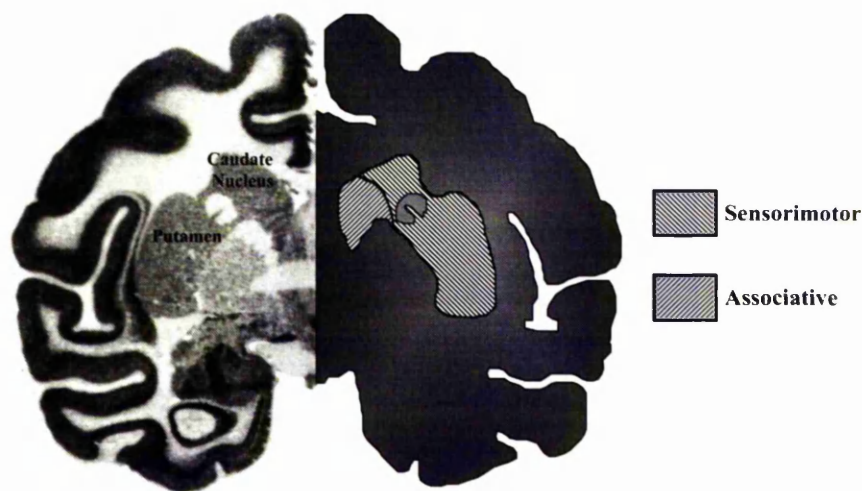


Figure 5.1 Diagrammatic representation of sensorimotor and associative regions in the caudal neostriatum of the macaque (*Macaca mulatta*)

Left hemisphere shows *in situ* hybridisation utilising an oligonucleotide probe targeted against G3PDH mRNA transcripts. Caudate nucleus and putamen are shown. Right hemisphere shows a diagrammatic representation illustrating sensorimotor and associative functional segregation within the neostriatum of the macaque (*Macaca mulatta*).

Levels of G3PDH control probe were also measured from rostral and caudal areas of the whole neostriatum. The mean value of PPE-A or PPE-B *in situ* hybridisation in each animal was divided by the G3PDH at that level for each animal to correct for any non-specific changes in transcription rate that may have occurred. Changes in transcription rate may be a consequence of non-specific RNase activity within the sections and temporal variations in preparation of the sections, both due to *post-mortem* delay and cryostat cutting, mounting and re-freezing. This ratio gives a semi-quantitative analysis of PPE-A and PPE-B expression levels in the neostriatum.

Utilising acetylcholinesterase histochemistry a template of striosome-matrix compartmentalisation was generated. This template of striosome-matrix compartmentalisation was applied to adjacent *in situ* hybridisation sections for both PPE-A and PPE-B expression. Average optical density readings for striosome and an area of identical size adjacent to the striosome area but within the matrix was measured.

5.2.6 Statistical analysis

Data are expressed as mean \pm SEM values. Parkinsonian rating scale for the dyskinetic and non-dyskinetic groups was analysed by non-parametric Mann-Whitney U-test. The length of time the macaques were parkinsonian was analysed by unpaired Student's t-test. Average optical density readings of *in situ* hybridisation signal were analysed between dyskinetic and non-dyskinetic MPTP-treated macaques by unpaired Student's t-test. In all tests significance was assigned when $P < 0.05$.

5.3 Results

5.3.1 Production of dopamine agonist-induced dyskinesia in the MPTP-treated non-human primate model of Parkinson's disease

Following MPTP-administration all eight rhesus macaques displayed marked motor deficits, indicative of a parkinsonian syndrome. Following stabilisation of the parkinsonian symptoms the macaques were split into two groups on the basis of their level of parkinsonism, such that there was no significant difference between the level of parkinsonism in each group ($P > 0.05$). One of the groups received doses of apomorphine capable of reversing the parkinsonian symptoms. Following repeated administration of this reversing dose of apomorphine all animals developed signs of 'peak-dose' dyskinesia. Three animals developed chorea (see section 1.4) of both the legs and arms, with one of the animals developing orofacial dyskinesia with tongue protrusions and increased vocalisations. The remaining macaque in the dyskinetic group developed severe dystonia of both the arms and legs (see section 1.4). This dystonia began in one leg, and later spread to encompass both legs and one arm. Following the first signs of dyskinesia all animals received three reversing doses of apomorphine per day for a further 14 days. The dyskinetic group of macaques were killed 20 minutes following the final apomorphine injection. The non-dyskinetic group of macaques received a dose of apomorphine known to reverse the parkinsonian symptoms and were killed 20 minutes post-injection. These animals showed no signs of dyskinesia before the terminal procedure.

Methodological considerations

Following *in situ* hybridisation utilising an oligonucleotide probe designed to target the mRNA transcript encoding the enkephalin precursor, pre-proenkephalin-A (PPE-A), a specific hybridisation signal restricted to the neostriatum (moderate to high) was observed (Figure 5.3.1.1, A). RNase pre-treatment prior to *in situ* hybridisation results in no hybridisation signal for PPE-A (Figure 5.3.1.1, B). Similarly, following *in situ* hybridisation utilising an oligonucleotide probe designed to target the mRNA transcript encoding the dynorphin precursor, pre-proenkephalin-B (PPE-B), a specific

hybridisation signal restricted to the neostriatum and a single layer around the cerebral cortex (moderate to low) was observed (Figure 5.3.1.2, A). RNase pre-treatment prior to *in situ* hybridisation results in virtually no hybridisation signal for PPE-B (Figure, 5.3.1.2, B).

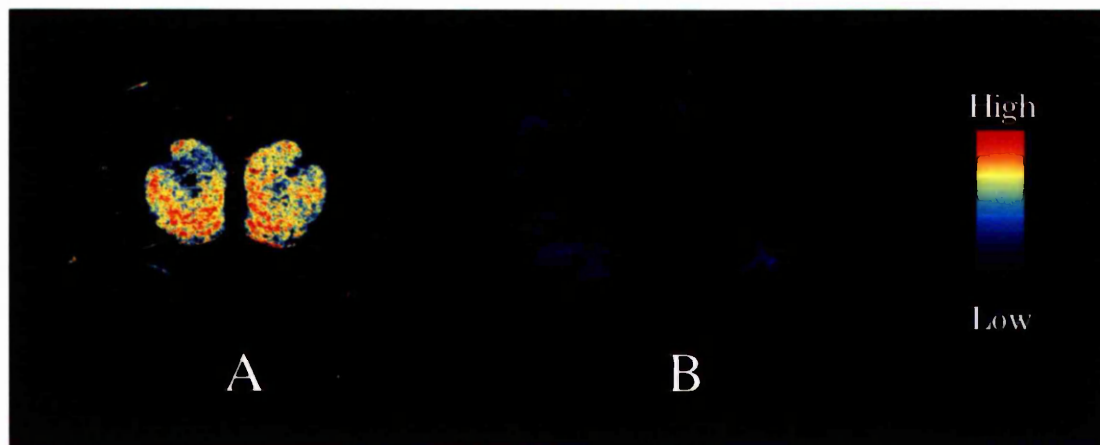


Figure 5.3.1.1 Effect of RNase pre-treatment on PPE-A hybridisation signal

Pseudocolour transformations of autoradiographs of in situ hybridisation utilising an oligonucleotide probe targeted against pre-proenkephalin-A (PPE-A) in striatal sections from the non-human primate (macaca mulatta) (A). Following RNase pre-treatment no hybridisation signal was observed (B).

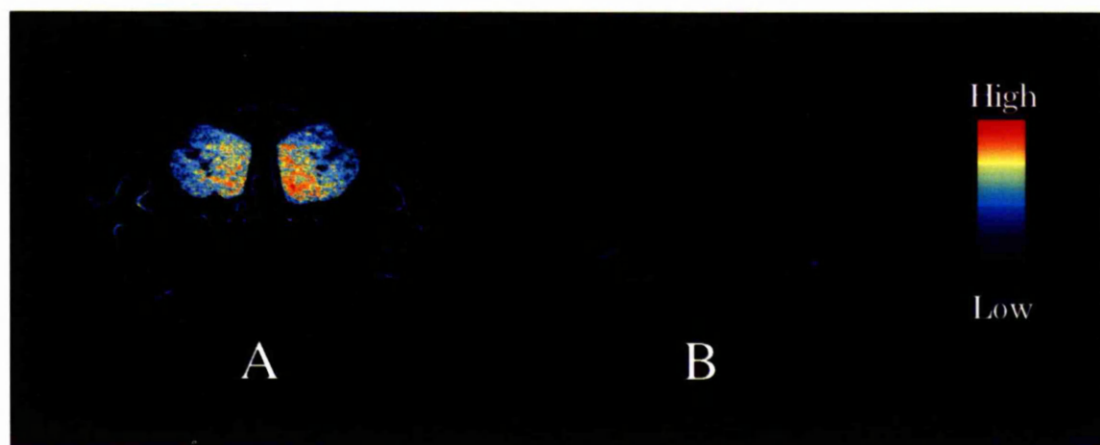


Figure 5.3.1.2 Effect of RNase pre-treatment on PPE-B hybridisation signal

Pseudocolour transformations of autoradiographs of in situ hybridisation utilising an oligonucleotide probe targeted against pre-proenkephalin-B (PPE-B) in striatal sections from the non-human primate (macaca mulatta) (A). Following RNase pre-treatment no hybridisation signal was observed (B).

5.3.2 Topographical distribution of pre-proenkephalin-A (PPE-A) in the MPTP-treated non-human primate model of dopamine-induced dyskinesia

In the non-human primate model of dopamine-induced dyskinesia, following analysis of sensorimotor, associative or limbic regions of the rostral neostriatum, PPE-A expression was significantly increased in sensorimotor (24%, $P < 0.05$) and associative regions (30%, $P < 0.05$), with a non-significant rise in the limbic nucleus accumbens (27%, Figures 5.3.2.1, 5.3.2.2), when compared to the non-dyskinetic MPTP-treated macaques following dopamine agonist-induced reversal of parkinsonian symptoms.

In the rostral neostriatum, both calbindin immunocytochemistry and acetylcholinesterase staining demonstrated striosome-matrix compartmentalisation, with pale non-staining striosome areas clearly visible within the positively-staining matrix region (Figure 5.3.2.3 B, C). PPE-A hybridisation signal showed a homogeneous distribution throughout the neostriatum (Figure 5.3.2.3, D). When analysed with respect to the striosome-matrix compartmentalisation, PPE-A expression showed no significant segregation between compartments (Figure 5.3.2.3, D). Following analysis with respect to striosome-matrix compartmentalisation, mean PPE-A expression was increased in the dyskinetic macaques when compared to the non-dyskinetic in both the striosome and matrix compartments of the neostriatum (60% and 84%, respectively). However, this increase was not significant (Figure 5.3.2.4).

In the caudal neostriatum, non-significant increases in mean PPE-A expression was observed in the sensorimotor and associative regions (20% and 24% respectively, figures 5.3.2.5, 5.3.2.6). Again, a homogeneous distribution of PPE-A mRNA expression was seen with respect to striosome-matrix compartmentalisation (Figures 5.3.2.5, 5.3.2.7), with no significant difference between the striosome or matrix compartments of the non-dyskinetic or dyskinetic primates being observed (Figure 5.3.2.8).

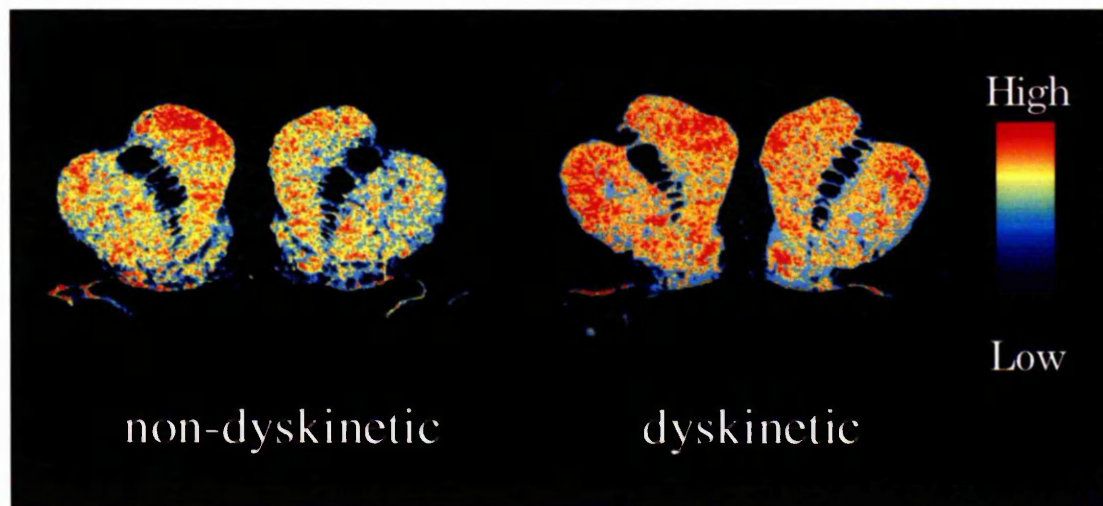


Figure 5.3.2.1 PPE-A hybridisation signal in the rostral neostriatum from non-dyskinetic or dyskinetic MPTP-treated macaques following apomorphine alleviation of parkinsonian symptoms

Pseudocolour transformations of autoradiographs of in situ hybridisation utilising an oligonucleotide probe targeted against pre-proenkephalin-A (PPE-A) in the rostral neostriatum from the MPTP-treated non-human primate, following either reversal of parkinsonian symptoms (non-dyskinetic) or displaying dopamine agonist-induced dyskinesias (dyskinetic).

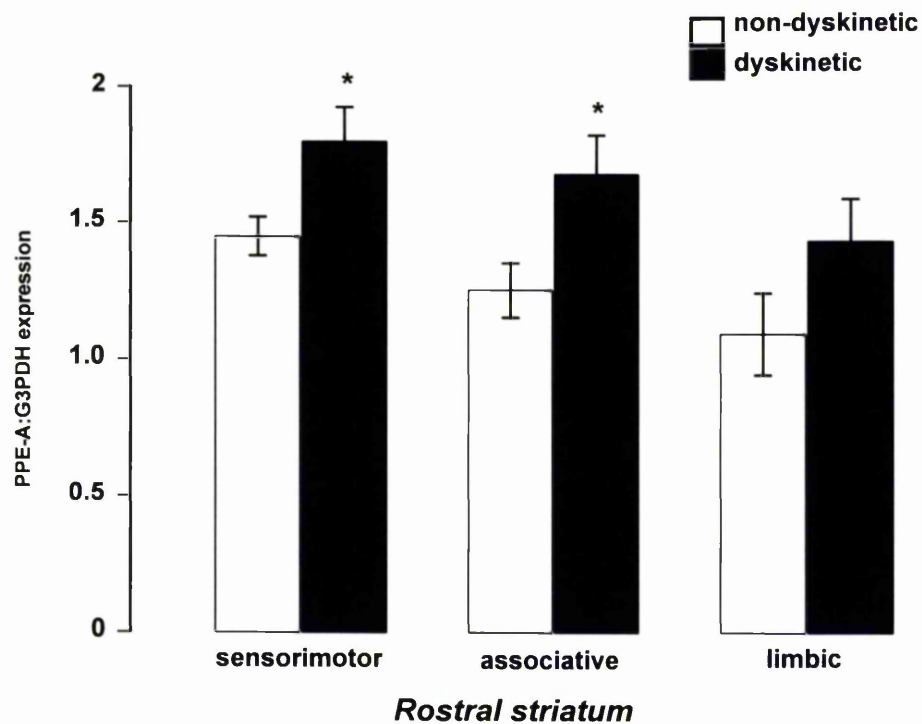


Figure 5.3.2.2 Graph showing the ratio of PPE-A:G3PDH expression in the sensorimotor, associative or limbic areas of the rostral neostriatum from non-dyskinetic or dyskinetic MPTP-treated macaques following apomorphine alleviation of parkinsonian symptoms

*Graph showing the ratio of PPE-A:G3PDH expression following in situ hybridisation utilising an oligonucleotide probe targeted against pre-proenkephalin-A (PPE-A) in the sensorimotor, associative or limbic areas in rostral neostriatum from the MPTP-treated non-human primate following either reversal of parkinsonian symptoms (non-dyskinetic, □) or displaying dopamine agonist-induced dyskinesia (dyskinetic, ■). Data are expressed as mean (\pm SEM) optical density ratios ($n = 4$, * $P < 0.05$ cf non-dyskinetic, unpaired Student's t -test).*

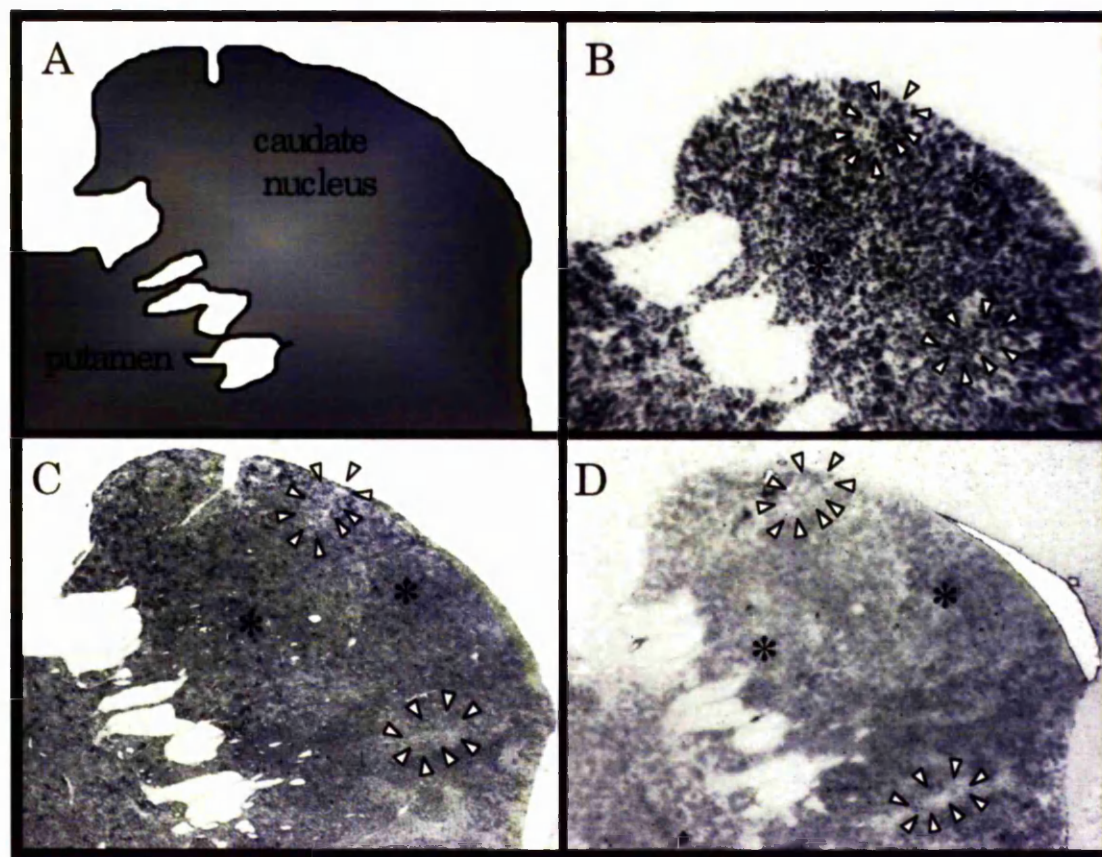


Figure 5.3.2.3 Illustration demonstrating striosome-matrix compartmentalisation in the rostral neostriatum with respect to PPE-A expression in the dyskinetic MPTP-treated non-human primate

PPE-A expression in the dyskinetic MPTP-treated non-human primate with respect to striosome-matrix compartmentalisation. Diagrammatic representation of the rostral caudate nucleus and putamen (A). In situ hybridisation utilising an oligonucleotide probe targeted against pre-proenkephalin-A (PPE-A) in the MPTP-treated non-human primate displaying dopamine agonist-induced dyskinesias (B). Striosome(>)-matrix() compartments demonstrated by acetylcholinesterase histochemistry (C). Striosome(>)-matrix(*) compartmentalisation demonstrated by calbindin immunocytochemistry (D). PPE-A mRNA expression displays a homogenous distribution with no segregation with regards striosome(>)-matrix(*) boundaries.*

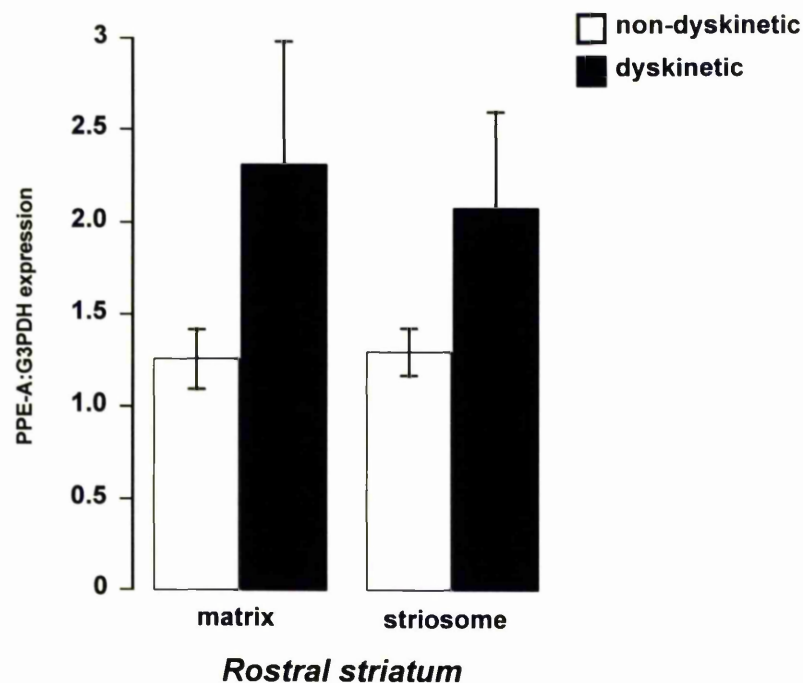


Figure 5.3.2.4 Graph showing the ratio of PPE-A:G3PDH expression in the striosome-matrix compartments in the rostral neostriatum of non-dyskinetic or dyskinetic MPTP-treated non-human primates

Graph showing the ratio of PPE-A:G3PDH expression following in situ hybridisation utilising an oligonucleotide probe targeted against pre-proenkephalin-A (PPE-A) in striosome-matrix compartments, as defined by acetylcholinesterase histochemistry, in the rostral neostriatum of the MPTP-treated non-human primate, following either reversal of parkinsonian symptoms (□) or displaying dopamine agonist-induced dyskinesias (■). Data are expressed as mean (± SEM) optical density ratios ($n = 4$, ns, $P > 0.05$ cf non-dyskinetic, unpaired Student's t -test).

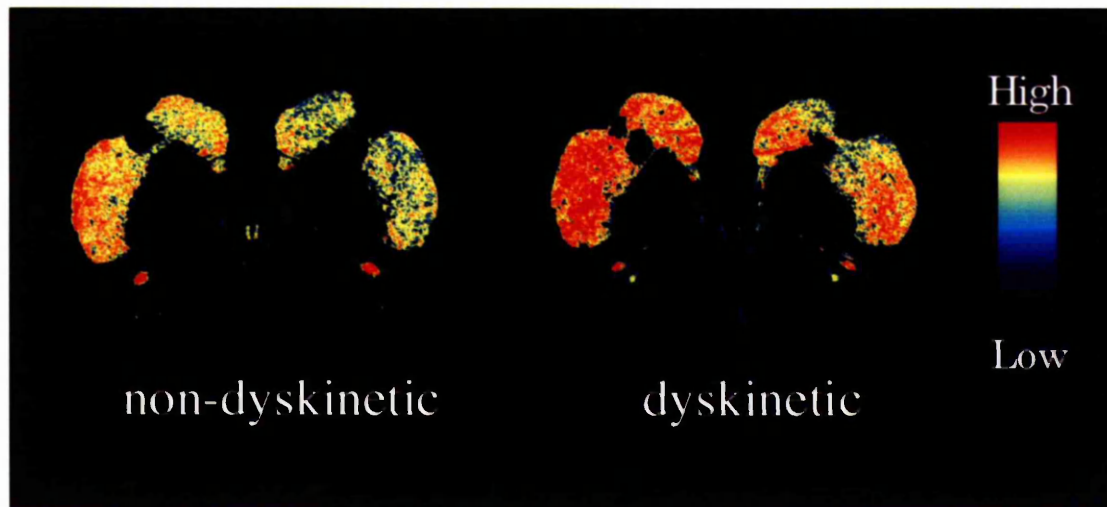


Figure 5.3.2.5 PPE-A hybridisation signal in the caudal neostriatum from non-dyskinetic or dyskinetic MPTP-treated macaques following apomorphine alleviation of parkinsonian symptoms

Pseudocolour transformations of autoradiographs of in situ hybridisation utilising an oligonucleotide probe targeted against pre-proenkephalin-A (PPE-A) in the caudal neostriatum from the MPTP-treated non-human primate, following either reversal of parkinsonian symptoms (non-dyskinetic) or displaying dopamine agonist-induced dyskinesias (dyskinetic).

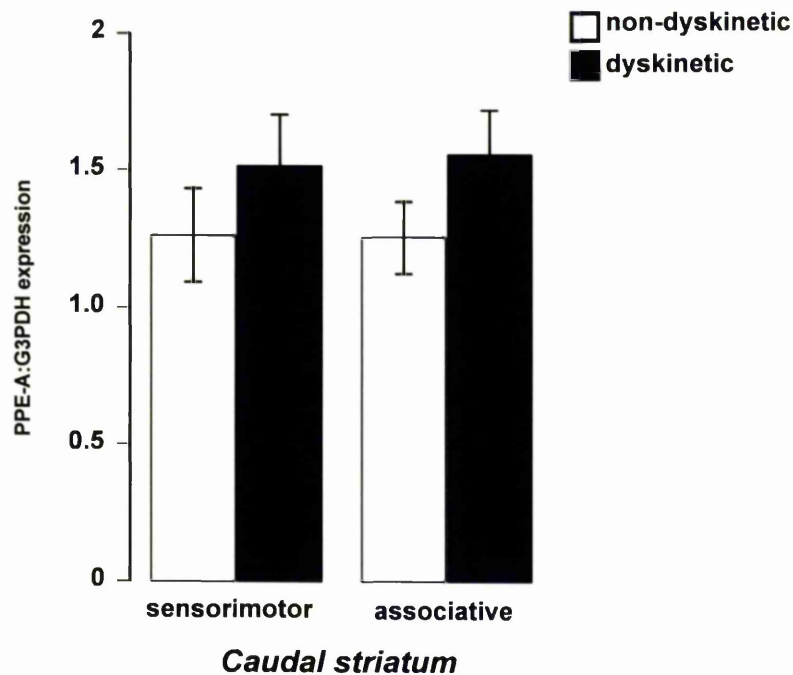


Figure 5.3.2.6 Graph showing the ratio of PPE-A:G3PDH expression in the sensorimotor or associative areas of the caudal neostriatum from non-dyskinetic or dyskinetic MPTP-treated macaques following apomorphine alleviation of parkinsonian symptoms

Graph showing the ratio of PPE-A:G3PDH expression following in situ hybridisation utilising an oligonucleotide probe targeted against pre-proenkephalin-A (PPE-A) in the sensorimotor or associative areas in caudal neostriatum from the MPTP-treated non-human primate, following either reversal of parkinsonian symptoms (non-dyskinetic, □) or displaying dopamine agonist-induced dyskinesias (dyskinetic, ■). Data are expressed as mean (\pm SEM) optical density ratios ($n = 4$, ns, $P > 0.05$ cf non-dyskinetic, unpaired Student's t -test).

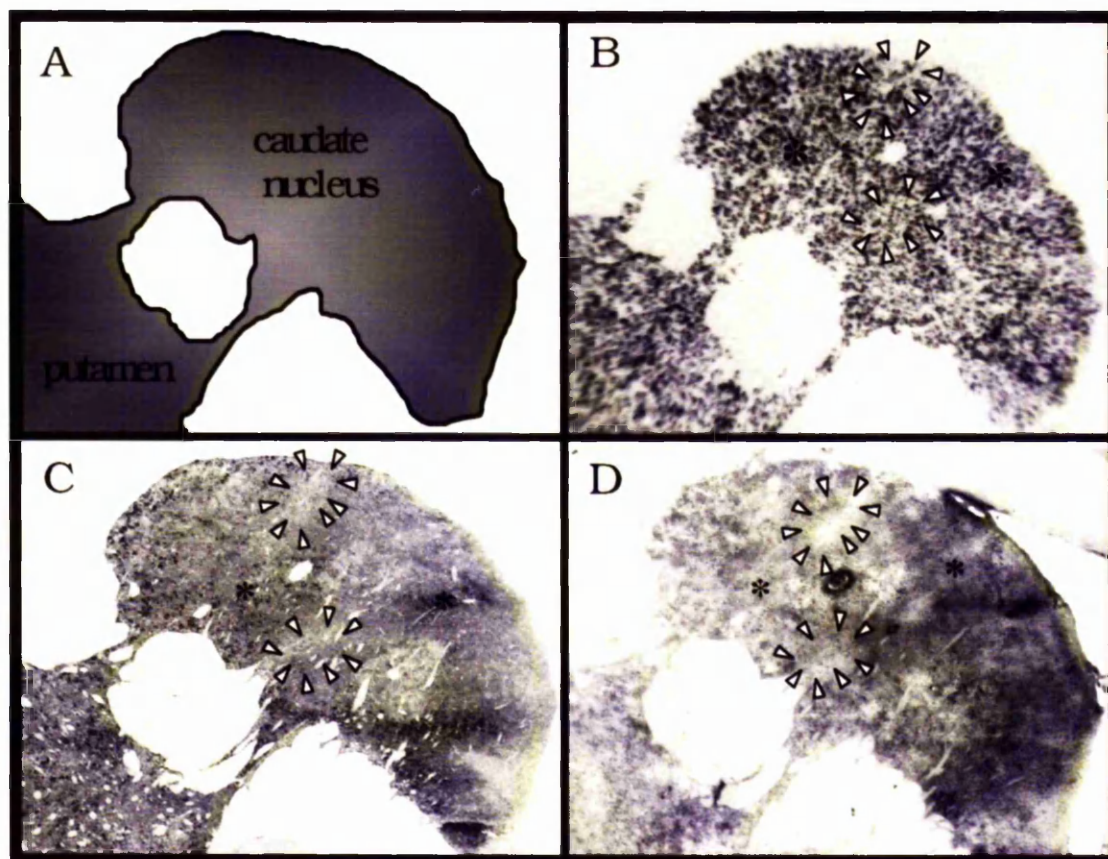


Figure 5.3.2.7 Illustration demonstrating striosome-matrix compartmentalisation in the caudal caudate nucleus with respect to PPE-A expression in the dyskinetic MPTP-treated non-human primate

PPE-A expression in the dyskinetic MPTP-treated non-human primate with respect to striosome-matrix compartmentalisation. Diagrammatic representation of the caudal caudate nucleus and putamen (A). In situ hybridisation utilising an oligonucleotide probe targeted against pre-proenkephalin-A (PPE-A) in the MPTP-treated non-human primate displaying dopamine agonist-induced dyskinesias (B). Striosome(▷)-matrix() compartments demonstrated by acetylcholinesterase histochemistry (C). Striosome(▷)-matrix(*) compartmentalisation demonstrated by calbindin immunocytochemistry (D). PPE-A mRNA expression displays a homogenous distribution with no segregation with regards striosome(▷)-matrix(*) boundaries.*

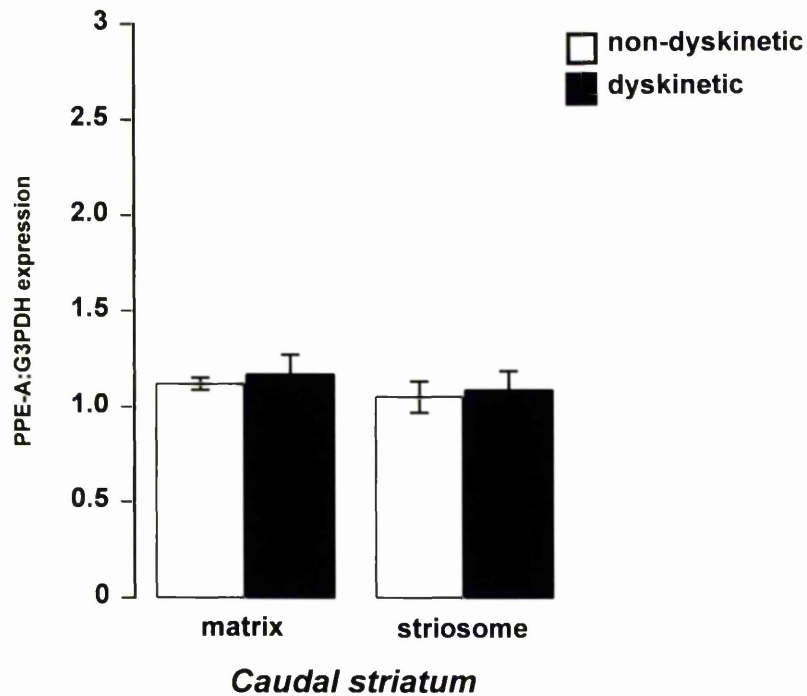


Figure 5.3.2.8 Graph showing the ratio of PPE-A:G3PDH expression in the striosome-matrix compartments of the caudal neostriatum from non-dyskinetic or dyskinetic MPTP-treated macaques following apomorphine alleviation of parkinsonian symptoms

Graph showing the ratio of PPE-A:G3PDH expression following in situ hybridisation utilising an oligonucleotide probe targeted against pre-proenkephalin-A (PPE-A) in striosome-matrix compartments as defined by acetylcholinesterase histochemistry in the caudal caudate nucleus of the MPTP-treated non-human primate, following either reversal of parkinsonian symptoms (non-dyskinetic, □) or displaying dopamine agonist-induced dyskinesias (dyskinetic, ■). Data are expressed as mean (\pm SEM) optical density ratios ($n = 4$, ns, $P > 0.05$ cf non-dyskinetic, unpaired Student's t -test).

5.3.4 Topographical distribution of pre-proenkephalin-B (PPE-B) in the MPTP-treated non-human primate model of dopamine-induced dyskinesia

In the non-human primate model of dopamine-induced dyskinesia, following analysis with respect to sensorimotor, associative or limbic regions of the rostral neostriatum, non-significant increases were seen in sensorimotor and associative regions (35% and 14%, respectively), with little alteration in the limbic nucleus accumbens (< 2% increase, figures, 5.3.3.1, 5.3.3.2).

PPE-B hybridisation signal showed a heterogeneous or 'patchy' distribution throughout the neostriatum (Figure 5.3.3.4, D). When observed with respect to striosome-matrix compartments, highest levels of PPE-B expression were observed to correspond to striosome compartments, with no high 'patches' of PPE-B expression seen in the matrix regions (Figure 5.3.3.4, D). Following analysis with respect to striosome-matrix compartments, a significant increase was seen in PPE-B mRNA expression in both the striosome and matrix compartments in the dyskinetic group compared with the non-dyskinetic group (matrix, 49%, $P < 0.05$, compared to non-dyskinetic, striosomes 69%, $P < 0.05$, compared to non-dyskinetic, figures 5.3.3.4, 5.3.3.5).

In the caudal neostriatum no-significant increases in PPE-B expression were seen in the sensorimotor and associative regions of the caudal neostriatum (Figure 5.3.2.7). Again, a heterogeneous or 'patchy' distribution was seen, with areas of high PPE-B mRNA expression restricted to the striosomes (Figure 5.3.3.9). When analysed with respect to striosome-matrix compartmentalisation PPE-B expression was non-significantly increased in both the striosomes and matrix compartments of the dyskinetic group when compared to the non-dyskinetic group (85% and 62% respectively, figure 5.3.3.10).

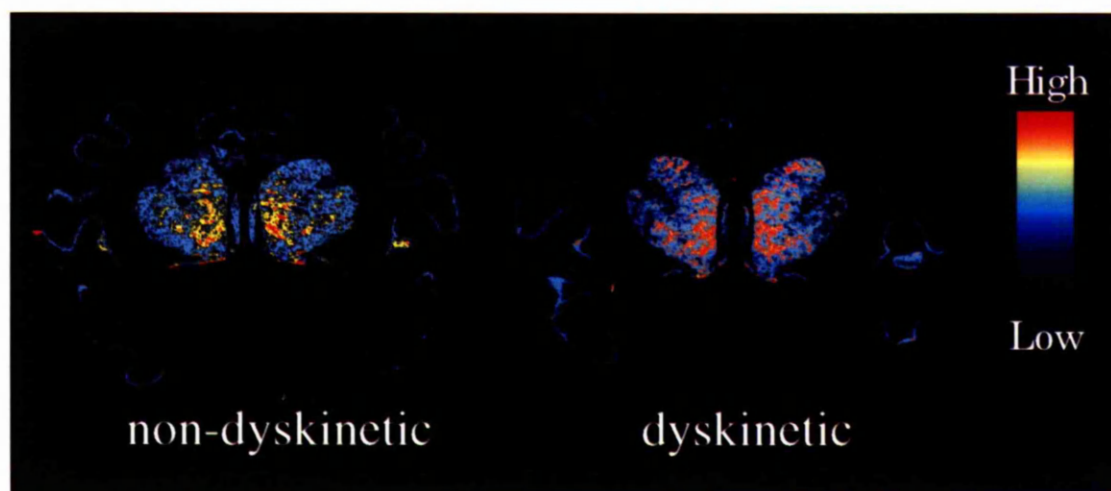


Figure 5.3.3.1 PPE-B hybridisation signal in the rostral neostriatum from non-dyskinetic or dyskinetic MPTP-treated macaques following apomorphine alleviation of parkinsonian symptoms

Pseudocolour transformations of autoradiographs of in situ hybridisation utilising an oligonucleotide probe targeted against pre-proenkephalin-B (PPE-B) in the rostral neostriatum from MPTP-treated non-human primate, following either reversal of parkinsonian symptoms (non-dyskinetic) or displaying dopamine agonist-induced dyskinesias (dyskinetic).

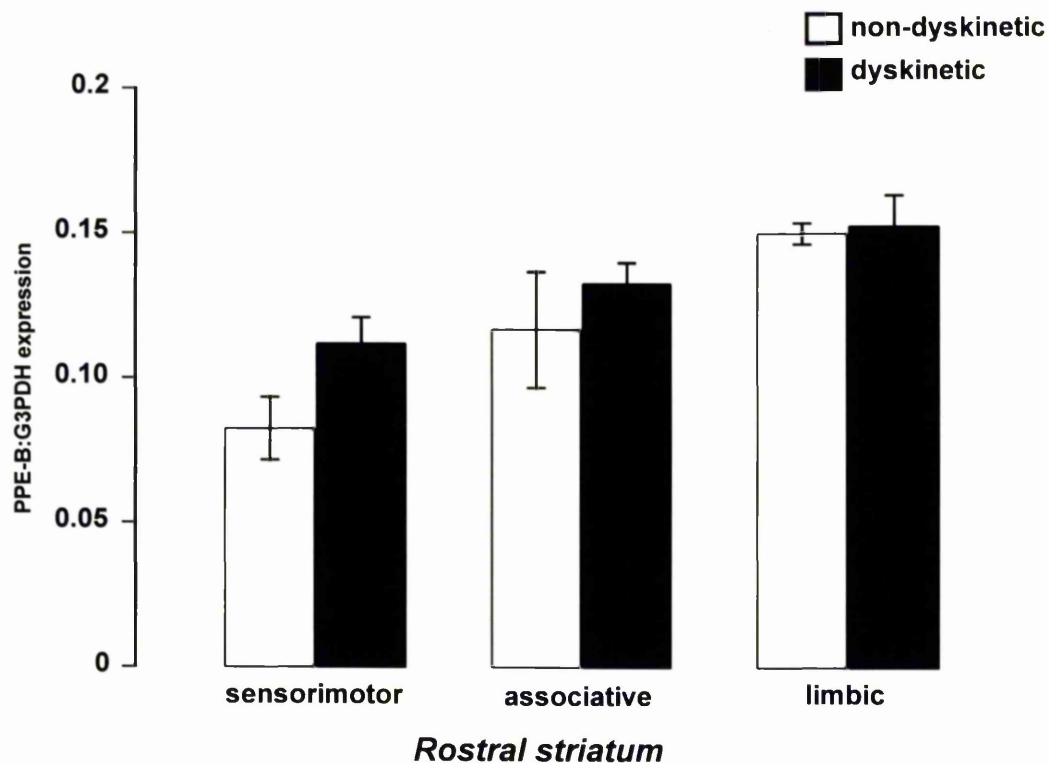


Figure 5.3.3.2 Graph showing the ratio of PPE-B:G3PDH expression in the sensorimotor, associative or limbic areas of the rostral neostriatum from non-dyskinetic or dyskinetic MPTP-treated macaques following apomorphine alleviation of parkinsonian symptoms

Graph showing the ratio of PPE-B:G3PDH expression following in situ hybridisation utilising an oligonucleotide probe targeted against pre-proenkephalin-B (PPE-B) in the sensorimotor, associative or limbic areas in rostral neostriatum from the MPTP-treated non-human primate, following either reversal of parkinsonian symptoms (non-dyskinetic, □) or displaying dopamine agonist-induced dyskinesias (dyskinetic, ■). Data are expressed as mean (\pm SEM) optical density ratios ($n = 4$, ns, $P > 0.05$ cf non dyskinetic, unpaired Student's t -test).

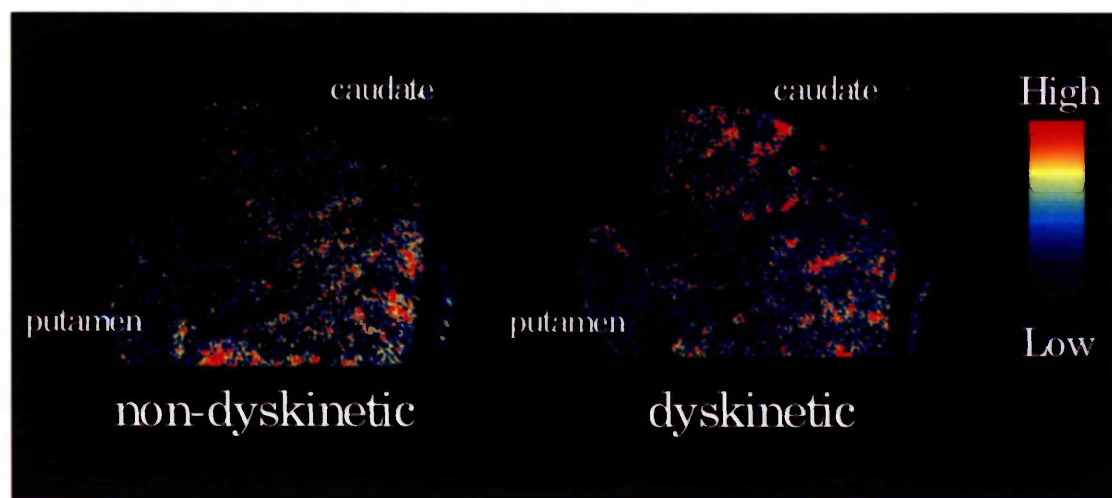


Figure 5.3.3.3 Enlargement of striatal section from figure 5.3.3.1 showing heterogeneous distribution of PPE-B hybridisation signal in the rostral neostriatum from non-dyskinetic or dyskinetic MPTP-treated macaques following apomorphine alleviation of parkinsonian symptoms

Pseudocolour transformations of autoradiographs of in situ hybridisation utilising an oligonucleotide probe targeted against pre-proenkephalin-B (PPE-B) in the rostral neostriatum from the MPTP-treated non-human primate, following either reversal of parkinsonian symptoms (non-dyskinetic) or displaying dopamine agonist-induced dyskinesias (dyskinetic). At higher magnification it can be seen that the signal is distributed in a 'patchy' heterogeneous manner.

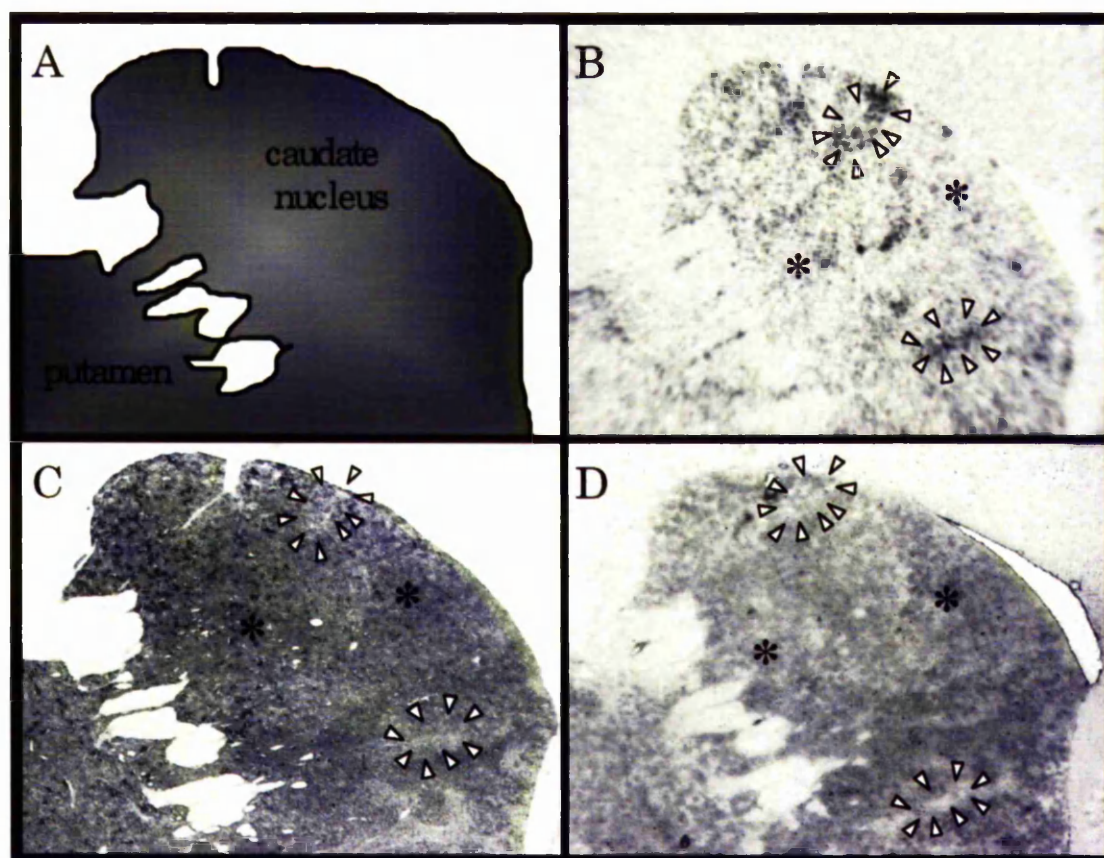


Figure 5.3.3.4 Illustration demonstrating striosome-matrix compartmentalisation in the rostral neostriatum with respect to PPE-B expression in the dyskinetic MPTP-treated non-human primate

PPE-B expression in the dyskinetic MPTP-treated non-human primate with respect to striosome-matrix compartmentalisation. Diagrammatic representation of the rostral caudate nucleus and putamen (A). In situ hybridisation utilising an oligonucleotide probe targeted against pre-proenkephalin-B (PPE-B) in the MPTP-treated non-human primate displaying dopamine agonist-induced dyskinesias (B). Striosome(>)-matrix() compartments demonstrated by acetylcholinesterase histochemistry (C). Striosome(>)-matrix(*) compartmentalisation demonstrated by calbindin immunocytochemistry (D). PPE-B mRNA expression displays a heterogeneous distribution with higher expression within the striosomal boundaries (>).*

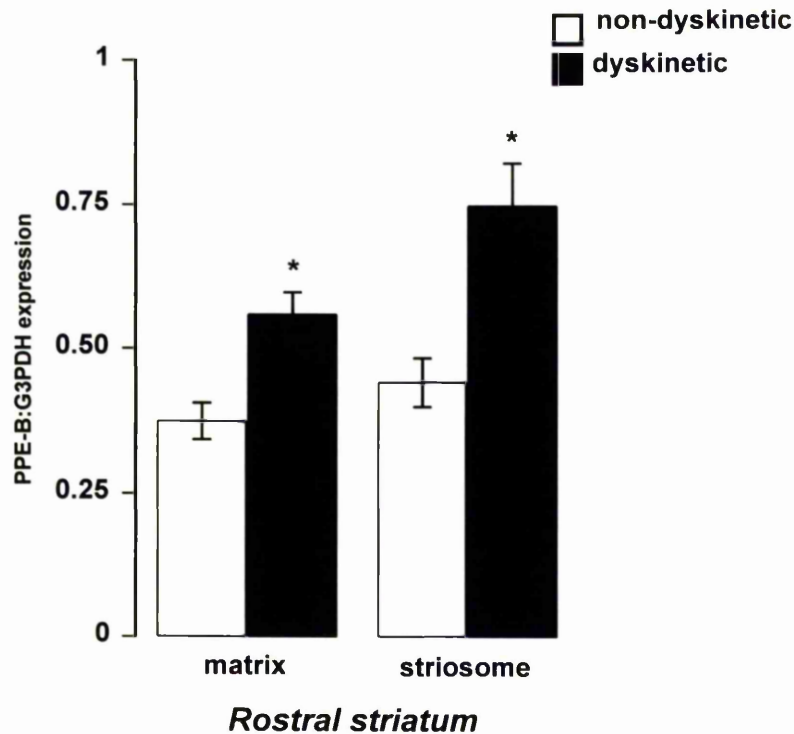


Figure 5.3.3.5 Graph showing the ratio of PPE-B:G3PDH expression in the striosome-matrix compartments in the rostral neostriatum from non-dyskinetic or dyskinetic MPTP-treated macaques following apomorphine alleviation of parkinsonian symptoms

*Graph showing the ratio of PPE-B:G3PDH expression following in situ hybridisation utilising an oligonucleotide probe targeted against pre-proenkephalin-B (PPE-B) in 'striosome - matrix' compartments, as defined by acetylcholinesterase histochemistry, in the rostral caudate nucleus from the MPTP-treated non-human primate, following either reversal of parkinsonian symptoms (non-dyskinetic, □) or displaying dopamine agonist-induced dyskinesias (dyskinetic, ■). Data are expressed as mean (\pm SEM) optical density ratios ($n = 4$, * $P < 0.05$ cf non-dyskinetic, unpaired Student's t -test).*

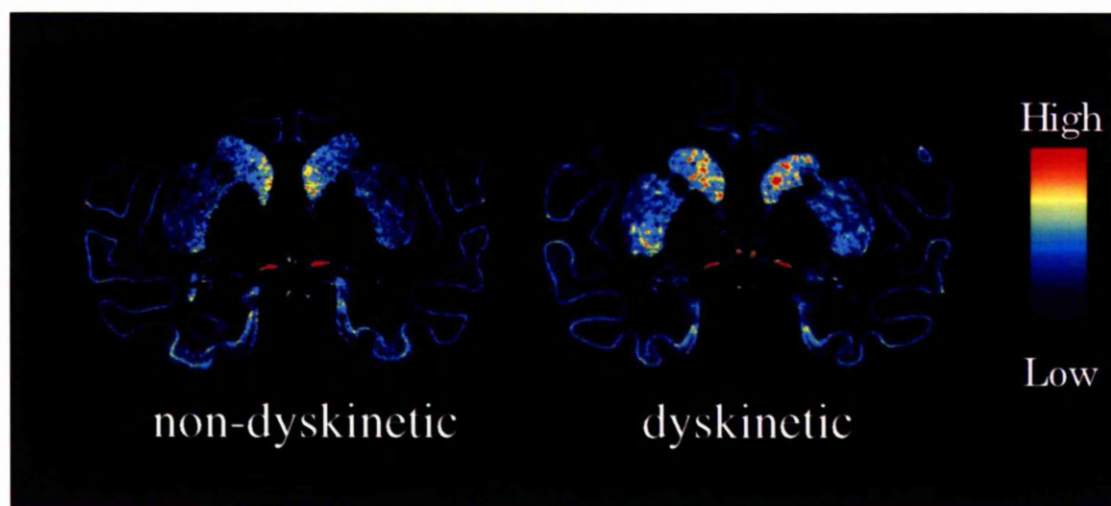


Figure 5.3.3.6 PPE-B hybridisation signal in the caudal neostriatum from non-dyskinetic or dyskinetic MPTP-treated macaques following apomorphine alleviation of parkinsonian symptoms

Pseudocolour transformations of autoradiographs of in situ hybridisation utilising an oligonucleotide probe targeted against pre-proenkephalin-B (PPE-B) in the caudal neostriatum from MPTP-treated non-human primate, following either reversal of parkinsonian symptoms (non-dyskinetic) or displaying dopamine agonist-induced dyskinesias (dyskinetic).

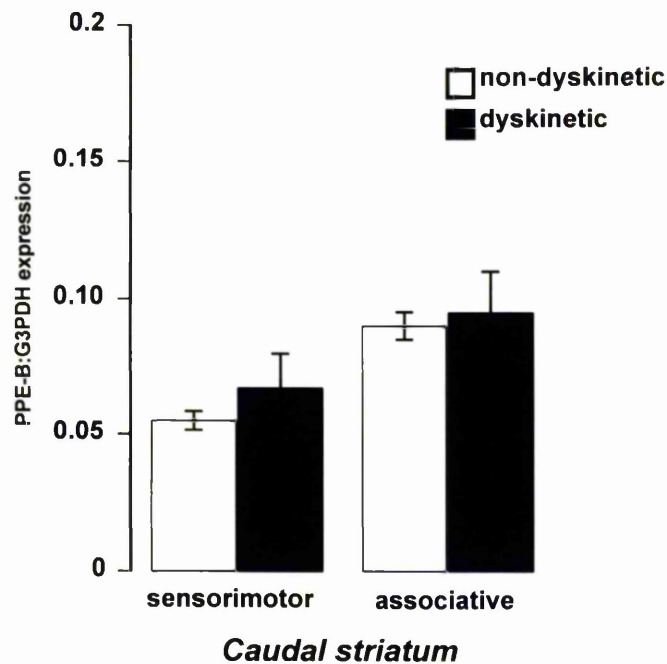


Figure 5.3.3.7 Graph showing the ratio of PPE-B:G3PDH expression in the sensorimotor or associative areas of the caudal neostriatum from non-dyskinetic or dyskinetic MPTP-treated macaques following apomorphine alleviation of parkinsonian symptoms

Graph showing the ratio of PPE-B:G3PDH expression following *in situ* hybridisation utilising an oligonucleotide probe targeted against pre-proenkephalin-B (PPE-B) in the sensorimotor or associative areas in caudal neostriatum from the MPTP-treated non-human primate, following either reversal of parkinsonian symptoms (non-dyskinetic, □) or displaying dopamine agonist-induced dyskinesias (dyskinetic, ■). Data are expressed as mean (\pm SEM) optical density ratios ($n = 4$, ns, $P > 0.05$, unpaired Student's *t*-test).

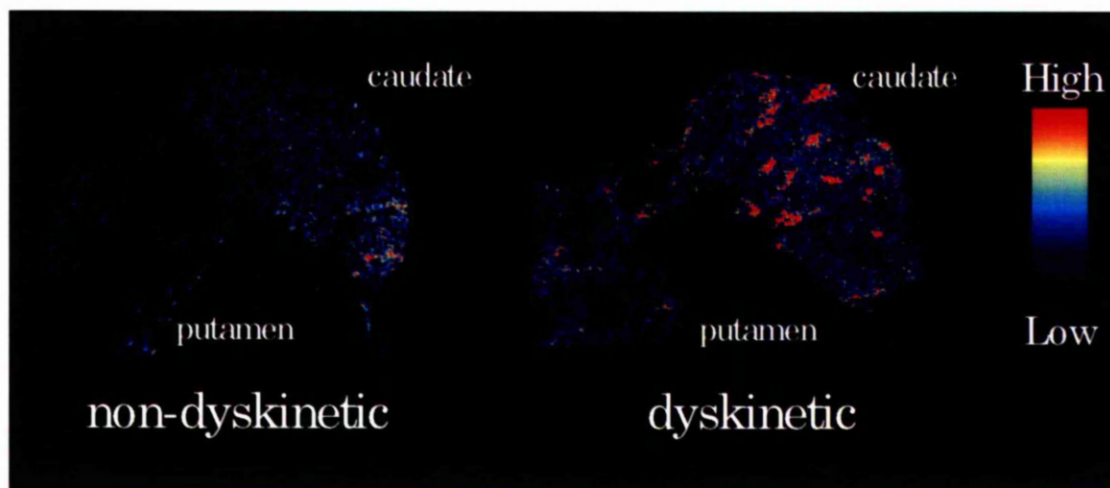


Figure 5.3.3.8 Enlargement of striatal section from figure 5.3.3.6 showing heterogeneous distribution of PPE-B hybridisation signal in the caudal neostriatum from non-dyskinetic or dyskinetic MPTP-treated macaques following apomorphine alleviation of parkinsonian symptoms

Pseudocolour transformations of autoradiographs of in situ hybridisation utilising an oligonucleotide probe targeted against pre-proenkephalin-B (PPE-B) in caudal neostriatum from the MPTP-treated non-human primate, following either reversal of parkinsonian symptoms (non-dyskinetic) or displaying dopamine agonist-induced dyskinesias (dyskinetic). At higher magnification it can be seen that the signal is distributed in a 'patchy' heterogeneous manner.

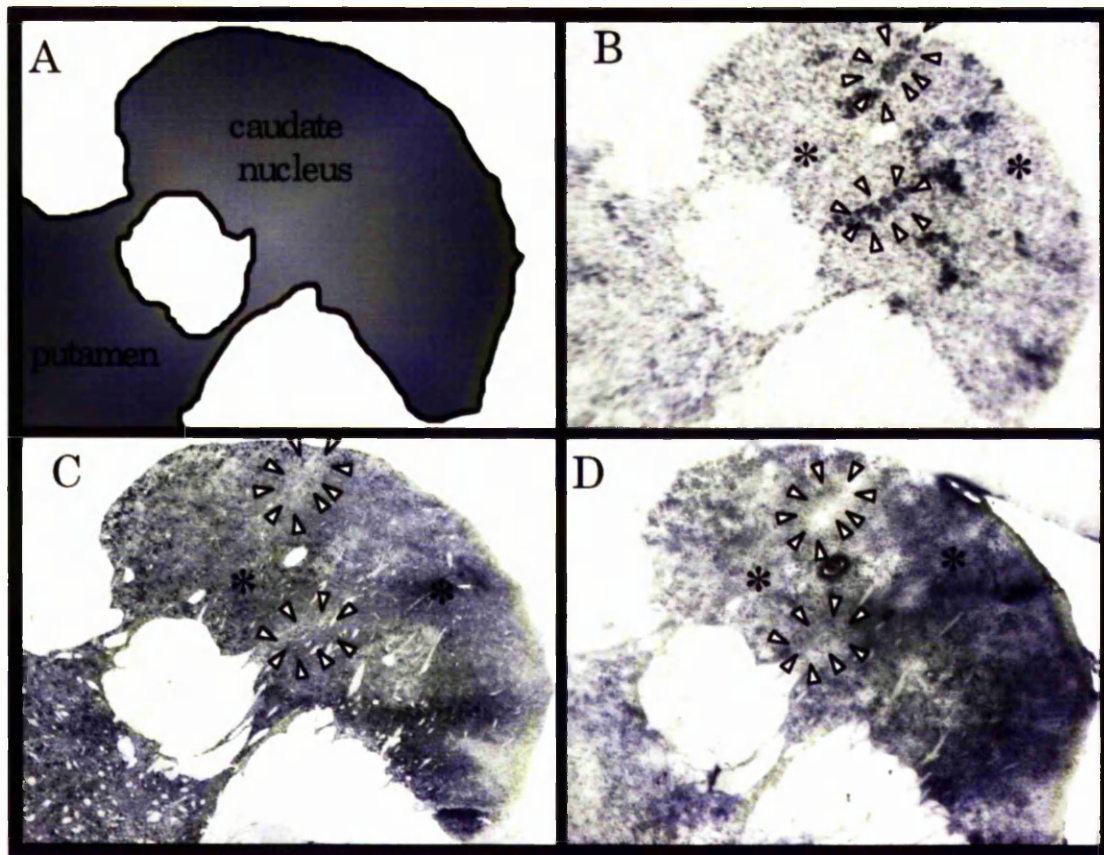


Figure 5.3.3.9 Illustration demonstrating striosome-matrix compartmentalisation in the caudal neostriatum with respect to PPE-B expression in the dyskinetic MPTP-treated non-human primate

PPE-B expression in the dyskinetic MPTP-treated non-human primate with respect to striosome-matrix compartmentalisation. Diagrammatic representation of the caudal caudate nucleus and putamen (A). In situ hybridisation utilising an oligonucleotide probe targeted against pre-proenkephalin-B (PPE-B) in the MPTP-treated non-human primate displaying dopamine agonist-induced dyskinesias (B). Striosome(>)-matrix() compartments demonstrated by acetylcholinesterase histochemistry (C). Striosome(>)-matrix(*) compartmentalisation demonstrated by calbindin immunocytochemistry (D). PPE-B mRNA expression displays a heterogeneous distribution with higher expression within the striosomal boundaries.*

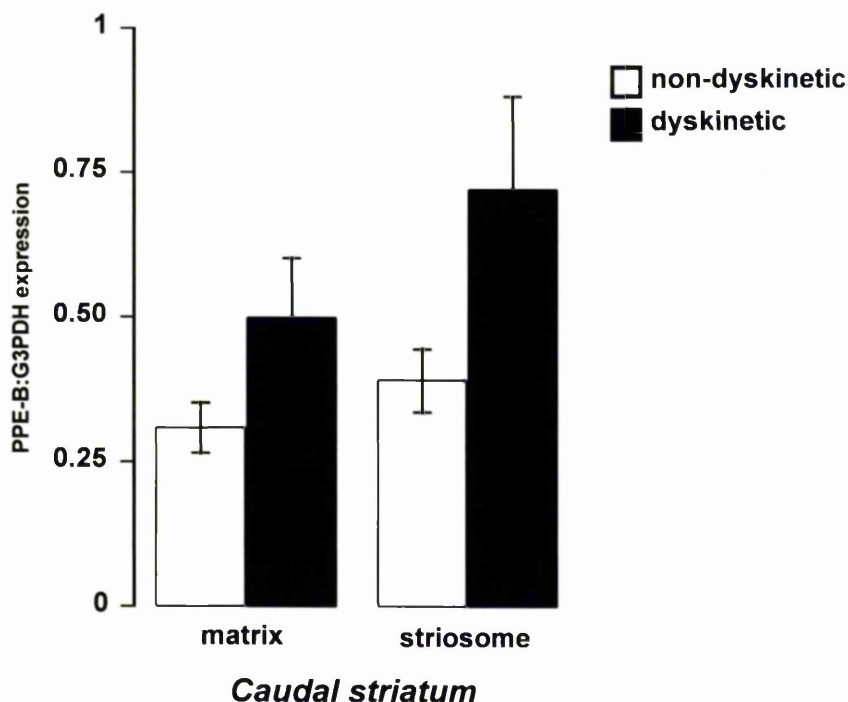


Figure 5.3.3.10 Graph showing the ratio of PPE-B:G3PDH expression in the striosome-matrix compartments of the caudal neostriatum from non-dyskinetic or dyskinetic MPTP-treated macaques following apomorphine alleviation of parkinsonian symptoms

Graph showing the ratio of PPE-B:G3PDH expression following in situ hybridisation utilising an oligonucleotide probe targeted against pre-proenkephalin-B (PPE-B) in 'striosome - matrix' compartments as defined by acetylcholinesterase histochemistry in the caudal caudate nucleus in striatal sections from the MPTP-treated non-human primate, following either reversal of parkinsonian symptoms (non-dyskinetic, □) or displaying dopamine agonist-induced dyskinesias (dyskinetic, ■). Data are expressed as mean (\pm SEM) optical density ratios ($n = 4$, ns, $P > 0.05$ cf non-dyskinetic group, unpaired Student's t -test).

5.4 Discussion

Methodological considerations

The MPTP-treated non-human primate was employed to investigate the changes in opioid neuropeptide precursors that underlie dopamine agonist-induced dyskinesia. Unlike the marmoset or rat model of L-DOPA-induced dyskinesia, this model produces symptoms of dyskinesias that are indistinguishable from those seen in parkinsonian patients following long-term dopamine-replacement therapy at doses that alleviate symptoms. MPTP was administered using a regime previously shown to result in parkinsonian symptoms, with a greater than 95% decrease in dopamine receptor uptake sites within the neostriatum as measured by [³H]mazindol radioligand binding, HPLC analysis of dopamine levels and tyrosine hydroxylase immunocytochemical studies (Mitchell *et al.*, 1985; Graham *et al.*, 1989b; Clarke *et al.*, 1989; Mitchell *et al.*, 1990, 1992).

The MPTP-treated macaques were split into two groups with no difference between level of parkinsonian, or time of they remained parkinsonian. Both groups were given increasing doses of apomorphine until a dose of apomorphine capable of reversing the parkinsonian symptoms was found. Once this dose had been achieved for all 8 macaques, 4 macaques were administered the direct dopamine-receptor agonist apomorphine three times a day, until dyskinesias were observed after every apomorphine injection. In three of the four animals the dyskinesia consisted of chorea of both the arms and legs, while the fourth developed dystonia in all limbs. In the group that developed dopamine-agonist induced dyskinesias, once dyskinesias were observed following every apomorphine injection, the animals were administered 3 apomorphine injections per day for 14 days in order to standardise the time period of dyskinesia.

All macaques, in both the dyskinetic and non-dyskinetic groups, were killed by an overdose of barbiturate 20 minutes following the final injection of an anti-parkinsonian dose of apomorphine. This was to coincide with the time of peak anti-parkinsonian or dyskinetic response that would have been observed following the final apomorphine injection.

To assess the specificity of the pre-proenkephalin-A (PPE-A) and pre-proenkephalin-B (PPE-B) oligonucleotide probes used in these *in situ* hybridisation studies several methodological considerations have been employed. To verify the specificity of the oligonucleotide probe for RNA, pre-treatment with RNase, an enzyme that specifically degrades single stranded RNA, was employed. Pre-treatment with RNase completely abolished the signal for PPE-A and PPE-B in macaque striatal sections (Figures 5.3.1.1, 5.3.1.2). The specificity of oligonucleotide probe sequences were verified using genbank and EMBL databases (Altschul *et al.*, 1993). Following *in situ* hybridisation in macaque sections, an identical pattern of specific binding to that seen in the rat was observed for both PPE-A and PPE-B.

Two adjacent sections on either side of the sections used for *in situ* hybridisation were used for acetylcholinesterase staining or calbindin immunocytochemistry. The acetylcholinesterase poor 'striosomes' coincided with acetylcholinesterase negative areas as previously described (Graybiel and Ragsdale, 1979), thus giving a map of striosome-matrix compartmentalisation for each *in situ* section. Utilising image analysis equipment, a template of acetylcholinesterase poor 'striosomes' was produced for each *in situ* section. This allowed average optical density readings to be taken for striosome-matrix compartments for each *in situ* hybridisation section. Since the classical striosome-matrix compartmentalisation does not remain as robust in the ventral neostriatum i.e. the nucleus accumbens (Meredith, 1996), the average optical density measurements for both PPE-A and PPE-B were obtained from only the dorsal neostriatum.

G3PDH was used to correct for any non-specific changes in transcription rate that occurred between animals, either due to non-specific RNase activity within the sections, temporal variations in preparation of the sections both due to *post-mortem* delay period and following cryostat cutting, mounting and re-freezing. This was achieved by dividing the mean of the probe of investigation values (PPE-A and PPE-B) from the non-dyskinetic or dyskinetic MPTP-treated macaques, by the mean value of the control probe G3PDH over the whole striatum for each individual animal. The final value is therefore expressed as a ratio of the mean probe of investigation relative to the mean of the G3PDH probe. This ratio gives a semi-quantitative analysis of PPE-A and PPE-B mRNA expression in the neostriatum.

Distribution of pre-proenkephalin-A

When average optical density measurements were made of the whole sensorimotor or associative areas of the striatum, or from the limbic nucleus accumbens, the ratio of PPE-A: G3PDH expression was increased in all areas in the dyskinetic group when compared to the non-dyskinetic MPTP-treated group (Figure 5.3.2.1). In the rostral striatum, this increase was significant in the sensorimotor and associative regions but non-significant in the limbic nucleus accumbens (Figure 5.3.2.2). In the caudal striatum, PPE-A expression was non-significantly increased in sensorimotor and associative regions of the striatum (Figures 5.3.2.5, 5.3.2.6). Herrero *et al.* in 1995 reported no significant alteration of PPE-A expression in MPTP-treated macaques following repeated L-DOPA/carbidopa administration (50/50 mg kg⁻¹ orally, twice daily for 4 months). However, analysis of the hybridisation signal was carried out by densitometric analysis of silver grains within individual neurons in either the caudate or putamen and not in the functionally-significant manner described in this chapter. Similarly, in the MPTP-treated common marmoset Jolkkonen *et al.* (1995) investigated PPE-A expression following repeated L-DOPA administration (12.5 mg kg⁻¹ orally, twice daily for 4 weeks). However, although these animals displayed L-DOPA-induced dyskinesias, no alteration in the MPTP-induced elevation of PPE-A expression was observed. Again in this study the PPE-A hybridisation signal was measured on the basis of caudate nucleus and putamen and not functionally-distinct regions. Furthermore, the marmosets remained parkinsonian for only four weeks before L-DOPA administration was started, unlike the set of experiments described in this chapter, whereby macaques remained in a stable parkinsonian state for a mean of eight months before apomorphine administration. Moreover, the marmosets in this study were sacrificed 24 hours following the last dose of L-DOPA, not when peak-dose dyskinesia would be expected. These temporal discrepancies, coupled with the possible species differences, may account for the lack of alteration in PPE-A expression seen following L-DOPA-induced dyskinesia in the marmoset study.

In the set of studies described in this chapter, when the PPE-A hybridisation signal was analysed with respect to striosome-matrix compartmentalisation, the mean PPE-A:G3PDH signal was increased, although non-significantly, in the dyskinetic animals in the rostral striatum. No difference in signal was observed with respect to

striosome-matrix compartmentalisation in either the dyskinetic or non-dyskinetic group (Figure 5.3.2.3). In the caudal striatum no significant increase in PPE-A expression was observed between the dyskinetic primates or the parkinsonian primates following apomorphine reversal of symptoms in either the striosomal or matrix compartment (Figure 5.3.2.6). The lack of any significant difference in PPE-A expression between striosome and matrix compartments is in agreement with previous studies in both non-human primates and human *post-mortem* studies that indicate no segregation of expression of PPE-A in either striosome or matrix compartments (Hurd and Herkenham, 1995). This homogenous distribution in PPE-A expression was also observed in the rat studies described in chapter 4. This distribution of PPE-B expression with regards striosome-matrix is also in agreement with data from the rat suggesting that PPE-A expression is not segregated to a specific subset of cells within the rat neostriatum (Gerfen, 1992). These data would suggest that in dopamine agonist-induced dyskinesias, although there is an increase in PPE-A expression in all areas within the neostriatum, the expression is not influenced by the conformities of striosome-matrix compartmentalisation but rather more by the functional segregation with regards to sensorimotor, associative and limbic functions. Topographically, this pattern of PPE-A expression is similar to that seen in the rat model of L-DOPA-induced dyskinesia, with significant increases seen in the most rostral sensorimotor and associative areas of the striatum and with little change in the limbic nucleus accumbens and more caudal neostriatum following repeated dopamine-replacement therapy.

Distribution of pre-proenkephalin-B

Analysis of average optical density measurements for the whole neostriatum with regards to functional segregation according to sensorimotor, association or limbic afferents, showed no significant difference in the ratio of PPE-B:G3PDH expression between the dyskinetic and the non-dyskinetic MPTP-treated primates (Figures 5.3.3.2, 5.3.3.7). However, within the rostral neostriatum of the dyskinetic primates, dark heterogeneous 'patches' of signal were observed. When analysed with respect to striosome-matrix compartmentalisation, a significant increase in the PPE-B expression was observed in the dyskinetic primates in both the striosomes and matrix of the dyskinetic group when compared to the non-dyskinetic MPTP-treated group (Figures

5.3.3.5). The greatest increase in PPE-B:G3PDH expression was present in the striosomes. However, this intense signal did not extend throughout the whole of the 'striosomes' but did remain within the 'striosomal' boundaries (Figures 5.3.3.4).

In the caudal neostriatum dark heterogeneous patches of signal were also observed, with the mean expression level of PPE-B:G3PDH also increased in both the striosomes and the matrix. However, these elevations were not significant (Figure 5.3.3.10). A preliminary study to investigate PPE-B expression in MPTP-treated non-human primates has demonstrated that following repeated L-DOPA administration and subsequent dyskinesia no alterations between the MPTP-treated group and the dyskinetic group were observed (Goulet *et al.*, 1996). However, these animals were not sacrificed during the time of peak-dose dyskinesias and had in fact had a washout period of three days. Another factor which may explain the discrepancy in this study compared to the one described in this chapter is the mode of analysis. Again, functional segregation or striosome-matrix compartmentalisation was not analysed, with only caudate nucleus and putamen measurements assessed.

Therefore, following repeated dopamine-replacement therapy in both the 6-OHDA-lesioned rat model and the dyskinetic MPTP-treated non-human primate model of Parkinson's disease, PPE-B expression is increased within the neostriatum. The heterogeneous pattern of PPE-B upregulation seen in the dyskinetic MPTP-treated macaque is unlike the homogeneous upregulation seen in the rat model of L-DOPA-induced dyskinesia. This may suggest that in the primate, a much more selective control of PPE-B expression is maintained. However, studies on *post-mortem* tissue indicate that in the human brain, PPE-B expression is higher in the striosomes than in the matrix (Hurd and Herkenham, 1995). This suggests that following repeated dopamine receptor agonist administration in the MPTP-treated non-human primate, PPE-B expression is increased in both the striosomes and the matrix.

In the rat, almost all striatopallidal neurons express enkephalin, while those neurons in the striatonigral pathway express dynorphin (Del Fiacco *et al.*, 1982; Vincent and Hokfelt, 1982; Beckstead and Kersey, 1985; Gerfen and Young, 1988; Gerfen *et al.*, 1988). However, in the primate brain, this distinction between peptides is not as differentiated, with dynorphin immunoreactivity present in the lateral segment of the globus pallidus and enkephalin immunoreactivity in the substantia nigra pars reticulata (Haber and Watson, 1985). However, the SNpr does contain a medial strip of only

dynorphinergic immunoreactivity (Haber and Watson, 1985, 1983). Although it is widely-held that only cells within the matrix provide the striatal efferent projections in both the rat and the primate, it has been demonstrated that some cells within the striosomes project to the SNpr and GPM (Gimenez-Amaya and Graybiel, 1987). This suggests that increased PPE-B expression in both the striosomes and matrix would produced an elevation in dynorphin in all projections areas of the PPE-B containing neurons.

The finding that PPE-B expression shows the highest increase in the striosomes as compared to the matrix may be linked to evidence suggesting increased D1 dopamine receptor binding within the striosomal compartments of both cats and primates (Besson *et al.*, 1988). As discussed in section 1.6 and 4.4, close links between dopamine D1 receptor activation and the control of PPE-B expression have been described. Increased activation of D1 receptors predominantly in the striosomal compartments may increase PPE-B expression. However, since in dopamine agonist-induced dyskinesia, an increase in PPE-B expression is observed in both the striosomes and matrix, together with the fact that D1 receptor binding is also found at high concentrations within the matrix, suggests further level control of PPE-B expression. This further level of control may arise from the cerebrocortical innervation of the striatum as both striosomes and matrix have been shown to receive efferent projections from different parts of the cerebral cortex (Ragsdale and Graybiel, 1981; Gerfen, 1984; McGeorge and Faull, 1989; Eblen and Graybiel, 1995). This alteration in corticostriatal transmission may underlie differential opioid peptide precursor expression and ultimately treatment-related dyskinesias.

Therefore, in a similar manner to the rodent model of L-DOPA-induced dyskinesia, in the MPTP-treated non-human primate, dopamine receptor agonist-induced dyskinesia produced elevated levels of both PPE-A and PPE-B expression within the neostriatum. In both the rat and primate model of dopamine agonist-induced dyskinesia, PPE-A expression was increased in the dorsal area of the rostral striatum. In a similar manner to the rat, the PPE-B signal was concentrated in the ventral areas of the striatum and the nucleus accumbens. The major differences between the rat and primate is the increase seen in both the striosomes and matrix in the dorsal neostriatum. In the rat, PPE-B expression was homogeneously increased following repeated L-DOPA-administration. However, in the dyskinetic primate, PPE-B expression is higher in the

striosomes. However, since this uneven distribution of PPE-B expression is also observed in the clinically-normal human brain, this discrepancy in distribution has probably little influence in the mechanisms underlying L-DOPA-induced dyskinesia.

Therefore, from the data presented in this chapter, it is clear that following dopamine agonist-induced dyskinesias in MPTP-treated non-human primates, there is an increase in the expression of both PPE-A and PPE-B. In conclusion, together with the rat data described in chapter 3 and 4, these data provide evidence to suggest that increased enkephalinergic and dynorphinergic transmission within the striatal efferents may play a role in L-DOPA-induced dyskinesias seen following repeated L-DOPA or dopamine-agonist administration in Parkinson's disease.

Chapter 6 :

General discussion

The key findings of this thesis will now be discussed with reference to their relevance in understanding the neural mechanisms underlying L-DOPA-induced dyskinesia and possible therapeutic approaches to Parkinson's disease that might not be associated with treatment-related dyskinesias.

Summary of major findings

In this thesis, a novel rodent model of L-DOPA-induced dyskinesia has been characterised. Repeated L-DOPA treatment of the 6-OHDA-lesioned rat models the cellular, biochemical, and pharmacological mechanisms underlying L-DOPA-induced dyskinesia in Parkinson's disease. This model exhibits an enhanced behavioural response to L-DOPA, and dopamine receptor agonists, that is distinct from the classically-observed dopamine agonist-induced rotational response (Figure 2.3.2.1). This enhanced behavioural response can be modulated by non-dopaminergic drugs in a manner similar to that seen in both primate models of L-DOPA-induced dyskinesia (Gomez-Mancilla and Bedard, 1993) and in parkinsonian patients displaying L-DOPA-induced dyskinesia (Bennett *et al.*, 1994; Bonifati *et al.*, 1994; Durif *et al.*, 1995, Figures 2.3.4.1-2.3.4.5). This rodent model may prove useful in studying the cellular and molecular mechanisms underlying L-DOPA-induced dyskinesia. Moreover, this model may be used to characterise whether *de novo* administration of novel anti-parkinsonian drugs are likely to have pro- or dyskinetic properties before they are introduced into the MPTP-treated non-human primate model of Parkinson's disease. This will allow a much faster screening for the pro-dyskinetic nature of novel anti-parkinsonian compounds and refine primate tests.

Northern blot hybridisation was used to demonstrate increased expression of pre-proenkephalin-A (PPE-A, the predominant precursor of enkephalin) and pre-proenkephalin-B (PPE-B, the precursor of dynorphin, Figures 3.3.3.4, 3.3.3.8) in the rodent model of L-DOPA-induced dyskinesia. Further investigation of these increases, utilising *in situ* hybridisation, showed a topographical arrangement in expression such that following L-DOPA treatment, PPE-A expression was increased in the most rostral neostriatum, and showed a dorsolateral (highest level of expression) to ventromedial gradient (lowest levels of expression, Figures 4.3.4.1-4.3.4.22). Furthermore, PPE-B expression was demonstrated to be increased throughout the neostriatum, again with

most significant increases in the most rostral neostriatum. PPE-B expression demonstrated a mediolateral gradient, with the greatest increases in the lateral neostriatum (Figures 4.3.5.1-4.3.5.22).

Treatment with drugs which do not elicit dyskinesias when given *de novo* to MPTP-treated primates or patients with Parkinson's disease, did not increase the expression of these neuropeptides (Figures 4.3.4.1-4.3.4.22 and 4.3.5.1-4.3.5.22). This finding further suggests, albeit indirectly, the involvement of the opioid neuropeptides enkephalin and dynorphin in dopamine receptor agonist-induced dyskinesias.

In a similar manner to the rat, an increase in both PPE-A and PPE-B expression in the neostriatum of the MPTP-treated non-human primate displaying treatment-related dyskinesias was also observed. In the rostral striatum, this increase was significant in the sensorimotor and associative regions. In the caudal striatum, PPE-A expression was non-significantly increased in sensorimotor or associative regions of the striatum (Figures 5.3.2.2, 5.3.2.6). No difference in PPE-A expression was observed with respect to striosome-matrix compartmentalisation in either the dyskinetic or non-dyskinetic group. In the caudal striatum, no significant increase in PPE-A expression was observed between the dyskinetic primates or the parkinsonian primates following apomorphine reversal of symptoms in either the striosomal or matrix compartment (Figures 5.3.2.4, 5.3.2.8). Analysis of average optical density measurements for the whole neostriatum with regarding functional segregation according to sensorimotor, association or limbic afferents, showed no significant difference in the ratio of PPE-B to G3PDH expression between the dyskinetic and the non-dyskinetic MPTP-treated primates (Figures 5.3.2.2, 5.3.2.6). However, when analysed with respect to striosome-matrix compartmentalisation, a significant increase in the PPE-B expression was observed in both the striosomes and matrix of the dyskinetic MPTP-treated primate group when compared to the non-dyskinetic MPTP-treated group. The greatest increase in PPE-B expression was observed in the striosomes (Figure 5.3.3.5). In the caudal neostriatum dark heterogeneous patches of PPE-B expression were also observed, with the mean expression level of PPE-B higher in both the striosomes and the matrix. However, these elevations were not significant (Figure 5.3.5.10).

Previous studies have demonstrated increases in both PPE-A expression and enkephalin peptide levels in *post-mortem* parkinsonian striatal tissue (De Ceballos *et al.*, 1993; Nisbet *et al.*, 1995). Since completing the work presented in this thesis, we have

also observed increased PPE-B expression in human *post-mortem* striatal tissue from patients with Parkinson's disease following long-term L-DOPA-treatment and displaying L-DOPA-induced dyskinesias when compared to age-matched, clinically-normal control tissue (Figure 6.1).

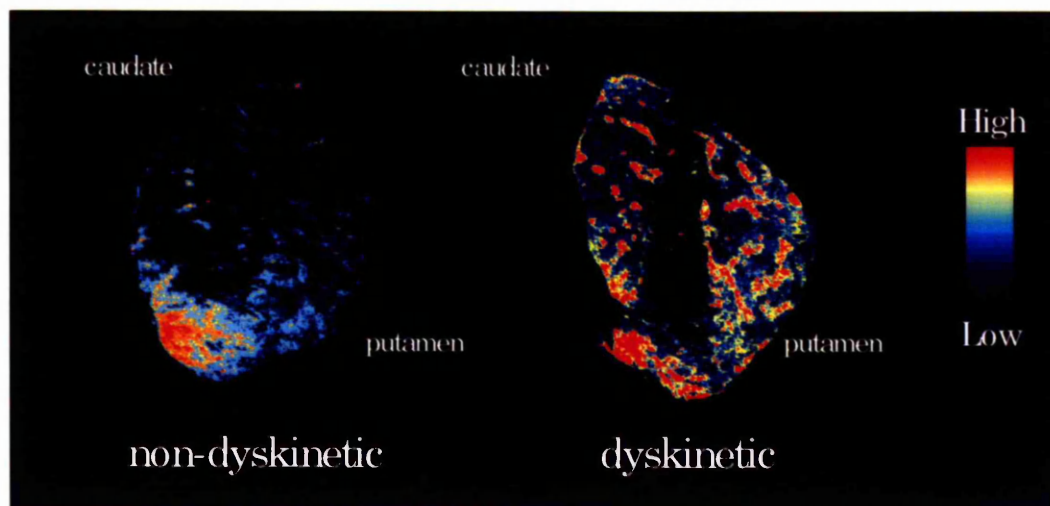


Figure 6.1 PPE-B hybridisation signal in the rostral neostriatum of parkinsonian patients following long-term L-DOPA therapy and displaying L-DOPA-induced dyskinesias

Pseudocolour transformation of autoradiographs of in situ hybridisation utilising an oligonucleotide probe targeted against pre-proenkephalin-B (PPE-B) in the rostral neostriatum of human parkinsonian patients following long-term L-DOPA therapy and displaying L-DOPA-induced dyskinesias prior to death (dyskinetic). Age-matched clinically-normal human neostriatum is also shown for comparison (non-dyskinetic).

Functional antagonism of the peptide products of PPE-A and PPE-B, by blocking kappa and delta opioid receptors respectively, attenuated the potentiated behavioural response or hyperkinesia seen in the rodent model of L-DOPA-induced dyskinesia. Thus, a reduction in the L-DOPA-induced hyperkinesia was demonstrated by administration of the non-selective opioid receptor antagonist naloxone (which blocks the effects of both enkephalin and dynorphin), *nor*-binaltorphimine, the selective kappa opioid receptor antagonist, and naltrindole, the selective delta opioid receptor antagonist (Figure 3.3.4.1-3.3.4.4).

Role of opioid peptides in L-DOPA-induced dyskinesia

In this thesis, it has been proposed that increased opioid peptide transmission in striatal efferents may, by two separate mechanisms, result in hyperkinesia in the rat or dyskinesia in patients, following long-term dopamine-replacement therapy. It is thought, from the experimental evidence to date, that all forms of dyskinesias result from a common neural mechanism, i.e. reduced activity of the medial segment of the globus pallidus, thus ultimately reducing the inhibitory drive of to the VA/VL thalamus (Crossman, 1987).

Increased peptidergic transmission in both the direct and indirect efferent projections of the striatum, may cause dyskinesia by two distinct mechanisms. These will now be discussed separately.

Role of enkephalin in L-DOPA-induced dyskinesia

It has been demonstrated that enkephalin-mediated opioid receptor activation can decrease GABA release within the rat globus pallidus (Maneuf *et al.*, 1994). This decrease in GABA is mediated through activation of delta opioid receptors on striatal efferents (Hill *et al.*, 1996). Therefore, increased enkephalinergic transmission in the striatopallidal pathway to the globus pallidus in rat, or lateral segment of the globus pallidus in the primate, could, by reduction of GABA release in the indirect striatal efferents, cause inhibition of GABA release in the lateral segment of the globus pallidus. This would increase the activity of the lateral segment of the globus pallidus and thus over-inhibit the subthalamic nucleus. Underactivity of the subthalamic nucleus would decrease glutamatergic excitation of the medial segment of the globus pallidus, thus causing underactivity of the GABAergic projection to the motor regions of the thalamus, ultimately causing dyskinesia (Figure 6.2). Administration of the delta opioid receptor antagonist, naltrindole, would block the inhibitory effects of enkephalin and increase the release of GABA in the lateral segment of the globus pallidus and thus reduce GABAergic over-inhibition of the subthalamic nucleus. This normalisation of subthalamic nucleus activity would subsequently restore normal activity of the output nuclei of the basal ganglia and thus reduce L-DOPA-induced hyperkinesia in the rat. This proposed mechanism bears many similarities with those underlying other forms of

dyskinesia (Crossman, 1987). Increased enkephalin could elicit dyskinesia in a similar manner to early stage Huntington's disease in which preferential loss of the GABAergic efferents to the lateral segment of the globus pallidus causes chorea (Sapp *et al.*, 1995; Richfield *et al.*, 1995). Similarly, injection of bicuculline into the lateral segment of the non-human primate globus pallidus (Jackson and Crossman, 1984) or inactivation of the subthalamic nucleus (Martin, 1927; Papez *et al.*, 1942; Whittier, 1949b; Anden *et al.*, 1995) also elicits dyskinesia.

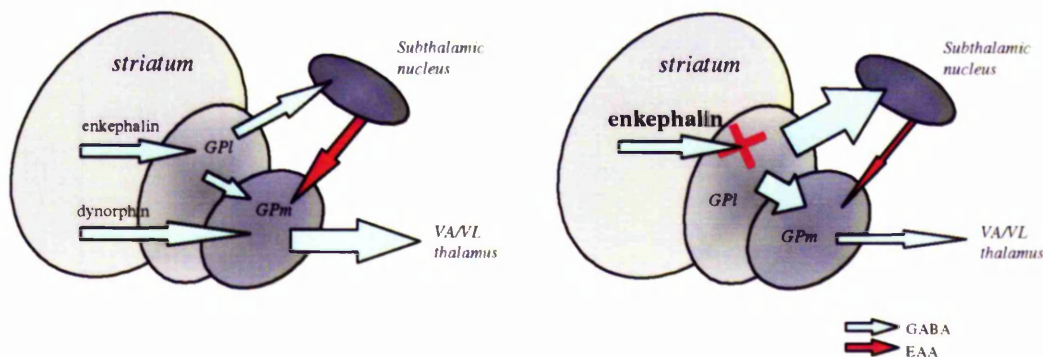


Figure 6.2 Diagrammatic representation of the effect of increased enkephalinergic transmission in striatal efferent projections on basal ganglia output

Role of dynorphin in L-DOPA-induced dyskinesia

In contrast to enkephalin, it has been demonstrated that kappa opioid receptor activation in the medial segment of the globus pallidus and substantia nigra pars reticulata in primate, or the substantia nigra pars reticulata of rats decreases glutamate release (Maneuf *et al.*, 1995, Hill and Brotchie, 1995, Hill *et al.*, 1996). Kappa opioid receptor mRNA is present in high concentrations in the subthalamic nucleus, with receptors located on the glutamatergic efferents in the medial segment of the globus pallidus (Zhu *et al.*, 1995). In L-DOPA-induced dyskinesia, increased dynorphinergic transmission within the medial segment of the globus pallidus could act on pre-synaptic kappa opioid receptors on subthalamic nucleus terminals to decrease glutamate release within the medial segment of the globus pallidus. Such an action would reduce the excitation of the medial segment of the globus pallidus. Increased dynorphinergic transmission in striatal efferents to the medial segment of the globus pallidus would

therefore act in a similar manner to injections of the glutamate antagonist kynurenate in the medial segment of the globus pallidus to elicit dyskinesia (Robertson *et al.*, 1989). Administration of the kappa opioid receptor antagonist, *nor*-binaltorphimine, would conversely increase the release of glutamate in the medial segment of the globus pallidus, resulting in increased activity of the output nuclei of the basal ganglia and thus reducing L-DOPA-induced hyperkinesia in the rat.

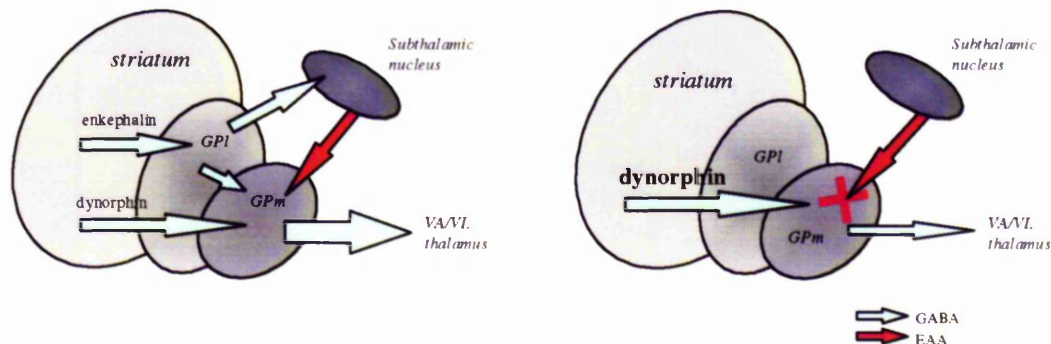


Figure 6.3 Diagrammatic representation of the effect of increased dynorphinergic transmission on basal ganglia output

Future strategies in the treatment of Parkinson's disease

From the discussion above it is apparent that, by two separate mechanisms, increased opioid peptide transmission in striatal efferents could reduce the activity of the output nuclei of the basal ganglia and ultimately underlie the dyskinesia observed following repeated dopamine-replacement in Parkinson's disease. Further work is required to investigate both the efferent localisation and release dynamics of the peptide products of PPE-A and PPE-B.

Several clinical studies have indicated the possible therapeutic utility of opioid receptor antagonists in the treatment of dyskinesias and other related syndromes e.g. tardive dyskinesia and Tourette's syndrome (Blum *et al.*, 1984; Lindenmayer *et al.*, 1988; Kurlan *et al.*, 1991). In the case of L-DOPA-induced dyskinesias, potentially exciting results have been reported. Two groups have independently described small scale clinical studies that have been successful in reducing L-DOPA-induced dyskinesias using intravenous administration of naloxone (Trabucchi *et al.*, 1982; Sandyk and Snider, 1986).

In these studies, patients showed a decreases in 'on' dyskinesias without loss of L-DOPA anti-parkinsonian efficacy. Patients also experienced an extended 'on' period, to a maximal 144%. It was also reported that the improvements included a shortened rigid phase, and that the 'on-off' fluctuations were more gradual. Conversely, in a more controlled experiment in the MPTP-treated primate model of Parkinson's disease, low doses of naloxone were ineffective at reducing L-DOPA-induced dyskinesias (Gomez-Mancilla and Bedard, 1993). However, comparison to the human studies suggests that the dose of naloxone used in this primate study may simply have been too low to be effective (Trabucchi *et al.*, 1982; Sandyk and Snider, 1986). Furthermore, oral administration of naltrexone, a longer acting analogue of naloxone, was ineffective in alleviating L-DOPA-induced dyskinesias (Rascol *et al.*, 1994). Intravenous administration of naloxone would no doubt deliver a higher peak plasma concentration in a shorter time and this may explain the observation of anti-dyskinetic effect in the two naloxone trials with no apparent reduction in dyskinesia in the naltrexone study. Nevertheless, a large scale prospective study remains to be carried out to investigate the possible role of opioid receptor antagonists in the treatment of L-DOPA-induced dyskinesias in Parkinson's disease. The possible role of mu opioid receptor activation in L-DOPA-induced dyskinesias remains uncertain, which brings into question the effectiveness of utilising a non-selective opioid receptor antagonist such as naloxone in the treatment of L-DOPA-induced dyskinesia. It is apparent that, under certain conditions, opioid receptor antagonists can reduce L-DOPA-induced dyskinesias. It is tempting to speculate that novel opioid receptor antagonists, perhaps with higher potency, longer duration of action and/or more selectivity towards kappa and delta opioid receptors may prove to be an effective treatment for L-DOPA-induced dyskinesias.

Therefore, in summary, evidence in this thesis suggests the intriguing possibility that novel opioid receptor antagonists acting primarily at the kappa and delta opioid receptor sites may provide a useful adjunct therapy to L-DOPA and dopamine receptor agonists in the treatment of Parkinson's disease.

References

- Aellig WH, Nuesch E. Comparative pharmacokinetic investigations with tritium-labeled ergot alkaloids after oral and intravenous administration in man. *Int J Clin Pharmacol Biopharm* 1977, 15 (3): 106-112
- Agid Y, Barroche G, Bonnet AM, Javoy-Agid F, Kato G, Lhermitte F, Pollak P, Signoret JL. Dopamine receptor stimulating agonists in the treatment of Parkinson's disease. *Biomedicine* 1979, 30 (2): 67-71
- Agid Y, Ruberg M, Dubois B, Javoy-Agid F. Biochemical substrates of mental disturbances in Parkinson's disease. In: Hassler RG, Christ JF, editors. *Advances in Neurology* 1984, 40: 211-218
- Akil H, Watson SJ. Neuromodulatory functions of the brain pro-opioid system. *Adv Biochem Psychopharmacol* 1980, 22: 435-445
- Albe-Fessard D, Guiot G, Lamarre Y, Arfel G. Activation of thalamocortical projections related to tremorogenic processes. In: Purpura DP, Yahr MD, editors. *The Thalamus*. Columbia University Press. New York 1996, 237-249
- Alexander GE, Crutcher MD, DeLong MR. Basal ganglia-thalamocortical circuits: parallel substrates for motor, oculomotor, 'prefrontal' and 'limbic' functions. *Prog Brain Res* 1990, 85: 119-146
- Alexander GE, DeLong MR, Strick PL. Parallel organization of functionally segregated circuits linking basal ganglia and cortex. *Annu Rev Neurosci* 1986, 9: 357-381
- Alheid GF, Heimer L. New perspectives in basal forebrain organisation of special relevance for neuropsychiatric disorders: the striatopallidal, amygdaloid and corticopetal components of substantia innominata. *Neuroscience* 1988, 27: 1-39
- Alreja M, Aghajanian GK. Opiates suppress a resting sodium-dependent inward current and activate an outward potassium current in locus coeruleus neurons. *J Neuroscience* 1993, 13 (8): 3525-3532
- Altschul SF, Gish W, Miller W, Myers EW, Lipman DJ. Basic local alignment search tool. *J Mol Biol* 1990, 215: 403-410
- Andren PE, Levin ED, Liminga U, Gunne L. Behavioral and neurochemical consequences of ibotenic acid lesion in the subthalamic nucleus of the common marmoset. *Brain Res Bull* 1995, 36 (3): 301-307
- Andy OJ. Thalamic stimulation for control of movement disorders. *Appl Neurophysiol* 1983, 46 (1-4): 107-111

- Angulo JA. Involvement of dopamine D1 and D2 receptors in the regulation of proenkephalin mRNA abundance in the striatum and accumbens of the rat brain. *J Neurochem* 1992, 58 (3): 1104-1109
- Angulo JA, Christoph GR, Manning RW, Burkhart BA, Davis LG. Reduction of dopamine receptor activity differentially alters striatal neuropeptide mRNA levels. *Adv Exp Med Biol* 1987, 221: 385-391
- Angulo JA, Coirini H, Ledoux M, Schumacher M. Regulation by dopaminergic neurotransmission of dopamine D2 mRNA and receptor levels in the striatum and nucleus accumbens of the rat. *Brain Res Mol Brain Res* 1991, 11 (2): 161-166
- Angulo JA, Davis LG, Burkhart BA, Christoph GR. Reduction of striatal dopaminergic neurotransmission elevates striatal proenkephalin mRNA. *Eur J Pharmacol* 1986, 130 (3): 341-343
- Angulo JA, Williams A, Ledoux M, Watanabe Y, McEwen BS. Elevation of striatal and accumbal preproenkephalin, preprotachikinin and preprodynorphin mRNA abundance subsequent to N-methyl-D-aspartate receptor blockade with MK-801. *Mol Brain Res* 1995, 29: 15-22
- Annett LE, Rogers DC, Hernandez TD, Dunnett SB. Behavioural analysis of unilateral monoamine depletion in the marmoset. *Brain* 1992, 115: 825-856
- Aoki C, Pickel VM. Neuropeptide Y-containing neurons in the rat striatum: ultrastructure and cellular relations with tyrosine hydroxylase-containing terminals and with astrocytes. *Brain Res* 1988, 459 (2): 205-225
- Araki M, McGeer PL, McGeer EG. Presumptive gamma-aminobutyric acid pathways from the midbrain to the superior colliculus studied by a combined horseradish peroxidase-gamma-aminobutyric acid transaminase pharmacohistochemical method. *Neuroscience* 1984, 13 (2): 433-439
- Arcari P, Martinelli R, Salvatore F. The complete sequence of a full length cDNA for human liver glyceraldehyde-3-phosphate dehydrogenase: evidence for multiple mRNA species. *Nuc Acid Res* 1984, 12(23): 9179- 9189
- Armstrong M, Daly AK, Cholerton S, Bateman DN, Idle JR. Mutant debrisoquine hydroxylation genes in Parkinson's disease. *Lancet* 1992, 339 (8800): 1017-1018
- Aronin N, Difiglia M, Graveland GA, Schwartz WJ, Wu JY. Localization of immunoreactive enkephalins in GABA synthesizing neurons of the rat neostriatum. *Brain Res* 1984, 300 (2): 376-380
- Asanuma C, Thach WR, Jones EG. Anatomical evidence for segregated focal groupings of efferent cells and their terminal ramifications in the cerebellothalamic pathway of the monkey. *Brain Res* 1983b, 286 (3): 267-297

- Asanuma C, Thach WR, Jones EG. Cytoarchitectonic delineation of the ventral lateral thalamic region in the monkey. *Brain Res* 1983a, 286 (3): 219-235
- Asselin MC, Soghomonian JJ, Cote PY, Parent A. Striatal changes in preproenkephalin mRNA levels in parkinsonian monkeys. *Neuroreport* 1994, 5(16): 2137-2140
- Augood SJ, Emson PC, Mitchell IJ, Boyce S, Clarke CE, Crossman AR. Cellular localisation of enkephalin gene expression in MPTP-treated cynomolgus monkeys. *Brain Res Mol Brain Res* 1989, 6 (1): 85-92
- Avidor-Reiss T, Bayewitch M, Levy R, Matus-Leibovitch N, Nevo I, Vogel Z. Adenylylcyclase supersensitization in mu-opioid receptor-transfected Chinese hamster ovary cells following chronic opioid treatment. *J Biol Chem* 1995, 270 (50): 29732-29738
- Aziz TZ, Peggs D, Agarwal E, Sambrook MA, Crossman AR. Subthalamic nucleotomy alleviates parkinsonism in the 1-methyl-4-phenyl-1,2,3,6-tetrahydropyridine (MPTP)-exposed primate. *Br J Neurosurg* 1992, 6: 575-582
- Aziz TZ, Peggs D, Sambrook MA, Crossman AR. Lesion of the subthalamic nucleus for the alleviation of 1-methyl-4-phenyl-1,2,3,6-tetrahydropyridine (MPTP)-induced parkinsonism in the primate. *Mov Dis* 1991, 6(4): 288-292
- Azmita EC, Gannon PJ. The primate serotonergic system: A review of human and animal studies and a report on *Macaca fascicularis*. In: Fahn S, editor. *Advances in Neurology*, New York: Raven Press, 1986, 43: 407-468
- Bakay RA, Fiandaca MS, Barrow DL, Schiff A, Collins DC. Preliminary report on the use of fetal tissue transplantation to correct MPTP-induced Parkinson-like syndrome in primates. *Appl Neurophysiol* 1985, 48 (1-6): 358-361
- Ballard PA, Tetrad JW, Langston JW. Permanent human parkinsonism due to 1-methyl-4-phenyl-1,2,3,6-tetrahydropyridine (MPTP): seven cases. *Neurology* 1985, 35 (7): 949-956
- Barbeau A. High-level levodopa therapy in severely akinetic parkinsonism patients: twelve years later. In: Rinne VK, Klinger M, Stamm G, editors. *Parkinson's disease: current progress, problems and management*. Amsterdam: Elsevier, 1980, 229-239
- Barbeau A. L-dopa therapy in Parkinson's disease - a critical review of nine years experience. *Can Med Assoc J* 1969, 101: 791-800
- Barbeau A. The clinical physiology of side effects in long-term L-dopa therapy. *Adv Neurol* 1974, 5: 347-365

- Barbeau A, Cloutier T, Roy M, Plasse L, Paris S, Poirier J. Ecogenetics of Parkinson's disease: 4-hydroxylation of debrisoquine. *Lancet* 1985, 2 (8466): 1213-1216
- Barbeau A, Roy M, Bernier G, Campanella G, Paris S. Ecogenetics of Parkinson's disease: prevalence and environmental aspects in rural areas. *Can J Neurol Sci* 1987, 14 (1): 36-41
- Bare LA, Mansson E, Yang DM. Expression of two variants of the human mu opioid receptor mRNA in SK-N-SH cells and human brain. *FEBS Lett* 1994, 354: 213-216
- Baron MS, Vitek JL, Bakay RAE, Green J, Kaneoke Y, Hashimoto T, Turner RS, Woodard JL, Cole SA, McDonald WM, DeLong MR. Treatment of advanced Parkinson's disease by posterior GPi pallidotomy: 1 year results of a pilot study. *Ann Neurol* 1996, 40(3): 355-366
- Bateman DN, Rawlins MD, Simpson JM. Extrapyramidal reactions to prochlorperazine and haloperidol in the United Kingdom. *Q J Med* 1986, 59 (230): 549-556
- Bayer SA, Altman J. Directions in neurogenetic gradients and patterns of anatomical connections in the telencephalon. *Prog Neurobiol* 1987, 29: 57-106
- Bayer SA. Neurogenesis in the olfactory tubercle and islands of Calleja in the rat. *Int J Dev Neurosci* 1985, 3: 135-147
- Bean AJ, Roth HR. Extracellular dopamine and neurotensin in rat prefrontal cortex in vivo: effects of medial forebrain bundle frequency, stimulation pattern and dopamine autoreceptors. *J Neuroscience* 1991, 11: 2694-2704
- Beaumont A, Metters KM, Rossier J, Hughes J. Identification of a proenkephalin precursor in striatal tissue. *J Neurochem* 1985, 44 (3): 934-940
- Beckett AH, Casey AF. Synthetic analgesics: stereochemical considerations. *J Pharm Pharmacol* 1954, 6: 986-1001
- Beckstead RM. A reciprocal axonal connection between the subthalamic nucleus and the neostriatum in the cat. *Brain Res* 1983a, 275 (1): 137-142
- Beckstead RM. Long collateral branches of substantia nigra pars reticulata axons to the thalamus, superior colliculus and reticular formation in monkey and cat: Multiple retrograde neuronal labeling with fluorescent dyes. *Neuroscience* 1983b, 10: 767-779
- Beckstead RM, Cruz CJ. Striatal axons to the globus pallidus, entopeduncular nucleus and substantia nigra come mainly from separate cell populations in cat. *Neuroscience* 1986, 19 (1): 147-58

- Beckstead RM, Domesick VB, Nauta WJ. Efferent connections of the substantia nigra and ventral tegmental area in the rat. *Brain Res* 1979, 175 (2): 191-217
- Beckstead RM, Frankfurter A. A direct projection from the retina to the intermediate gray layer of the superior colliculus demonstrated by anterograde transport of horseradish peroxidase in monkey, cat and rat. *Exp Brain Res* 1983, 52: 261-268
- Beckstead RM, Kersey KS. Immunohistochemical demonstration of differential substance P-, met-enkephalin-, and glutamic-acid-decarboxylase-containing cell body and axon distributions in the corpus striatum of the cat. *J Comp Neurol* 1985, 232 (4): 481-498
- Bedard P, Parkes JD, Marsden CD. Nomifensine in Parkinson's disease. *Br J Clin Pharmacol* 1977, 4 (2): 187S-190S
- Bedard PJ, Di Paolo T, Falardeau P, Boucher R. Chronic treatment with L-DOPA, but not bromocriptine induces dyskinesia in MPTP-parkinsonian monkeys. Correlation with [3 H]Spiperone binding. *Brain Res* 1986, 379: 294-299
- Benabid AL, Pollak P, Gervason C, Hoffmann D, Gao DM, Hommel M, Perret JE, de Rougemont J. Long-term suppression of tremor by chronic stimulation of the ventral intermediate thalamic nucleus. *Lancet* 1991, 337: 403-406
- Benabid AL, Pollak P, Louveau A, Henry S, de Rougemont J. Combined (thalamotomy and stimulation) stereotactic surgery of the VIM thalamic nucleus for bilateral Parkinson disease. *Appl Neurophysiol* 1987, 50 (1-6): 344-346
- Benabid AL, Pollak P, Seigneuret E, Hoffmann D, Gay E, Perret J. Chronic VIM thalamic stimulation in Parkinson's disease, essential tremor and extra-pyramidal dyskinesias. *Acta Neurochir* 1993, 58: 39-44
- Benitez J, Ladero JM, Jimenez-Jimenez FJ, Martinez C, Puerto AM, Valdivielso MJ, Llerena A, Cobaleda J, Munoz JJ. Oxidative polymorphism of debrisoquine in Parkinson's disease. *J Neurol Neurosurg Psychiatry* 1990, 53 (4): 289-292
- Bennett BD, Bolam JP. Characterization of calretinin-immunoreactive structures in the striatum of the rat. *Brain Res* 1993, 609 (1-2): 137-148
- Bennett JP, Landow ER, Dietrich S, Schuh LA. Suppression of dyskinesias in advanced Parkinson's disease: Moderate daily clozapine doses provide long-term dyskinesia reduction. *Mov Dis* 1994, 9(4): 409-414
- Bennett JP, Landow ER, Schuh LA. Suppression of dyskinesias in advanced Parkinson's disease. *Neurology* 1993, 43: 1551-1555

- Ben-Shachar D, Eshel G, Finberg JP, Youdim MB. The iron chelator desferrioxamine (Desferal) retards 6-hydroxydopamine-induced degeneration of nigrostriatal dopamine neurons. *J Neurochem* 1991, 56 (4): 1441-1444
- Berendse HW, Groenewegen HJ. Organization of the thalamostriatal projections in the rat, with special emphasis on the ventral striatum. *J Comp Neurol* 1990, 299 (2): 187-228
- Berendse HW, Groenewegen HJ. Restricted cortical termination fields of the midline and intralaminar thalamic nuclei in the rat. *Neuroscience* 1991, 42 (1): 73-102
- Berendse HW, Groenewegen HJ, Lohman AHM. Compartmental distribution of ventral striatal neurons projecting to the mesencephalon in the rat. *J Neurosci* 1992, 12: 2079-2103
- Bergman H, Wichmann T, DeLong MR. Reversal of experimental parkinsonism by lesions of the subthalamic nucleus. *Science* 1990, 249 (4975):1436-1438
- Berman YL, Juliano L, Devi LA. Purification and characterization of a dynorphin-processing endopeptidase. *J Biol Chem* 1995, 270 (40): 23845-23850
- Besson MJ, Graybiel AM, Nastuk MA. [³H] SCH 23390 binding to dopamine D1 receptors in the basal ganglia of the cat and primate: delineation of striosomal compartments and pallidal and nigral subdivisions. *Neuroscience* 1988, 26(1): 101-119
- Bevan P. Repeated apomorphine treatment causes behavioural supersensitivity and dopamine D2 receptor hyposensitivity. *Neurosci Lett* 1983, 25: 185-189
- Blanchet PJ, Calon F, Martel JC, Bedard PJ, Di Paolo T, Walters RR, Piercey MF. Continuous administration decreases and pulsatile administration increases behavioral sensitivity to a novel dopamine D2 agonist (U-91356A) in MPTP-exposed monkeys. *J Pharmacol Exp Ther* 1995, 272 (2): 854-859
- Bloom F, Segal D, Ling N, Guillemin R. Endorphins: profound behavioural effects in rats suggest new etiological factors in mental illness. *Science* 1976, 194: 630-632
- Bloom FE. The endorphins: A growing family of pharmacologically pertinent peptides. *Ann Rev Pharmacol Toxicol* 1983, 22: 151-170
- Blum I, Munitz H, Shalev A, Roberts E. Naloxone may be beneficial in the treatment of tardive dyskinesia. *Clin Neuropharmacol* 1984, 7 (3): 265-267
- Bocchetta A, Corsini GU. Parkinson's disease and pesticides. *Lancet* 1986, 2 (8516): 1163

- Bonifati V, Fabrizio E, Cipriani R, Vanacore N, Meco G. Buspirone in levodopa-induced dyskinesias. *Clin Neuropharmacol* 1994, 17 (1):73-82
- Boraud T, Bezard E, Bioulac B, Gross C. High frequency stimulation of the internal globus pallidus (GPi) simultaneously improves parkinsonian symptoms and reduces the firing frequency of GPi neurons in the MPTP-treated monkey. *Neurosci Lett* 1996, 215(1): 17-20
- Bouyer JJ, Park DH, Joh TH, Pickel VM. Chemical and structural analysis in the relation between cortical inputs and tyrosine hydroxylase-containing terminals in the rat neostriatum. *Brain Res* 1984, 302: 267-275
- Boyce S, Kelly E, Reavill C, Jenner P, Marsden CD. Repeated administration of N-methyl-4-phenyl 1,2,5,6-tetrahydropyridine to rats is not toxic to striatal dopamine neurones. *Biochem Pharmacol* 1984, 33 (11): 1747-1752
- Bracha HS, Shults C, Glick SD, Kleinman JE. Spontaneous asymmetric circling behavior in hemi-parkinsonism, a human equivalent of the lesioned-circling rodent behavior. *Life Sci* 1987, 40 (11): 1127-1130
- Bradbury AJ, Costall B, Domeney AM, Testa B, Jenner PG, Marsden CD, Naylor RJ. The toxic actions of MPTP and its metabolite MPP⁺ are not mimicked by analogues of MPTP lacking an N-methyl moiety. *Neurosci Lett* 1985, 61: 121-126
- Breese GR, Chase TN, Kopin IJ. Metabolism of tyramine-³H and octopamine-³H by rat brain. *Biochem Pharmacol* 1969, 18 (4): 863-869
- Breese GR, Traylor TD. Effect of 6-hydroxydopamine on brain norepinephrine and dopamine evidence for selective degeneration of catecholamine neurons. *J Pharmacol Exp Ther* 1970, 174 (3): 413-420
- Breslin MB, Lindberg I, Benjannet S, Mathis JP, Lazure C, Seidah NG. Differential processing of proenkephalin by prohormone convertases 1(3) and 2 and furin. *J Biol Chem* 1993, 268 (36): 27084-27093
- Brog JS, Salyapongse A, Deutch AY, Zahm DS. The patterns of afferent innervation of the core and shell in the 'accumbens' part of the rat ventral striatum: immunohistochemical detection of retrogradely transported fluoro-gold. *J Comp Neurol* 1993, 338 (2): 255-278
- Brogden RN, Carmine AA, Heel RC, Speight TM, Avery GS. Domperidone. A review of its pharmacological activity, pharmacokinetics and therapeutic efficacy in the symptomatic treatment of chronic dyspepsia and as an antiemetic. *Drugs* 1982, 24 (5): 360-400

- Brooks DJ, Ibanez V, Sawle GV, Playford ED, Quinn N, Mathias CJ, Lees AJ, Marsden CD, Bannister R, Frackowiak RS. Striatal D2 receptor status in patients with Parkinson's disease, striatonigral degeneration, and progressive supranuclear palsy, measured with ^{11}C -raclopride and positron emission tomography. *Ann Neurol* 1992, 31 (2): 184-192
- Brooks DJ, Torjanski N, Burn DJ. Ropinirole in the symptomatic treatment of Parkinson's disease. *J Neural Transm Suppl* 1995, 45: 231-238
- Brotchie JM, Crossman AR. D- ^3H aspartate and ^{14}C GABA uptake in the basal ganglia of rats following lesions in the subthalamic region suggest a role for excitatory amino acid but not GABA-mediated transmission in subthalamic nucleus efferents. *Exp Neurol* 1991, 113 (2): 171-181
- Brotchie JM, Mitchell IJ, Sambrook MA, Crossman AR. Alleviation of parkinsonism by antagonism of excitatory amino acid transmission in the medial segment of the globus pallidus in rat and primate. *Mov Dis* 1991, 6: 133-138
- Buchwald A, Price DD, Vernon L, Hull CD. Caudate intracellular response to thalamic and cortical inputs. *Exp Neurol* 1973, 38: 311
- Bucy JC, Case TJ. Athetosis II: surgical treatment of unilateral athetosis. *Arch Neurol Psychiatr* 1937, 37: 983
- Bunzow JR, Saez C, Mortrud M, Bouvier C, Williams JT, Low M, Grandy DK. Molecular cloning and tissue distribution of a putative member of the rat opioid receptor gene family that is not a mu, delta or kappa opioid receptor type. *FEBS Lett* 1994, 347 (2-3): 284-288
- Burns RS, Chiueh CC, Markey SP, Ebert MH, Jacobowitz DM, Kopin IJ. A primate model of parkinsonism: Selective destruction of dopaminergic neurons in the pars compacta of the substantia nigra by N-methyl-4-phenyl-1,2,3,6-tetrahydropyridine. *Proc Natl Acad Sci USA* 1983, 80: 4546-4550
- Burton K, Calne DB. Dopamine agonists and Parkinson's disease. *Clin Neurol Neurosurg* 1984, 86(3): 172-177
- Butcher LL, Hodge GK. Postnatal development of acetylcholinesterase in the caudate-putamen nucleus and substantia nigra of rats. *Brain Res* 1976, 106 (2): 223-240
- Caboche J, Vernier P, Julien JF, Rogard M, Mallet J, Besson MJ. Parallel decreases of glutamate acid decarboxylase and proenkephalin mRNA in the rat striatum following chronic treatment with a dopaminergic D1 antagonist and D2 agonist. *J Neurochem* 1991, 56: 428-435
- Cadet JL. The iminodipropionitrile (IDPN)-induced dyskinetic syndrome: behavioral and biochemical pharmacology. *Neurosci Biobehav Rev* 1989, 13 (1): 39-45

- Calne DB, Teychenne PF, Claveria LE. Bromocriptine in Parkinsonism. *BMJ* 1974, 4: 442-444
- Calne DB, Burton K, Beckman J, Martin WR. Dopamine agonists in Parkinson's disease. *Can J Neurol Sci* 1984, 11: 221-224
- Calne DB, Plotkin C, Williams AC, Nutt JG, Neophytides A, Teychenne PF. Long-term treatment of parkinsonism with bromocriptine. *Lancet* 1978, 1 (8067): 735-738
- Calon F, Goulet M, Blanchet PJ, Martel JC, Piercey MF, Bedard PJ, Di Paolo T. Levodopa or D2 agonist induced dyskinesia in MPTP monkeys: correlation with changes in dopamine and GABA_A receptors in the striatopallidal complex. *Brain Res* 1995, 680 (1-2): 43-52
- Campbell K, Bjorklund A. Prefrontal corticostriatal afferents maintain increased enkephalin gene expression in the dopamine-denervated rat striatum. *Eur J Neurosci* 1994, 6 (8): 1371-1383
- Canteras NS, Shammah-Lagnado SJ, Silva BA, Ricardo JA. Afferent connections of the subthalamic nucleus: a combined retrograde and anterograde horseradish peroxidase study in the rat. *Brain Res* 1990, 513 (1): 43-59
- Caparros-Lefebvre D, Blond S, Vermersch P, Pecheux N, Guieu JD, Petit H. Chronic thalamic stimulation improves tremor and levodopa induced dyskinesias in Parkinson's disease. *J Neurol Neurosurg Psychiatry* 1993, 56 (3): 268-273
- Carey RJ. Naloxone reverses L-DOPA induced overstimulation effects in a Parkinson's disease animal model analogue. *Life Sci* 1991, 48: 1303-1308
- Carlsson A, Lindqvist M, Magnusson T. 2,4-Dihydroxyphenylalanine and 5-hydroxytryptophan as reserpine antagonists. *Nature* 1957, 180: 1200
- Carpenter MB, Peter P. Nigrostriatal and nigrothalamic fibres in the rhesus monkey. *J Comp Neurol* 1972, 144: 93-166
- Carpenter MB, Strominger N. Efferent fibres of the subthalamic nucleus in the monkey. A comparison of the efferent projections of the subthalamic nucleus, substantia nigra and globus pallidus. *Am J Anat* 1967, 121: 41-72
- Carpenter MB, Whittier JR, Mettler FA. Analysis of choreoid hyperkinesia in the rhesus monkey. *J Comp Neurol* 1950, 303: 293-332
- Carpenter MB. Ballism associated with partial destruction of the subthalamic nucleus of Luys. *Neurology* 1955, 5: 504
- Carpenter MB. Interconnections between the corpus striatum and brain stem nuclei. In: McKenzie JS, Kemm RE, Wilcock LN, editors. *The basal ganglia: structure and function*. Advances in behavioural biology 29 Plenum Press 1984: 1-68

- Carpenter MB, Baton RR, Carleton SC, Keller JT. Interconnections and organization of pallidal and subthalamic nucleus neurons in the monkey. *J Comp Neurol* 1981, 197 (4): 579-603
- Carpentier AF, Bonnet AM, Vidailhet M, Agid Y. Improvement of levodopa-induced dyskinesia by propranolol in Parkinson's disease. *Neurology* 1996, 46 (6): 1548-1551
- Carroll CB, Hollaway V, Brochie JM, Mitchell IJ. Neurochemical and behavioural investigations of the NMDA receptor-associated glycine site in the rat striatum: functional implications for the treatment of parkinsonian symptoms. *Psychopharmacology* 1995, 119: 55-65
- Carter DA, Fibiger HC. The projections of the entopeduncular nucleus and globus pallidus in rat as demonstrated by autoradiography and horseradish peroxidase histochemistry. *J Comp Neurol.* 1978, 177: 113-124
- Casey DE, Povlsen UJ, Meidahl B, Gerlack J. Neuroleptic-induced tardive dyskinesia and parkinsonism: changes during several years of continuing treatment. *Psychopharmacol Bull* 1986, 22: 250-253
- Ceballos I, Lafon M, Javoy-Agid F, Hirsch E, Nicole A, Sinet PM, Agid Y. Superoxide dismutase and Parkinson's disease. *Lancet* 1990, 335 (8696): 1035-1036
- Chang HT, Kita H, Kitai ST. The fine structure of the rat subthalamic nucleus: an electron microscopic study. *J Comp Neurol.* 1983, 221: 113-123
- Chang HT. Dopamine-acetylcholine interaction in the rat striatum: a dual-labeling immunocytochemical study. *Brain Res Bull* 1988, 21 (2): 295-304
- Chavkin C, James IF, Goldstein A. Dynorphin is a specific endogenous ligand of the kappa opioid receptor. *Science* 1982, 215 (4531): 413-415
- Chen CL, Dionne FT, Roberts JL. Regulation of the pro-opiomelanocortin mRNA levels in rat pituitary by dopaminergic compounds. *Proc Natl Acad Sci USA.* 1983, 80(8): 2211-2215
- Chen Y, Mestek A, Liu J, Hurley JA, Yu L. Molecular cloning and functional expression of a mu-opioid receptor from rat brain. *Mol Pharmacol* 1993, 44 (1): 8-12
- Cheng J, Roques BP, Gacel GA, Huang E, Pasternak GW. Kappa₃ opiate receptor binding in the mouse and rat. *Eur J Pharmacol* 1992, 226 (1): 15-20
- Chesselet MF, Graybiel AM. Striatal neurons expressing somatostatin-like immunoreactivity: evidence for a peptidergic interneuronal system in the cat. *Neuroscience* 1986, 17 (3): 647-671

- Chiba K, Peterson LA, Castagnoli KP, Trevor AJ, Castagnoli N. Studies on the molecular mechanism of bioactivation of the selective nigrostriatal toxin 1-methyl-4-phenyl-1,2,3,6-tetrahydropyridine. *Drug Metab Dispos* 1985, 13 (3): 342-347
- Chiueh CC, Markey SP, Burns RS, Johannessen JN, Jacobowitz DM, Kopin IJ. Neurochemical and behavioral effects of 1-methyl-4-phenyl-1,2,3,6-tetrahydropyridine (MPTP) in rat, guinea pig, and monkey. *Psychopharmacol Bull* 1984, 20 (3): 548-553
- Chomczynski P, Sacchi N. Single-step method of isolation of RNA by acid guanidinium thiocyanate-phenol-chloroform extraction. *Analyt Biochem* 1987, 162: 156-159
- Chritin M, Feuerstein C, Savasta M. Time-course of changes in striatal levels of DA uptake sites, DA D2 receptor and preproenkephalin mRNAs after nigrostriatal dopaminergic denervation in the rat. *Brain Res Mol Brain Res* 1993, 19 (4): 318-322
- Civelli O, Douglass J, Goldstein A, Herbert E. Sequence and expression of the rat prodynorphin gene. *Proc Natl Acad Sci USA*. 1985, 82: 4291-4295
- Clark JA, Lui L, Price M, Hersh B, Edelson M, Pasternak GW. K opiate receptor multiplicity: Evidence for two U50 488-sensitive κ_1 subtypes and a novel κ_3 subtype. *J Pharmacol Exp Ther* 1989, 251: 461-468
- Clarke CE, Sambrook MA, Mitchell IJ, Crossman AR. Levodopa-induced dyskinesia and response fluctuations in primates rendered parkinsonian with 1-methyl-4-phenyl-1,2,3,6-tetrahydropyridine (MPTP). *J Neurol Sci* 1987, 79: 273-280
- Clough CG, Bergmann KJ, Yahr MD. Cholinergic and dopaminergic mechanisms in Parkinson's disease after long-term L-DOPA administration. *Adv Neurol* 1984, 40: 131-140
- Cohen G. The pathobiology of Parkinson's disease: biochemical aspects of dopamine neuron senescence. *J Neural Transm* 1983, 19: 89-103
- Cohen GA, Doze VA, Madison DV. Opioid inhibition of GABA release from presynaptic terminals of rat hippocampal interneurons. *Neuron* 1992, 9 (2): 325-335
- Collingridge GL, Davis J. Actions of substance P and opiates in the rat substantia nigra. *Neuropharmacology* 1982, 21: 715-719
- Cole DG, Kobierski LA, Konradi C, Hyman SE. 6-hydroxydopamine lesions of rat substantia nigra up-regulate dopamine-induced phosphorylation of the cAMP-response element-binding protein in striatal neurons. *Proc Natl Acad Sci USA* 1994, 91: 9631-9635

- Comb M, Birnberg NC, Seasholtz A, Herbert E, Goodman HM. A cyclic AMP- and phorbol ester-inducible DNA element. *Nature* 1986, 323: 353-356
- Comb M, Mermod N, Hyman SE, Pearlberg J, Ross ME. Proteins bound at adjacent DNA elements act synergistically to regulate human proenkephalin cAMP inducible transcription. *EMBO J.* 1988, 7: 3793-3805
- Comb M, Seeburg PH, Adelman J, Eiden L, Herbert E. Primary structure of the human Met- and Leu-enkephalin precursor and its mRNA. *Nature* 1982, 295 (5851): 663-666
- Cools AR, Jaspers R, Schwarz M, Sontag KH, Vrijmoed-de Vries M, van der Bercken J. Basal ganglia and switching programs. In: McKenzie JS, Kemm RE, Wilcock LN, editors. *The Basal Ganglia. Advances in Behavioural Biology* 1984, 27: 513-544
- Cooper DR, Marrel C, Testa B, van de Waterbeemd H, Quinn N, Jenner P, Marsden CD. L-Dopa methyl ester: a candidate for chronic systemic delivery of L-Dopa in Parkinson's disease. *Clin Neuropharmacol* 1984, 7 (1): 89-98
- Cooper ERA. The development of the substantia nigra. *Brain* 1946, 69: 22-33
- Cooper IS, Bravo GJ. Anterior choroidal artery occlusion, chemopallidectomy in parkinsonism: a consecutive series of 700 operations. In: Fields WS, editor. *Pathogenesis and treatment of parkinsonism. Springfield (III): Thomas* 1985, 325-363
- Corbett AD, Paterson SJ, McKnight AT, Magnan J, Kosterlitz HW. Dynorphin₁₋₈ and dynorphin₁₋₉ are ligands for the kappa-subtype of opiate receptor. *Nature* 1982, 299 (5878): 79
- Costa E, Mocchetti I, Supattapone S, Snyder SH. Opioid peptide biosynthesis: enzymatic selectivity and regulatory mechanisms. *FASEB* 1987, 1 (1): 16-20
- Cote TE, Felder R, Kebejian JW, Sekura RD, Reisine T, Affolter HU. D2 dopamine receptor-mediated inhibition of pro-opiomelanocortin synthesis in rat intermediate lobe. Abolition by pertussis toxin or activators of adenylate cyclase. *J Biol Chem* 1986, 261 (10): 4555-4561
- Cotzias GC, Papavasiliou PS, Gellene R. Modification of parkinsonism: chronic treatment with L-dopa. *N Engl J Med* 1969, 280: 337-345
- Cotzias GC, Papavasiliou PS, Tolosa ES, Mendez JS, Bell-Midura M. Treatment of Parkinson's disease with aporphines. Possible role of growth hormone. *N Engl J Med* 1976, 294 (11): 567-572
- Cotzias GC, Van Woert MH, Schiffer LM. Aromatic amino acids and modification of parkinsonism. *N Engl J Med* 1967, 276 (7): 374-379

- Cowan RL, Wilson CJ, Emson P, Heizmann CW. Parvalbumin-containing GABAergic interneurons in the rat neostriatum. *J Comp Neurol* 1990, 302: 197-205
- Crossman AR, Clarke CE, Boyce S, Robertson RG, Sambrook MA. MPTP-induced parkinsonism in the monkey: Neurochemical pathology, complications of treatment and pathophysiological mechanisms. *Can J Neurol Sci* 1987, 14: 428-435
- Crossman AR, Mitchell IJ, Sambrook MA, Jackson A. Chorea and myoclonus in the monkey induced by gamma-aminobutyric acid antagonism in the lentiform complex: the site of drug action and a hypothesis for the neural mechanism of chorea. *Brain* 1988, 111: 1211-1233
- Crossman AR, Sambrook MA, Jackson A. Experimental hemiballismus in the baboon produced by injection of a gamma-aminobutyric acid antagonist into the basal ganglia. *Neurosci Lett* 1980, 20: 369-372
- Crossman AR, Sambrook MA, Jackson A. Experimental hemichorea/hemiballismus in the monkey. Studies on the intracerebral site of action in a drug-induced dyskinesia. *Brain* 1984, 107, 579-596
- Crossman AR. A hypothesis on the pathophysiological mechanisms that underlie levodopa- or dopamine agonist-induced dyskinesias in Parkinson's disease: Implications for future strategies in treatment. *Mov Dis* 1990, 5(2): 100-108
- Crossman AR. Primate models of dyskinesia: the experimental approach to the study of basal ganglia-related involuntary movement disorders. *Neuroscience* 1987, 21: 1-40
- Cuello AC, Paxinos G. Evidence for a long leu-enkephalin striopallidal pathway in the rat brain. *Nature* 1978, 271: 178-180
- Damier P, Hirsch EC, Agid Y, Graybiel AM. Topographical progression of Parkinson's disease in the substantia nigra. *Mov Dis* 1996, 11 (1): Abs P603: 163
- Date I, Ohmoto T. Neural transplantation and trophic factors in Parkinson's disease: Special reference to chromaffin cell grafting, NGF support from pretranshectral nerve, and encapsulated dopamine-secreting cell grafting. *Exp Neurol* 1996, 137 (2): 333-344
- Davis TL, Roznoski M, Burns RS. Acute effects of COMT inhibition on L-DOPA pharmacokinetics in patients treated with carbidopa and selegiline. *Clin Neuropharmacol* 1995, 18 (4): 333-337
- Davis TL, Roznoski M, Burns RS. Effects of tolcapone in Parkinson's patients taking L-dihydroxyphenylalanine/carbidopa and selegiline. *Mov Dis* 1995, 10 (3): 349-351
- De Ceballos ML, Fernandez A, Jenner P, Marsden CD. Parallel alterations in Met-enkephalin and substance P levels in medial globus pallidus in Parkinson's disease patients. *Neurosci Lett* 1993, 160 (2): 163-166

- Del Fiacco M, Paxinos G, Cuello AC. Neostriatal enkephalin-immunoreactive neurones project to the globus pallidus. *Brain Res* 1982, 231 (1): 1-17
- De Olmos JS, Ingram WR. The projection field of the stria terminalis in the rat brain: An experimental study. *J Comp Neurol* 1972, 146: 304-334
- DeLong MR, Georgopoulos AP, Crutcher MD. Cortico-basal ganglia relations and coding of motor performance. *Exp Brain Res* 1983, 7: 30-40
- DeLong MR, Georgopoulos AP. Motor functions of the basal ganglia as revealed by studies of single activity in the behaving primate. *Adv Neurol* 1979, 24: 131-140
- DeLong MR, Crutcher MD, Georgopoulos AP. Primate globus pallidus and subthalamic nucleus: functional organization. *J Neurophysiol* 1985, 53 (2): 530-543
- DeLong MR, Georgopoulos AP, Crutcher MD, Mitchell SJ, Richardson RT, Alexander GE. Functional organization of the basal ganglia: contributions of single-cell recording studies. *Ciba Found Symp* 1984, 107: 64-82
- Deniau JM, Chevalier G. The lamellar organisation of the rat substantia nigra pars reticulata: distribution of projections neurons. *Neuroscience* 1992, 46: 361-377
- Deutch AY, Cameron DS. Pharmacological characterization of dopamine systems in the nucleus accumbens core and shell. *Neuroscience* 1992, 46 (1): 49-56
- De Vito JL, Anderson ME. An autoradiographic study of efferent connections of the globus pallidus in *Macaca mulatta*. *Exp Brain Res* 1982, 46 (1): 107-117
- Dexter DT, Carter CJ, Wells FR, Javoy-Agid F, Agid Y, Lees A, Jenner P, Marsden CD. Basal lipid peroxidation in substantia nigra is increased in Parkinson's disease. *J Neurochem* 1989, 52 (2): 381-389
- Di Chiara G, Imperato A. Opposite effects of mu and kappa opiate agonists on dopamine release in the nucleus accumbens and in the dorsal caudate of freely moving rats. *J Pharmacol Exp Ther* 1988, 244: 1067-1080
- Di Figlia M, Aronin N. Ultrastructural features of immunoreactive somatostatin neurons in the rat caudate nucleus. *J Neurosci* 1982, 2 (9): 1267-1274
- Di Mauro S. Mitochondrial involvement in Parkinson's disease: the controversy continues. *Neurology* 1993, 43 (11): 2170-2172
- Dogali M, Fazzini E, Kolodny E, Eidelberg D, Sterio D, Devinsky D, Bevic A. Stereotatic ventral pallidotomy for Parkinson's disease. *Neurology* 1995, 45: 753-761

- Dolphin AC, Jenner P, Sawaya CB, Marsden CD, Testa B. The effect of bromocriptine on locomotor activity and cerebral catecholamines in rodents. *J Pharm Pharmacol* 1977, 29: 727-734
- Doucet G, Descarries L, Garcia S. Quantification of dopamine innervation in adult rat neostriatum. *Neuroscience* 1986, 19(2): 427-445
- Douglass J, McKinzie AA, Pollock KM. Identification of multiple DNA elements regulating basal and protein kinase A-induced transcriptional expression of the rat prodynorphin gene. *Mol Endocrinol* 1994, 8: 333-344
- Douglass J, McMurray CT, Garrett JE, Adelman JP, Calavetta L. Characterization of the rat prodynorphin gene. *Mol Endocrinol* 1989, 3 (12): 2070-2078
- Dovosin RC, Yahr MD. Encephalitis and parkinsonism. *Arch Neurology* 1965, 12: 227-239
- Dray A, Davis J, Oakley NR, Tongroach P, Vellucci S. The dorsal and medial raphe projections to the substantia nigra in the rat: Electrophysiological, biochemical and behavioural observations. *Brain Res* 1978, 151: 431-442
- Drouin J, Chamberland M, Charron J, Jeannotte L, Nemer M. Structure of the rat pro-opiomelanocortin (POMC) gene. *FEBS Lett* 1985, 193 (1): 54-58
- Dube L, Smith AD, Bolam JP. Identification of synaptic terminals of thalamic or cortical origin in contact with distinct medium-size spiny neurons in the rat neostriatum. *J Comp Neurol* 1988, 267: 455-471
- Duggan MJ, Stephenson FA. Biochemical evidence for the existence of gamma-aminobutyrateA receptor iso-oligomers. *J Biol Chem* 1990, 265 (7): 3831-3835
- Dupuy A, Lindberg I, Zhou Y, Akil H, Lazure C, Chretien M, Seidah NG, Day R. Processing of prodynorphin by the prohormone convertase PC1 results in high molecular weight intermediate forms. Cleavage at a single arginine residue. *FEBS Lett* 1994, 337 (1): 60-65
- Durif F, Vidailhet M, Bonnet AM, Blin J, Agid Y. Levodopa-induced dyskinesias are improved by fluoxetine. *Neurology* 1995, 45 (10): 1855-1858
- Duvoisin RC. Cholinergic-anticholinergic antagonism in parkinsonism. *Arch Neurol* 1967, 17 (2): 124-36
- Eblen F, Graybiel AM. Highly restricted origin of prefrontal cortical inputs to striosomes in the macaque monkey. *J Neurosci* 1995, 15 (9): 5999-6013

- Ebmeier KP, Mutch WJ, Calder SA, Crawford JR, Stewart L, Besson JO. Does idiopathic parkinsonism in Aberdeen follow intrauterine influenza? *J Neurol Neurosurg Psychiatry* 1989, 52 (7): 911-913
- Emson PC, Arregui A, Clement-Jones V, Sandberg BE, Rossor M. Regional distribution of methionine-enkephalin and substance P-like immunoreactivity in normal human brain and in Huntington's disease. *Brain Res* 1980, 199 (1): 147-160
- Engber TM, Susel Z, Kuo S, Gerfen CR, Chase TN. Levodopa replacement therapy alters enzyme activities in striatum and neuropeptide content in striatal output neurons of 6-hydroxydopamine lesioned rats. *Brain Res* 1991, 552: 113-118
- Ericsson AD. Potentiation of the L-Dopa effect in man by the use of catechol-O-methyltransferase inhibitors. *J Neurol Sci* 1971, 14 (2): 193-197
- Errami M, Nicoullon A. Development of a micromethod to study the Na⁺-independent L-[³H]glutamic acid binding to rat striatal membranes. II. Effects of selective striatal lesions and deafferentations. *Brain Res* 1986, 366 (1-2): 178-86
- Fahn S. The tardive syndromes: Phenomenology, concepts on pathology and treatment. In: Fahn S, Marsden CD, Jankovic J, editors. A comprehensive review of movement disorders for the clinical practitioner. 1994, 141-181
- Fahn S, Cote LJ, Snider SR, Barrett RE, Isgreen WP. The role of bromocriptine in the treatment of parkinsonism. *Neurology* 1979, 29 (8): 1077-1083
- Fallon JH, Moore RY. Catecholamine innervation of the basal forebrain. VI. Topography of the dopamine projection to the basal forebrain and neostriatum. *J Comp Neurol* 1979, 180: 545-580
- Fearnley JM, Lees AJ. Striatonigral degeneration. A clinicopathological study. *Brain* 1990, 113 (6): 1823-1842
- Feger J, Crossman AR. Identification of different subpopulations of neostriatal neurones projecting to globus pallidus or substantia nigra in the monkey: a retrograde fluorescence double-labelling study. *Neurosci Lett* 1984, 49 (1-2): 7-12
- Figueredo-Cardenas G, Anderson KD, Chen Q, Veenman CL, Reiner A. Relative survival of striatal projection neurons and interneurons after intrastriatal injection of quinolinic acid in rats. *Exp Neurol* 1994, 129 (1): 37-56
- Flaherty AW, Graybiel AM. Output architecture of the primate putamen. *J Neuroscience* 1993, 13(8): 3222-3237
- Folkerth RD, Durso R. Survival and proliferation of nonneural tissues, with obstruction of cerebral ventricles, in a parkinsonian patient treated with fetal allografts. *Neurology* 1996, 46 (5): 1219-1225

- Fonne-Pfister R, Bargetzi MJ, Meyer UA. MPTP, the neurotoxin inducing Parkinson's disease, is a potent competitive inhibitor of human and rat cytochrome P450 isozymes (P450bufI, P450db1) catalyzing debrisoquine 4-hydroxylation. *Biochem Biophys Res Commun* 1987, 148 (3): 1144-1150
- Fonnum F, Gottesfeld Z, Grofova I. Distribution of glutamate decarboxylase, choline acetyl-transferase and aromatic amino acid decarboxylase in the basal ganglia of normal and operated rats. Evidence for striatopallidal, striatoentopeduncular and striatonigral GABAergic fibres. *Brain Res* 1978, 143 (1): 125-138
- Fonnum F, Paulsen RE. Comparison of transmitter amino acid levels in rat globus pallidus and neostriatum during hypoglycemia or after treatment with methionine sulfoximine or gamma-vinyl gamma-aminobutyric acid. *J Neurochem* 1990, 54 (4) 1253-1257
- Forno LS, DeLanney LE, Irwin I, Langston JW. Similarities and differences between MPTP-induced parkinsonism and Parkinson's disease Neuropathologic considerations. In: Narabayashi H, Nagatsu T, Yanagisawa N, Mizuno Y, editors. *Parkinson's disease from basic research to treatments. Advances in Neurology* 1993, 60 Chapter 101: 600-608
- Forno LS, DeLanney LE, Irwin I, Langston JW, Ricaurte GA. Locus coeruleus lesions and eosinophilic inclusions in MPTP-treated monkeys. *Ann Neurology* 1986, 20: 449-445
- Forno LS, Langston JW, DeLanney LE, Irwin I. An electron microscopic study of MPTP-induced inclusion bodies in an old monkey. *Brain Res* 1988, 448: 150-157
- Franceschi M, Cecchetto R, Panerai AE. Plasma beta-endorphin and beta-lipotrophin in patients with Parkinson's disease. *Clinical Neuropharmacology* 1986, 9: 549-555
- Francois C, Yelnik J, Percheron G, Tande D. Calbindin D-28k as a marker for the associative cortical territory of the striatum in macaque. *Brain Res* 1994, 633 (1-2): 331-336
- Frayne SE, Mitchell IJ, Sharp PT, Sambrook MA, Crossman AR. Distribution of enkephalin gene in the striatum of the parkinsonian primate: implications for dopamine agonist induced dystonia. *Mol Neuropharmacol* 1991, 1: 53-58
- Freed WJ. Functional brain tissue transplantation: reversal of lesion-induced rotation by intraventricular substantia nigra and adrenal medulla grafts, with a note on intracranial retinal grafts. *Biol Psychiatry* 1983, 18 (11): 1205-1267
- Freed WJ, Ko GN, Niehoff DL, Kuhar MJ, Hoffer BJ, Olson L, Cannon-Spoor HE, Morihisa JM, Wyatt RJ. Normalization of spiroperidol binding in the denervated rat striatum by homologous grafts of substantia nigra. *Science* 1983, 222: 937-939

- Freund TF, Powell JG, Smith AD. Tyrosine hydroxylase-immunoreactive boutons in synaptic contacts with identified striatonigral neurons, with particular reference to dendritic spines. *Neuroscience* 1984, 13: 1189-1216
- Fried G, Terenius L, Hokfelt T, Goldstein M. Evidence for differential localization of noradrenaline and neuropeptide Y in neuronal storage vesicles isolated from rat vas deferens. *J Neurosci* 1985, 5 (2): 450-458
- Friedman JH, Lannon MC. Clozapine-responsive tremor in Parkinson's disease. *Mov Dis* 1990, 5 (3): 225-229
- Fuchs V, Coper H. Modification of different morphine actions by 6-hydroxydopamine and 6-hydroxydopamine plus desmethylinipramine. *Psychopharmacol* 1980, 67 (2): 181-188
- Fukuda K, Kato S, Morikawa H, Shoda T, Mori K. Functional coupling of the delta-, mu-, and kappa-opioid receptors to mitogen-activated protein kinase and arachidonate release in Chinese hamster ovary cells. *J Neurochem* 1996, 67 (3): 1309-1316
- Futami T, Takakusaki K, Kitai ST. Glutamatergic and cholinergic inputs from the pedunculopontine tegmental nucleus to dopamine neurons in the substantia nigra pars compacta. *Neurosci Res* 1995, 21 (4): 331-342
- Fuxe K, Agnati L. Two principle modes of electrochemical communication in the brain: volume versus wiring transmission. In: Fuxe K, Agnati L, editors. *Volume transmission in the brain: Novel mechanisms for neural transmission*, New York Raven Press, 1991: 1-9
- Gancher ST, Nutt JG, Woodward WR. Peripheral pharmacokinetics of levodopa in untreated, stable, and fluctuating parkinsonian patients. *Neurology* 1987, 37 (6): 940-944
- Gannon RL, Terrian DM. Presynaptic modulation of glutamate and dynorphin release by excitatory amino acids in the guinea-pig hippocampus. *Neuroscience* 1991a, 41 (2-3): 401-410
- Gannon RL, Terrian DM. U-50,488H inhibits dynorphin and glutamate release from guinea pig hippocampal mossy fiber terminals. *Brain Res* 1991b, 548 (1-2): 242-247
- Gasbarri A, Campana E, Pacitti C, Hajdu F, Tombol T. Organization of the projections from the ventral tegmental area of Tsai to the hippocampal formation in the rat. *J Hirnforsch* 1991, 32 (4): 429-437
- Gauchy C, Desban M, Krebs MO, Glowinski J, Kemel ML. Role of dynorphin-containing neurons in the presynaptic inhibitory control of the acetylcholine-evoked release of dopamine in the striosomes and the matrix of the cat caudate nucleus. *Neuroscience* 1991, 41 (2-3): 449-458

- Geminiani G, Fetoni V, Genitrini S, Giovannini P, Tamma F, Caraceni T. Carbergoline in Parkinson's disease complicated by motor fluctuations. *Mov Dis* 1996, 11(5): 495-500
- Gerfen CR. The neostriatal mosaic: multiple levels of compartmental organization. *Trends Neurosci* 1992, 15 (4): 133-139
- Gerfen CG, Young III WS. Distribution of striatonigral and striatopallidal peptidergic neurons in both patch and matrix compartments: an in situ hybridisation histochemistry and fluorescent retrograde tracing study. *Brain Res* 1988, 460: 161-167
- Gerfen CR, McGinty JF, Young III WS. Dopamine differentially regulates dynorphin, substance P and enkephalin expression in striatal neurons: In situ hybridisation histochemical analysis. *J Neurosci* 1991, 11: 1016-1031
- Gerfen CR, Staines WA, Arbuthnott GW, Fibiger HD. Crossed connections of the substantia nigra in the rat. *J Comp Neurol* 1982, 207: 283-303
- Gerfen CR. The neostriatal mosaic. I. Compartmental organisation of projections from the striatum to the substantia nigra in the rat. *J Comp Neurol*. 1985: 236, 454-476
- Gerfen CR. The neostriatal mosaic: Compartmentalization of corticostriatal input and striatonigral output system. *Nature* 1984, 311: 461-464
- Gerfen CR, Engber TM, Mahan LC, Susel Z, Chase TN, Monsma FJ Jr, Sibley DR D1 and D2 dopamine receptor-regulated gene expression of striatonigral and striatopallidal neurons *Science* 1990, 250 (4986): 1429-1432
- Gibb WR, Lees AJ. Anatomy, pigmentation, ventral and dorsal subpopulations of the substantia nigra, and differential cell death in Parkinson's disease. *J Neurol Neurosurg Psychiatry* 1991, 54 (5): 388-396
- Gibb WR, Lees AJ. The relevance of the Lewy body to the pathogenesis of idiopathic Parkinson's disease. *J Neurol Neurosurg Psychiatry* 1988, 51: 745-752
- Gimenez-Amaya JM, Graybiel AM. Compartmental origins of the striatopallidal projection in the primate. *Neuroscience* 1990, 34(1): 111-126
- Gnanalingham KK, Robertson RG. Chronic continuous and intermittent L-3,4-dihydroxyphenylalanine treatments differentially affect basal ganglia function in 6-hydroxydopamine lesioned rats: an autoradiographic study using [³H] Flunitrazepam. *Neuroscience* 1993, 57: 673-681
- Golbe LI. The genetics of Parkinson's disease: a reconsideration. *Neurology* 1990, 40 (10): 7-14

- Golding D, Bayraktaroglu E. Exocytosis of secretory granules. A probable mechanism for the release of neuromodulators in invertebrates neuropil. *Experientia* 1984, 40: 1277-1280
- Goldman PS, Nauta WJH. An intricately patterned prefronto-caudate projection in the rhesus monkey. *J Comp Neurol* 1977, 171: 369-386
- Goldstein A, Judson BA, Sheehan P. Cellular and metabolic tolerance to an opioid narcotic in mouse brain. *Br J Pharmacol* 1973, 47 (1): 138-140
- Goldstein A, Naidu A. Multiple opioid receptors: ligand selectivity profiles and binding site signatures. *Mol Pharmacol* 1989, 36(2): 265-272
- Gomez-Mancilla B, Bedard PJ. Effect of nondopaminergic drugs on L-DOPA-induced dyskinesias in MPTP-treated monkeys. *Clin Neuropharm* 1993, 16(5): 418-427
- Gonya-Magee T, Anderson ME. An electrophysiological characterization of projections from the pedunclopontine area to entopeduncular nucleus and globus pallidus in the cat. *Exp Brain Res*, 1983: 49 (2): 269-279
- Goulet M, Morisset M, Falardeau P, Bedard PJ, Di Paolo T. *In situ* hybridisation of prodynorphin mRNA in the caudate-putamen of MPTP monkeys: effect of chronic treatment with L-DOPA and with the D2 agonist U91356A. *Society for Neuroscience Abstract* 1996, 22, P89.2
- Graham DG. Catecholamine toxicity: a proposal for the molecular pathogenesis of manganese neurotoxicity and Parkinson's disease. *Neurotoxicology* 1984, 5 (1): 83-95
- Graham WC, Clarke CE, Boyce S, Sambrook MA, Crossman AR, Woodruff GN. Autoradiographic studies in animal models of hemi-parkinsonism reveal dopamine D2 but not D1 receptor supersensitivity. II. Unilateral intra-carotid infusion of MPTP in the monkey (*Macaca fascicularis*). *Brain Res* 1990a, 514 (1): 103-110
- Graham WC, Crossman AR, Woodruff GN. Autoradiographic studies in animal models of hemi-parkinsonism reveal dopamine D2 but not D1 receptor supersensitivity. I. 6-OHDA lesions of ascending mesencephalic dopaminergic pathways in the rat. *Brain Res* 1990b, 514 (1): 93-102
- Graham WC, Robertson RG, Sambrook MA, Crossman AR. Injection of excitatory amino acid antagonists into the medial pallidal segment of a 1-methyl-4-phenyl-1,2,3,6-tetrahydropyridine (MPTP)-treated primate reverses motor symptoms of parkinsonism. *Life Sci* 1990c, 47: PL91-PL97
- Graveland GA, Di Figlia M. The frequency and distribution of medium-sized neurons with indented nuclei in the primate and rodent neostriatum. *Brain Res* 1985, 327: 307-311

- Graybiel AM. Neuropeptides in the basal ganglia. *Res Publ Assoc Res Nerv Ment Dis* 1986, 64: 135-161
- Graybiel AM, Aosaki T, Flaherty AW, Kimura M. The basal ganglia and adaptive motor control. *Science* 1994, 265 (5180): 1826-1831
- Graybiel AM, Ragsdale CW. Histochemically distinct compartments in the striatum of human, monkey and cat demonstrated by acetylcholinesterase staining. *PNAS* 1979, 75: 5723-5726
- Griffiths PD, Sambrook MA, Perry R, Crossman AR. Changes in benzodiazepine and acetylcholine receptors in the globus pallidus in Parkinson's disease. *J Neurol Sci* 1990, 100: 131-136
- Groenewegen HJ, Berendse HW. Connections of the subthalamic nucleus with ventral striatopallidal parts of the basal ganglia in the rat. *J Comp Neurol* 1990, 294 (4): 607-622
- Groenewegen HJ, Berendse HW, Wolters JG, Lohman AH. The anatomical relationship of the prefrontal cortex with the striatopallidal system, the thalamus and the amygdala: evidence for a parallel organization. *Prog Brain Res* 1990, 85: 95-116
- Groenewegen HJ, Russchen FT. Organization of the efferent projections of the nucleus accumbens to pallidal, hypothalamic, and mesencephalic structures: A tracing and immunohistochemical study in the cat. *J Comp Neurol* 1984, 223: 347-367
- Groenewegen HJ, Vermeulen-Van der Zee E, te Kortschot A, Witter MP. Organization of the projections from the subiculum to the ventral striatum in the rat. A study using anterograde transport of *Phaseolus vulgaris* leucoagglutinin. *Neuroscience* 1987, 23 (1): 103-120
- Grofova I, Rinvik E. Cortical and pallidal projections to the nucleus ventralis lateralis thalami. Electron microscopical studies in the cat. *Anat Embryol* 1974, 146: 113-132
- Gudjonsson O, Sanz E, Alvan G, Aquilonius SM, Reviriego J. Poor hydroxylator phenotypes of debrisoquine and S-mephenytoin are not over-represented in a group of patients with Parkinson's disease. *Br J Clin Pharmacol* 1990, 30 (2): 301-302
- Gunne LM, Barany S. Haloperidol-induced tardive dyskinesia in monkeys. *Psychopharmacology* 1976, 50: 237-240
- Gupta M, Felten DL, Gash DM. MPTP alters central catecholamine neurons in addition to the nigrostriatal system. *Brain Res Bull* 1984, 13 (6): 737-742
- Haber S, Elde R. Correlation between Met-enkephalin and substance P immunoreactivity in the primate globus pallidus. *Neuroscience* 1981 6 (7): 1291-1297

- Haber SN, Groenewegen HJ, Grove EA, Nauta WJ. Efferent connections of the ventral pallidum: evidence of a dual striato pallidofugal pathway. *J Comp Neurol* 1985, 235 (3): 322-335
- Haber SN, Watson SJ. The comparative distribution of enkephalin, dynorphin and substance P in the human globus pallidus and basal forebrain. *Neuroscience* 1985, 14 (4): 1011-1024
- Haber SN, Watson SJ. The comparison between enkephalin-like and dynorphin-like immunoreactivity in both monkey and human globus pallidus and substantia nigra. *Life Sci* 1983, 33 (1): 33-36
- Haber SN, Wolfe DP, Groenewegen HJ. The relationship between ventral striatal efferent fibers and the distribution of peptide-positive woolly fibers in the forebrain of the rhesus monkey. *Neuroscience* 1990, 39 (2): 323-338
- Hajji MD, Salin P, Kerkerian-Le Goff L. Chronic dizocilpine maleate (MK-801) treatment suppresses the effects of nigrostriatal dopamine deafferentation on enkephalin but not on substance P expression in the rat striatum. *Eur J Neurosci* 1996, 8 (5): 917-926
- Hamilton WJ, Mossman, HW. Human embryology. Williams and Wilkins, Baltimore. 1972, Chapter 12: 376-378
- Hanaway J, McConnell JA, Netskey MG. Histogenesis of the substantia nigra, ventral tegmental area of Tsai and interpeduncular nucleus: an autoradiographic study of the mesencephalon in the rat. *J Comp Neurol* 1971, 142: 59-73
- Hantraye P, Riche D, Maziere M, Isacson O. A Primate model of Huntington's disease: Behavioural and anatomical studies of unilateral excitotoxic lesions of the caudate-putamen in the baboon. *Experimental Neurology* 1990, 108: 91-104
- Harding AE. Genetic aspects of autosomal dominant late onset cerebellar ataxia. *J Med Genet* 1981, 18 (6): 436-441
- Harding AE. The clinical features and classification of the late onset autosomal dominant cerebellar ataxias. A study of 11 families, including descendants of the 'the Drew family of Walworth'. *Brain* 1982, 105 (1): 1-28
- Hariz MI. Correlation between clinical outcome and size and site of the lesion in computed tomography guided thalamotomy and pallidotomy. *Stereotact Funct Neurosurg* 1990, 54-55: 172-185
- Harris PL. Bromocriptine and hallucinations. *Ann Intern Med* 1984, 101 (1): 149

- Hassler R, Haug P, Nitsch C, Kim JS, Paik K. Effect of motor and premotor cortex ablation on concentrations of amino acids, monoamines, and acetylcholine and on the ultrastructure in rat striatum. A confirmation of glutamate as the specific corticostriatal transmitter. *J Neurochem* 1982, 38 (4): 1087-1098
- Haywood CA, Cowey A. Effects on visual search of lesions of the superior colliculus in infant or adult rats. *Exp Brain Res* 1987, 65: 523-529
- Hazrati LN, Parent A. Contralateral pallidothalamic and pallidotegmental projections in primates: an anterograde and retrograde labeling study. *Brain Res* 1991, 567: 212-223
- Hazrati LN, Parent A. Differential patterns of arborization of striatal and subthalamic fibers in the two pallidal segments in primates. *Brain Res* 1992, 598 (1-2): 311-315
- Hazrati LN, Parent A. Projection from the external pallidum to the reticular thalamic nucleus in the squirrel monkey. *Brain Res* 1991, 550 (1): 142-146
- Hazrati LN, Parent A, Mitchell S, Haber SN. Evidence for interconnections between the two segments of the globus pallidus in primates: a PHA-L anterograde tracing study. *Brain Res* 1990, 533 (1): 171-175
- Heikkila RE, Cabbat FS, Manzino L, Duvoisin RC. Effects of 1-methyl-4-phenyl-1,2,5,6-tetrahydropyridine on neostriatal dopamine in mice. *Neuropharmacology* 1984, 23 (6): 711-713
- Heikkila RE, Duvoisin RC, Finberg JP, Youdim MB. Prevention of MPTP-induced neurotoxicity by AGN-1133 and AGN-1135, selective inhibitors of monoamine oxidase-B. *Eur J Pharmacol* 1985a, 116 (3): 113-117
- Heikkila RE, Hess A, Duvoisin RC. Dopaminergic neurotoxicity of 1-methyl-4-phenyl-1,2,5,6-tetrahydropyridine (MPTP) in the mouse: relationships between monoamine oxidase, MPTP metabolism and neurotoxicity. *Life Sci* 1985b, 36 (3): 231-236
- Heikkila RE, Manzino L, Cabbat FS, Duvoisin RC. Studies on the oxidation of the dopaminergic neurotoxin 1-methyl-4-phenyl-1,2,5,6-tetrahydropyridine by monoamine oxidase B. *J Neurochem* 1985c, 45 (4): 1049-54
- Heimer L, Zahm DS, Churchill L, Kalivas PW, Wohltmann C. Specificity in the projection patterns of accumbal core and shell in the rat. *Neuroscience* 1991, 41 (1): 89-125
- Herkenham MS, Pert CB. Mosaic distribution of opiate receptors, parafascicular projections and acetylcholinesterase in the rat striatum. *Nature* 1981, 291: 415-418

- Herrera-Marschitz M, Christensson-Nylander I, Sharp T, Staines W, Reid T, Hokfelt T, Terenius L, Ungerstedt U. Striato-nigral dynorphin and substance P pathways in the rat II. Functional analysis. *Exp Brain Res* 1986, 64: 193-207
- Herrera-Marschitz M, Hokfelt T, Ungerstedt U, Terenius L. Functional studies with the opioid peptide dynorphin : Acute effects of injections into the substantia nigra reticulata of naive rats. *Life Sci* 1983, 33: 555-558
- Herrera-Marschitz M, Hokfelt T, Ungerstedt U, Terenius L, Goldstein M. Effect of intranigral injections of dynorphin, dynorphin fragments and alpha-neo-endorphin on rotational behavior in the rat. *Eur J Pharmacol* 1984, 102: 213-227
- Herrero MT, Augood SJ, Hirsch EC, Javoy-Agid F, Luquin MR, Agid Y, Obeso JA, Emson PC Effects of L-DOPA on preproenkephalin and preprotachykinin gene expression in the MPTP-treated monkey striatum. *Neuroscience* 1995, 68 (4): 1189-1198
- Hill MP, Brochie JM. Modulation of glutamate release by a k-opioid receptor agonist in rodent and primate striatum. *Eur J Pharmacol* 1995, 281: R1-R2
- Hill MP, Hille CJ, Maneuf YP, Brochie JM. Modulation of glutamate transmission in the basal ganglia by enadoline, a selective kappa-opioid receptor agonist, in the marmoset and rat. In: Ohye O, Kimura M, McKenzie J, editors. *The basal ganglia V* 1996, 165-171
- Hirai T, Nagaseki Y, Kawashima Y, Wada H, Tsukahara Y, Imai S, Ohye C. Large neurons in the thalamic ventrolateral mass in humans and monkeys. *App Neurophysiol* 1982, 45: 245-250
- Hirai T, Ohye C, Nagaseki Y, Matsumara M. Cytometric analysis of the thalamic ventralis intermedius nucleus in humans. *J Neurophysiol* 1989, 61: 478-487
- Hoehn MM, Yahr MD. Parkinsonism: Onset, progression, and mortality. *Neurology* 1967, 17: 427-442
- Hoehn MM. Result of chronic levodopa therapy and its modification by bromocriptine in Parkinson's disease. *Acta Neurol Scand* 1985, 71: 97-106
- Hokfelt T, Ungerstedt U. Specificity of 6-hydroxydopamine induced degeneration of central monoamine neurones: An electron and fluorescence microscopic study with special reference to intracerebral injection on the nigro-striatal dopamine system. *Brain Res* 1973, 60: 269-297
- Holt V. Opioid peptide processing and receptor selectivity. *Ann Rev Pharmacol Toxicol* 1986, 26: 59-77

- Homer DW, Pert A. The actions of opiates in the rat substantia nigra: An electrophysiological analysis. *Peptides* 1983, 4: 603-608
- Hong J, Yang T, Gillin J, Costa E. Effects of long-term administration of antipsychotic drugs on enkephalinergic neurons. *Adv Biochem Psychopharmacol* 1980, 24: 223-232
- Hoover JE, Strick PL. Multiple output channels in the basal ganglia. *Science* 1993, 259: 819-821
- Horikawa S, Takai T, Toyosato M, Takahashi H, Noda M, Kakidani H, Kubo T, Hirose T, Inayama S, Hayashida H, Miyata T, Numa S. Isolation and structural organization of the human preproenkephalin B gene. *Nature* 1983, 306 (5943): 611-614
- Hornykiewicz O. Dopamine (3-hydroxytyramine) and brain function. *Pharmacol rev* 1966, 18 (2): 925-964
- Hornykiewicz O. Imbalance of brain monoamines and clinical disorders. *Prog Brain Res* 1982, 55: 419-29
- Horowski R, Wachtel H. Direct dopaminergic action of lisuride hydrogen maleate, an ergot derivative, in mice. *Eur J Pharmacol* 1976, 36 (2): 373-383
- Horrocks PM, Vicary DJ, Rees JE, Parkes JD, Marsden CD. Anticholinergic withdrawal and benzhexol treatment in Parkinson's disease. *J Neurol Neurosurg Psychiatry* 1973, 36 (6): 936-941
- Howells RD, Kilpatrick DL, Bhatt R, Monahan JJ, Poonian M, Udenfriend S. Molecular cloning and sequence determination of rat preproenkephalin cDNA: sensitive probe for studying transcriptional changes in rat tissues. *Proc Natl Acad Sci U S A* 1984, 81 (23): 7651-7655
- Hubble JP, Koller WC, Cutler NR, Sramek JJ, Friedman J, Goetz C, Ranhosky A, Korts D, Elvin A. Pramipexole in patients with early Parkinson's disease. *Clin Neuropharmacol* 1995, 18 (4): 338-347
- Huerta MF, Weber JT, Rothstein LR, Harting JK. Subcortical connections of area 17 in the tree shrew: an autoradiographic analysis. *Brain Res* 1985, 340 (1): 163-170
- Hughes J. Isolation of an endogenous compound from the brain with pharmacological properties similar to morphine. *Brain Res* 1975a, 88 (2): 295-308
- Hughes J, Smith T, Morgan B, Fothergill L. Purification and properties of enkephalin - the possible endogenous ligand for the morphine receptor. *Life Sci* 1975c, 16 (12): 1753-1758

- Hughes J, Smith TW, Kosterlitz HW, Fothergill LA, Morgan BA, Morris HR. Identification of two related pentapeptides from the brain with potent opiate agonist activity. *Nature* 1975b, 258 (5536): 577-580
- Humpel M, Toda T, Oshino N, Pommerenke G. The pharmacokinetics of lisuride hydrogen maleate in rat, rabbit and rhesus monkey. *Eur J Drug Metab Pharmacokinet* 1981, 6 (3): 207-219
- Huntington's Disease Collaborative Research Group. A novel gene containing a trinucleotide repeat that is expanded and unstable on Huntington's disease chromosomes. *Cell* 1993, 72 (6): 971-983
- Hurd YL, Herkenham M. The human neostriatum shows compartmentalization of neuropeptide gene expression in dorsal and ventral regions: an in situ hybridization histochemical analysis. *Neuroscience* 1995, 64 (3): 571-586
- Hurley KM, Herbet H, Moga MM, Saper CB. Efferent projections of the infralimbic cortex of the rat. *J Comp Neurol* 1991, 308: 249-276
- Ilinsky IA, Jouandest MJ, Goldman-Rakic PS. Organisation of the nigrothalamocortical system in the rhesus monkey. *J Comp Neurol* 1985, 256: 315-330
- Ilinsky IA, Kultas-Ilinsky K. Sagittal cytoarchitectonic maps of the *Macaca mulatta* thalamus with a revised nomenclature of the motor-related nuclei validated by observations on their connectivity. *J Comp Neurol* 1987, 262 (3): 331-364
- Imai H, Steindler DA, Kitai ST. The organisation of divergent axonal projections from the midbrain raphe nuclei in the rat. *J Comp Neurol* 1986, 243: 363-380
- Inagaki S, Parent A. Distribution of enkephalin-immunoreactive neurons in the forebrain and upper brainstem of the squirrel monkey. *Brain Res* 1985, 359 (1-2): 267-80
- Inagaki S, Parent A. Distribution of substance P and enkephalin-like immunoreactivity in the substantia nigra of rat, cat and monkey. *Brain Res Bull* 1984, 13 (2): 319-329
- Inzelberg R, Nisipeanu P, Rabey MJ, Korczyn AD. Long-term tolerability and efficacy of cabergoline, a new long-acting dopamine agonist, in Parkinson's disease. *Mov Dis* 1995, 10 (5): 604-607
- Isacson O, Riche D, Hantraye P, Sofroniew MV, Maziere M. A primate model of Huntington's disease: cross-species implantation of striatal precursor cells to the excitotoxically lesioned baboon caudate-putamen. *Exp Brain Res* 1989, 75 (1): 213-220

- Iverfeldt K, Serfozo P, Diaz Arnesto L, Bartfai T. Differential release of coexisting neurotransmitters: frequency dependence of the efflux of substance P, thyrotropin releasing hormone and [3H]serotonin from tissue slices of rat ventral spinal cord. *Acta Physiol Scand* 1989, 137 (1): 63-71
- Iwahori N. A golgi study on the subthalamic nucleus of the cat. *J Comp Neurol* 1978, 182: 383-398
- Izenwasser S, Buzas B, Cox BM. Differential regulation of adenylyl cyclase activity by mu and delta opioids in rat caudate putamen and nucleus accumbens. *J Pharmacol Exp Ther* 1993, 267 (1): 145-152
- Izzo PN, Bolam JP. Cholinergic synaptic input to different parts of spiny striatonigral neurons in the rat. *J Comp Neurol* 1988, 269 (2): 219-234
- Jaber M, Fournier MC, Bloch B. Reserpine treatment stimulates enkephalin and D2 dopamine receptor gene expression in the rat striatum. *Brain Res Mol Brain Res* 1992, 15 (3-4): 189-194.
- Jaber M, Normand E, Bloch B. Effect of reserpine treatment on enkephalin mRNA level in the rat striatum: an in situ hybridization study. *Brain Res Mol Brain Res* 1995, 32 (1): 156-160
- Jaber M, Tison F, Fournier MC, Bloch B. Differential influence of haloperidol and sulpiride on dopamine receptors and peptide mRNA levels in the rat striatum and pituitary. *Brain Res Mol Brain Res* 1994, 23: 14-20
- Jackson A, Crossman AR. Experimental choreoathetosis produced by injection of a gamma-aminobutyric acid antagonist into the lentiform nucleus in the monkey. *Neurosci Lett* 1984, 46: 41-45
- Jacquet YF, Marks N. The C-fragment of beta-lipotropin: an endogenous neuroleptic or antipsychotogen? *Science* 1976, 194: 632-635
- Jankovic J, Marsden CD. Therapeutic strategies in Parkinson's disease. In: Jankovic J, Tolosa E, editors. *Parkinson's disease and movement disorders* 1988, 45-119
- Jankovic J, Orman J. Tetrabenazine therapy of dystonia, chorea, tics, and other dyskinesias. *Neurology* 1988, 38 (3): 391-394
- Jankovic J, Rohaidy H. Motor, behavioral and pharmacologic findings in Tourette's syndrome. *Can J Neurol Sci* 1987, 14 (3): 541-546
- Javitch JA, Strittmatter SM, Snyder SH. Differential visualization of dopamine and noradrenaline uptake sites in rat brain using ³H-mazindol autoradiography. *J Neuroscience* 1985, 5: 1513-1521

- Javoy-Agid F, Ruberg M, Taquet H, Bokobza B, Agid Y, Gaspar P, Berger B, N'Guyen-Legros J, Alvarez C, Gray F, Escourolle R, Scatton B, Rouquier L. Biochemical neuropathology of Parkinson's disease. In: Hassler RG, Christ JF, editors. *Advances in Neurology* 1984, 40 : 1891-1892
- Jenner P, Dexter DT, Sian J, Schapira AH, Marsden CD. Oxidative stress as a cause of nigral cell death in Parkinson's disease and incidental Lewy body disease. *Ann Neurol* 1992, 32: S82-87
- Jeon BS, Jackson-Lewis V, Burke RE. 6-Hydroxydopamine lesion of the rat substantia nigra: time course and morphology of cell death. *Neurodegeneration* 1995, 4 (2): 131-137
- Jeste DV, Lohr JB, Clarke K, Wyatt RJ. Pharmacological treatment of tardive dyskinesia in the 1980s. *J Clin Psychopharmacol* 1988, 8: 38S-48S
- Jiang HK, McGinty JF, Hong JS. Differential modulation of striatonigral dynorphin and enkephalin by dopamine receptor subtypes. *Brain Res* 1990, 507 (1): 57-64
- Jimenez-Castellanos J, Graybiel AM. Compartmental origins of striatal efferent projections in the cat. *Neuroscience* 1989, 32 (2): 297-321
- Jimenez-Castellanos J, Graybiel AM. Subdivisions of the dopamine-containing A8-A9-A10 complex identified by their differential mesostriatal innervation of striosomes and extrastriosomal matrix. *Neuroscience* 1987b, 23 (1): 223-242
- Jimenez-Castellanos J, Graybiel AM. Subdivisions of the primate substantia nigra pars compacta detected by acetylcholinesterase histochemistry. *Brain Res* 1987a, 437 (2): 349-354
- Johannessen JN, Chiueh CC, Burns RS, Markey SP. Differences in the metabolism of MPTP in the rodent and primate parallel differences in sensitivity to its neurotoxic effects. *Life Sci* 1985, 36 (3): 219-224
- Johnson WG, Hodge SE, Duvoisin R. Twin studies and the genetics of Parkinson's disease: a reappraisal. *Mov Dis* 1990, 5 (3): 187-194
- Jolkkonen J, Jenner P, Marsden CD. L-DOPA reverses altered gene expression of substance P but not enkephalin in the caudate-putamen of common marmosets treated with MPTP. *Brain Res Mol Brain Res* 1995, 32 (2): 297-307
- Jones EG. Some aspects of the organization of the thalamic reticular complex. *J Comp Neurol* 1975, 162 (3): 285-308
- Jongen-Relo AL, Groenewegen HJ, Vroon P. Evidence for a multi-compartmental histochemical organization of the nucleus accumbens in the rat. *J Comp Neurol* 1993, 337: 267-276

- Jurgens U. The efferent and afferent connections of the supplementary motor area. *Brain Res* 1984, 300 (1): 63-81
- Jurna I. Reserpine rigidity in the rat: a model for the analysis of antiparkinson drugs. *Naunyn Schmiedebergs Arch Exp Pathol Pharmacol* 1968, 259 (2): 181
- Kakidani H, Furutani Y, Takahashi H, Noda M, Morimoto Y, Hirose T, Asai M, Inayama S, Nakanishi S, Numa S. Cloning and sequence analysis of cDNA for porcine beta-neo-endorphin/dynorphin precursor. *Nature* 1982, 298 (5871): 245-249
- Kartzinel R, Teychenne P, Gillespie MM. Bromocriptine and levodopa (with or without carbidopa) in parkinsonism. *Lancet* 1976, 2(7980): 272-275
- Kashihara K, Akiyama K, Ishihara T, Shiro Y, Shohmori T. Levodopa but not bromocriptine induces AP-1 and CREB DNA-binding activity in the dopamine-depleted striatum of the rat. *Life Sci* 1996, 58(10): 159-170
- Kawada Y, Ogawa N, Asanuma M, Mori A. Neuropeptide levels in discrete brain regions in the iminodipropionitrile-induced persistent dyskinesia rat model. *Regul Pept* 1995, 55 (1): 103-110
- Kawaguchi Y. Physiological, morphological, and histochemical characterization of three classes of interneurons in rat neostriatum. *J Neurosci* 1993, 13 (11): 4908-4923
- Kawaguchi Y, Wilson CJ, Emson PC. Projection subtypes of rat neostriatal matrix cells revealed by intracellular injection of biocytin. *J Neurosci* 1990, 10 (10): 3421-3438
- Kelley AE, Domesick VB, Nauta WJ. The amygdalostriatal projection in the rat: an anatomical study by anterograde and retrograde tracing methods. *Neuroscience* 1982, 7 (3): 615-630
- Kemp JM, Powell TPS. Cortico-striate projections in the monkey. *Brain* 1970, 93: 525-546
- Kemp JM, Powell TPS. The termination of fibres from the cerebral cortex and thalamus upon dendritic spines in the caudate nucleus: a study with the Golgi method. *Phil Trans R Soc* 1971, 262: 429-439
- Kenny AJ. Regulatory peptide metabolism at cell surfaces: the key role of endopeptidase-24.11. *Biomed Biochim Acta* 1986, 45 (11-12): 1503-1513
- Kieffer BL. Recent advances in molecular recognition and signal transduction of active peptides: receptors for opioid peptides. *Cell Mol Neurobiol* 1995, 15 (6): 615-634

- Kilpatrick IC, Starr MS, Fletcher A, James TA, MacLeod NK. Evidence for a GABAergic nigrothalamic pathway in the rat. I. Behavioural and biochemical studies. *Exp Brain Res* 1980, 40 (1): 45-54
- Kim JS, Hassler R, Haug P, Paik KS. Effect of frontal cortex ablation on striatal glutamic acid level in the rat. *Brain Res* 1977, 132: 370-374
- Kim R, Nakano K, Jayaraman A, Carpenter MB. Projections of the globus pallidus and adjacent structures: an autoradiographic study in the monkey. *J Comp Neurol* 1976, 169 (3): 263-290
- Kincaid AE, Penney JB, Young AB, Newman SW. Evidence for a projection from the globus pallidus to the entopeduncular nucleus in the rat. *Neuroscience Letters* 1991, 128: 121-125
- Kinouchi HW, Pasternak GW. Evidence for kappa, opioid receptor multiplicity in the guinea pig cerebellum. *Eur J Pharmacol* 1991, 207: 135-141
- Kita H, Kitai ST. Parvalbumin-immunoreactive neurons in the rat neostriatum: A light and electron microscopic study. *Brain Res.* 1990, 536: 1-15
- Kita H, Chang HT, Kitai ST. Pallidal inputs to subthalamus: intracellular analysis. *Brain Res* 1983, 264 (2): 255-265
- Kita H, Kitai ST. Efferent projections of the subthalamic nucleus in the rat: light and electron microscopic analysis with the PHA-L method. *J Comp Neurol* 1987, 260 (3): 435-452
- Kitai ST. Anatomy and physiology of the neostriatum. *Adv Biochem Psychopharmacol* 1981, 30: 1-21
- Kitai ST, Kocsis JD, Wood J. Origin and characteristics of the cortico-caudate afferents: An anatomical and electrophysiological study. *Brain Res.* 1976, 118: 137-141
- Klitenick MA, Deutch AY, Churchill L, Kalivas PW. Topography and functional role of dopaminergic projections from the ventral mesencephalic tegmentum to the ventral pallidum. *Neuroscience* 1992, 50: 371-386
- Klockgether T, Turski L. NMDA antagonists potentiate antiparkinsonian actions of L-DOPA in monoamine-depleted rats. *Ann Neurology* 1990, 28: 539-546
- Koller W, Herbst G, Anderson D, Wack R, Gordon J. Quinpirole hydrochloride, a potential anti-parkinsonism drug. *Neuropharmacology* 1987, 26 (8): 1031-1036

- Koller W, Vetere-Overfield B, Gray C, Alexander C, Chin T, Dolezal J, Hassanein R, Tanner C. Environmental risk factors in Parkinson's disease. *Neurology* 1990; 40 (8): 1218-1221
- Koller WC. Pharmacologic treatment of parkinsonian tremor. *Arch Neurol* 1986; 43 (2): 126-127
- Koller WC, Pahwa R. Treating motor fluctuations with controlled-release levodopa preparations. *Neurology* 1994; 44 (7): S23-28
- Kornhuber J, Bormann J, Hubers M, Rusche K, Riederer P. Effects of the 1-amine-adamantanes at the MK-801 binding site of the NMDA receptor gated ion channel: a human postmortem study. *Eur J Pharmacology* 1991; 206: 297-300
- Kosterlitz HW, Paterson SJ, Robson LE. Characterisation of the kappa subtype of opiate receptor in the guinea pig brain, *Br J Pharmacol* 1981; 68: 333-342
- Kosterlitz HW, Waterfield AA. Differential effects of drugs on the acetylcholine output from the myenteric plexus and the responses of the longitudinal muscle of the guinea-pig ileum. *Br J Pharmacol* 1972; 46 (3): 569-570
- Krauthamer GM, Krol JG, Grunweg BS. Effect of superior colliculus lesions on sensory unit responses in the intralaminar thalamus of the rat. *Brain Res* 1992; 576: 277-286
- Kubota Y, Inagaki S, Kito S, Shimada S, Okayama T, Hatanaka H, Pelletier G, Takagi H, Tohyama M. Neuropeptide Y-immunoreactive neurons receive synaptic inputs from dopaminergic axon terminals in the rat neostriatum. *Brain Res* 1988; 458 (2): 389-393
- Kubota Y, Inagaki S, Shimada S, Kito S, Eckenstein F, Tohyama M. Neostriatal cholinergic neurons receive direct synaptic inputs from dopaminergic axons. *Brain Res* 1987; 413 (1): 179-184
- Kubota Y, Kawaguchi Y. Spatial distributions of chemically identified intrinsic neurons in relation to patch and matrix compartments of rat neostriatum. *J Comp Neurol* 1993; 332 (4): 499-513
- Kuhlenbeck H. The derivatives of the thalamus ventralis in the human brain and their relation to the so-called subthalamus. *Mil Surgeon*. 1948; 102: 433
- Kuhlenbeck H, Haymaker W. The derivatives of the hypothalamus in the human brain, their relation to the extrapyramidal and autonomic systems. *Mil Surgeon*. 1949; 105: 26

- Kultas-Ilinsky K, Ilinsky IA. Fine structure of the magnocellular subdivision of the ventral anterior thalamic nucleus (VAmc) of *Macaca mulatta*: II organisation of nigrothalamic afferents as revealed with EM autoradiography. *J Comp Neurol* 1990, 294: 479-489
- Kurlan R, Majumdar L, Deeley C, Mudholkar GS, Plumb S, Como PG. A controlled trial of propoxyphene and naltrexone in patients with Tourette's syndrome. *Ann Neurol* 1991, 30: 19-23
- Kurnzel H. Projections from the primary somatosensory cortex to basal ganglia and thalamus in the monkey. *Exp Brain Res* 1977, 30: 481-492
- Kurnzle H. An autoradiographic analysis of the efferent connections from premotor and adjacent prefrontal regions (areas 6 and 9) in macaca fascicularis. *Brain Behav Evol* 1978, 15 (3) 185-234
- Kurnzle H. Bilateral projections from precentral motor cortex to the putamen and other parts of the basal ganglia. An autoradiographic study in *Macaca fascicularis*. *Brain Res* 1975, 88: 195-209
- L'Hereault S, Barden N. Monoaminergic regulation of proopiomelanocortin messenger RNA concentrations in primary cell cultures of rat hypothalamus. *Brain Res Mol Brain Res* 1991, 9(4): 327-332
- Labandeira-Garcia JL, Rozas G, Lopez-Martin E, Liste I, Guerra MJ. Time course of striatal changes induced by 6-hydroxydopamine lesion of the nigrostriatal pathway, as studied by combined evaluation of rotational behaviour and striatal Fos expression. *Exp Brain Res* 1996, 108: 69-84
- Lang AE, Blair RDG. Anticholinergic drugs and amantidine in the treatment of Parkinson's disease. In: Calne DB, editor. *Drugs for the treatment of Parkinson's disease*. Berlin: Springer-Verlag, 1989: 307-323
- Langdon N, Malcolm PN, Parkes JD. Comparison of levodopa with carbidopa, and levodopa with domperidone in Parkinson's disease. *Clin Neuropharmacol* 1986, 9 (5): 440-447
- Lannes B, Bernard V, Bloch B, Micheletti G. Chronic treatment with dizocilpine maleate increases the number of striatal neurons expressing the D2 receptor gene. *Neuroscience* 1995, 65(2): 431-438
- Lapper SR, Bolam JP. Input from the frontal cortex and the parafascicular nucleus to cholinergic interneurons in the dorsal striatum of the rat. *Neuroscience* 1992, 51 (3): 533-545
- Lavoie B, Parent A. Immunohistochemical study of the serotonergic innervation of the basal ganglia in the squirrel monkey. *J Comp Neurol* 1990, 299: 1-16

Lavoie B, Parent A. Pedunculopontine nucleus in the squirrel monkey: cholinergic and glutamatergic projections to the substantia nigra. *J Comp Neurol* 1994c, 344 (2): 232-241

Lavoie B, Parent A. Pedunculopontine nucleus in the squirrel monkey: distribution of cholinergic and monoaminergic neurons in the mesopontine tegmentum with evidence for the presence of glutamate in cholinergic neurons. *J Comp Neurol* 1994a, 344 (2): 190-209

Lavoie B, Parent A. Pedunculopontine nucleus in the squirrel monkey: projections to the basal ganglia as revealed by anterograde tract-tracing methods. *J Comp Neurol* 1994b, 344 (2): 210-231

Lazareno S, Mariott DB, Nahorski SR. Differential effects of selective and non-selective neuroleptics on intracellular and extracellular cyclic AMP accumulation in rat striatal slices. *Brain Res* 1985, 361: 91-98

Le Moine C, Bloch B. D1 and D2 dopamine receptor gene expression in the rat striatum: sensitive cRNA probes demonstrate prominent segregation of D1 and D2 mRNAs in distinct neuronal populations of the dorsal and ventral striatum. *J Comp Neurol* 1995, 355 (3): 418-426

Le Moine C, Normand E, Guitteny AF, Fouque B, Teoule R, Bloch B. Dopamine receptor gene expression by enkephalin neurons in rat forebrain. *Proc Natl Acad Sci U S A* 1990, 87 (1): 230-234

Le Witt PA, Ward CD, Larsen TA, Raphaelson MI, Newman RP, Foster N, Dambrosia JM, Calne DB. Comparison of pergolide and bromocriptine therapy in parkinsonism. *Neurology* 1983, 33 (8): 1009-1014

Le Doux MS, Lorden JF, Ervin JM. Cerebellectomy eliminates the motor syndrome of the genetically dystonic rat. *Exp Neurol* 1993, 120 (2): 302-310

Le Doux MS, Lorden JF, Ervin JM. Inferior olive serotonin and norepinephrine levels during development in the genetically dystonic rat. *Brain Res Bull* 1994, 33 (3): 299-305

Lees AJ. Comparison of therapeutic effects of levodopa, levodopa and selegiline, and bromocriptine in patients with early, mild Parkinson's disease: three year interim report. *BMJ* 1993, 307: 469-472

Lees AJ, Stern GM. Sustained bromocriptine therapy in previously untreated patients with Parkinson's disease. *J Neurol Neurosurg Psychiatry* 1981, 44: 1020-1023

Lees AJ: Parkinson's Disease Research Group of the United Kingdom Comparison of therapeutic effects and mortality data of levodopa and levodopa combined with selegiline in patients with early, mild Parkinson's disease. *BMJ* 1995, 311 (7020): 1602-1607

- Lehmann J, Langer SZ. The striatal cholinergic interneuron: synaptic target of dopaminergic terminals? *Neuroscience* 1983, 10: 1105-1120
- Lenz FA, Dostrowski JO, Tasker RR, Yamashiro K, Kwan HC, Murphy JT. Single-unit analysis of the human ventral thalamic nuclear group: somatosensory responses. *J Neurophysiol* 1988, 59: 299-316
- Lera G, Vaamonde J, Rodriguez M, Obeso JA. Cabergoline in Parkinson's disease: long-term follow-up. *Neurology* 1993, 43 (12): 2587-2590
- Levy R, Herrero MT, Ruberg M, Villares J, Faucheux B, Guridi J, Guillen J, Luquin MR, Javoy-Agid F, Obeso JA, Hirsch EC. Effects of nigrostriatal denervation and L-DOPA therapy on the GABAergic neurons of the striatum in MPTP-treated monkeys and Parkinson's disease: An *in situ* hybridisation study of GAD67 mRNA. *Eur J Neuroscience* 1995a, 7: 1199-1209
- Levy R, Vila M, Herrero MT, Faucheux B, Agid Y, Hirsch EC. Striatal expression of substance P and methionin-enkephalin in genes in patients with Parkinson's disease. *Neurosci Lett* 1995b, 199 (3): 220-224
- Le Witt PA, Miller LP, Levine RA, Lovenberg W, Newman RP, Papavasiliou A, Rayes A, Eldridge R, Burns RS. Tetrahydrobiopterin in dystonia: identification of abnormal metabolism and therapeutic trials. *Neurology* 1986, 36 (6) 760-764
- L'Hereault S, Barden N. Regulation of proopiomelanocortin messenger RNA concentrations by opioid peptides in primary cell cultures of rat hypothalamus. *Brain Res Mol Brain Res* 1991, 10 (2): 115-121
- Li S, Sivam S, Hong J. Regulation of the concentration of dynorphin A₁₋₁₈ in the striatonigral pathway by the dopaminergic system. *Brain Res* 1986, 398: 390-392
- Li SJ, Sivam SP, McGinty JF, Jiang HK, Douglass J, Calavetta L, Hong JS. Regulation of the metabolism of striatal dynorphin by the dopaminergic system. *J Pharmacol Exp Ther* 1988, 246 (1): 403-408
- Lieberman A, Kupersmith M, Estey E, Goldstein M. Treatment of Parkinson's disease with bromocriptine. *N Engl J Med* 1976, 295 (25):1400-1404
- Liles SL, Updyke BV. Projection of the digit and wrist area of precentral gyrus to the putamen: relation between topography and physiological properties of neurons in the putamen. *Brain Res* 1985, 339: 245-255
- Limousin P, Pollak P, Benazzouz A, Hoffmann D, Le Bas JF, Broussolle E, Perret JE, Benabid AL. Effect on parkinsonian signs and symptoms of bilateral subthalamic nucleus stimulation. *Lancet* 1995, 345: 91-95

- Linazasoro G, Guridi J, Gorospe A, Ramos E, Mozo A, Obeso JA. Posterioventral pallidotomy in Parkinson's disease : Clinical results in 27 patients. *Mov Dis* 1996, Vol 11 (1) Abs P904: 240
- Linden R, Perry VH. Massive retinotectal projection in rats. *Brain Res* 1983, 272:145-149
- Lindenmayer JP, Gardner E, Goldberg E, Opler LA, Kay SR, van Praag HM, Weiner M, Zukin S. High-dose naloxone in tardive dyskinesia. *Psychiatry Res* 1988, 26: 19-28
- Lindvall O. Neural transplantation. *Cell Transplant* 1995, 4 (4): 393-400
- Lindvall O, Bjorklund A. Transplantation strategies in the treatment of Parkinson's disease: experimental basis and clinical trials. *Acta Neurol Scand* 1989, 126: 197-210
- Linert W, Herlinger E, Jameson RF, Kienzl E, Jellinger K, Youdim MB. Dopamine, 6-hydroxydopamine, iron, and dioxygen: their mutual interactions and possible implication in the development of Parkinson's disease. *Biochim Biophys Acta* 1996, 1316 (3): 160-168
- Liu Y, Roghani A, Edwards RH. Gene transfer of a reserpine-sensitive mechanism of resistance to N-methyl-4-phenylpyridinium. *Proc Natl Acad Sci U S A* 1992, 89 (19): 9074-9078
- Loeffler JP, Kley N, Pittius CW, Holtt V. Regulation of proopiomelanocortin (POMC) mRNA levels in primary pituitary cultures. *NIDA Res Monograph* 1986, 75: 397-400
- Lord J, Waterfield A, Hughes J, Kosterlitz H. Endogenous opioid peptides: multiple agonists and receptors. *Nature* 1977, 267: 495-499
- Loscher W, Fisher JE Jr, Schmidt D, Fredow G, Honack D, Iturrian WB. The sz mutant hamster: a genetic model of epilepsy or of paroxysmal dystonia? *Mov Dis* 1989, 4 (3): 219-232
- Loschmann PA, Lange KW, Kunow M, Rettig KJ, Jahnig P, Honore T, Turski L, Wachtel H, Jenner P, Marsden CD. Synergism of the AMP-antagonist NBQX and the NMDA-antagonist CPP with L-DOPA in models of Parkinson's disease. *J Neural Transm* 1991, 3: 203-213
- Lozano AM, Lang AE, Galvez-Jimenez N, Miyasaki J, Duff J, Hutchinson WD, Dostrovsky JO. Effect of GPi pallidotomy on motor function in Parkinson's disease. *Lancet* 1995, 346: 1383-1387

- Lucking CB, Kosel S, Mehraein P, Graeber MB. Absence of the mitochondrial A7237T mutation in Parkinson's disease. *Biochem Biophys Res Commun* 1995, 211 (2): 700-704
- Lundberg JM, Hedlund B, Anggard A, Fahrenkrug J. Costorage of peptides and classical transmitters in neurons. In: Bloom SR, Bartfai T, Lindenlaub, editors. *Systemic role of regulatory peptides*. Stuttgart: Schattauer 1982, 93-119
- Madrazo I, Leon V, Torres C, Aguilera MC, Varela G, Alvarez F, Fraga A, Drucker-Colin R, Ostrosky F, Skurovich M, Franco R. Transplantation of fetal substantia nigra and adrenal medulla to the caudate nucleus in two patients with Parkinson's disease. *N Engl J Med* 1988, 318 (1): 51
- Maj J, Rogoz Z, Skuza G, Sowinska H, Superata J. Behavioural and neurochemical effects of Ro 40-7592, a new COMT inhibitor with a potential therapeutic activity in Parkinson's disease. *J Neural Transm Park Dis Dement Sect* 1990, 2 (2): 101-112
- Maneuf YP, Mitchell IJ, Crossman AR, Brotchie JM. Functional implications of kappa opioid receptor-mediated modulation of glutamate transmission in the output regions of the basal ganglia in rodent and primate models of Parkinson's disease. *Brain Res* 1995, 683: 102-108
- Maneuf YP, Mitchell IJ, Crossman AR, Woodruff GN, Brotchie JM. On the role of enkephalin cotransmission in the GABAergic striatal efferents to the globus pallidus. *Exp Neurol* 1994, 125: 65-71
- Mansour A, Fox CA, Akil H, Watson SJ. Opioid-receptor mRNA expression in the rat CNS: anatomical and functional implications. *Trends Neurosci* 1995, 18(1): 22-29
- Mansour A, Fox CA, Burke S, Meng F, Thompson RC, Akil H, Watson SJ. Mu, delta, and kappa opioid receptor mRNA expression in the rat CNS: an in situ hybridization study. *J Comp Neurol* 1994, 350 (3): 412-438
- Maraganore DM, Harding AE, Marsden CD. A clinical and genetic study of familial Parkinson's disease. *Mov Dis* 1991, 6 (3): 205-211
- Marder K, Tang MX, Mejia H, Alfaro B, Cote L, Louis E, Groves J, Mayeux R. Risk of Parkinson's disease among first-degree relatives: A community-based study. *Neurology* 1996, 47 (1): 155-160
- Marin C, Chase TN. Effects of SCH 32615, an enkephalinase inhibitor, on D-1 and D-2 dopamine receptor-mediated behaviors. *Neuropharmacology* 1995, 34 (6): 677-682
- Markey SP, Colburn RW, Kopin IJ, Aamodt RL. Distribution and excretion in the rat and monkey of [82Br] bromocriptine. *J Pharmacol Exp Ther* 1979, 211 (1): 31-35
- Marmot MJ. Mortality in Parkinson's disease. In: Rose CF, Capildeo R, editors. *Research progress in Parkinson's disease*. London Libby 1987, Chapter 2: 9-16

- Marsden CD, Obeso JA. The functions of the basal ganglia and the paradox of stereotaxic surgery in Parkinson's disease. *Brain* 1994, 117: 877-897
- Marsden CD. Parkinson's disease. *Journal of Neurology, Neurosurgery and Psychiatry*. 1994, 57: 627-681
- Marsden CD, Parkes JD. 'On-off' effects in patients with Parkinson's disease on chronic levodopa therapy. *Lancet* 1976, 1: 292-296
- Martin JP. Hemichorea resulting from a local lesion of the brain (syndrome of body of Luys). *Brain* 1927, 50: 637-651
- Martin WR. Opioid antagonists. *Pharmacol Rev* 1967, 19 (4): 463-521
- Marttila RJ, Kaprio J, Koskenvuo M, Rinne UK. Parkinson's disease in a nationwide twin cohort. *Neurology* 1988, 38 (8): 1217-1219
- Marttila RJ, Rinne UK. Epidemiology of Parkinson's disease-an overview. *J Neural Transm* 1981, 51 (1-2): 135-148
- Matsumoto RR, Brinsfield KH, Patrick RL, Walker JM. Rotational behavior mediated by dopaminergic and nondopaminergic mechanisms after intranigral microinjection of specific mu, kappa and delta opioid agonists. *J Pharmacol Exp Ther* 1988a, 246: 296-203
- Matsumoto RR, Lohof AM, Patrick RL, Walker JM. Dopamine-independent motor behavior following microinjection of rimorphin in the substantia nigra. *Brain Res* 1988b, 444: 67-74
- Matsumura M, Tremblay L, Richard H, Filion M. Activity of pallidal neurons in the monkey during dyskinesia induced by injection of bicuculline in the external pallidum. *Neuroscience* 1995, 65 (1): 59-70
- Matteoli M, Haimann C, Torri TF, Polak JM, Ceccarelli B, De Camilli P. Differential effect of alpha-latrotoxin on exocytosis from small synaptic vesicles and from large dense-core vesicles containing calcitonin gene-related peptide at the frog neuromuscular junction. *Proc Natl Acad Sci USA* 1988, 85: 7366-7370
- Mattia A, Vanderah T, Mosberg HI, Porreca F. Lack of antinociceptive cross-tolerance between [D-Pen², D-Pen⁵] enkephalin and [D-Ala²]deltorphin II in mice: evidence for delta receptor sub-types. *J Pharmacol Exp Ther*. 1991, 258: 583-587
- Mattock C, Marmot M, Stern G. Could Parkinson's disease follow intra-uterine influenza?: a speculative hypothesis *J Neurol Neurosurg Psychiatry* 1988, 51 (6): 753-756

- McDonald AJ. Topographical organisation of amygdaloid projections to the caudatoputamen, nucleus accumbens, and related striatal-like areas of the rat brain. *Neuroscience*. 1991, 44: 15-33
- McGeorge AJ, Faull RL. The organization of the projection from the cerebral cortex to the striatum in the rat. *Neuroscience* 1989, 29 (3): 503-537
- Meltzer HY, Matsubara S, Lee JC. Classification of typical and atypical antipsychotic drugs on the basis of dopamine D1, D2 and serotonin pKi values. *J Pharmacol Exp Ther* 1989, 251: 238-246
- Meredith GE, Pattiselanno A, Groenewegen HJ, Haber SN. Shell and core in monkey and human nucleus accumbens identified with antibodies to calbindin-D_{28k}. *J Comp Neurol* 1996, 365:628-639
- Merello M, Lees AJ, Webster R, Bovingdon M, Gordin A. Effect of entacapone, a peripherally acting catechol-O-methyltransferase inhibitor, on the motor response to acute treatment with levodopa in patients with Parkinson's disease. *J Neurol Neurosurg Psychiatry* 1994, 57 (2): 186-189
- Messersmith DJ, Gu J, Dubner J, Douglass J, Iadarola MJ. Basal and inducible transcriptional activity of an upstream AP-1/CRE element (DYNCRE3) in the prodynorphin promoter. *Mol Cell Neurosci* 1994, 5: 238-245
- Messersmith DJ, Kim DJ, Gu J, Dubner R, Iadarola MJ. c-Jun activation of the DYNCRE3 site in the prodynorphin promoter. *Brain Res Mol Brain Res* 1996, 40: 15-21
- Mesulam MM, Geula C, Bothwell MA, Hersh LB. Human reticular formation: cholinergic neurons of the pedunculopontine and laterodorsal tegmental nuclei and some cytochemical comparisons to forebrain cholinergic neurons. *J Comp Neurol* 1989, 283 (4): 611-633
- Meunier JC, Mollereau C, Toll L, Suaudeau C, Moisand C, Alvinerie P, Butour JL, Guillemot JC, Ferrara P, Monsarrat B, Mazarguil H, Vassart G, Parmentier M, Costentin J. Isolation and structure of the endogenous agonist of opioid receptor-like ORL1 receptor. *Nature* 1995, 377 (6549): 532-535
- Meyer B. Encephalitis after measles with severe parkinsonian rigidity. *BMJ* 1943, 1:508
- Miller WC, DeLong MR. Altered tonic activity of neurons in the globus pallidus and subthalamic nucleus in the primate MPTP model of parkinsonism. In: Carpenter MB, Jayaraman A, editors. *The Basal Ganglia II*, New York: Plenum 1987: 415-427

Miller WC, DeLong MR. Parkinsonian symptomatology. An anatomical and physiological analysis. *Ann N Y Acad Sci* 1988, 515: 287-302

Min BH, Augustin LB, Felsheim RF, Fuchs JA, Loh HH. Genomic structure analysis of promoter sequences of a mouse mu opioid receptor gene. *Proc Natl Acad Sci USA* 1994, 91: 9081-9085

Miotto K, Magendzo K, Evens CJ. Molecular characterisation of opioid receptors. In: Tseng LF, editor. *The pharmacology of opioid peptides*, Singapore Harwood Acad. 1995: 142-167

Mitchell IJ, Boyce S, Sambrook MA, Crossman AR. A 2-deoxyglucose study of the effects of dopamine agonists on the parkinsonian primate brain: Implications for the neural mechanisms that mediate dopamine agonist-induced dyskinesia. *Brain* 1992b, 115: 809-824

Mitchell IJ, Cross AJ, Sambrook MA, Crossman AR. Sites of the neurotoxic action of 1-methyl-4-phenyl-1,2,3,6-tetrahydropyridine in the macaque monkey include the ventral tegmental area and the locus coeruleus. *Neuroscience Lett* 1985, 61: 195-200

Mitchell IJ, Crossman AR, Liminga U, Andren P, Gunne LM. Regional changes in 2-deoxyglucose uptake associated with neuroleptic-induced tardive dyskinesia in the cebus monkey. *Mov Dis* 1992a, 7: 32-37

Mitchell IJ, Hughes N, Carroll CB, Brotchie JM. Reversal of parkinsonian symptoms by intrastriatal and systemic manipulations of excitatory amino acid transmission in the bilateral 6-OHDA lesioned marmoset. *Behav Pharmacol* 1995, 6: 492-507

Mitchell IJ, Jackson A, Sambrook MA, Crossman AR. Common neural mechanisms in experimental chorea and hemiballismus in the monkey. Evidence from 2-deoxyglucose autoradiography. *Brain Res* 1985, 339: 346-350

Mitchell IJ, Jackson A, Sambrook MA, Crossman AR. The role of the subthalamic nucleus in experimental chorea: evidence from 2-deoxyglucose metabolic mapping and horseradish peroxidase tracing studies. *Brain* 1989, 112: 1533-1548

Mizuno N, Ueyama T, Itoh K, Satoda T, Tashiro T, Shigemoto R. Direct projections from the subthalamic nucleus of Luys to the spinal cord in the Japanese monkey. *Neurosci Lett* 1988, 89 (1): 13-18

Mocchetti I, Naranjo J, Costa E. Regulation of striatal enkephalin turnover in rats receiving antagonists of specific dopamine subtypes. *J Pharmacol Exp Ther* 1987, 241: 1120-1124

Molho ES, Factor SA, Weiner WJ, Sanchez-Ramos JR, Singer C, Shulman L, Brown D, Sheldon C. The use of pramipexole, a novel dopamine (DA) agonist, in advanced Parkinson's disease. *J Neural Transm Suppl* 1995, 45: 225-230

- Mollereau C, Parmentier M, Mailleux P, Butour JL, Moisand C, Chalon P, Caput D, Vassart G, Meunier JC. ORL1, a novel member of the opioid receptor family. Cloning, functional expression and localization. *FEBS Lett* 1994, 341 (1): 33-38
- Monakow KH, Akert K, Kunzle H. Projections of the precentral motor cortex and other cortical areas of the frontal lobe to the subthalamic nucleus in the monkey. *Exp Brain Res* 1978, 33 (3-4): 395-403
- Moon-Edley S, Graybiel AM. The afferent and efferent connections of the feline nucleus tegmenti pedunculopontinus pars compacta. *J Comp Neurol.* 1983 217: 187-215
- Morales-Olivas FJ, Palop V, Rubio E, Esplagues J. Hypotensive action and alpha-adrenolytic properties of a new dopaminergic agonist, CU 32-085, in the rat. *Arch int Pharmacodyn* 1984, 272: 71-78
- Morris BJ, Herz A, Holtt V. Localization of striatal opioid gene expression, and its modulation by the mesostriatal dopamine pathway: an in situ hybridization study. *J Mol Neurosci* 1989, 1 (1): 9-18
- Morrish PK, Sawle GV, Brooks DJ. The rate of progression of Parkinson's disease. A longitudinal [^{18}F]DOPA PET study. *Adv Neurol* 1996, 69: 427-31
- Muenter MD, Sharpless NS, Tyce GM, Darley FL. Patterns of dystonia ('I-D-I' and 'D-I-D') in response to l-dopa therapy for Parkinson's disease. *Mayo Clin Proc* 1977, 52 (3): 163-174
- Mulder AH, Wardeh G, Hogenboom F, Frankhuyzen AL. Kappa- and delta-opioid receptor agonists differentially inhibit striatal dopamine and acetylcholine release. *Nature* 1984, 308 (5956): 278-280
- Murray AM, Waddington JL. The induction of grooming and vacuous chewing by a series of selective D-1 dopamine receptor agonists: two directions of D-1:D-2 interaction. *Eur J Pharmacol* 1989, 160 (3): 377-384
- Murthy KS, Makhlouf GM. Opioid mu, delta, and kappa receptor-induced activation of phospholipase C-beta 3 and inhibition of adenylyl cyclase is mediated by Gi2 and G(o) in smooth muscle. *Mol Pharmacol* 1996, 50 (4): 870-877
- Myers HR. Surgical procedure for postencephalitic tremor with notes on the physiology of premotor fibres. *Arch. Neurol Psychiat* 1940, 44: 455-459
- Nakanishi S, Inoue A, Kita T, Nakamura M, Chang AC, Cohen SN, Numa S. Nucleotide sequence of cloned cDNA for bovine corticotropin-beta-lipotropin precursor. *Nature* 1979, 278 (5703): 423-427

- Narabayashi H. Stereotaxic Vim thalamotomy for treatment of tremor. *Eur Neurol* 1989, 29 (1): 29-32
- Narabayashi H, Okuma T, Shikiba S. Procaine oil blocking of the globus pallidus. *Arch Neurol Psychiatry* 1956, 75: 36-48
- Narabayashi H, Yokochi F, Nakajima Y. Levodopa-induced dyskinesia and thalamotomy. *J Neurol Neurosurg Psych* 1984, 47: 831-839
- Nauta WJH, Cole M. Efferent projections of the subthalamic nucleus: An autoradiographic study in monkey and cat. *J Comp Neurol* 1978, 180: 1-16
- Nauta WJH, Domesick VB. Crossroads of the limbic and striatal circuitry: hypothalamo-nigral connections. In: Livingston KE, Hornykiewicz O, editors. *Limbic mechanisms*. Plenum, New York, 1978: 75-93
- Nauta WJH, Mehler WR. Projections of the lentiform nucleus in the monkey. *Brain Res* 1966, 1: 3-42
- Needham PL, Skill MJ, Cowan A, Redfern RJ, Heal DJ. Reserpinization severs the cooperative but not the oppositional interaction between D1 and D2 receptors. *Neuropharmacology* 1993, 32 (6): 515-517
- Nisbet AP, Eve DJ, Kingsbury AE, Daniel SE, Marsden CD, Lees AJ, Foster OJF. Glutamate decarboxylase-67 messenger RNA expression in normal human basal ganglia and in Parkinson's disease. *Neuroscience* 1996, 75 (2): 389-406
- Nisbet AP, Foster OJ, Kingsbury A, Eve DJ, Daniel SE, Marsden CD, Lees AJ. Preproenkephalin and preprotachykinin messenger RNA expression in normal human basal ganglia and in Parkinson's disease. *Neuroscience* 1995, 66 (2): 361-376
- Nishi M, Takeshima H, Mori M, Nakagawara K, Takeuchi T. Structure and chromosomal mapping of genes for the mouse kappa-opioid receptor and an opioid receptor homologue (MOR-C). *Biochem Biophys Res Commun* 1994, 205 (2): 1353-1357
- Noda M, Teranishi Y, Takahashi H, Toyosato M, Notake M, Nakanishi S, Numa S. Isolation and structural organization of the human preproenkephalin gene. *Nature* 1982, 297 (5865): 431-434
- Nutt JG. Levodopa-induced dyskinesia. *Neurology* 1990, 40: 340-245
- Nutt JG, Carter JH, Woodward WR. Effect of brief levodopa holidays on the short-duration response to levodopa: evidence for tolerance to the antiparkinsonian effects. *Neurology* 1994, 44 (9): 1617-1622

- Nutt JG, Woodward WR, Hammerstad JP, Carter JH, Anderson JL. The "on-off" phenomenon in Parkinson's disease. Relation to levodopa absorption and transport. *N Engl J Med* 1984, 310 (8): 483-488
- Nyberg F, Terenius L. Enzymatic inactivation of neuropeptides. In: HJ Heriksen, editor. Degredation of biogenic substances: physiology and pathophysiology. CRC Press Boca Raton AnnArbor Boston 1991: 189-200
- Oertel WH, Nitsch C, Mugnaini E. Immunocytochemical demonstration of the GABA-ergic neurons in rat globus pallidus and nucleus entopeduncularis and their GABA-ergic innervation. *Adv Neurol* 1984, 40: 91-98
- Ogawa N, Mizukawa K, Haba K, Sato H. Neurotransmitter and receptor alterations in the rat persistent dyskinesia model induced by iminodipropionitrile. *Eur Neurol* 1990, 30 Suppl 1: 31-40
- Ohye C. Anatomy and physiology of the thalamic nucleus ventralis intermedius. In: Ito M, editor. Integrative control functions of the brain. Kodansha, Tokyo. 1978, Vol 1:152-163
- Ohye C. Thalamus. In: Paxinos G, editor. The human nervous system. Academic press, New York. 1990, 439-468
- Ohye C, Narabayashi H. Physiological study of the presumed ventralis intermedius neurons in the human thalamus. *J Neurosurg* 1979, 50: 290-297
- Ohye C, Shibasaki T, Hirai T, Wada H, Hirato M, Kawashima Y. Further physiological observations on the ventralis intermedius neurons in the human thalamus. *J Neurophysiol* 1989, 61 (3): 488-500
- Olanow CW. A rationale for monoamine oxidase inhibition as neuroprotective therapy for Parkinson's disease. *Mov Dis* 1993, 8 (1): S1-7
- Olanow CW, Fahn S, Langston JW, Godbold J. Selegiline and mortality in Parkinson's disease. *Ann Neurol* 1996, 40 (6): 841-845
- Olsson M, Nikkhah G, Bentlage C, Bjorklund A. Forelimb akinesia in the rat parkinson model: Differential effects of dopamine agonists and nigral transplants as assessed by a new stepping test. *J Neurosci* 1995, 15(5): 3863-3875
- Ovadia A, Zhang Z, Gash DM. Increased susceptibility to MPTP toxicity in middle-aged rhesus monkeys. *Neurobiol Aging* 1995, 16 (6): 931-937
- Owen AD, Schapira AH, Jenner P, Marsden CD. Oxidative stress and Parkinson's disease. *Ann N Y Acad Sci* 1996, 786: 217-223

- Ozawa T, Tanaka M, Ino H, Ohno K, Sano T, Wada Y, Yoneda M, Tanno Y, Miyatake T, Tanaka T. Distinct clustering of point mutations in mitochondrial DNA among patients with mitochondrial encephalomyopathies and with Parkinson's disease. *Biochem Biophys Res Commun* 1991, 176 (2): 938-946
- Palkovits M, Jacobowitz DM. Topographic atlas of catecholamine and acetylcholinesterase-containing neurons in the rat brain. II. Hindbrain (mesencephalon, rhombencephalon). *J Comp Neurol* 1974, 157 (1): 29-42
- Pan HS, Frey KA, Young AB, Penney JB. Changes in [3H]muscimol binding in substantia nigra, entopeduncular nucleus, globus pallidus, and thalamus after striatal lesions as demonstrated by quantitative receptor autoradiography. *J Neurosci* 1983, 3 (6): 1189-1198
- Pan HS, Penny JB, Young AB. γ -Aminobutyric acid and benzodiazepine receptor changes induced by unilateral 6-hydroxydopamine lesions of the medium forebrain bundle. *J Neurochem* 1985, 45: 1396-1404
- Papa SM, Boldry RC, Engber TM, Kask AM, Chase TN. Reversal of levodopa-induced motor fluctuations in experimental parkinsonism by NMDA receptor blockade. *Brain Res* 1995, 701 (1-2): 13-18
- Papa SM, Chase TN. Levodopa-induced dyskinesias improved by a glutamate antagonist in Parkinsonian monkeys *Ann Neurol* 1996, 39 (5): 574-578
- Papez JW, Bennett AE, Cash PT. Hemichorea (hemiballismus) associated with a pallidal lesion involving afferent and efferent connections of the subthalamic nucleus. *Arch Neurology Psychiatry* 1942, 47: 667-676
- Pare D, Hazrati LN, Parent A, Steriade M. Substantia nigra pars reticulata projects to the reticular thalamic nucleus of the cat: a morphological and electrophysiological study. *Brain Res* 1990, 535 (1): 139-146
- Parent A, Smith Y. Differential dopaminergic innervation of the two pallidal segments in the squirrel monkey (*Saimiri sciureus*). *Brain Res* 1987a, 426: 397-400
- Parent A, Smith Y. Organisation of efferent projections of the subthalamic nucleus in the squirrel monkey as revealed by retrograde labelling methods. *Brain Res* 1987b, 436: 296-310.
- Parent A. Comparative anatomy of the serotonergic systems. *J Physiol* 1981, 77 (2-3): 147-156
- Parent A, Asselin MC, Cote PY. Dopaminergic regulation of peptide gene expression in the striatum of normal and parkinsonian monkeys. *Advances in Neurology* 1996, 69: 73-77

- Parent A, Bouchard C, Smith Y. The striatopallidal and striatonigral projections: two distinct fiber systems in primate. *Brain Res* 1984, 303 (2): 385-390
- Parent A, De Bellefeuille L. The pallidointralaminar and pallidonigral projections in primate as studied by retrograde double-labeling method. *Brain Res* 1983, 278 (1-2): 11-27
- Parent A, Descarries L, Beaudet A. Organisation of ascending serotonin systems in the adult rat brain. A radiographic study after intraventricular administration of [³H]5-hydroxytryptamine. *Neuroscience* 1981, 6: 115-138
- Parent A, Hazrati LN. Functional anatomy of the basal ganglia. II. The place of subthalamic nucleus and external pallidum in basal ganglia circuitry. *Brain Res Brain Res Rev* 1995b, 20 (1): 128-54
- Parent A, Hazrati LN. Functional anatomy of the basal ganglia. I. The cortico-basal ganglia-thalamo-cortical loop. *Brain Res Brain Res Rev* 1995a, 20 (1): 91-127
- Parent A, Hazrati LN. Multiple striatal representation in primate substantia nigra. *J Comp Neurol* 1994, 344 (2): 305-320
- Parent A, Smith Y, Filion M, Dumas J. Distinct afferents to internal and external pallidal segments in the squirrel monkey. *Neurosci Lett* 1989, 96 (2): 140-144
- Park MR, Lighthall JW, Kitai ST. Recurrent inhibition in the rat neostriatum. *Brain Res* 1980, 194 (2): 359-369
- Parkes JD. Adverse effects of antiparkinsonian drugs. *Drugs* 1981, 21 (5): 341-353
- Parkes JD. Bromocriptine in the treatment of parkinsonism. *Drugs* 1979, 17 (5): 365-382
- Parkes JD. Bromocriptine. *Adv Drug Res* 1977, 12: 247-344
- Parkes JD, Baxter RC, Curzon G, Knill-Jones RP, Knott PJ, Marsden CD, Tattersall R, Vollum D. Treatment of Parkinson's disease with amantadine and levodopa. A one-year study. *Lancet* 1971, 1 (709): 1083-1086
- Parkes JD, Baxter RC, Marsden CD, Rees JE. Comparative trial of benzhexol, amantadine, and levodopa in the treatment of Parkinson's disease. *J Neurol Neurosurg Psychiatry* 1974, 37 (4): 422-426
- Parkes JD, Debono AG, Marsden CD. Bromocriptine in Parkinsonism: long-term treatment dose response, and comparison with levodopa. *J Neurol Neurosurg Psychiatry* 1976, 39: 1101-1108
- Parkes JD, Schachter M, Marsden CD, Smith B, Wilson A. Lisuride in parkinsonism. *Ann Neurol* 1981, 9 (1): 48-52

- Parkes JD, Tarsy D, Marsden CD, Bovill KT, Phipps JA, Rose P, Asselman P. Amphetamines in the treatment of Parkinson's disease. *J Neurol Neurosurg Psychiatry* 1975, 38 (3): 232-237
- Parkinson J. An essay on the shaking palsy. Sherwood, Neely and Jones, London 1817
- Parkinson Study Group. Effect of deprenyl on the progression of disability in early Parkinson's disease. *N Engl J Med* 1989, 321,1364-1371
- Parkinson Study Group. Effects of tocopherol and deprenyl on the progression of disability in early Parkinson's disease. *N Engl J Med* 1993, 328,176-183
- Parkinson Study Group. Impact of deprenyl and tocopherol treatment on Parkinson's disease in DATATOP patients requiring levodopa. *Ann Neurol* 1996, 39 (1): 37-45
- Pasik P, Pasik T, Pecci-Saavedra JP, Holstein GR, Yahr MD. Serotonin in pallidal neuronal circuits: an immunocytochemical study in monkeys. *Adv Neurol*. 1984, 40:63-76
- Pasternak GW, Wood PL. Multiple mu opiate receptors. *Life Sci* 1986, 38: 1889-1898
- Pauls DL, Raymond CL, Stevenson JM, Leckman JF. A family study of Gilles de la Tourette syndrome. *Am J Hum Genet* 1991, 48 (1): 154-163
- Paxinos G, Watson C. The rat brain in stereotatic coordinates (2nd edition). Academic Press Limited, 1986
- Pearce RK, Jackson M, Smith L, Jenner P, Marsden CD. Chronic L-DOPA administration induces dyskinesias in the 1-methyl-4-phenyl-1,2,3,6-tetrahydropyridine-treated common marmoset (*Callithrix Jacchus*). *Mov Dis* 1995, 10 (6): 731-740
- Pearce RKB, Banerji T, Jackson M, Jenner P, Marsden CD. Cholinergic manipulation of L-DOPA-induced chorea and dystonia in the MPTP-treated common marmoset. *Movement disorders Abstract* 1996, Vol 11 (1), P200: 60
- Pennartz CMA, Dolleman-Van der Weel MJ, Lopes da Silva FH. Differential membrane properties and dopamine effects in the shell and core of the rat nucleus accumbens studied *in vitro*. *Neurosci Lett* 1992, 136: 109-112
- Perlow MJ, Freed WJ, Hoffer BJ, Seiger A, Olson L, Wyatt RJ. Brain grafts reduce motor abnormalities produced by destruction of nigrostriatal dopamine system. *Science* 1979, 204 (4393): 643-647

- Perry TL, Godin DV, Hansen S. Parkinson's disease: a disorder due to nigral glutathione deficiency? *Neurosci Lett* 1982, 33 (3): 305-310
- Pert CB, Kuhar MJ, Snyder SH. Opiate receptors: Autoradiographic localisation in rat brain. *Proc. Natl. Acad. Sci. USA*. 1976, 73: 3729-3733
- Pert CB, Snyder SH. Opiate receptor: demonstration in nervous tissue. *Science* 1973, 179 (77): 1011-1014
- Pfeiffer A, Herz A. Demonstration and distribution of an opiate binding site in rat brain with high affinity for ethylketocyclazocine and SKF 10,047. *Biochem Biophys Res Commun* 1981, 101 (1): 38-44
- Phelps PE, Vaughn JE. Immunocytochemical localisation of choline acetyltransferase in the ventral striatum: A light microscopic study. *J Neurocytol.* 1986, 15: 595-617
- Phillipson OT, Griffiths AC. The topographic order of inputs to nucleus accumbens in the rat. *Neuroscience* 1985, 16 (2): 275-296
- Pinter MM, Helscher RJ. Therapeutic effect of clozapine in psychotic decompensation in idiopathic Parkinson's disease. *J Neural Transm Park Dis Dement Sect* 1993, 5 (2): 135-146
- Pittius CW, Seizinger BR, Mehraein P, Pasi A, Herz A. Proenkephalin-A-derived peptides are present in human brain. *Life Sci* 1983, 33 (Suppl 1), 41-44
- Poirier J, Roy M, Campanella G, Cloutier T, Paris S. Debrisoquine metabolism in parkinsonian patients treated with antihistamine drugs. *Lancet* 1987, 2: 386
- Poirier LJ. Experimental and histological study of midbrain dyskinesias *J Physiology* 1960, 23: 534-551
- Polizos P, Englehardt DM, Hoffman SP, Waizer J. Neurological consequences of psychotropic drug withdrawal in schizophrenic children. *J Autism Child Schizo* 1973, 3: 247-253
- Pollack AE, Wooten GF. D2 dopaminergic regulation of striatal preproenkephalin mRNA levels is mediated at least in part through cholinergic interneurons. *Brain Res Mol Brain Res* 1992, 13 (1-2): 35-41
- Pollak P, Benabid AL, Gervason CL, Hoffmann D, Seigneuret E, Perret J. Long-term effects of chronic stimulation of the ventral intermediate thalamic nucleus in different types of tremor. *Adv Neurol* 1993, 60: 408-413.
- Portoghese PS. A new concept on the mode of interaction of narcotic analgesics with receptors. *J Med Chem* 1965, 8 (5): 609-616

- Portoghese PS, Lipkowski AW, Takemori AE. Binaltorphimine and nor-binaltorphimine, potent and selective kappa-opioid receptor antagonists. *Life Sci* 1987, 40 (13): 1287-1292
- Portoghese PS, Sultana M, Takemori AE. Naltrindole, a highly selective and potent non-peptide delta opioid receptor antagonist. *Eur J Pharmacol* 1988, 146 (1): 185-186
- Poskanzer DC, Schwab RS. Cohort analysis of Parkinson's syndrome: evidence for a single etiology related to subclinical infection about 1920. *J Chron Dis* 1963, 16: 961-973
- Powell TPS, Cowan WM. A study of thalamo-striate relations in the monkey. *Brain* 1956, 79: 364
- Powell TPS, Cowan WM. The connexions of the midline and intralaminar nuclei of the thalamus of the rat. *J Anat Lond* 1954, 88, 307
- Przedborski S, Kostic V, Jackson-Lewis V, Naini AB, Simonetti S, Fahn S, Carlson E, Epstein CJ, Cadet JL. Transgenic mice with increased Cu/Zn-superoxide dismutase activity are resistant to N-methyl-4-phenyl-1,2,3,6-tetrahydropyridine-induced neurotoxicity. *J Neurosci* 1992, 12 (5): 1658-1667
- Przedborski S, Wright M, Fahn S, Cadet JL. Quantitative autoradiographic changes in 5-[³H]HT-labeled 5-HT₁ serotonin receptors in discrete regions of brain in the rat model of persistent dyskinesias induced by iminodipropionitrile (IDPN). *Neurosci Lett* 1990, 116 (1-2): 51-57
- Przedborski S, Wright M, Fahn S, Cadet JL. Regional changes in brain 5-HT_{1A} serotonin receptors in the rat model of persistent spasmodic dyskinesias induced by iminodipropionitrile. *Brain Res* 1989, 504 (2): 311-314
- Putnam TJ. Treatment of unilateral paralysis agitans by section of the lateral pyramidal tract. *Arch Neurol Psychiatr* 1940, 44: 950
- Pycock CJ. Turning behaviour in animals. *Neuroscience* 1980, 5: 461-514
- Rafols JA, Fox CA. The neurons in the primate subthalamic nucleus: a Golgi and electron microscopic study. *J Comp Neurol*. 1976, 168: 75-112
- Ragsdale CW, Graybiel AM. The fronto-striatal projection in the cat and monkey and its relationship to inhomogeneities established by acetylcholinesterase histochemistry. *Brain Res* 1981, 208: 259-266
- Rascol O, Fabre N, Blin O, Poulik J, Sabatini U, Senard JM, Ane M, Montastru JL, Rascol A. Naltrexone, an opiate antagonists, fails to modify motor symptoms in patients with Parkinson's disease. *Mov Dis* 1994, 9(4): 437-440

Rascol O, Rai S, Sabatini U, Chollet P, Celsis P, Montastruc JL. Cortical overactivation in dyskinetic parkinsonian patients. *Mov Dis abstract* 1996, 11(1): 61

Rascol O, Lees AJ, Senard JM, Pirtosek Z, Montastruc JL, Fuell D. Ropinirole in the treatment of levodopa-induced motor fluctuations in patients with Parkinson's disease. *Clin Neuropharmacol* 1996, 19 (3): 234-245

Ravenholt RT, Foege WH. 1918 influenza, encephalitis lethargica, parkinsonism. *Lancet* 1982, 2 (8303): 860-864

Reches A, Jiang D, Fahn S. Catechol-O-methyltransferase inhibition by U-0521 increases striatal utilization of levodopa. *Naunyn Schmiedebergs Arch Pharmacol* 1982, 320 (1): 34-37

Redgrave P, Mitchell IJ, Dean P. Descending projections from the superior colliculus in rat: A study using orthograde transport of wheatgerm-agglutinin conjugated horseradish peroxidase. *Exp Brain Res* 1987, 68: 147-149

Redgrave P, Odekunle A, Dean P. Tectal cells of origin of predorsal bundle in rat: location and segregation from ipsilateral descending pathway. *Exp Brain Res* 1986, 63: 279-293

Redmond DE, Sladek JR Jr, Roth RH, Collier TJ, Elsworth JD, Deutch AY, Haber S. Fetal neuronal grafts in monkeys given methyl-phenyltetrahydropyridine. *Lancet* 1986, 1: 1125-1127

Reid M, Herrera-Marschitz M, Hokfelt T, Terenius L, Ungerstedt U. Differential modulation of striatal dopamine release by intranigral injection of gamma-aminobutyric acid (GABA), dynorphin A and substance P. *Eur J Pharmacol* 1988, 147: 411-420

Reinscheid RK, Nothacker HP, Bourson A, Ardati A, Henningsen RA, Bunzow JR, Grandy DK, Langen H, Monsma FJ Jr, Civelli O. Orphanin FQ: a neuropeptide that activates an opioid-like G protein-coupled receptor. *Science* 1995, 270 (5237): 792-794

Ricaurte GA, Langston JW, DeLanney LE, Irwin I, Brooks JD. Dopamine uptake blockers protect against the dopamine depleting effect of 1-methyl-4-phenyl-1,2,3,6-tetrahydropyridine (MPTP) in the mouse striatum. *Neurosci Lett* 1985, 59 (3): 259-264

Richfield EK, Maguire-Zeiss KA, Vonkeman HE, Voorn P. Preferential loss of preproenkephalin versus preprotachykinin neurons from the striatum of Huntington's disease patients. *Ann Neurol* 1995, 38: 852-861

- Riederer P, Lange KW, Kornhuber J, Jellinger K. Glutamate receptor antagonism: neurotoxicity, anti-kinetic effects, and psychosis. *J Neural Transm Suppl* 1991, 34: 203-210
- Riederer P, Sofic E, Rausch WD, Schmidt B, Reynolds GP, Jellinger K, Youdim MB. Transition metals, ferritin, glutathione, and ascorbic acid in parkinsonian brains. *J Neurochem* 1989, 52 (2): 515-520
- Rinne UK. Early combination of bromocriptine and levodopa in the treatment of Parkinson's disease: A 5-year follow-up. *Neurology* 1987, 37: 826-828
- Robertson RG, Farmery SM, Sambrook MA, Crossman AR. Dyskinesia in the primate following injection of an excitatory amino acid antagonist into the medial segment of the globus pallidus. *Brain Res* 1989, 476: 317-322
- Robertson RG, Graham WC, Sambrook MA, Crossman AR. Further investigations into the pathophysiology of MPTP-induced parkinsonism in the primate: an intracerebral microdialysis study of γ -aminobutyric acid in the lateral segment of the globus pallidus. *Brain Res* 1991, 563: 278-280
- Robledo P, Feger J. Excitatory influence of rat subthalamic nucleus to substantia nigra pars reticulata and the pallidal complex: electrophysiological data. *Brain Res* 1990, 518 (1-2): 47-54
- Rodnitzky RL. The use of Sinemet CR in the management of mild to moderate Parkinson's disease. *Neurology* 1992, 42 (Supp 1): 44-50
- Roques BP, Noble F. Dual inhibitors of enkephalin-degrading enzymes (neutral endopeptidase 24.11 and aminopeptidase N) as potential new medications in the management of pain and opioid addiction. *NIDA Res Monogr* 1995, 147: 104-145
- Rose G, Gerhardt G, Stromberg I, Olson L, Hoffer B. Monoamine release from dopamine-depleted rat caudate nucleus reinnervated by substantia nigra transplants: an in vivo electrochemical study. *Brain Res* 1985, 341 (1): 92-100
- Rouillard C, Bedard PJ, Falardeau P, Dipaolo T. Behavioural and biochemical evidence for a different effect of repeated administration of L-DOPA and bromocriptine on denervated versus non-denervated striatal dopamine receptors. *Neuropharmacology* 1987, 26(11): 1601-1606
- Rouzaire-Dubois B, Scarnati E. Bilateral corticosubthalamic nucleus projections: an electrophysiological study in rats with chronic cerebral lesions. *Neuroscience* 1985, 15 (1): 69-79
- Royce GJ, Laine EJ. Efferent connections of the caudate nucleus, including cortical projections of the striatum and other basal ganglia: an autoradiographic and horseradish peroxidase investigation in the cat. *J Comp Neurol* 1984, 226 (1): 28-49

- Ruottinen HM, Rinne UK. Effect of one month's treatment with peripherally acting catechol-O-methyltransferase inhibitor, entacapone, on pharmacokinetics and motor response to levodopa in advanced parkinsonian patients. *Clin Neuropharmacol* 1996, 19 (3): 222-233
- Russchen FT, Price JL. Amygdalostriatal projections in the rat. Topographical organization and fiber morphology shown using the lectin PHA-L as an anterograde tracer. *Neurosci Lett* 1984, 47 (1): 15-22
- Rye DB, Saper CB, Lee HJ, Wainer BH. Pedunculopontine tegmental nucleus of the rat: Cytoarchitecture, cytochemistry, and some extrapyramidal connections of the mesopontine tegmentum. *J Comp Neurol* 1987, 259: 483-528
- Saavedra JM. Distribution of serotonin and synthesizing enzymes in discrete areas of the brain. *Fed Proc* 1977, 36 (8): 2134-2141
- Sadikot AF, Parent A, Francois C. The centre median and parafascicular thalamic nuclei project respectively to the sensorimotor and associative-limbic striatal territories in the squirrel monkey. *Brain Res* 1990, 510 (1): 161-165
- Sakai K, Gash DM. Effect of bilateral 6-OHDA lesions of the substantia nigra on locomotor activity in the rat. *Brain Res* 1994, 633: 144-150
- Salin P, Hajji MD, Goff LK. Bilateral 6-hydroxydopamine-induced lesion of the nigrostriatal dopamine pathway reproduces the effects of unilateral lesion on substance P but not on enkephalin expression in the rat basal ganglia. *Eur J Neurosci* 1996, 8: 1746-1757
- Sambrook J, Fritsch EF, Maniatis T. *Molecular cloning: A laboratory manual*. Cold Spring Harbor Laboratory Press, Cold Spring Harbor, NY. 1986
- Sandy MS, Armstrong M, Tanner CM, Daly AK, Di Monte DA, Langston JW, Idle JR. CYP2D6 allelic frequencies in young-onset Parkinson's disease. *Neurology* 1996, 47 (1): 225-30
- Sandyk R. Nomifensine in advanced parkinsonism. *Clin Neuropharmacol* 1985, 8 (3): 296-297
- Sandyk R, Snider SN. Naloxone treatment of l-dopa-induced dyskinesias in Parkinson's disease. *Am J Psychiatry* 1986, 143(1): 118
- Sapp E, Ge P, Aizawa H, Bird E, Penney J, Young AB, Vonsattel JP, Difiglia M. Evidence for a preferential loss of enkephalin immunoreactivity in the external globus pallidus in low grade Huntington's disease using high resolution image analysis. *Neuroscience* 1995, 64(2): 397-404

Schachter M, Bedard P, Debono AG, Jenner P, Marsden CD, Price P, Parkes JD, Keenan J, Smith B, Rosenthaler J, Horowski R, Dorow R. The role of D-1 and D-2 receptors. *Nature* 1980, 286 (5769): 157-159

Schapira AH, Cooper JM, Dexter D, Clark JB, Jenner P, Marsden CD. Mitochondrial complex I deficiency in Parkinson's disease. *J Neurochem* 1990, 54 (3): 823-827

Schell CB, Strick PL. The origin of thalamic inputs to the arcuate premotor and supplementary motor areas. *J Neurosci* 1984, 4: 539-560

Schiller MR, Mende-Mueller L, Moran K, Meng M, Miller KW, Hook VY. 'Prohormone thiol protease' (PTP) processing of recombinant proenkephalin. *Biochemistry* 1995, 34 (25): 7988-7995

Schmidhammer H, Burkard WP, Eggstein-Aeppli L, Smith CF. Synthesis and biological evaluation of 14-alkoxymorphinans. 2. (-)-N-(cyclopropylmethyl)-4,14-dimethoxymorphinan-6-one, a selective mu opioid receptor antagonist. *J Med Chem* 1989, 32 (2): 418-421

Schonenecker VM. Ein eigentumliches syndrom im oralen Bereich bei Megaphenapplikation. *Nervenarzt* 1957, 28: 35-43

Schuh LA, Bennett JP. Suppression of dyskinesias in advanced Parkinson's disease. I. Continuous intravenous levodopa shifts dose response for production of dyskinesias but not for relief of parkinsonism in patients with advanced Parkinson's disease. *Neurology* 1993, 43 (8): 1545-1550

Schwab RS, England AC. Amantadine HCL (Symmetrel) and its relation to Levodopa in the treatment of Parkinson's disease. *Trans Am Neurol Assoc* 1969a, 94: 85-90

Schwab RS, England AC, Poskanzer DC, Young RR. Amantadine in the treatment of Parkinson's disease. *JAMA* 1969b, 208 (7): 1168-1170

Schwab RS, Poskanzer DC, England AC, Young RR. Amantadine in Parkinson's disease. Review of more than two years' experience. *JAMA* 1972, 222 (7): 792-795

Seiger A, Olson L. Late prenatal ontogeny of central monoamine neurons in the rat: Fluorescence histochemical observations. *Z Anat Entwicklungsgesch* 1973, 140 (3): 281-318

Seizinger BR, Grimm C, Holtt V, Herz A. Evidence for a selective processing of proenkephalin B into different opioid peptide forms in particular regions of rat brain and pituitary. *J Neurochem* 1984, 42 (2): 447-457

- Sesack SR, Pickel VM. In the rat medial nucleus accumbens, hippocampal and catecholaminergic terminals converge on spiny neurons and are in apposition to each other. *Brain Res* 1990, 527: 266-279
- Shaner RF. Development of the finer structure and fiber connections of the globus pallidus, corpus of Luys and substantia nigra, in the pig. *J Comp Neurol* 1936, 64:213-225
- Shaw KM, Lees AJ, Stern GM. The impact of treatment with levodopa in Parkinson's disease. *Q J Med* 1980, 49: 283-293
- Shinonaga Y, Takada M, Mizuno N. Topographical organisation of collateral projections from the basolateral amygdaloid nucleus to both the prefrontal cortex and nucleus accumbens in the rat. *Neuroscience* 1994, 58: 389-397
- Silverman PB. Sensitisation, response fluctuation and long-term effect of SKF-82958 and bromocriptine in the hemi-parkinsonian rat. *Eur J Pharmacol* 1992, 229: 235-240
- Simon EJ, Hiller JM, Edelman I. Stereospecific binding of the potent narcotic analgesic (3H) Etorphine to rat-brain homogenate. *Proc Natl Acad Sci U S A* 1973, 70 (7): 1947-1949
- Singer HS, Hahn IH, Krowiak E, Nelson E, Moran T. Tourette's syndrome: a neurochemical analysis of postmortem cortical brain tissue. *Ann Neurol* 1990, 27 (4): 443-446
- Singer HS, Rosenberg LA. Development of behavioral and emotional problems in Tourette syndrome. *Pediatr Neurol* 1989, 5 (1): 41-44
- Smart D, Lambert DG. delta-Opioids stimulate inositol 1,4,5-trisphosphate formation, and so mobilize Ca^{2+} from intracellular stores, in undifferentiated NG108-15 cells. *J Neurochem* 1996, 66 (4): 1462-1467
- Smith CA, Gough AC, Leigh PN, Summers BA, Harding AE, Maraganore DM, Sturman SG, Schapira AH, Williams AC, Maraganore DM. Debrisoquine hydroxylase gene polymorphism and susceptibility to Parkinson's disease. *Lancet* 1992, 339 (8806): 1375-1377
- Smith JAM, Leslie FM, Broide RS, Loughlin SE. Long-term changes in striatal opioid systems after 6-hydroxydopamine lesion of rat substantia nigra. *Neuroscience* 1993, 55(4): 935-951
- Smith Y, Bolam JP. Convergence of synaptic inputs from the striatum and globus pallidus onto identified nigrocollicular cells in the rat: A double anterograde labelling study. *Neuroscience* 1991, 44: 45-74

- Smith Y, Hazrati LN, Parent A. Efferent projections of the subthalamic nucleus in the squirrel monkey as studied by the PHA-L anterograde tracing method. *J Comp Neurol* 1990, 294: 306-326
- Smith Y, Bolam JP. Neurons of the substantia nigra reticulata receive a dense GABA-containing input from the globus pallidus in the rat. *Brain Res* 1989, 493 (1): 160-167
- Smith Y, Bolam JP. The output neurones and the dopaminergic neurones of the substantia nigra receive a GABA-containing input from the globus pallidus in the rat. *J Comp Neurol* 1990, 296 (1): 47-64
- Smith Y, Parent A, Seguela P, Descarries L. Distribution of GABA-immunoreactive neurons in the basal ganglia of the squirrel monkey (*Saimiri sciureus*). *J Comp Neurol* 1987a, 259 (1): 50-64.
- Sofic E, Riederer P, Heinsen H, Beckmann H, Reynolds GP, Hebenstreit G, Youdim MB. Increased iron (III) and total iron content in post mortem substantia nigra of parkinsonian brain. *J Neural Transm* 1988, 74 (3): 199-205
- Soghomonian JJ, Descarries L, Watkins KC. Serotonin innervation in adult rat neostriatum. II. Ultrastructural features: A autoradiographic and immunocytochemical study. *Brain Res* 1989, 481: 67-86
- Soghomonian JJ, Pedault S, Blanchet PJ, Goulet M, Di Paolo T, Bedard PJ. L-DOPA regulates glutamate decarboxylase mRNA levels in MPTP-treated monkeys. *Mol Brain Res* 1996, 39: 237-240
- Soghomonian JJ. Differential regulation of glutamate decarboxylase and preproenkephalin mRNA levels in the rat striatum. *Brain Res* 1994, 640 (1-2): 146-54
- Somers DL, Beckstead RM. N-methyl-D-aspartate receptor antagonism alters substance P and met5-enkephalin biosynthesis in neurons of the rat striatum. *J Pharmacol Exp Ther* 1992, 262 (2): 823-833
- Somogyi P, Hodgson AJ, Smith AD. An approach to tracing neuron networks in the cerebral cortex and basal ganglia: Combination of Golgi staining, retrograde transport of horseradish peroxidase and anterograde degeneration of synaptic boutons in the same material. *Neuroscience* 1979, 4: 1805-1852
- Somogyi P, Smith AD. Projection of the neostriatal spiny neurons to the substantia nigra: Application of a combined Golgi-staining and horseradish peroxidase transport procedure at both light and electron microscopic levels. *Brain Res* 1979, 178: 3-15
- Sonnenberg JL, Rauscher III FJ, Morgan JJ, Curran T. Regulation of proenkephalin by fos and jun. *Science* 1989, 246: 1622-1625

- Spanagel R, Herz A, Shippenberg TS. Opposing tonically active endogenous opioid systems modulate the mesolimbic dopaminergic pathway. *Proc Natl Acad Sci U S A* 1992, 89 (6): 2046-2050
- Spanagel R, Herz A, Shippenberg TS. The effects of opioid peptides on dopamine release in the nucleus accumbens: an in vivo microdialysis study. *J Neurochem* 1990, 55 (5): 1734-1740
- Spann BM, Grofova I. Origin of ascending and spinal pathways from the nucleus tegmenti pedunculopontinus in the rat. *J Comp Neurol*. 1989, 283: 13-27
- Specht LA, Pickel VM, Joh TH, Reis DJ. Light-microscopic immunocytochemical localization of tyrosine hydroxylase in prenatal rat brain. II. Late ontogeny. *J Comp Neurol* 1981b, 199 (2): 255-276
- Specht LA, Pickel VM, Joh TH, Reis DJ. Light-microscopic immunocytochemical localization of tyrosine hydroxylase in prenatal rat brain. I. Early ontogeny. *J Comp Neurol* 1981a, 199 (2): 233-253
- Spencer HJ. Antagonism of cortical excitation of striatal neurons by glutamic acid diethylester: Evidence for glutamic acid as an excitatory transmitter in the rat striatum. *Brain Res* 1986, 102: 91-101
- Spiegel EA, Wycis HT. Pallidothalamotomy in chorea. *Arch Neurol Psychiat* 1950, 64: 295-296
- Spina MB, Cohen G. Dopamine turnover and glutathione oxidation: implications for Parkinson disease. *Proc Natl Acad Sci U S A* 1989, 86 (4): 1398-1400
- Stanton GB, Goldberg ME, Bruce CJ. Frontal eye field efferents in the macaque monkey: I. Subcortical pathways and topography of striatal and thalamic terminal fields. *J Comp Neurol* 1988, 271 (4): 473-492
- Stenevi U, Bjorklund A, Svendgaard NA. Transplantation of central and peripheral monoamine neurons to the adult rat brain: techniques and conditions for survival. *Brain Res* 1976, 114 (1): 1-20
- Steriade M, Deschenes M. The thalamus as a neuronal oscillator. *Brain Res* 1984, 320 (1): 1-63
- Stern AS, Jones BN, Shively JE, Stein S, Udenfriend S. Two adrenal opioid polypeptides: proposed intermediates in the processing of proenkephalin. *Proc Natl Acad Sci U S A* 1981, 78 (3): 1962-1966
- Stern Y, Langston JW. Intellectual changes in patients with MPTP-induced parkinsonism. *Neurology* 1985, 35: 1506-1509

- Stoessl AJ, Mak E, Calne DB. (+)-4-Propyl-9-hydroxynaphthoxazine (PHNO), a new dopaminomimetic, in treatment of parkinsonism. *Lancet* 1985, 2: 1330-1331
- Stoof JC, De Boer T, Sminia P, Mulder AH. Stimulation of D2-dopamine receptors in rat neostriatum inhibits the release of acetylcholine and dopamine but does not affect the release of gamma-aminobutyric acid, glutamate or serotonin. *Eur J Pharmacol* 1982b, 84: 211-214
- Stoof JC, Keabian JW. Independent in vitro regulation by the D-2 dopamine receptor of dopamine-stimulated efflux of cyclic AMP and K^+ -stimulated release of acetylcholine from rat neostriatum. *Brain Res* 1982a, 250 (2): 263-270
- Stoof JC, Keabian JW. Opposing roles for D-1 and D-2 dopamine receptors in efflux of cyclic AMP from rat neostriatum. *Nature* 1981, 294: 366-368
- Stoof JC, Keabian JW. Two dopamine receptors biochemistry, physiology and pharmacology. *Life Sci* 1984, 35: 2281-2296
- Stoof JC, Verheijden PFHM, Leysen JE. Stimulation of D2-receptors in rat nucleus accumbens slices inhibits dopamine and acetylcholine release but not cyclic AMP formation. *Brain Res* 1987, 423, 364-368
- Stringer JL, Greenfield LJ, Hackett JT, Guyenet PG. Blockade of long-term potentiation by phencyclidine and sigma opiates in the hippocampus in vivo and in vitro. *Brain Res* 1983, 280 (1): 127-138
- Stromberg I, Herrera-Marschitz M, Ungerstedt U, Ebendal T, Olson L. Chronic implants of chromaffin tissue into the dopamine-denervated striatum. Effects of NGF on graft survival, fiber growth and rotational behavior. *Exp Brain Res* 1985, 60 (2): 335-349
- Stromberg U, Svensson TM. Further studies on the mode of action of amantidine. *Acta Pharmacol Toxicol* 1971, 30: 161-171
- Surmeier DJ, Song WJ, Yan Z. Coordinated expression of dopamine receptors in neostriatal medium spiny neurons. *J Neurosci* 1996, 16(20): 6579-6591
- Sweet RD, Lee JE, Spiegel HE, McDowell F. Enhanced response to low doses of levodopa after withdrawal from chronic treatment. *Neurology* 1972, 22 (5): 520-525
- Takada M, Li ZK, Hattori T. Long descending direct projection from the basal ganglia to the spinal cord: a revival of the extrapyramidal concept. *Brain Res* 1987, 436 (1): 129-135
- Takada M, Nishihama MS, Nishihama CC, Hattori T. Two separate neuronal populations of the rat subthalamic nucleus project to the basal ganglia and pedunculopontine tegmental region. *Brain Res* 1988, 442 (1): 72-80

- Tang F, Costa E, Schwartz JP. Increase of proenkephalin mRNA and enkephalin content of rat striatum after daily injection of haloperidol for 2 to 3 weeks. *Proc Natl Acad Sci U S A* 1983, 80 (12): 3841-3844
- Tasker RR, Doorly T, Yamashiro K. Thalamotomy in generalised dystonia. In: Fahn S, editor. *Advances in Neurology. Dystonia 2* 1988, 50: 615-631
- Tassin JP, Cheramy A, Blanc G, Thierry AM, Glowinski F. Topographical distribution of dopaminergic innervation and of dopaminergic receptors in the rat striatum. I Microestimation of [³H] dopamine uptake and dopamine content in microdiscs. *Brain Res* 1976, 107: 291-301
- Taylor MD, De Ceballos ML, Rose S, Jenner P, Marsden CD. Effects of a unilateral 6-hydroxydopamine lesion and prolonged L-3,4-dihydroxyphenylalanine treatment on peptidergic systems in rat basal ganglia. *Eur J Pharmacol* 1992, 219: 183-192
- Terenius L. Characteristics of the 'receptor' for narcotic analgesics in synaptic plasma membrane fraction from rat brain. *Acta Pharmacol Toxicol* 1973, 33 (5): 377-384
- Thomas KL, Rose S, Jenner P, Marsden CD. Dissociation of the striatal D-2 dopamine receptor from adenylyl cyclase following 6-hydroxydopamine-induced denervation. *Biochem Pharmacol* 1992, 44(1): 73-82
- Thureson-Klien A, Klein RL. Exocytosis from neuronal large dense-core vesicles. *Int Rev Cytol* 1990, 121: 67-126
- Tolosa ES, Martin WE, Cohen HP. Dyskinesias during levodopa therapy. *Lancet* 1975a, 1 (7921): 1381-1382
- Tolosa ES, Martin WE, Cohen HP, Jacobson RL. Patterns of clinical response and plasma dopa levels in Parkinson's disease. *Neurology* 1975b, 25 (2): 177-183
- Torczynski R, Bollon AP, Fuke M. Nucleotide sequence of the 5'-terminal region of rat 18S ribosomal DNA. *Mol Gen Genet* 1983, 191(3): 427-429
- Torczynski R, Fuke M, Bollon AP. Cloning and sequencing of a human 18S ribosomal RNA gene. *DNA* 1985, 4(4): 283-291
- Tork I. Anatomy of the serotonergic system. *Ann N Y Acad Sci* 1990, 600: 9-34
- Trabucchi M, Bassi S, Frattola L. Effect of naloxone on the 'on-off' syndrome in patients receiving long-term levodopa therapy. *Arch Neurol* 1982, 39: 120-121
- Tsu RC, Chan JS, Wong YH. Regulation of multiple effectors by the cloned delta-opioid receptor: stimulation of phospholipase C and type II adenylyl cyclase. *J Neurochem* 1995, 64 (6): 2700-2707

- Ueda H, Miyamae T, Fukushima N, Takeshima H, Fukuda K, Sasaki Y, Misu Y. Opioid mu- and kappa-receptor mediate phospholipase C activation through Gi1 in *Xenopus* oocytes. *Brain Res Mol Brain Res* 1995, 32 (1): 166-170
- Ueda H, Miyamae T, Hayashi C, Watanabe S, Fukushima N, Sasaki Y, Iwamura T, Misu Y. Protein kinase C involvement in homologous desensitization of delta-opioid receptor coupled to Gi1-phospholipase C activation in *Xenopus* oocytes. *J Neurosci* 1995, 15 (11):7485-7499
- Uhl GR, Navia B, Douglas J. Differential expression of preproenkephalin and prodynorphin mRNA in striatal neurons: High levels of preproenkephalin expression depend on cerebral cortical afferents. *J Neuroscience* 1988, 8(12): 4755-4764
- Uhler M, Herbert E, D'Eustachio P, Ruddle FD. The mouse genome contains two nonallelic pro-opiomelanocortin genes. *J Biol Chem* 1983, 258 (15): 9444-9453
- Ungerstedt U. 6-hydroxy-dopamine induced degeneration of central monoamine neurons. *Eur J Pharmacol* 1968, 5: 107-110
- Ungerstedt U. Adipsia and aphagia after 6-hydroxydopamine induced degeneration of the nigro-striatal dopamine system. *Acta Physiol Scand Suppl* 1971a, 367: 95-122
- Ungerstedt U. Postsynaptic supersensitivity after 6-hydroxy-dopamine induced degeneration of the nigro-striatal dopamine system. *Acta Physiol Scand Suppl* 1971b, 367: 69-93
- Ungerstedt U. Striatal dopamine release after amphetamine or nerve degeneration revealed by rotational behaviour. *Acta Physiol Scand Suppl* 1971c, 367:49-68
- Ungerstedt U, Arbuthnott GW. Quantitative recording of rotational behavior in rats after 6-hydroxy-dopamine lesions of the nigrostriatal dopamine system. *Brain Res* 1970, 24 (3): 485-93
- Uno M, Yoshida M. Monosynaptic inhibition of thalamic neurons produced by stimulation of the pallidal nucleus in cats. *Brain Res* 1975, 99 (2): 377-380
- Uretsky NJ, Seiden LS. Effect of alpha-methyl dopa on the reserpine-induced suppression of motor activity and the conditioned avoidance response. *J Pharmacol Exp Ther* 1969, 168 (1): 153-162
- Vaamonde J, Luquin MR, Obeso JA. Subcutaneous lisuride infusion in Parkinson's disease. Response to chronic administration in 34 patients. *Brain* 1991, 114: 601-617
- van der Drift JH. Long-term clinical experience with levodopa and anticholinergics: therapeutic considerations. In: Lakke JP, editor. *Parkinson's disease*. Amsterdam, Excerpta Medica, 1977, 111-116

- van der Kooy D, Carter DA. The organisation of the efferent projections and striatal afferents of the entopeduncular nucleus and adjacent areas in the rat. *Brain Res.* 1981, 211: 15-36
- van der Kooy D, Hattori T. Dorsal raphe cells with collateral projections to the caudate-putamen and substantia nigra: A fluorescent retrograde double labeling study in the rat. *Brain Res.* 1980a, 186: 1-7
- van der Kooy D, Hattori T. Single subthalamic nucleus neurons project to both the globus pallidus and substantia nigra in rat. *J Comp Neurol.* 1980b, 192: 751-768
- Vankova M, Arluison M, Leviel V, Tramu G. Afferent connections of the rat substantia nigra pars lateralis with special reference to peptide-containing neurons of the amygdalo-nigral pathway. *J Chem Neuroanat* 1992, 5 (1): 39-50
- Varastet M, Riche D, Maziere M, Hantraye P. Chronic MPTP treatment reproduces in baboons the differential vulnerability of mesencephalic dopaminergic neurons observed in Parkinson's disease. *Neuroscience* 1994, 63 (1), 47-56
- Verhage M, Sandman H, Mosselvelde F, van de Velde M, Hengst PA, Lopes da Silva FH, Ghijsen WE. Perfusion of immobilized isolated nerve terminals as a model for the regulation of transmitter release: release of different, endogenous transmitters, repeated stimulation, and high time resolution. *J Neurochem* 1992, 58 (4): 1313-1320
- Verhagen-Metman L, Blanchet PJ, Mouradian MM, Chase TN. Dextromethorphan and levodopa combination therapy in parkinsonian patients with response fluctuations. *Mov Dis abstract* 1996, 11(1): 687
- Vertes RP. A PHA-L analysis of ascending projections of the dorsal raphe nucleus in the rat. *J Comp Neurol* 1991, 313 (4): 643-668
- Vila M, Levy R, Herrero MT, Ruberg M, Faucheux B, Obeso JA, Agid Y, Hirsch EC. Consequences of nigrostriatal denervation on the functioning of the basal ganglia in human and non-human primates: An *in situ* hybridisation study of cytochrome oxidase subunit 1 mRNA. *J Neuroscience* 1997, 17(2): 765-773
- Vincent SR, Hokfelt T, Christensson I, Terenius L. Dynorphin-immunoreactive neurons in the central nervous system of the rat. *Neurosci Lett* 1982a, 33 (2): 185-190
- Vincent SR, Hokfelt T, Christensson I, Terenius L. Immunohistochemical evidence for a dynorphinergic immunoreactive strionigral pathway. *Eur J Pharmacol* 1982b, 85: 251-252
- Vogt C, Vogt O. Thalamusstudien I-III. *J Psychol Neurol.* 1941, 50: 32
- Von Voigtlander PF, Moore KE. Dopamine: release from the brain in vivo by amantidine. *Science* 1971, 174: 408-410

- Voorn P, Roest G, Groenewegen HJ. Increase of enkephalin and decrease of substance P immunoreactivity in the dorsal and ventral striatum of the rat after midbrain 6-hydroxydopamine lesions. *Brain Res* 1987, 412 (2): 391-396
- Vuillet J, Dimova R, Nieoullon A, Goff LK. Ultrastructural relationships between choline acetyltransferase- and neuropeptide Y-containing neurons in the rat striatum. *Neuroscience* 1992, 46 (2): 351-360
- Vuillet J, Kerkerian L, Kachidian P, Bosler O, Nieoullon A. Ultrastructural correlates of functional relationships between nigral dopaminergic or cortical afferent fibers and neuropeptide Y-containing neurons in the rat striatum. *Neurosci Lett* 1989, 100 (1-3): 99-104
- Vuillet J, Kerkerian L, Salin P, Nieoullon A. Ultrastructural features of NPY-containing neurons in the rat striatum. *Brain Res* 1989, 477 (1-2): 241-251
- Waddington JL. Effects of nomifensine and desipramine on the sequelae of intracerebrally-injected 6-OHDA and 5,6-DHT. *Pharmacol Biochem Behav* 1980, 13 (6): 915-917
- Waddington JL, Cross AJ, Gamble SJ, Bourne RC. Spontaneous orofacial dyskinesia and dopaminergic function in rats after 6 months of neuroleptic treatment. *Science* 1983, 220 (4596): 530-532
- Waddington JL, Gamble SJ. Emergence of apomorphine-induced 'vacuous chewing' during 6 months continuous treatment with fluphenazine decanoate. *Eur J Pharmacol* 1980, 68 (3): 387-388
- Wagner JJ, Terman GW, Chavkin C. Endogenous dynorphins inhibit excitatory neurotransmission and block LTP induction in the hippocampus. *Nature* 1993, 363 (6428): 451-454
- Walker JM, Thompson LA, Frascella J, Friederich MW. Opposing effects of mu and kappa opiates on the firing rate of dopamine cells in the substantia nigra of the rat. *Eur J Pharmacol* 1987, 134: 53-59
- Walker RH, Arbuthnott GW, Baughman RW, Graybiel AM. Dendritic domains of medium spiny neurons in the primate striatum: relationships to striosomal borders. *J Comp Neurol* 1993, 337 (4): 614-628
- Wamsley JK, Young WS, Kuhar MJ. Immunohistochemical localization of enkephalin in rat forebrain. *Brain Res* 1980, 190 (1): 153-174
- Ward CD, Duvoisin RC, Ince SE, Nutt JD, Eldridge R, Calne DB. Parkinson's disease in 65 pairs of twins and in a set of quadruplets. *Neurology* 1983, 33 (7): 815-824

- Weiner WJ, Koller WC, Perlik S, Nausieda PA, Klawans HL. The role of transient levodopa withdrawal ('drug holiday') in the management of Parkinson's disease. In: Rose CF, Capildeo R, editors. Research Progress in Parkinson's disease 1987, Chapter 35: 275-281
- Weiss S, Sebben M, Garcia-Sainz JA, Bockaert J. D2-dopamine receptor-mediated inhibition of cyclic AMP formation in striatal neurons in primary culture. *Mol Pharmacol* 1985, 27 (6): 595-599
- Weisskopf MG, Zalutsky RA, Nicoll RA. The opioid peptide dynorphin mediates heterosynaptic depression of hippocampal mossy fibre synapses and modulates long-term potentiation. *Nature* 1993b, 365 (6442): 188
- Weisskopf MG, Zalutsky RA, Nicoll RA. The opioid peptide dynorphin mediates heterosynaptic depression of hippocampal mossy fibre synapses and modulates long-term potentiation. *Nature* 1993a, 362 (6419): 423-427
- Werz MA, Macdonald RL. Dynorphin reduces calcium-dependent action potential duration by decreasing voltage-dependent calcium conductance. *Neurosci Lett* 1984, 46 (2): 185-190
- Werz MA, MacDonald RL. Opioid peptides selective for mu- and delta-opiate receptors reduce calcium-dependent action potential duration by increasing potassium conductance. *Neurosci Lett* 1983, 42 (2): 173-178
- Wesemann W, Sturm G, Funfgeld EW. Distribution of metabolism of the potential anti-parkinson drug memantine in the human. *J Neural Transm Suppl* 1980, (16): 143-148
- Wester K, Hauglie-Hanssen E. Stereotaxic thalamotomy: experiences from the levodopa era. *J Neurol Neurosurg Psychiatry* 1990, 53 (5): 427-430
- Westlund KN, Denney RM, Kochersperger LM, Rose RM, Abell CW. Distinct monoamine oxidase A and B populations in primate brain. *Science* 1985, 230 (4722): 181-183
- Whim MD, Lloyd PE. Frequency-dependent release of peptide cotransmitters from identified cholinergic motor neurons in *Aplysia*. *Proc Natl Acad Sci U S A* 1989, 86 (22): 9034-9038
- White JD, Gall CM, McKelvy JF. Proenkephalin is processed in a projection-specific manner in the rat central nervous system. *Proc Natl Acad Sci U S A* 1986, 83 (18): 7099-7103
- Whittier JR. Ballisim and the subthalamic nucleus (nucleus hypothalamicus corpus Luysii). *Arch. Neurol. Psychiat* 1947, 58: 672

- Whittier JR, Mettler FA. Studies on the subthalamus of rhesus monkey. II. Hyperkinesia and other physiological effects of subthalamic lesions, with special reference to the subthalamic nucleus of Luys. *J Comp Neurol* 1949b, 90: 319-372
- Whittier JR, Mettler FA. Studies on the subthalamus of the rhesus monkey. I. Anatomy and fiber connections of the subthalamic nucleus of Luys. *J Comp Neurol* 1949a, 90: 281-318
- Wichmann T, DeLong MR. Pathophysiology of parkinsonian motor abnormalities. *Adv Neurol* 1993, 60: 53-61
- Widner H, Tetud J, Rehncrona S, Snow BJ, Brundin P, Bjorklund A, Lindvall O, Langston JW. Fifteen months' follow-up on bilateral embryonic mesencephalic grafts in two cases of severe MPTP-induced parkinsonism. *Adv Neurol* 1993, 60: 729-733
- Wieland S, Lucki I. Altered behavioral responses mediated by serotonin receptors in the genetically dystonic (dt) rat. *Brain Res Bull* 1991, 26 (1): 11-16
- Wilkinson DG. The theory and practice of *in situ* hybridisation. In: Wilkinson DG, editor. *In situ* hybridisation: A practical approach. IRL Press, Oxford University Press, 1992, Chapter 1: 9-10
- Williams JT, Egan TM, North RA. Enkephalin opens potassium channels on mammalian central neurones. *Nature* 1982, 299 (5878): 74-77
- Wilson CJ, Chang HT, Kitai ST. Firing patterns and synaptic potentials of identified giant aspiny interneurons in the rat neostriatum. *J Neurosci* 1990, 10 (2): 508-519
- Wilson CJ, Groves PM. Fine structure and synaptic connections of the common spiny neuron of the rat neostriatum: a study employing intracellular injection of horseradish peroxidase. *J Comp Neurol* 1980, 194: 599-615
- Wong GF, Gray CS, Hassanein RS, Koller WC. Environmental risk factors in siblings with Parkinson's disease. *Arch Neurol* 1991, 48 (3): 287-289
- Wooten GF, Collins RC. Metabolic effects of unilateral lesion of the substantia nigra. *J Neurosci* 1981, 1 (3): 285-291
- Wuster M, Schulz R, Herz A. Specificity of opioids towards the mu-, delta- and epsilon-opiate receptors. *Neurosci Lett* 1979, 15 (2-3): 193-198
- Wyss JM, Sripanidkulchai K. The topography of the mesencephalic and pontine projections from the cingulate cortex of the rat. *Brain Res* 1984, 293 (1): 1-15
- Yamasaki DSG, Krauthamer GM, Rhoades RW. Superior collicular projections to intralaminar thalamus in rat. *Brain Res.* 1986, 378: 223-233

- Ye FQ, Allen PS, Martin WR. Basal ganglia iron content in Parkinson's disease measured with magnetic resonance. *Mov Dis* 1996, 11 (3): 243-249
- Yelnik J, Percheron G. Subthalamic neurons in primates: a quantitative and comparative analysis. *Neuroscience* 1979, 4: 17171-1743
- Youdim MB, Ben-Shachar D, Riederer P. Is Parkinson's disease a progressive siderosis of substantia nigra resulting in iron and melanin induced neurodegeneration? *Acta Neurol Scand* 1989, 126: 47-54
- Youdim MB, Riederer P. The role of iron in senescence of dopaminergic neurons in Parkinson's disease. *J Neural Transm* 1993, 40: 57-67
- Young AB, Bromberg MB, Penney JB. Decreased glutamate uptake in subcortical areas deafferented by sensorimotor cortical ablation in the cat. *J Neurosci* 1981, 1: 241-249
- Young III WS, Bonner TI, Brann MR. Mesencephalic dopamine neurons regulate the expression of neuropeptide mRNAs in the rat forebrain. *Proc Natl Acad Sci USA* 1986, 83: 9827-9831
- Zaborszky L, Alheid GF, Beinfeld MC, Eiden LE, Heimer L, Plakovits M. Cholecystokinin innervation of the ventral striatum: A morphological and radioimmunological study. *Neuroscience* 1985, 14: 427-453
- Zagon IS, Gibo DM, McLaughlin PJ. Ontogeny of zeta (zeta), the opioid growth factor receptor, in the rat brain. *Brain Res* 1992, 596 (1-2): 149-156
- Zagon IS, McLaughlin PJ. Naloxone modulates body and organ growth of rats: dependency on the duration of opioid receptor blockade and stereospecificity. *Pharmacol Biochem Behav* 1989, 33 (2): 325-328
- Zahm DS. Ventral striatopallidal parts of the basal ganglia in the rat. II. Compartmentalisation of the ventral pallidal efferents. *Neuroscience* 1989, 30: 33-50
- Zahm DS, Brog JS. On the significance of subterritories in the 'accumbens' part of the rat ventral striatum. *Neuroscience* 1992, 50 (4): 751-767
- Zamir N, Palkovits M, Brownstein MJ. Distribution of immunoreactive dynorphin A1-8 in discrete nuclei of the rat brain: comparison with dynorphin A. *Brain Res* 1984a, 307 (1-2): 61-68
- Zamir N, Palkovits M, Brownstein M. Distribution of immunoreactive Met-enkephalin-Arg6-Gly7-Leu8 and Leu-enkephalin in discrete regions of the rat brain. *Brain Res* 1985, 326 (1): 1-8

- Zamir N, Palkovits M, Weber E, Brownstein MJ. Distribution of immunoreactive dynorphin B in discrete areas of the rat brain and spinal cord. *Brain Res* 1984c, 300 (1): 121-127
- Zamir N, Skofitsch G, Bannon MJ, Helke CJ, Kopin IJ, Jacobowitz DM. Primate model of Parkinson's disease: alterations in multiple opioid systems in the basal ganglia. *Brain Res* 1984, 322 (2): 356-360
- Zamir N, Weber E, Palkovits M, Brownstein M. Differential processing of prodynorphin and proenkephalin in specific regions of the rat brain. *Proc Natl Acad Sci U S A* 1984b, 81 (21): 6886-6889
- Zeng BY, Jolkkonen J, Jenner P, Marsden CD. Chronic L-DOPA treatment differentially regulates gene expression of glutamate decarboxylase, preproenkephalin and preprotachykinin in the striatum of 6-hydroxydopamine-lesioned rat. *Neuroscience* 1995, 66 (1): 19-28
- Zhu J, Chen C, Xue JC, Kunapuli S, DeRiel JK, Liu-Chen LY. Cloning of a human kappa opioid receptor from the brain. *Life Sci* 1995, 56 (9): 201-207
- Zukin RS, Eghbali M, Olive D, Unterwald EM, Tempel A. Characterisation and visualisation of rat and guinea pig brain K opioid receptors: Evidence for K₁ and K₂ opioid receptors. *Proc Natl Acad Sci U.S.A.* 1988, 85: 4061- 4065
- Zurawski G, Benedik M, Kamb BJ, Abrams JS, Zurawski SM, Lee FD. Activation of mouse T-helper cells induces abundant preproenkephalin mRNA synthesis. *Science* 1986, 232 (4751): 772-775

